3. CHAPTER 3 - RESULTS AND DISCUSSIONS

3.1. FIELD EXPOSURE TESTS OF STONE SAMPLES

3.1.1. MINERALOGICAL-PETROGRAPHIC CHARACTERISATION OF STONE SAMPLES

3.1.1.1. Visual assessment and Observation of thin sections by Polarized Light Microscopy (PLM)

Carrara Marble

Macroscopic Observation

Marble selected for this study is white Carrara Marble, commercially classified as "Marmo Bianco Carrara C/D (White Carrara Marble C/D)" (Primavori, 2015) (Figure 3.1). It was extracted from the Massa Carrara area, located in the western Apuan Alps. This medium-fine grained metamorphic stone ranges from pearly white to light grey in colour but the variety C/D stands out from C for the not perfectly white groundmass. Many thin dark grey veins and grey patches up to centimetre size are observable with naked eyes all over the stone surface. This dark veins with a predominant sub parallel orientation along with small graphite crystals of nanometre dimension testify the bio-constructed origin of protolite. The material is compact and no surface pores are detectable. Hoverer, it is known that the degradation produces a decohesion of the granules and thus a secondary porosity can occur.

Figure 3. 1 Slab of Carrara Marble

Observation of thin sections by Polarized Light Microscopy

This lithotype is characterised by an granoblastic texture with polygonal crystals of average size of 300 µm, without preferential crystallographic orientation (isotropic matrix) crossed by anisotropic thick white and less abundant thin black veins. The crystals of white and black veins are mainly hypidioblastic and to a lesser extent idioblastic, with linear or rounded edges. Carbonate (calcite and rare dolomite) dimension range is between 40 µm and 700 µm while the dimension of quartz, muscovite, opaque minerals (magnetite and pyrite) are often < 40 µm (Figure 3.2).

The main mineral of the stone is the calcite, colourless in plane polarised light (PPL) and characterised by high birefringence and rhombohedral cleavage. Fluid inclusions are observable in some calcite crystals at reflected light (Figure 3.2 B, C). Moreover, carbon crystallised as graphite is visible as dark areas between grains both in plane and crossed polarised light. This can suggest that the protolith was a bituminous limestone.

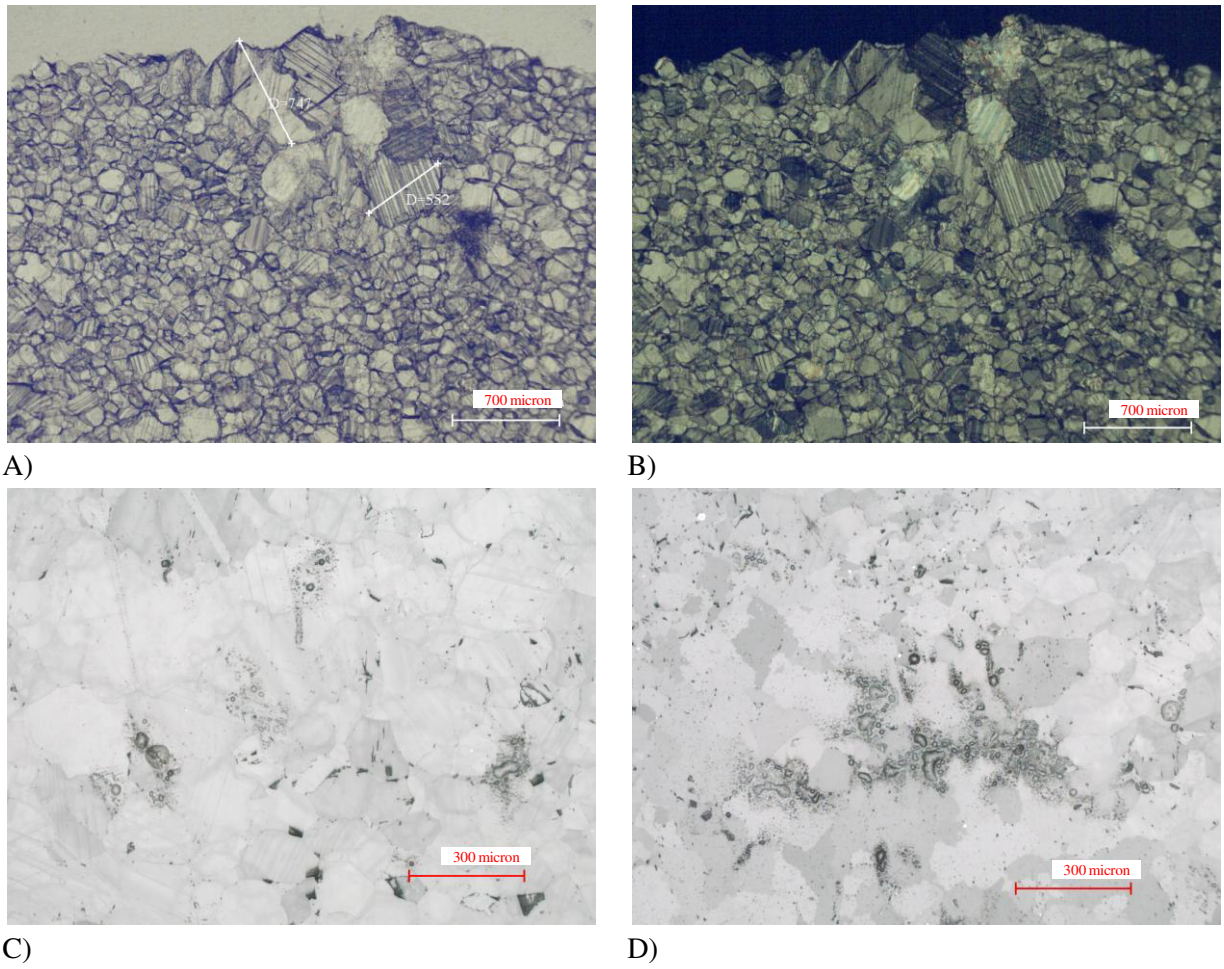

A) B)

C) D)

Figure 3.2 Micrographs (OM) of thin section of Carrara Marble before exposure in PPL (A) and CPL (B). C and D shows the presence of fluid inclusions along calcite crystals in white veins (PPL).

Grey patches and veins are recognised by optical microscopy as turbid dark areas in transmitted light while it is possible to recognise their xenoblastic calcite crystals only with reflected light (Figure 3.3).
Several opaque minerals, often xenoblastic but sometimes also with spherical or polygonal habit, are observable mainly in or along the edge of veins/patches (Figure 3.3). In reflected light, many of these are white and luminescent in PPL and dark in CPL, likely identified as pyrite.

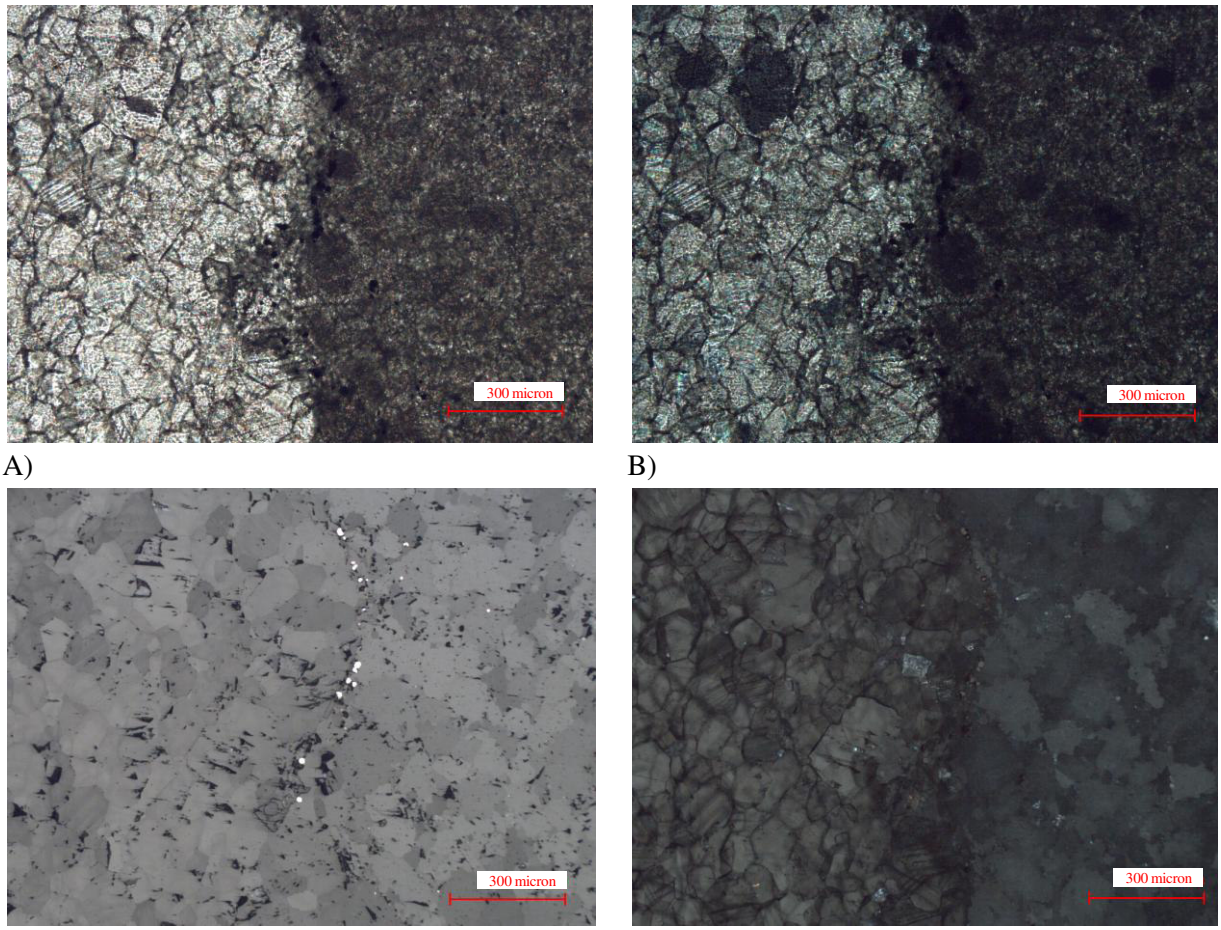

A) B)

C) D)

Figure 3.3 Grey patch (on the right) observed by optical microscopy in transmitted (A, B) and reflected light (C, D) (PPL in A and C while CPL in B and D). Opaque minerals are visible along the edge of veins as luminescent in PPL (C) while opaque dark grey in CPL (D).

Rosso Ammonitico Veronese

Macroscopic observation

Limestone selected for this research is a Rosso Ammonitico Veronese extracted from Valpolicella area, in the venetian Prealps close to Verona (Bosellini et al., 1967). Regarding the commercial classification, this lithotype is a sedimentary rock identified as Verona Red Marble (as hereafter called) and in particular as "Nembro Limestone" that represents the lowest stratigraphic unit of the Rosso Ammonitico Veronese Formation deposited in the Middle-Upper Jurassic (170-140 million years ago).

This lithotype is a nodular rose limestone, more reddish in some areas while more greyish-greenish in others (Figure 3.4). Many discontinuities between nodules are visible as veins and styloitic joints of mainly red but also greenish and white colour. Some orange-yellow patches are observable all over the surface. The material appears in general compact and no surface macropores are detectable while a surface roughness is observed also due to the presence of micro and meso pores.

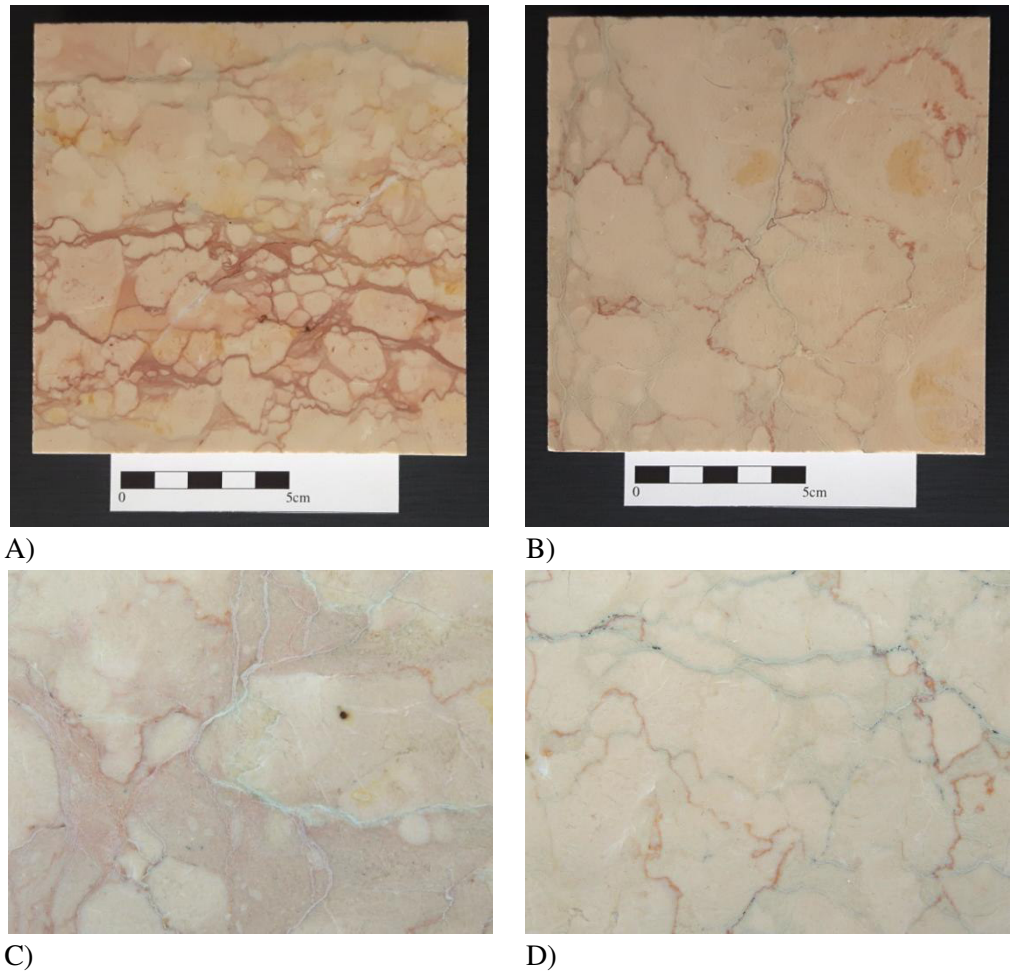

Figure 3.4 Slabs of Verona Red Marble more pinkish and with red veins (A and detail in C) and lighter in colour with the presence of greenish-grey veins in addition to red ones (B and detail in D).

A high macroporosity is also conferred by the numerous veins and the stylolite peaks. The presence of insoluble minerals, such as oxides and hydroxides, clay minerals and sulphides within the stylolite peaks makes the Verona Red Marble less permeable despite the presence of very large planar discontinuities.

Observation of thin sections by Polarized Light Microscopy

Thin section analysis shows that the analysed lithotype is a pseudo-nodular biomicritic limestone (Figure 3.5 A). Optical microscopy allows to identify a carbonate mud (micrite) that contains microfossils such as fragments of thin pelagic bivalves shells, crinoids, ostracods, radiolarians and some primitive planktonic foraminifera (probably *Conoglobigerina* sp.) (Figure 3.5 B-E). Moreover, it was observed that fragments of thin lamellibranches prevail in some areas. Considering the texture, it is classified as wackestone (Duhman, 1962).

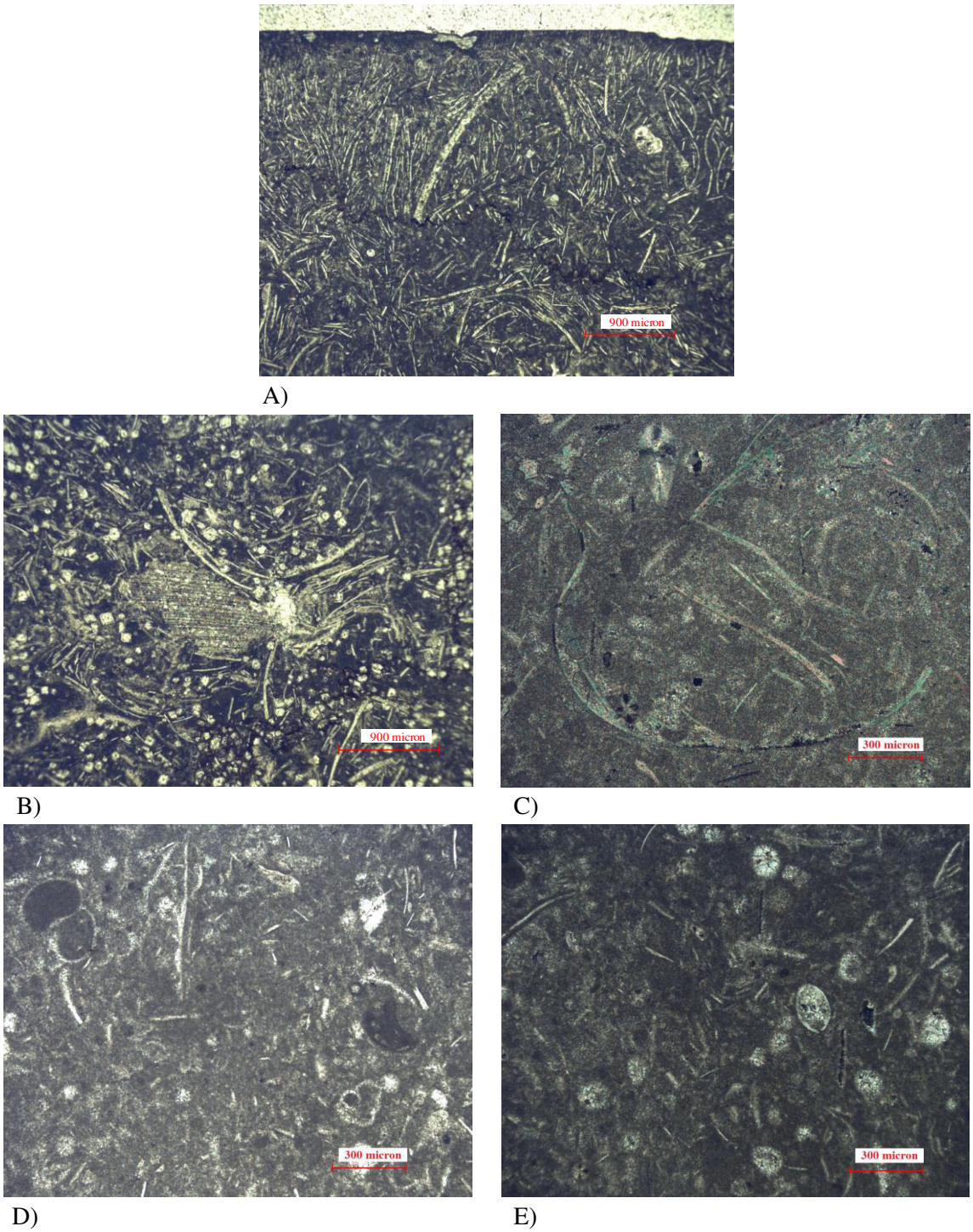

Figure 3.5 Optical micrographs of Rosso Ammonitico Veronese (A, B, D plane-polarised light and C, E cross-polarised light). A) General overview of the limestone. B-E) examples of fragments of lamellibranches shells, crinoids, ostracods, radiolarians and some primitive planktonic foraminifera detected in the micritic mud.

Both stylolitic joins and sparry-calcite veins are observable (Figure 3.6 A-D). Re-crystallisation of well-formed rhomb-shaped crystals are abundant along stylolitic joints but they are observable also in the matrix (Figure 3.6 C-F). Nevertheless, further analyses are necessary to discriminate if they are crystals of dolomite or sparry calcite. Moreover, brownish-red veins observed in stylolitic joints suggest the presence of oxides or hydroxides of Fe or Mg.

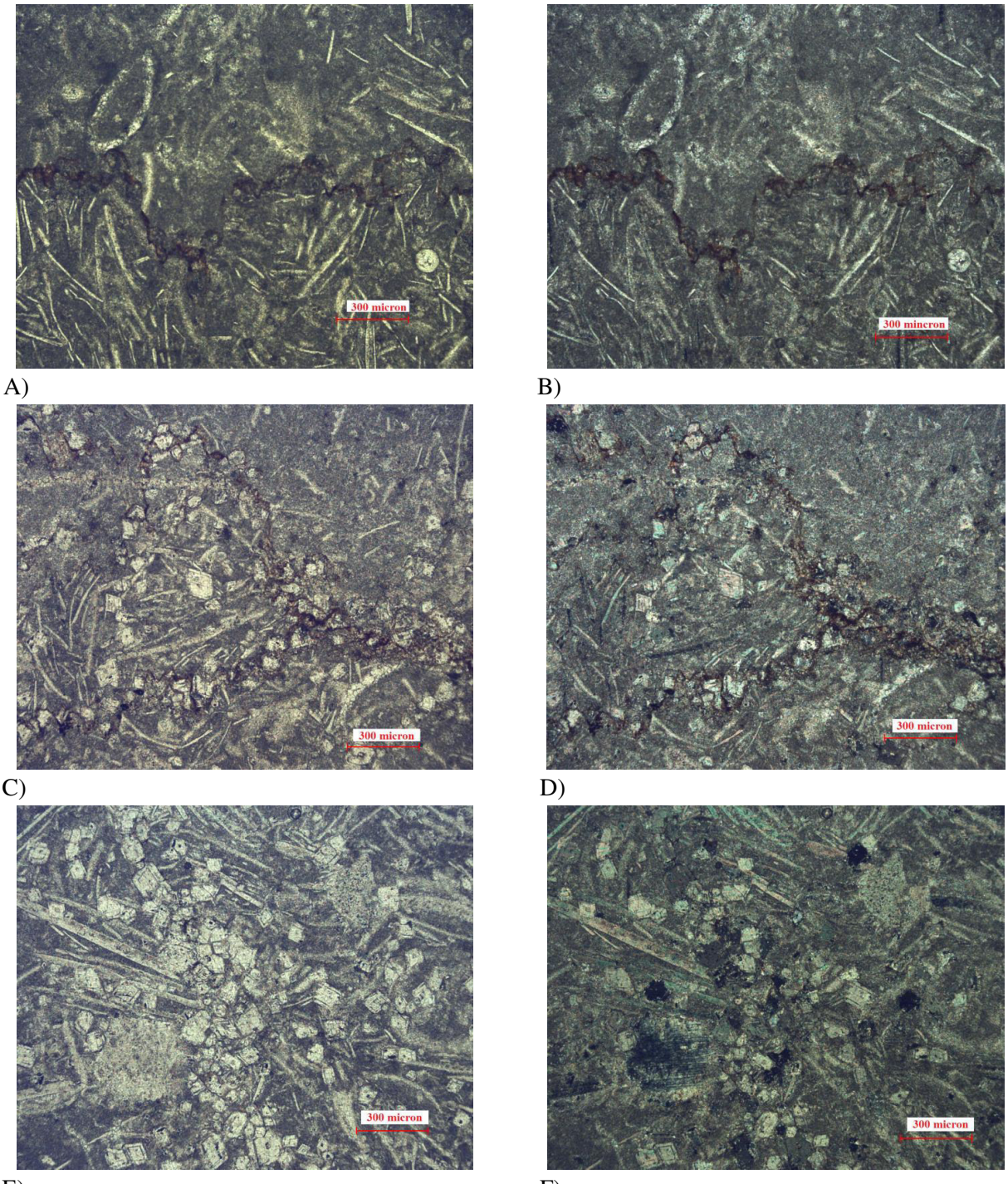

Figure 3.6 Optical micrographs of Rosso Ammonitico Veronese (A, C, E, G plane-polarised light and B, D, F, H cross-polarised light). A-D) brownish-red stylolitic joints, along which crystallisation of dolomite is sometimes observable (C-D). Euhedral to subeuhedral zoned dolomite crystals present in veins (E-F) but also in the matrix.

3.1.1.2. X-Ray Powder Diffraction (XRPD)

The XRD patterns of Carrara Marble and Verona Red Marble samples are shown in Figure 3.7-3.9. In Carrara Marble sample (Figure 3.7), the highest-intensity diffractions are indicative of calcite (d_{104} = 3.02 Å, JCPDS: 01-072-1652), dolomite (d_{104} = 2.88 Å, JCPDS: 01-071-1662) and quartz (d_{011} = 3.29 Å, JCPDS: 01-079-1914). Further information about the diffraction data are reported in Annex 1.

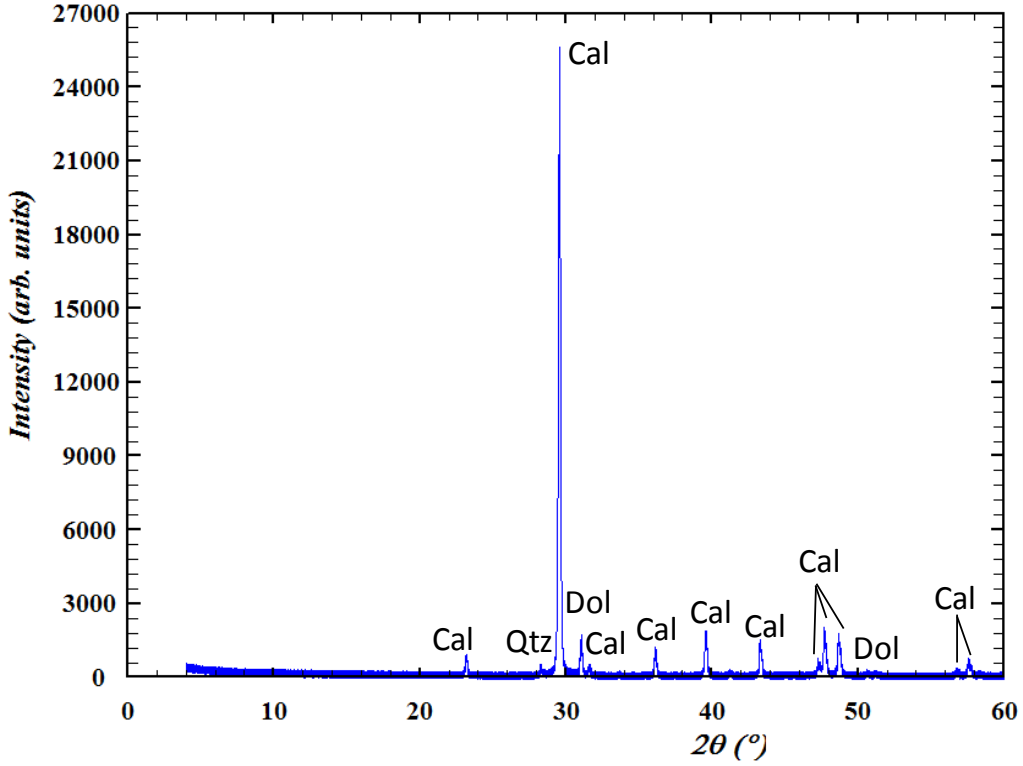

Figure 3.7 Diffractogram of Carrara Marble sample.

Two samples of Verona Red Marble were assessed: one characterised by more greyish colour (NBE1) and one with more reddish colour (NBE2). The highest-intensity peaks of both samples are indicative of calcite (d_{104} = 3.02 Å, JCPDS: 01-072-1652); in NBE2 sample the presence of dolomite was also detected (d_{104} = 2.88 Å, JCPDS: 01-074-1687) (Figure 3.8, 3.9). Moreover, powders diffraction patterns of both samples show a small peak (d= 3.16 Å) that probably refers to hydrated magnesium carbonate. More information about powders diffraction data are reported in Annex 1.

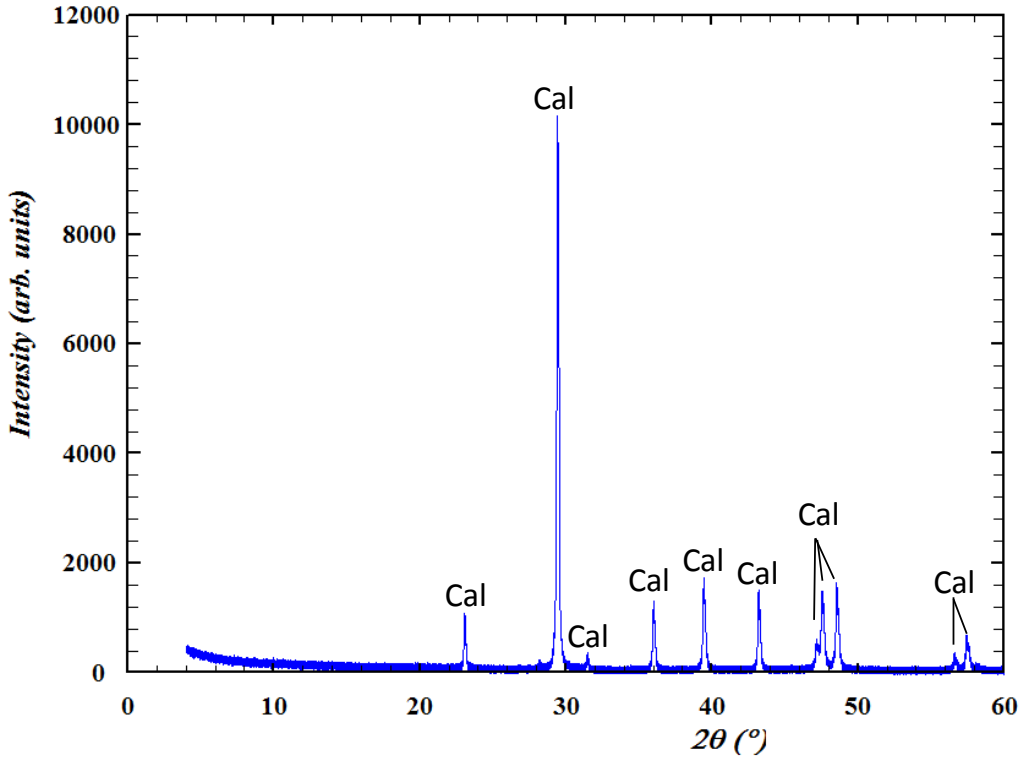

Figure 3.8 Diffractogram of NBE1 sample.

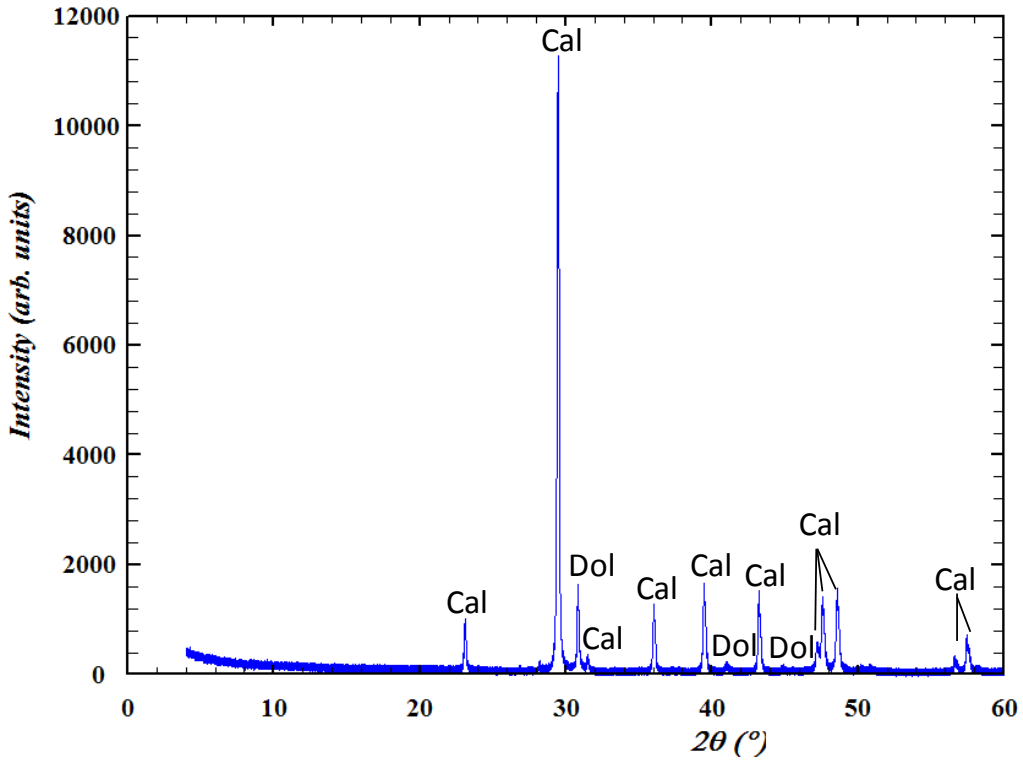

Figure 3.9 Diffractogram of NBE2 sample.

3.1.1.3. X-Ray Fluorescence Spectroscopy (XRF)

X-Ray fluorescence was performed on marble and limestone samples for a comprehensive mineralogical and chemical characterisation of the lithotypes exposed.
Table 3.1 shows results of major and trace elements detected on 3 samples of Carrara Marble (CBE_1, CBE_2 and CBE_3) and 6 of Verona Red Marble (sample with more greyish colour: NBE1_1, NBE1_2 and NBE1_3; more reddish sample: NBE2_1, NBE2_2 and NBE2_3).
Results proved that Carrara Marble is mainly composed by CaO followed by SiO_2 and MgO (Table 3.1). These outputs confirm the presence of calcite (CaO), dolomite (CaO and MgO) and quartz (SiO_2) already detected by XRPD. Moreover, small quantity of Sr (mean: 136.13 ppm) and S (mean: 44.20 ppm) prevailed among other trace elements.
Concentrating upon limestone, the highest value was of CaO followed by SiO_2, MgO (mainly in more reddish sample - NBE2), Al_2O_3 and Fe_2O_3. CaO and MgO prove the presence of calcium and magnesium carbonate previously identified by XRPD (subchapter 3.1.1.2) while the detected percentages of SiO_2, Al_2O_3 and Fe_2O_3 suggest the possible presence of small quantity of kaolinite. Among trace elements, Sr (mean: 98.53 ppm) showed the highest value.

LITHOTYPE	CARRARA MARBLE			VERONA RED MARBLE					
SAMPLE	CBE1_1	CBE1_ 2	CBE1_3	NBE1_1	NBE1_2	NBE1_3	NBE2_1	NBE2_2	NBE2_3
SiO_2	2.93	2.90	2.86	3.85	3.84	3.88	3.79	3.84	3.89
TiO_2	0.00	0.00	0.00	0.02	0.02	0.02	0.02	0.02	0.02
AL_2O_3	0.47	0.46	0.45	0.74	0.74	0.75	0.73	0.73	0.73
Fe_2O_3	0.49	0.49	0.48	0.59	0.59	0.59	0.68	0.67	0.68
MnO	0.00	0.00	0.00	0.04	0.04	0.04	0.04	0.04	0.04
MgO	1.59	1.57	1.58	0.39	0.39	0.39	1.36	1.43	1.41
CaO	52.93	52.96	52.72	51.55	51.64	51.86	50.24	50.59	50.28
Na_2O	0.05	0.05	0.05	0.04	0.04	0.05	0.05	0.05	0.05
K_2O	0.00	0.00	0.00	0.22	0.22	0.23	0.19	0.19	0.18
P_2O_5	0.01	0.01	0.01	0.04	0.04	0.04	0.05	0.05	0.05
LOI	41.52	41.56	41.84	42.51	42.42	42.14	42.87	42.39	42.65
Totale	99.99	100.00	99.99	99.99	99.98	99.99	100.02	100.00	99.98
Anhyd.	58.47	58.44	58.15	57.48	57.56	57.85	57.15	57.61	57.33
Ba	0.00	0.00	0.00	0.00	0.00	0.00	0.00	0.00	0.00
Ce	3.10	8.10	14.30	21.80	19.40	17.90	21.30	25.00	19.50
Co	0.00	0.00	0.00	0.00	0.00	0.00	0.00	0.00	0.00
Cr	0.00	0.00	0.00	0.00	0.00	0.00	0.00	0.00	0.00
Cu	8.10	1.60	0.70	7.90	7.00	6.00	8.80	7.80	8.70
Ga	0.00	0.00	0.00	0.00	0.00	0.00	0.00	0.00	0.00
Hf	0.50	0.30	0.70	0.50	0.70	0.80	0.60	0.40	0.40
La	16.10	0.00	17.40	46.90	30.60	40.20	46.50	0.00	30.20
Nb	3.30	4.80	5.20	4.40	4.50	5.60	5.30	5.60	5.10
Nd	0.00	0.00	0.00	0.00	0.20	0.30	0.00	0.00	0.00
Ni	0.00	0.00	0.00	0.00	0.00	0.00	0.00	0.00	0.00
Pb	16.20	17.30	12.70	18.60	20.50	18.60	16.80	16.70	18.40
Rb	1.30	1.70	1.20	3.80	4.10	4.10	3.50	3.40	3.90
S	0.00	57.80	74.80	0.00	0.00	0.00	0.00	0.00	0.00
Sc	0.00	0.00	0.00	0.00	0.00	0.00	0.00	0.00	0.00
Sr	133.30	138.40	136.70	91.40	99.60	98.90	99.80	101.50	100.00
Th	0.50	0.40	1.00	1.60	1.00	1.20	2.70	0.00	4.00
V	7.20	6.80	7.40	13.70	11.70	8.90	12.60	11.80	10.60
Y	1.80	2.40	1.30	14.40	14.30	14.70	10.70	12.70	10.50
Zn	0.00	0.00	0.00	0.00	0.00	0.00	0.00	0.00	0.00
Zr	0.00	0.00	0.00	2.70	3.90	3.90	1.40	3.30	4.50

Table 3.1 Major (wt%) and trace (ppm) element analyses of Carrara Marble and Verona Red Marble.

3.1.1.4. Mercury Intrusion Porosimetry (MIP)

Considering the porosimetry analysis, both lithotypes are characterised by a low porosity and it is noticeable slightly higher values of accessible porosity in Carrara Marble (between 1.11 % and 1.66 %) than in Verona Red Marble (from 0.05 % to 0.34 %), as shown in Table 3.2.

LITHOTYPE	SAMPLE	ACCESSIBLE POROSITY (%)	INACCESSIBLE POROSITY (%)	AVERAGE PORE DIAMETER (µm)	MEDIAN PORE DIAMETER (µm)	MODEL PORE DIAMETER (µm)
CARRARA MARBLE	CBE_1	1.66	0.01	0.4742	0.9602	1.7450
	CBE_2	1.11	0.02	0.3131	0.4372	0.2434
	CBE_3	1.46	0.00	0.5637	2.1501	10.2940
VERONA RED MARBLE	NBE1_1	0.09	0.02	0.3717	3.4557	5.0212
	NBE1_2	0.08	0.02	0.7608	1.1967	0.8343
	NBE1_3	0.05	0.03	1.2440	2.5267	2.8127
	NBE2_1	0.13	0.00	0.2936	0.9128	0.4680
	NBE2_2	0.34	0.03	0.0960	0.1462	0.0803
	NBE2_3	0.13	0.02	0.4358	1.6754	8.5057

Table 3.2 Porosity and pore size diameter of the marble and limestone.

In Carrara Marble, most of pore diameter was included in a range of 0.1000-10.0000 µm with mean pore diameter between 0.3131 µm and 0.5637 µm. Mean values exceeded threshold of micropores range (i.e. diameter of 0.2 µm) based on Cardell et al. (2003). However, some differences were detected in modal pore diameter (Table 3.2) and pore size distributions among replicas (Figure 3.10). Figure 3.10 shows a multimodal distribution of pore size in sample CBE_1 (with most pores having a diameter between 0.2661 µm and 4.2036 µm), a unimodal distribution around 0.2661 µm in sample CBE_2 and a bimodal distribution in CBE_3 (with the highest peak around 11.4673 µm and a smaller one at 0.2661 µm).

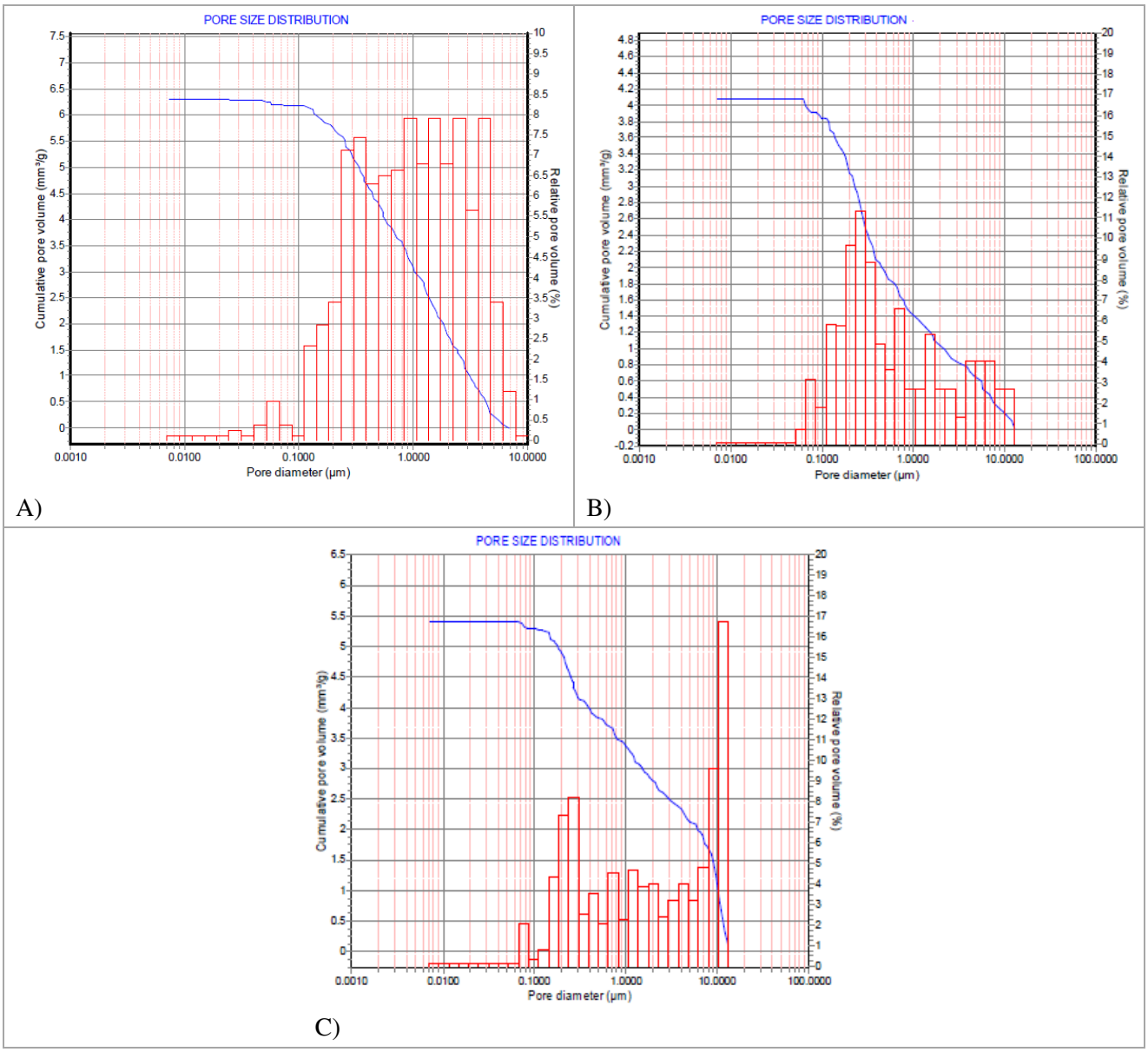

Figure 3.10 Pore size distribution of Carrara Marble samples: multimodal for CBE_1 (A), unimodal for CBE_2 (B) and bimodal for CBE_3 (C).

Porosimetry highlighted that Verona Red Marble samples were characterised by a pore diameter included in a range 0.0131-11.4673 µm, values that are considered as micro- and mesoporisity by Cadell et al. (2003). Mean pore diameters of the three replicas were between 0.2936 µm and 1.2440 µm but differences have been observed in modal pore diameter (Table 3.2) and in size distribution (Figure 3.11). In this regard, all three specimens of sample with more greyish appearance (NBE1) displayed a multimodal distribution with at least 64 % of relative volume comprised in the range 1.0000-10.0000 µm while replicas of more reddish specimen (NBE2) showed slightly higher concentration of pores with smaller dimension (20-67 % of relative volume was between 0.1000 µm and 1.0000 µm). Figure 3.11 displays also a unimodal distribution of pore size in sample NBE2_1 (around 0.1611 µm) and NBE2_2 (around 0.0759 µm) and a multimodal distribution mostly concentrated in the range 1.0000-10.0000 µm in NBE2_3.

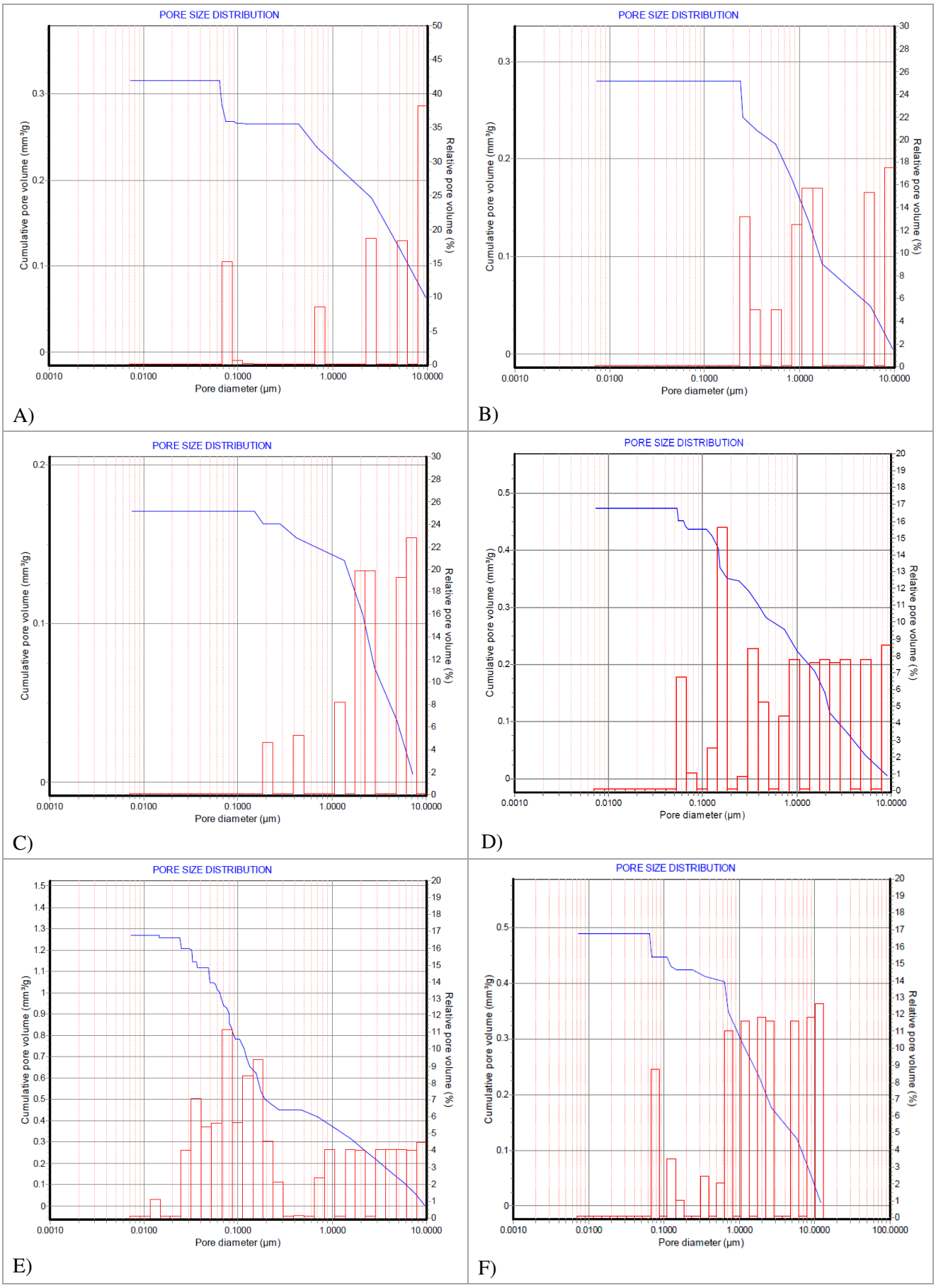

Figure 3.11 Pore size distribution of Verona Red Marble samples: multimodal for NBE1_1 (A), NBE1_2 (B), NBE1_3 (C), and NBE2_3 (F) and unimodal for NBE2_1 (D) and NBE2_2 (E).

Porosity features supply useful information about decay of stone materials because it is widely recognised that the higher the porosity of stones, the faster the degradation (Amoroso, 2002). Beside total porosity, also pore size distribution affects deterioration phenomena of stone materials. Camuffo (2014) declared that physical effects (such as frost) are more likely to occur in materials characterised by a pore radius below 0.1 µm while in pores with radius higher than 1 µm and contaminated by soluble salts, the physicochemical effect that determines the equilibrium pressure for solutions may also cause condensation at lower relative humidity. Furthermore, Arnold and Zehnder (1991) observed a higher crystallization of salts in pores with a diameter in the range 1-10 µm. As the considered lithotypes have low porosity, they are not particularly vulnerable to decohesion linked to salt crystallization and freeze-thaw cycles.

Final remarks:

- Carrara Marble and Verona Red Marble are both compact stones, characterised by a low accessible porosity (mean values respectively of 1.41 % and 0.13 %).
- As the considered lithotypes have low porosity, they are not particularly vulnerable to decohesion linked to salt crystallization and freeze-thaw cycles.

3.1.2. COLORIMETRIC ANALYSIS

Colorimetric analysis has been performed to understand how the appearance of Carrara Marble and Verona Red Marble was changed during the exposure period and depending on the different sites.
The analysis was carried out on (Table 3.3):

- samples before exposure. For this stage, the choice of specimens took into consideration the representativeness of stone as well as the aesthetic homogeneity of samples;
- selected specimens after 6, 12, 18 and 24 months of their location outdoor.

A portable spectrophotometer (subchapter 2.1.2) allowed to measure in situ values of luminosity (L*), red-green component (a*) and blue-yellow component (b*). The results were compared in order to verify the total colour change (ΔE*) occurred at different time of exposure.
The colorimetric data were acquired including and excluding the specular component of light (respectively SCI and SCE). As previously said (subchapter 2.1.2), sample's surface features condition how the wavelengths of light reflect off that object and thus affect its appearance by human sight. Therefore, I decide to display the results including both specular and diffused reflected light, making them unaffected by any surface conditions.
It is noteworthy that the values reported below are the averages of measures carried out on 5 different points of the sample, repeated five times.

SITE	SAMPLE	BEFORE EXPOSURE	AFTER 6 MONTHS OF EXPOSURE	AFTER 12 MONTHS OF EXPOSURE	AFTER 18 MONTHS OF EXPOSURE	AFTER 24 MONTHS OF EXPOSURE
BOLOGNA	BCH1	V	V	V	V	-
	BCH9	V	-	-	-	V
	BCO1	V	-	V	V	V
	BCO9	V	-	-	-	-
	BCV1	V	-	V	V	V
	BCV9	V	-	-	-	-
FERRARA	PTCH1	V	V	V	V	-
	PTCH17	-	-	-	V	V
	PTCH18	V	-	-	-	-
	PTCO1	V	-	V	V	V
	PTCO3	-	-	-	V	V
	PTCO18	V	-	-	-	-
	PTCV1	V	-	V	V	V
	PTNH1	V	V	V	V	-
	PTNH6	V	-	-	-	-
	PTNH9	V	-	-	-	-
	PTNH12	V	-	-	-	-
	PTNH14	V	-	-	-	-
	PTNH16	V	-	-	-	-
	PTNH18	V	-	-	V	V
	PTNH21	V	-	-	-	-
	PTNO1	V	-	V	V	-
	PTNO3	V	-	-	-	-
	PTNO6	V	-	-	-	-
	PTNO8	V	-	-	-	-
	PTNO10	V	-	-	V	V
	PTNO15	V	-	-	-	-
	PTNO18	V	-	-	-	-
	PTNO22	V	-	-	-	-
	PTNV1	V	-	V	V	V
	PTNV13	V	-	-	-	-
FLORENCE	SMCH7	V	-	-	-	-
	SMCH9	V	-	-	-	-
	SMCH10	V	V	V	V	V
	SMCH12	V	-	-	-	-
	SMCH16	V	-	-	-	-
	SMCO3	V	-	-	-	-
	SMCO9	V	-	-	-	-
	SMCO10	V	-	V	V	V
	SMCO18	V	-	-	-	-
	SMCV5	V	-	-	-	-
	SMCV9	V	-	-	-	-
	SMCV10	V	-	V	V	V
	SMCV15	V	-	-	-	-

Table 3.3 Specimens, subdivided in different sites and times of measurement, examined with colorimetric analysis. The sign "V" ("-") means that the analysis was (not) carried out on the sample.

Before exposure

Average colour parameters of Carrara Marble were measured on the selected specimens and are displayed in Table 3.4.

Considering Verona Red Marble, the significant heterogeneity of this stone (i.e. more reddish appearance of some samples, the presence of yellow stains as well as of greenish ones in others) forced me to selected more reddish and aesthetically homogeneous samples (PTNH1, PTNH18, PTNO1, PTNO18, PTNV1) to average the colorimetric parameters reported in Table 3.4. Considering the CIELAB colour space (subchapter 2.1.2), it is clearly understandable that Carrara Marble has a light colour while Verona Red Marble displays lower lightness and a hue that results from a combination of red and yellow components.

	L*	a*	b*
Carrara Marble	89.60	-0.46	0.14
Verona Red Marble	67.29	7.27	16.65

Table 3.4 Average colorimetric parameters of samples of Carrara Marble and Verona Red Marble measured before their exposure.

BOLOGNA

Colorimetric data measured on surface of samples exposed in Bologna at different exposure time are reported in Table A2.1 (Annex 2).

After 6 months of exposure

After 6 months of exposure, colorimetric analysis was carried out on sample horizontally exposed.

Considering the mean value of measurements performed in 5 different points, the exposure of Carrara Marble to the environment led to a decrease of lightness ($\Delta L^* = -5.09 \pm 1.10$) and to a slight variation of b* parameter towards more positive value (2.34 ± 0.23) while almost no change affected a* parameter ($\Delta a^* = 0.42 \pm 0.04$) (Figure 3.12). The variation of total colour reaches an average value of 5.65 ± 0.93.

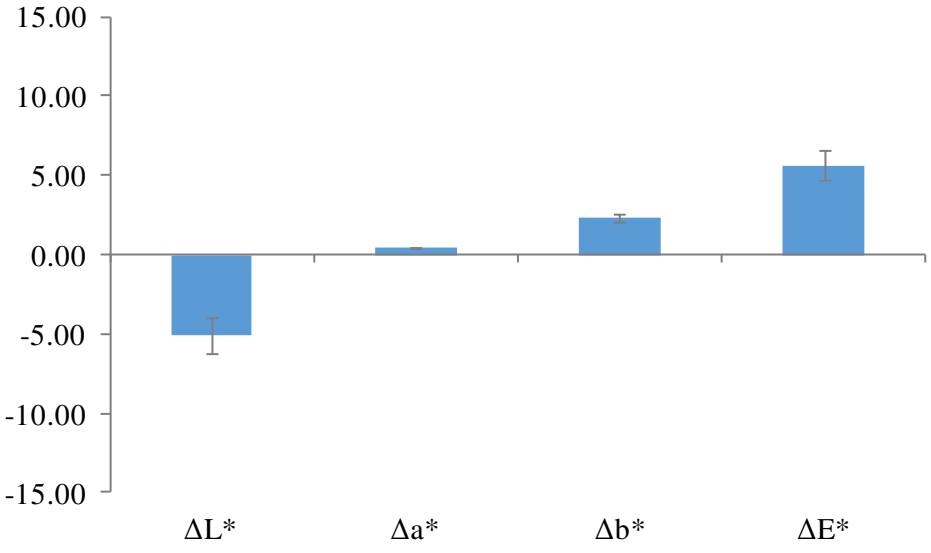

*Figure 3.12 Mean variation of the colorimetric CIE L*a*b* parameters and of total colour appearance (ΔE*) of Carrara Marble samples horizontally exposed in Bologna for 6 months compared to samples before exposure. Grey bars indicate the relative standard deviation.*

After 12 months of exposure

After 12 months from the start of exposure, colorimetric analysis was performed on samples placed with different orientation. Those horizontally and obliquely exposed show the highest and similar change of total colour ($\Delta E^* = 7.00 \pm 1.59$ and $\Delta E^* = 7.09 \pm 1.80$, respectively) induced mainly by a variation of lightness towards negative values (-5.69 ± 1.42 and -5.95 ± 1.72) and more positive measures of b* coordinate (4.02 ± 0.78 and 3.78 ± 0.70) (Figure 3.13). On the contrary, colorimetric parameters of samples vertically exposed remain almost unchanged ($\Delta E^* = 0.67 \pm 0.58$).

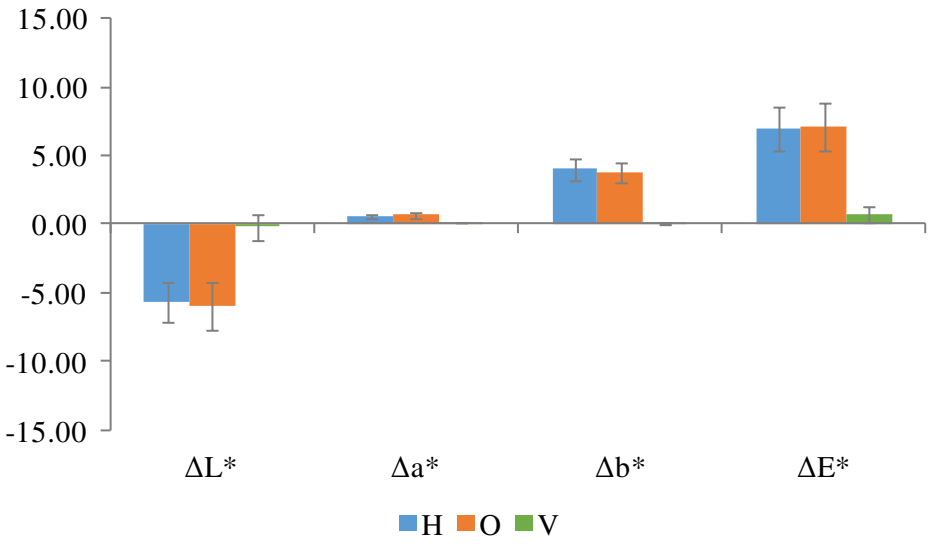

*Figure 3.13 Mean variation of the colorimetric CIE L*a*b* parameters and of total colour appearance (ΔE*) of Carrara Marble samples exposed in Bologna for 12 months compared to samples before exposure. Blue columns refer to samples horizontally placed, orange ones to those exposed obliquely and green ones to specimens placed vertically. Grey bars indicate the relative standard deviation.*

After 18 months of exposure

At the end of 18 months of exposure, lightness and b* parameter are the colorimetric variables mainly modified (Figure 3.14). In particular, horizontal, oblique and vertical samples underwent a decrease of L* parameter compared to the initial value (-3.82 ± 1.18, -4.27 ± 1.15 and -2.66 ± 3.16, respectively) as well as a shift of b* toward positive values for samples horizontally and obliquely exposed (2.31 ± 0.38 and 2.73 ± 0.14) while toward lightly negative values for vertical sample (-0.07 ± 0.11). On the contrary, almost no change affected a* parameter, which never exceeded 1.00. However, the total colour change of all samples remains below 5.16.

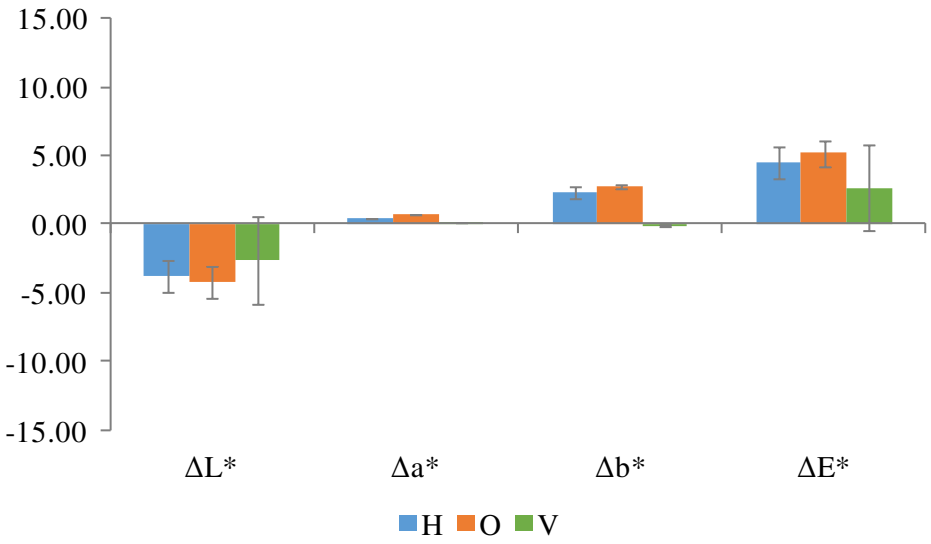

*Figure 3.14 Mean variation of the colorimetric CIE L*a*b* parameters and of total colour appearance (ΔE*) of Carrara Marble samples exposed in Bologna for 18 months compared to samples before exposure. Blue columns refer to samples horizontally placed, orange ones to those exposed obliquely and green ones to specimens placed vertically. Grey bars indicate the relative standard deviation.*

After 24 months of exposure

Horizontal and oblique samples exposed for 24 months underwent a similar variation of total colour (7.90 ± 4.85 and 8.63 ± 2.11, respectively) while the colour of vertical specimen remained much more similar to that of stone before exposure (0.71 ± 0.11) (Figure 3.15). In particular, horizontal and oblique specimens were subjected to a decrease of L* parameter (-6.17 ± 4.66 and -7.43 ± 2.10, respectively) and a variation of b* toward positive values (4.70 ± 1.92 and 4.30 ± 0.70, respectively) compared to the initial value while changes of a* parameter were negligible.

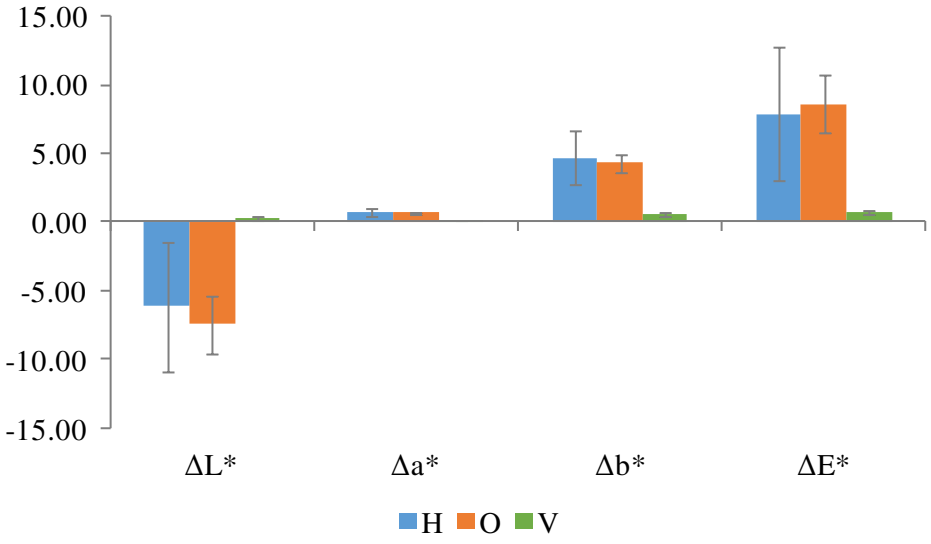

*Figure 3. 15 Mean variation of the colorimetric CIE L*a*b* parameters and of total colour appearance (ΔE*) of Carrara Marble samples exposed in Bolgona for 24 months compared to samples before exposure. Blue columns refer to samples horizontally placed, orange ones to those exposed obliquely and green ones to specimens placed vertically. Grey bars indicate the relative standard deviation.*

Comparison

Taking into consideration the variation of each colorimetric parameter during the complete exposure time, it appears that in general terms horizontal and oblique samples underwent the highest change and that the main colour coordinates subjected to variation were L* and b* (Figure 3.16).

Both horizontal and oblique samples underwent a similar decrease of lightness ($\Delta L^* < 0$) in respect to the initial value before exposure, with a general increasing trend over time (till to -7.43) (Figure 3.16). Change of L* was much more controlled in vertical samples (till to -2.66) and it was toward negative values after 12 and 18 months while a slight shift toward whitening ($\Delta L^* > 0$) happened after 24 months of exposure (0.33).

During the exposure period, a* coordinate remained almost unchanged ($\Delta a^* < 1$) and the limited variations were towards positive values (Figure 3.16). Moreover, a shift toward yellow component ($\Delta b^* > 0$) was recorded in horizontal and oblique samples with a general increasing trend over time (till to 4.70 and 4.30, respectively), with exception of samples exposed for 18 months that underwent a slight decrease. On the contrary, the variation of b* parameter of vertical samples is nearly imperceptible in all the period (remaining below 1.00) (Figure 3.16).

Considering the contribution of all colorimetric parameters, total colour variation was higher and in general increasing over time in horizontal and oblique samples reaching values till to 7.90 and 8.63, respectively.

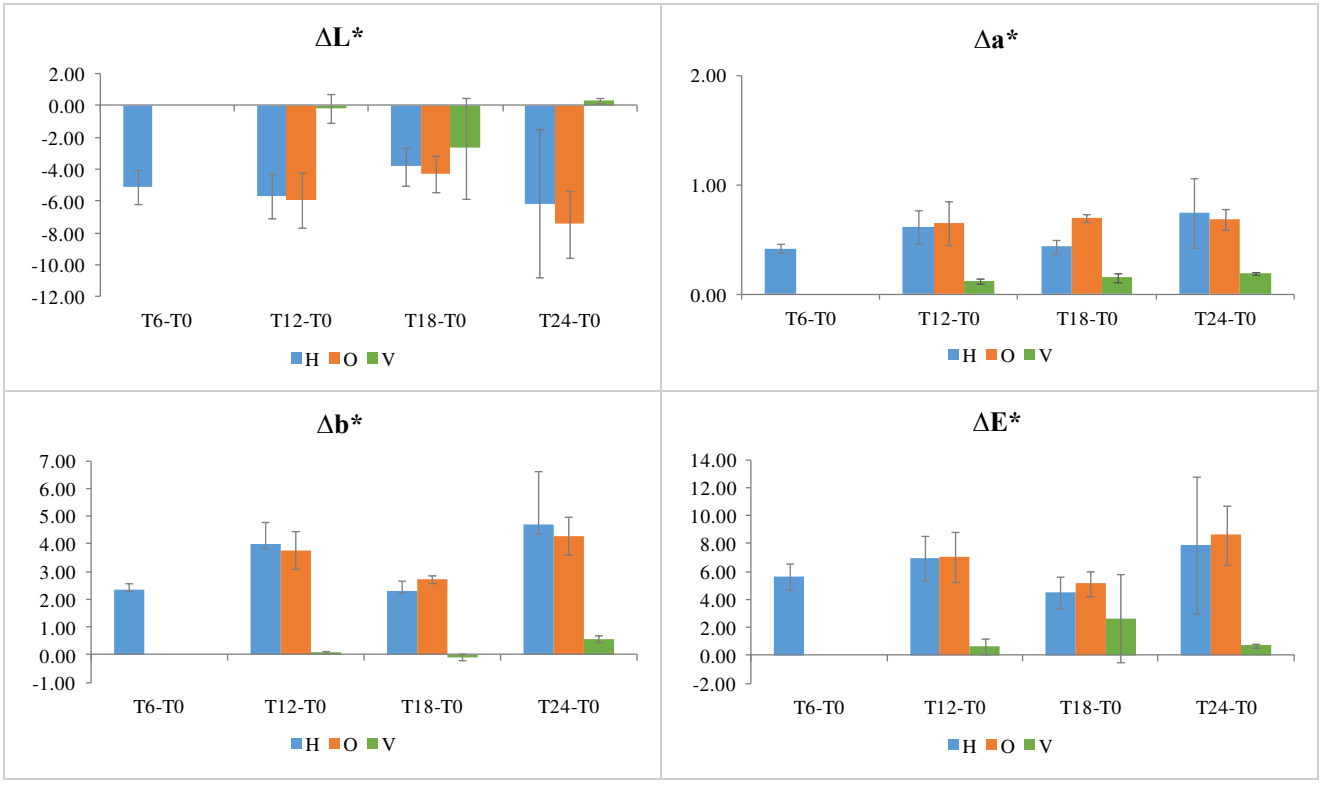

*Figure 3.16 Mean variation of the colorimetric CIE L*a*b* parameters and of total colour appearance (ΔE*) of Carrara Marble specimens after various time of exposure in Bologna. Blue, orange and green columns refer respectively to samples horizontally, obliquely and vertically placed. Grey bars indicate the relative standard deviation.*

FERRARA

CARRARA MARBLE

Colorimetric data measured on surface of marble specimens exposed in Ferrara at different exposure time are reported in Table A2.2 (Annex 2).

After 6 months of exposure

At the end of the first 6 months of exposure, colorimetric analysis carried out on horizontal specimens shows a significant variation of total colour respected to before exposure ($\Delta E^* = 10.88 \pm 1.39$).

In particular, these changes are mainly due to the variation of lightness followed by b* parameter: ΔL^* shifted toward negative value (-9.73±1.37) and Δb^* toward the yellow component (4.82±0.53) (Figure 3.17). The variation of a* parameter, toward positive value, remained below 1 unit (0.65±0.09).

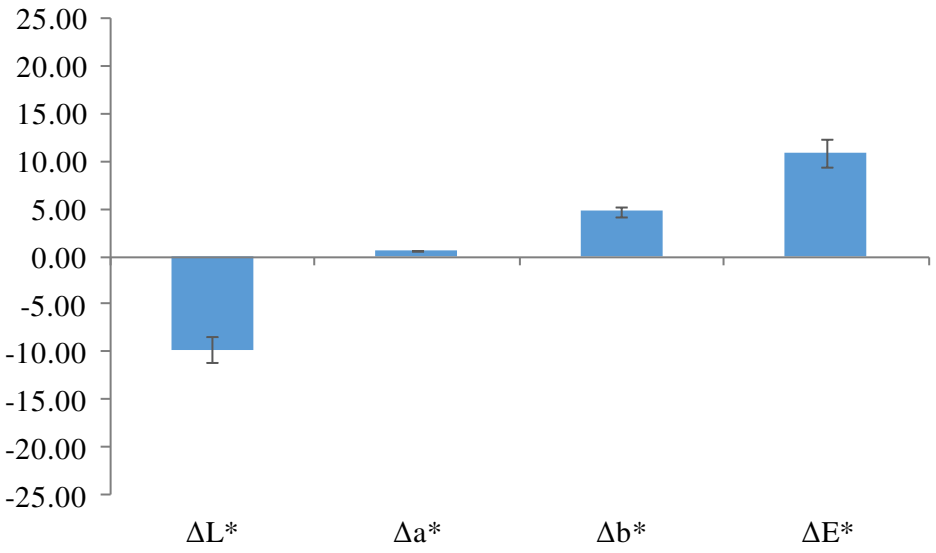

*Figure 3.17 Mean variation of the colorimetric CIE L*a*b* parameters and of total colour appearance (ΔE*) of Carrara Marble samples horizontally exposed in Ferrara for 6 months compared to samples before exposure. Grey bars indicate the relative standard deviation.*

After 12 months of exposure

The exposure of samples for 1 year induced a variation of total colour higher in horizontal samples than in oblique and vertical specimens (i.e., 13.60 ± 1.87, 2.44 ± 1.21 and 1.28 ± 0.31) (Figure 3.18). Horizontally and obliquely exposed samples underwent a shift toward darkening (-12.07 ± 1.94 and -1.57 ± 1.42) respected to the initial values while a light increase of lightness was detected in vertical sample (1.26 ± 0.32). Furthermore, blue-yellow component was modified towards positive values in all samples (6.17 ± 0.50, 1.65 ± 0.43 and 0.08 ± 0.16) while Δa^* remained very low (0.94 ± 0.08, 0.38 ± 0.02 and 0.15 ± 0.02 for horizontal, oblique and vertical samples) (Figure 3.18).

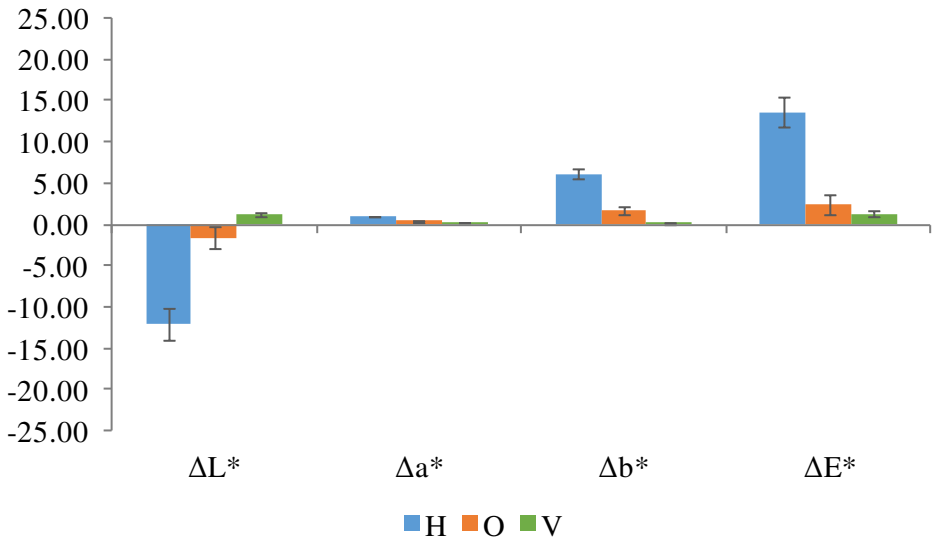

*Figure 3.18 Mean variation of the colorimetric CIE L*a*b* parameters and of total colour appearance (ΔE*) of Carrara Marble samples exposed in Ferrara for 12 months compared to samples before exposure. Blue, orange and green columns refer respectively to samples horizontally, obliquely and vertically placed. Grey bars indicate the relative standard deviation.*

After 18 months of exposure

After 18 months of exposure, the variation of total colour become more evident in horizontal and also in oblique samples (19.35 ± 3.11 and 12.39 ± 0.89) while it remains almost unchanged in vertical specimen (1.26 ± 0.32) (Figure 3.19). Figure 3.19 shows also considerable shift towards negative values of L* (-17.63 ± 3.22 and -10.71 ± 0.95) and towards positive ones of b* (7.84 ± 0.49 and 6.15 ± 0.16) for horizontal and oblique samples respected to values before exposure. On the contrary, the exposure outdoor of vertical sample did not change its colour coordinates that remained below 1.00.

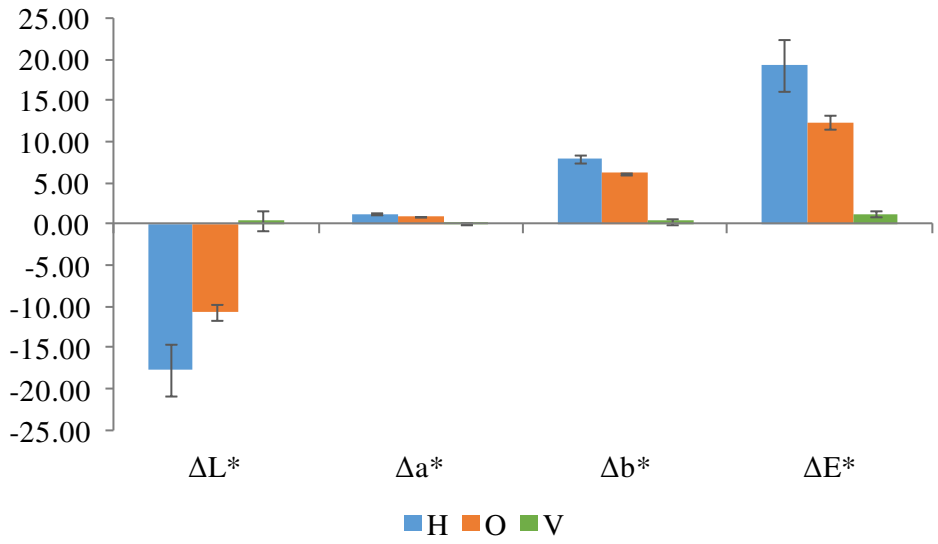

*Figure 3.19 Mean variation of the colorimetric CIE L*a*b* parameters and of total colour appearance (ΔE*) of Carrara Marble samples exposed in Ferrara for 18 months compared to samples before exposure. Blue, orange and green columns refer respectively to samples horizontally, obliquely and vertically placed. Grey bars indicate the relative standard deviation.*

After 24 months of exposure

After 24 months of exposure, higher total colour variation was observed for horizontal and oblique samples (20.78 ± 1.46 and 15.28 ± 2.59, respectively) while vertical sample maintained a colour much more similar to that belonged to stone before exposure (1.05 ± 0.33) (Figure 3.20). Figure 3.20 displays also that higher change of colorimetric parameters pertained L* and b* and affected mainly horizontal and oblique specimens. In particular, horizontal and oblique samples underwent a decrease of lightness (ΔL* < 0) (-18.57 ± 1.53 and -13.32 ± 2.75, respectively) as well as a shift of b* toward more positive values (i.e. 9.19 ± 0.28 and 7.32 ± 0.37).

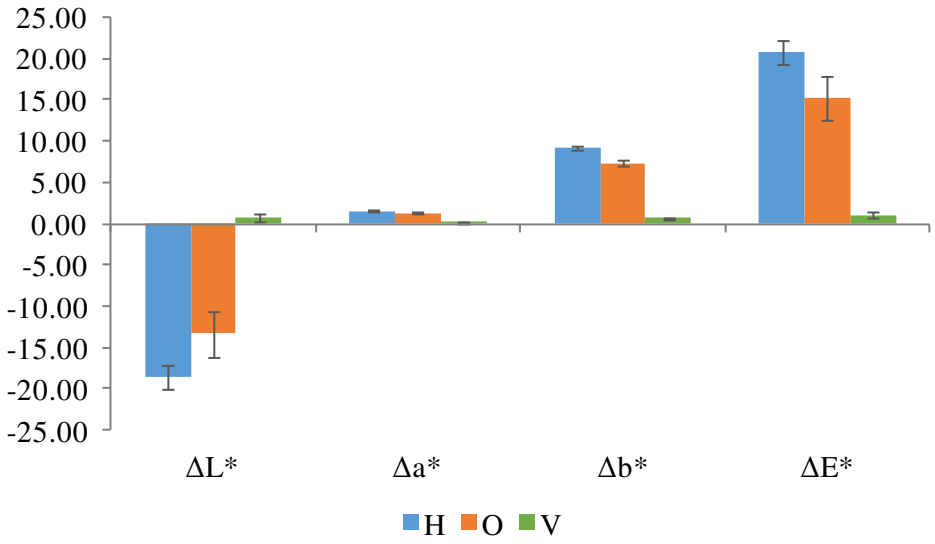

*Figure 3.20 Mean variation of the colorimetric CIE L*a*b* parameters and of total colour appearance (ΔE*) of Carrara Marble samples exposed in Ferrara for 24 months compared to samples before exposure. Blue, orange and green columns refer respectively to samples horizontally, obliquely and vertically placed. Grey bars indicate the relative standard deviation.*

Comparison

The comparison of colour variation of Carrara Marble samples exposed in Ferrara respected to their features before exposure shows that horizontal specimens were subjected to the highest ΔE* in all the exposure time (10.88, 13.60, 19.35 and 20.78, respectively), with an increasing value over time (Figure 3.21). For oblique samples, ΔE* remained low during the second semester of exposure (2.44) while it grew during the next 6 and 12 months (12.39 and 15.28). On the contrary total colour change remained constant in vertical samples for all the period (1.28, 1.26 and 1.05).

As already reported, L* parameter, followed by b*, underwent the highest changes during the whole studied time in respect to the initial colorimetric values of the marble. In particular, a gradual increase of ΔL* towards negative values is detectable on horizontal samples during the exposure period, reaching its maximum value after 24 months of exposure (i.e. ΔL* = -18.57) while oblique specimens display always a change towards blackening (ΔL* < 0) but lower and constant during the first year (around -1.57) and more evident after 18 and 24 months (-10.71 and -13.32). On the contrary, vertical samples underwent a stable shift toward white (ΔL* > 0) but imperceptible (around 1.00) all over the considered period. A similar trend is also discernible comparing Δb* of all the samples but always towards positive value (shift toward yellow): the change of b* is higher and continuous in horizontal samples (from 4.82 to 9.19), increasing over time in oblique samples (from 1.65 to 7.32) and very few over time in vertical samples (always below 1.00) (Figure

3.21). Variation of a* results very small (always below 1.55) and always towards positive values independently from time of analysis and orientation of the samples.

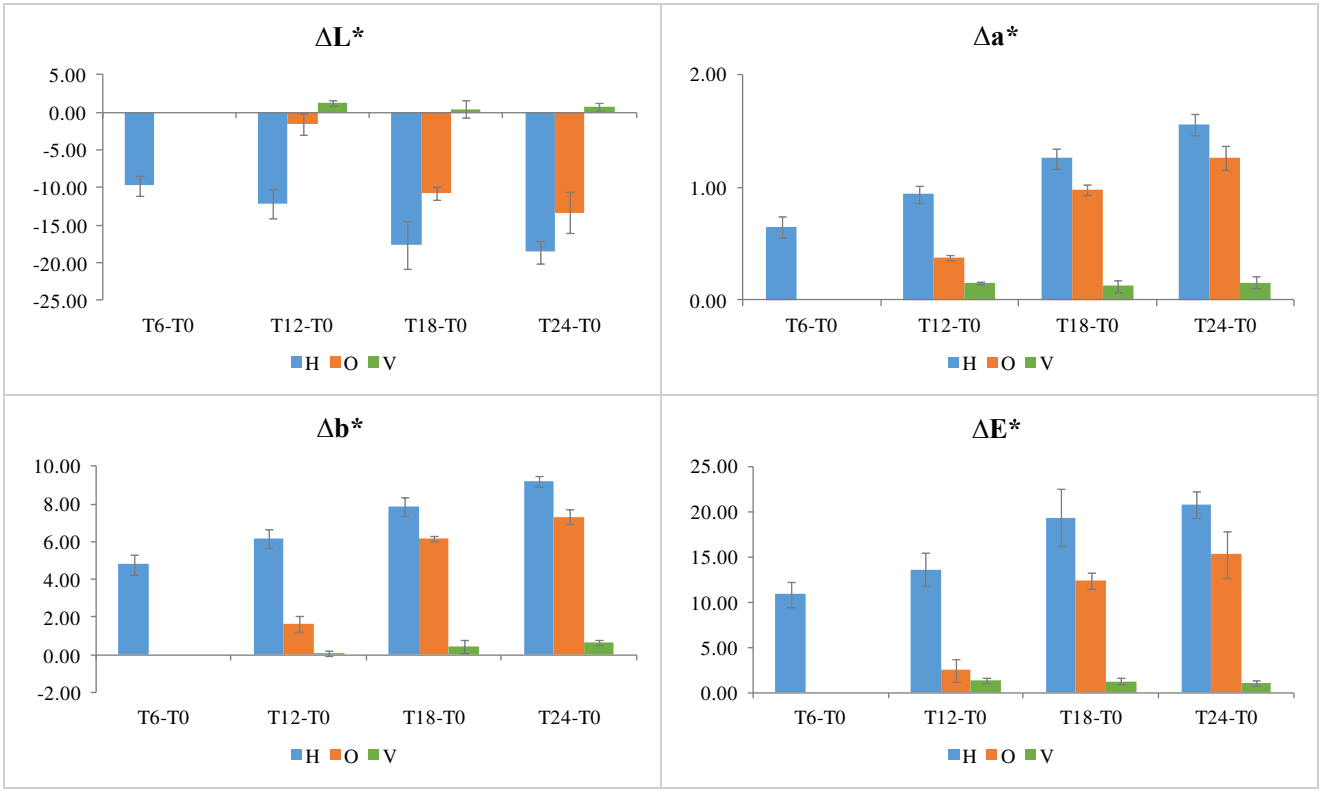

*Figure 3.21 Mean variation of the colorimetric CIE L*a*b* parameters and of total colour appearance (ΔE*) of Carrara Marble specimens after various time of exposure in Ferrara. Blue, orange and green columns refer respectively to samples horizontally, obliquely and vertically placed. Grey bars indicate the relative standard deviation.*

VERONA RED MARBLE

Results of colorimetric analysis performed on the surface of limestone samples exposed in Ferrara at different exposure time are reported in Table A2.3 (Annex 2).

After 6 months of exposure

After 6 months of exposure, colorimetric analysis was carried out on sample horizontally exposed. In general, a slight variation of total colour was detected (ΔE* = 4.20 ± 0.79) (Figure 3.22). Considering each colorimetric coordinates, all of them underwent a shift towards negative values, higher for L* and b* parameters (-3.65 ± 0.95 and -1.61 ± 0.58, respectively) and negligible for a* (-0.58 ± 1.05).

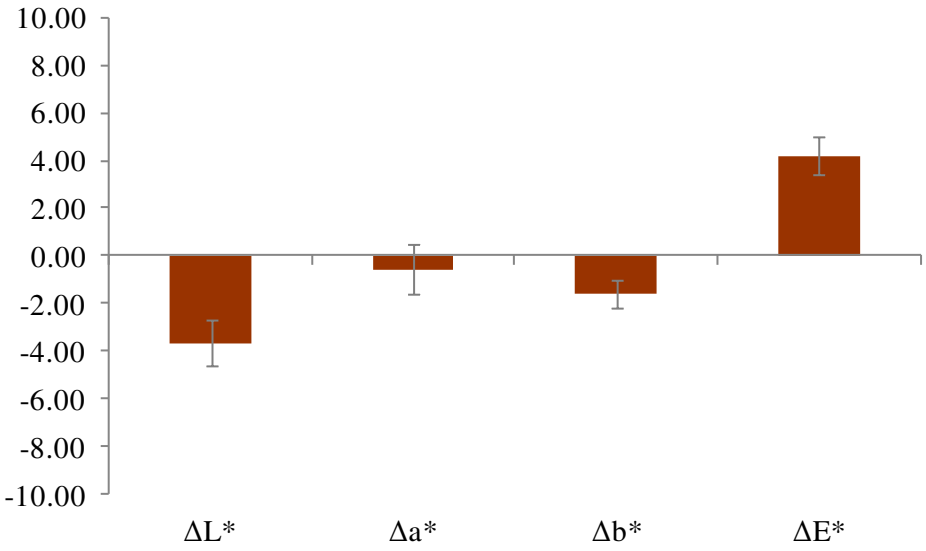

*Figure 3.22 Mean variation of the colorimetric CIE L*a*b* parameters and of total colour appearance (ΔE*) of Verona Red Marble samples horizontally exposed in Ferrara for 6 months compared to samples before exposure. Grey bars indicate the relative standard deviation.*

After 12 months of exposure

The variation of total colour measured on surface of specimens exposed for 12 months is similar in all samples (around 3.00) and some differences are detectable on L*, a* and b* parameters (Figure 3.23). Considering the lightness, horizontal sample underwent a small shift toward blackening (i.e. ΔL* = -1.48 ± 1.97) while in oblique and vertical samples the change was toward more positive values (0.78 ± 2.26 and 2.39 ± 2.12, respectively). Moreover, mean variation of a* remained around -1.00 in all three samples while b* underwent a shift towards negative values, higher in oblique sample (-2.52 ± 0.25) and quite similar in horizontal (-1.70 ± 0.59) and vertical ones (-1.32 ± 0.29).

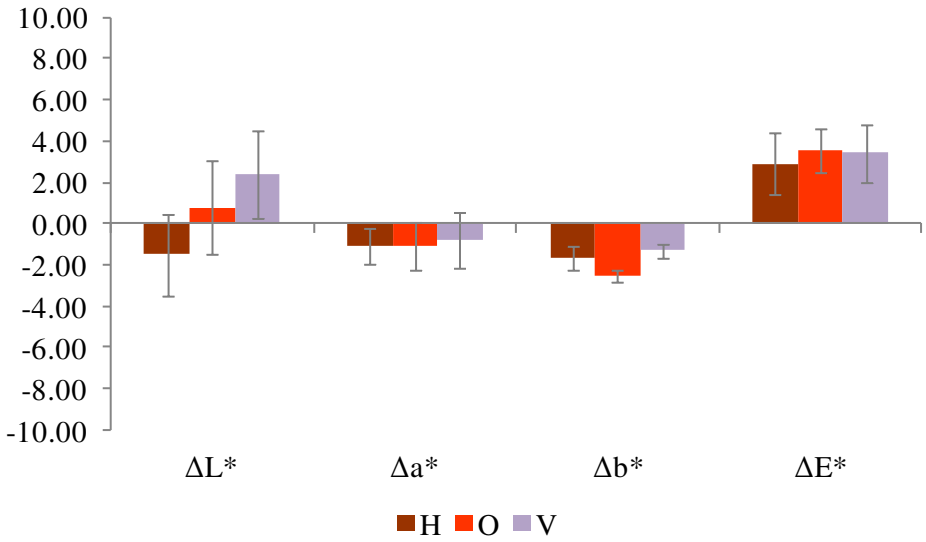

*Figure 3.23 Mean variation of colorimetric CIE L*a*b* parameters and total colour (ΔE*) of Verona Red Marble samples exposed in Ferrara for 12 months compared to samples before exposure. Brown, red and lilac columns refer respectively to samples horizontally, obliquely and vertically placed. Grey bars indicate the relative standard deviation.*

After 18 months of exposure

Changes of total colour are more evident after 18 months of exposure: the variations are all towards positive values, major in horizontal samples (7.74 ± 0.81) than on oblique and vertical ones (3.75 ± 1.22 and 3.20 ± 1.02) (Figure 3.24).

Considering ΔL*, horizontal and oblique specimens underwent a shift toward blackening (-7.00 ± 0.70 and -2.80 ± 1.13) while vertical one toward a more positive measure (1.48 ± 1.88). Analysing a* change, it shifted towards negative values in all samples, remaining below -3.00 in horizontal, oblique and vertical samples (-2.27 ± 0.58, -0.73 ± 0.36 and -0.72 ± 0.72). Moreover, horizontal and vertical samples were subjected to a change toward the blue component (-2.38 ± 0.28 and -1.99 ± 1.20, respectively) while the oblique one toward yellow (2.21 ± 1.04) (Figure 3.24).

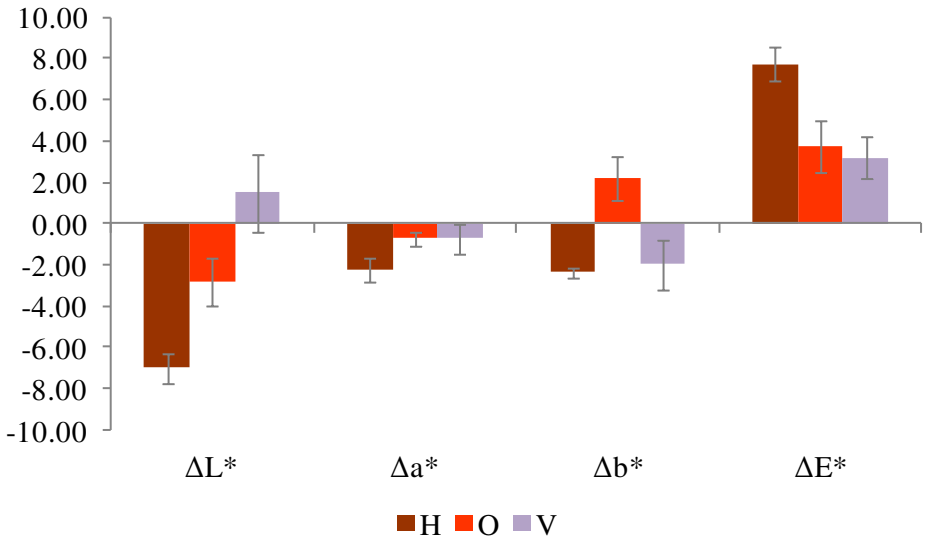

*Figure 3.24 Mean variation of colorimetric CIE L*a*b* parameters and total colour (ΔE*) of Verona Red Marble samples exposed in Ferrara for 18 months compared to samples before exposure. Brown, red and lilac columns refer respectively to samples horizontally, obliquely and vertically placed. Grey bars indicate the relative standard deviation.*

After 24 months of exposure

The exposure outdoor of limestone samples for 24 months led to a variation of total colour higher for horizontal specimens (7.62 ± 1.29) than for oblique and vertical ones (4.38 ± 1.19 and 4.19 ± 1.05) (Figure 3.25).

Considering the change of L* respect to that assessed before exposure, horizontal and oblique specimens were subjected to a shift toward negative values (-6.76 ± 1.33 and -3.59 ± 1.80) while vertical sample toward a more positive value (2.37 ± 1.37) (Figure 3.25). Moreover, samples displayed a variation of a* toward negative values independently from the orientation (-2.37 ± 0.66, -1.29 ± 0.7 and -0.86 ± 0.80 for horizontal, oblique and vertical specimens, respectively) and a shift toward blue component happened in horizontal and vertical specimen (-2.47 ± 0.53 and -3.11 ± 0.67) but toward the yellow one in oblique sample (0.25 ± 1.81).

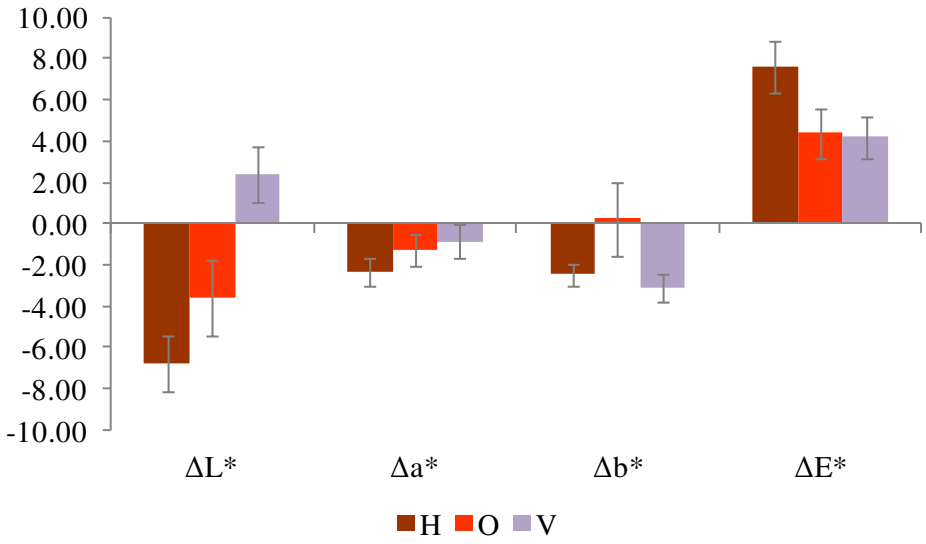

*Figure 3.25 Mean variation of colorimetric CIE L*a*b* parameters and total colour (ΔE*) of Verona Red Marble samples exposed in Ferrara for 24 months compared to samples before exposure. Brown, red and lilac columns refer respectively to samples horizontally, obliquely and vertically placed. Grey bars indicate the relative standard deviation.*

Comparison

In general, during the exposure period, horizontal samples underwent the highest change in total colour with a decreasing trend after 12 months of exposure (2.91) respect to the previous 6 months (4.20) and an increase after 18 months (7.74) and 24 months (7.62) (Figure 3.26). On the contrary, ΔE* of oblique and vertical samples remained almost constant over time (between 3.41 and 4.38).

In particular, the assessment of lightness over time highlights a shift toward blackening (ΔL* < 0) in horizontal samples, higher for analyses performed after 6 (-3.65), 18 (-7.00) and 24 (-6.76) months of exposure (Figure 3.26). Oblique samples displays a very light variation toward positive value after 12 months of exposure (0.78) but negative after 18 and 24 months (-2.80 and -3.59, respectively) while it is positive for vertical samples (2.39, 1.48 and 2.37).

The change of red-green component underwent a shift towards negative value over all time but remaining always below -3.00 in all samples. Also Δb* shifted towards negative values slightly increasing overtime, higher in vertical samples (till to -3.11), except for analysis performed on oblique specimen after 18 and 24 months of exposure that showed a positive change (2.21 and 0.25) respect the initial value (Figure 3.26).

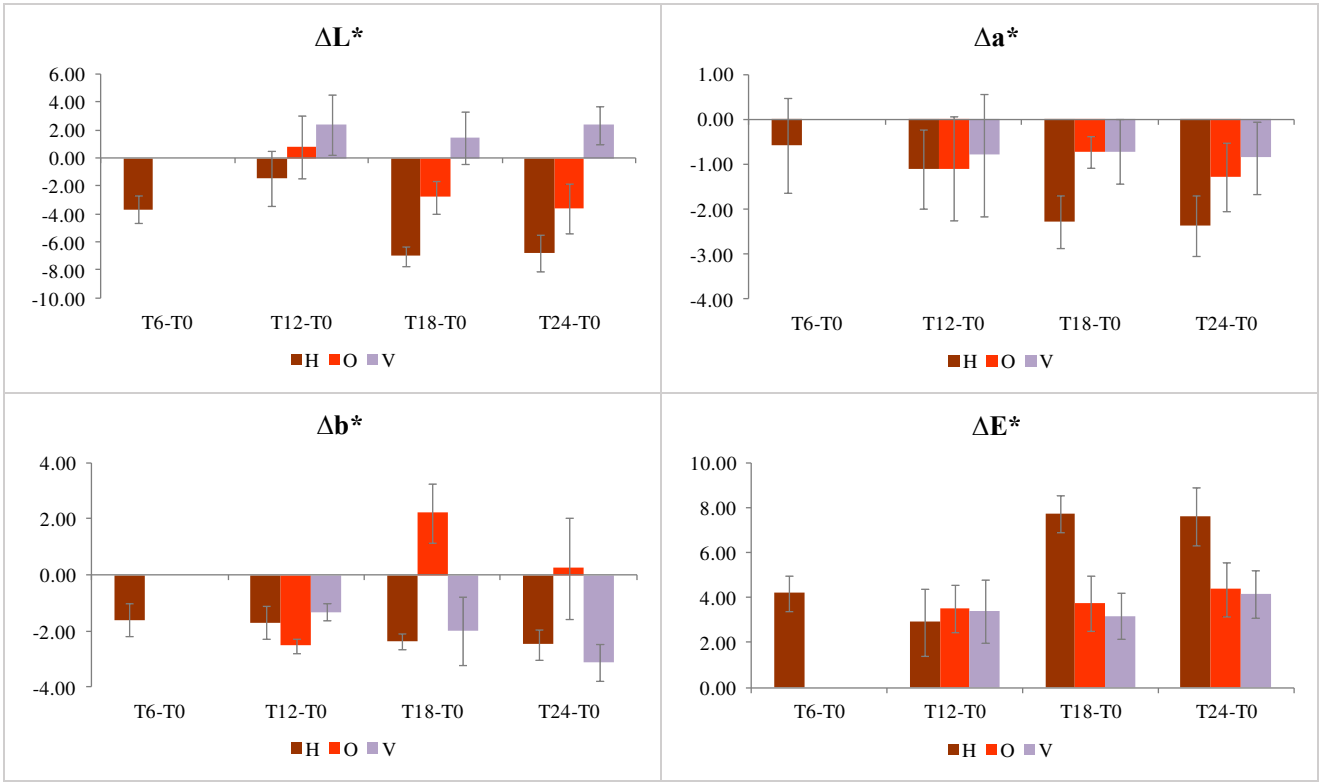

*Figure 3.26 Mean variation of the colorimetric CIE L*a*b* parameters and total colour (ΔE*) of Verona Red Marble specimens after various time of exposure in Ferrara. Brown, red and lilac columns refer respectively to samples horizontally, obliquely and vertically placed. Grey bars indicate the relative standard deviation.*

FLORENCE

Colorimetric data measured on surface of marble specimens exposed in Florence at different exposure time are reported in Table A2.4 (Annex 2).

After 6 months of exposure

At the end of the first 6 months of exposure, horizontal sample underwent colorimetric analysis. Figure 3.27 shows an important change of total colour (13.97 ± 1.60), mainly induced by a shift to blackening (ΔL* = -13.47 ± 1.52). Considering the two chroma coordinates, b* underwent a shift toward the yellow component (3.62 ± 0.51) while a* remained almost equal to the initial value.

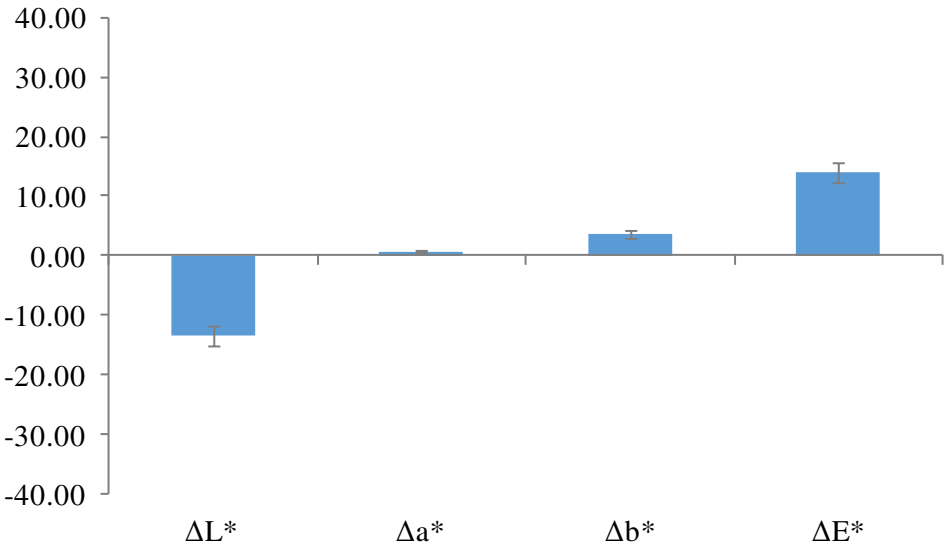

*Figure 3.27 Mean variation of the colorimetric CIE L*a*b* parameters and of total colour appearance (ΔE*) of Carrara Marble samples horizontally exposed in Florence for 6 months compared to samples before exposure. Grey bars indicate the relative standard deviation.*

After 12 months of exposure

After 12 months from the beginning of the exposure, a change in total colour occurred much higher in horizontal (15.88 ± 1.39) and oblique (13.24 ± 2.37) samples than in vertical ones (1.68 ± 0.65) (Figure 3.28). All samples underwent a shift to blackening respected to before exposure, more pronounced in horizontal (-15.06 ± 1.33) and oblique (-12.68 ± 2.22) specimens. Blue-yellow component of horizontal and oblique samples varied towards positive values (4.96 ± 0.40 and 3.71 ± 0.85) while that of vertical sample remained almost stable (-0.19 ± 0.06). a* component underwent a light variation towards positive values but remaining below 1.00.

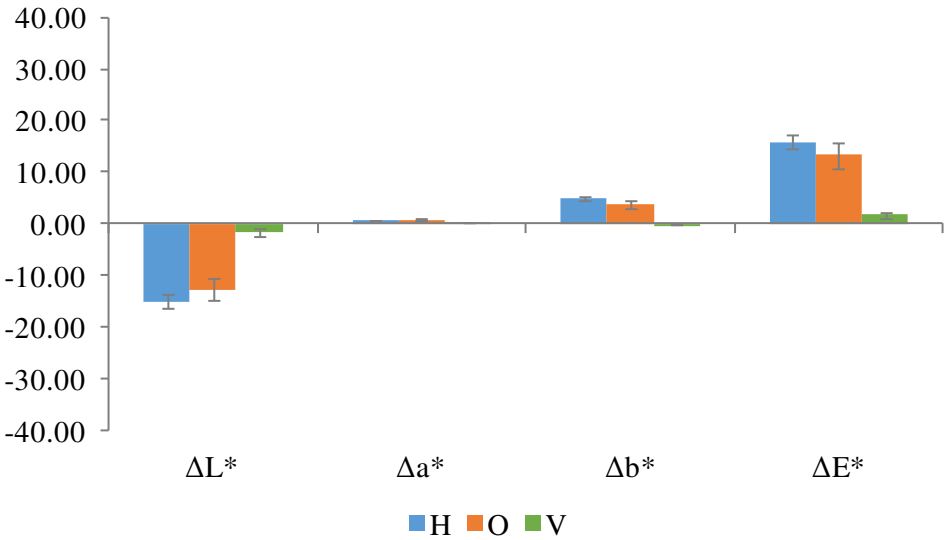

*Figure 3.28 Mean variation of the colorimetric CIE L*a*b* parameters and of total colour appearance (ΔE*) of Carrara Marble samples exposed in Florence for 12 months compared to samples before exposure. Blue, orange and green columns refer respectively to samples horizontally, obliquely and vertically placed. Grey bars indicate the relative standard deviation.*

After 18 months of exposure

After 18 months of exposure, the differences of CIE L*a*b* parameters in respect to the initial value become more evident (Figure 3.29). Horizontal and oblique samples underwent an intense blackening (-27.68 ± 1.82 and -20.18 ± 2.15) and a shift to yellow component (6.99 ± 0.28 and 5.25 ± 0.81), causing an important change of E* (28.59 ± 1.83 and 20.89 ± 2.29). On the contrary, colour parameters of vertical specimen remained essentially similar to the initial ones.

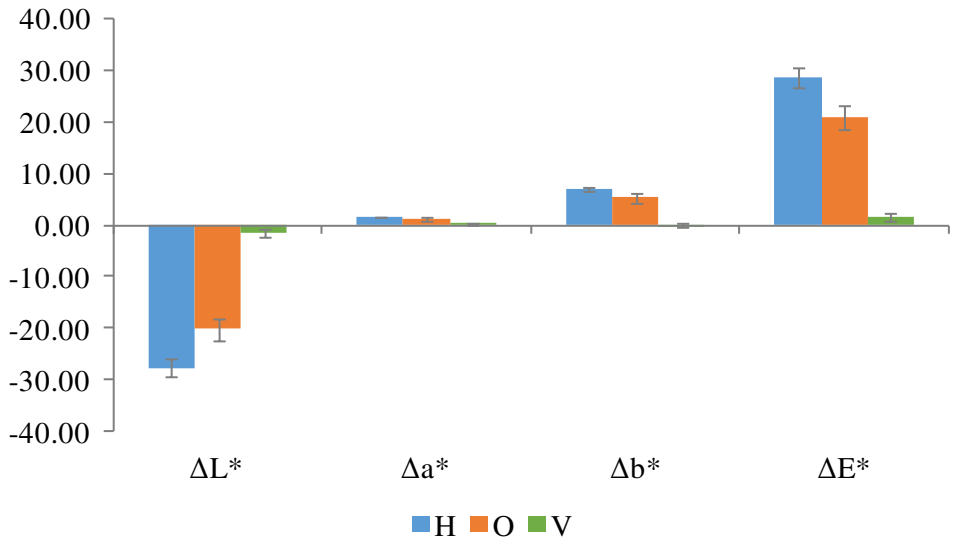

*Figure 3.29 Mean variation of the colorimetric CIE L*a*b* parameters and of total colour appearance (ΔE*) of Carrara Marble samples exposed in Florence for 18 months compared to samples before exposure. Blue, orange and green columns refer respectively to samples horizontally, obliquely and vertically placed. Grey bars indicate the relative standard deviation.*

After 24 months of exposure

The exposure outdoor of samples for 24 months led to an evident variation of total colour for horizontal and oblique samples (31.19 ± 1.95 and 26.05 ± 1.36), induced mainly by a change of lightness toward negative values (-29.96 ± 1.92 and -24.88 ±1.37) and secondly by a shift of b* toward the yellow component (8.49 ± 0.37 and 7.53 ± 0.24) (Figure 3.30). In contrast, colour parameters of vertical specimen remained basically similar to the initial ones.

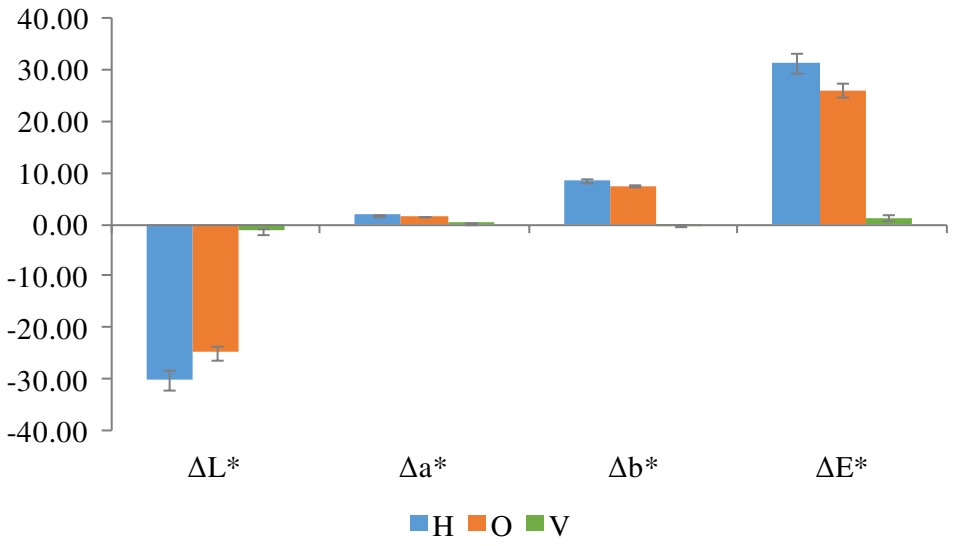

*Figure 3.30 Mean variation of the colorimetric CIE L*a*b* parameters and of total colour appearance (ΔE*) of Carrara Marble samples exposed in Florence for 24 months compared to samples before exposure. Blue, orange and green columns refer respectively to samples horizontally, obliquely and vertically placed. Grey bars indicate the relative standard deviation.*

Comparison

During the whole exposure time, horizontal samples underwent the highest variation of total colour, with an increasing value over time (13.97, 15.88, 28.59 and 31.19, respectively) (Figure 3.31). Also oblique samples show a similar trend with mean values of ΔE* higher than 13.00 (i.e. 13.24, 20.89 and 26.05 after 12, 18 and 24 months of exposure). On the contrary, total colour of vertical samples was not subjected to a conspicuous change, remaining constant around 1.50 (Figure 3.31).

Taking into consideration the measures of lightness of all samples exposed in Florence over time (Figure 3.31), it was appreciable a general shift toward blackening (ΔL* < 0) in respect to initial values, more evident and increasing over time in horizontal (-13.47, 15.06, -27.68 and -29.96) and oblique (-12.68, -20.18 and -24.88 after 12, 18 and 24 months of exposure) samples while more stable and restricted in vertical ones (-1.64, -1.47 and -1.31 after 12, 18 and 24 months of exposure). Moreover, changes of a* parameter were generally low (always below 2.00) during all exposure time, slightly higher in horizontal and oblique specimens. On the contrary, the variation toward the yellow component (Δb* > 0) of horizontal and oblique samples was more noticeable and it gradually increased over time. However, vertical samples continued to display a value very similar to the original one (Figure 3.31).

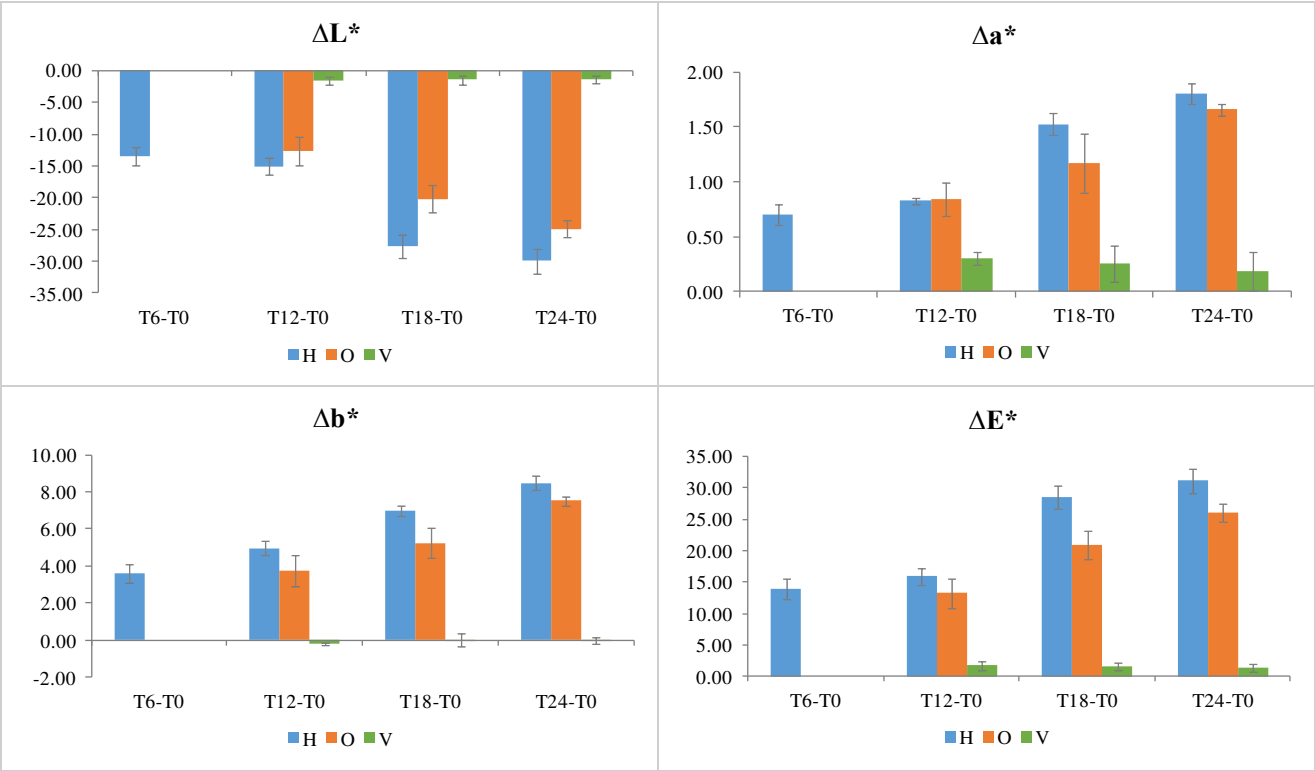

*Figure 3.31 Mean variation of the colorimetric CIE L*a*b* parameters and of total colour appearance (ΔE*) of Carrara Marble specimens after various time of exposure in Florence. Blue, orange and green columns refer respectively to samples horizontally, obliquely and vertically placed. Grey bars indicate the relative standard deviation.*

GENERAL COMPARISON

The comparison of colorimetric analysis performed on Carrara Marble horizontal samples in different sites after 6 months of exposure with that carried out before exposure shows as lightness underwent an evident shift towards negative values, with increasing difference from Bologna (-5.09) to Ferrara (-9.73) and Florence (-13.47) while Δb* moved to positive values without exceeding 5.00 (Figure 3.32). Also the variation of a* parameter was positive but they never reached 1.00. Moreover, the combination of the three colour parameters highlights that total colour change is higher in sample exposed in Florence followed by Ferrara and last Bologna. In addition, all samples underwent a change of total colour higher than the value of acceptability ($\Delta E^* \leq 5$) mentioned by Miliani et al. (2007) for colour change of treated stone considered in absence of more proper limit for stone soiling on the basis of published literature.

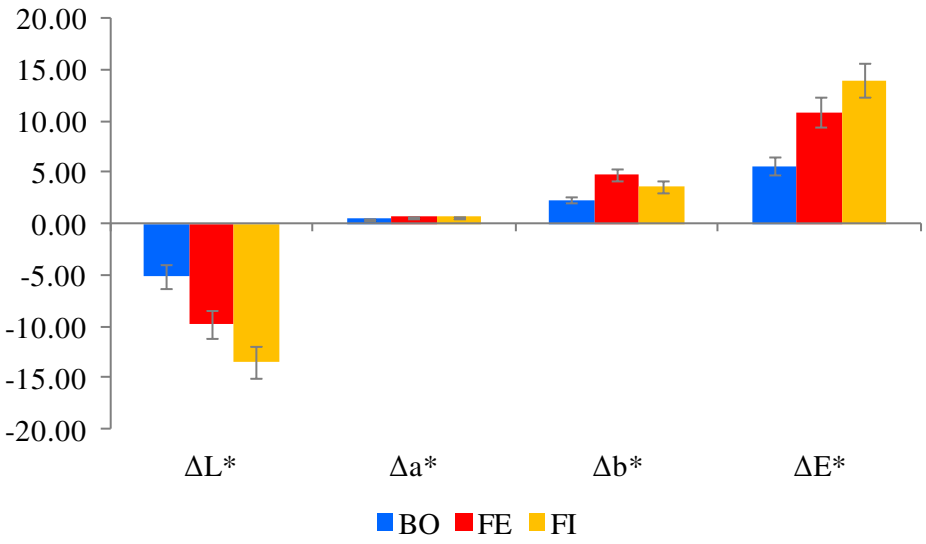

*Figure 3.32 Mean variation of the colorimetric CIE L*a*b* parameters and of total colour appearance (ΔE*) of horizontal Carrara Marble specimens exposed for 6 months in different locations compared to samples before exposure. Blue, red and ochre columns refer respectively to samples exposed in Bologna (BO), Ferrara (FE) and Florence (FI). Grey bars indicate the relative standard deviation.*

Also after 1 year of exposure higher change of colorimetric parameters was observed mainly in horizontal samples but also on those obliquely exposed in all sites (Figure 3.33).
Compared to the initial measures, total colour of horizontal samples changed till 15.88 in Florence despite 13.60 and 7.00 of Ferrara and Bologna, exceeding anyway ΔE* values referred to the period 6-0 months. The analysed ΔE* were minor in oblique samples and even more in vertical ones (Figure 3.33). Moreover, ΔE* was above the limit of acceptability (Miliani et al., 2007) for all horizontal samples and in general for oblique ones (with exception of that exposed in Ferrara).
Considering each parameter, L* was subjected to relevant variation towards negative values (with the exception of vertical sample exposed in Ferrara), higher in specimens exposed in Florence (Figure 3.33). Red-green component underwent a shift towards positive value in all samples but remaining low ($\Delta a^* < 1.00$). A change toward the yellow component was detectable in horizontal and oblique samples (with values between 1.65 and 6.17) while it is around 1.00 in vertical ones.

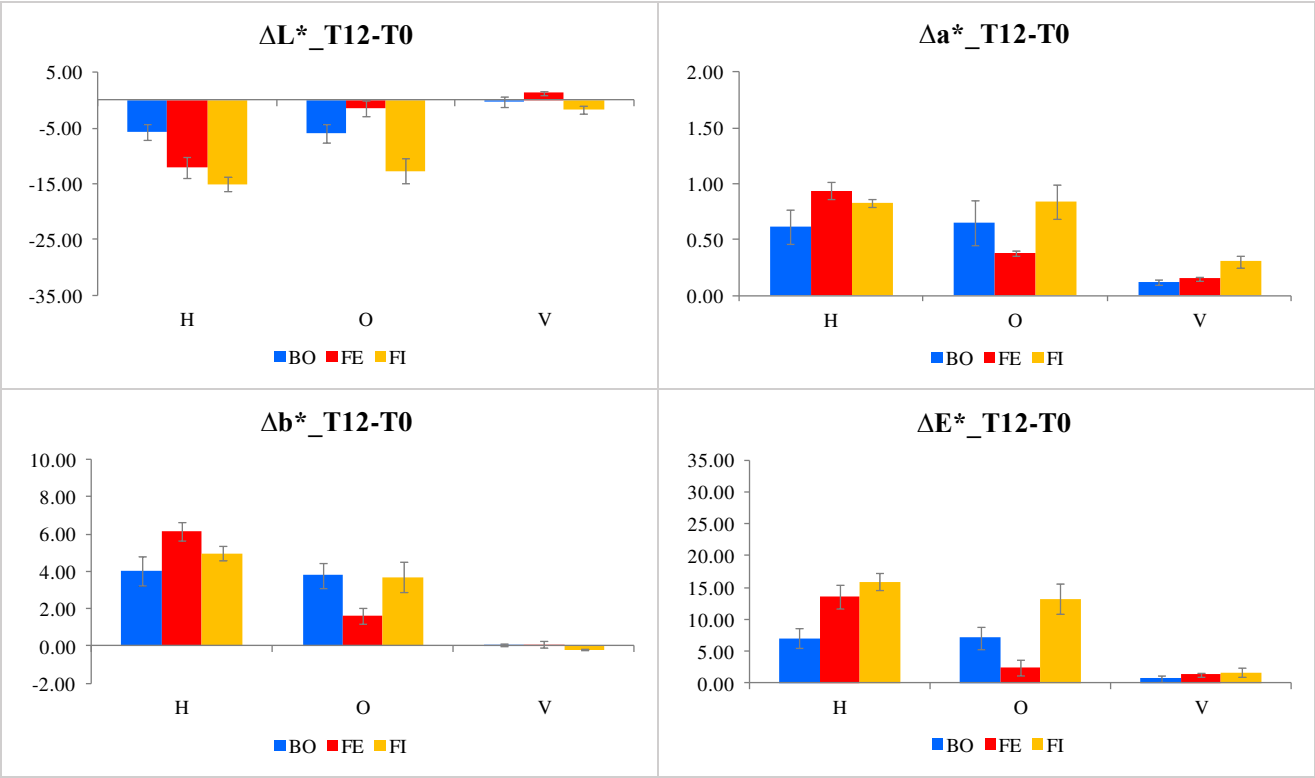

*Figure 3.33 Mean variation of the colorimetric CIE L*a*b* parameters and of total colour appearance (ΔE*) of horizontal, oblique and vertical Carrara Marble specimens exposed for 12 months in different sites compared to samples before exposure. Blue, red and ochre columns refer respectively to samples exposed in Bologna (BO), Ferrara (FE) and Florence (FI). Grey bars indicate the relative standard deviation.*

Except for vertical specimens that remained very comparable to sample before exposure, the comparison of colorimetric analyses performed after 18 months of exposure and before exposure highlights as the trend of ΔL*, Δa*, Δb* and ΔE* among different exposure locations remained similar, more discernible in horizontal than oblique samples (Figure 3.34). Specifically, L* underwent a shift toward blackening both in horizontal and oblique samples mainly in Florence (-27.68 and -20.18), followed by Ferrara (-17.63 and -10.71) and Bologna (-3.82 and -4.27). A slight shift towards positive values is detectable for a* parameters, again higher in Florence than in Ferrara and in Bologna, and for b*, more evident in Ferrara (till to 7.84 in horizontal sample and 6.15 in oblique one) followed by Florence and Bologna. Finally, ΔE* shows an increasing value from Bologna to Ferrara and Florence both on horizontal and oblique specimens, generally always overcoming limit of acceptability defined by Miliani et al. (2007).

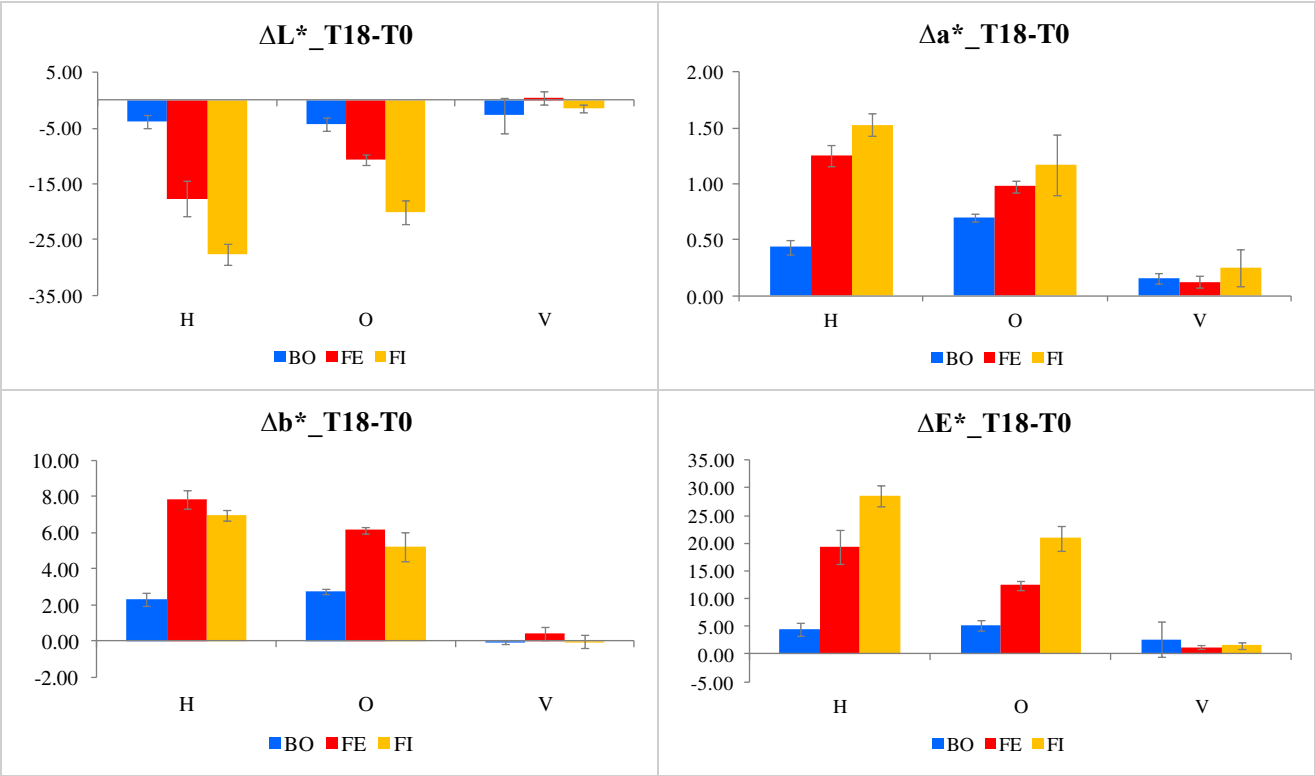

*Figure 3.34 Mean variation of the colorimetric CIE L*a*b* parameters and of total colour appearance (ΔE*) of horizontal, oblique and vertical Carrara Marble specimens exposed for 18 months in different sites compared to samples before exposure. Blue, red and ochre columns refer respectively to samples exposed in Bologna (BO), Ferrara (FE) and Florence (FI). Grey bars indicate the relative standard deviation.*

Differences of CIE L*a*b* parameters after 24 months of exposure in respect to the initial value become more evident mainly for horizontal and oblique samples while vertical samples remained much more similar to marble appearance before exposure (Figure 3.35). In particular, horizontal and oblique specimens underwent a change of total colour not acceptable by human sight (Miliani et al., 2007), more evident in Florence than Ferrara and Bologna and mostly caused by a change of L* toward blackening (between -6.17 and -29.6) and a shift of b* toward yellow component (between 4.40 and 9.19) (Figure 3.35).

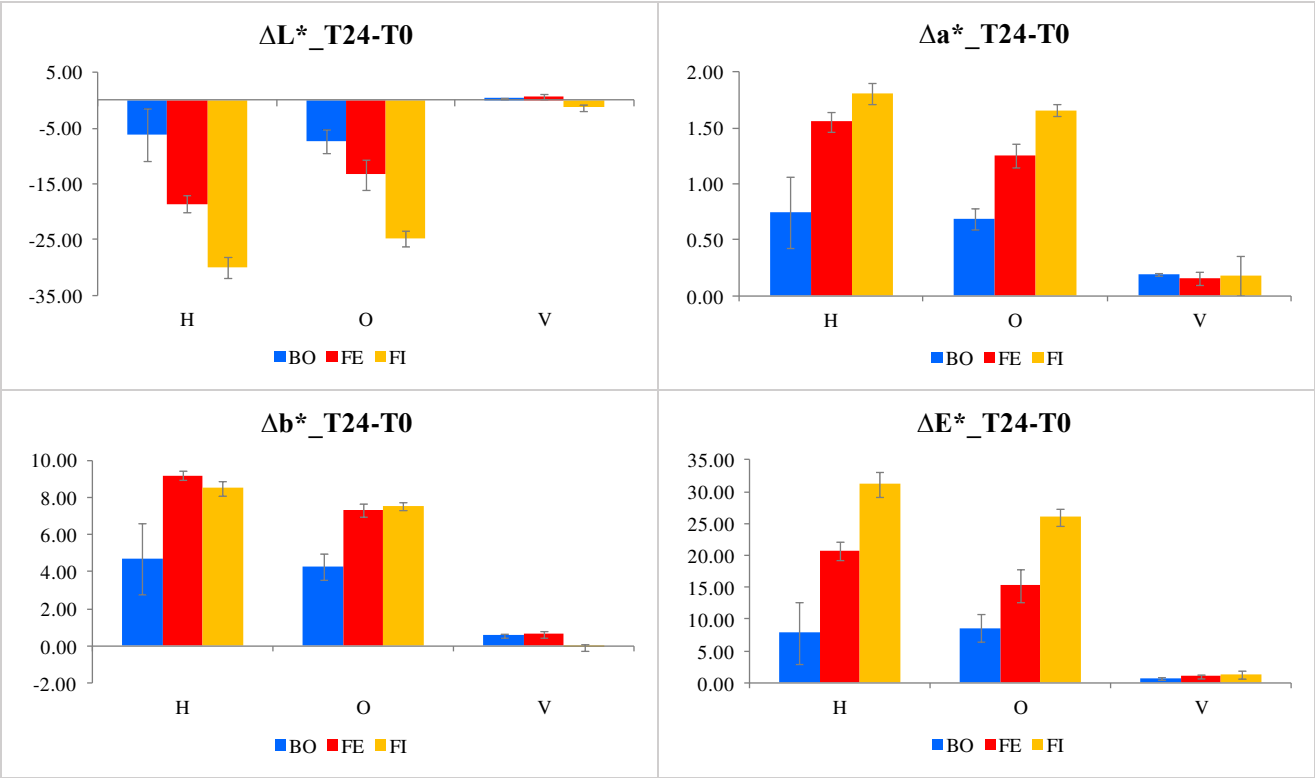

*Figure 3.35 Mean variation of the colorimetric CIE L*a*b* parameters and of total colour appearance (ΔE*) of horizontal, oblique and vertical Carrara Marble specimens exposed for 24 months in different sites compared to samples before exposure. Blue, red and ochre columns refer respectively to samples exposed in Bologna (BO), Ferrara (FE) and Florence (FI). Grey bars indicate the relative standard deviation.*

Considering the same site of exposure (i.e. Ferrara) but different stone substrates, Figure 3.36 displays the difference of colorimetric parameters of horizontal samples between 6 months after exposure and before exposure: besides Δa* whose both values are close to 0.00, all the other parameters underwent a change higher in Carrara Marble than in Verona Red Marble. In particular, both lithotypes showed a shift toward blackening (ΔL* < 0) while b* modified towards positive value for marble but to negative ones for limestone. Therefore ΔE* reached 10.88 in Carrara Marble and 4.20 in limestone.

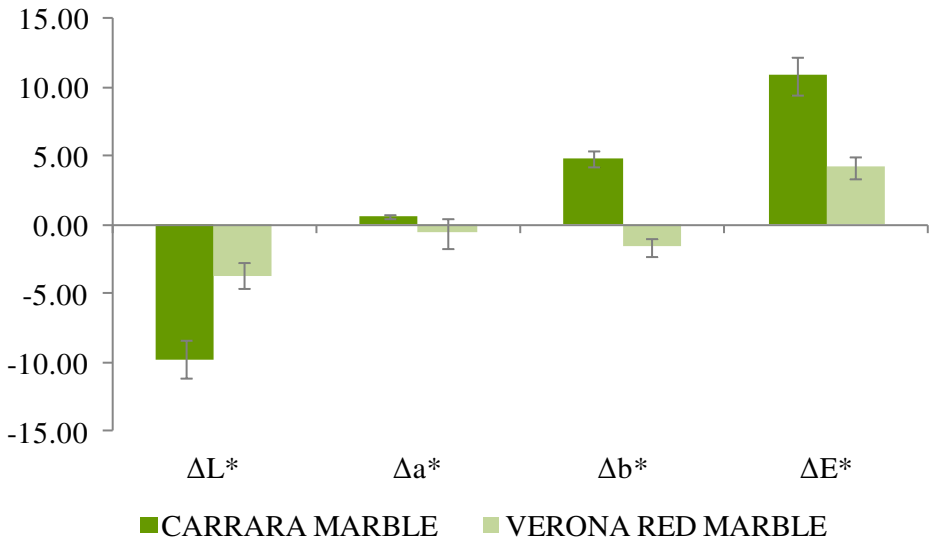

*Figure 3.36 Mean variation of the colorimetric CIE L*a*b* parameters and of total colour appearance (ΔE*) of horizontal specimens exposed for 6 months in Ferrara compared to samples before exposure. Dark and light green columns refer respectively to Carrara and Verona Red Marbles. Grey bars indicate the relative standard deviation.*

Extending the time of exposure to 12 months, Figure 3.37 shows an evident mean change of E* respect to the value before exposure in horizontal Carrara Marble sample (13.60), almost 5 times higher that recorded for horizontal limestone sample (2.91). On the contrary, for oblique and vertical specimens the differences of ΔE* between the two lithotypes are moderate, slightly higher in Verona Red Marble than in Carrara Marble. Comparing L* parameter of the two stones, a change towards negative values is detectable in both horizontal samples, much higher in Carrara Marble (-12.07) than in limestone (-1.48), opposed values in oblique specimens (-1.57 for marble and 0.78 for limestone) and towards light positive values in both vertical samples (Figure 3.37).

Focusing on a* coordinate, Carrara Marble underwent a shift towards positive values, which gradually decrease from horizontal to oblique and vertical samples, while Δa* of Verona Red Marble remained almost constant around -1 (Figure 3.37). The higher relative standard deviations of limestone are likely ascribable to the intrinsic feature of the substrate, characterised by more reddish or more greenish veins.

Finally, Δb* shifted toward yellow coordinate in Carrara Marble samples, more in horizontal one (6.17), while it changed towards negative but rather constant values in limestone specimens (around -1.85) (Figure 3.37).

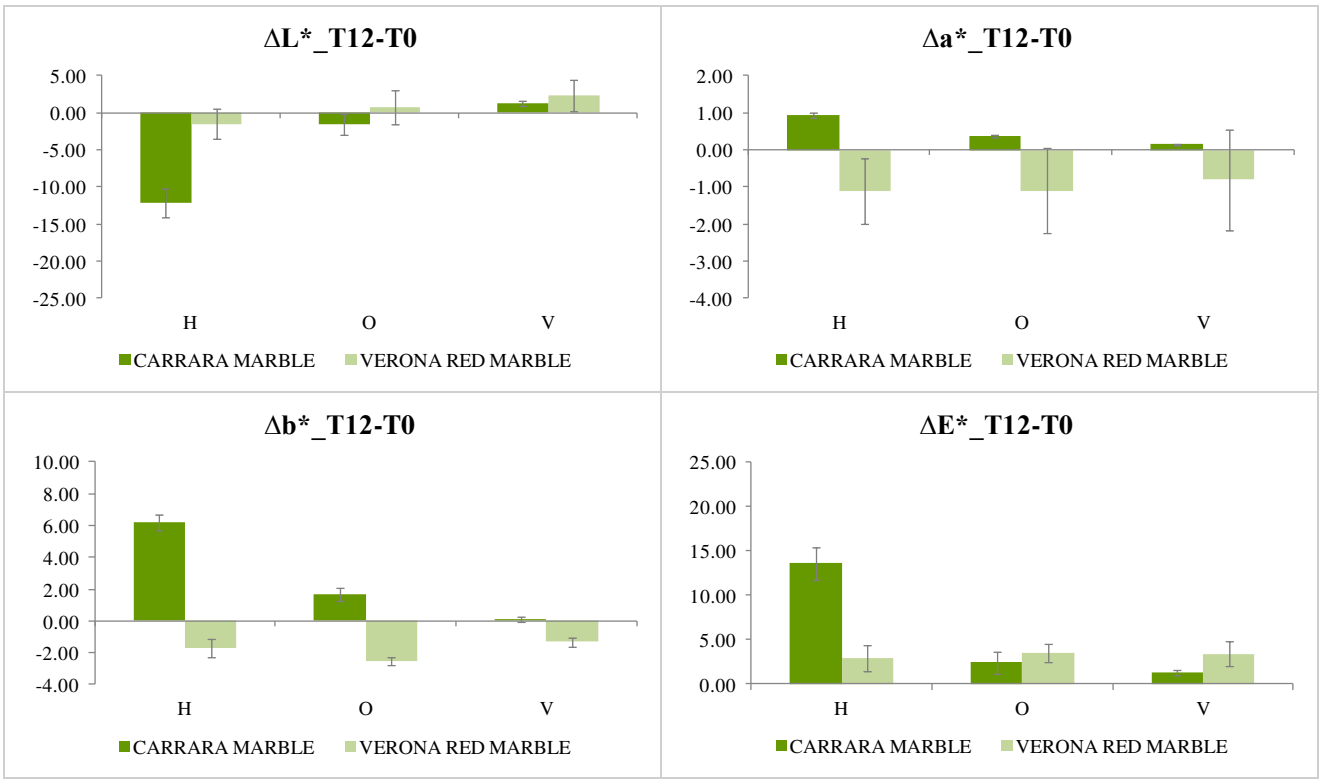

*Figure 3.37 Mean variation of the colorimetric CIE L*a*b* parameters and of total colour appearance (ΔE*) of specimens exposed for 12 months in Ferrara compared to samples before exposure. Dark and light green columns refer respectively to Carrara and Verona Red Marbles. Grey bars indicate the relative standard deviation.*

The difference of total colour of samples exposed for 18 months respect to values measured before exposure increased in horizontal and oblique samples of Carrara Marble (19,35 and 12,39) and in horizontal specimen of Verona Red Marble (7,74) while it remained almost similar to values measure after 12 months of exposure in all the other samples (Figure 3.38). In particular, L* of both lithotypes underwent an evident shift towards negative values in horizontal (-17,63 and -7,00, respectively for marble and limestone) and oblique samples (-10,71and -2,80, respectively for marble and limestone) but small and towards positive values in vertical specimens (0,47 for marble and 1,48 for limestone). Moreover, a* was subject to a variation towards positive values in all marble samples and toward negative measure in each limestone specimen. Considering blue-yellow coordinate, Figure 3.38 shows a change of values towards yellow for all Carrara Marble samples and for oblique limestone specimen while toward the blue component for horizontal and vertical limestone samples.

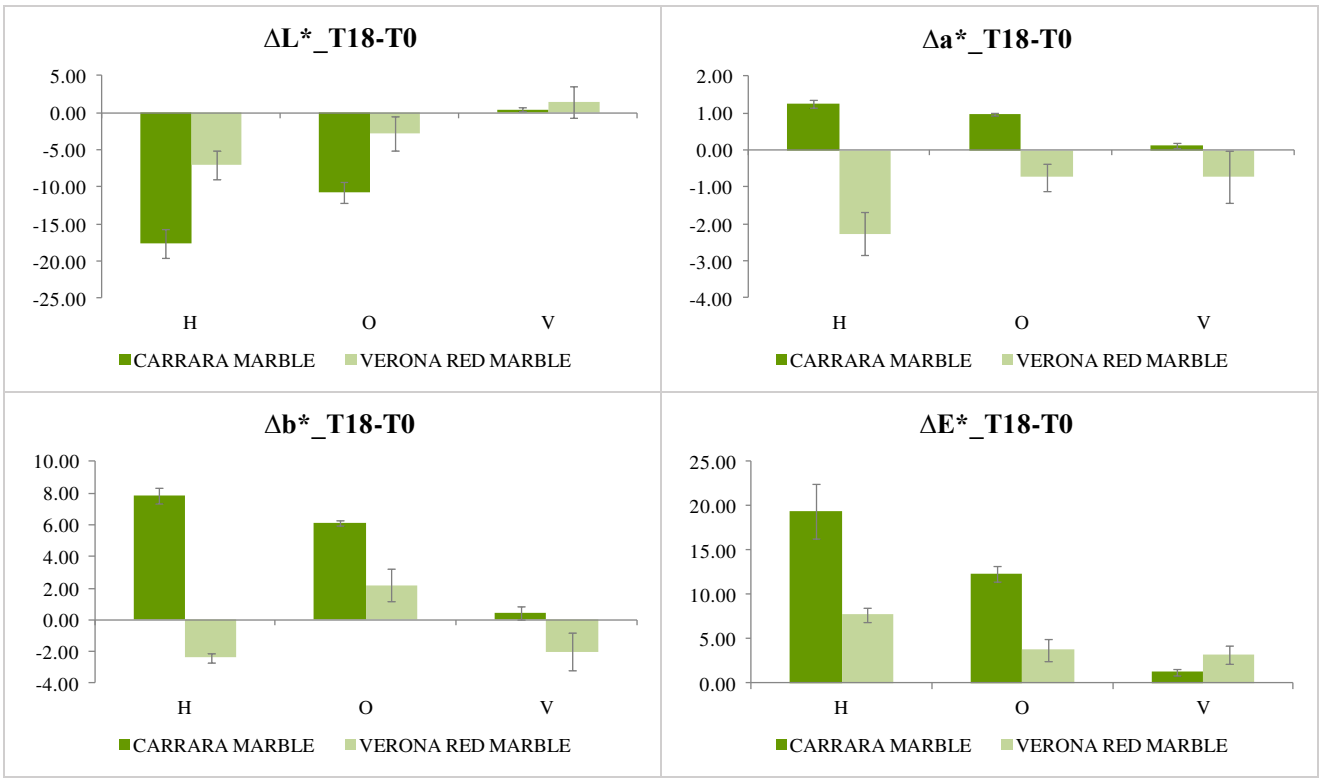

*Figure 3.38 Mean variation of the colorimetric CIE L*a*b* parameters and of total colour appearance (ΔE*) of specimens exposed for 18 months in Ferrara compared to samples before exposure. Dark and light green columns refer respectively to Carrara and Verona Red Marbles. Grey bars indicate the relative standard deviation.*

Figure 3.39 displays colorimetric differences among marble and limestone samples exposed for 24 months respect to colour features of lithotypes before exposure. Also after 24 months of exposure, Carrara Marble samples horizontally and obliquely placed confirmed to be more susceptible to a change of total colour (till to 20.78 and 15.28, respectively) than to the equivalent limestone samples (7.62 and 4.38) while limestone vertical specimens underwent higher ΔE* than the vertical marble one. Moreover, both horizontal samples and marble oblique one exceeded the acceptability limit of total colour change for human sight (Miliani et al., 2007).

Focusing on ΔL*, a slight whitening effect (ΔL* > 0) affected both vertical samples while all horizontal and oblique specimens underwent blackening (ΔL* < 0) more evident in marble samples and in those horizontally exposed (Figure 3.39).

Considering chroma values (Figure 3.39), Δa* slightly changed toward negative value in limestone samples and to positive ones in marble while higher change happened in b* parameter mainly in marble samples. In this regard, horizontal and oblique marble specimens were subjected to Δb* toward positive values till to 9.19 and 7.32, respectively.

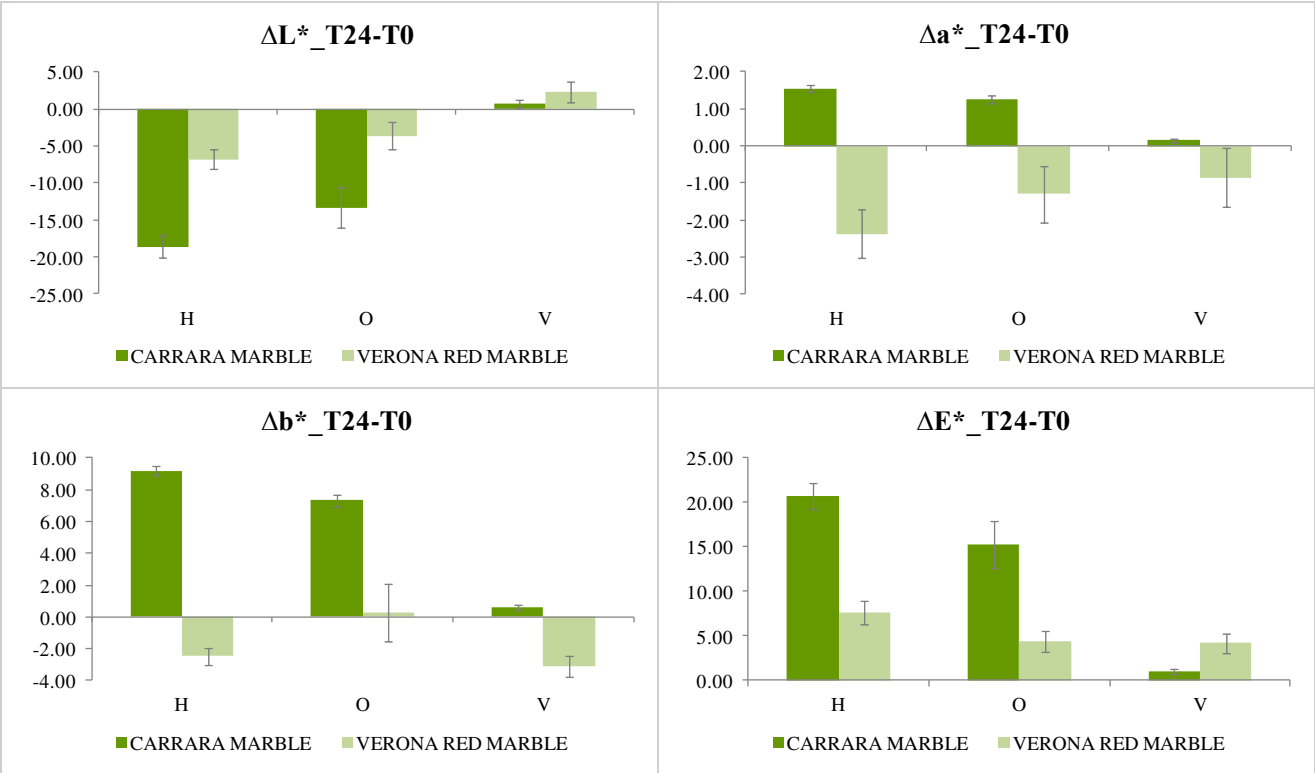

*Figure 3.39 Mean variation of the colorimetric CIE L*a*b* parameters and of total colour appearance (ΔE*) of specimens exposed for 24 months in Ferrara compared to samples before exposure. Dark and light green columns refer respectively to Carrara and Verona Red Marbles. Grey bars indicate the relative standard deviation.*

Final remarks:

- Results proved that Carrara Marble underwent higher colour vulnerability than Verona Red Marble. In general, horizontal and oblique marble samples often exceeded the acceptability limit of total colour change for human sight (Miliani et al., 2007).
- In general, total colour change of marble samples increased over time in all site, reaching higher values in Florence (till to 31.19).
- Horizontal samples, followed by oblique ones, were more subjected to colour change.
- ΔE* was mainly induced by a variation of lightness and secondly by change of blue-yellow parameter that led to a blackening effect and a shift toward yellow component of marble surface, respectively.

3.1.3. TOTAL DEPOSITED PARTICULATE (TDP)

The amount of particulate matter deposited per surface unit on stone samples was calculated by dividing the weight of particulate matter mechanically removed from each stone sample (then utilised for carbon speciation, see subchapter 3.1.5) by the area of exposed surface of stone specimen (i.e. 144 cm^2). The complete list of investigated samples is reported in Table 3.5.

SITE	SAMPLE	AFTER 6 MONTHS OF EXPOSURE	AFTER 12 MONTHS OF EXPOSURE	AFTER 18 MONTHS OF EXPOSURE	AFTER 24 MONTHS OF EXPOSURE	WEIGHT OF DEPOSITED PM (mg)
BOLOGNA	BCH10	V	-	-	-	18,2
	BCH12	-	V	-	-	32,2
	BCO2	-	V	-	-	29,6
	BCH8	-	-	V	-	9,3
	BCO10	-	-	V	-	20,1
	BCH14	-	-	-	V	24,5
	BCO5	-	-	-	V	13,7
FERRARA	PTCH21	V	-	-	-	30,7
	PTNH21	V	-	-	-	20,1
	PTCH23	-	V	-	-	63,8
	PTNH17	-	V	-	-	46,8
	PTNO12	-	V	-	-	36,0
	PTCO12	-	V	-	-	37,8
	PTCH4	-	-	V	-	120,8
	PTNH4	-	-	V	-	73,7
	PTCO5	-	-	V	-	86,2
	PTNO14	-	-	V	-	64,4
	PTCH5	-	-	-	V	141,8
	PTNH11	-	-	-	V	114,4
	PTCO4	-	-	-	V	108,2
	PTNO16	-	-	-	V	68,4
FLORENCE	SMCH1	V	-	-	-	37,4
	SMCO1	V	-	-	-	40,8
	SMCH4	-	V	-	-	57,7
	SMCO4	-	V	-	-	51,2
	SMCH5	-	-	V	-	106,6
	SMCO5	-	-	V	-	86,4
	SMCH8	-	-	-	V	194,2
	SMCO8	-	-	-	V	146,5

Table 3.5 Specimens, subdivided in different sites and times of measurement, from which the accumulated particulate matter was collected and weighted (reported in the last column). The sign "V" ("-") means that particulate matter was (not) collected from the exposed surface of sample.

<u>BOLOGNA</u>

Table 3.6 shows the amount of particulate per surface unit deposited on stone samples exposed in Bologna after different exposure time. The highest TDP of horizontal samples (223.61 µg cm^{-2}) was measured after 12 months of exposure while TDP was lower during the other considered period. TDP of oblique samples

reached the highest value after 12 months of exposure (205.56 µg cm^{-2}) and gradually decreased after 18 and 24 months of exposure up to 94.79 µg cm^{-2} (Table 3.6).

	EXPOSURE TIME (month)	SAMPLE	TDP (µg cm^{-2})
H	6	BCH10	126.39
H	12	BCH12	223.61
O		BCO2	205.56
H	18	BCH8	64.58
O		BCO10	139.58
H	24	BCH14	170.14
O		BCO5	94.79

Table 3.6 Total deposited particulate (TDP) accumulated on horizontal (H) and oblique (O) Carrara Marble samples exposed in Bologna at different exposure time (6, 12, 18, 24 months).

FERRARA

Table 3.7 displays the amount of particulate matter per surface unit deposited on the exposed surface of CM and VRM samples located in Ferrara after different exposure time.

		CM		VRM	
	EXPOSURE TIME (month)	SAMPLE	TDP (µg cm^{-2})	SAMPLE	TDP (µg cm^{-2})
H	6	PTCH21	213.19	PTNH21	139.58
H	12	PTCH23	443.06	PTNH17	325.00
O		PTCO12	262.50	PTNO12	250.00
H	18	PTCH4	838.89	PTNH4	511.81
O		PTCO5	598.61	PTNO14	447.22
H	24	PTCH5	984.79	PTNH11	794.44
O		PTCO4	751.39	PTNOI6	474.72

Table 3.7 Total deposited particulate (TDP) accumulated on horizontal (H) and oblique (O) Carrara Marble (CM) and Verona Red Marble (VRM) samples exposed in Ferrara at different exposure time (6, 12, 18, 24 months).

It can be observed that TDP on horizontal Carrara Marble samples increased over time from 213.19 µg cm^{-2} after 6 months to 984.79 µg cm^{-2} after 24 months of exposure. Also horizontal limestone specimens

underwent a gradual increase of deposited PM per surface unit over time but with lower values respect to marble (from 139.58 µg cm^{-2} after 6 months to 794.44 µg cm^{-2} after 24 months).
Higher TDP was observed also on oblique CM samples than on oblique limestone ones, mainly after 18 and 24 months of exposure. The increasing trend of TDP over time of both oblique specimens was anyway minor than those detected on the corresponding horizontal samples. Therefore, PM deposition affected mostly horizontal samples probably because of higher influence of gravitational settling on horizontal surfaces.

FLORENCE

TDP of horizontal and oblique samples exposed in Florence are reported in Table 3.8.

	EXPOSURE TIME (month)	SAMPLE	TDP (µg cm^{-2})
H	6	SMCH1	259.72
O		SMCO1	283.33
H	12	SMCH4	400.69
O		SMCO4	355.56
H	18	SMCH5	740.28
O		SMCO5	600.00
H	24	SMCH8	1348.26
O		SMCO8	1017.29

Table 3.8 Total deposited particulate (TDP) accumulated on horizontal (H) and oblique (O) Carrara Marble samples exposed in Florence at different exposure time (6, 12, 18, 24 months).

TDP of horizontal samples increased over time passing from 259.72 µg cm^{-2} after 6 months of exposure to 1348.26 µg cm^{-2} after 24 months. Also oblique samples were characterised by a growing TDP over time (from 283.33 µg cm^{-2} after 6 months to 1017.29 µg cm^{-2} after 24 months of exposure) but with smaller values than the corresponding horizontal samples.

COMPARISON

The comparison of TDP among different sites shows that horizontal samples exposed in Bologna never reached 225.00 µg cm^{-2} while TDP detected in horizontal specimens exposed Ferrara and Florence almost always exceeded this value (Figure 3.40 A). In particular, the amount of particulate matter deposited per surface unit on horizontal specimens exposed in Ferrara and Florence underwent an increasing trend over time reaching the highest values after 24 months of exposure (984.79 µg cm^{-2} and 1348.26 µg cm^{-2}, respectively).
Considering the same exposure site, also horizontal limestone specimens underwent a gradual increase of TDP over time but with slightly lower values respect to marble ones (Figure 3.40 A). As both lithotypes are characterised by low porosity (subchapter 3.1.1.4) and polished surface, TDP differences can be due to

different stone texture (micritic for limestone and granoblastic for marble - subchapter 3.1.1.1) that led higher compactness to Verona Red Marble.

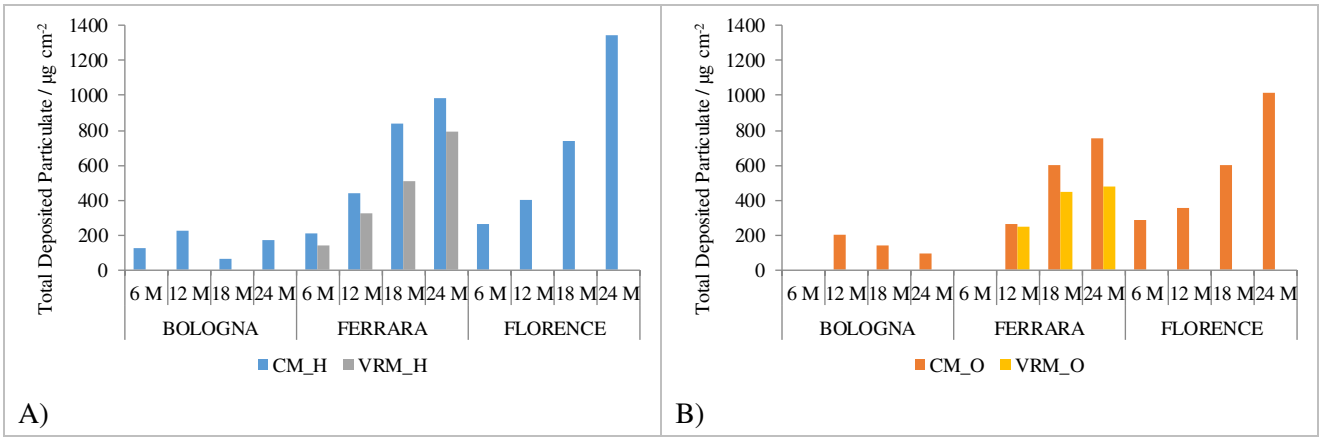

Figure 3.40 Comparison of the amount of particulate matter deposited per surface unit on CM and VRM horizontal (A) and oblique (B) samples exposed in Bologna, Ferrara and Florence at different exposure time (6, 12, 18, 24 months).

Concentrating upon oblique samples, TDP was detected in Bologna and Ferrara after 12, 18 and 24 months of exposure while after all time periods in Florence (Figure 3.40 B). TDP increased over time in samples exposed in Ferrara and Florence (but with lower values than the corresponding horizontal samples) while it displayed a decreasing trend in specimens exposed in Bologna.

Therefore, the deposition of coarse particles by gravitation settling on horizontal surfaces may explain the general higher TDP detected in horizontal samples. In addition, results shows as particulate matter deposition prevailed in Ferrara and Florence as TDP increased over time on stones surface while natural removal processes (e.g. wind) along with accumulation occurred after 18 and 24 months of exposure in Bologna.

3.1.4. ION CHROMATOGRAPHY (IC)

Ion chromatography of the material deposited on stone specimens was performed in each exposure site every 6 months from the starting of stone exposure, using stone samples with different orientation, whenever a suitable amount of particulate matter was accumulated on their surface. The complete list of analysed samples is reported in Table 3.9.

SITE	SAMPLE	AFTER 6 MONTHS OF EXPOSURE	AFTER 12 MONTHS OF EXPOSURE	AFTER 18 MONTHS OF EXPOSURE	AFTER 24 MONTHS OF EXPOSURE
BOLOGNA	BCH11	V	-	-	-
	BCH13	-	V	-	-
	BCO3	-	V	-	-
	BCH7	-	-	V	-
	BCO11	-	-	V	-
	BCH6	-	-	-	V
	BCO12	-	-	-	V
	BCV2	-	-	-	V
FERRARA	PTCH22	V	-	-	-
	PTNH22	V	-	-	-
	PTCH18	-	V	-	-
	PTNH19	-	V	-	-
	PTNO11	-	V	-	-
	PTCO11	-	V	-	-
	PTCH12	-	-	V	-
	PTNH12	-	-	V	-
	PTCO6	-	-	V	-
	PTNO15	-	-	V	-
	PTCH13	-	-	-	V
	PTNH13	-	-	-	V
	PTCO7	-	-	-	V
	PTCO20	-	-	-	V
	PTNO17	-	-	-	V
	PTNO20	-	-	-	V
	PTCV2	-	-	-	V
	PTNV3	-	-	-	V
FLORENCE	SMCH2	V	-	-	-
	SMCO2	V	-	-	-
	SMCH3	-	V	-	-
	SMCO3	-	V	-	-
	SMCH6	-	-	V	-
	SMCO6	-	-	V	-
	SMCH7	-	-	-	V
	SMCO7	-	-	-	V
	SMCV3	-	-	-	V

Table 3.9 Specimens, subdivided in different sites and times of measurement, examined with IC. The sign "V" ("-") means that the analysis was (not) carried out on the sample.

Please note that the reported concentration of water-soluble ions in ppb refers to analysed data normalised to the selected volume of 100 mL.

BOLOGNA

Concentrations of water-soluble ions (ppm) measured in material deposited on marble samples exposed in Bologna at different exposure time are reported in Table A3.1 (Annex 3).

After 6 months of exposure

Investigation about water-soluble ions was performed only on horizontally exposed specimen. Considering anions, the deposited matter resulted to be composed mainly by chloride ion – Cl^- – followed by nitrate ion – NO_3^- – and few sulphate ion – SO_4^{2-} – (Figure 3.41). The analysis of cations revealed the prevalence of sodium ion – Na^+ – over calcium ion – Ca^{2+} – and magnesium ion – Mg^{2+} – while the detected amount of potassium ion – K^+ – and ammonium ion – NH_4^+ – is negligible (Figure 3.41).

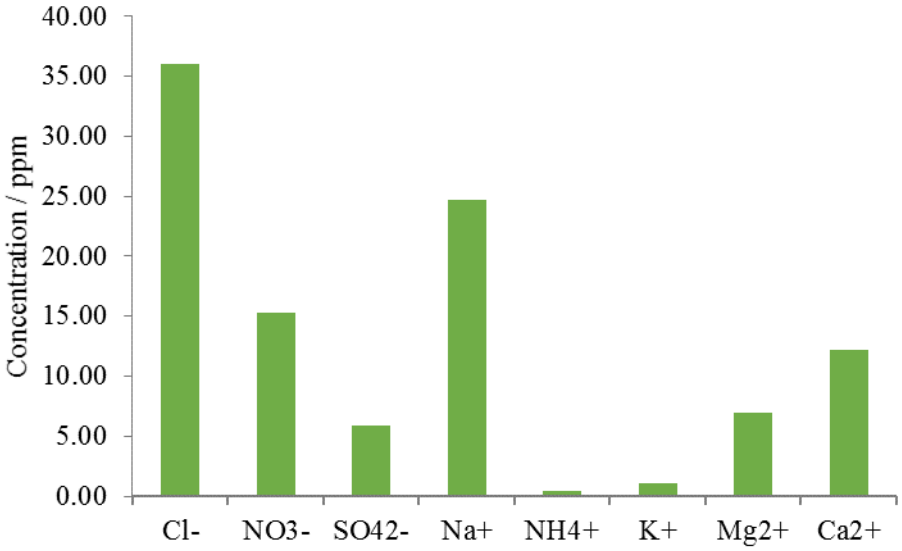

Figure 3.41 Soluble ions concentrations (ppm) measured in material accumulated on sample horizontally exposed for 6 months in Bologna.

Moreover, Table 3.10 reports the amount of soluble ions detected in the solute of the solution per surface unit.

	Cl^- (µg cm^{-2})	NO_3^- (µg cm^{-2})	SO_4^{2-} (µg cm^{-2})	Na^+ (µg cm^{-2})	NH_4^+ (µg cm^{-2})	K^+ (µg cm^{-2})	Mg^{2+} (µg cm^{-2})	Ca^{2+} (µg cm^{-2})
BCH11	25.00	10.65	4.11	17.16	0.30	0.74	4.86	8.46

Table 3.10 Soluble ions concentrations per surface unit measured in material deposited on sample horizontally exposed for 6 months in Bologna.

After 12 months of exposure

Concentration of soluble ions was measured in material deposited on horizontal and oblique samples. Figure 3.42 shows that Cl^- (26.35 ppm) of the deposit accumulated on horizontal samples was detected with higher concentration respect to the other anions (15.35 ppm for NO_3^- and 8.05 ppm for SO_4^{2-}). Moreover, it exceeded also the concentration of all cations analysed on the same sample. Among cations, Na^+ (22.86 ppm) was more abundant than Mg^{2+} and K^+ (5.08 ppm and 1.75 ppm, respectively) while NH_4^+ and Ca^{2+} were below the limit of detection.

Material deposited on oblique stone sample was characterised by the prevalence of Cl^- among anionic species and Na^+ among cations but with lower concentration respect to those measured on horizontal sample: 21.35 ppm and 20.36 ppm, respectively (Figure 3.42). Considering the other ions, there are no big differences respect to values measured in the horizontal sample but it was possible to detect NH_4^+ (0.22 ppm) and Ca^{2+} (4.88ppm).

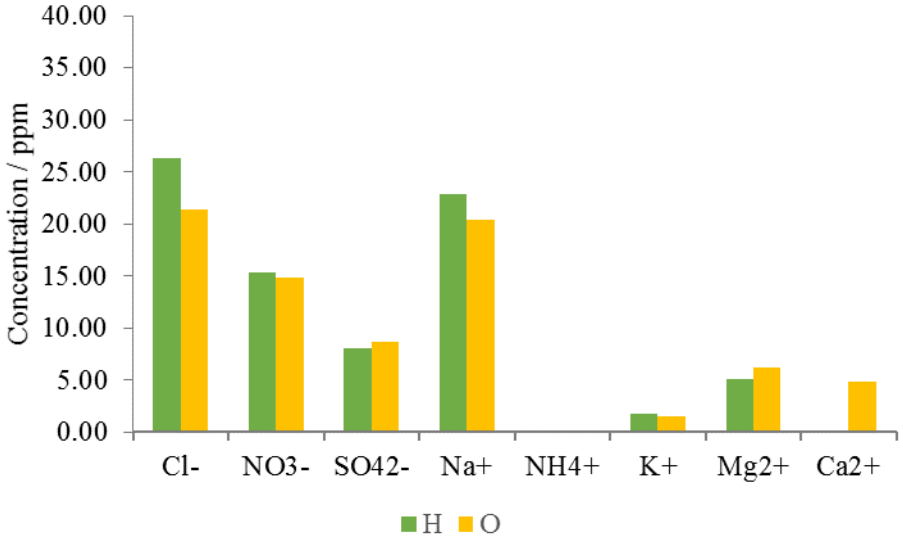

Figure 3.42 Soluble ions concentrations (ppm) measured in material accumulated on sample horizontally (green) and obliquely (ochre) exposed for 12 months in Bologna.

Data of each ion measured per surface unit are reported in Table 3.11 and show a similar trend to the related concentration reported in ppm.

	Cl^- (µg cm^{-2})	NO_3^- (µg cm^{-2})	SO_4^{2-} (µg cm^{-2})	Na^+ (µg cm^{-2})	NH_4^+ (µg cm^{-2})	K^+ (µg cm^{-2})	Mg^{2+} (µg cm^{-2})	Ca^{2+} (µg cm^{-2})
BCH13	18.30	10.66	5.59	15.88	<LOD	1.22	3.53	<LOD
BCO3	14.83	10.29	6.02	14.14	0.15	1.06	4.32	3.39

Table 3.11 Soluble ions concentrations per surface unit measured in material deposited on horizontal and oblique samples exposed for 12 months in Bologna. <LOD means below the limit of detection.

After 18 months of exposure

The analysis of the material accumulated on horizontal and oblique samples displays rather significant amount of Cl^-, Na^+ and Ca^{2+} in both samples but with always higher values in horizontal specimen than in the oblique one (Figure 3.43). Sulphate ion was detected with slightly higher concentration in the oblique sample (6.25 ppm) than the horizontal one (4.43 ppm) while similar values on both samples were assessed for K^+ (0.55 ppm for BCH7 and 0.65 ppm for BCO11) and Mg^{2+} (5.94 ppm for BCH7 and 5.61 ppm for BCO11). Moreover, NO_3^- and NH_4^+ were below the limit of detection in both samples.

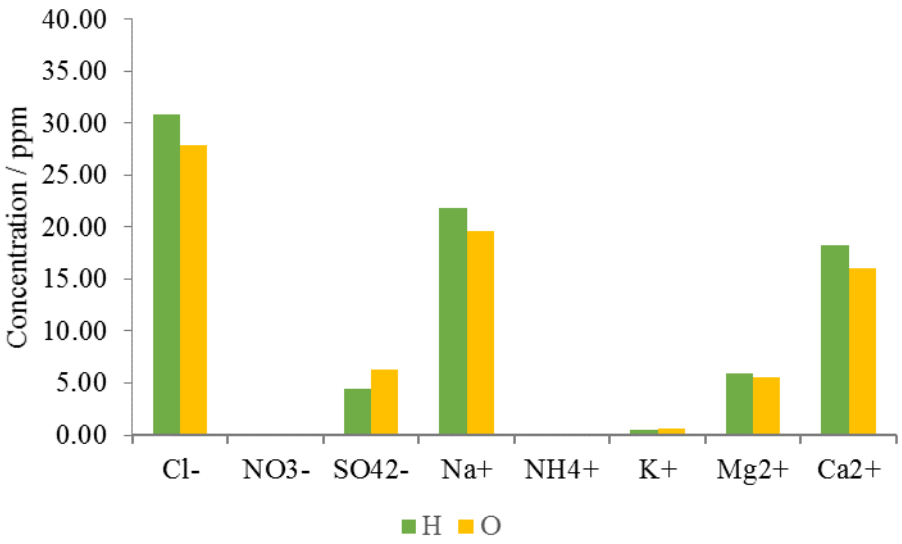

Figure 3.43 Soluble ions concentrations (ppm) measured in material accumulated on sample horizontally (green) and obliquely (ochre) exposed for 18 months in Bologna.

Finally, Table 3.12 shows the concentration of all water-soluble ions per unit of surface detected on the material accumulated horizontally and obliquely exposed samples.

	Cl^- (µg cm^{-2})	NO_3^- (µg cm^{-2})	SO_4^{2-} (µg cm^{-2})	Na^+ (µg cm^{-2})	NH_4^+ (µg cm^{-2})	K^+ (µg cm^{-2})	Mg^{2+} (µg cm^{-2})	Ca^{2+} (µg cm^{-2})
BCH7	21.46	<LOD	3.08	15.13	<LOD	0.38	4.13	12.67
BCO11	19.40	<LOD	4.34	13.61	<LOD	0.45	3.90	11.15

Table 3.12 Soluble ions concentrations per surface unit measured in material deposited on horizontal and oblique samples exposed for 18 months in Bologna. <LOD means below the limit of detection.

After 24 months of exposure

After 24 months of exposure, ion chromatography was carried out on the material deposited on horizontal, oblique and vertical samples. The results show in general low values in all the analysed specimens (Figure 3.44). In particular, ion concentration detected on material accumulated on vertical sample was always below 1.00 ppm. Considering other samples, among anions SO_4^{2-} is more abundant than Cl^- (0.97 ppm of horizontal sample and 1.68 ppm on the oblique one) and NO_3^- (2.10 ppm of horizontal sample and 2.00 ppm on the oblique one), with higher value on oblique specimen (4.22 ppm) respect to the horizontal one (2.68 ppm). Taking into consideration cations, Ca^{2+} was more abundant (5.87 ppm on horizontal sample and 4.77 ppm of the oblique one) than Na^+ (0.62 ppm on horizontal sample and 1.03 ppm of the oblique one) while all the other cationic fractions were close to 0.00 ppm.

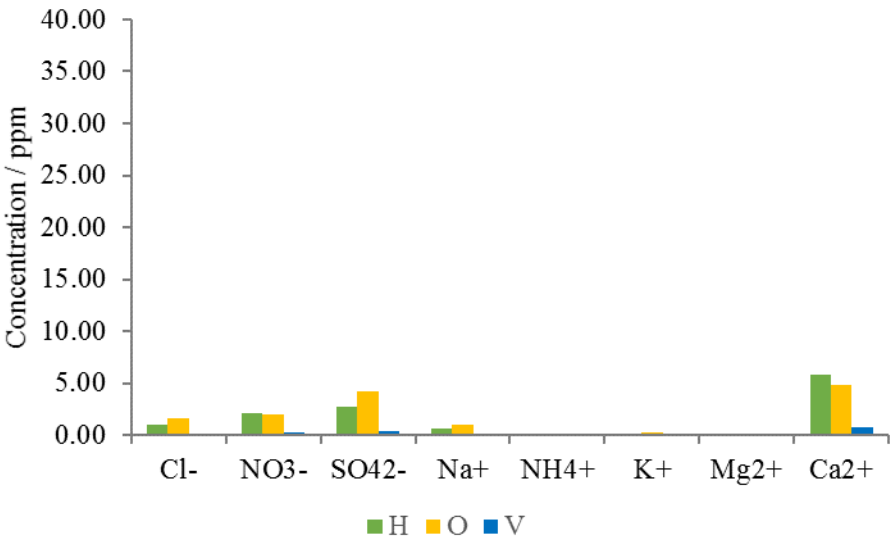

Figure 3.44 Soluble ions concentrations (ppm) measured in material accumulated on sample horizontally (green), obliquely (ochre) and vertically (blue) exposed for 24 months in Bologna.

Observing ion concentration per surface unit (Table 3.13), it is evident that all values were very low.

	Cl^- (µg cm^{-2})	NO_3^- (µg cm^{-2})	SO_4^{2-} (µg cm^{-2})	Na^+ (µg cm^{-2})	NH_4^+ (µg cm^{-2})	K^+ (µg cm^{-2})	Mg^{2+} (µg cm^{-2})	Ca^{2+} (µg cm^{-2})
BCH6	0.67	1.46	1.86	0.43	0.01	0.05	0.12	4.08
BCO12	1.17	1.39	2.93	0.72	<LOD	0.16	0.14	3.31
BCV2	0.08	0.18	0.28	0.04	<LOD	0.00	0.02	0.54

Table 3.13 Soluble ions concentrations per surface unit measured in material deposited on horizontal, oblique and vertical samples exposed for 24 months in Bologna. <LOD means below the limit of detection.

Comparison

Comparing anions concentration per surface unit detected in all specimens at different exposure time, it is evident that in general lower values of all anions were measured in all samples after 24 months of exposure respect to samples assessed during previous months. Moreover, Cl^- was the most abundant anion measured in horizontal and oblique samples till 18 months of exposure, reaching values between 14.83 µg cm^{-2} and 25.00 µg cm^{-2} (Figure 3.45) while SO_4^{2-} prevailed over other anions on samples remained exposed for 24 months.
Concentrating upon the variation over time of each anion, Cl^- concentration decreased after 12 ad 24 months of exposure while higher values were measured after 6 and 18 months of exposure, reaching higher amount on horizontal samples than in the oblique ones (with exception analysis on specimens exposed for 24 months whose values were similar). NO_3^- analysed on horizontal and oblique samples remained alike after 6 and 12 months of exposure (around 10.53 µg cm^{-2}), decreased below limit of detection after 18 months and underwent a slight growth after 24 of exposure (about 2.40 µg cm^{-2}). Finally, the amount of anions detected on vertical sample after 24 months of exposure was negligible.

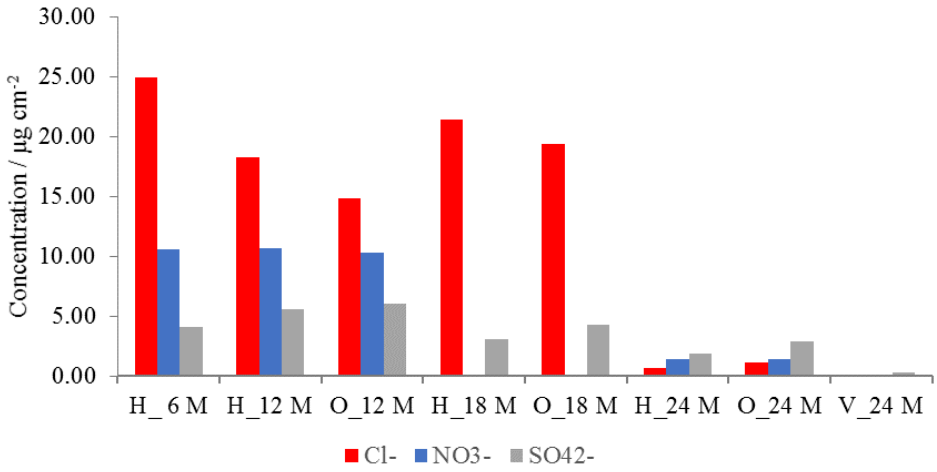

Figure 3.45 Concentration of soluble anions per surface unit (µg cm^{-2}) measured in material accumulated on horizontal (H), oblique (O) and vertical (V) samples remained exposed for 6, 12, 18 and 24 months in Bologna.

Na^+, Mg^{2+} and Ca^{2+} were cations detected with higher concentration in all samples considering different exposure time and orientation. Na^+ showed higher concentration among other cationic species for horizontal and oblique samples analysed till 18 months of exposure (with values between 17.16 µg cm^{-2} and 13.61 µg cm^{-2}) while samples exposed for 24 months were characterised by the predominance of Ca^{2+} (around 3.70 µg cm^{-2}) (Figure 3.46). The concentration per surface unit of Na^+ gradually decreased within 18 months of exposure with slightly higher values on horizontal samples than the oblique ones, followed by a radical drop after 24 months of exposure. Considering Ca^{2+} amount per surface unit, it underwent a decrease after 12 and 24 months of exposure while higher values were measured after 6 and 18 months of exposure, in general with higher values on horizontal specimens (with the exception of horizontal sample exposed for 12 months where Ca^{2+} was below the detection limit). The amount of Mg^{2+} per surface unit was rather constant (around 4.15 µg cm^{-2}) on horizontal and oblique specimens within 18 months of exposure while then it decreased around 0.00 µg cm^{-2}. NH_4^+ and K^+ displayed concentration close to 0.00 µg cm^{-2} or below limit of detection all over the period.

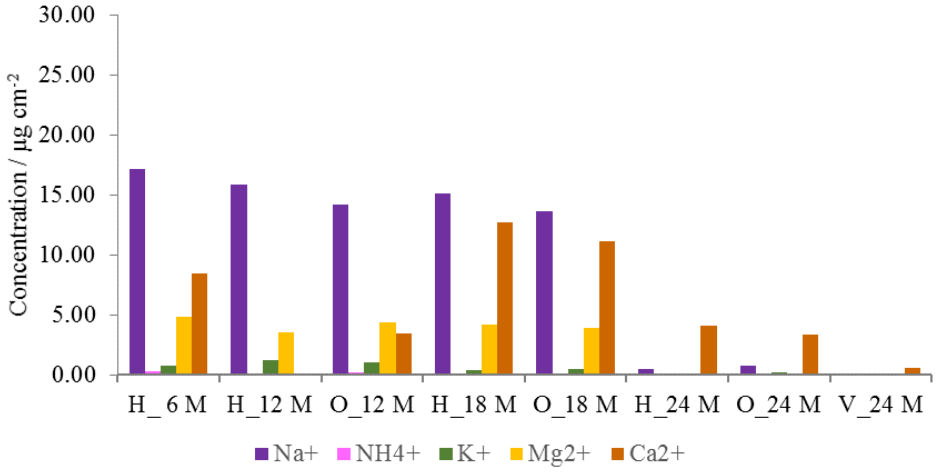

Figure 3.46 Concentration of soluble cations per surface unit (µg cm^{-2}) measured in material accumulated on horizontal (H), oblique (O) and vertical (V) samples remained exposed for 6, 12, 18 and 24 months in Bologna.

FERRARA

CARRARA MARBLE

Concentrations of water-soluble ions (ppm) measured in material deposited on marble samples exposed in Ferrara at different exposure time are reported in Table A3.2 (Annex 3).

After 6 months of exposure

Investigation of water-soluble ions was performed only on horizontally exposed specimen. Among anions, Cl^- was measured with higher concentration followed by NO_3^- and SO_4^{2-} (Figure 3.47). Moreover, Na^+ and Ca^{2+} were abounding while the concentration of NH_4^+, K^+ and Mg^{2+} were lower (Figure 3.47).

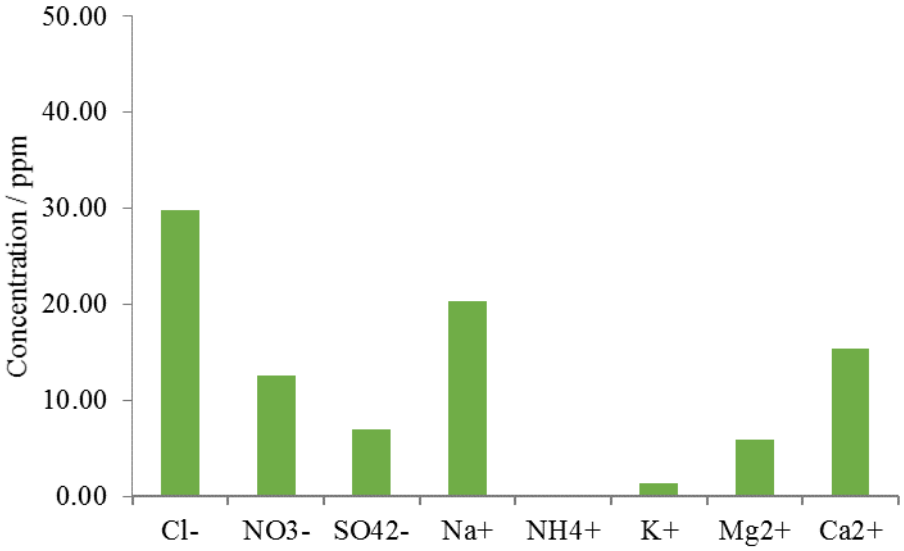

Figure 3.47 Soluble ions concentrations (ppm) measured in material accumulated on Carrara Marble sample horizontally exposed for 6 months in Ferrara.

The amount of soluble ions per surface unit of sample exposed for 6 months, reported in Table 3.14, confirms the prevalence of Cl^-, Na^+ and Ca^{2+}.

	Cl^- (µg cm^{-2})	NO_3^- (µg cm^{-2})	SO_4^{2-} (µg cm^{-2})	Na^+ (µg cm^{-2})	NH_4^+ (µg cm^{-2})	K^+ (µg cm^{-2})	Mg^{2+} (µg cm^{-2})	Ca^{2+} (µg cm^{-2})
PTCH22	20.71	8.74	4.86	14.08	0.10	0.99	4.07	10.68

Table 3.14 Soluble ions concentration per surface unit measured in material deposited on Carrara Marble sample horizontally exposed for 6 months in Ferrara.

After 12 months of exposure

Horizontal sample exposed for 12 months was characterised by the prevalence of Cl^- among anions even if the amount of NO_3^- and SO_4^{2-} was not so unlike (Figure 3.48). Among cations, Na^+ was detected with the highest concentration while the others were lower or below the detection limit.

The concentrations of Cl^-, Na^+ and Mg^{2+} measured on the oblique sample were slightly higher those detected on horizontal specimen, thus suggesting a likely common source (Figure 3.48). On the contrary, NO_3^-, SO_4^{2-} and K^+ were lower on oblique samples than the values measured in the horizontal sample. Finally, also here NH_4^+ was below limit of detection while an appreciable quantity of Ca^{2+} was assessed.

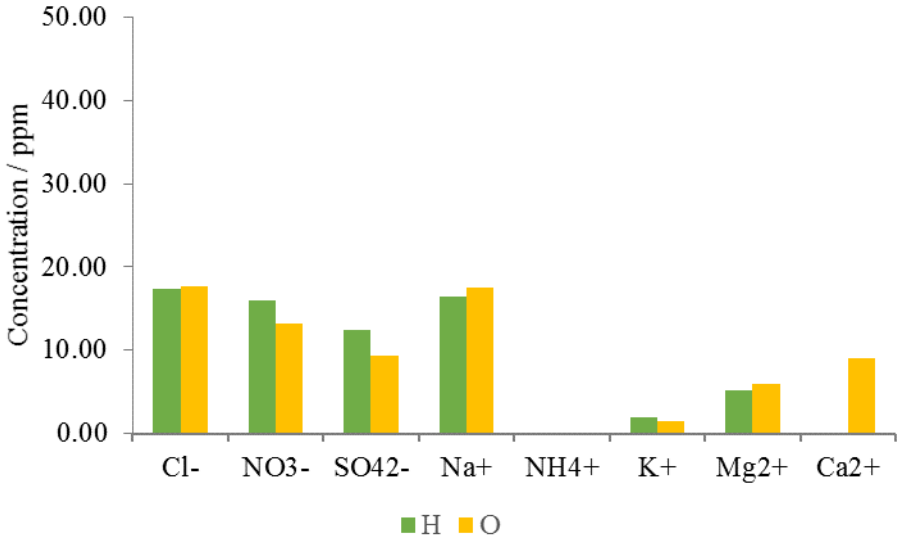

Figure 3.48 Soluble ions concentrations (ppm) measured in material accumulated on Carrara Marble samples horizontally (green) and obliquely (ochre) exposed for 12 months in Ferrara.

Furthermore, Table 3.15 shows concentration of ions per surface unit calculated for both samples.

	Cl^- (µg cm^{-2})	NO_3^- (µg cm^{-2})	SO_4^{2-} (µg cm^{-2})	Na^+ (µg cm^{-2})	NH_4^+ (µg cm^{-2})	K^+ (µg cm^{-2})	Mg^{2+} (µg cm^{-2})	Ca^{2+} (µg cm^{-2})
PTCH18	12.00	11.10	8.59	11.43	<LOD	1.33	3.57	<LOD
PTCO11	12.22	9.11	6.47	12.11	<LOD	1.08	4.18	6.29

Table 3.15 Soluble ions concentrations per surface unit measured in material deposited on horizontal and oblique Carrara Marble samples exposed for 12 months in Ferrara. <LOD means below the limit of detection.

After 18 months of exposure

Observing the concentrations of anions measured on horizontal and oblique samples, Cl^- remained the most abundant (31.64 ppm in horizontal specimen and 28.04 ppm in the oblique one) but also the amount of SO_4^{2-} was considerable (18.98 ppm in horizontal sample and 23.66 ppm in oblique one) while NO_3^- was lower (13.21 ppm in horizontal specimen and 12.13 ppm in the oblique one) (Figure 3.49).

Considering cations, similar values of Na^+, Mg^{2+} and Ca^{2+} were measured in horizontal (23.77 ppm, 6.52 ppm and 17.01, respectively) and oblique (22.46 ppm, 6.66 ppm and 17.04 ppm) samples while lower amount of NH_4^+ and K^+ was detected in oblique specimen (0.09 ppm and 1.63 ppm) than the horizontal one (2.55 ppm and 3.92, respectively) (Figure 3.49).

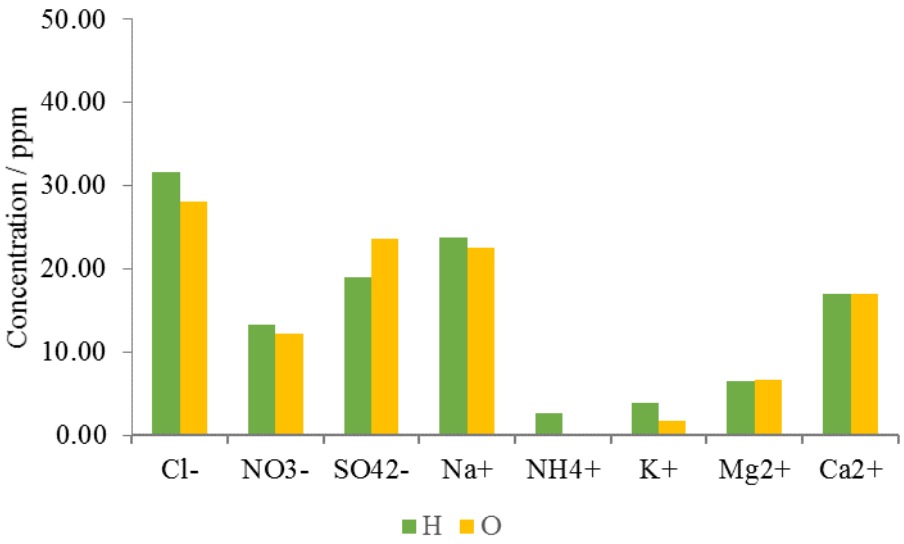

Figure 3.49 Soluble ions concentrations (ppm) measured in material accumulated on Carrara Marble samples horizontally (green) and obliquely (ochre) exposed for 18 months in Ferrara.

Furthermore, Table 3.16 displays ions concentration per surface unit of both samples highlighting the prevalence of Cl^- and SO_4^{2-} among anions and Na^+ and Ca^{2+} among cations.

	Cl^- ($\mu g\ cm^{-2}$)	NO_3^- ($\mu g\ cm^{-2}$)	SO_4^{2-} ($\mu g\ cm^{-2}$)	Na^+ ($\mu g\ cm^{-2}$)	NH_4^+ ($\mu g\ cm^{-2}$)	K^+ ($\mu g\ cm^{-2}$)	Mg^{2+} ($\mu g\ cm^{-2}$)	Ca^{2+} ($\mu g\ cm^{-2}$)
PTCH12	21.97	9.18	13.18	16.51	1.77	2.72	4.53	11.81
PTCO6	19.47	8.42	16.43	15.60	0.06	1.13	4.62	11.83

Table 3.16 Soluble ions concentrations per surface unit measured in material deposited on horizontal and oblique Carrara Marble samples exposed for 18 months in Ferrara.

After 24 months of exposure

After 24 months of exposure, ion chromatography was carried out on material deposited on horizontal, oblique and vertical samples exposed on the roof terrace and on oblique specimen located at window balcony (here indicated as O_W). Figure 3.50 shows that anions measured on the horizontal samples had quite similar concentration while Ca^{2+} stood out from the other cations.

Sample obliquely exposed on roof terrace was characterised by high concentration of SO_4^{2-} and Ca^{2+} while other ions were lower or imperceptible (Figure 3.50). In contrast, much lower values for all ions were detected in oblique sample exposed in window balcony.

Finally, vertical sample was characterised by rather considerable amount of SO_4^{2-} and Ca^{2+} while the other ionic species were lower or below limit of detection (NH_4^+) (Figure 3.50).

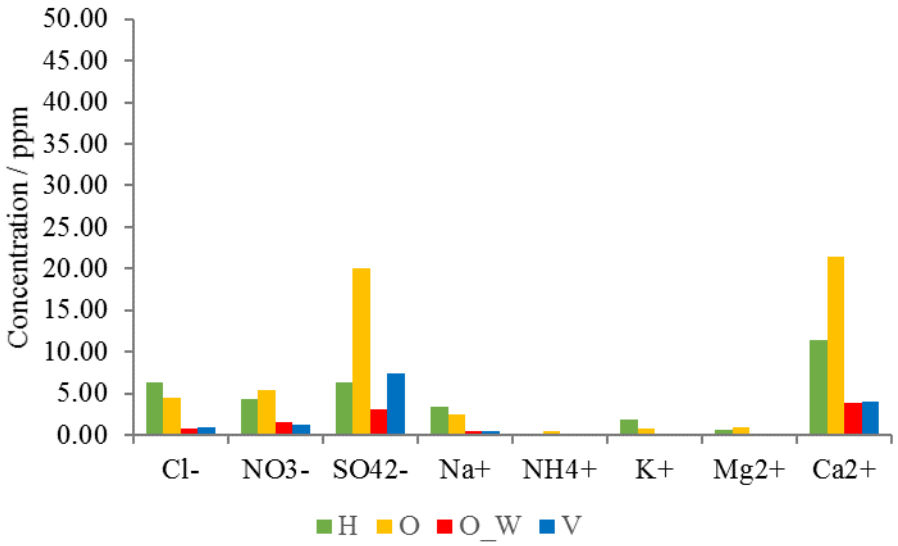

Figure 3.50 Soluble ions concentrations (ppm) measured in material accumulated on Carrara Marble samples exposed for 24 months in Ferrara. Green, ochre and blue bars refer to samples horizontally, obliquely and vertically located on the roof terrace while red bars to specimen obliquely placed on window balcony.

Furthermore, soluble ions concentrations per surface unit shows as SO_4^{2-} and Ca^{2+} prevailed over the other ions in all samples, indicating probable ongoing sulphation process, while noticeable values of Cl^- and Na^+ on horizontal sample suggest the presence of halite (Table 3.17).

	Cl^- (µg cm^{-2})	NO_3^- (µg cm^{-2})	SO_4^{2-} (µg cm^{-2})	Na^+ (µg cm^{-2})	NH_4^+ (µg cm^{-2})	K^+ (µg cm^{-2})	Mg^{2+} (µg cm^{-2})	Ca^{2+} (µg cm^{-2})
PTCH13	4.36	3.01	4.38	2.34	0.12	1.31	0.38	7.94
PTCO7	3.06	3.78	13.94	1.72	0.32	0.56	0.65	14.84
PTCO20 *	0.51	1.10	2.11	0.26	0.03	0.10	0.14	2.63
PTCV2	0.60	0.87	5.11	0.32	<LOD	0.09	0.09	2.76

*Table 3.17 Soluble ions concentrations per surface unit measured in material deposited on horizontal, oblique and vertical Carrara Marble samples exposed for 24 months on the roof terrace in Ferrara. * refers to specimen obliquely placed on window balcony. <LOD means below the limit of detection.*

Comparison

Focusing on anions concentration per surface unit measured in all samples at different exposure time, Cl^- was the most abundant anion measured in horizontal and oblique samples till 18 months of exposure, ranging between 12.00 µg cm^{-2} and 21.97 µg cm^{-2} with higher values detected after 6 and 18 months of exposure, while a drop of values was assessed after 24 months of exposure. The comparison of concentrations shows higher values on horizontal samples than the oblique and vertical ones with exception of measurements performed after 12 months of exposure that provided similar values (Figure 3.51).

NO_3^- analysed on horizontal samples was rather constant (around 9.67 µg cm^{-2}) after 6, 12 and 18 months of exposure while a decreased was measured after 24 months of exposure. In general, oblique specimens showed similar values of NO_3^- to horizontal samples with exception of samples analysed after 12 months where NO_3^- was higher on horizontal sample (Figure 3.51). Moreover, values measured on O_W and vertical samples after 24 months of exposure were the lowest ones detected among all analysed samples.

Considering SO_4^{2-}, it increased in horizontal and oblique specimens within 18 months (Figure 3.51) while lower values were measured after 24 months of exposure. Furthermore, SO_4^{2-} values of oblique samples exceeded those measured on horizontal specimen after 18 and 24 months of exposure. Please, note that is valid for oblique sample exposed in the roof terrace because much lower value was detected for O_W. concentration detected on vertical sample was not negligible.

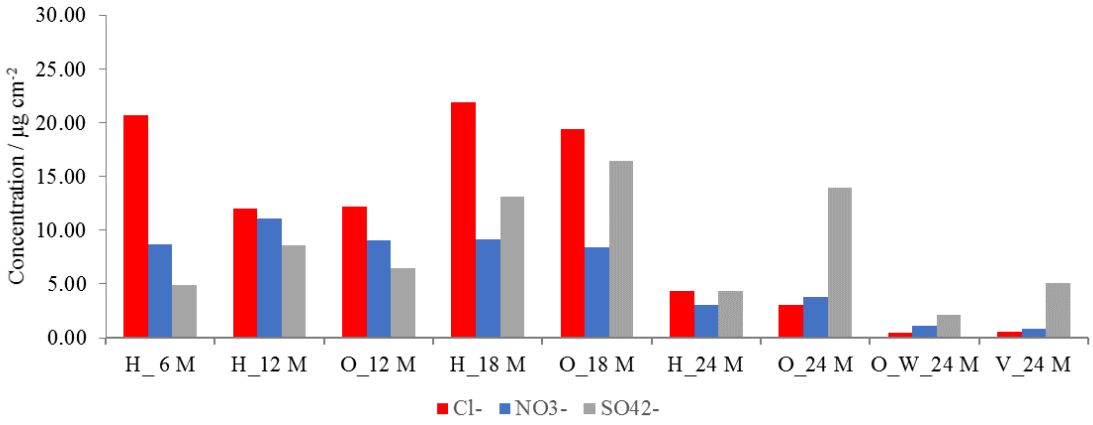

Figure 3.51 Concentration of soluble anions per surface unit (µg cm^{-2}) measured in material accumulated on horizontal (H), oblique (O) and vertical (V) Carrara Marble samples remained exposed for 6, 12, 18 and 24 months in Ferrara. O_W refers to oblique sample exposed on window balcony.

Figure 3.52 compares the cationic species measured on samples with different orientations and exposure time. Within first 18 months Na^+ prevailed over the other cations in all samples, with a slight decrease after 12 months of exposure followed by a growth after 18 month of exposure while its values fell down in all samples after 24 months of exposure. Moreover, Ca^{2+} was detected in rather high amount over all analysed period, with increasing values over time for oblique specimens, with exception of O_W that was lower and similar to the concentration of vertical sample. Considering horizontal samples, analysis shows lower values of Ca^{2+} after 12 and 24 months of exposure.
Mg^{2+} displayed a rather constant amount (4.20 µg cm^{-2}) in all samples during the first 18 months of exposure while lower values were detected on samples with different orientation after 24 months of exposure.
Finally, values of K^+ were very low (below 2.72 µg cm^{-2}) in all samples as well as NH_4^+, whose concentration was often below limit of detection.

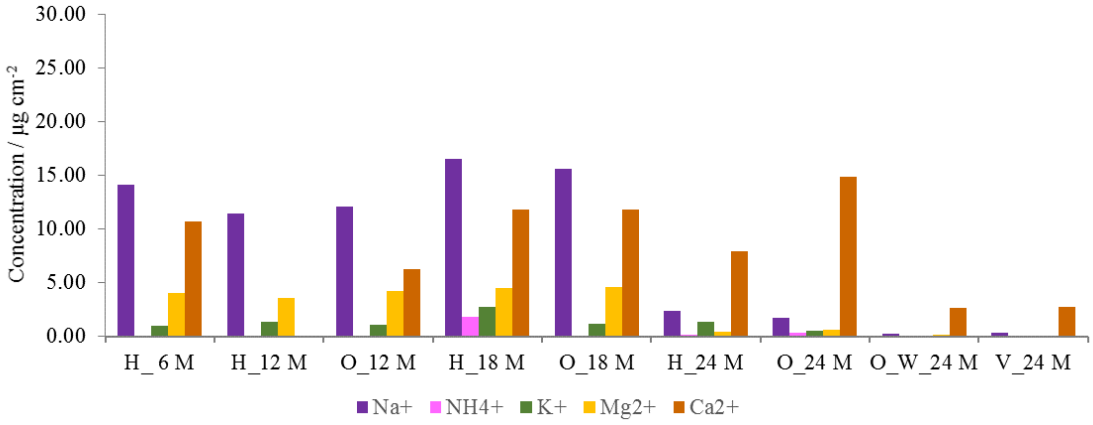

Figure 3.52 Concentration of soluble cations per surface unit (µg cm^{-2}) measured in material accumulated on horizontal (H), oblique (O) and vertical (V) Carrara Marble samples remained exposed for 6, 12, 18 and 24 months in Ferrara. O_W refers to oblique sample exposed on window balcony.

VERONA RED MARBLE

Concentrations of water-soluble ions (ppm) measured in material deposited on limestone samples exposed in Ferrara at different exposure time are reported in Table A3.3 (Annex 3).

After 6 months of exposure

Ion chromatography was performed only on horizontally exposed specimen after 6 months of exposure. Among anions, Cl^- was detected with higher concentration followed by NO_3^- and SO_4^{2-} (Figure 3.53). Moreover, Na^+ was higher than Ca^{2+}, Mg^{2+}, K^+ and NH_4^+ (Figure 3.53).

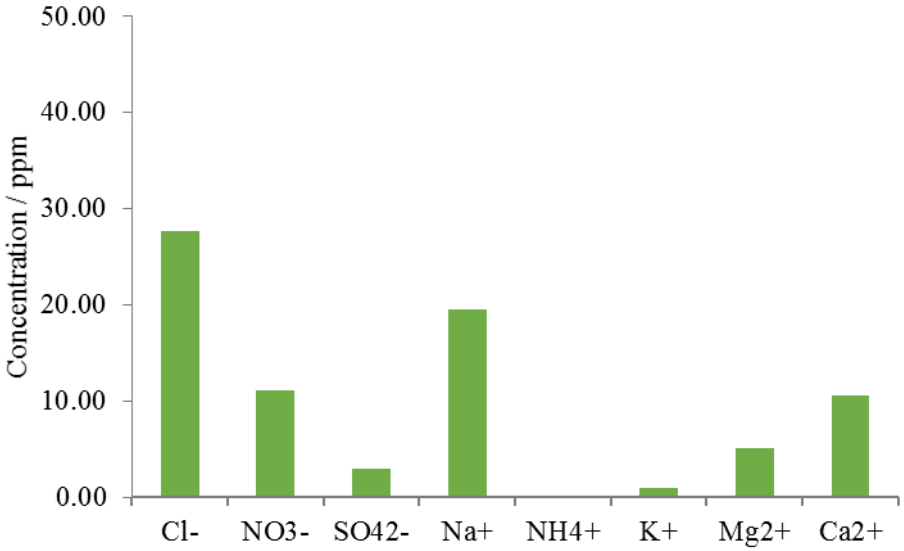

Figure 3.53 Soluble ions concentrations (ppm) measured in material accumulated on Verona Red Marble sample horizontally exposed for 6 months in Ferrara.

Table 3.18, presenting soluble-ions concentration per surface unit, shows higher values of Cl^-, NO_3^-, Na^+ and Ca^{2+}.

	Cl^- (µg cm^{-2})	NO_3^- (µg cm^{-2})	SO_4^{2-} (µg cm^{-2})	Na^+ (µg cm^{-2})	NH_4^+ (µg cm^{-2})	K^+ (µg cm^{-2})	Mg^{2+} (µg cm^{-2})	Ca^{2+} (µg cm^{-2})
PTNH22	19.24	7.69	2.05	13.58	0.04	0.70	3.55	7.31

Table 3.18 Soluble ions concentration per surface unit measured in material deposited on Verona Red Marble sample horizontally exposed for 6 months in Ferrara.

After 12 months of exposure

Anions concentration of horizontal and oblique samples shows higher values for Cl^-, followed by NO_3^- and SO_4^{2-} (Figure 3.54). In particular, horizontal samples (22.24 ppm, 17.04 ppm and 6.53 ppm, respectively) always displayed higher amount than the oblique ones (19.61 ppm, 13.30 ppm and 4.76 ppm).

Concentrating upon cations, a rather high amount of Na^+ was measured in both samples, slightly more in horizontal specimen than the oblique one (Figure 3.54). Ca^{2+} was detected only on oblique sample while it was below limit of detection in horizontal sample. Moreover, Mg^{2+} had similar values in both samples (6.34 ppm and 6.61 ppm on horizontal and oblique samples, respectively) while the concentration of NH_4^+ and K^+

were lower (0.27 ppm and 1.68 ppm on horizontal specimen and 0.01 ppm and 1.47 ppm on the oblique one).

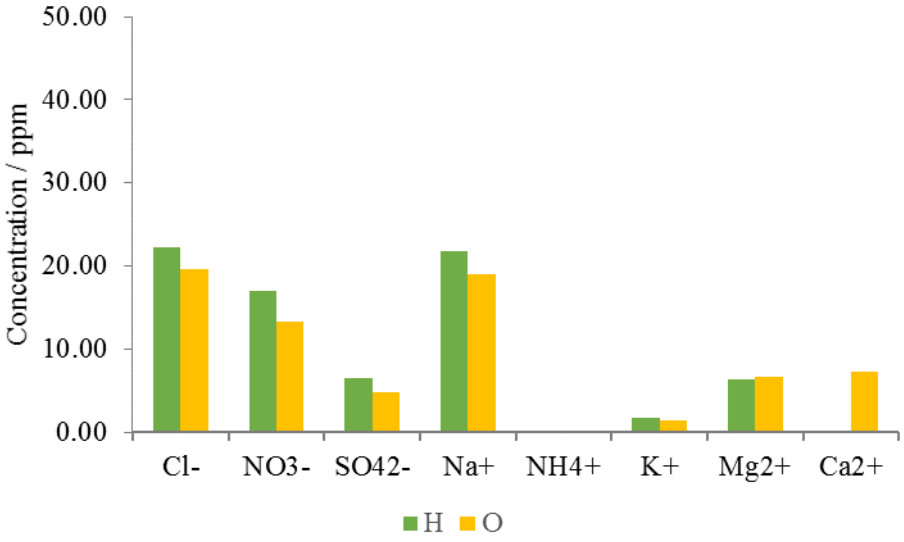

Figure 3.54 Soluble ions concentrations (ppm) measured in material accumulated on Verona Red Marble samples horizontally (green) and obliquely (ochre) exposed for 6 months in Ferrara.

Soluble-ion concentration per surface unit (Table 3.19) shows the prevalence of Cl^-, NO_3^- and Na^+ among other ions.

	Cl^- ($\mu g\ cm^{-2}$)	NO_3^- ($\mu g\ cm^{-2}$)	SO_4^{2-} ($\mu g\ cm^{-2}$)	Na^+ ($\mu g\ cm^{-2}$)	NH_4^+ ($\mu g\ cm^{-2}$)	K^+ ($\mu g\ cm^{-2}$)	Mg^{2+} ($\mu g\ cm^{-2}$)	Ca^{2+} ($\mu g\ cm^{-2}$)
PTNH19	15.44	11.83	4.54	15.14	0.19	1.17	4.40	<LOD
PTNO11	13.61	9.24	3.31	13.17	0.01	1.02	4.59	5.03

Table 3.19 Soluble ions concentration per surface unit measured in material deposited on Verona Red Marble samples horizontally and obliquely exposed for 12 months in Ferrara. <LOD means below the limit of detection.

After 18 months of exposure

Among anions, Figure 3.55 displays a clear predominance of Cl^- over NO_3^- and SO_4^{2-} on horizontal sample while lower concentrations were detected on the oblique specimen. Moreover, horizontal sample was characterised by abounding amount of Ca^{2+}, K^+ and Na^+. On the contrary the concentration of K^+ in the oblique sample was much lower (1.00 ppm) while rather high amount of Na^+ and Ca^{2+} were measured (Figure 3.55). Furthermore, NH_4^+ and Mg^{2+} displayed lower values than the other cations in both samples.

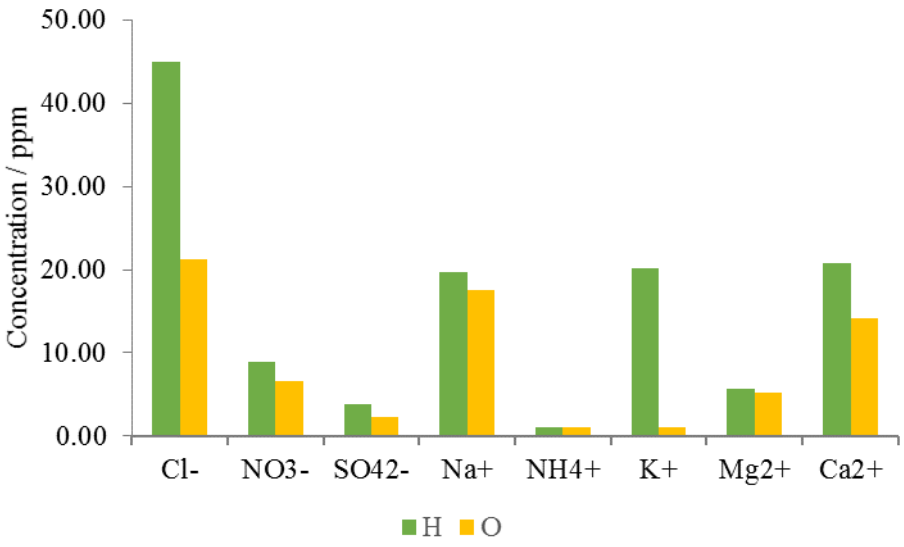

Figure 3.55 Soluble ions concentrations (ppm) measured in material accumulated on Verona Red Marble samples horizontally (green) and obliquely (ochre) exposed for 6 months in Ferrara.

Ions concentration per surface unit (Table 3.20) shows the clear abundance of Cl^- (31.28 µg cm^{-2}) and similar values of Na^+, K^+ and Ca^{2+} (around 14.04 µg cm^{-2}) on the horizontal sample while the prevalence of Cl^-, Na^+ and Ca^{2+} on oblique sample.

	Cl^- (µg cm^{-2})	NO_3^- (µg cm^{-2})	SO_4^{2-} (µg cm^{-2})	Na^+ (µg cm^{-2})	NH_4^+ (µg cm^{-2})	K^+ (µg cm^{-2})	Mg^{2+} (µg cm^{-2})	Ca^{2+} (µg cm^{-2})
PTNH12	31.28	6.22	2.63	13.71	0.75	13.95	3.96	14.47
PTNO15	14.81	4.59	1.55	12.13	0.71	0.69	3.60	9.88

Table 3.20 Soluble ions concentration per surface unit measured in material deposited on Verona Red Marble samples horizontally and obliquely exposed for 18 months in Ferrara.

After 24 months of exposure

After 24 months of exposure, ion chromatography was carried out on material deposited on horizontal, oblique and vertical samples exposed on the roof terrace and on oblique specimen located at window balcony (here indicated as O_W). In general, ion concentration detected after 24 months of exposure in all analysed samples was rather low (Figure 3.56). Moreover, comparing anions of all samples SO_4^{2-} of vertical sample stood out for higher value as well as Ca^{2+} prevailed over other cations, mainly on the horizontal specimen.

Concentrating upon each sample, SO_4^{2-} was slightly more abundant than NO_3^- and Cl^- on horizontal sample while among cations it was characterised by higher concentration of Ca^{2+} and lower amount of Na^+, NH_4^+, K^+ and Mg^{2+}.

Both oblique samples were characterised by low concentration of anions and cations, with slightly higher values on sample placed in the roof terrace (Figure 3.56). Only Ca^{2+} had a more considerable amount (6.48 ppm and 3.46 ppm on horizontal and oblique samples, respectively).

On vertical sample, SO_4^{2-} and Ca^{2+} prevailed over the other ions that displayed values below 1 ppm.

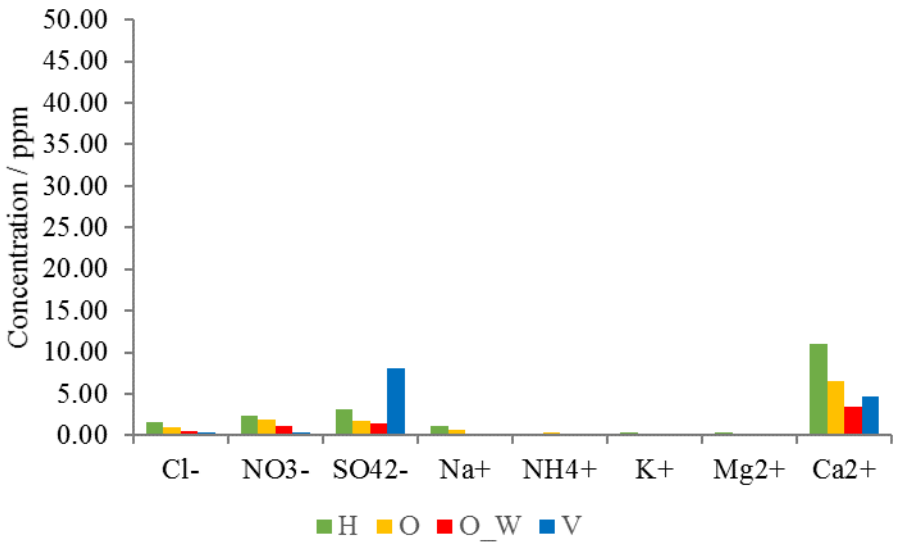

Figure 3.56 Soluble ions concentrations (ppm) measured in material accumulated on Verona Red Marble samples exposed for 24 months in Ferrara. Green, ochre and blue bars refer to samples horizontally, obliquely and vertically located on the roof terrace while red bars to specimen obliquely placed on window balcony.

Observing ion concentration per surface unit of all samples (Table 3.21), it is evident that in general SO_4^{2-} prevailed over the other anions, mainly on the vertical sample, while among cations Ca^{2+} displayed higher values mostly on the horizontal specimen while other cation amount was lower 1 µg cm^{-2} in all samples.

	Cl^- (µg cm^{-2})	NO_3^- (µg cm^{-2})	SO_4^{2-} (µg cm^{-2})	Na^+ (µg cm^{-2})	NH_4^+ (µg cm^{-2})	K^+ (µg cm^{-2})	Mg^{2+} (µg cm^{-2})	Ca^{2+} (µg cm^{-2})
PTNH13	1.07	1.69	2.16	0.76	<LOD	0.30	0.29	7.69
PTNO17	0.69	1.34	1.23	0.52	0.21	0.09	0.19	4.50
PTNO20 *	0.31	0.84	1.02	0.17	0.08	0.08	0.06	2.40
PTNV3	0.21	0.26	5.65	0.14	<LOD	0.06	0.05	3.27

*Table 3.21 Soluble ions concentrations per surface unit measured in material deposited on horizontal, oblique and vertical Verona Red Marble samples exposed for 24 months on the roof terrace in Ferrara. * refers to specimen obliquely placed on window balcony. <LOD means below the limit of detection.*

Comparison

Concentrating upon soluble anions concentration per surface unit measured in samples with different orientation and exposure time, Cl^- was the most abundant anion measured in horizontal and oblique samples till 18 months of exposure, ranging between 13.61 µg cm^{-2} and 31.28 µg cm^{-2}, with lower values measured on oblique samples (Figure 3.57). After a first general reduction at 12 moths of exposure, Cl^- concentration drastically decreased after 24 months of exposure in all samples.

Figure 3.57 shows also an increasing trend of NO_3^- amount after 12 months of exposure (reaching 11.83 µg cm^{-2}) followed by an incessant decrease in all samples of subsequent analysed periods. Among different orientation of exposure, horizontal samples showed higher concentration respect to the others.

Considering SO_4^{2-}, its concentration increased after 12 months and underwent a slight decrease after 18 months on both horizontal and oblique samples. Horizontal and oblique samples after 24 months displayed similar values to those measured on the related specimens exposed for 18 months. Furthermore, SO_4^{2-}

concentration measured on vertical sample after 24 months showed the highest value ever measured on Verona Red Marble specimens.

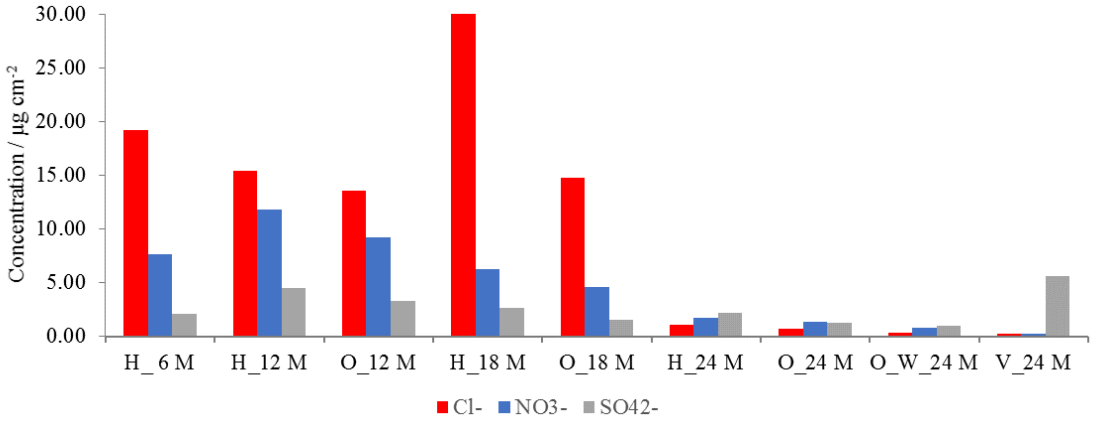

Figure 3.57 Concentration of soluble anions per surface unit (µg cm^{-2}) measured in material accumulated on horizontal (H), oblique (O) and vertical (V) Verona Red Marble samples remained exposed for 6, 12, 18 and 24 months in Ferrara. O_W refers to oblique sample exposed on window balcony.

The comparison of cation concentration per surface unit among all samples (Figure 3.58) shows abundant and rather similar values of Na^+ in all samples within 18 months of exposure (between 12.13 µg cm^{-2} and 15.14 µg cm^{-2}) while an evident drop in concentration happened after 24 months of exposure in samples with different orientation.

In general, Ca^{2+} was detected in rather high amount during all analysed period, with exception on horizontal sample exposed for 12 months (that was below limit of detection), reaching the highest value after 18 months of exposure for both horizontal and oblique samples.

Mg^{2+} displayed a rather constant amount (4.02 µg cm^{-2}) in all samples during the first 18 months of exposure while it decreased lower than 1.00 µg cm^{-2} in all samples measured after 24 months of exposure.

Concentrations of K^+ and NH_4^+ were always very low in all analysed specimens with different orientation, with exception of K^+ detected on horizontal sample exposed for 18 months (13.95 µg cm^{-2}).

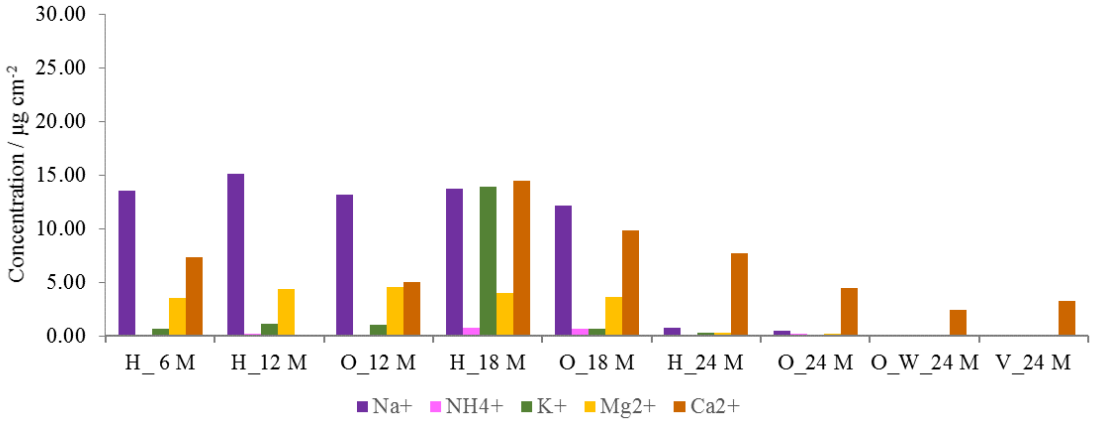

Figure 3.58 Concentration of soluble cations per surface unit (µg cm^{-2}) measured in material accumulated on horizontal (H), oblique (O) and vertical (V) Verona Red Marble samples remained exposed for 6, 12, 18 and 24 months in Ferrara. O_W refers to oblique sample exposed on window balcony.

FLORENCE

The amount of water-soluble ions (ppm) measured in material deposited on marble samples exposed in Florence at different exposure time is reported in Table A3.4 (Annex 3).

After 6 months of exposure

Ion concentration was measured on horizontal and oblique samples exposed in Florence for 6 months. Considering the analysis of material accumulated on horizontal sample (Figure 3.59), Cl^- was detected with higher concentration than the other anions. Among cations, Na^+ and Ca^{2+} were abounding while lower values of Mg^{2+}, K^+ and NH_4^+ were measured.

Ion chromatography performed on oblique sample shows an ion trend similar to that detected on horizontal samples but with always lower concentrations (Figure 3.59).

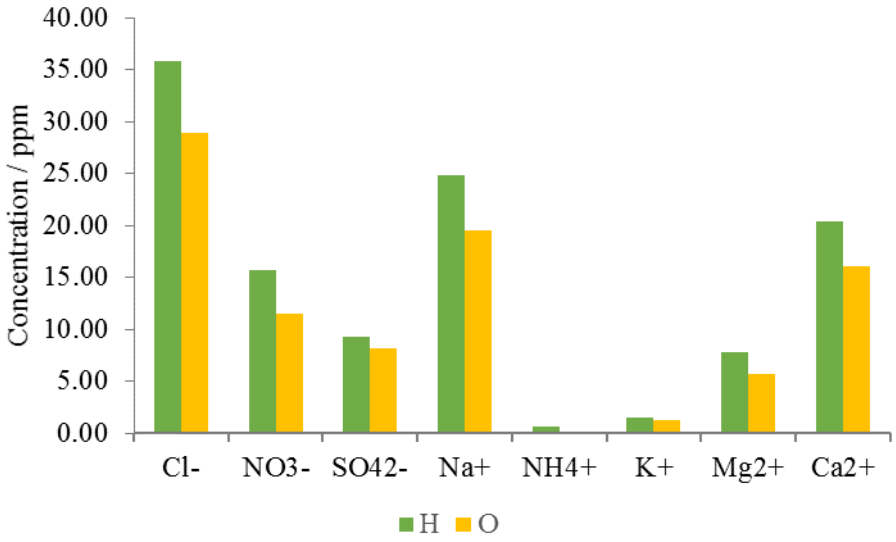

Figure 3.59 Soluble ions concentrations (ppm) measured in material accumulated on sample horizontally (green) and obliquely (ochre) exposed for 6 months in Florence.

Table 3.22 presents that concentration of different ions per unit surface of horizontal sample were higher than those detected on oblique samples but both samples were characterised by higher values of Cl^-, Na^+ and Ca^{2+}.

	Cl^- (µg cm^{-2})	NO_3^- (µg cm^{-2})	SO_4^{2-} (µg cm^{-2})	Na^+ (µg cm^{-2})	NH_4^+ (µg cm^{-2})	K^+ (µg cm^{-2})	Mg^{2+} (µg cm^{-2})	Ca^{2+} (µg cm^{-2})
SMCH2	24.91	10.91	6.46	17.27	0.46	1.05	5.43	14.12
SMCO2	20.07	7.98	5.69	13.52	<LOD	0.87	3.97	11.15

Table 3.22 Soluble ions concentrations per surface unit measured in material deposited on horizontal and oblique samples exposed for 6 months in Florence. <LOD means below the limit of detection.

After 12 months of exposure

Deposit material analysed on stone samples exposed for 12 months displays clear higher concentration of each ion on oblique sample than the horizontal one (Figure 3.60). In this regard, among anions 32.33 ppm of Cl^-, 13.99 ppm of NO_3^- and 14.65 ppm of SO_4^{2-} were measured on oblique sample respect to 14.78 ppm, 6.36

ppm and 5.71 ppm of the horizontal sample (Figure 3.60). Moreover, high concentration of Na^+ was detected (29.48 ppm and 11.81 ppm on horizontal and oblique samples, respectively) while the other cations concentration was lower (K^+ and Mg^{2+}) or below limit of detection in both samples (NH_4^+ and Ca^{2+}).

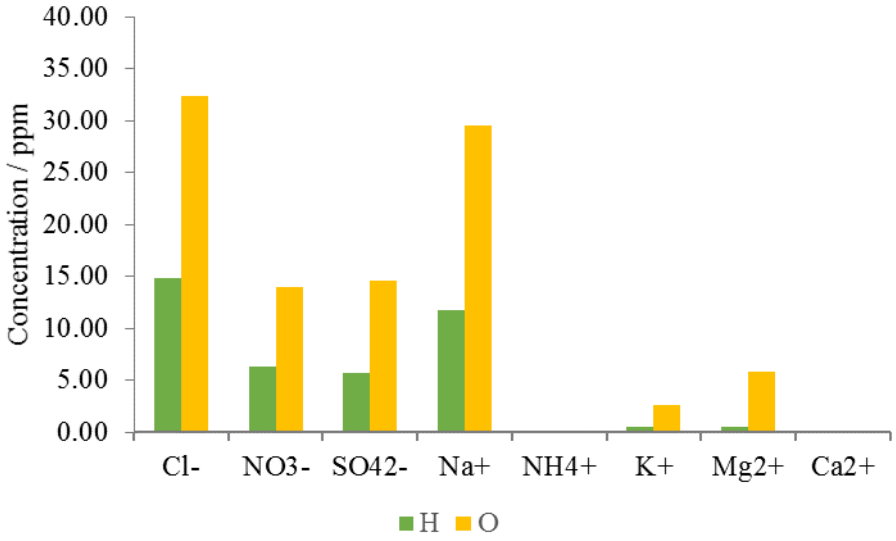

Figure 3.60 Soluble ions concentrations (ppm) measured in material accumulated on sample horizontally (green) and obliquely (ochre) exposed for 12 months in Florence.

Ion concentration per surface unit of all samples (Table 3.23) displays in general higher values of all ions on oblique sample with exception for NH_4^+ and Ca^{2+}, whose values of both specimens were lower limit of detection. Furthermore, the prevalence of Cl^- and Na^+ is evident in both samples.

	Cl^- (µg cm^{-2})	NO_3^- (µg cm^{-2})	SO_4^{2-} (µg cm^{-2})	Na^+ (µg cm^{-2})	NH_4^+ (µg cm^{-2})	K^+ (µg cm^{-2})	Mg^{2+} (µg cm^{-2})	Ca^{2+} (µg cm^{-2})
SMCH3	10.27	4.41	3.97	8.20	<LOD	0.40	0.34	<LOD
SMCO3	22.45	9.71	10.17	20.47	<LOD	1.82	4.08	<LOD

Table 3.23 Soluble ions concentrations per surface unit measured in material deposited on horizontal and oblique samples exposed for 12 months in Florence. <LOD means below the limit of detection.

After 18 months of exposure

Anions concentrations measured on horizontal sample exposed for 18 months were characterised by higher values of Cl^- followed by SO_4^{2-} and NO_3^- while among cations Na^+ and Ca^{2+} prevailed over the other cations (Figure 3.61).

Furthermore, the concentrations of ions detected on oblique sample were really close to those obtained from horizontal sample, with exception of Ca^{2+} that was higher on oblique specimen (Figure 3.61).

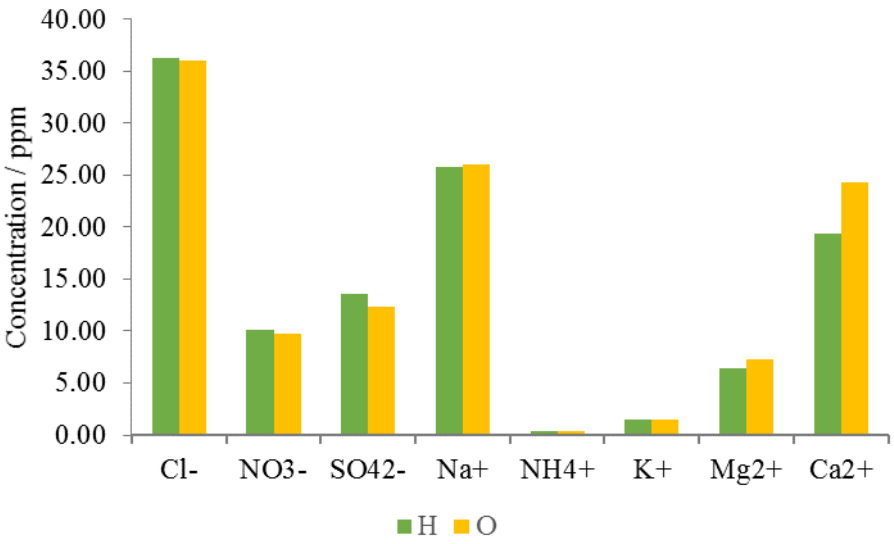

Figure 3.61 Soluble ions concentrations (ppm) measured in material accumulated on sample horizontally (green) and obliquely (ochre) exposed for 18 months in Florence.

Ion concentration per surface unit of all samples (Table 3.24) displays in general similar values of ions on both samples with exception for Ca^{2+}, that was higher on oblique sample. Additionally, the prevalence of Cl^-, Na^+ and Ca^{2+} is perceptible in both samples.

	Cl^- ($\mu g\ cm^{-2}$)	NO_3^- ($\mu g\ cm^{-2}$)	SO_4^{2-} ($\mu g\ cm^{-2}$)	Na^+ ($\mu g\ cm^{-2}$)	NH_4^+ ($\mu g\ cm^{-2}$)	K^+ ($\mu g\ cm^{-2}$)	Mg^{2+} ($\mu g\ cm^{-2}$)	Ca^{2+} ($\mu g\ cm^{-2}$)
SMCH6	25.22	7.07	9.42	17.91	0.25	1.07	4.50	13.43
SMCO6	24.98	6.81	8.55	18.04	0.28	1.01	5.05	16.92

Table 3.24 Soluble ions concentrations per surface unit measured in material deposited on horizontal and oblique samples exposed for 18 months in Florence.

After 24 months of exposure

After 24 months of exposure, ion chromatography was carried out on the material deposited on horizontal, oblique and vertical sample. In general, SO_4^{2-} prevailed over the other anions, showing higher value on oblique sample (15.98 ppm) than horizontal (13.82 ppm) and vertical (8.73 ppm) ones. Concentration of Cl^- and NO_3^- were similar on horizontal (6.04 ppm and 5.37 ppm) and oblique (4.26 ppm and 4.27 ppm) samples while lower values were measured on vertical sample (0.83 ppm and 2.44 ppm) (Figure 3.62).

Among cations, Ca^{2+} overcame in all samples, with higher value on oblique specimen (22.84 ppm) respect to horizontal (15.92 ppm) and vertical (6.34 ppm) ones (Figure 3.62). Moreover, Na^+ was appreciable for oblique (3.31 ppm) and horizontal (3.23 ppm) specimens while it was low on vertical sample (0.49 ppm). Finally, the other measured cations were negligible for all samples.

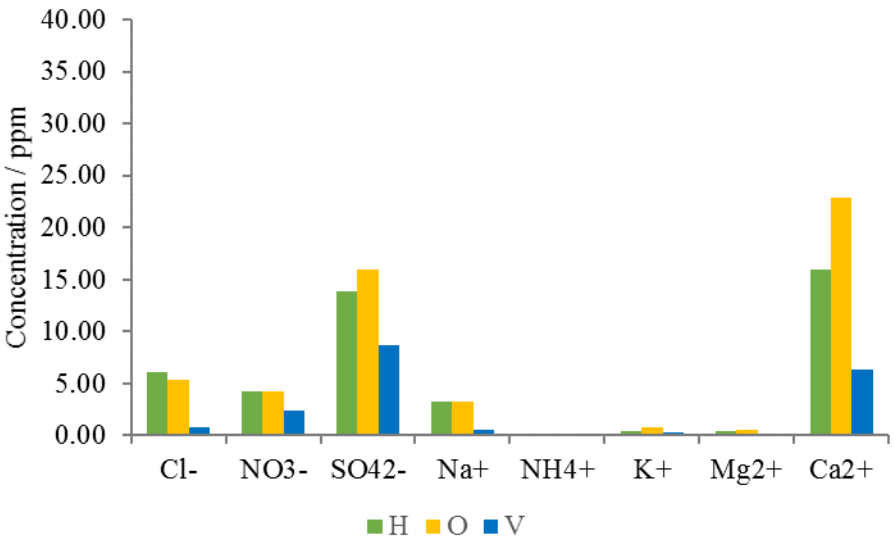

Figure 3.62 Soluble ions concentrations (ppm) measured in material accumulated on sample horizontally (green), obliquely (ochre) and vertically (blue) exposed for 24 months in Ferrara.

Comparing ion concentration per surface unit (Table 3.25), each sample was characterised by the prevalence of SO_4^{2-} and Ca^{2+} among other ions and in particular, more abundant values were detected on oblique specimen.

	Cl^- (µg cm^{-2})	NO_3^- (µg cm^{-2})	SO_4^{2-} (µg cm^{-2})	Na^+ (µg cm^{-2})	NH_4^+ (µg cm^{-2})	K^+ (µg cm^{-2})	Mg^{2+} (µg cm^{-2})	Ca^{2+} (µg cm^{-2})
SMCH7	4.19	2.96	9.60	2.24	0.16	0.28	0.26	11.06
SMCO7	3.73	2.96	11.10	2.30	0.02	0.58	0.37	15.86
SMCV3	0.58	1.70	6.07	0.34	<LOD	0.24	0.06	4.41

Table 3.25 Soluble ions concentrations per surface unit measured in material deposited on horizontal, oblique and vertical samples exposed for 24 months in Florence. <LOD means below the limit of detection.

Comparison

Comparing anions concentration per surface unit detected in all specimens at different exposure time (Figure 3.63), high values of Cl^- were measured in all samples within 18 months of exposure (with values between 10.27 µg cm^{-2} and 25.22 µg cm^{-2}) while a decrease happened on all samples remained exposed for 24 months.

NO_3^-, ranging between 1.70 µg cm^{-2} and 10.91 µg cm^{-2} considering all samples, showed the highest value for horizontal sample after 6 months of exposure (10.91 µg cm^{-2}) and for oblique sample after 12 months 9.71 µg cm^{-2} while lower values were measured after 24 months of exposure in all samples.

SO_4^{2-} showed concentration rather constant over time (with values between 3.97 µg cm^{-2} and 11.10 µg cm^{-2}), slightly higher on oblique samples after 12 and 24 months of exposure.

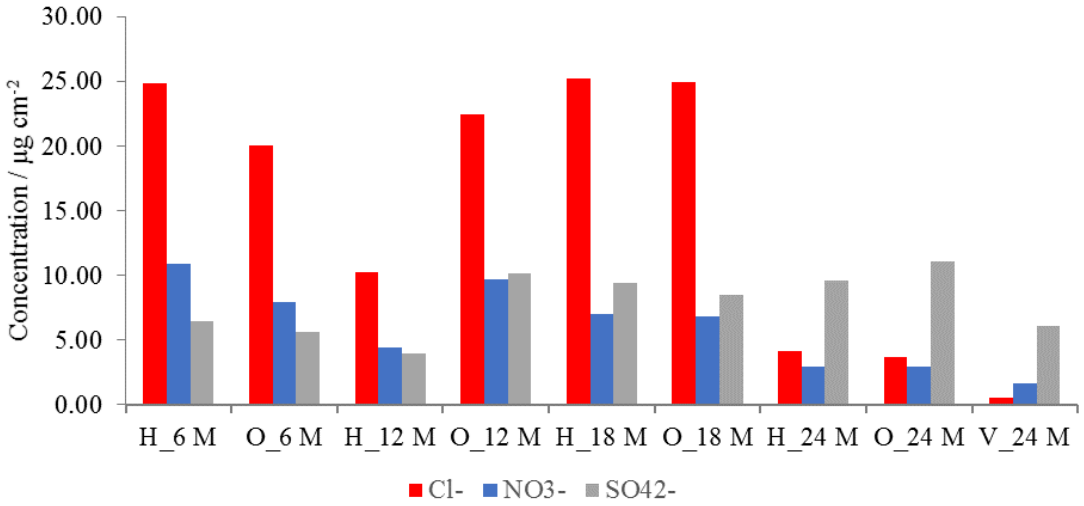

Figure 3.63 Concentration of soluble anions per surface unit (µg cm^{-2}) measured in material accumulated on horizontal (H), oblique (O) and vertical (V) samples remained exposed for 6, 12, 18 and 24 months in Florence.

Among cations, Na^+ and Ca^{2+} prevailed over time in all samples (Figure 3.64). In particular, Na^+ was more abundant within first 18 months of exposure both in horizontal and oblique samples while Ca^{2+} was detected all over the period (between 4.41 µg cm^{-2} and 16.92 µg cm^{-2}) with exception of measurement after 12 months (<LOD). Moreover, Ca^{2+} displayed higher values on oblique samples than horizontal one during last 2 examined periods.

Mg^{2+} remained in general rather constant in all samples (median value of 4.29 µg cm^{-2}) within 18 months of exposure while it diminished in all samples after 24 months of exposure.

Finally, NH_4^+ and K^+ concentrations were negligible over time because they remained below 2.00 µg cm^{-2} (K^+) or 1.00 µg cm^{-2} (NH_4^+) in all samples.

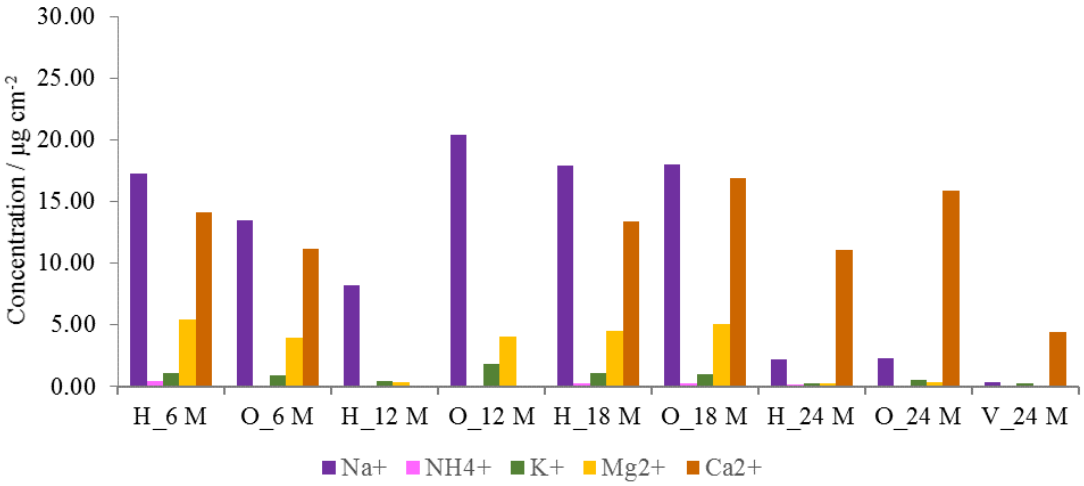

Figure 3.64 Concentration of soluble cations per surface unit (µg cm^{-2}) measured in material accumulated on horizontal (H), oblique (O) and vertical (V) samples remained exposed for 6, 12, 18 and 24 months in Florence.

GENERAL COMPARISON

Concentring upon amount of anions measured per surface unit on all horizontal Carrara Marble samples (Figure 3.65 A), Cl^- was more abundant than NO_3^- and SO_4^{2-} in all sites within 18 months of exposure, with slight decrease after 12 months of exposure, while its concentration underwent a clear drop after 24 months of exposure. Concentration of NO_3^- was in general rather constant in all site and exposure time, with lower values after 24 months of exposure. Moreover, SO_4^{2-} presented lower concentration than NO_3^- within 12 months of exposure while then it exceeded values of NO_3^- (after 18 months) and also Cl^- (after 24 months of exposure) in all exposure sites. In general, Ferrara and Florence showed higher values of SO_4^{2-} than Bologna.
Among cations (Figure 3.65 B), Na^+ prevailed over the other cations within 18 months of exposure in all sites. Also Ca^{2+} was detected in considerable amount in all exposure sites and periods with exception of samples analysed after 12 months of exposure, whose values were below the detection limit. Considering ion chromatography results after 6 and 24 months of exposure, Ca^{2+} amount gradually increased passing from Bologna to Ferrara and Florence while more similar values in all sites were measured after 18 months of exposure.
Furthermore, amount of Mg^{2+} proved to be almost constant within 18 months of exposure while it visibly decreased after 24 months of exposure. Small quantity of K^+ and much lower of NH_4^+ was assessed in all sites over time.

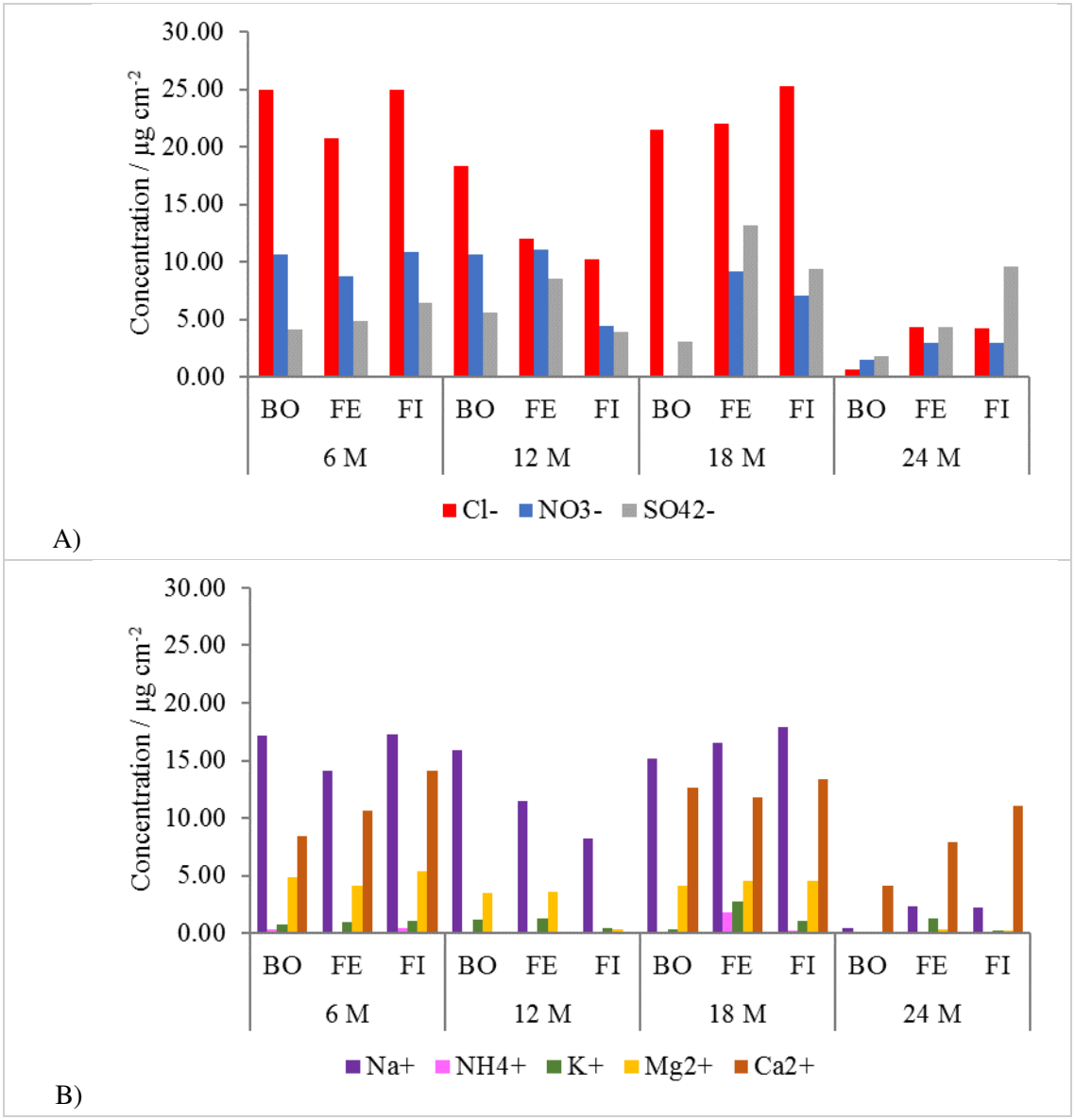

Figure 3.65 Concentration of anions (A) and cations (B) per surface unit measured on the exposed surface of Carrara Marble stone samples horizontally exposed in Bologna (BO), Ferrara (FE) and Florence (FI) for 6, 12, 18 and 24 months.

Figure 3.66 compare ion concentration per surface unit measured on oblique Carrara Marble specimens in all sites at different exposure time. Given that ion chromatography of oblique samples after 6 months of exposure was performed only on samples exposed in Florence, also for oblique specimens Cl^- displayed higher values than NO_3^- and SO_4^{2-} in all sites within 18 months of exposure, while its general decrease was measured after 24 months of exposure (Figure 3.66 A).

Concentration of NO_3^- was in general rather constant in all site and exposure time, with lower values after 24 months of exposure. Moreover, SO_4^{2-} was in general lower than the amount of NO_3^- within 12 months of exposure (excepted sample exposed in Florence for 12 months) while it exceeded values of NO_3^- (after 18 months) and also Cl^- (after 24 months of exposure) in all exposure sites. In general, Ferrara and Florence showed higher values of SO_4^{2-} than Bologna.

Focusing on cations (Figure 3.66 B), Na^+ prevailed over the other cations within 18 months of exposure in all site while after 24 months the most abounding cation was Ca^{2+}. Moreover, Ca^{2+} was detected in considerable quantity in all exposure sites and periods with exception of samples analysed after 12 months of exposure. Ca^{2+} amount was higher on samples exposed in Florence, followed by Ferrara, than those placed in Bologna.

Furthermore, amount of Mg^{2+} was almost constant within 18 months of exposure while it clearly decreased after 24 months of exposure. Finally, all sites had few concentration of K^+ and negligible amount of NH_4^+ over time.
As already written, concentration of all ions measured on sample exposed on the roof terrace was higher than that measured on sample located on the window balcony.

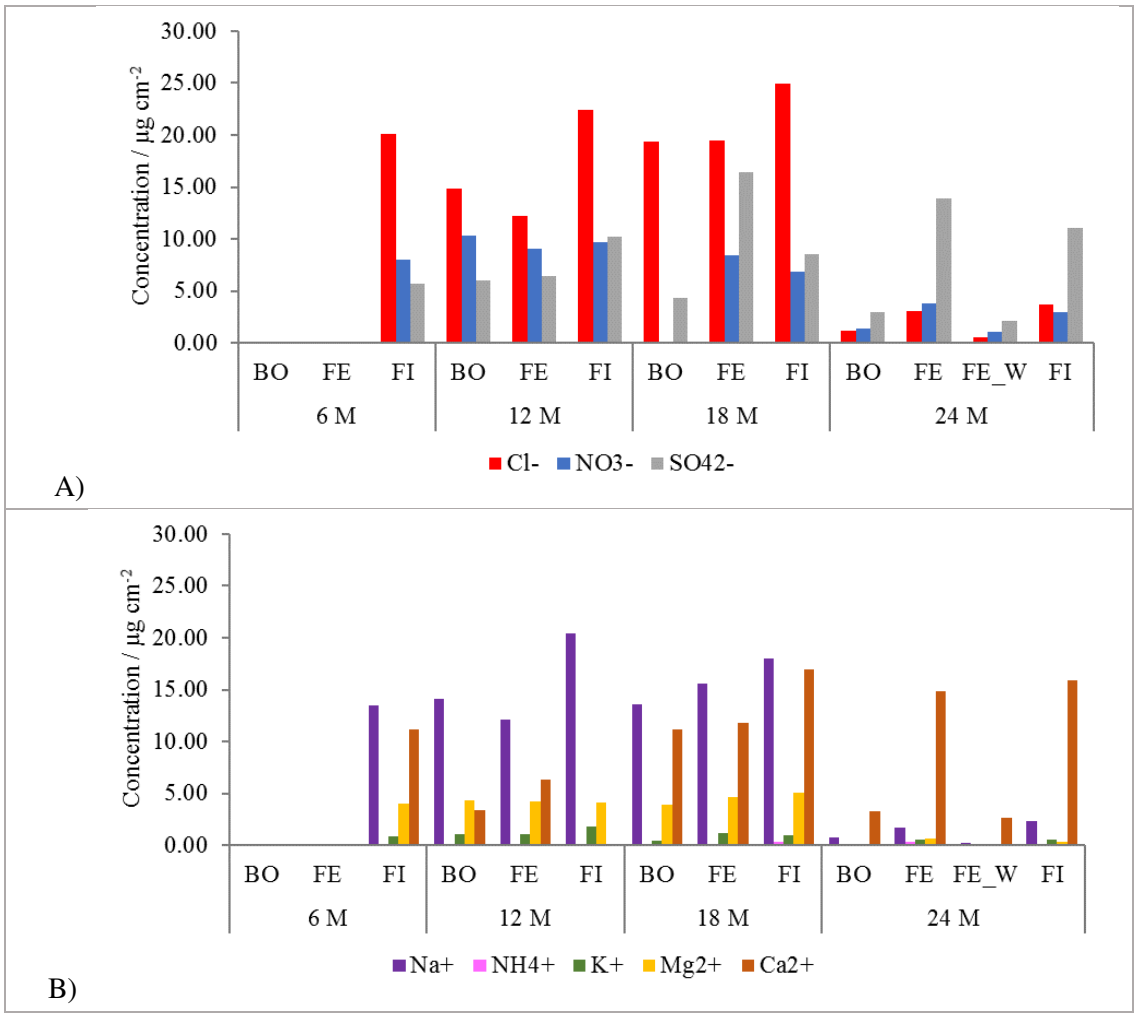

Figure 3.66 Concentration of anions (A) and cations (B) per surface unit measured on the exposed surface of Carrara Marble stone samples obliquely exposed in Bologna (BO), Ferrara (FE) and Florence (FI) for 6, 12, 18 and 24 months. Fe_W refers to oblique sample exposed on window balcony in Ferrara for 24 months.

Finally, concentrations of ions measured on vertical specimens after 24 months of exposure were very low in all samples (Figure 3.67). In particular, values of all ions measured on sample exposed in Bologna were close to 0.00 µg cm^{-2} while SO_4^{2-} and Ca^{2+} were slightly higher detected in samples located in Florence than those exposed in Ferrara.

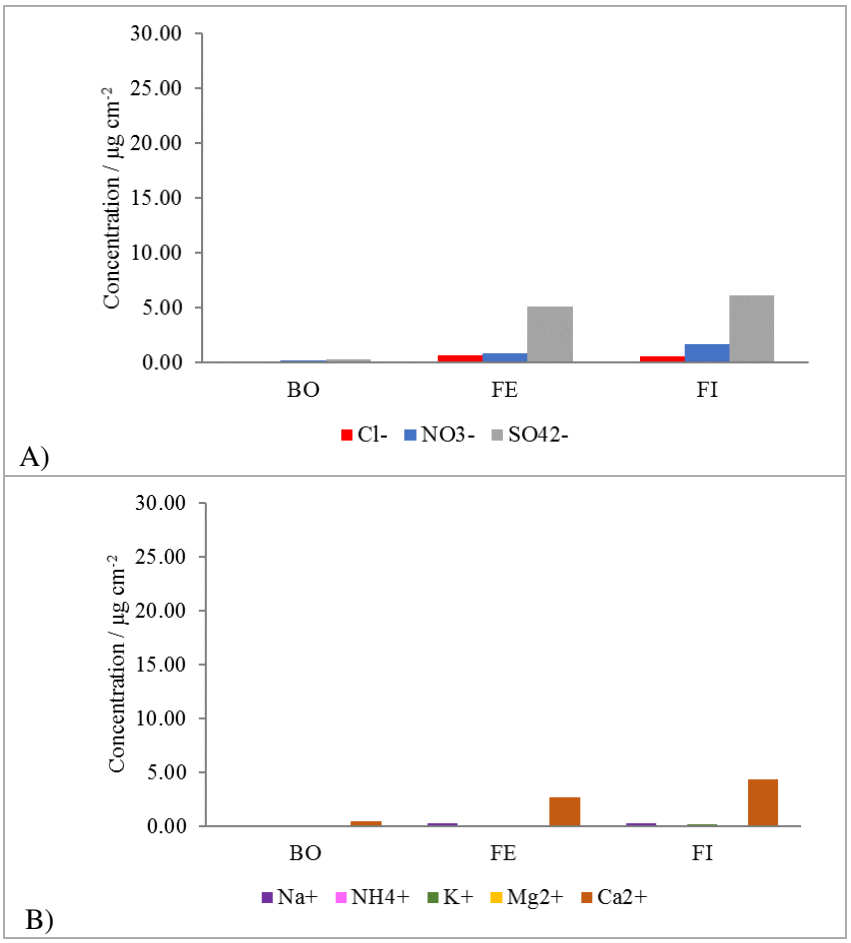

Figure 3.67 Concentration of anions (A) and cations (B) per surface unit measured on the exposed surface of Carrara Marble stone samples vertically exposed in Bologna (BO), Ferrara (FE) and Florence (FI) for 24 months.

The comparison of anions measured on horizontal samples of different lithotypes exposed in the same location shows in general the prevalence of Cl^- over NO_3^- and SO_4^{2-} in both kind of stones during each analysed period, with exception of Carrara Marble samples after 24 months of exposure where SO_4^{2-} reached concentration similar to Cl^- (Figure 3.68 A). In particular, Cl^- of Carrara Marble sample was slightly more abounding than that assessed on Verona Red Marble specimens after 6 and 24 months of exposure while the contrary happened after 12 and 18 months of exposure. Moreover, the amount of NO_3^- was similar on samples of both lithotypes, with slightly higher values on the marble than the limestone. Finally, amount of SO_4^{2-} measured on Carrara Marble was double that detected on Verona Red Marble during the considered periods, reaching even 5 times higher concentration after 18 months of exposure.

Comparing cations concentration measured on both lithotypes (Figure 3.68 B), Na^+ prevailed over the other cations within 18 months of exposure for both Carrara Marble and Verona Red Marble samples. In particular, analysis on the marble revealed slightly higher amount of Na^+ after 6, 18 and 24 months respect to the limestone.

Ca^{2+} was generally rather abundant in both kind of samples, with exception after 12 months of exposure that reached values below limit of detection. However, the reciprocal correlation of its concentration measured on both kinds of stone changed over time because Ca^{2+} was higher on marble sample after 6 months of exposure, below on marble specimen after 18 months of exposure and similar on both lithotypes after 24 months.

Mg^{2+} displayed similar values on both stones over time as well as also K^+ with exception of the considerable value detected in limestone after 18 months of exposure. Finally, NH_4^+ was always very low in both lithotypes during different exposure time.

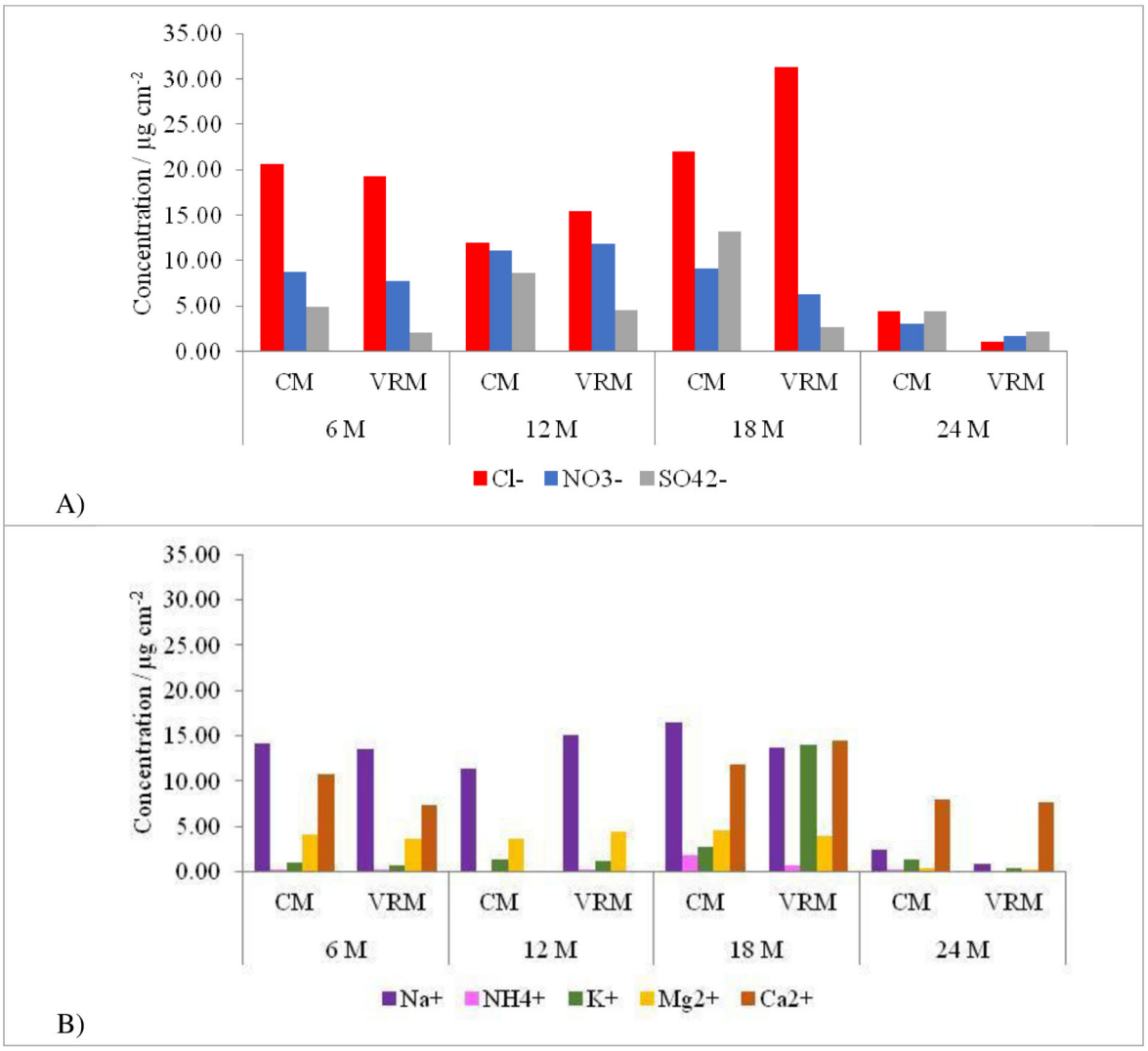

Figure 3.68 Concentration of anions (A) and cations (B) per surface unit measured on the exposed surface of Carrara Marble (CM) and Verona Red Marble (VRM) stone samples horizontally exposed in Ferrara for 6, 12, 18 and 24 months.

The trend of anions concentration per surface unit of Carrara Marble and Verona Red Marble samples obliquely exposed in Ferrara for different time (Figure 3.69 A) was similar to that detected for the same kind specimens horizontally exposed (Figure 3.68 A), with the prevalence of Cl^- over NO_3^- and SO_4^{2-} in both kind of stones after 12 and 18 months of exposure. Nevertheless, marble sample analysed after 18 months of exposure displayed a much higher concentration of SO_4^{2-} than that measured on limestone specimen as well as a more abounding amount of SO_4^{2-} was measured on Carrara Marble sample exposed for 24 months on the roof terrace than the other marble and limestones samples exposed both on the terrace and on window balcony (Figure 3.69 A). In particular, in this last case the concentration of SO_4^{2-} exceeded also the amount of the other anions.

Na^+ was the most abundant cation measured on oblique marble and limestone after 12 and 18 moths of exposure (Figure 3.69 B). Also Ca^{2+} was abundant in both lithotypes, slightly higher on the Carrara Marble samples after 12 and 18 months of exposure. This difference became more substantial after 24 months of exposure when Ca^{2+} concentration, higher than that of the other cations, reached the highest value ever

reached in Ferrara among marble and limestone samples. Moreover, the concentration of Mg^{2+}, K^{+} and NH_4^{+} remained individually constant after 12 and 18 months of exposure with similar values in both lithotypes (around 4 µg cm^{-2}, about 1 µg cm^{-2} and below 1 µg cm^{-2}, respectively) while it decreased close to zero after 24 months of exposure.

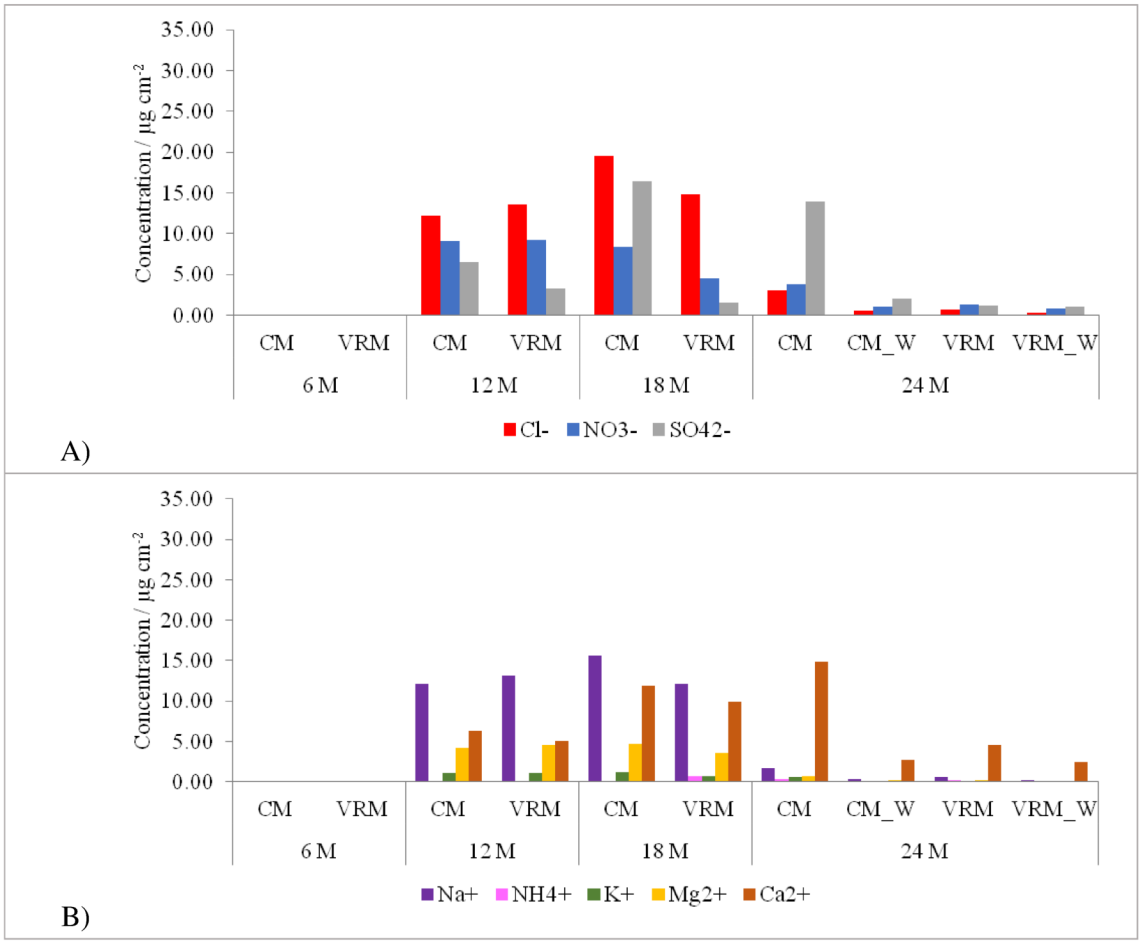

Figure 3.69 Concentration of anions (A) and cations (B) per surface unit measured on the exposed surface of Carrara Marble (CM) and Verona Red Marble (VRM) stone samples obliquely exposed in Ferrara for 6, 12, 18 and 24 months. CM_W and VRM_W refer to oblique sample exposed on window balcony in Ferrara for 24 months.

Ion amount detected on samples vertically exposed for 24 months resulted very low independently from the kind of stone (Figure 3.70). In particular, small concentration of SO_4^{2-} and Ca^{2+} were detected on both lithotypes, suggesting the possible presence of underway sulphation process.

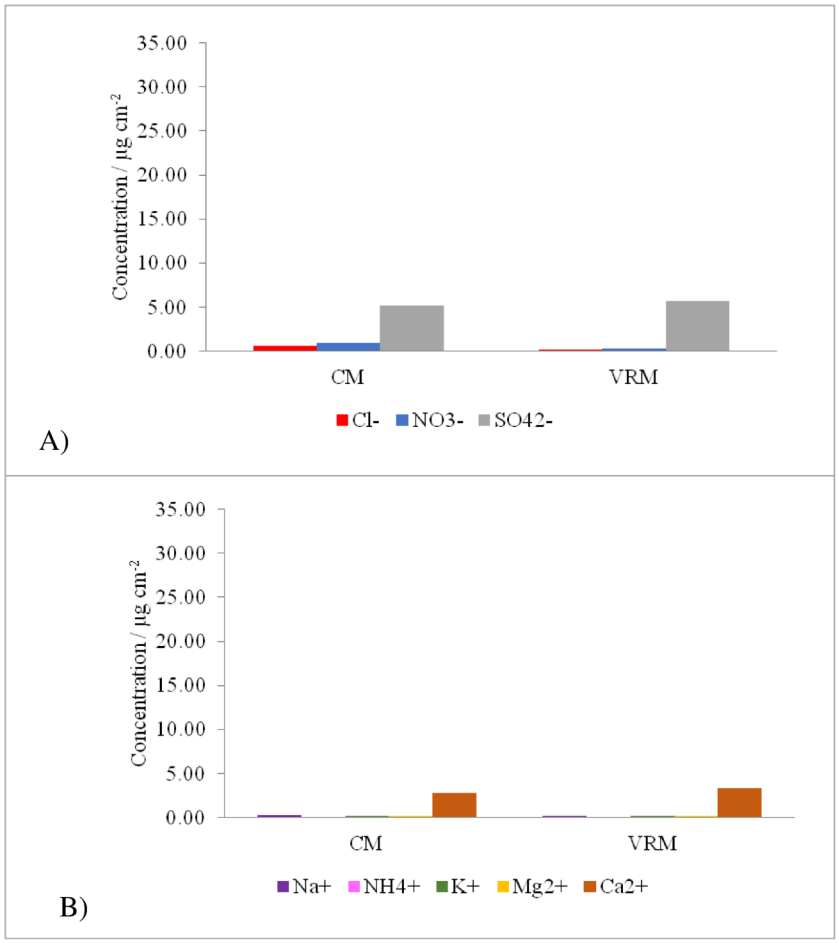

Figure 3.70 Concentration of anions (A) and cations (B) per surface unit measured on the exposed surface of Carrara Marble (CM) and Verona Red Marble (VRM) stone samples vertically exposed in Ferrara for 24 months.

Final remarks:

- Concentrating upon Carrara Marble samples, the amount of Cl^- measured per surface unit prevailed over the other anions (up to 25.22 µg cm^{-2}) in horizontal and oblique samples in all sites within 18 months of exposure. Besides a general reduction of ion concentration after 24 months in all sites, SO_4^{2-} was more abundant than the other anions, suggesting an ongoing sulphation process, with general higher values in Ferrara (till 13.94 µg cm^{-2}) and Florence (up to 9.60 µg cm^{-2}). Among cations, significant concentration per surface unit of Na^+, followed by Ca^{2+}, were detected in samples exposed in all sites within 18 months while Ca^{2+} prevailed over the other cations after 24 months of exposure.
- Ion chromatography performed on vertical marble specimens after 24 months of exposure showed lower ion concentration than the corresponding horizontal and oblique specimens. In particular, values of all ions measured on sample exposed in Bologna were close to 0.00 µg cm^{-2} while the concentration per surface unit of SO_4^{2-} and Ca^{2+} was slightly higher in samples located in Florence than those exposed in Ferrara.
- Soluble ions detected in material accumulated on Verona Red Marble showed a trend similar to that observed in marble samples exposed in the same site (i.e. Ferrara), characterised in general by the prevalence of Cl^-, Na^+ and Ca^{2+} within 18 months of exposure. In addition to a common reduction of ion amount, material deposited on limestone samples analysed after 24 months of exposure was dominated by SO_4^{2-} and Ca^{2+}, likely indicating an ongoing sulphation process. In particular, the concentration of SO_4^{2-} was much higher on marble samples than on limestone ones, suggesting a higher reactivity of marble to sulphation process.
- The sources of major soluble ions detected on the surface of stone samples could be attributed to marine origin and de-icing salts (Cl^-, SO_4^{2-}, Na^+ and Ca^{2+}), resuspended dust (mainly Ca^{2+}) and vehicular traffic beside industry (SO_4^{2-} and NO_3^-).

3.1.5. CARBON SPECIATION AND RELATED ISOTOPIC ANALYSIS

Quantification of carbon fractions and the related isotopic ratio were performed on material deposited on exposed surface of stone specimens in order to assess the different carbon components and achieve information about their possible emission sources.
The analysis was carried out by thermally-based separation every 6 months on the material mechanically removed from the whole exposed surface of a sample from each exposure site and for each orientation, whenever a suitable amount of particulate was observed on specimens surface (cf. subchapter 2.1.2). Unfortunately, no data about carbon fractions of stone slabs vertically exposed are available because the quantity of the material deposited on them was always insufficient to be analysed by EA-IRMS. The complete list of investigated samples is reported in Table 3.5.

<u>BOLOGNA</u>

The amount of carbon fractions measured as weight percent of material accumulated on marble samples exposed in Bologna at different exposure time is reported in Table A4.1 (Annex 4).

After 6 months of exposure
Investigation about carbon content was performed only on specimen horizontally exposed. The deposited matter resulted to be composed by 14.70 wt% of total carbon, characterised by a slight predominance of NCC (8.55 wt%) over CC (6.15 wt%) (Figure 3.71). Specifically, the non-carbonate fraction was constituted by 7.38 wt% of OC and 1.17 wt% of EC with a OC/EC ratio of 6. Calculating the different carbon portions as percentage of TC, OC represents half of TC while CC is 42 % and EC 8 %. Moreover, knowledge about the quantity of each carbon fraction deposited per unit of surface on sample ($C_{surface}$) can provide further information about the possible deterioration of a stone surface exposed outdoor (Figure 3.71).

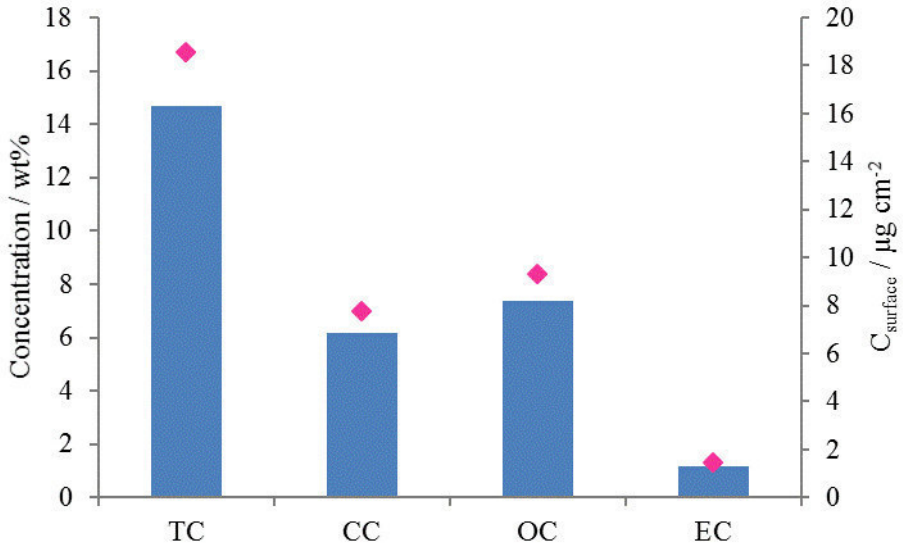

Figure 3.71 Blue bars indicate TC, CC, OC and EC concentrations weighted in powder deposit collected from sample horizontally exposed for 6 months in Bologna while pink rhombuses represent the amount of each carbon fraction per surface unit of the same sample.

Finally, the measured ($\delta^{13}C_{TC}$, $\delta^{13}C_{CC}$ and $\delta^{13}C_{OC}$) and calculate ($\delta^{13}C_{EC}$) isotopic ratios were respectively -14.7 ‰, 0.9 ‰, -25.48 ‰ and -28.7 ‰ (Table 3.26).

	$TC_{surface}$ ($\mu g\ cm^{-2}$)	$CC_{surface}$ ($\mu g\ cm^{-2}$)	$OC_{surface}$ ($\mu g\ cm^{-2}$)	$EC_{surface}$ ($\mu g\ cm^{-2}$)	$\delta^{13}C_{TC}$ (‰)	$\delta^{13}C_{CC}$ (‰)	$\delta^{13}C_{OC}$ (‰)	$\delta^{13}C_{EC}$ (‰)	OC/EC
BCH10	18.58	7.77	9.33	1.48	-14.7	0.9	-25.5	-28.7	6

Table 3.26 Information related to carbon fractions (carbon fractions measured as weight per surface unit, isotopic ratios and OC/EC) of horizontal Carrara Marble sample after 6 months of exposure in Bologna.

After 12 months of exposure

The exposure outdoor of samples for 12 months in Bologna led the analysis of carbon fractions of the particulate matter deposited on both horizontal and oblique specimens. Figure 3.72 shows a slightly higher concentration of TC in horizontal sample (16.61 wt%) than in tilted one (15.93 wt%). In particular, CC of the material collected from horizontal and oblique samples (6.03 wt% and 5.43 wt%) accounted respectively for 36 % and 34 % of TC while NCC prevailed (10.58 wt% and 10.50 wt%). Furthermore, OC was detected in higher amount than EC in both samples, displaying a OC/EC ratio of 2 and 15 for horizontal and oblique samples, respectively (Table 3.27). Considering the different samples orientation, TC, CC and EC were more concentrated in horizontal specimen while OC prevailed in oblique sample (9.83 wt% respect to 7.54 wt% of horizontal sample) (Figure 3.72).

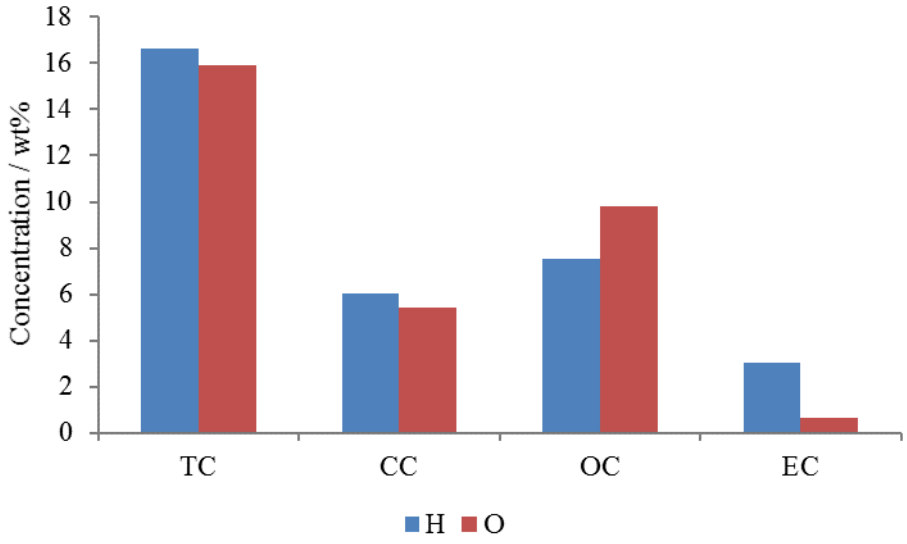

Figure 3.72 TC, CC, OC and EC concentrations detected in powder deposit collected from samples horizontally (blue) and obliquely (red) exposed for 12 months in Bologna.

Moreover, similar $\delta^{13}C$ values for each carbon fraction were assessed in both samples (see Table 3.27). The same table displays also the amount of each carbon portion accumulated per surface unit of stone ($C_{surface}$) (Table 3.27).

	$TC_{surface}$ ($\mu g\ cm^{-2}$)	$CC_{surface}$ ($\mu g\ cm^{-2}$)	$OC_{surface}$ ($\mu g\ cm^{-2}$)	$EC_{surface}$ ($\mu g\ cm^{-2}$)	$\delta^{13}C_{TC}$ (‰)	$\delta^{13}C_{CC}$ (‰)	$\delta^{13}C_{OC}$ (‰)	$\delta^{13}C_{EC}$ (‰)	OC/EC
BCH12	37.15	13.49	16.87	6.79	-16.3	0.7	-25.3	-27.7	2
BCO2	32.74	11.17	20.20	1.37	-16.8	0.1	-25.5	-26.5	15

Table 3.27 Information related to carbon fractions (carbon fractions measured as weight per surface unit, isotopic ratios and OC/EC) of horizontal and oblique Carrara Marble samples after 12 months of exposure in Bologna.

After 18 months of exposure

The material accumulated on horizontal sample resulted to be composed by 14.64 wt% of TC, 7.08 wt% of CC and 7.57 wt% of NCC (Figure 3.73). The latter was characterised by the prevalence of OC (5.74 wt%) over EC (1.82 wt%). Therefore, considering the percentage of each carbon fraction related to TC, CC (48 %) slightly prevailed over OC (39 %) and EC (12 %). The analysis of material deposited on the sample obliquely exposed showed a concentration of TC (14.25 wt%) similar to that measured on horizontal sample (Figure 3.73) but with a clear prevalence of NNC (8.42 wt%) over CC (5.82 wt%). In particular, OC (7.57 wt%) was much higher than EC (0.85 wt%) and they corresponded to 53 % and 6 % of TC respect to 41 % of CC.

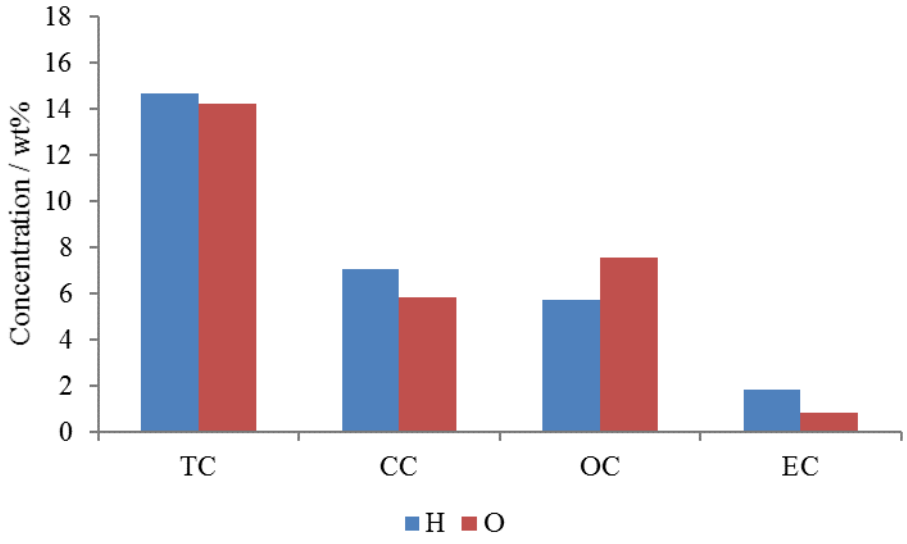

Figure 3.73 TC, CC, OC and EC concentrations detected in powder deposit collected from samples horizontally (blue) and obliquely (red) exposed for 18 months in Bologna.

Furthermore, $\delta^{13}C$ of both samples were similar with positive values for $\delta^{13}C_{CC}$ while more negative for $\delta^{13}C_{OC}$ and $\delta^{13}C_{EC}$ (Table 3.28).

Finally, the calculated amount of each carbon fraction per surface unit highlighted higher values for oblique sample than for horizontal one of all C portions (Table 3.28) because the quantity of material deposited on oblique specimen (20.1 mg) was much higher that of horizontal sample (9.3 mg).

	$TC_{surface}$ ($\mu g\ cm^{-2}$)	$CC_{surface}$ ($\mu g\ cm^{-2}$)	$OC_{surface}$ ($\mu g\ cm^{-2}$)	$EC_{surface}$ ($\mu g\ cm^{-2}$)	$\delta^{13}C_{TC}$ (‰)	$\delta^{13}C_{CC}$ (‰)	$\delta^{13}C_{OC}$ (‰)	$\delta^{13}C_{EC}$ (‰)	OC/EC
BCH8	9.46	4.57	3.71	1.18	-13.4	1.1	-25.8	-30.8	3
BCO10	19.89	8.13	10.57	1.19	-14.8	0.9	-25.6	-25.3	9

Table 3.28 Information related to carbon fractions (carbon fractions measured as weight per surface unit, isotopic ratios and OC/EC) of horizontal and oblique Carrara Marble samples after 18 months of exposure in Bologna.

After 24 months of exposure

The material accumulated on horizontal sample resulted to be composed by 12.73 wt% of TC, 6.58 wt% of CC and 6.16 wt% of NCC (Figure 3.74). However, the small amount of collected particulate matter was not enough for analyse the concentration of OC and EC. Higher concentration of TC (21.10 wt%) was detected in deposit of oblique sample (Table 3.29 and Figure 3.74). In particular, OC represented 49 % of TC followed by EC (33 %) and CC (19 %).

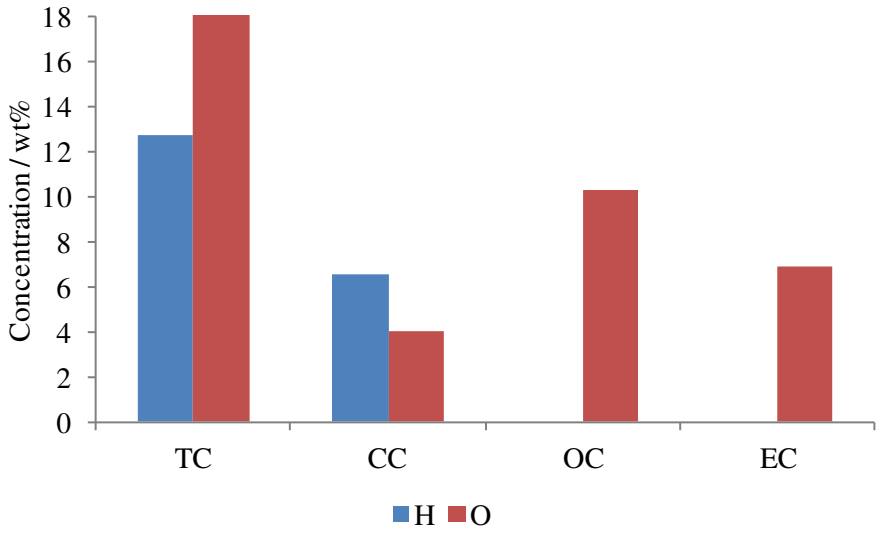

Figure 3.74 TC, CC, OC and EC concentrations detected in powder deposit collected from samples horizontally (blue) and obliquely (red) exposed for 24 months in Bologna.

TC isotopic ratio of oblique sample was more negative than that measured in the horizontal one (Table 3.29).

	$TC_{surface}$ ($\mu g\ cm^{-2}$)	$CC_{surface}$ ($\mu g\ cm^{-2}$)	$OC_{surface}$ ($\mu g\ cm^{-2}$)	$EC_{surface}$ ($\mu g\ cm^{-2}$)	$\delta^{13}C_{TC}$ (‰)	$\delta^{13}C_{CC}$ (‰)	$\delta^{13}C_{OC}$ (‰)	$\delta^{13}C_{EC}$ (‰)	OC/EC
BCH14	21.67	11.19	n.d.	n.d.	-12.7	1.6	n.d.	n.d.	n.d.
BCO5	20.00	3.78	9.72	6.50	-21.6	1.1	-26.1	-28.0	1

Table 3.29 Information related to carbon fractions (carbon fractions measured as weight per surface unit, isotopic ratios and OC/EC) of horizontal and oblique Carrara Marble samples after 24 months of exposure in Bologna. n.d. stands for not detected.

Considering carbon fraction per surface unit (Table 3.29), $TC_{surface}$ was slightly higher in horizontal sample (21.67 $\mu g\ cm^{-2}$) than in oblique one (20.00 $\mu g\ cm^{-2}$).

Comparison

Considering the amount of carbon fractions of material accumulated on stone samples during different time of exposure, TC remained always between 14.25 wt% and 21.10 wt% both for samples exposed horizontally and obliquely (when available).

Moreover, the percentage of OC per TC is higher than CC/TC, with exception of the horizontal sample analysed after 18 months of exposure, while EC/TC displays always the lowest value (Figure 3.75) Also CC/TC of horizontal sample analysed after 24 months is significant (52%) but EC and OC concentrations were not detected.

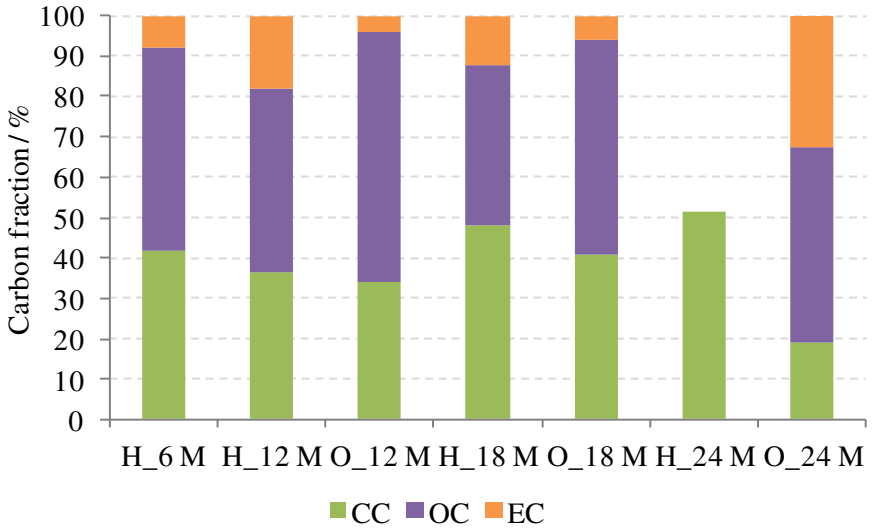

Figure 3.75 CC (green), OC (purple) and EC (orange) fractions calculated as percentages of TC measured in the material deposited on horizontal (H) and oblique (O) stone samples exposed for 6, 12, 18 and 24 months in Bologna.

Figure 3.76 aims to clarify how much carbon portions were accumulated on the whole exposed surface of stone specimens during the investigated period. In general, the trend of each carbon fraction detected on horizontal specimens shows increasing values till 12 months of exposure followed by a decrease after 18 months of exposure and an increase after 24 months. This tendency is observable also in samples obliquely exposed (Figure 3.76). It is noteworthy that the horizontal sample exposed for 12 months recorded the highest amount of EC ever among all analysed samples while the oblique sample of the same exposure period showed the highest quantity of OC ever. On the contrary the overall lowest values of each carbon fraction were detected in the particulate matter collected from horizontal sample remained exposed for 18 months, with exception of CC amount that reached the lowest value on oblique sample after 24 months of exposure (Figure 3.76).

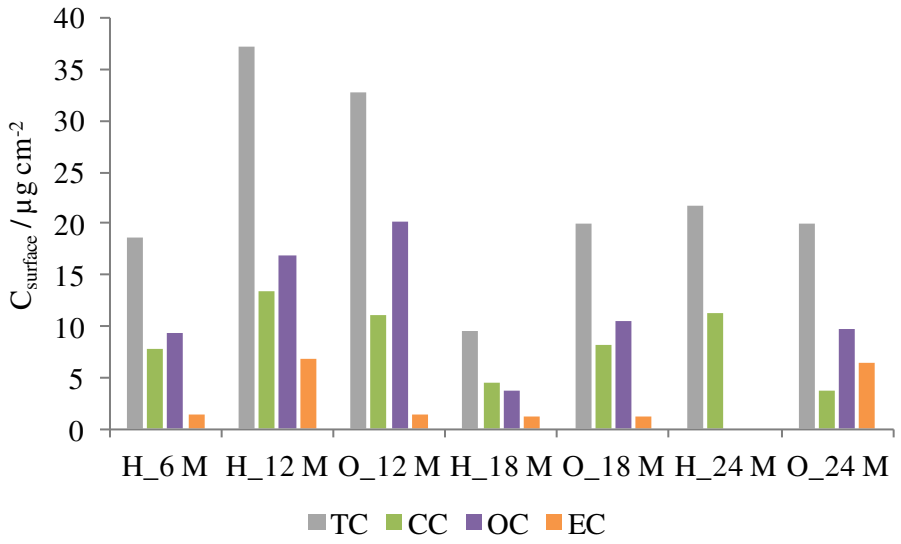

Figure 3.76 Carbon fraction amount per surface unit calculated on the material collected from the exposed surface of stone samples horizontally (H) and obliquely (O) exposed for 6, 12, 18 and 24 months in Bologna. Grey, green, purple and orange refer respectively to $TC_{surface}$, $CC_{surface}$, $OC_{surface}$ and $EC_{surface}$.

Considering $\delta^{13}C$ of all samples, the isotopic ratios remained almost constant for all samples during all the analysed periods (Tables 3.26-3.29). $\delta^{13}C_{TC}$ remained between -12.7 ‰ of horizontal sample exposed for 24 months and -21.6 ‰ of oblique specimen exposed for 24 months. $\delta^{13}C_{CC}$ is always around 0.0 ‰ while $\delta^{13}C_{OC}$ and $\delta^{13}C_{EC}$ are more negative: around -25.0 ‰ and between -25.3 ‰ and -30.8 ‰, respectively.

FERRARA

CARRARA MARBLE

The amount of carbon fractions measured as weight percent of material accumulated on marble samples exposed in Ferrara at different exposure time is reported in Table A4.2 (Annex 4).

After 6 months of exposure

The amount of deposited material was considered enough for carbon speciation only on horizontally exposed sample. The elemental analyser detected 15.72 wt% of TC, 3.22 wt% of CC and 12.40 wt% of NCC (Figure 3.77). The latter was composed mainly of OC (11.24 wt%) and only slightly of EC (1.16 wt%). OC/EC ratio, equal to 10, highlights the prevalence of OC (Table 3.30). Furthermore, Figure 3.77 displays also the amount of each carbon fraction per surface unit deposited on the stone slab.

The evaluation of different carbon portions as percentage of TC underlines that OC represented almost one third of TC (72 %) while CC is 21 % and EC 7 %.

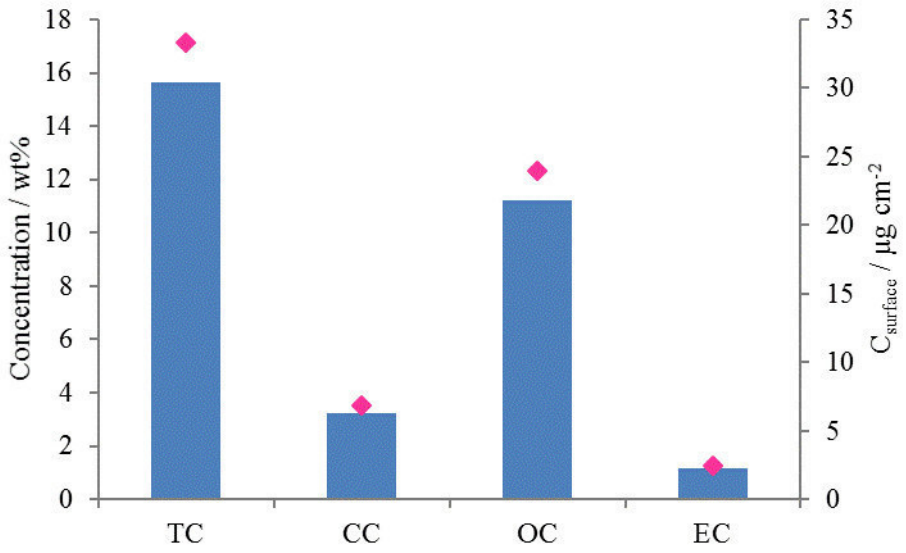

Figure 3.77 Blue bars indicate TC, CC, OC and EC concentrations weighted in powder deposit collected from Carrara Marble sample horizontally exposed for 6 months in Ferrara while pink rhombuses represent the related amount of each carbon fraction per surface unit of the same sample.

Considering the isotopic ratios, $\delta^{13}C_{CC}$ resulted -0.7 ‰ while $\delta^{13}C_{OC}$ and $\delta^{13}C_{EC}$ were increasingly negative (-24.8 ‰ and -29.5 ‰, respectively) (Table 3.30).

	$TC_{surface}$ (µg cm^{-2})	$CC_{surface}$ (µg cm^{-2})	$OC_{surface}$ (µg cm^{-2})	$EC_{surface}$ (µg cm^{-2})	$\delta^{13}C_{TC}$ (‰)	$\delta^{13}C_{CC}$ (‰)	$\delta^{13}C_{OC}$ (‰)	$\delta^{13}C_{EC}$ (‰)	OC/EC
PTCH21	33.30	6.87	23.96	2.47	-20.2	-0.7	-24.8	-29.5	10

Table 3.30 Information related to carbon fractions (carbon fractions measured as weight per surface unit, isotopic ratios and OC/EC) of horizontal Carrara Marble sample after 6 months of exposure in Ferrara.

After 12 months of exposure

The exposure outdoor of samples for 12 months in Ferrara led the analysis of carbon fractions of the particulate matter deposited on both horizontal and oblique specimens. TC analysed in the particulate matter deposited on horizontal stone sample was 16.91 wt%, whose 73 % consisted of NCC (54 % OC and 19 % EC) and the remaining 27% of CC (Figure 3.78). The OC/EC ratio confirmed that OC is almost double EC.
The analysis of material deposited on the obliquely exposed sample showed a concentration of TC (16.56 wt%), CC (3.91 wt%) and NCC (12.65 wt%) similar to that measured on horizontal sample (Figure 3.78). Nevertheless, a higher amount of OC (11.37 wt%) over EC (1.27 wt%) was detected on oblique specimen than in the horizontal one (Figure 3.78). This is clear also observing OC/EC ratio (i.e. 9) and the calculated percentage of NCC components respect to TC (69 % of OC and 8 % of EC).

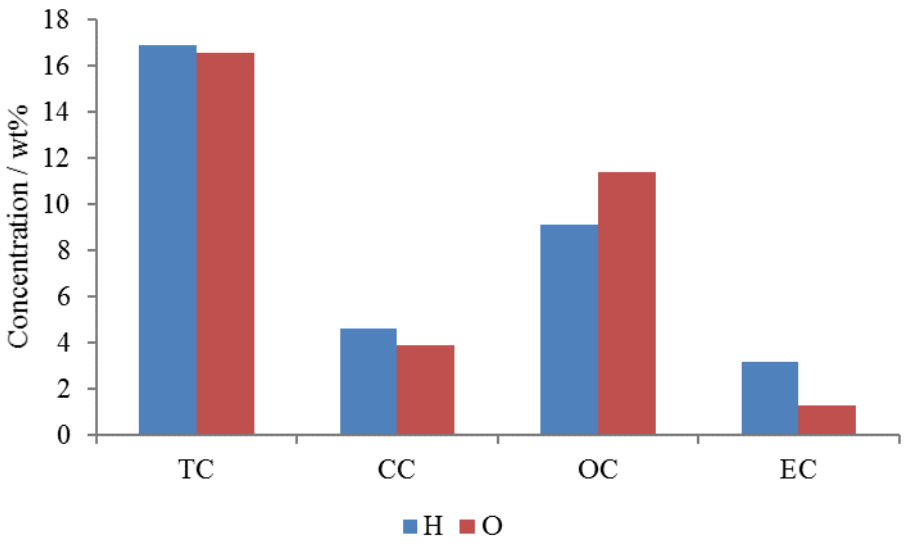

Figure 3.78 TC, CC, OC and EC concentrations detected in powder deposit collected from Carrara Marble samples horizontally (blue) and obliquely (red) exposed for 12 months in Ferrara.

However, considering the quantity of material collected from the two samples, the amount of carbon fractions calculated per surface unit showed that $TC_{surface}$ of horizontal specimen is almost double that of oblique sample (74.90 µg cm^{-2} and 43.47 µg cm^{-2}) and therefore all the other $C_{surface}$ fractions resulted higher in the horizontal sample than the oblique one (Table 3.31).

	$TC_{surface}$ (µg cm^{-2})	$CC_{surface}$ (µg cm^{-2})	$OC_{surface}$ (µg cm^{-2})	$EC_{surface}$ (µg cm^{-2})	$\delta^{13}C_{TC}$ (‰)	$\delta^{13}C_{CC}$ (‰)	$\delta^{13}C_{OC}$ (‰)	$\delta^{13}C_{EC}$ (‰)	OC/EC
PTCH23	74.90	20.51	40.32	14.07	-18.3	1.0	-24.5	-28.5	3
PTCO12	43.47	10.27	29.85	3.34	-19.0	0.3	-25.2	-22.7	9

Table 3.31 Information related to carbon fractions (carbon fractions measured as weight per surface unit, isotopic ratios and OC/EC) of horizontal and oblique Carrara Marble samples after 12 months of exposure in Ferrara.

The measured $\delta^{13}C_{CC}$ of both samples was around 0.0 ‰ while the isotope ratios of OC and EC components were more negative ($\delta^{13}C_{OC}$ was between -24.5 ‰ and -25.2 ‰ and $\delta^{13}C_{EC}$ between -28.5 ‰ and -22.7 ‰, respectively for the horizontal and oblique samples) (Table 3.31).

After 18 months of exposure

The material accumulated on horizontal marble sample after 18 months of exposure was composed by 14.11 wt% of TC, 3.10 wt% of CC, 8.11 wt% of OC and 2.90 wt% of EC (11.01 wt% of NCC), as shown in Figure 3.79. In particular, OC was the dominant component of TC (57 %) while EC and CC accounted for a similar percentage to TC (21 % and 22 %, respectively). Considering the proportion of the NCC components, OC/EC ratio is equal to 3.

Figure 3.79 displays also that the amount of TC (14.22 wt%) and OC (11.85 wt%) measured on oblique sample was slightly higher than that of horizontal specimen while slightly lower values were recorded for CC (2.37 wt%) and EC (2.51 wt%), always attesting the prevalence of NCC (83 %) over CC (17 %) respect to TC.

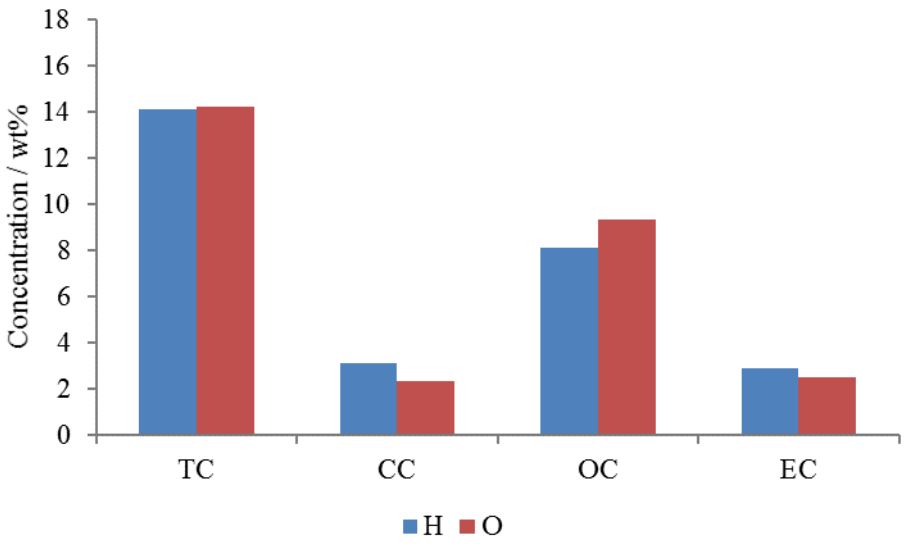

Figure 3.79 TC, CC, OC and EC concentrations detected in powder deposit collected from Carrara Marble samples horizontally (blue) and obliquely (red) exposed for 18 months in Ferrara.

However, the abundance evaluation of each carbon component to all the collected material and related to surface unit highlighted higher $C_{surface}$ of all components in horizontal sample than the oblique one (Table 3.32).

	$TC_{surface}$ ($\mu g\ cm^{-2}$)	$CC_{surface}$ ($\mu g\ cm^{-2}$)	$OC_{surface}$ ($\mu g\ cm^{-2}$)	$EC_{surface}$ ($\mu g\ cm^{-2}$)	$\delta^{13}C_{TC}$ (‰)	$\delta^{13}C_{CC}$ (‰)	$\delta^{13}C_{OC}$ (‰)	$\delta^{13}C_{EC}$ (‰)	OC/EC
PTCH4	118.35	26.02	68.02	24.32	-20.0	-1.1	-26.0	-23.4	3
PTCO5	85.10	14.16	55.91	15.03	-19.9	0.4	-25.9	-16.6	4

Table 3.32 Information related to carbon fractions (carbon fractions measured as weight per surface unit, isotopic ratios and OC/EC) of horizontal and oblique Carrara Marble samples after 18 months of exposure in Ferrara.

Considering the isotopic ratios in Table 3.32 $\delta^{13}C_{TC}$ was very similar in both samples while higher differences were observable in $\delta^{13}C_{EC}$, equal to -23.4 ‰ in the horizontal sample and -16.6 ‰ in the oblique one.

After 24 months of exposure

The material accumulated on horizontal marble sample after 24 months of exposure was composed by 15.51 wt% of TC, 1.80 wt% of CC, 7.00 wt% of OC and 6.72 wt% of EC (13.72 wt% of NCC), as shown in Figure 3.80. Considering the related percentage to TC, OC (45 %) and EC (43 %) percentage were similar and both were higher than that of CC (12 %).

Figure 3.80 displays also that the amount of OC (7.67 wt%) and CC (2.06 wt%) measured on oblique sample was slightly higher that of horizontal specimen while slightly lower values were recorded for TC (13.68 wt%) and EC (3.96 wt%), always attesting the prevalence of NCC (85 %) over CC (15 %) respect to TC.

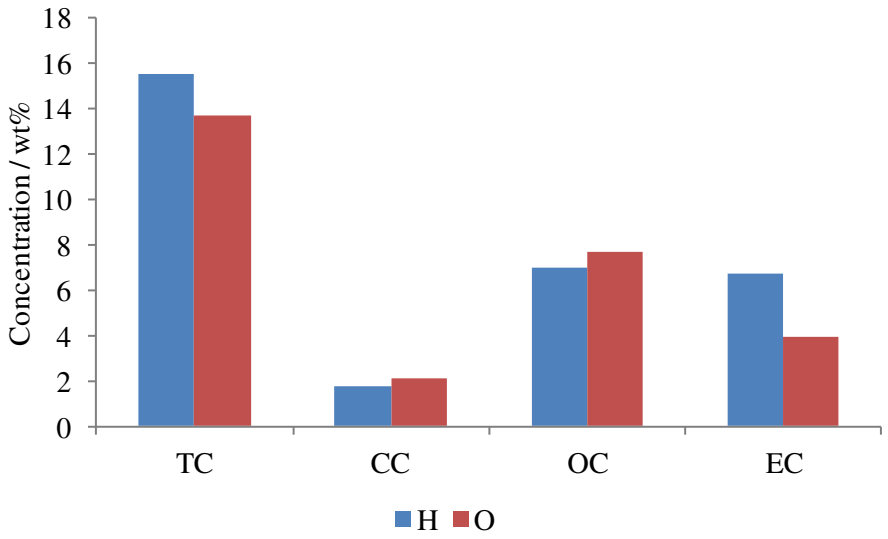

Figure 3.80 TC, CC, OC and EC concentrations detected in powder deposit collected from Carrara Marble samples horizontally (blue) and obliquely (red) exposed for 24 months in Ferrara.

$C_{surface}$ of all fractions resulted higher in horizontal sample than in the oblique one (Table 3.33). Moreover, the isotopic ratio of all carbon fractions was similar in both samples (Table 3.33).

	$TC_{surface}$ ($\mu g\ cm^{-2}$)	$CC_{surface}$ ($\mu g\ cm^{-2}$)	$OC_{surface}$ ($\mu g\ cm^{-2}$)	$EC_{surface}$ ($\mu g\ cm^{-2}$)	$\delta^{13}C_{TC}$ (‰)	$\delta^{13}C_{CC}$ (‰)	$\delta^{13}C_{OC}$ (‰)	$\delta^{13}C_{EC}$ (‰)	OC/EC
PTCH5	152.75	17.68	68.94	66.14	-20.7	-0.7	-25.4	-21.2	1
PTCO4	102.82	15.50	57.59	29.72	-20.4	-1.3	-25.4	-20.7	2

Table 3.33 Information related to carbon fractions (carbon fractions measured as weight per surface unit, isotopic ratios and OC/EC) of horizontal and oblique Carrara Marble samples after 24 months of exposure in Ferrara.

Comparison

Comparing the amount of carbon fractions of material accumulated on stone samples during different exposure time, TC remained always between 13.68 wt% and 16.91 wt% both for samples exposed horizontally and obliquely (when available).

In general, OC was the main component of TC in all analysed samples, contributing always to more than half of TC, with exception of deposited particulate matter on horizontal sample after 24 month of exposure (Figure 3.81). Moreover, considering the components of NCC, OC/EC ratio decreased during the exposure time in both horizontal and oblique samples (Tables 3.30-3.33). Along with a natural increase of EC/TC over time, it should be considered that the deposit samples collected after 24 months of exposure was analysed using 400°C rather than 430°C as temperature to detect OC concentration. This can lead to an additional increase of EC respect to OC.

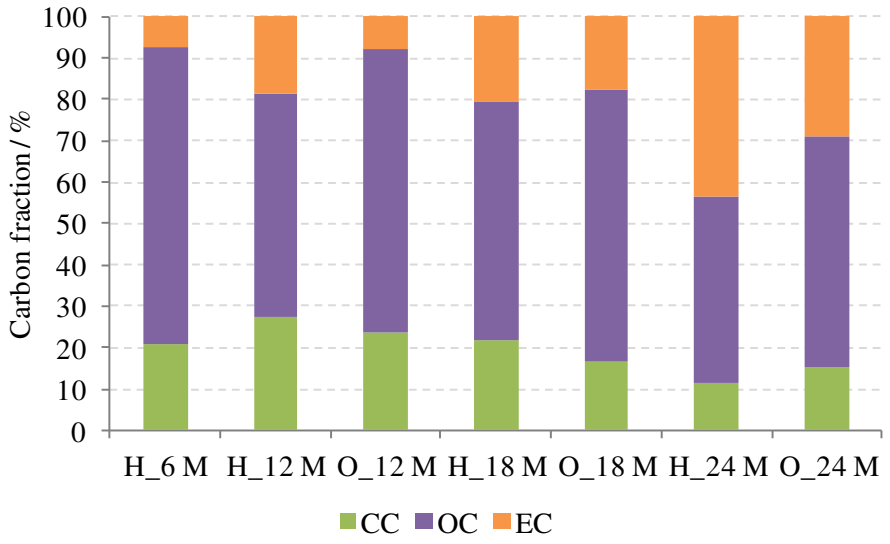

Figure 3.81 CC (green), OC (purple) and EC (orange) fractions calculated as percentages of TC measured in the material deposited on horizontal (H) and oblique (O) Carrara Marble stone samples exposed for 6, 12, 18 and 24 months in Ferrara.

Taking into consideration $C_{surface}$, both horizontal and oblique specimens underwent a gradual increase of $TC_{surface}$ over time, showing higher values in horizontal samples than in the corresponding oblique one (Figure 3.82). Also all the other $C_{surface}$ fractions display a similar increasing trend over time of both kinds of samples, with exception of OC and CC fractions of deposit exposed for 24 months that remained almost similar to the values of the previous period (Figure 3.82).

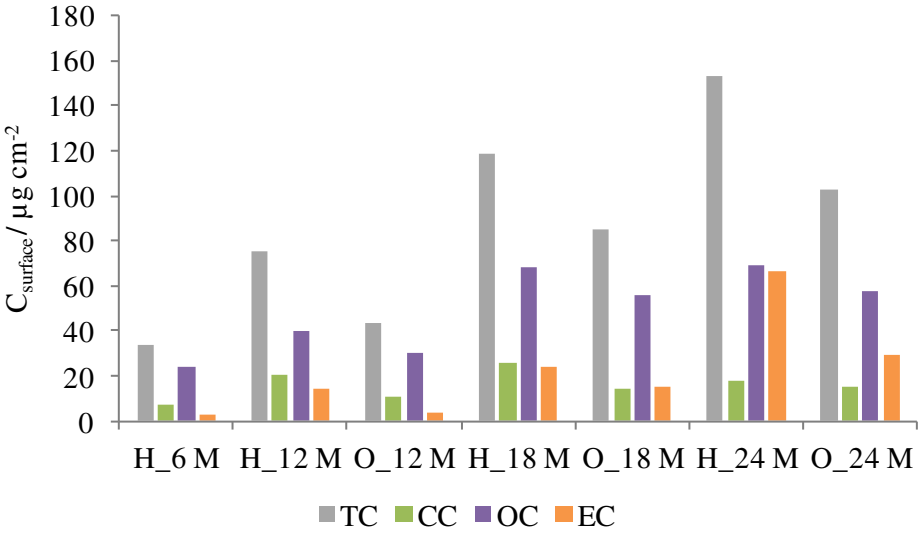

Figure 3.82 Carbon fraction amount per surface unit calculated on the material collected from the exposed surface of Carrara Marble stone samples horizontally (H) and obliquely (O) exposed for 6, 12, 18 and 24 months in Ferrara. Grey, green, purple and orange refer respectively to $TC_{surface}$, $CC_{surface}$, $OC_{surface}$ and $EC_{surface}$.

Finally, $\delta^{13}C_{TC}$ remained constant in all sample of all exposure time in between -20.7 ‰ of horizontal sample exposed for 24 months and -18.3 of horizontal specimen exposed for 12 months (Tables 3.30-3.33). $\delta^{13}C_{CC}$ and $\delta^{13}C_{OC}$ remained constant in all analysed samples with mean value of -0.3 ‰ and -25.3 ‰, respectively.

Furthermore, $\delta^{13}C_{EC}$ varied towards lightly more positive values over time on horizontal samples (from -29.5 ‰ calculated after 6 months to -21.2 after 24 months of exposure) and remained more stable over time on oblique specimens (around -20.0).

VERONA RED MARBLE

The amount of carbon fractions measured as weight percent of material accumulated on limestone samples exposed in Ferrara at different exposure time is reported in Table A4.3 (Annex 4).

After 6 months of exposure

The amount of material accumulated on Verona Red Marble samples after 6 months of exposure was such few to not allow the analyses on oblique sample and measure only partially the carbon fractions on horizontal sample. The material deposited in the analysed sample was composed of 16.86 wt% of TC, 3.37 wt% of CC and the remaining 13.50 wt% of NCC (Figure 3.83). In particular, NCC accounted for 80 % of TC while CC for 20 %. Figure 3.83 shows also values of $C_{surface}$ of TC (23.54 µg cm^{-2}), CC (4.70 µg cm^{-2}) and NCC (18.84 µg cm^{-2}). Moreover, it was possible to calculate the isotopic ratio of TC (-21.1 ‰) and CC (-0.5 ‰) (Table 3.34).

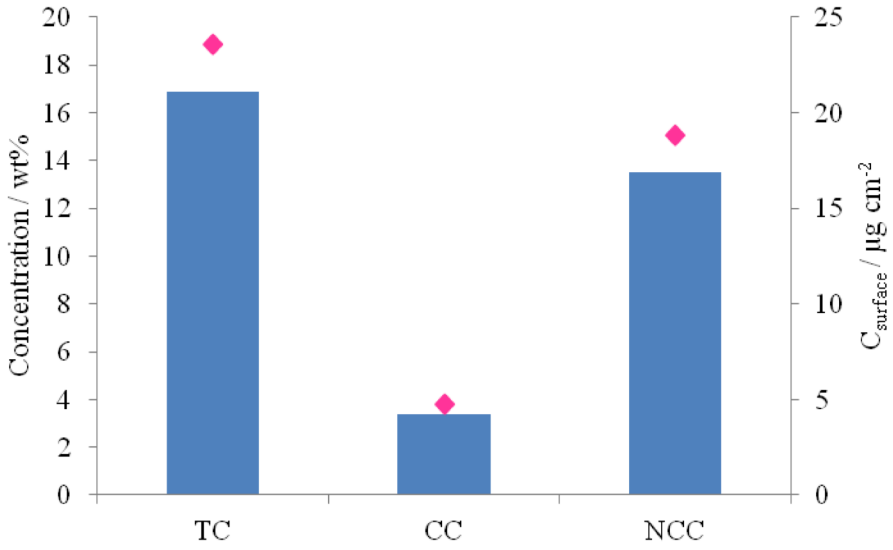

Figure 3.83 Blue bars indicate TC, CC and NCC concentrations weighted in powder deposit collected from Verona Red Marble sample horizontally exposed for 6 months in Ferrara while pink rhombuses represent the related amount of each carbon fraction per surface unit of the same sample.

	$TC_{surface}$ (µg cm^{-2})	$CC_{surface}$ (µg cm^{-2})	$OC_{surface}$ (µg cm^{-2})	$EC_{surface}$ (µg cm^{-2})	$\delta^{13}C_{TC}$ (‰)	$\delta^{13}C_{CC}$ (‰)	$\delta^{13}C_{OC}$ (‰)	$\delta^{13}C_{EC}$ (‰)	OC/EC
PTNH21	23.54	4.70	n.d.	n.d.	-21.1	-0.5	n.d.	n.d.	n.d.

Table 3.34 Information related to carbon fractions (carbon fractions measured as weight per surface unit, isotopic ratios and OC/EC) of horizontal Verona Red Marble sample after 6 months of exposure in Ferrara.

After 12 months of exposure

Respect to time of investigation, the exposure outdoor of samples for 12 months let the accumulation of atmospheric material enough for the analysis of carbon fractions on both horizontal (46.8 mg) and oblique (36.0 mg) samples.

The particulate matter deposited on the horizontal sample was composed by 17.16 wt% of TC, 2.79 wt% of CC, 9.26 wt% of OC and 5.11 wt% of EC (Figure 3.84). Specifically, TC was made up mainly of OC (54 %), followed by EC (30 %) and CC (16 %).

The weight % of TC and CC related to the measured portion of oblique sample was similar to that assess in the horizontal specimen (Figure 3.84). On the contrary, concerning the NCC components of oblique sample, OC (14.30 wt%) was much more abundant than EC (1.98 wt%), having an OC/EC ratio of 7 respect to 2 calculated for the horizontal sample. Moreover, OC accounted for 75 % of TC, CC for 14% and EC for 10 %.

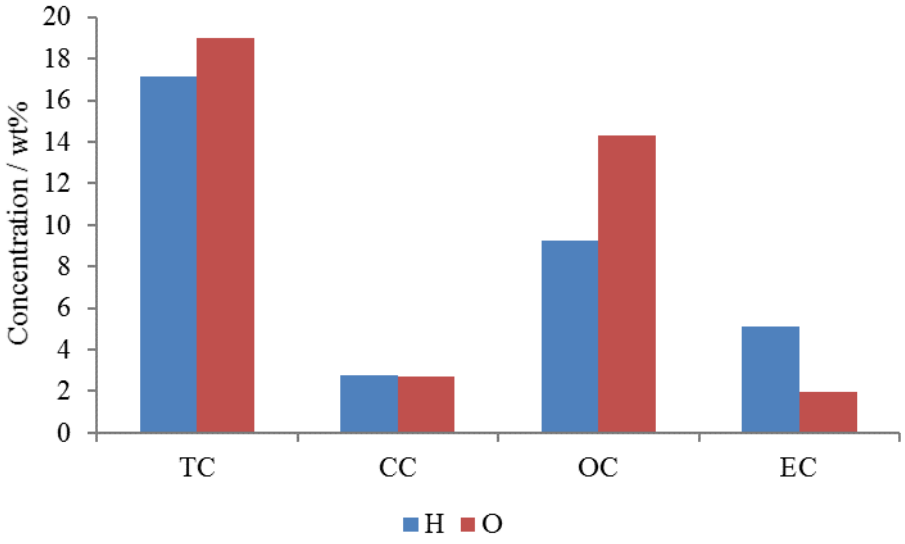

Figure 3.84 TC, CC, OC and EC concentrations detected in material collected from Verona Red Marble samples horizontally (blue) and obliquely (red) exposed for 12 months in Ferrara.

However, the amount of carbon fractions calculated per surface unit shows that $C_{surface}$ fractions of horizontal specimen were higher than those detected from the oblique sample with exception for $OC_{surface}$ (Table 3.35). Moreover, each isotopic fraction of horizontal samples was similar to that of the oblique one, with increasingly more negative value from $\delta^{13}C_{CC}$ to $\delta^{13}C_{OC}$ and $\delta^{13}C_{EC}$ (Table 3.35). $\delta^{13}C_{TC}$ is equal to -21.7 ‰ in both sample.

	$TC_{surface}$ ($\mu g\ cm^{-2}$)	$CC_{surface}$ ($\mu g\ cm^{-2}$)	$OC_{surface}$ ($\mu g\ cm^{-2}$)	$EC_{surface}$ ($\mu g\ cm^{-2}$)	$\delta^{13}C_{TC}$ (‰)	$\delta^{13}C_{CC}$ (‰)	$\delta^{13}C_{OC}$ (‰)	$\delta^{13}C_{EC}$ (‰)	OC/EC
PTNH17	55.76	9.07	30.10	16.60	-21.7	-1.1	-24.4	-28.1	2
PTNO12	47.43	6.72	35.75	4.96	-21.7	-0.9	-25.1	-25.7	7

Table 3.35 Information related to carbon fractions (carbon fractions measured as weight per surface unit, isotopic ratios and OC/EC) of horizontal and oblique Verona Red Marble samples after 12 months of exposure in Ferrara.

After 18 months of exposure

The material deposited on the horizontal sample was composed by 13.90 wt% of TC, 2.75 wt% of CC, 11.38 wt% of OC and 0 wt% of EC (Figure 3.85).

Also the analysis performed on oblique sample showed C fractions results similar to those analysed on the horizontal sample with 14.87 wt% of TC, 3.13 wt% of CC, 11.42 wt% of OC and 0.32 wt% of EC (Figure 3.85). Considering the NCC fraction, OC represents 77 % of TC while EC only 2 %.

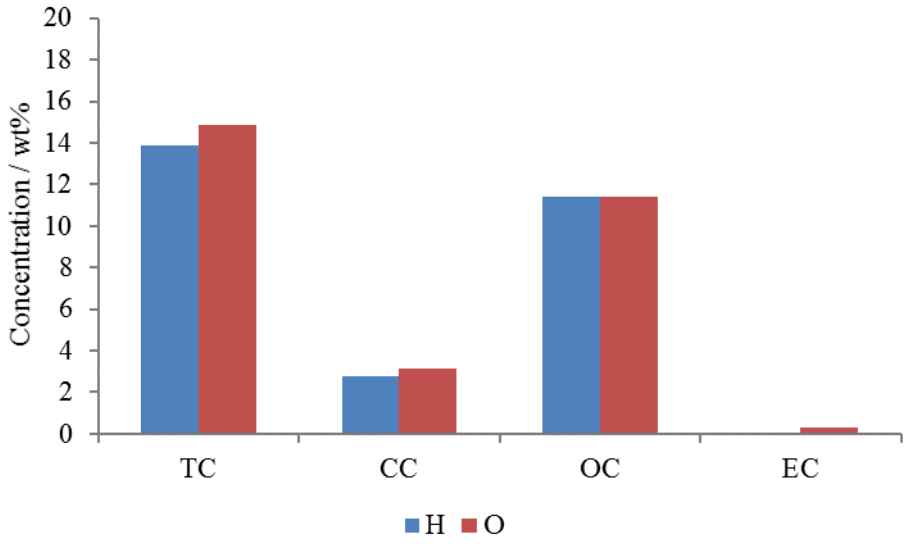

Figure 3.85 TC, CC, OC and EC concentrations detected in material collected from Verona Red Marble samples horizontally (blue) and obliquely (red) exposed for 18 months in Ferrara.

Furthermore, the quantity of carbon fractions calculated per surface unit in horizontal sample was higher than that measured in the oblique one, with $TC_{surface}$ equals to 71.14 µg cm^{-2} and 66.49 µg cm^{-2}, respectively (Table 3.36).

	$TC_{surface}$ (µg cm^{-2})	$CC_{surface}$ (µg cm^{-2})	$OC_{surface}$ (µg cm^{-2})	$EC_{surface}$ (µg cm^{-2})	$\delta^{13}C_{TC}$ (‰)	$\delta^{13}C_{CC}$ (‰)	$\delta^{13}C_{OC}$ (‰)	$\delta^{13}C_{EC}$ (‰)	OC/EC
PTNH4	71.14	14.06	58.25	0.00	-20.1	-0.4	-25.9	n.a.	n.a.
PTNO14	66.49	13.99	51.09	1.41	-20.6	-0.6	-26.0	-22.6	36

Table 3.36 Information related to carbon fractions (carbon fractions measured as weight per surface unit, isotopic ratios and OC/EC) of horizontal and oblique Verona Red Marble samples after 18 months of exposure in Ferrara. n.a. means not available data.

Table 3.36 reports also the isotopic ratios of each carbon fraction of both samples, evidencing similar values for each C component.

After 24 months of exposure

Particulate matter deposited on the horizontal sample was composed by 13.40 wt% of TC, 2.08 wt% of CC, 8.00 wt% of OC and 3.32 wt% of EC (Figure 3.86). Specifically, TC was made up mainly of OC (59.7 %), followed by EC (24.8 %) and CC (15.5 %).

In general, the weight percent of carbon fraction of particulate matter collected from oblique sample was slightly higher than that assess on the horizontal specimen, with exception of CC (Figure 3.86). In particular, OC accounted for 62.89 % of TC, CC for 12.13 % and EC for 24.98 % but OC/EC (equals to 3) was similar to then calculated for horizontal sample (i.e. 2).

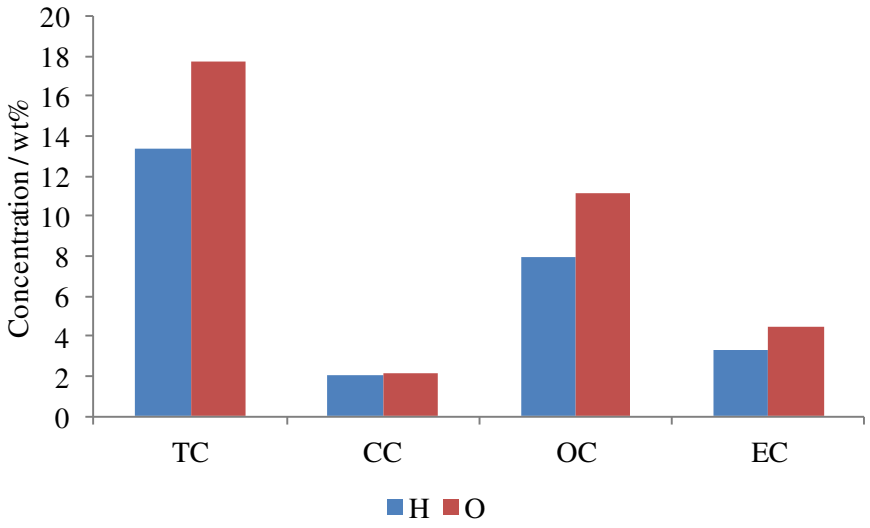

Figure 3.86 TC, CC, OC and EC concentrations detected in material collected from Verona Red Marble samples horizontally (blue) and obliquely (red) exposed for 24 months in Ferrara.

Furthermore, the quantity of carbon fractions calculated per surface unit in horizontal sample was higher than that measured in the oblique one, with $TC_{surface}$ equals to 106.47 µg cm^{-2} and 84.24 µg cm^{-2}, respectively (Table 3.37). Table 3.37 reports also the isotopic ratios of each carbon fraction of both samples, evidencing similar values for each C component.

	$TC_{surface}$ (µg cm^{-2})	$CC_{surface}$ (µg cm^{-2})	$OC_{surface}$ (µg cm^{-2})	$EC_{surface}$ (µg cm^{-2})	$\delta^{13}C_{TC}$ (‰)	$\delta^{13}C_{CC}$ (‰)	$\delta^{13}C_{OC}$ (‰)	$\delta^{13}C_{EC}$ (‰)	OC/EC
PTNH11	106.47	16.55	63.56	26.37	-21.0	-0.6	-25.1	-23.7	2
PTNOI6	84.24	10.22	52.98	21.04	-21.6	-0.9	-25.3	-22.2	3

Table 3.37 Information related to carbon fractions (carbon fractions measured as weight per surface unit, isotopic ratios and OC/EC) of horizontal and oblique Verona Red Marble samples after 24 months of exposure in Ferrara.

Comparison

Comparing the amount of carbon fractions of material accumulated on stone samples during different exposure time, TC remained always between 13.40 wt% and 18.97 wt% both for samples exposed horizontally and obliquely (when available) (Tables 3.34-3.37).

Comparing horizontal and oblique samples over time, OC is the main component of TC in all analysed specimens, contributing always to more than half of TC, apart from the horizontal sample exposed for 6 months of which was possible to detect only NCC (Figure 3.87). Moreover, OC amount increased so much after 18 months of exposure respect to EC that OC/EC ratio increased during the exposure time in both horizontal and oblique samples reaching up to 36 (Tables 3.34-3.37). However, after 24 months of exposure there was an increase of EC, as shown in Figure 3.87. It has to remain that deposit samples collected after 24

months of exposure was analysed using 400°C rather than 430°C as temperature to detect OC concentration and thus this could have influenced the higher amount of EC respect to OC.

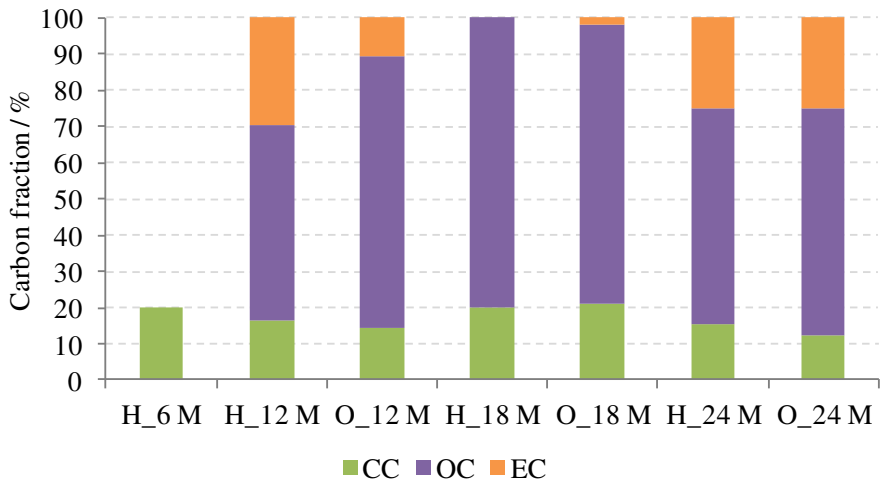

Figure 3.87 CC (green), OC (purple) and EC (orange) fractions calculated as percentages of TC measured in the material deposited on horizontal (H) and oblique (O) Verona Red Marble stone samples exposed for 6, 12, 18 and 24 months in Ferrara.

Concerning upon $C_{surface}$, both horizontal and oblique specimens underwent a gradual increase of $TC_{surface}$ over time, showing higher values in horizontal samples than in the corresponding oblique ones (Figure 3.88). Moreover, $CC_{surface}$ resulted almost similar in horizontal and oblique samples, with a slight increase over time, while $EC_{surface}$ resulted less in oblique specimen than in the horizontal one, when detected. In general, $OC_{surface}$ increased over time with higher concentration on the horizontal samples respect to the oblique ones (Figure 3.88).

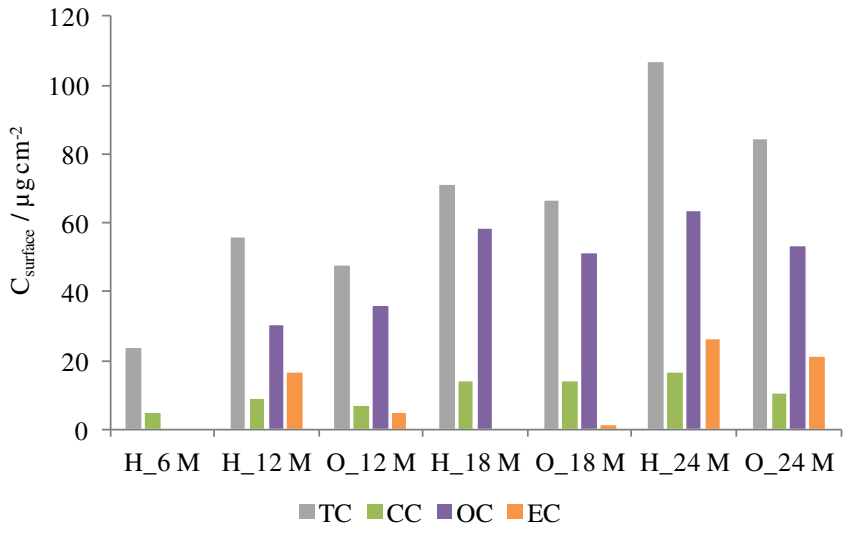

Figure 3.88 Carbon fraction amount per surface unit calculated on the material collected from the exposed surface of Verona Red Marble stone samples horizontally (H) and obliquely (O) exposed for 6, 12, 18 and 24 months in Ferrara. Grey, green, purple and orange refer respectively to $TC_{surface}$, $CC_{surface}$, $OC_{surface}$ and $EC_{surface}$.

Finally, $\delta^{13}C_{TC}$ remained constant around -21.1 ‰ in all sample (Tables 3.34-3.37). Also $\delta^{13}C_{CC}$ and $\delta^{13}C_{OC}$ remained constant in all analysed samples with mean value of -0.71 ‰ and -25.29 ‰, respectively. When detected, $\delta^{13}C_{EC}$ varied from -28.1 ‰ calculated after 12 months on horizontal sample to -22.2 ‰ after 24 months of exposure on oblique specimen.

FLORENCE

The amount of carbon fractions measured as weight percent of material accumulated on marble samples exposed in Florence at different exposure time is reported in Table A4.4 (Annex 4).

After 6 months of exposure

The exposure outdoor of stone samples in Florence caused the deposition of particulate matter enough to allow the analysis of carbon fractions both on horizontal and oblique samples. The material deposited on the exposed surface of horizontal specimen was composed of 12.34 wt% of TC, 4.51 wt% of CC and 6.67 wt% of OC and 1.16 wt% of EC (Figure 3.89). Therefore, TC was made up mainly of OC (54 %) followed by CC (37 %) and EC (9 %). Figure 3.89 shows also that the particulate matter collected from the oblique sample was composed by 11.72 wt% of TC, 5.63 wt% of CC and 6.09 wt% of NCC. In particular, CC (48 %) was the predominant part of TC while OC accounted for 43% and EC for 9% of TC.

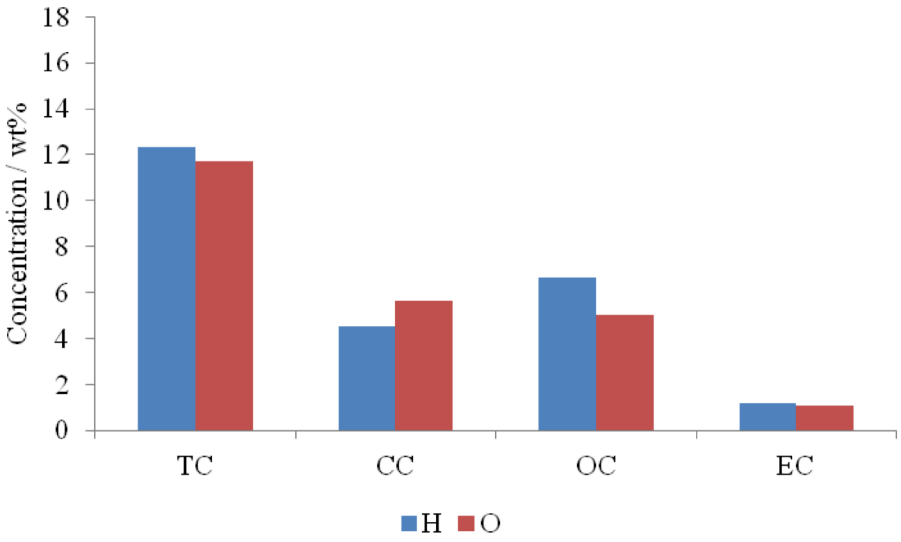

Figure 3.89 TC, CC, OC and EC concentrations detected in material collected from samples horizontally (blue) and obliquely (red) exposed for 6 months in Florence.

Table 3.38 displays a similar amount of $TC_{surface}$ measured on samples with different orientation, with a slight prevalence on oblique sample (33.20 µg cm^{-2}) than on the horizontal specimen (32.04 µg cm^{-2}). In particular, oblique sample showed a higher $CC_{surface}$ than the horizontal specimen and a similar $EC_{surface}$, while $OC_{surface}$ was slightly higher in the horizontal sample (Table 3.38).

Moreover, the isotopic ratios of both samples were quite similar with exception of $\delta^{13}C_{EC}$, more positive for the horizontal sample than for the oblique one (Table 3.38).

	$TC_{surface}$ ($\mu g\ cm^{-2}$)	$CC_{surface}$ ($\mu g\ cm^{-2}$)	$OC_{surface}$ ($\mu g\ cm^{-2}$)	$EC_{surface}$ ($\mu g\ cm^{-2}$)	$\delta^{13}C_{TC}$ (‰)	$\delta^{13}C_{CC}$ (‰)	$\delta^{13}C_{OC}$ (‰)	$\delta^{13}C_{EC}$ (‰)	OC/EC
SMCH1	32.04	11.70	17.33	3.01	-15.6	-0.9	-25.4	-16.0	6
SMCO1	33.20	15.96	14.22	3.02	-13.2	0.0	-25.5	-25.7	5

Table 3.38 Information related to carbon fractions (carbon fractions measured as weight per surface unit, isotopic ratios and OC/EC) of horizontal and oblique Carrara Marble samples after 6 months of exposure in Florence.

After 12 months of exposure

Sample horizontally exposed for 12 months in Florence underwent a deposition of particulate matter composed of 14.5 wt% of TC, 2.73 wt% of CC and 11.77 wt% of NCC (Figure 3.90). In particular, OC accounted for 59 % of TC, EC for 23 % and CC for 19 %.

Carbon fractions detected on the oblique sample were slightly lower than those of the horizontal sample with the exception of CC portion (Figure 3.90). Moreover, considering the percentage of each carbon fraction over TC, OC (59 %) prevailed followed by CC (24 %) and EC (17 %).

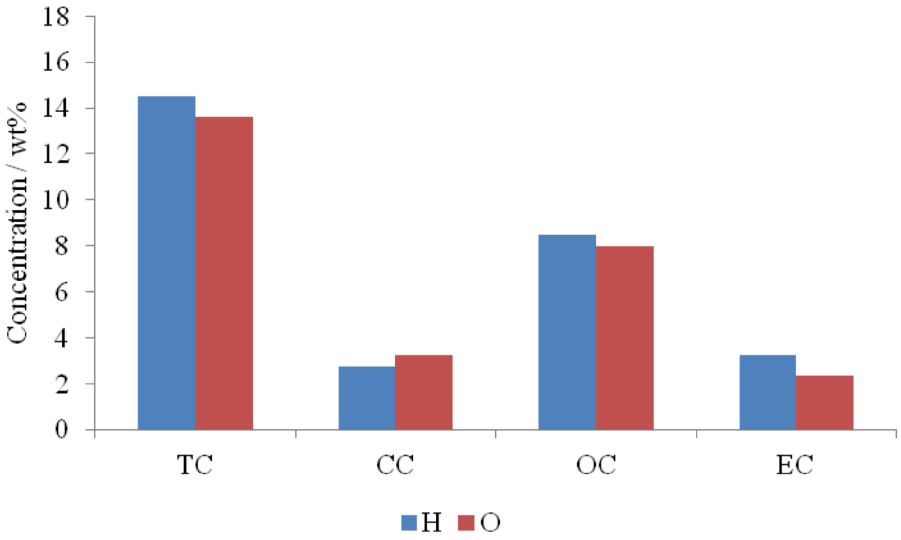

Figure 3.90 TC, CC, OC and EC concentrations detected in material collected from samples horizontally (blue) and obliquely (red) exposed for 12 months in Florence.

Taking into consideration the $C_{surface}$, higher $TC_{surface}$ accumulated on the horizontal sample than the oblique one but with the prevalence of OC over CC and EC in both samples (Table 3.39).

	$TC_{surface}$ ($\mu g\ cm^{-2}$)	$CC_{surface}$ ($\mu g\ cm^{-2}$)	$OC_{surface}$ ($\mu g\ cm^{-2}$)	$EC_{surface}$ ($\mu g\ cm^{-2}$)	$\delta^{13}C_{TC}$ (‰)	$\delta^{13}C_{CC}$ (‰)	$\delta^{13}C_{OC}$ (‰)	$\delta^{13}C_{EC}$ (‰)	OC/EC
SMCH4	58.10	10.94	34.06	13.10	-18.4	0.3	-25.8	-14.8	3
SMCO4	48.38	11.44	28.48	8.46	-19.3	-1.4	-24.9	-24.6	3

Table 3.39 Information related to carbon fractions (carbon fractions measured as weight per surface unit, isotopic ratios and OC/EC) of horizontal and oblique Carrara Marble samples after 12 months of exposure in Florence.

Finally, the isotopic ratio of each carbon fraction were similar in both samples although some differences were observable in $\delta^{13}C_{EC}$, equal to -14,8 in the horizontal specimen and -24,6 in the oblique one (Table 3.39).

After 18 months of exposure

The exposure for 18 months of horizontal stone sample led to the accumulation of particulate matter composed by 9.91 wt% of TC, 4.00 wt% of CC, 4.95 wt% of OC and 0.96 wt% of EC (Figure 3.91). In particular, TC was composed by 50 % of OC, 40 % of CC and 10% of EC.

Also oblique specimen displayed similar values to those of horizontal sample, with a slight higher amount of CC and OC but a reduction of EC (Figure 3.91). Therefore, it is noteworthy the clear prevalence of OC over EC (OC/EC equals to 20).

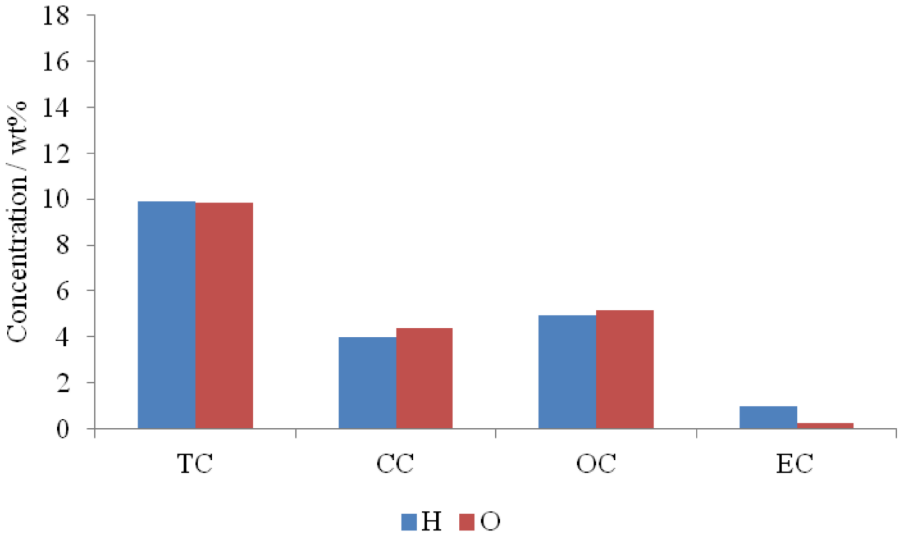

Figure 3.91 TC, CC, OC and EC concentrations detected in material collected from samples horizontally (blue) and obliquely (red) exposed for 18 months in Florence.

However, the amount of carbon fractions calculated per surface unit resulted higher for all carbon fractions in horizontal sample than in the oblique one, as presented in Table 3.40.

	$TC_{surface}$ (µg cm^{-2})	$CC_{surface}$ (µg cm^{-2})	$OC_{surface}$ (µg cm^{-2})	$EC_{surface}$ (µg cm^{-2})	$\delta^{13}C_{TC}$ (‰)	$\delta^{13}C_{CC}$ (‰)	$\delta^{13}C_{OC}$ (‰)	$\delta^{13}C_{EC}$ (‰)	OC/EC
SMCH5	73.36	29.62	36.64	7.10	-15.3	-1.6	-25.9	-17.7	5
SMCO5	58.91	26.27	31.06	1.58	-14.6	-1.4	-25.2	-23.7	20

Table 3.40 Information related to carbon fractions (carbon fractions measured as weight per surface unit, isotopic ratios and OC/EC) of horizontal and oblique Carrara Marble samples after 18 months of exposure in Florence.

Considering the isotopic ratio, similar values related to each carbon fractions were measured in both samples (Table 3.40). Only $\delta^{13}C_{EC}$ was more positive in the horizontal sample (-17.7 ‰) than in the oblique one (-23.7 ‰).

After 24 months of exposure

Particulate deposited on horizontal sample exposed for 24 months was composed by 8.95 wt% of TC, 3.86 wt% of CC, 3.10 wt% of OC and 1.99 wt% of EC (Figure 3.92). In particular, TC was composed by 43 % of CC, 35 % of OC and 22% of EC.

Also oblique specimen displayed similar values to those of horizontal sample, with slightly higher concentration of EC (Figure 3.92). Thus OC/EC identified in oblique samples (equal to 1) was half than that detected in the horizontal sample (equal to 2).

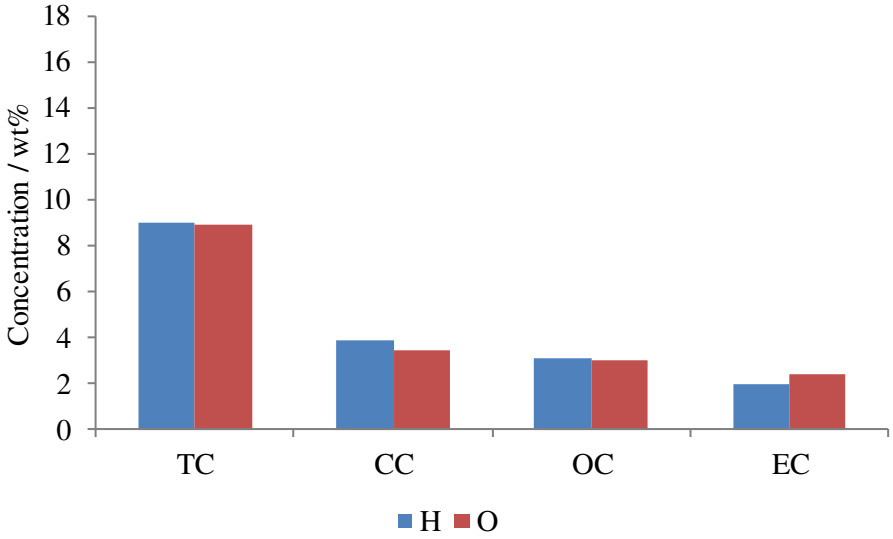

Figure 3.92 TC, CC, OC and EC concentrations detected in material collected from samples horizontally (blue) and obliquely (red) exposed for 24 months in Florence.

Nevertheless, the amount of carbon fractions calculated per surface unit resulted higher for all carbon fractions in horizontal sample than in the oblique one, as presented in Table 3.41. The same Table shows also similar isotopic ratio of each carbon fraction among different samples.

	$TC_{surface}$ (µg cm^{-2})	$CC_{surface}$ (µg cm^{-2})	$OC_{surface}$ (µg cm^{-2})	$EC_{surface}$ (µg cm^{-2})	$\delta^{13}C_{TC}$ (‰)	$\delta^{13}C_{CC}$ (‰)	$\delta^{13}C_{OC}$ (‰)	$\delta^{13}C_{EC}$ (‰)	OC/EC
SMCH8	120.63	52.00	41.80	26.84	-13.4	-0.8	-26.0	-18.3	2
SMCO8	90.12	34.87	30.52	24.73	-14.2	-0.9	-26.1	-18.4	1

Table 3.41 Information related to carbon fractions (carbon fractions measured as weight per surface unit, isotopic ratios and OC/EC) of horizontal and oblique Carrara Marble samples after 24 months of exposure in Florence.

Comparison

The quantity of carbon fractions deposited on all analysed stone samples in Florence remained always between 8.86 wt% and 14.50 wt%, with higher values measured on samples exposed for 12 months (Table 3.38-3.41). In particular, this increase detected after 12 months of exposure seems to be mainly induced by NCC, which reached values of 11.77 wt% in the horizontal sample and 10.39 wt% in the oblique one, while CC fraction is higher in the other periods of analysis (Table 3.38-3.41).

This trend is also confirmed by Figure 3.93 that evaluates the percentage of each carbon fraction over TC. Furthermore, OC represented always half or more of TC, with exception of oblique samples measured after 6 and 24 month of exposure.

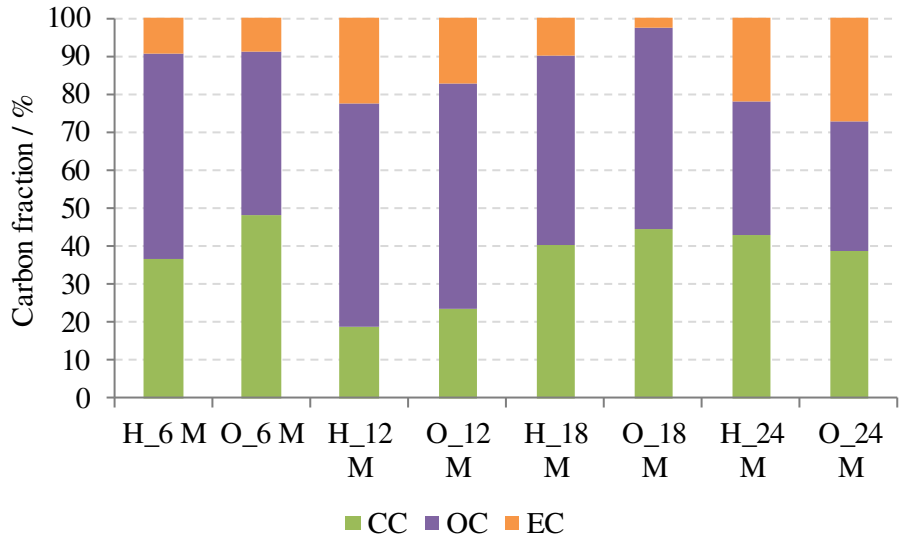

Figure 3.93 CC (green), OC (purple) and EC (orange) fractions calculated as percentages of TC measured in the material deposited on horizontal (H) and oblique (O) stone samples exposed for 6, 12, 18 and 24 months in Florence.

However, $C_{surface}$ of stone samples highlighted an increase of $TC_{surface}$ and $OC_{surface}$ over time for both horizontal and oblique samples (Figure 3.94). $CC_{surface}$ underwent a decrease after 12 months of exposure for then regained after 18 and 24 months of exposure while $EC_{surface}$ showed a higher value after 12 and 24 months of exposure. $OC_{surface}$ and $EC_{surface}$ were slightly higher in the horizontal samples than the oblique ones all over time.

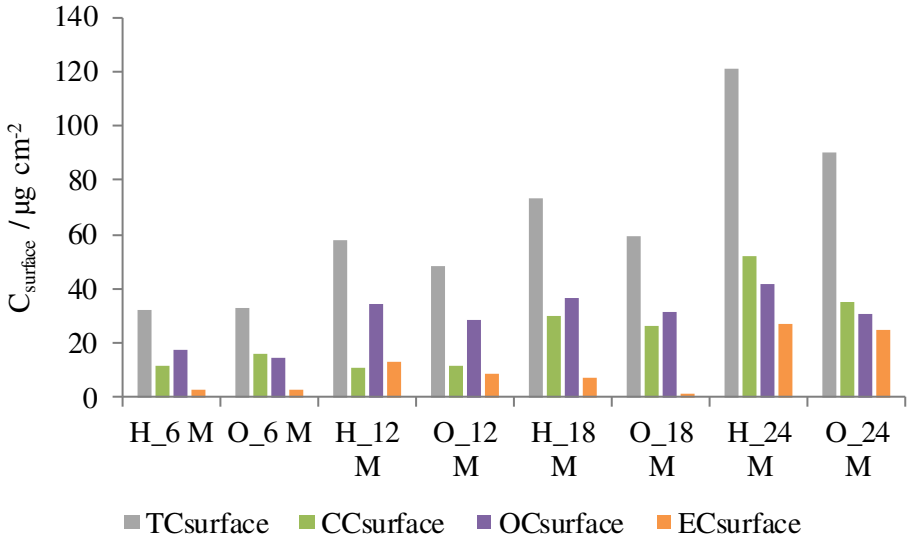

Figure 3.94 Carbon fraction amount per surface unit calculated on the material collected from the exposed surface of stone samples horizontally (H) and obliquely (O) exposed for 6, 12, 18 and 24 months in Florence. Grey, green, purple and orange refer respectively to $TC_{surface}$, $CC_{surface}$, $OC_{surface}$ and $EC_{surface}$.

Finally, $\delta^{13}C_{TC}$ of both samples was always between -19.3 ‰ and -13.2 ‰, with slightly more positive values after 6 and 24 months of exposure, while the isotopic ratio of CC was always around -0,8 ‰ and that

of OC around -25,6 ‰. On the contrary, some differences were perceived in $\delta^{13}C_{EC}$ because it resulted more positive in horizontal specimens (between -17.7 ‰ and -14.8 ‰) than the oblique ones (between -25.7 ‰ and -18.4 ‰).

GENERAL COMPARISON

The comparison of the amounts of accumulated TC per surface unit on horizontal Carrara Marble samples highlights that Ferrara recorded the highest $TC_{surface}$ in each studied period while Bologna the lowest one; Florence shows an intermediate trend (Figure 3.95). In particular, a gradual increase over time of $TC_{surface}$ was detected in Ferrara and Florence samples while Bologna underwent to an increase of $TC_{surface}$ after 6 and 12 months of exposure followed by a decrease after 18 months and a slight increase after 24 months. Also $TC_{surface}$ of oblique samples exposed in Ferrara and Florence progressively increased over time while oblique specimen exposed in Bologna underwent a decrease of $TC_{surface}$ after 18 and 24 months of exposure (Figure 3.95). $TC_{surface}$ of oblique sample analysed after 18 months in Bologna resulted higher (19,89 µg cm^{-2}) than the value measured on the equivalent horizontal sample (9,46 µg cm^{-2}) while all other $TC_{surface}$ analysed on oblique samples were similar or lower than that measured on the corresponding horizontal specimens.
All values of $CC_{surface}$ related to different exposure time, site and orientation remained always between 4.00 µg cm^{-2} and 52.00 µg cm^{-2}. On the contrary, the tendency of $OC_{surface}$ measured in all kind of samples is very similar to that of $TC_{surface}$, but with lower values (i.e. between 3.00 µg cm^{-2} and 69.00 µg cm^{-2} in horizontal samples and between 9.00 µg cm^{-2} and 58.00 µg cm^{-2} in the oblique ones). Thus, higher values of $OC_{surface}$ for each exposure period were detected in Ferrara while the lowest ones in Bologna for both horizontal and oblique samples (Figure 3.95).
$EC_{surface}$ of all studied samples remained always between 1.00 µg cm^{-2} and 67.00 µg cm^{-2}, showing an increasing trend over time in Ferrara where was reached the highest value ever for both kind of samples after 24 months of exposure (Figure 3.95).

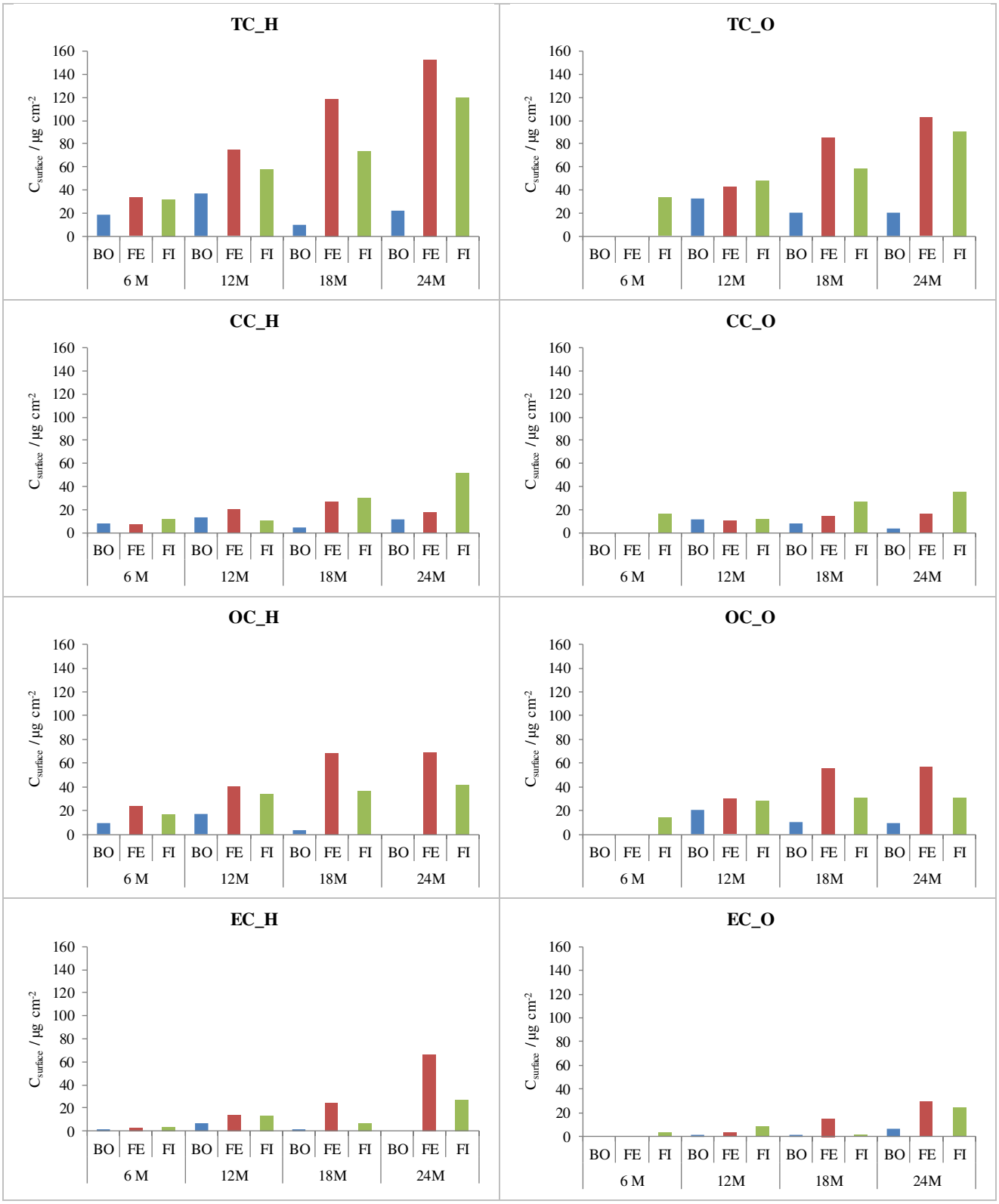

Figure 3.95 Carbon fractions amount per surface unit calculated on the material collected from the exposed surface of Carrara Marble stone samples horizontally (H) and obliquely (O) exposed in different exposure sites for 6, 12, 18 and 24 months. Blue, red and green bars refer respectively to samples exposed in Bologna (BO), Ferrara (FE) and Florence (FI). Carbon analysis was not possible for oblique samples exposed in Bologna and Ferrara for 6 months.

The assessment of the percentage of each carbon fraction respect to TC highlights that NCC always prevails over CC for both horizontal and oblique Carrara Marble samples in all the exposure sites, with exception of

horizontal sample exposed in Bologna and the oblique one placed in Ferrara after 24 months (Figure 3.96). Considering all the analysed carbon fractions, in general EC was detected with the lowest concentration in both horizontal (7-23 %) and oblique (3-33 %) samples exposed for different exposure time in different sites while OC resulted to be in general the predominant component (35-72 % for horizontal samples and 29-69 % for the oblique ones) (Figure 3.96). Nevertheless, some exceptions were identified: horizontal sample exposed for 12 months in Florence was mainly composed by OC (59 %) followed by EC (23 %) and CC (19 %) while the prevalence of CC was evaluated in the horizontal specimen exposed for 18 months in Bologna, in horizontal ones exposed for 24 months in all sites, in the oblique one exposed for 6 months in Florence and in the oblique ones exposed in Ferrara and Florence after 24 months.

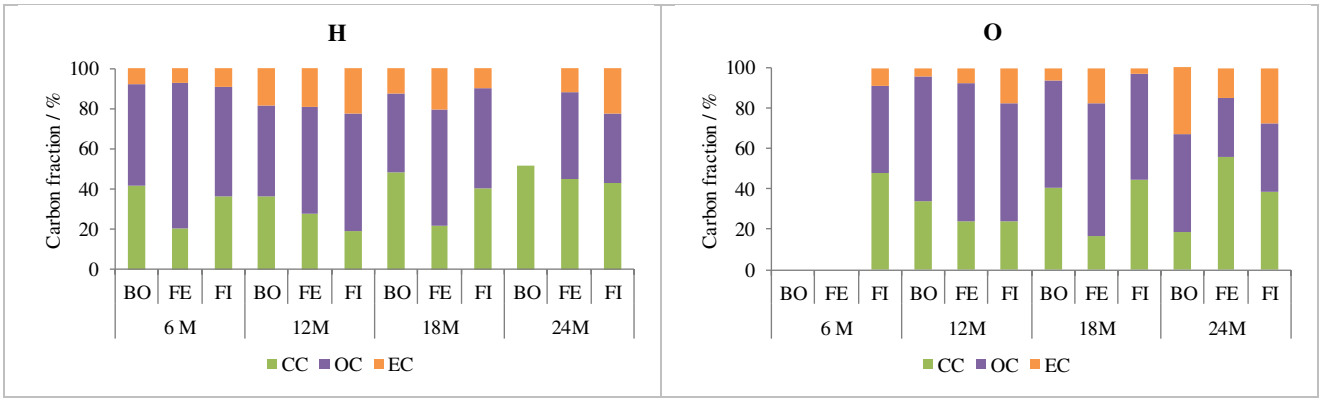

Figure 3.96 CC (green), OC (purple) and EC (orange) fractions calculated as percentages of TC measured in the material deposited on horizontal (H) and oblique (O) Carrara Marble stone samples exposed for 6, 12, 18 and 24 months in Bologna (BO), Ferrara (FE) and Florence (FI). Carbon analysis was not possible for oblique samples exposed in Bologna and Ferrara for 6 months.

Observing the isotopic ratio measured on all horizontal samples at different exposure time, $\delta^{13}C_{TC}$ always ranged between -20.7 ‰ and -13.4 ‰, showing slightly more negative values in samples collected from Ferrara (Figure 3.97). $\delta^{13}C_{CC}$ continuously remained constant around 0.0 ‰ in all sites and also $\delta^{13}C_{OC}$ displayed stable values in each sites over time but more negative (mean equals to -25.5 ‰) than those of $\delta^{13}C_{CC}$ (Figure 3.97). On the contrary, $\delta^{13}C_{EC}$ underwent the highest variations among exposure sites, with more positive measures in Florence (mean -16.7 ‰) than in Bologna (average -29,1 ‰) and Ferrara (mean -25,6 ‰).

$\delta^{13}C_{TC}$ measured in oblique samples are similar to those evaluated in horizontal specimens with values between -20.4 ‰ and -12.7 ‰: Other affinities were detected in the isotopic ratios of the other carbon fractions: $\delta^{13}C_{CC}$ and $\delta^{13}C_{OC}$ always remained around -0.2 ‰ and -25.5 ‰, respectively. $\delta^{13}C_{EC}$, in general, displayed values similar to those of $\delta^{13}C_{OC}$ in samples exposed in Bologna and Florence while more positive measures are observable in specimens exposed in Ferrara (Figure 3.97).

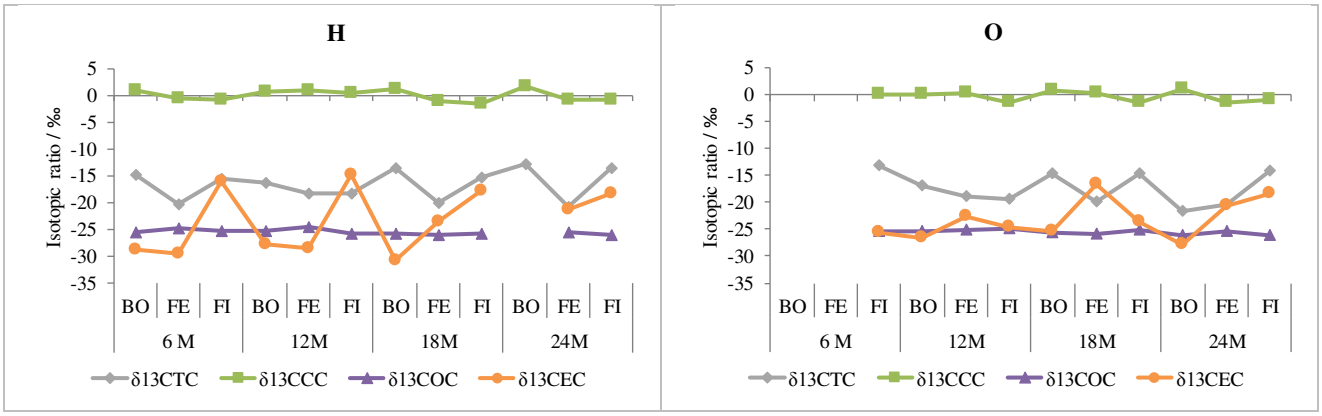

Figure 3.97 Isotopic ratio identified on the material collected from the exposed surface of Carrara Marble stone samples horizontally (H) and obliquely (O) exposed in Bologna (BO), Ferrara (FE) and Florence (FI) for 6, 12, 18 and 24 months. Grey rhombuses, green squares, purple triangles and orange circles represent respectively $\delta^{13}C_{TC}$, $\delta^{13}C_{CC}$, $\delta^{13}C_{OC}$ and $\delta^{13}C_{EC}$. Carbon analysis was not possible for oblique samples exposed in Bologna and Ferrara for 6 months.

Moreover, the comparison of carbon fractions detected on different kind of stone exposed in Ferrara is summarised in Figure 3.98. Carbon fractions on oblique samples of marble and limestone after 6 months of exposure were not analysed as the deposited material was too low. $TC_{surface}$ of horizontal Carrara Marble samples remained always higher than that detected on limestone specimens throughout the analysed period. Concentrating upon oblique specimens, $TC_{surface}$ was similar for both lithotypes after 12 months of exposure while it revealed slightly higher value on marble sample after 18 and 24 months of exposure. Nevertheless, both lithotypes showed an increasing trend over time both for horizontal and oblique specimens but with higher values on horizontal samples.

$CC_{surface}$ of horizontal samples gradually increased for both lithotypes till 18 months and values detected after 24 months remained close to those of 18 months, always displaying more abounding concentration for Carrara Marble than Verona Red Marble (Figure 3.98). Also oblique specimens underwent a growth over time for both lithotypes, though $CC_{surface}$ was higher on marble than on limestone after 12 months of exposure while their values were similar after 18 and 24 months of exposure.

As already said, the amount of material accumulated on Verona Red Marble horizontal sample after 6 months of exposure was not enough to detect the fractions of NCC. $OC_{surface}$ analysed on horizontal samples was always higher on marble than on limestone samples, independently from the time of exposure, and both lithotypes showed higher $OC_{surface}$ after 18 and 24 months that after 12 months of exposure. This trend is also appreciable for oblique specimens of both lithotypes.

Values of $EC_{surface}$ were rather similar on both lithotypes after 12 months of exposure considering both horizontal and oblique samples but more abundant on horizontal specimens. On contrast, $OC_{surface}$ was higher on marble samples than on limestone ones after 18 and 24 months of exposure for both different orientations of samples.

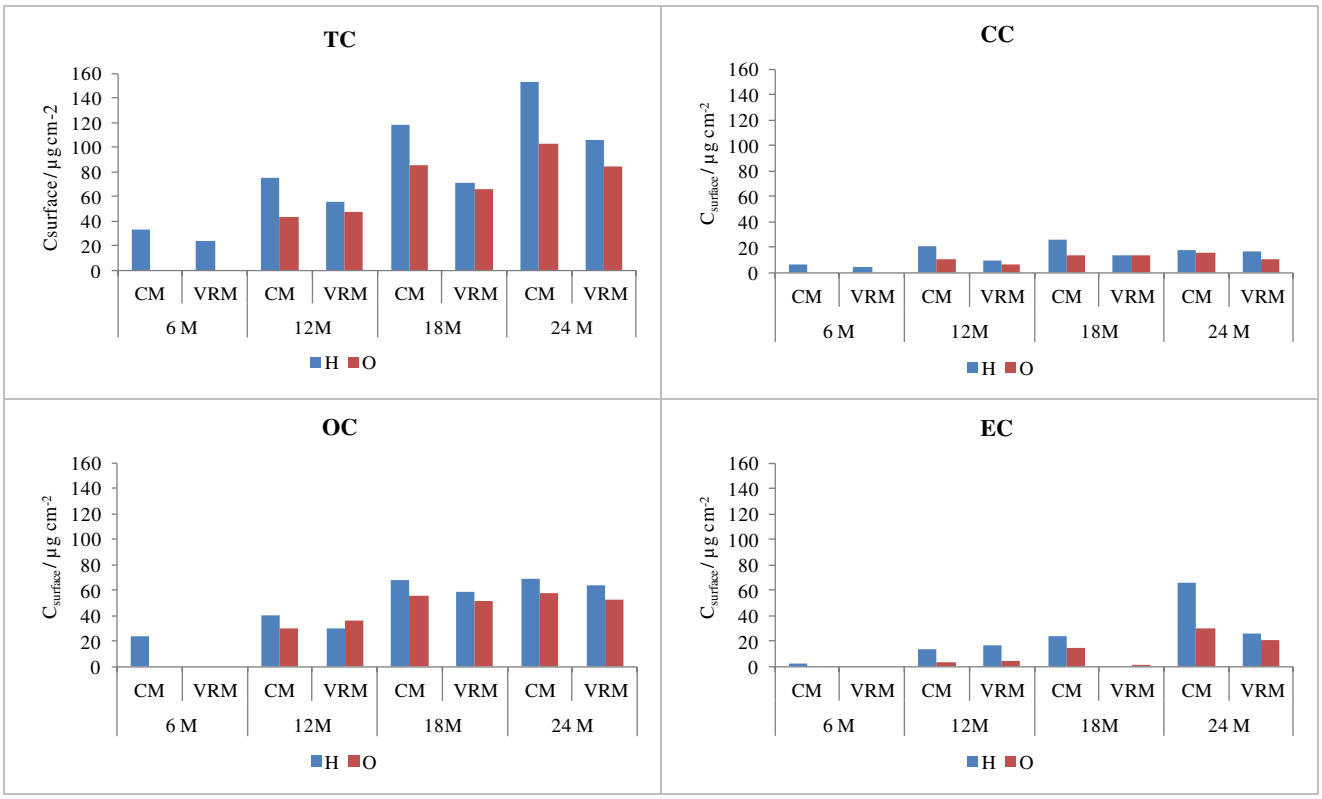

Figure 3.98 Carbon fractions amount per surface unit calculated on the material collected from the exposed surface of Carrara Marble (CM) and Verona Red Marble (VRM) stone samples horizontally (blue) and obliquely (red) exposed in Ferrara for 6, 12, 18 and 24 months.

The percentage of each carbon fraction respect to TC highlights that NCC always prevails over CC for both Carrara Marble and Verona Red Marble samples horizontally and obliquely exposed (Figure 3.99). In this regard, NCC, when detectable, was always predominantly composed by OC while EC represented the lowest portion, with exception of deposit analysed on limestone after 24 months of exposure. Considering horizontal samples, OC ranged between 45 % and 72 % for marble samples and between 16 % and 80 % for limestone ones while EC remained between 7 % and 43 % for marble samples and between 0 % and 60 % for limestone ones, thus highlighting a more intense variation of carbon fractions on limestone over time. Oblique samples experienced higher accumulation of OC on limestone samples respect to the corresponding marble specimen of the same exposure period, always remaining by far higher than EC, with exception of deposit analysed on limestone after 24 months of exposure (Figure 3.99)

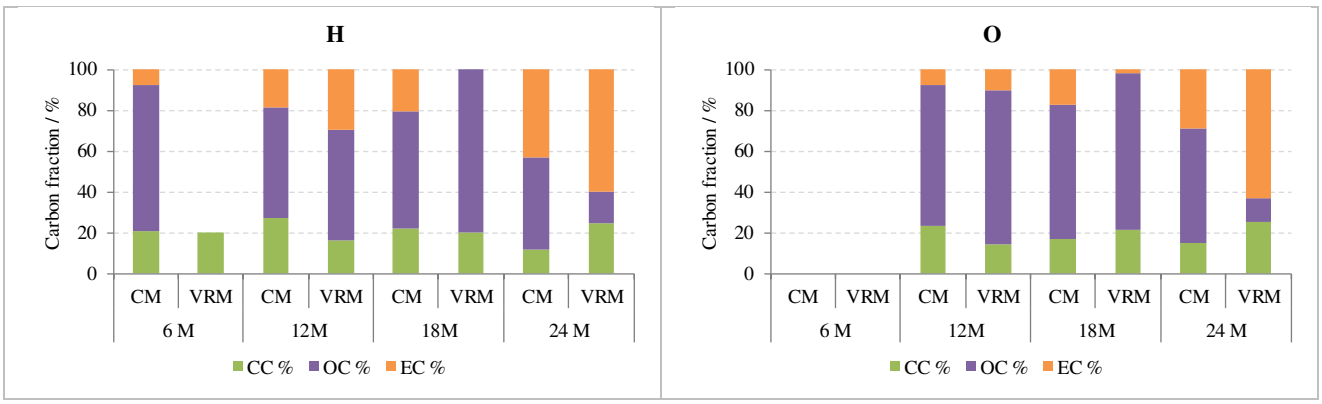

Figure 3.99 CC (green), OC (purple) and EC (orange) fractions calculated as percentages of TC measured in the material deposited on horizontal (H) and oblique (O) Carrara Marble (CM) and Verona Red Marble (VRM) stone samples exposed for 6, 12, 18 and 24 months in Ferrara. Carbon analysis was not possible for oblique samples exposed for 6 months.

Comparing the isotopic ratio assessed on horizontal samples at different exposure time (Figure 3.100), both lithotypes showed similar value of $\delta^{13}C_{TC}$ over time, slightly more positive in Carrara Marble samples (mean value: -19.8 ‰) than in Verona Red Marble ones (average: -21.0 ‰). Moreover, similarities among lithotypes over time were detected for $\delta^{13}C_{CC}$ (constant around 0.0 ‰), $\delta^{13}C_{OC}$ (mean value equals to -25.2 ‰ and -25.1 ‰ for marble and limestone, respectively) and $\delta^{13}C_{EC}$ (average value equals to -25.6 ‰ and -25.9 ‰ for marble and limestone, respectively).
$\delta^{13}C_{TC}$ measured in oblique samples were similar to those evaluated in horizontal specimens with mean values between -19.8 ‰ for marble and -21.3 ‰ for limestone samples. Also $\delta^{13}C_{CC}$ and $\delta^{13}C_{OC}$ remained stable over time and similar to those of horizontal specimens independently from the lithotype (around 0.0 ‰ and -25.5 ‰, respectively). However, $\delta^{13}C_{EC}$ showed differences based on stone type, reaching more positive values on marble samples (-20.0 ‰) than on limestone ones (-23.5 ‰).

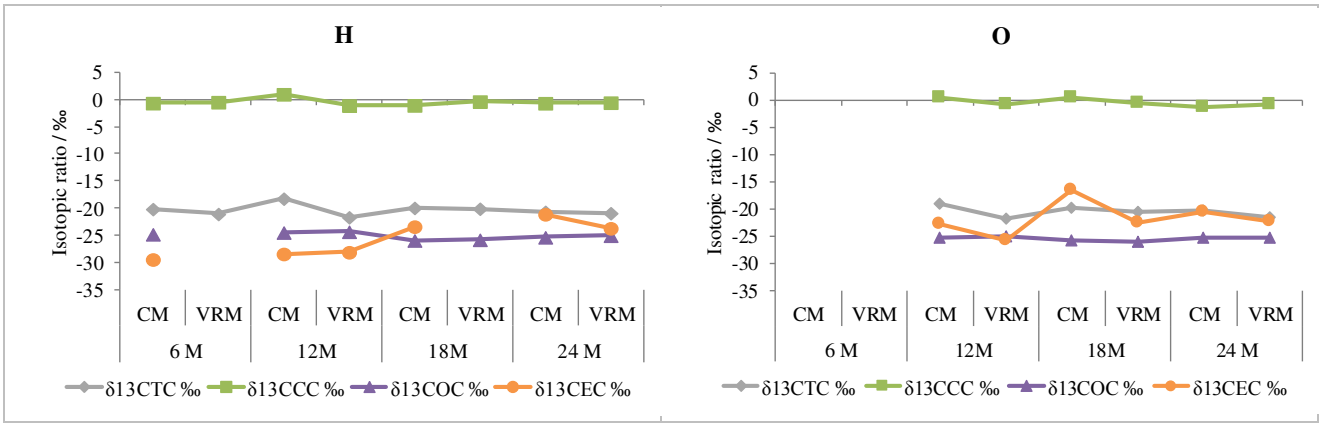

Figure 3.100 Isotopic ratio identified on the material collected from the exposed surface of Carrara Marble (CM) and Verona Red Marble (VRM) stone samples horizontally (H) and obliquely (O) exposed in Ferrara for 6, 12, 18 and 24 months. Grey rhombuses, green squares, purple triangles and orange circles represent respectively $\delta^{13}C_{TC}$, $\delta^{13}C_{CC}$, $\delta^{13}C_{OC}$ and $\delta^{13}C_{EC}$. Carbon analysis was not possible for oblique samples exposed for 6 months.

CONSIDERATIONS ABOUT ISOTOPIC RATIO

Relative proportion of stable carbon isotopes is different in each carbon reservoirs and thus it can provide useful information about the sources of emission of atmospheric aerosol. The carbon cycle involves active exchange of CO_2 among the atmosphere, terrestrial ecosystem and the surface of oceans. In general, $\delta^{13}C$ of the atmospheric CO_2 is around -8 ‰ but during photosynthesis, carbon fixed in plant tissue is significantly depleted in ^{13}C respect to the atmospheric value, leading the terrestrial biosphere to reach an average $\delta^{13}C$ of -26 ‰ (https://www.esrl.noaa.gov/). However, differences in carbon assimilation pathways in plants (i.e. C3- and C4-plants) cause a variation in $\delta^{13}C$. Most terrestrial plants are C3-plants and have a $\delta^{13}C$ between -30 ‰ and -20 ‰ while C4-plants (maize in temperate regions, aquatic plants, desert plants, salt marsh plants, and tropical grasses) are less depleted in ^{13}C, showing a $\delta^{13}C$ from -18 ‰ to -10 ‰ (Cachier, 1989). Therefore, combustion and biogenic emissions of these different group of plants produce aerosol with different $\delta^{13}C$ signatures.
Considering minerals, calcite is enriched in ^{13}C by around 10 ‰ respect to CO_2 at 20°C. As a consequence sedimentary carbonates normally have $\delta^{13}C$ values ranging from 0 ‰ to 1 ‰. Moreover, metamorphic processes normally cause a decrease in $\delta^{13}C$ values but carbonates retain the isotopic signature of the pre-metamorphic material (Salmimen, 2014).
Fossil fuels, which basically derive from ancient plants, display different $\delta^{13}C$ related to the $\delta^{13}C$ of the kerogen that depends on the types of organisms preserved and on the substrate on which was lain. So,

Widory (2006) studied the $\delta^{13}C$ in fossil fuel and combustibles used in Paris characterized by values between –25 ‰ to –23 ‰ for coal, between -29 ‰ and -26 ‰ for liquid fuels and between -40 ‰ and -28 ‰ for natural gas (composed by 90 % of methane and 8 % of ethane). However, the isotopic signature of the aerosol could be the same of the source but oxidation and aging of aerosol can provide isotopic changes (Figure 3.101). Compounds originated from oxidation processes are generally depleted in heavier isotopes (Martinsson et al., 2017 and related references). Furthermore, photochemical aging of organic aerosol leads to a loss of organic carbon from the particles and thus to a gradual enrichment in ^{13}C of the remaining aerosol phase (Mašalaitė et al., 2017).

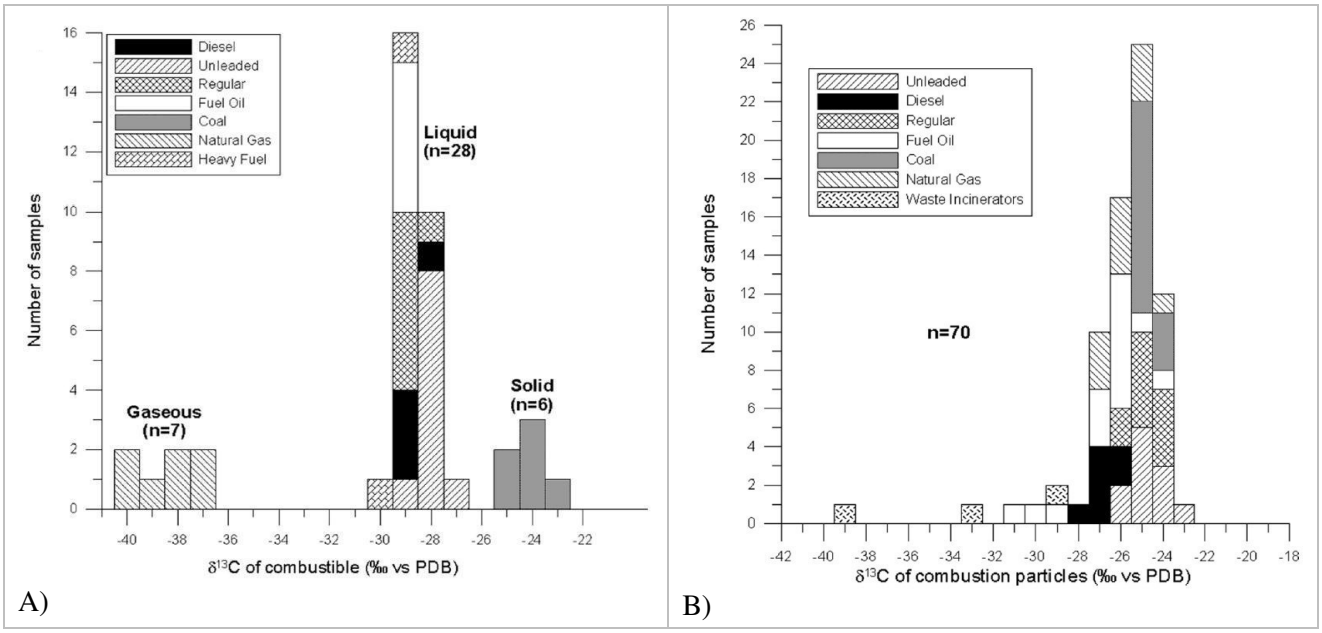

Figure 3.101 $\delta^{13}C$ distributions in fuels and combustibles (A) and of combustion particles (B). From Widory (2006).

Therefore, it is often difficult to assess the major sources of carbonaceous aerosol because there is a considerable overlap of $\delta^{13}C$ signatures within the sources of fossil fuel combustion even if liquid fuels and even more gaseous ones are more depleted than solid combustibles. Fossil fuel sources in turn overlap with the $\delta^{13}C$ values of C3 plants that are released as biogenic aerosol or from biomass burning.

Moreover, the provenance of fossil fuels resulted to have a great importance in indentify the related $\delta^{13}C$. Globally, $\delta^{13}C$ of crude petroleum shows fairly high degree of variability (between -19 ‰ and -35 ‰) depending on the geographic origin (Mašalaitė et al., 2012). For example, Eastern Europe reliant on Russian gasoline/diesel whose combustion emissions display a typical $\delta^{13}C$ (from -29 ‰ to -27 ‰) that differs from $\delta^{13}C$ typical of biomass burning (between -26 ‰ and -25‰). On contrast, Western Europe fuels are more enriched in heavier carbon isotopes (thus having more positive $\delta^{13}C$ value) than fuel of Russian origin as confirmed by $\delta^{13}C$ of diesel (-27 ‰) and unleaded gasoline (-25 ‰) particles measured in Paris by Widory (2006).

The study of carbon isotopic ratio of each carbon fraction is useful to distinguish the possible sources as EC is recognise to be a marker of incomplete combustion of fossil fuels and thus $\delta^{13}C_{EC}$ can be ascribable to fewer possible sources. On the contrary, higher uncertainty is found in identifying $\delta^{13}C_{OC}$ because OC may originate from a large number of factors such as various biogenic sources and combustion.

All these information obtained from literature help to recognise the likely sources of carbon fractions detected in different exposure sites over time. Concentrating upon CC, the related $\delta^{13}C$ ranged always around -0.3 ± 0.9 ‰, confirming the provenance from soil dust or stone substrate during the removal of deposited material.

$\delta^{13}C_{OC}$ remained constant in deposit collected from all samples independently from location and exposure time, showing a mean value of -25.5 ± 0.5 ‰. This means a temporal continuity of OC in all selected sites over time that suggest a significant contribution of vehicular traffic along with biogenic sources.
More discrepancies among sites are present for $\delta^{13}C_{EC}$. Bologna displayed a similar $\delta^{13}C_{EC}$ value both on horizontal and oblique samples over time (with exception after 24 months of exposure) and the related mean value is around -27.8 ± 1.9 ‰. Comparing with data acquired in literature, it could be related to a constant emission source such as traffic and in particular to diesel emissions. On contrast, Ferrara was characterised by a slight variation of $\delta^{13}C_{EC}$ over time with more positive values after 18 and 24 months of exposure. $\delta^{13}C_{EC}$ values detected from the deposit accumulated on horizontal and oblique specimens were between -29.5 ‰ and -16.6 ‰ with a mean value of -23.7 ± 3.8 ‰. Therefore, here the responsible combustion sources could be different (e.g. gasoline, diesel, natural gas and biomass burning) and it is difficult to discriminate. Finally, atmospheric material studied in Florence revealed differences among horizontal and oblique samples. $\delta^{13}C_{EC}$ analysed on horizontal specimens remained constant over time but was enriched in heavier carbon isotopes (mean value: -16.7 ± 1.6 ‰) respect to the average value assessed on oblique samples (-23.1 ± 3.2 ‰).

Final remarks:

- In general, the analysis of $TC_{surface}$ of material deposited on all Carrara Marble samples showed always the highest values in Ferrara specimens and the lowest ones in those exposed in Bologna. Moreover, a gradual increase over time of $TC_{surface}$ was identified in Ferrara and Florence samples.
- The percentage of each carbon fraction respect to TC measured in marble specimens highlights a general prevalence of NCC over CC. In particular, the concentration of OC almost always prevailed over that of EC as displayed also by OC/EC that ranged from 1 to 20.
- The comparison of carbon fractions detected on different kind of stone exposed in Ferrara displayed higher $TC_{surface}$ in Carrara Marble samples than in limestone specimens throughout the analysed period and independently from orientation. Both lithotypes showed an increasing trend over time both for horizontal and oblique specimens. In particular, NCC always prevailed over CC also for material accumulated on Verona Red Marble and it was commonly composed by prevailing OC over EC.
- The isotopic ratio of all analysed CC remained always constant around -0.3 ± 0.9 ‰, confirming the provenance of CC from soil dust or stone substrate. Also $\delta^{13}C_{OC}$ showed stable values (average equals to -25.5 ± 0.5 ‰) independently from location, lithotype and exposure time. Therefore, the continuity of OC in all selected sites over time suggests a significant contribution of vehicular traffic along with biogenic sources. Finally, more variety of $\delta^{13}C_{EC}$ among sites, exposure time and stones makes the distinction among combustion sources more difficult.

3.1.6. ENVIRONMENTAL SCANNING ELECTRON MICROSCOPY (ESEM-EDX)

Material deposited on the surface of stone samples exposed for 24 months in different exposure sites and with different orientation was analysed with Environmental Scanning Electron Microscopy equipped whit EDS x-ray microanalysis in order to identify its morphology and chemical composition.
Table 3.42 displays all analysed specimens and main results are reported hereafter.

SITE	SAMPLE	ORIENTATION
BOLOGNA	BCH16	Horizontal
	BCO6	Oblique
FERRARA	PTCH3	Horizontal
	PTCO7	Oblique
	PTCO19	Oblique - windowsill
	PTCV3	Vertical
	PTNH3	Horizontal
	PTNO17	Oblique
	PTNO19	Oblique - windowsill
FLORENCE	SMCH12	Horizontal
	SMCO11	Oblique
	SMCV4	Vertical

Table 3.42 Specimens, subdivided in different sites, examined with ESEM-EDX.

<u>BOLOGNA</u>

The observation was concentrated upon horizontal and oblique samples as there was enough material for the analysis. In general, assessment of material deposited on samples exposed in Bologna revealed the prevalence of soil and mineral dust particles along with biological particles (Figure 3.102 A).
Among inorganic material, mineral particles of different composition were observed in all analysed samples, showing higher dimension (up to 70 μm) in horizontal sample. This is possible because coarse particles are preferably deposited by gravitational settling that affects mainly horizontal surface. Most of these particles are composed by Si, Al, K and Na, as shown in Figures 3.102 B-3.104.

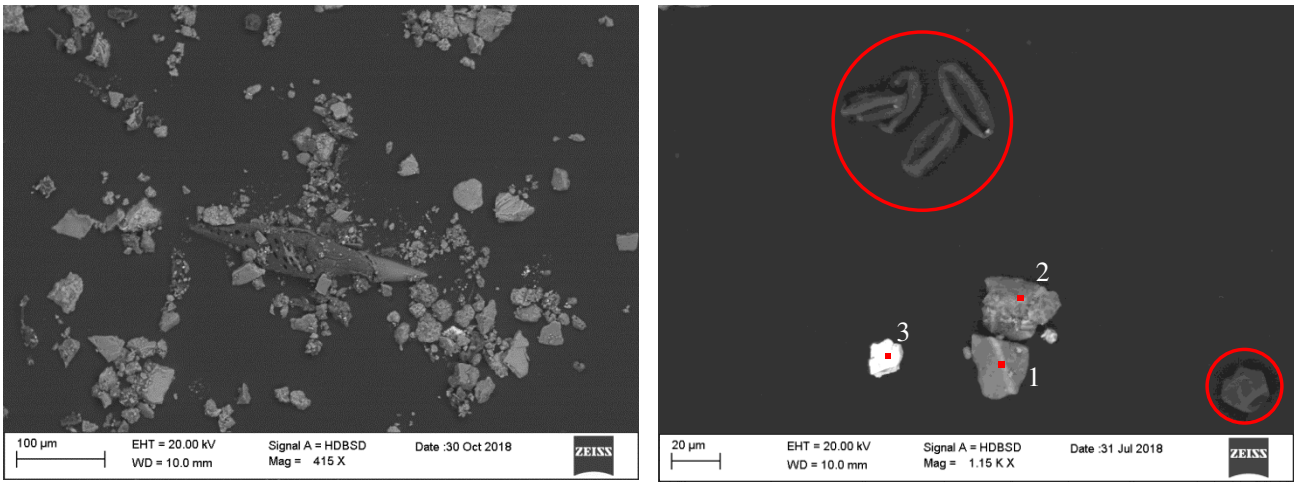

A) B)

Figure 3.102 ESEM photomicroghraph of portion of material deposited on BCH16 sample. A) Overview of a portion of deposited material with a big (250 µm long), pointed biological particle in the centre surrounded by inorganic particles. B) Biological particles (probably pollens) are encircled. Numbered particles are inorganic, mineral fragments. Red dots represent the points of EDS analysis.

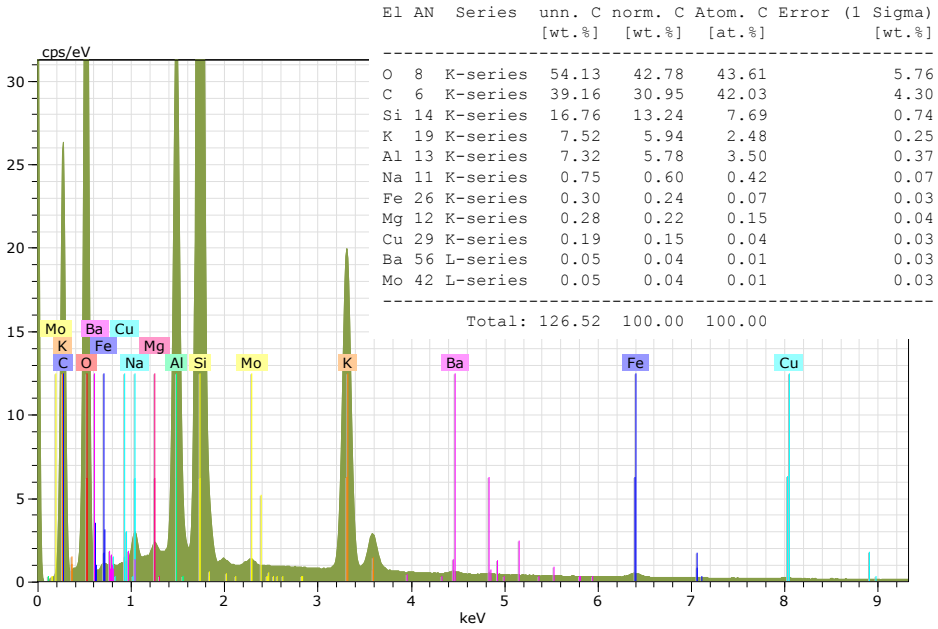

El	AN	Series	unn. C [wt.%]	norm. C [wt.%]	Atom. C [at.%]	Error (1 Sigma) [wt.%]
O	8	K-series	54.13	42.78	43.61	5.76
C	6	K-series	39.16	30.95	42.03	4.30
Si	14	K-series	16.76	13.24	7.69	0.74
K	19	K-series	7.52	5.94	2.48	0.25
Al	13	K-series	7.32	5.78	3.50	0.37
Na	11	K-series	0.75	0.60	0.42	0.07
Fe	26	K-series	0.30	0.24	0.07	0.03
Mg	12	K-series	0.28	0.22	0.15	0.04
Cu	29	K-series	0.19	0.15	0.04	0.03
Ba	56	L-series	0.05	0.04	0.01	0.03
Mo	42	L-series	0.05	0.04	0.01	0.03
		Total:	126.52	100.00	100.00	

Figure 3.103 ESEM-EDS spectrum of point 1 shown in Figure 3.102B.

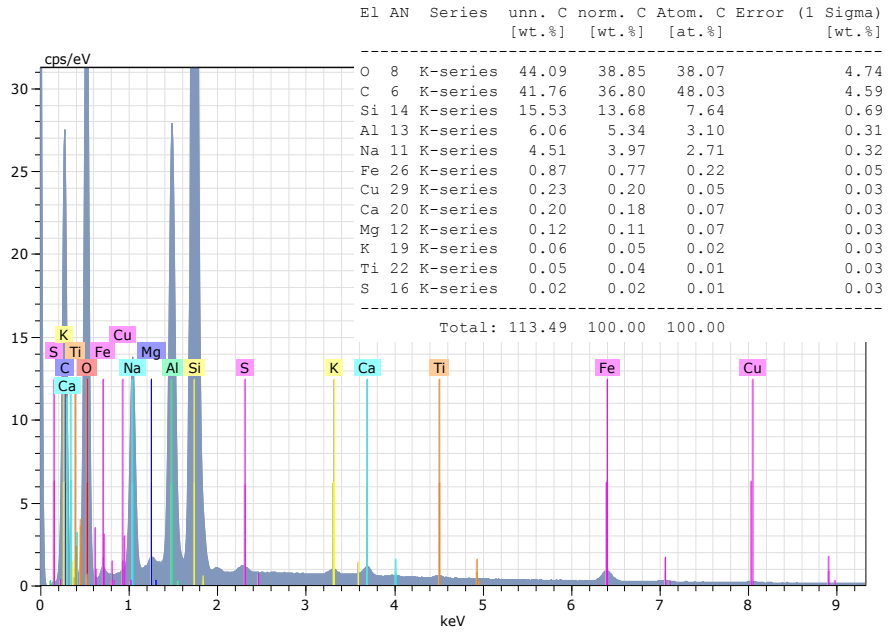

El	AN	Series	unn. C [wt.%]	norm. C [wt.%]	Atom. C [at.%]	Error (1 Sigma) [wt.%]
O	8	K-series	44.09	38.85	38.07	4.74
C	6	K-series	41.76	36.80	48.03	4.59
Si	14	K-series	15.53	13.68	7.64	0.69
Al	13	K-series	6.06	5.34	3.10	0.31
Na	11	K-series	4.51	3.97	2.71	0.32
Fe	26	K-series	0.87	0.77	0.22	0.05
Cu	29	K-series	0.23	0.20	0.05	0.03
Ca	20	K-series	0.20	0.18	0.07	0.03
Mg	12	K-series	0.12	0.11	0.07	0.03
K	19	K-series	0.06	0.05	0.02	0.03
Ti	22	K-series	0.05	0.04	0.01	0.03
S	16	K-series	0.02	0.02	0.01	0.03
Total:			113.49	100.00	100.00	

Figure 3.104 ESEM-EDS spectrum of point 2 shown in Figure 3.102B.

Among other mineral fragments, also barium sulphate was identified (Figures 3.102 B, 3.105), probably deriving from hills surrounding Bologna.

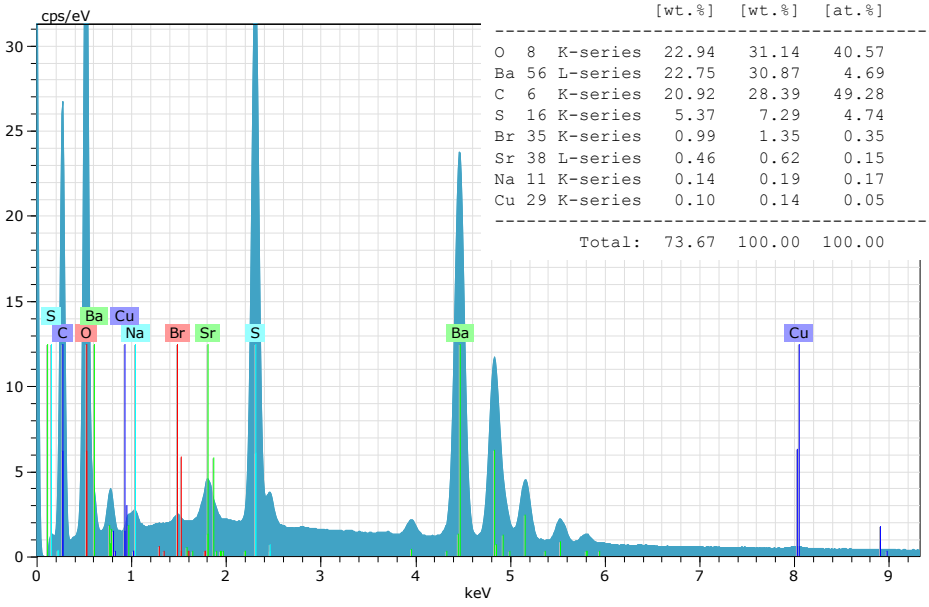

El	AN	Series	unn. C [wt.%]	norm. C [wt.%]	Atom. C [at.%]	Error (1 Sigma) [wt.%]
O	8	K-series	22.94	31.14	40.57	2.46
Ba	56	L-series	22.75	30.87	4.69	0.65
C	6	K-series	20.92	28.39	49.28	2.29
S	16	K-series	5.37	7.29	4.74	0.22
Br	35	K-series	0.99	1.35	0.35	0.06
Sr	38	L-series	0.46	0.62	0.15	0.04
Na	11	K-series	0.14	0.19	0.17	0.03
Cu	29	K-series	0.10	0.14	0.05	0.03
Total:			73.67	100.00	100.00	

Figure 3.105 ESEM-EDS spectrum of point 3 shown in Figure 3.102 B.

Furthermore, microscopic observation allowed to detect the presence of aggregated material of small dimension (from 20 µm to submicrometers) that consist of a mixture of mineral fragments (e.g. aluminosilicates and carbonates) deriving from soil dust (Figures 3.106-3.109).

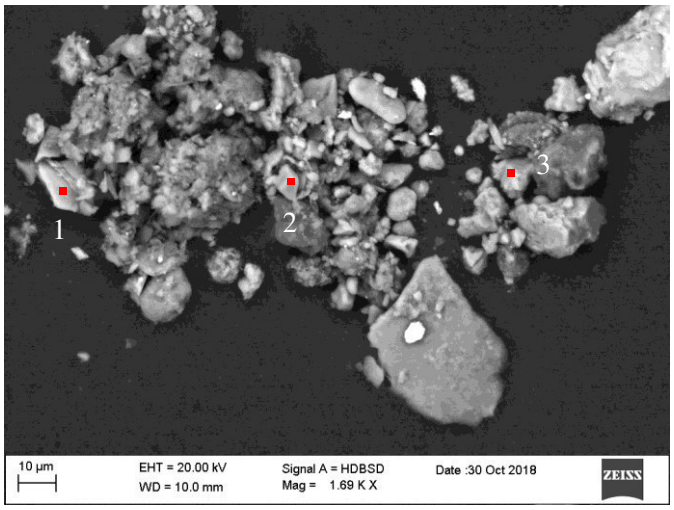

Figure 3.106 ESEM photomicroghraph of aggregated material deposited on BCH16 sample. Red dots represent the points of EDS analysis.

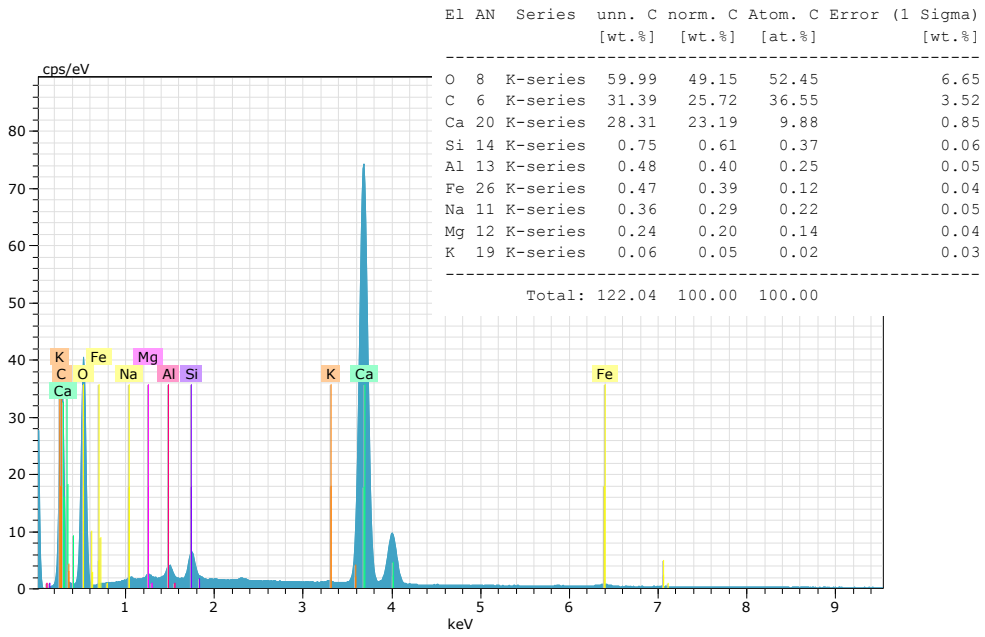

El	AN	Series	unn. C [wt.%]	norm. C [wt.%]	Atom. C [at.%]	Error (1 Sigma) [wt.%]
O	8	K-series	59.99	49.15	52.45	6.65
C	6	K-series	31.39	25.72	36.55	3.52
Ca	20	K-series	28.31	23.19	9.88	0.85
Si	14	K-series	0.75	0.61	0.37	0.06
Al	13	K-series	0.48	0.40	0.25	0.05
Fe	26	K-series	0.47	0.39	0.12	0.04
Na	11	K-series	0.36	0.29	0.22	0.05
Mg	12	K-series	0.24	0.20	0.14	0.04
K	19	K-series	0.06	0.05	0.02	0.03
		Total:	122.04	100.00	100.00	

Figure 3.107 ESEM-EDS spectrum of point 1 shown in Figure 3.106.

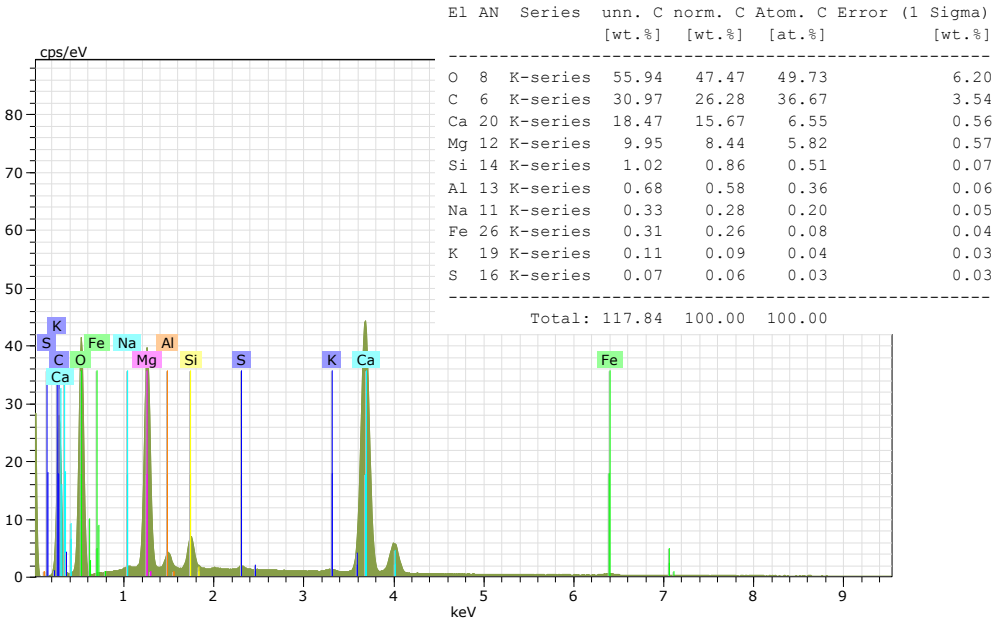

El	AN	Series	unn. C [wt.%]	norm. C [wt.%]	Atom. C [at.%]	Error (1 Sigma) [wt.%]
O	8	K-series	55.94	47.47	49.73	6.20
C	6	K-series	30.97	26.28	36.67	3.54
Ca	20	K-series	18.47	15.67	6.55	0.56
Mg	12	K-series	9.95	8.44	5.82	0.57
Si	14	K-series	1.02	0.86	0.51	0.07
Al	13	K-series	0.68	0.58	0.36	0.06
Na	11	K-series	0.33	0.28	0.20	0.05
Fe	26	K-series	0.31	0.26	0.08	0.04
K	19	K-series	0.11	0.09	0.04	0.03
S	16	K-series	0.07	0.06	0.03	0.03
Total:			117.84	100.00	100.00	

Figure 3.108 ESEM-EDS spectrum of point 2 shown in Figure 3.106.

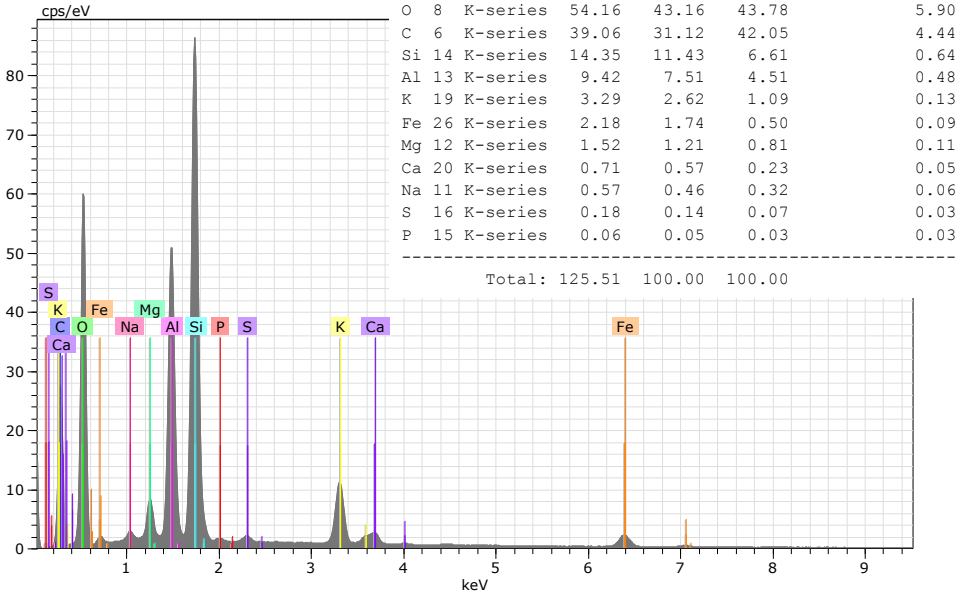

El	AN	Series	unn. C [wt.%]	norm. C [wt.%]	Atom. C [at.%]	Error (1 Sigma) [wt.%]
O	8	K-series	54.16	43.16	43.78	5.90
C	6	K-series	39.06	31.12	42.05	4.44
Si	14	K-series	14.35	11.43	6.61	0.64
Al	13	K-series	9.42	7.51	4.51	0.48
K	19	K-series	3.29	2.62	1.09	0.13
Fe	26	K-series	2.18	1.74	0.50	0.09
Mg	12	K-series	1.52	1.21	0.81	0.11
Ca	20	K-series	0.71	0.57	0.23	0.05
Na	11	K-series	0.57	0.46	0.32	0.06
S	16	K-series	0.18	0.14	0.07	0.03
P	15	K-series	0.06	0.05	0.03	0.03
Total:			125.51	100.00	100.00	

Figure 3.109 ESEM-EDS spectrum of point 3 shown in Figure 3.106.

In addition, fly-ash (Figure 3.112) and iron-rich (Figure 3.111) particles were also identified (Figure 3.110). Both have a spherical shape but fly-ash particles have a smooth surface and are composed mainly of silicon and aluminium with minor amounts of Mg, Fe, Ti and S (Figure 3.11). They are representative of coal, wood and oil combustion (Ausset et al., 1998; Urosevic et al., 2012; Bonazza and Sabbioni, 2016). The detected iron-rich particles had different dimension (from less than 2 µm till to 10 µm), a dendritic surface (Figure 3.113) and a composition made mainly of Fe with the presence also of other metals (e.g. Zn, Cu, Mn, Cr) (Figures 3.111, 3.115). Fe-rich particles can be related to combustion processes of fossil fuels or emissions from metallurgical high temperature processes (Esbert et al., 2001; Weinbruch et al., 2014).

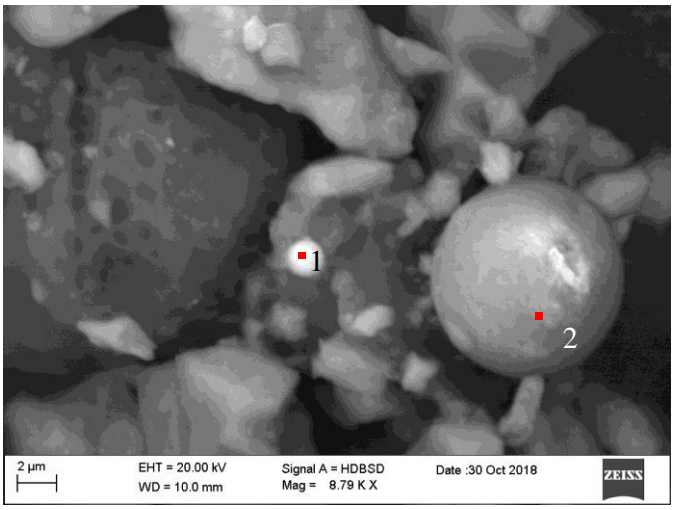

Figure 3.110 ESEM photomicroghraph of material deposited on BCH16 sample. Particle 1 and 2 are Fe-rich and fly-ash particles, respectively. Red dots represent the points of EDS analysis.

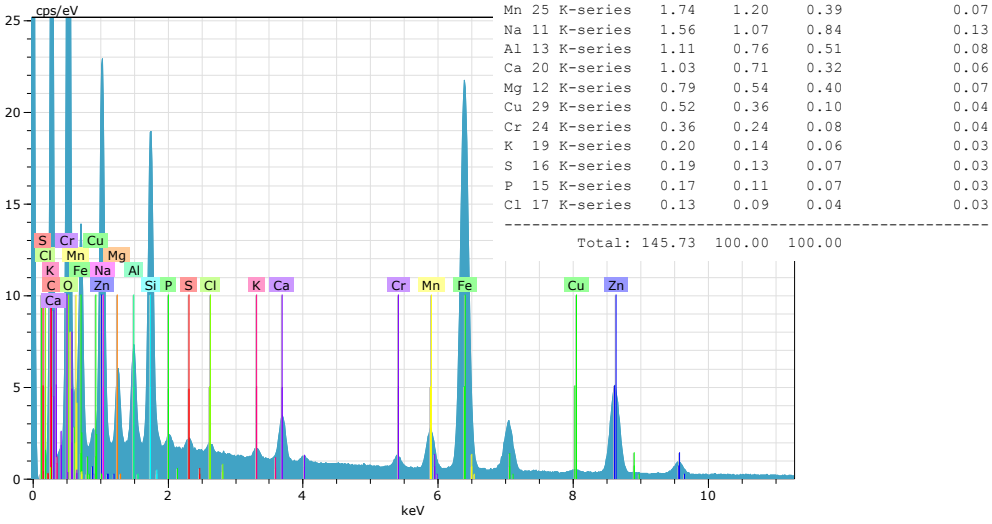

El	AN	Series	unn. C [wt.%]	norm. C [wt.%]	Atom. C [at.%]	Error (1 Sigma) [wt.%]
C	6	K-series	48.95	33.59	50.35	5.46
O	8	K-series	48.67	33.40	37.58	5.33
Fe	26	K-series	23.17	15.90	5.13	0.64
Zn	30	K-series	13.89	9.53	2.62	0.41
Si	14	K-series	3.24	2.23	1.43	0.16
Mn	25	K-series	1.74	1.20	0.39	0.07
Na	11	K-series	1.56	1.07	0.84	0.13
Al	13	K-series	1.11	0.76	0.51	0.08
Ca	20	K-series	1.03	0.71	0.32	0.06
Mg	12	K-series	0.79	0.54	0.40	0.07
Cu	29	K-series	0.52	0.36	0.10	0.04
Cr	24	K-series	0.36	0.24	0.08	0.04
K	19	K-series	0.20	0.14	0.06	0.03
S	16	K-series	0.19	0.13	0.07	0.03
P	15	K-series	0.17	0.11	0.07	0.03
Cl	17	K-series	0.13	0.09	0.04	0.03
		Total:	145.73	100.00	100.00	

Figure 3.111 ESEM-EDS spectrum of point 1 shown in Figure 3.110.

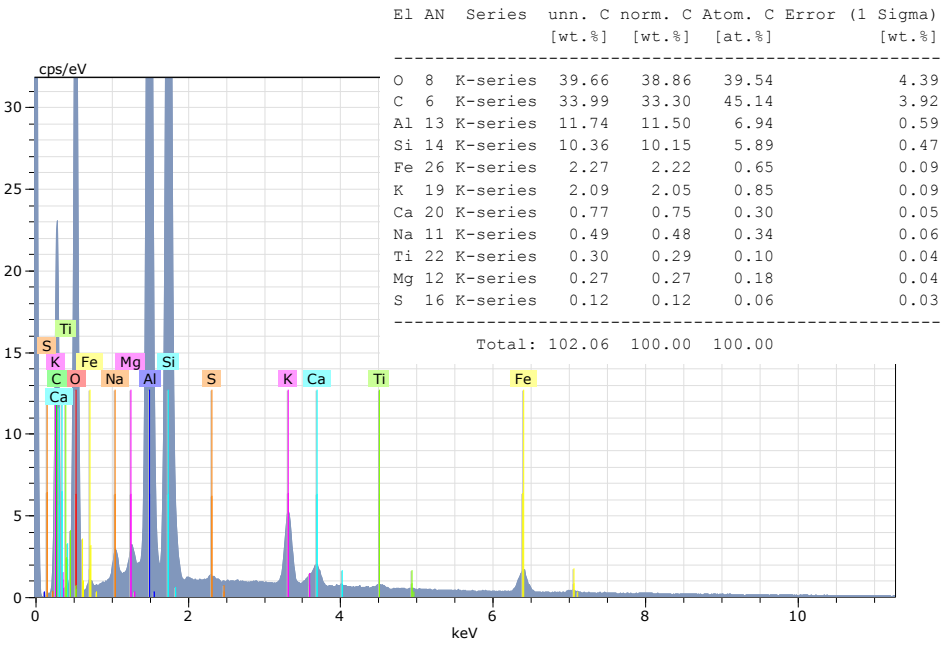

El	AN	Series	unn. C [wt.%]	norm. C [wt.%]	Atom. C [at.%]	Error (1 Sigma) [wt.%]
O	8	K-series	39.66	38.86	39.54	4.39
C	6	K-series	33.99	33.30	45.14	3.92
Al	13	K-series	11.74	11.50	6.94	0.59
Si	14	K-series	10.36	10.15	5.89	0.47
Fe	26	K-series	2.27	2.22	0.65	0.09
K	19	K-series	2.09	2.05	0.85	0.09
Ca	20	K-series	0.77	0.75	0.30	0.05
Na	11	K-series	0.49	0.48	0.34	0.06
Ti	22	K-series	0.30	0.29	0.10	0.04
Mg	12	K-series	0.27	0.27	0.18	0.04
S	16	K-series	0.12	0.12	0.06	0.03
		Total:	102.06	100.00	100.00	

Figure 3.112 ESEM-EDS spectrum of point 2 shown in Figure 3.110.

Furthermore, Fe-rich particle was also detected together with carbonaceous particle (Figures 3.113-3.115). This last had a sub-spherical porous surface with circular pores and was mainly composed by C (Figure 3.114). Carbonaceous particles are mostly related to oil or distilled oil combustion in domestic heating systems and electric power plants (Sabbioni, 1995) and to vehicle exhaust (Chabas and Lefevre, 2000).

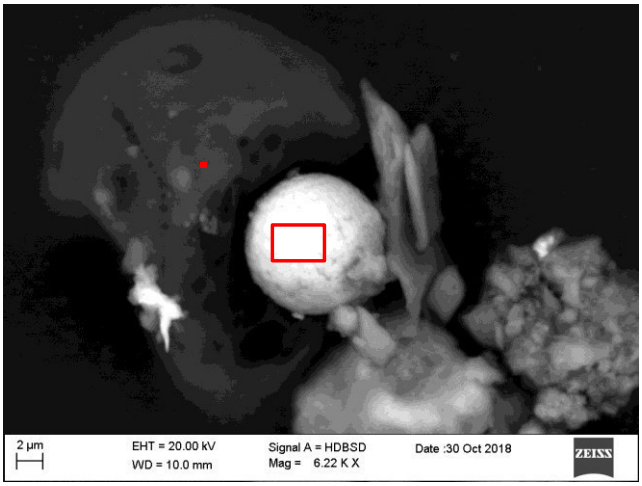

Figure 3.113 ESEM photomicroghraph of material deposited on BCH16 sample. On the left there is a carbonaceous particle with a spongy structure while in the centre a Fe-rich particle with dendritic surface. Red dot and red rectangle represent areas of EDS analysis.

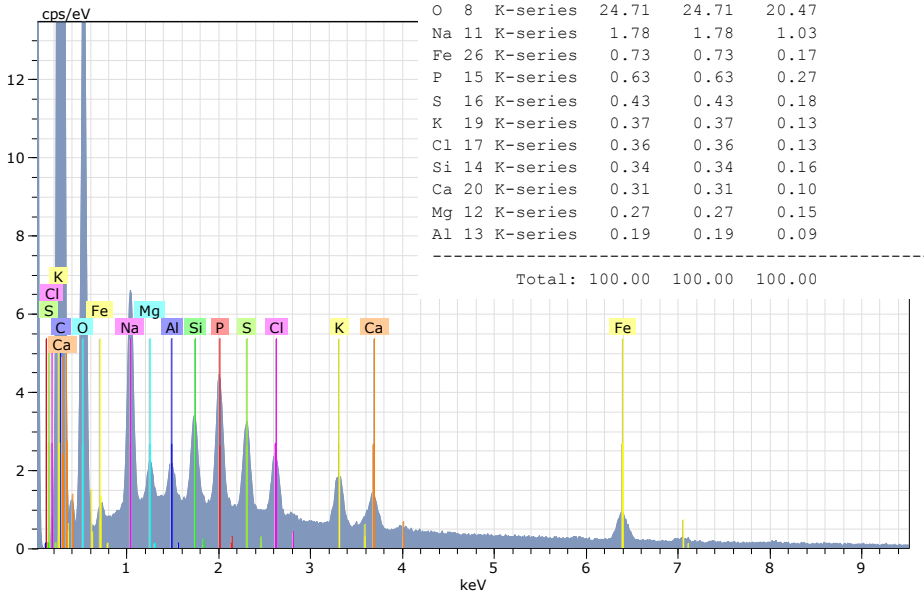

El	AN	Series	unn. C [wt.%]	norm. C [wt.%]	Atom. C [at.%]	Error (1 Sigma) [wt.%]
C	6	K-series	69.88	69.88	77.12	7.51
O	8	K-series	24.71	24.71	20.47	2.92
Na	11	K-series	1.78	1.78	1.03	0.14
Fe	26	K-series	0.73	0.73	0.17	0.05
P	15	K-series	0.63	0.63	0.27	0.05
S	16	K-series	0.43	0.43	0.18	0.04
K	19	K-series	0.37	0.37	0.13	0.04
Cl	17	K-series	0.36	0.36	0.13	0.04
Si	14	K-series	0.34	0.34	0.16	0.04
Ca	20	K-series	0.31	0.31	0.10	0.04
Mg	12	K-series	0.27	0.27	0.15	0.04
Al	13	K-series	0.19	0.19	0.09	0.03
		Total:	100.00	100.00	100.00	

Figure 3.114 ESEM-EDS spectrum of point shown in Figure 3.113.

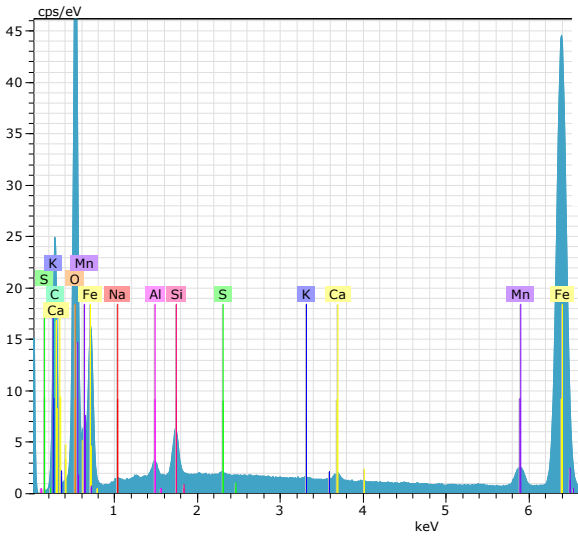

El	AN	Series	unn. C [wt.%]	norm. C [wt.%]	Atom. C [at.%]	Error (1 Sigma) [wt.%]
Fe	26	K-series	45.24	39.13	14.23	1.22
O	8	K-series	39.72	34.36	43.60	4.35
C	6	K-series	27.98	24.20	40.91	3.22
Mn	25	K-series	1.37	1.19	0.44	0.06
Si	14	K-series	0.68	0.59	0.42	0.05
Al	13	K-series	0.24	0.21	0.16	0.04
Na	11	K-series	0.18	0.15	0.14	0.04
Ca	20	K-series	0.11	0.10	0.05	0.03
S	16	K-series	0.05	0.05	0.03	0.03
K	19	K-series	0.04	0.03	0.02	0.03
		Total:	115.60	100.00	100.00	

Figure 3.115 ESEM-EDS spectrum of area shown in Figure 3.113.

Among biological particles, many spherical/sub-spherical pollens were observed (Figures 3.102 B, 3.116 A) while elongated, 15 µm length carbon-rich, clud-shaped particles may be identified as *Alteraria* spores (Figure 3.116 B).

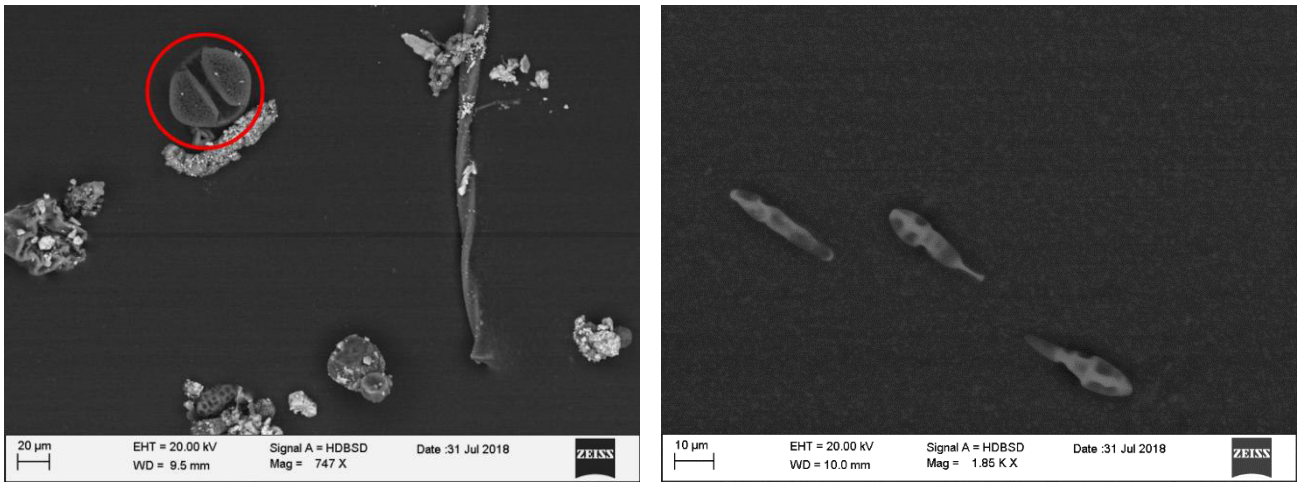

A) B)

Figure 3.116 ESEM photomicroghraph of portion of material deposited on BCO6 (A) and BCH16 (B) samples. A) Red circle highlights the presence of a Pinaceae pollen. B) Biological particles likely recognised as Alternaria spores.

Finally, many well-formed, cubic, small (each face around 2 µm long or smaller) salt particles were observed in the material collected from oblique sample (Figures 3.117-3.120). Cubic shape suggests that they probably were halite crystals and chemical analysis confirmed their Na- and Cl-rich composition. Salt particles were found on the surface of soil dust fragments, suggesting their provenance from atmospheric transport as sea spray or de-icing salt. It has to be considered that Bologna can rarely be reached by marine air masses (more frequently in wintertime) because of its distance from the coast (> 100 km) and the weak circulation of this region. Therefore, Tositti et al. (2014) attributed the seasalt component detected in Bologna during another monitoring campaign mostly to de-icing salts. Furthermore, Peré-Trepat et al. (2007) found that de-icing salts have higher dimension than marine salt and that the first one can be observed togheter with crustal elements that identify the sand commonly spread with the salt.

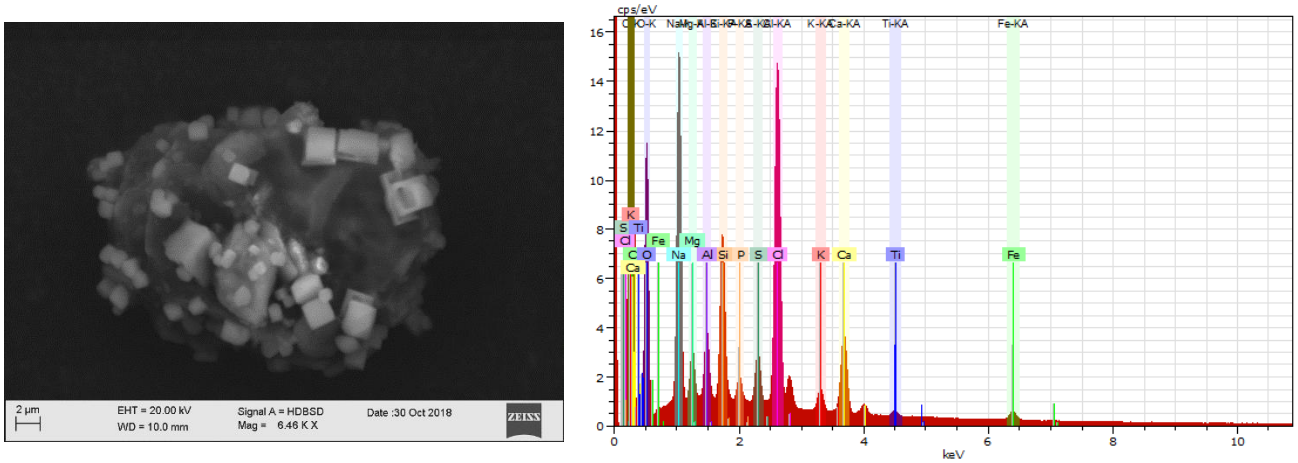

Figure 3.117 ESEM photomicroghraph of portion of material deposited on BCO6 with related ESEM-EDS spectrum. Lighter cubic particles are NaCl crystals.

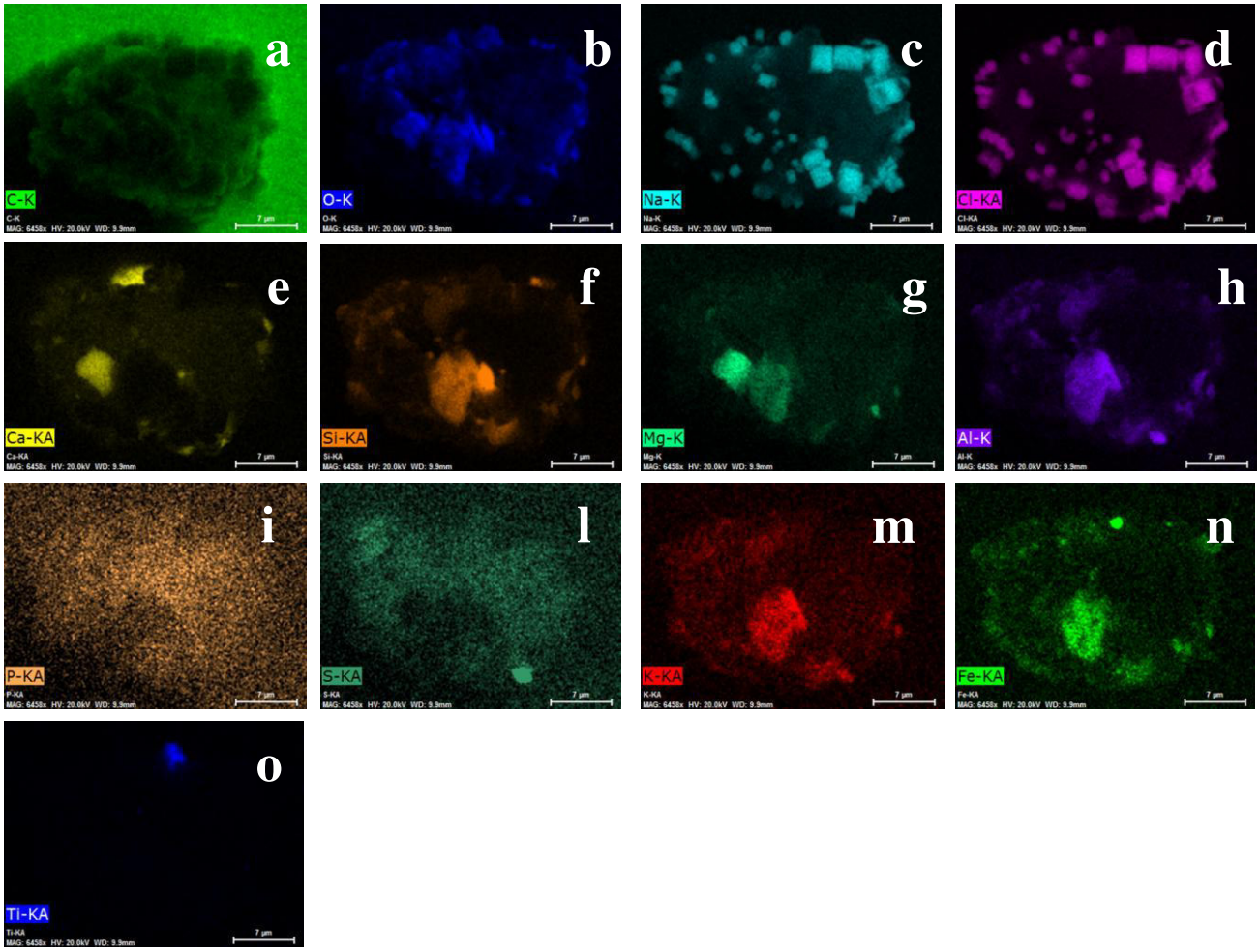

Figure 3.118 Photomicrographs of BCO6 sample representing the EDS-maps analyses carried out on the area shown in Figure 3.117: a. EDS-map of C; b. EDS map of O; c. EDS map of Na; d. EDS map of Cl; e. EDS map of Ca; f. EDS map of Si; g. EDS map of Mg; h. EDS map of Al; i. EDS map of P; l. EDS map of S; m. EDS map of K; n. EDS map of Fe; o. EDS map of Ti.

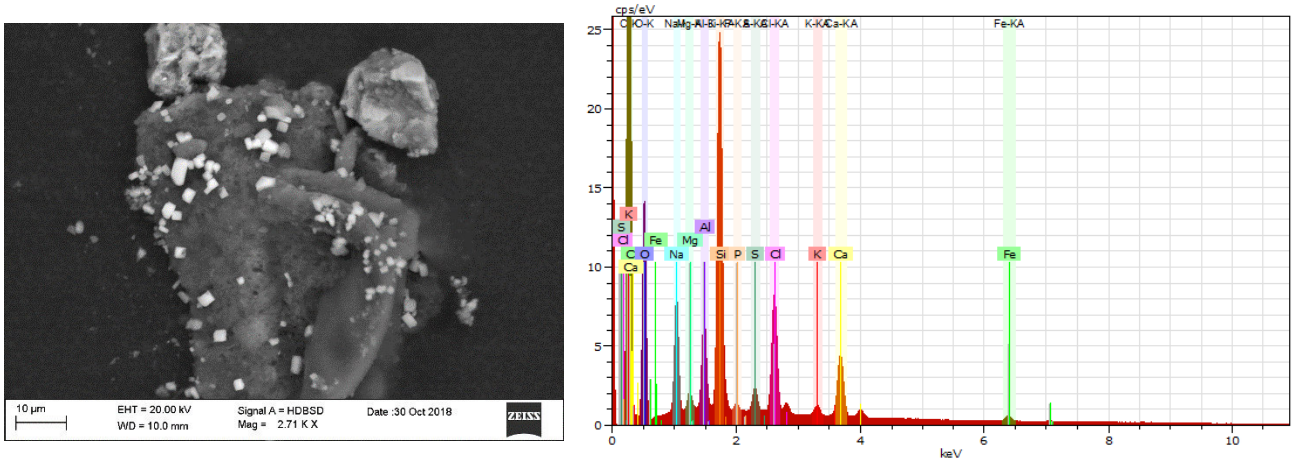

Figure 3.119 ESEM photomicroghraph of portion of material deposited on BCO6 with related ESEM-EDS spectrum. Lighter cubic NaCl crystals are attached on the surface of Si-rich particle.

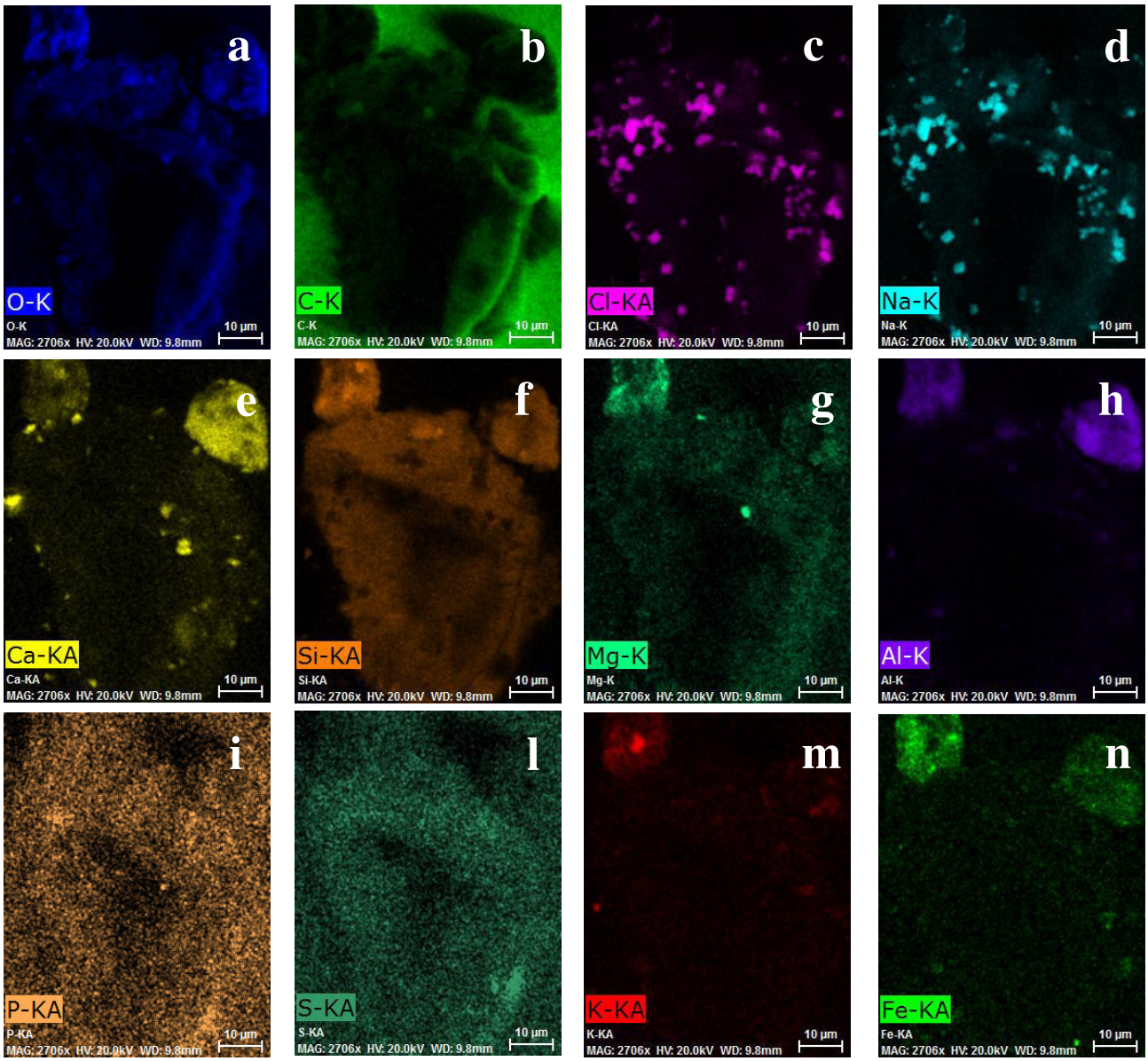

Figure 3.120 Photomicrographs of BCO6 sample representing the EDS-maps analyses carried out on the area shown in Figure 3.119: a. EDS-map of C; b. EDS map of O; c. EDS map of Cl; d. EDS map of Na; e. EDS map of Ca; f. EDS map of Si; g. EDS map of Mg; h. EDS map of Al; i. EDS map of P; l. EDS map of S; m. EDS map of K; n. EDS map of Fe.

FERRARA

Observation of material deposited on the surface of samples exposed in Ferrara displayed a conspicuous presence of biogenic particles, mineral fragments and soil dust aggregates.

The analysis of a portion of the material accumulated on horizontal Carrara Marble sample (Figure 3.121) showed prevailing carbonates and aluminosilicates, typical components of soil dust (Figure 3.122). In addition, spherical metal oxide particles (Fe-rich) of different dimension (from 1 µm to 12 µm) were also detected (Figure 3.122), proving emissions from anthropogenic sources.

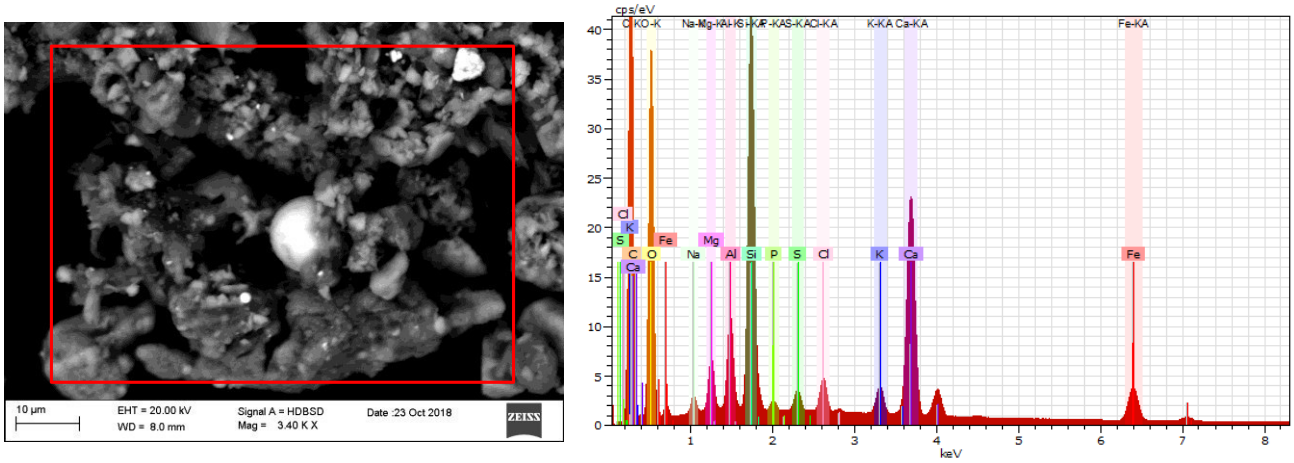

Figure 3.121 ESEM photomicroghraph of portion of material deposited on PTCH3 with related ESEM-EDS spectrum. Besides aluminosilicates and carbonates a spherical iron oxide particle is detectable in the centre. Red rectangle shows the area subjected to EDS-maps.

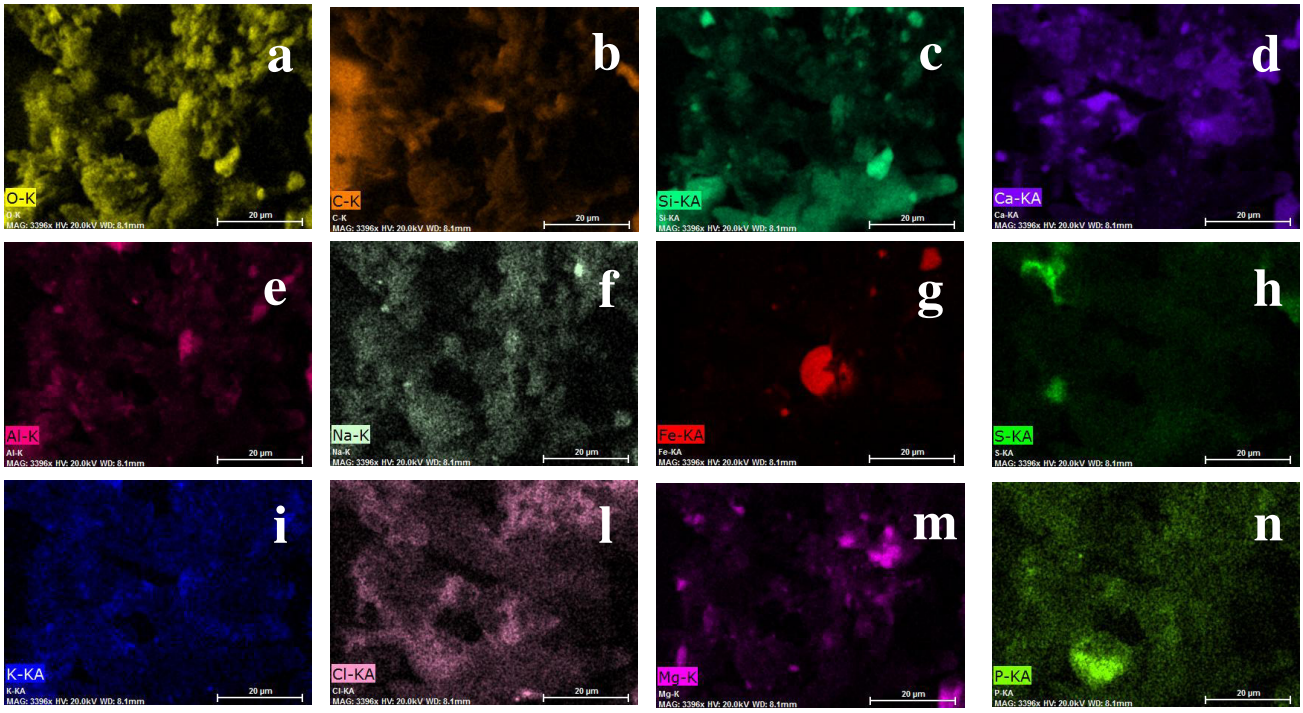

Figure 3.122 Photomicrographs of PTCH3 sample representing the EDS-maps analyses carried out on the area shown in Figure 3.121: a. EDS-map of O; b. EDS map of C; c. EDS map of Si; d. EDS map of Ca; e. EDS map of Al; f. EDS map of Na; g. EDS map of Fe; h. EDS map of S; i.. EDS map of K; l. EDS map of Cl; m. EDS map of Mg; n. EDS map of P.

Small fragments of minerals and metallic particles were detected as assembled material also on oblique samples exposed on windowsill, sometimes having a spherical shape probably induce by wind rolling (Figure 3.123).

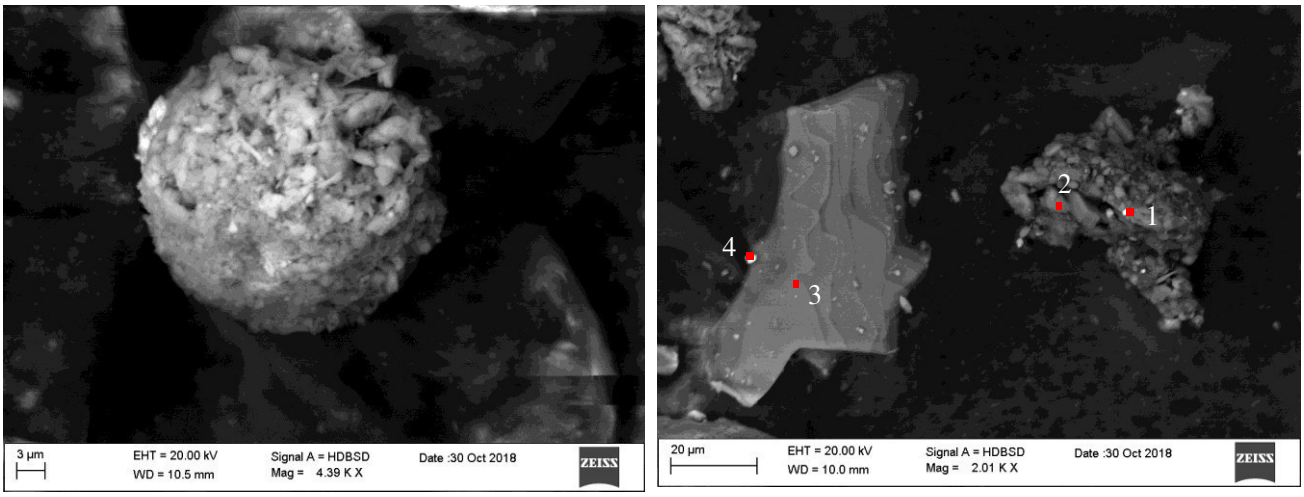

A) B)

Figure 123 ESEM photomicroghraph of portion of material deposited on PTCO19 sample. A) Spherical aggregate material. B) Laminated mineral fragment on the left and aggregate material on the right. Red dots represent the points of EDS analysis.

Chemical analysis of another examples of these aggregated materials confirms the presence of carbonate (in this case calcium carbonate but mixed Mg and Ca carbonate was also identified) as well as Fe-rich particles with irregular shape deriving from soil dust (Figures 3.124, 3.125).

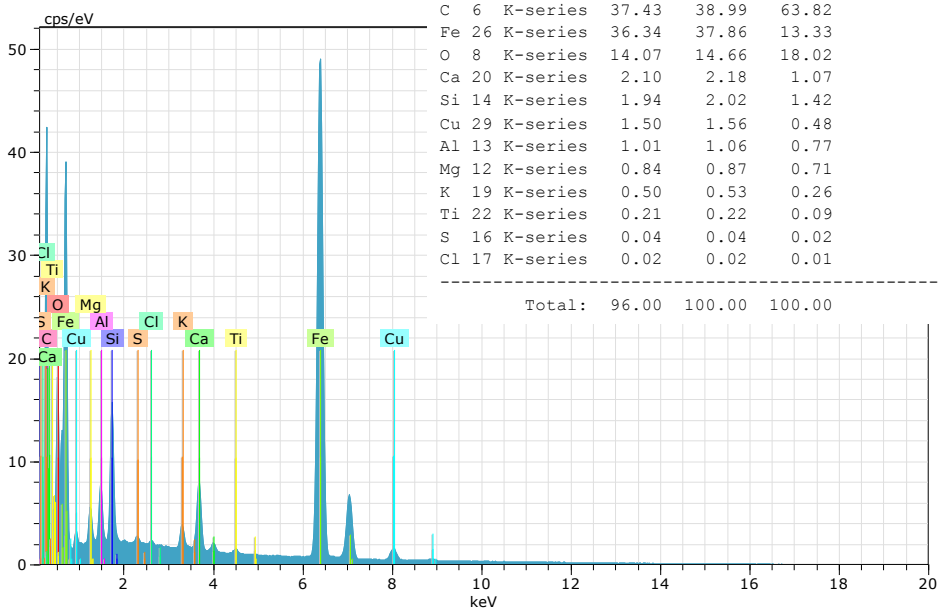

El	AN	Series	unn. C [wt.%]	norm. C [wt.%]	Atom. C [at.%]	Error (1 Sigma) [wt.%]
C	6	K-series	37.43	38.99	63.82	4.15
Fe	26	K-series	36.34	37.86	13.33	0.99
O	8	K-series	14.07	14.66	18.02	1.64
Ca	20	K-series	2.10	2.18	1.07	0.09
Si	14	K-series	1.94	2.02	1.42	0.11
Cu	29	K-series	1.50	1.56	0.48	0.07
Al	13	K-series	1.01	1.06	0.77	0.07
Mg	12	K-series	0.84	0.87	0.71	0.07
K	19	K-series	0.50	0.53	0.26	0.04
Ti	22	K-series	0.21	0.22	0.09	0.03
S	16	K-series	0.04	0.04	0.02	0.03
Cl	17	K-series	0.02	0.02	0.01	0.03
		Total:	96.00	100.00	100.00	

Figure 3.124 ESEM-EDS spectrum of point 1 shown in Figure 3.123 B.

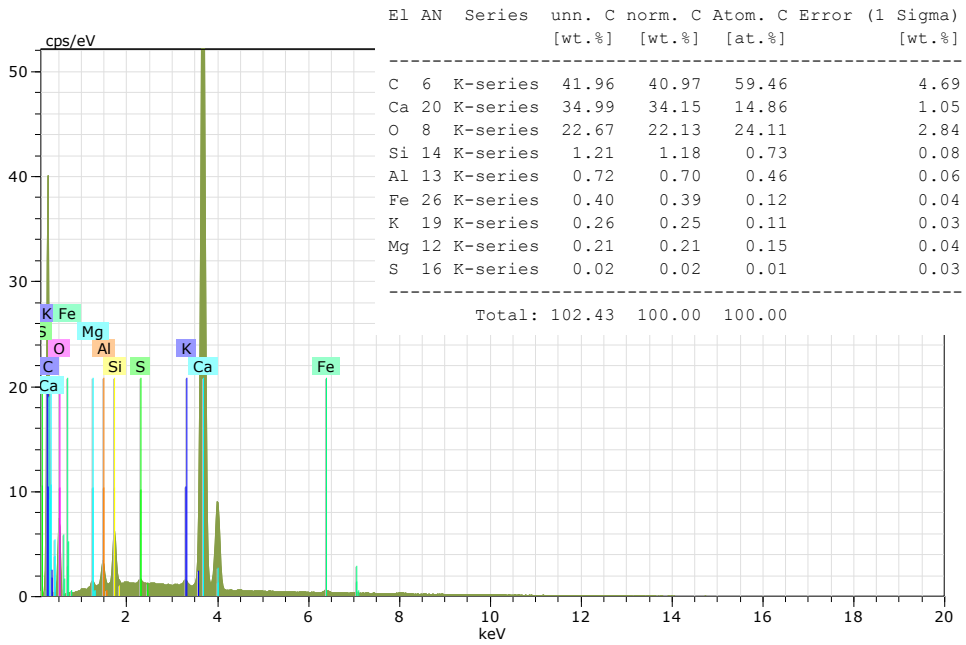

El	AN	Series	unn. C [wt.%]	norm. C [wt.%]	Atom. C [at.%]	Error (1 Sigma) [wt.%]
C	6	K-series	41.96	40.97	59.46	4.69
Ca	20	K-series	34.99	34.15	14.86	1.05
O	8	K-series	22.67	22.13	24.11	2.84
Si	14	K-series	1.21	1.18	0.73	0.08
Al	13	K-series	0.72	0.70	0.46	0.06
Fe	26	K-series	0.40	0.39	0.12	0.04
K	19	K-series	0.26	0.25	0.11	0.03
Mg	12	K-series	0.21	0.21	0.15	0.04
S	16	K-series	0.02	0.02	0.01	0.03
Total:			102.43	100.00	100.00	

Figure 3.125 ESEM-EDS spectrum of point 2 shown in Figure 3.123 B.

Figure 3.123 B displays the presence also of a phyllosilicate 82 µm long, composed mainly by Al, Si and K and a small pyrite (Figures 3.126, 3.127).

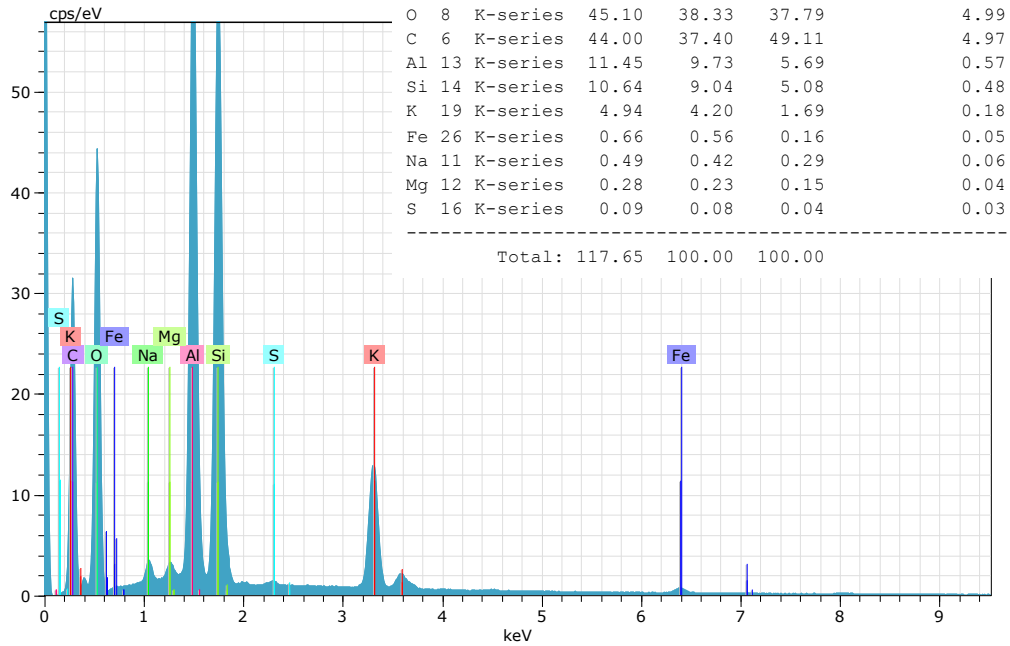

El	AN	Series	unn. C [wt.%]	norm. C [wt.%]	Atom. C [at.%]	Error (1 Sigma) [wt.%]
O	8	K-series	45.10	38.33	37.79	4.99
C	6	K-series	44.00	37.40	49.11	4.97
Al	13	K-series	11.45	9.73	5.69	0.57
Si	14	K-series	10.64	9.04	5.08	0.48
K	19	K-series	4.94	4.20	1.69	0.18
Fe	26	K-series	0.66	0.56	0.16	0.05
Na	11	K-series	0.49	0.42	0.29	0.06
Mg	12	K-series	0.28	0.23	0.15	0.04
S	16	K-series	0.09	0.08	0.04	0.03
Total:			117.65	100.00	100.00	

Figure 3.126 ESEM-EDS spectrum of point 3 shown in Figure 3.123 B.

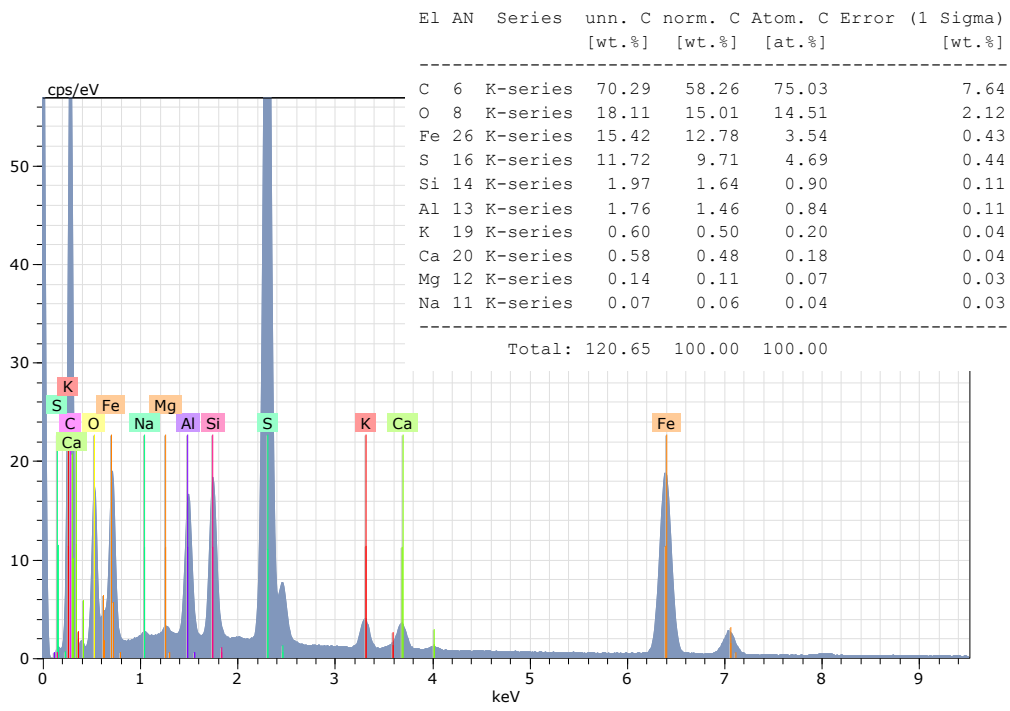

El	AN	Series	unn. C [wt.%]	norm. C [wt.%]	Atom. C [at.%]	Error (1 Sigma) [wt.%]
C	6	K-series	70.29	58.26	75.03	7.64
O	8	K-series	18.11	15.01	14.51	2.12
Fe	26	K-series	15.42	12.78	3.54	0.43
S	16	K-series	11.72	9.71	4.69	0.44
Si	14	K-series	1.97	1.64	0.90	0.11
Al	13	K-series	1.76	1.46	0.84	0.11
K	19	K-series	0.60	0.50	0.20	0.04
Ca	20	K-series	0.58	0.48	0.18	0.04
Mg	12	K-series	0.14	0.11	0.07	0.03
Na	11	K-series	0.07	0.06	0.04	0.03
		Total:	120.65	100.00	100.00	

Figure 3.127 ESEM-EDS spectrum of point 4 shown in Figure 3.123 B.

Fe-rich particles were found not only with spherical shape but also as irregular fragments of around 3 till to 20 µm length (Figures 3.128-3.130). These particles can be interpreted as metal oxides/hydroxides of terrigenous origin or from building materials.

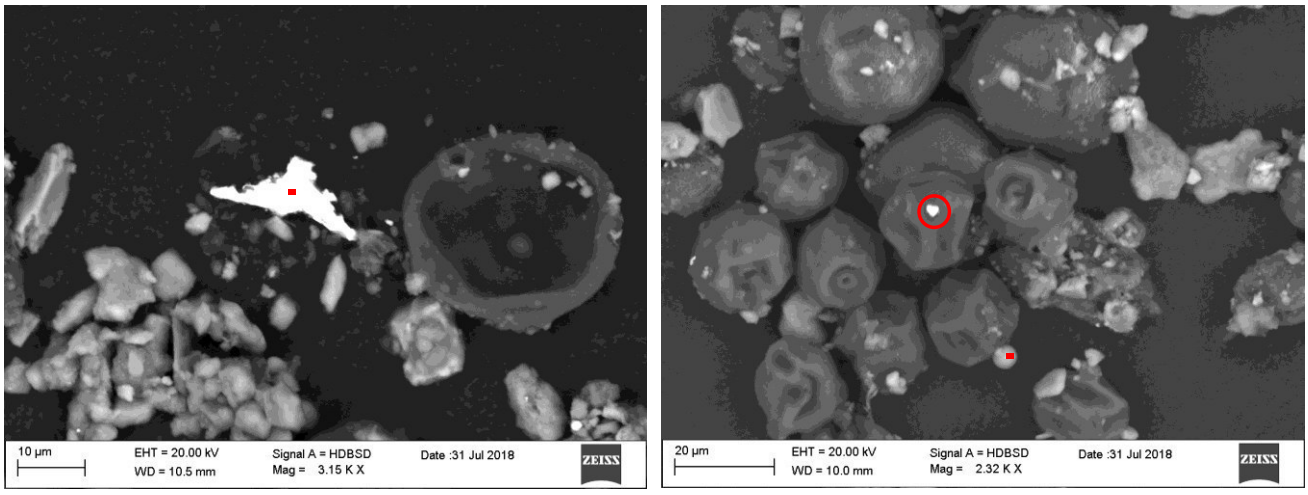

A) B)

Figure 128 ESEM photomicroghraph of portion of material deposited on PTNO17 sample. Pollens (sub-spherical dark particles), Fe-rich particles (bright fragments), aluminosilicates particle (round and light) along with mineral fragments are visible. Red dots and red circle represent the points of EDS analysis.

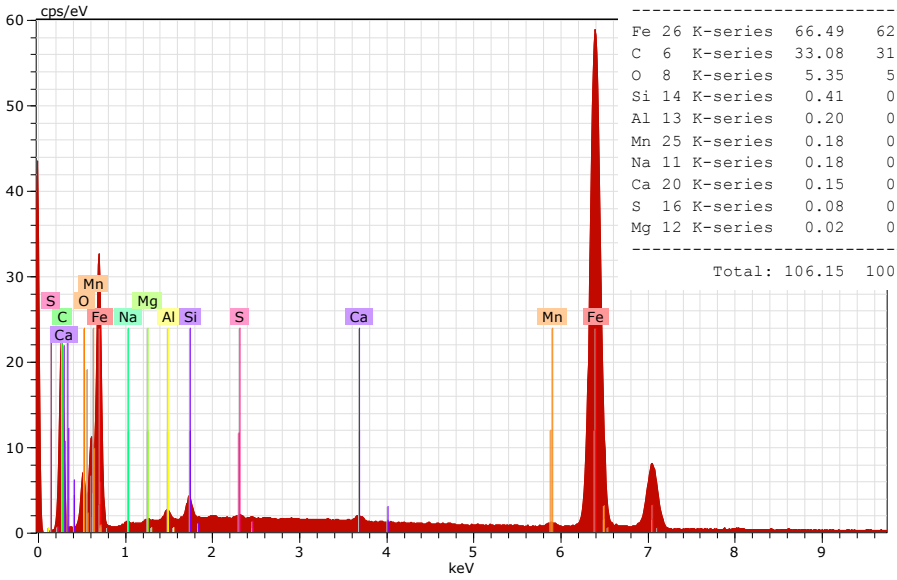

El	AN	Series	unn. C [wt.%]	norm. C [wt.%]	Atom. C [at.%]	Error (1 Sigma) [wt.%]
Fe	26	K-series	66.49	62.63	27.56	1.79
C	6	K-series	33.08	31.17	63.76	4.18
O	8	K-series	5.35	5.04	7.75	0.82
Si	14	K-series	0.41	0.39	0.34	0.05
Al	13	K-series	0.20	0.19	0.17	0.04
Mn	25	K-series	0.18	0.17	0.08	0.03
Na	11	K-series	0.18	0.17	0.18	0.04
Ca	20	K-series	0.15	0.14	0.09	0.03
S	16	K-series	0.08	0.08	0.06	0.03
Mg	12	K-series	0.02	0.02	0.02	0.03
Total:			106.15	100.00	100.00	

Figure 3.129 ESEM-EDS spectrum of point shown in Figure 3.128 A.

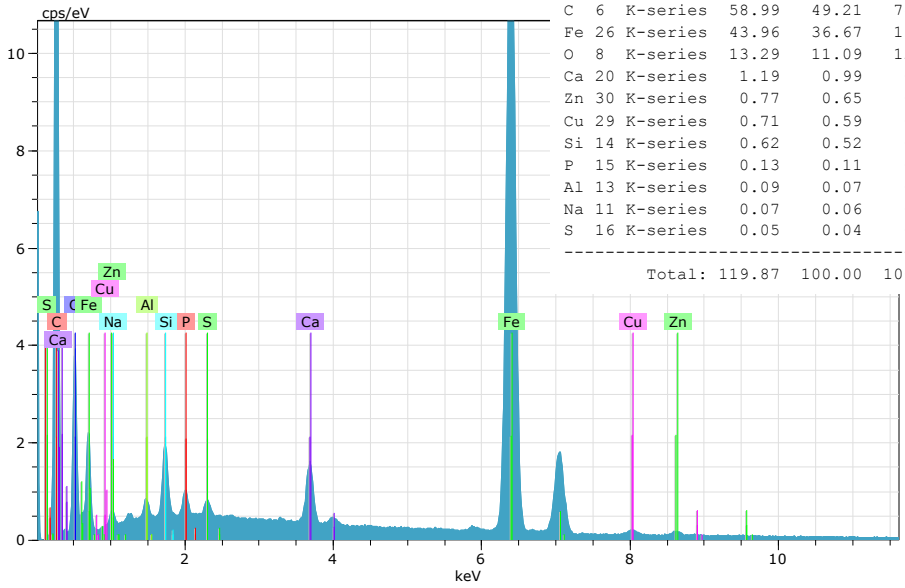

El	AN	Series	unn. C [wt.%]	norm. C [wt.%]	Atom. C [at.%]	Error (1 Sigma) [wt.%]
C	6	K-series	58.99	49.21	74.23	6.65
Fe	26	K-series	43.96	36.67	11.90	1.19
O	8	K-series	13.29	11.09	12.56	1.70
Ca	20	K-series	1.19	0.99	0.45	0.06
Zn	30	K-series	0.77	0.65	0.18	0.05
Cu	29	K-series	0.71	0.59	0.17	0.05
Si	14	K-series	0.62	0.52	0.33	0.05
P	15	K-series	0.13	0.11	0.06	0.03
Al	13	K-series	0.09	0.07	0.05	0.03
Na	11	K-series	0.07	0.06	0.05	0.03
S	16	K-series	0.05	0.04	0.02	0.03
Total:			119.87	100.00	100.00	

Figure 3.130 ESEM-EDS spectrum of circle shown in Figure 3.128 B.

Some spherical, aluminosilicate particles were also identified (Figures 3.128 B, 3.131).

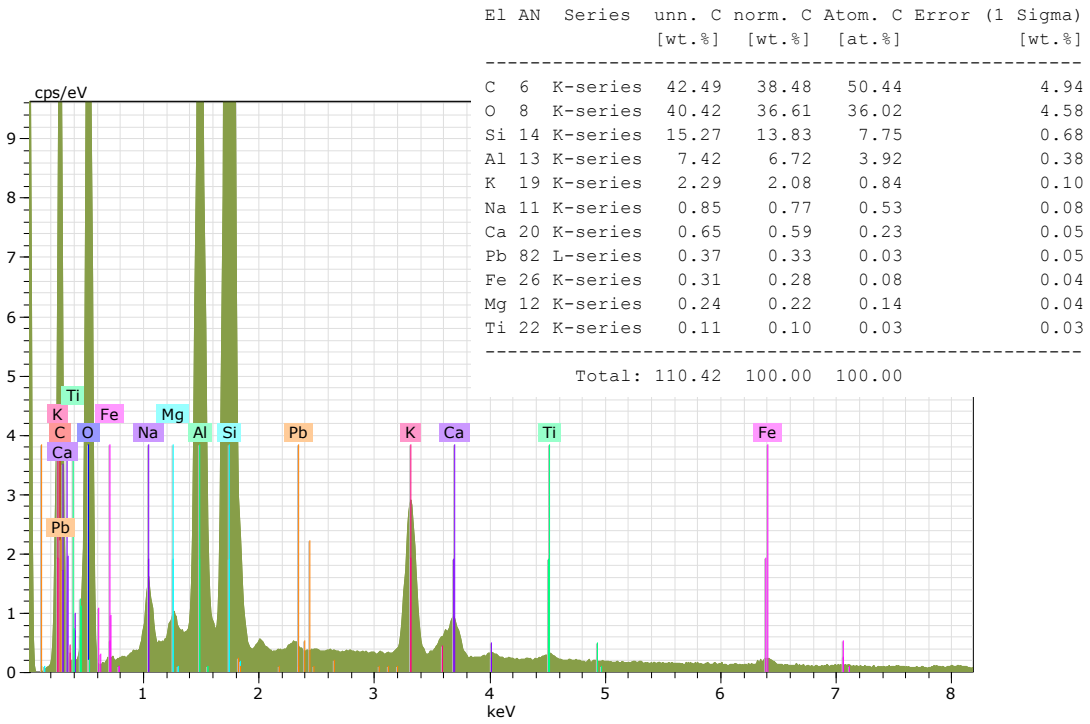

El	AN	Series	unn. C [wt.%]	norm. C [wt.%]	Atom. C [at.%]	Error (1 Sigma) [wt.%]
C	6	K-series	42.49	38.48	50.44	4.94
O	8	K-series	40.42	36.61	36.02	4.58
Si	14	K-series	15.27	13.83	7.75	0.68
Al	13	K-series	7.42	6.72	3.92	0.38
K	19	K-series	2.29	2.08	0.84	0.10
Na	11	K-series	0.85	0.77	0.53	0.08
Ca	20	K-series	0.65	0.59	0.23	0.05
Pb	82	L-series	0.37	0.33	0.03	0.05
Fe	26	K-series	0.31	0.28	0.08	0.04
Mg	12	K-series	0.24	0.22	0.14	0.04
Ti	22	K-series	0.11	0.10	0.03	0.03
		Total:	110.42	100.00	100.00	

Figure 3.131 ESEM-EDS spectrum of point shown in Figure 3.128 B.

No differences were detected on the accumulated material of horizontal and oblique samples. However, higher presence of biological particles was observed on samples exposed on the terrace than those placed on the windowsill.

FLORENCE

The observation was concentrated upon horizontal and oblique samples as higher amount of material had deposited on them than on vertical samples.

Material accumulated on surface of specimens exposed in Florence is mainly composed by mineral fragments and soil dust particles. In this regard, the analysis of a portion of material deposited on horizontal sample (Figures 3.132, 3.133) confirmed the presence of carbonates, aluminosilicates and sulphates, typical of mineral dust. A spherical Fe-rich particle, detectable on the left of Figure 3.132 and with a diameter of 16 µm, can confirm emissions from anthropogenic sources while small particles of Na and Cl identified the presence of salt crystals deriving from sea spray or de-icing salts spread on road during wintertime.

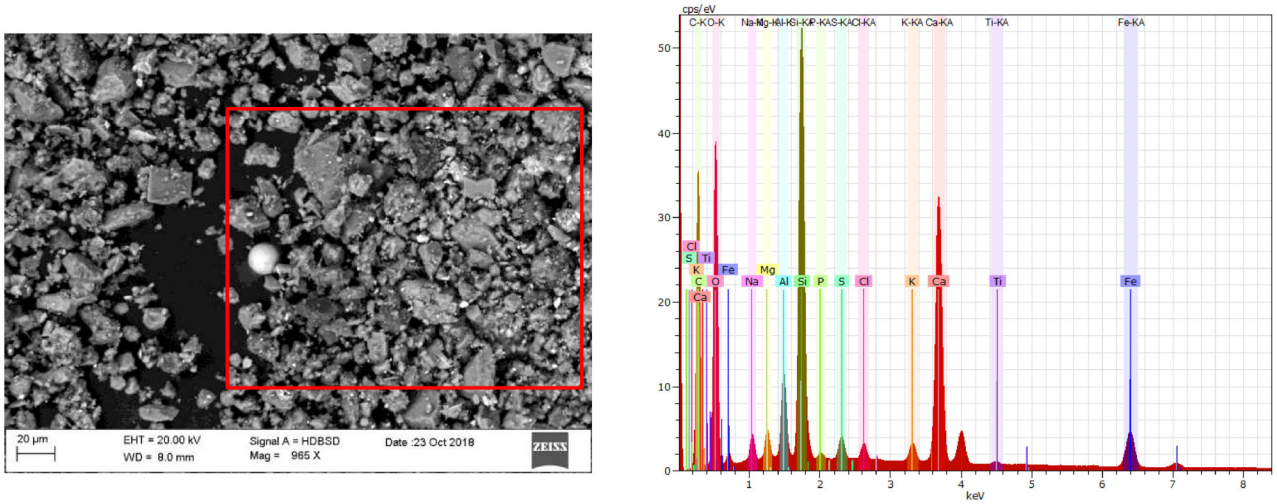

Figure 3.132 ESEM photomicroghraph of portion of material deposited on SMCH12 with related ESEM-EDS spectrum. Besides aluminosilicates and carbonates a spherical iron oxide particle is detectable in the centre. Red rectangle shows the area subjected to EDS-maps.

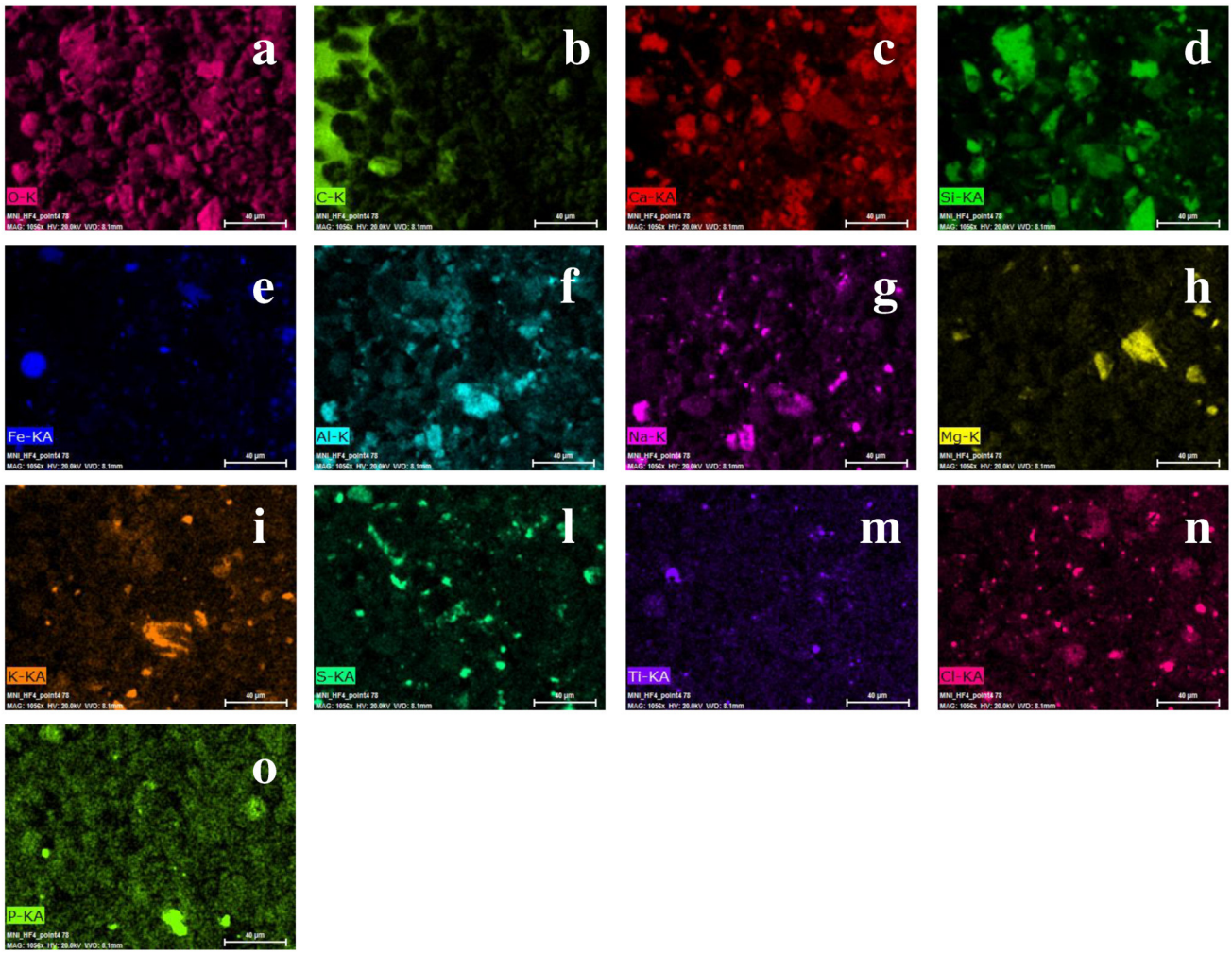

Figure 3.133 Photomicrographs of SMCH12 sample representing the EDS-maps analyses carried out on the area shown in Figure 3.132: a. EDS-map of O; b. EDS map of C; c. EDS map of Ca; d. EDS map of Si; e. EDS map of Fe; f. EDS map of Al; g. EDS map of Na; h. EDS map of Mg; i.. EDS map of K; l. EDS map of S; m. EDS map of Ti; n. EDS map of Cl; o. EDS map of P.

Figure 3.134 shows the presence of a laminated mineral (phyllosilicate), around 70 µm long (A), and aggregate material (B) with a spherical shape (with a diameter of 28 µm) also on oblique sample.

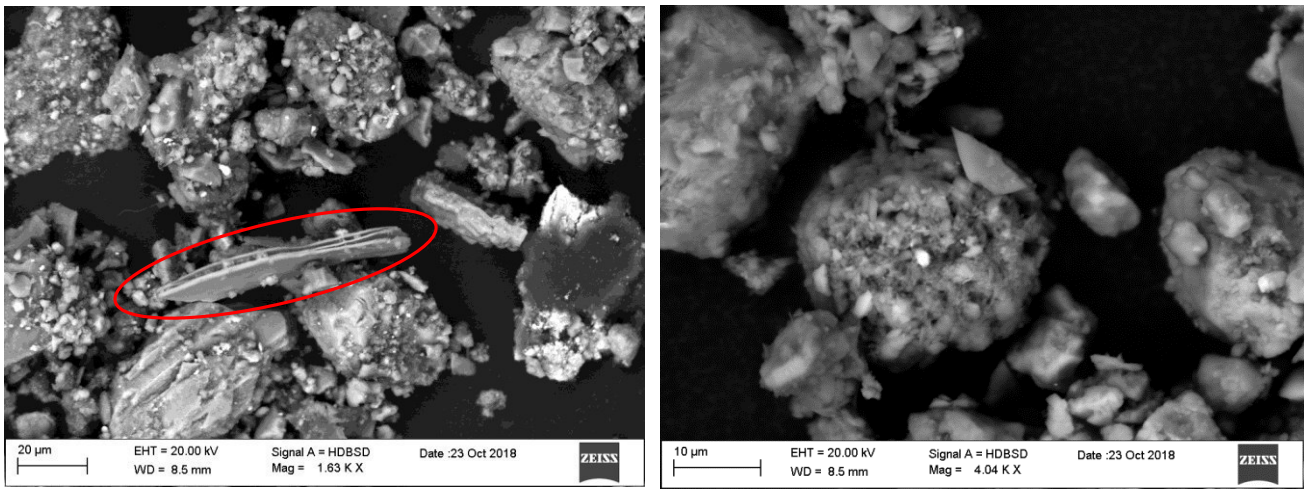

Figure 3.134 ESEM photomicroghraph of portion of material deposited on SMCO11 sample. A) Laminated mineral highlighted by red circle. B) Spherical aggregate material.

Carbonaceous particles of around 11 µm of diameter were recognised by their spherical/sub-spherical shape, spongy appearance and C-rich composition (Figure 3.135 A, 3.136). They are products of vehicle exhaust (Chabas and Lefevre, 2000) and of oil combustion in domestic heating systems and electric power plants (Sabbioni, 1995).
Also aluminosilicates particles, characterised by smooth, round surface with a diameter up to 10 µm were observed in the deposited material (Figure 3.135 B, 3.137) as consequence of coal combustion (Sabbioni, 1995) and wood burning (Ausset et al., 1998).

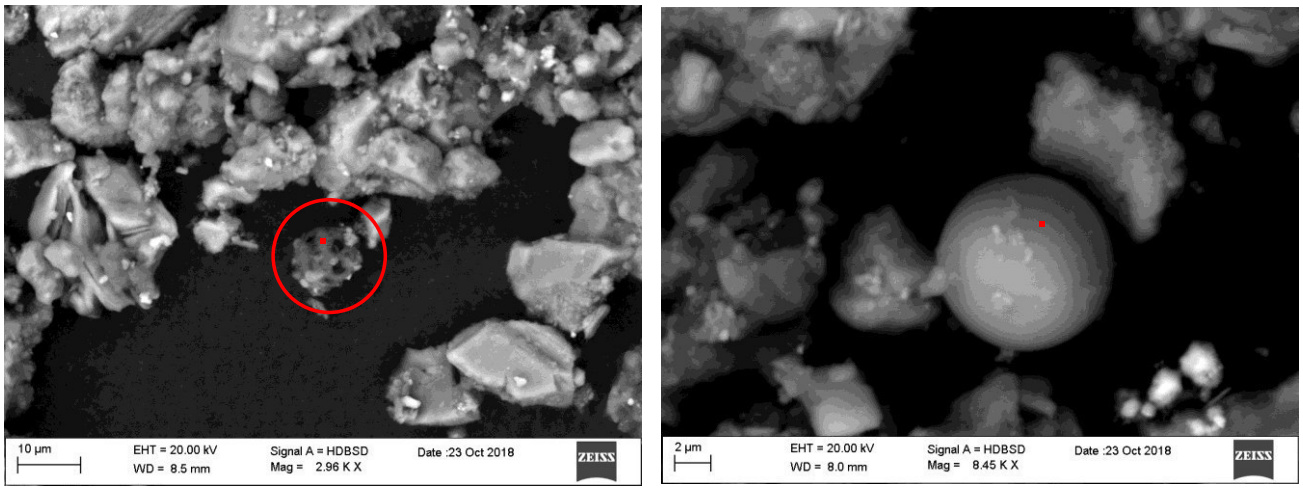

A) B)

Figure 3.135 ESEM photomicroghraph of portion of material deposited on SMCO11 (A) and SMCH12 (B) samples. A) Carbonaceous particle with a spongy structure encircled in red. B)Aluminosilicate particle with smooth, round surface. Red dots represent areas of EDS analysis.

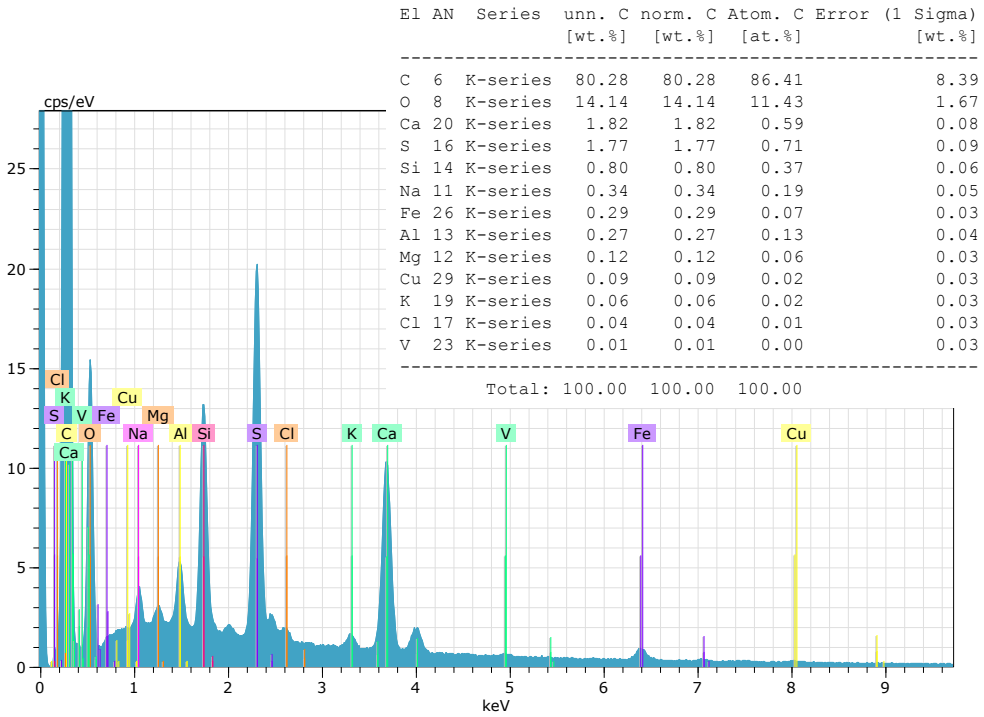

Figure 3.136 ESEM-EDS spectrum of point shown in Figure 3.135 A.

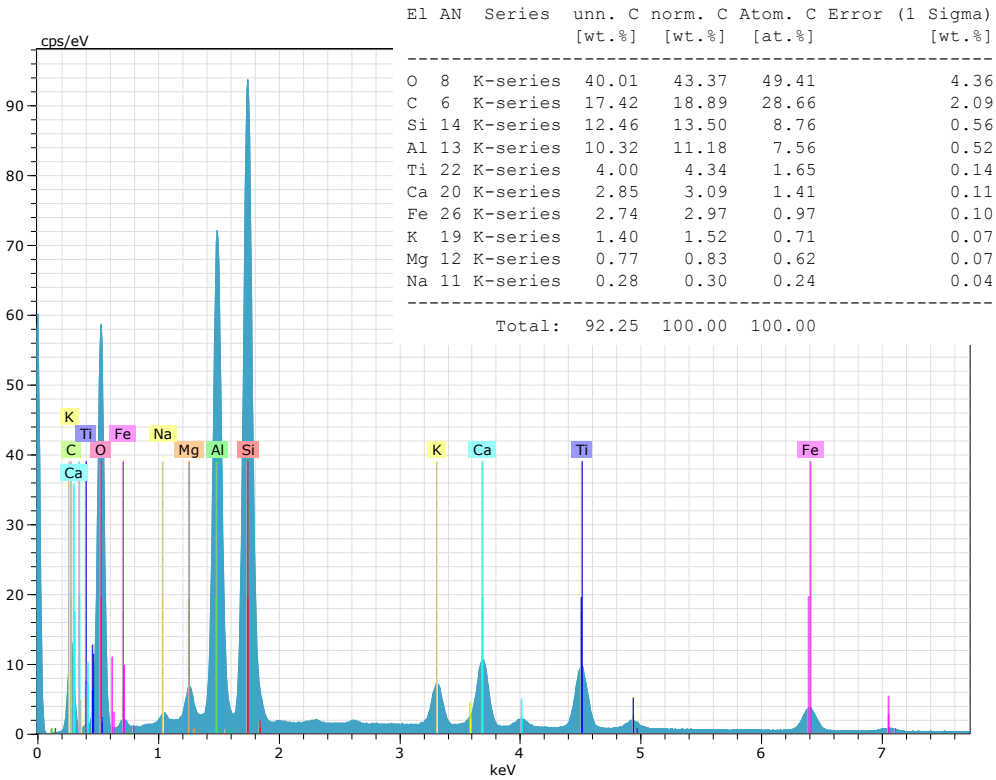

Figure 3.137 ESEM-EDS spectrum of point shown in Figure 3.135 B.

Other spherical particles of around 20 µm diameter stood out from the others for a dendritic appearance and a Fe-rich composition (Figures 3.138 A, 3.139). These particles can be related to combustion processes of fossil fuels or emissions from metallurgical high temperature processes (Esbert et al., 2001; Weinbruch et al., 2014). Moreover, analysis of deposited material highlighted the presence of other particles with Fe-rich

composition but irregular shapes (Figures 3.138 B, 3.140). These reached a dimension till 70 µm and could represent metal oxides/hidroxides from soil dust or building materials. In addition to these, other smaller particles (around 1 µm) were characterised by different metal composition, such as tungsten probably released by hard-metal facility (Figures 3.138 B, 3.141).

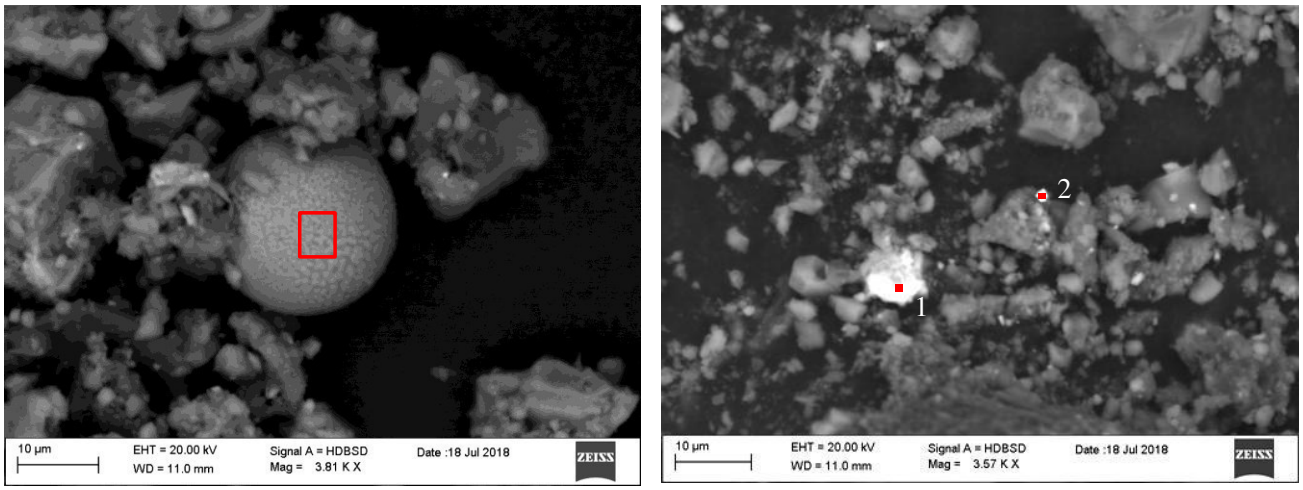

A) B)

Figure 3.138 ESEM photomicroghraph of portion of material deposited on SMCO11 sample. A) Spherical Fe-rich particle with dendritic surface. B)Metal-rich particles with irregular shapes. Red rectangle and dots represent areas of EDS analysis.

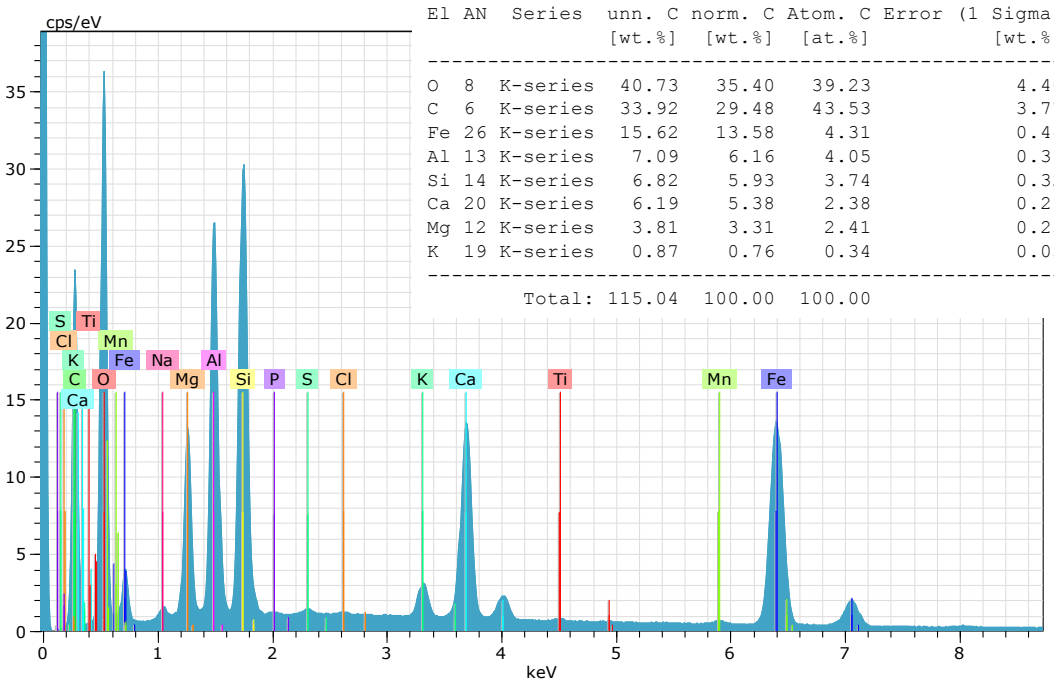

El	AN	Series	unn. C [wt.%]	norm. C [wt.%]	Atom. C [at.%]	Error (1 Sigma) [wt.%]
O	8	K-series	40.73	35.40	39.23	4.40
C	6	K-series	33.92	29.48	43.53	3.77
Fe	26	K-series	15.62	13.58	4.31	0.44
Al	13	K-series	7.09	6.16	4.05	0.36
Si	14	K-series	6.82	5.93	3.74	0.32
Ca	20	K-series	6.19	5.38	2.38	0.21
Mg	12	K-series	3.81	3.31	2.41	0.23
K	19	K-series	0.87	0.76	0.34	0.05
		Total:	115.04	100.00	100.00	

Figure 3.139 ESEM-EDS spectrum of point shown in Figure 3.138 A.

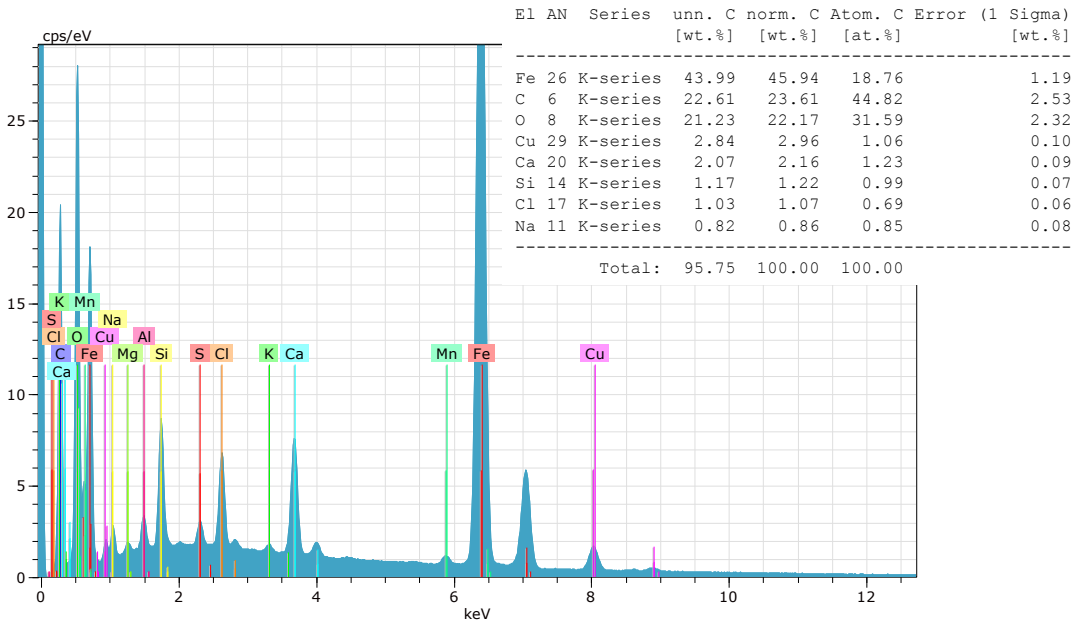

El	AN	Series	unn. C [wt.%]	norm. C [wt.%]	Atom. C [at.%]	Error (1 Sigma) [wt.%]
Fe	26	K-series	43.99	45.94	18.76	1.19
C	6	K-series	22.61	23.61	44.82	2.53
O	8	K-series	21.23	22.17	31.59	2.32
Cu	29	K-series	2.84	2.96	1.06	0.10
Ca	20	K-series	2.07	2.16	1.23	0.09
Si	14	K-series	1.17	1.22	0.99	0.07
Cl	17	K-series	1.03	1.07	0.69	0.06
Na	11	K-series	0.82	0.86	0.85	0.08
Total:			95.75	100.00	100.00	

Figure 3.140 ESEM-EDS spectrum of point 1 shown in Figure 3.138 B.

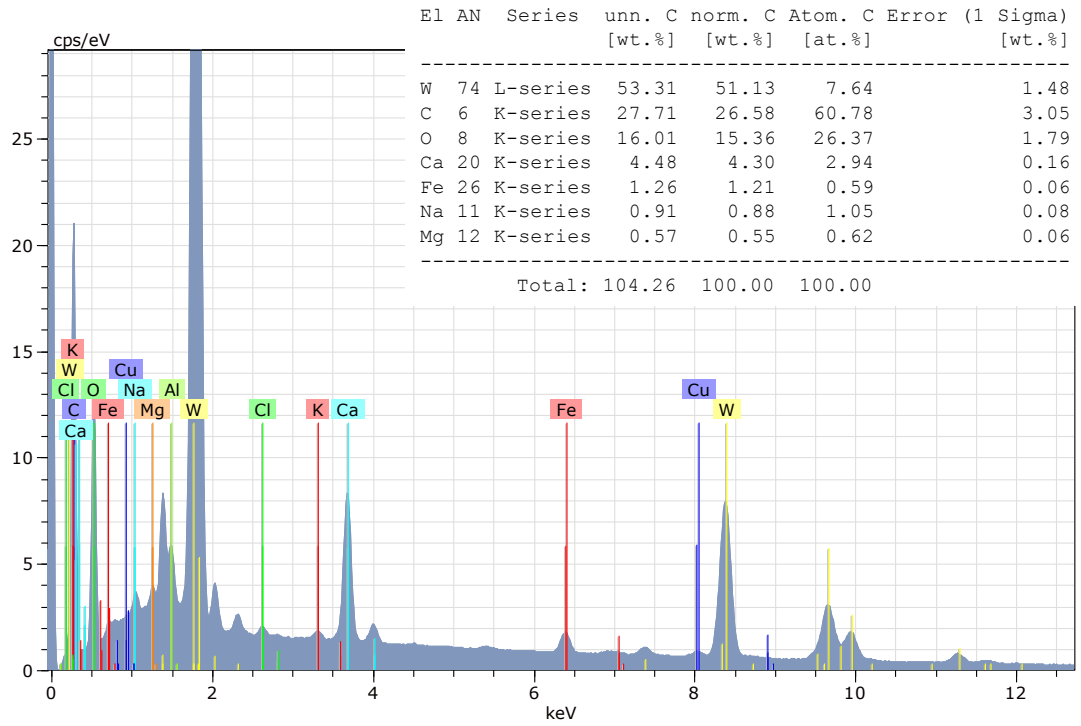

El	AN	Series	unn. C [wt.%]	norm. C [wt.%]	Atom. C [at.%]	Error (1 Sigma) [wt.%]
W	74	L-series	53.31	51.13	7.64	1.48
C	6	K-series	27.71	26.58	60.78	3.05
O	8	K-series	16.01	15.36	26.37	1.79
Ca	20	K-series	4.48	4.30	2.94	0.16
Fe	26	K-series	1.26	1.21	0.59	0.06
Na	11	K-series	0.91	0.88	1.05	0.08
Mg	12	K-series	0.57	0.55	0.62	0.06
Total:			104.26	100.00	100.00	

Figure 3.141 ESEM-EDS spectrum of point 2 shown in Figure 3.138 B.

Finally, less biological particles were detected in material deposited in Florence than in the other sites. Figure 3.142 displays an olive tree leaf trichome, typical of Tuscany region.

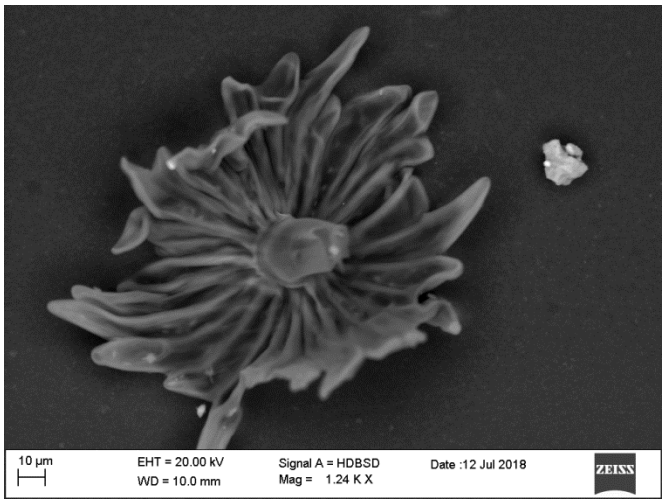

Figure 3.142 ESEM photomicroghraph of olive tree leaf trichome deposited on sample SMCV4.

Final remarks:

- Assessment of material accumulated on surface of samples exposed in all three sites for 24 months revealed to be mainly composed by mineral and soil dust particles. They can derive from soil resuspension and erosion of surrounding building materials.
- Fly-ash particles with diameter up to 10 µm were identified in all sites. They are characterised by spherical shape, smooth surface and are composed mainly by silicon and aluminium. They are representative of coal, wood and oil combustion (Ausset et al., 1998; Urosevic et al., 2012; Bonazza and Sabbioni, 2016).
- Dendritic surface, spherical shape and Fe-rich composition allowed to detected iron-rich particles (from less than 2 µm till to 10 µm of diameter), related to combustion processes of fossil fuels or emissions from metallurgical high temperature processes (Esbert et al., 2001; Weinbruch et al., 2014). In Ferrara and Florence, microscopic observation recognised other Fe-rich particles but with irregular shapes, likely interpreted as metal oxides/hydroxides from soil dust or erosion of building materials.
- Carbonaceous particles (10 µm of diameter) were recognised in Bologna and Florence by their spherical/sub-spherical shape, spongy appearance and C-rich composition. They are products of vehicle exhaust (Chabas and Lefevre, 2000) and of oil combustion in domestic heating systems and electric power plants (Sabbioni, 1995).
- Particles composed mainly by Na and Cl identified the presence of salt crystals deriving from sea spray or de-icing salts spread on road during wintertime (detected mainly in Bologna).
- Higher presence of biological particles were detected on samples exposed in Ferrara and Bologna.

3.1.7. INDUCTIVELY COUPLED PLASMA MASS SPECTROMETRY (ICP-MS)

Inductively Coupled Plasma Mass Spectrometry provides useful information for investigating the possible sources of trace elements. For this reason, chemical analysis was carried out on particulate accumulate on the exposed surface of horizontal stone specimens for 24 months. Moreover, ICP-MS results were compared with those obtained from substrate samples in order to understand whether each detected element derive from lithotypes or from atmospheric particulate. Results discussion have been concentrated on heavy metals (As, Cd, Co, Cr, Cu, Fe, Mn, Mo, Ni, Pb, Sb, Sn, Ti, U, V and Zn) as they are indicative of anthropogenic pollution sources (Belfiore et al., 2013).

STONE SUBSTRATES

Table 3.43 reports the amount of element detected of Carrara Marble (CM) and Verona Red Marble (VRM) substrates.
Considering elements detected with a concentration higher than 100 ppm, elemental analysis showed as Ca followed by Mg and Sr were the main components of Carrara Marble while Ca followed by Mg, K, Al, Fe, Mn and P constituted the majority of limestone sample.

	CM (ppm)	VRM (ppm)
Li	0.232	0.704
Be	0.015	0.042
B	0.070	2.03
Na	10.7	63.5
Mg	5231	4003
Al	90.5	1034
P	14.0	105
K	73.4	1157
Ca	332308	260543
Sc	0.378	1.060
Ti	3.08	46.4
V	0.331	1.69
Cr	1.34	3.19
Mn	23.6	335
Fe	84.2	616
Co	1.05	1.08
Ni	4.29	6.49
Cu	0.624	1.44
Zn	<LOD	5.15
Ga	0.043	0.290
As	16.8	13.5
Se	0.420	0.265
Rb	0.310	3.16
Sr	118	76.1
Mo	0.057	0.331
Ag	<LOD	<LOD
Cd	0.425	0.388
Sn	0.176	0.149
Sb	0.017	0.153
Te	0.407	0.317
Ba	1.29	6.35
Hg	<LOD	<LOD
Tl	<LOD	<LOD
Pb	2.66	2.01
Bi	<LOD	<LOD
U	0.219	0.070

Table 3.43 Concentration of trace elements of Carrara Marble (CM) and Verona Red Marble (VRM) samples. <LOD means below limit of detection (i.e. <0.0001 ppm).

DEPOSITED MATERIAL

Table 3.44 displays element concentration measured on the material collected from specimens horizontally exposed in Bologna (BO_C), Ferrara (PT_C1 and PT_C2 from Carrara Marble samples, PT_N1 and PT_N2 from Verona Red Marble samples) and Florence (SM_C1 and SM_C2) for 24 months.

EXP. SITE	BOLOGNA	FERRARA				FLORENCE	
LITHOTYPE	CM	CM	CM	VRM	VRM	CM	CM
SAMPLE	BO_C (ppm)	PT_C1 (ppm)	PT_C2 (ppm)	PT_N1 (ppm)	PT_N2 (ppm)	SM_C1 (ppm)	SM_C2 (ppm)
Li	9.34	11.2	9.30	16.2	13.8	12.3	11.3
Be	0.432	0.669	0.547	0.721	0.579	0.841	0.725
B	15.5	14.4	12.4	11.6	9.88	12.4	9.58
Na	2258	4778	4314	4715	4267	6284	6142
Mg	5447	10324	9329	16770	15952	7167	7735
Al	7459	10787	10039	18649	17047	13584	13496
P	968	1019	984	1564	1317	692	602
K	4186	5487	5243	7926	6817	6828	5855
Ca	180756	119511	118684	69189	62214	137337	133122
Sc	2.89	1.47	3.93	4.93	4.97	2.24	2.74
Ti	789	764	700	1140	951	1124	981
V	21.1	25.8	24.5	40.9	35.3	36.4	33.1
Cr	40.9	55.2	52.4	88.3	76.2	131	120
Mn	200	239	228	263	272	471	428
Fe	8228	9616	9441	16547	14903	21847	19607
Co	5.15	4.89	4.60	7.35	6.10	8.15	6.67
Ni	21.7	26.5	26.8	45.4	39.4	40.8	33.5
Cu	186	153	151	242	224	595	595
Zn	1705	722	799	795	960	419	641
Ga	6.97	8.72	82.3	13.5	331	14.7	275
As	12.1	9.88	9.32	9.61	8.11	12.3	11.2
Se	0.921	0.891	2.44	1.12	6.94	1.15	5.22
Rb	19.3	32.2	28.9	44.7	37.0	28.0	25.8
Sr	154	161	232	178	925	270	659
Mo	6.80	5.40	5.66	7.53	6.42	13.6	12.0
Ag	0.625	1.13	1.00	1.91	1.74	2.21	2.31
Cd	1.05	1.05	1.19	1.81	1.62	2.07	1.78
Sn	19.5	27.8	26.8	41.1	34.0	86.0	65.4
Sb	4.04	4.88	15.4	21.3	5.08	78.6	63.1
Te	0.257	0.134	0.171	0.200	0.216	0.252	0.253
Ba	156	239	2588	313	10668	468	9981
Hg	0.093	0.052	0.051	0.114	0.124	0.084	0.072
Tl	0.155	0.148	0.138	0.240	0.200	0.211	0.183
Pb	167	847	125	759	76.1	176	63.1
Bi	0.716	1.25	1.01	1.41	1.43	2.53	2.64
U	8.75	6.65	6.01	0.957	0.830	1.16	1.06

Table 3.44 Concentration of elements measured on material deposited on samples horizontally exposed in Bologna, Ferrara, Florence.

COMPARISON

In order to distinguish whether the elements measured on deposited material derived mostly from atmospheric deposition or they were related to the composition of stone substrate, the ratio between the amount of each element analysed on the deposit and that detected from the related stone substrate was calculated and it is presented in Table 3.45. Values equal or close to 1 indicates that the element is strictly

related to stone substrate while much higher value means that the element found in the deposit is enriched due to atmospheric deposition respect to the stone sample.

	BO_C/CM	PT_C1 /CM	PT_C2/CM	PT_N1/VRM	PT_N2/VRM	SM_C1/CM	SM_C2/CM
Li	40	48	40	23	20	53	49
Be	29	45	37	17	14	56	49
B	220	204	177	6	5	176	136
Na	211	445	402	74	67	586	573
Mg	1	2	2	4	4	1	1
Al	82	119	111	18	16	150	149
P	69	73	70	15	13	49	43
K	57	75	71	7	6	93	80
Ca	1	0	0	0	0	0	0
Sc	8	4	10	5	5	6	7
Ti	256	248	228	25	21	365	319
V	64	78	74	24	21	110	100
Cr	31	41	39	28	24	97	89
Mn	9	10	10	1	1	20	18
Fe	98	114	112	27	24	259	233
Co	5	5	4	7	6	8	6
Ni	5	6	6	7	6	10	8
Cu	299	245	242	168	155	954	954
Zn	-	-	-	154	186	-	-
Ga	162	203	1919	47	1141	342	6418
As	1	1	1	1	1	1	1
Se	2	2	6	4	26	3	12
Rb	62	104	93	14	12	90	83
Sr	1	1	2	2	12	2	6
Mo	119	94	99	23	19	237	209
Ag	-	-	-	-	-	-	-
Cd	2	2	3	5	4	5	4
Sn	111	158	152	275	228	489	372
Sb	234	283	892	139	33	4556	3659
Te	1	0	0	1	1	1	1
Ba	121	186	2011	49	1681	364	7757
Hg	-	-	-	-	-	-	-
Tl	-	-	-	-	-	-	-
Pb	63	319	47	377	38	66	24
Bi	-	-	-	-	-	-	-
U	40	30	27	14	12	5	5

Table 3.45 Ratio between concentration of each element measured on material accumulated on stone samples and that assessed on stone substrate. In some samples all the detected concentration of some element (-) come from atmospheric deposition.

Concentrating upon heavy metals (As, Cd, Co, Cr, Cu, Fe, Mn, Mo, Ni, Pb, Sb, Sn, Ti, U, V and Zn), the analysis highlighted that specimen exposed in Bologna for 24 months was enriched mostly in Cu, Ti, Sb, Mo, Sn (between 300 and 100 times more than their amount found in stone substrate) followed by Fe, V, Pb, U and Cr (between 100 and 10 times more than stone substrate) (Figure 3.143). The amount of Zn measured in the deposited material (1705 ppm) is ascribable totally to the atmospheric deposition as it was not detected

in marble substrate. On the contrary, As seems to be mainly related to stone substrate as indicated by the ratio value close to 1.
Zn, Cu, Sn and Sb were found to be products of tire and brake abrasion (Thorpe and Harrison, 2008; Telloli, 2014). Cu along with V are emitted also from diesel engines (Lucarelli et al., 2004; Tositti et al., 2014) and Sb has been attributed also to road traffic, incinerators, metal production and domestic and industrial coal and fuel combustion (Cal-Prieto et la., 2001). Fe, Pb and Zn are recognised to be related to lead gasoline emissions while Cu, Ni, Cr and V are more common in oil combustible, diesel and gasoline (Belfiore et al., 2013). Mo is utilised for alloys production but it is released also from traffic-related source. On the contrary, Ti is mostly related to soil dust along with Al, Si, Ca, Sr and Mg (Lucarelli et al., 2004; Thorpe and Harrison, 2008) even if Ebert et al. (2012) attributed the origin of fly-ash particles rich in Fe and Ti to metallurgical high temperature processes. Therefore, the analysed heavy metals are linked to the major impact of vehicular traffic.

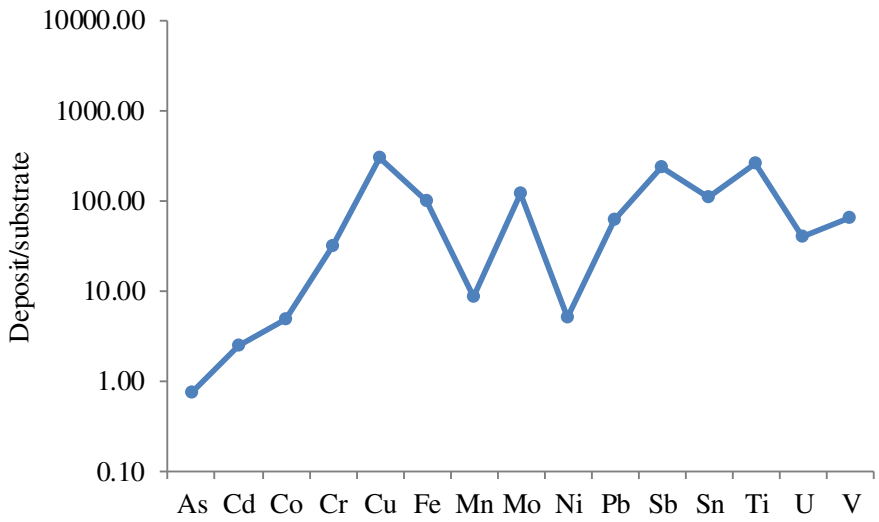

Figure 3.143 Ratio of heavy metals concentration measured in material deposited on sample exposed in Bologna and in Carrara Marble substrate.

Carrara Marble samples exposed in Ferrara underwent an enrichment mostly of Sb, Ti, Cu, Pb, Sn, Fe (with values between 900 and 100 times higher that analysed on the substrate) followed by Mo, V, Cr, Mn and U (between 100 and 10 times more than stone substrate) (Figure 3.144 A). Moreover, deposited material enriched the exposed specimens with Zn (722 and 799 ppm) as it was not detected in the stone substrate. The significant enrichment of these elements suggests that the emissions from mobile combustion sources highly affected the material accumulated on stone samples, probably linked to the congested street Via Porta Mare. Furthermore, also the substantial enrichment of Ba (equals to 186 and 2011 for PT_C1 and PT_C2, respectively) confirms the impact of vehicular traffic as Ba, along with Cu, is ascribable to brake pad wear (Comite et al., 2017).
Also limestone samples exposed in Ferrara were enriched with Sn, Pb, Zn, Cu, Sb (values between 400 and 100 times higher than the substrate) followed by Ti, V, Cr, Fe, Mo and U (values between 100 and 10 times higher than limestone substrate) (Figure 3.144 B).

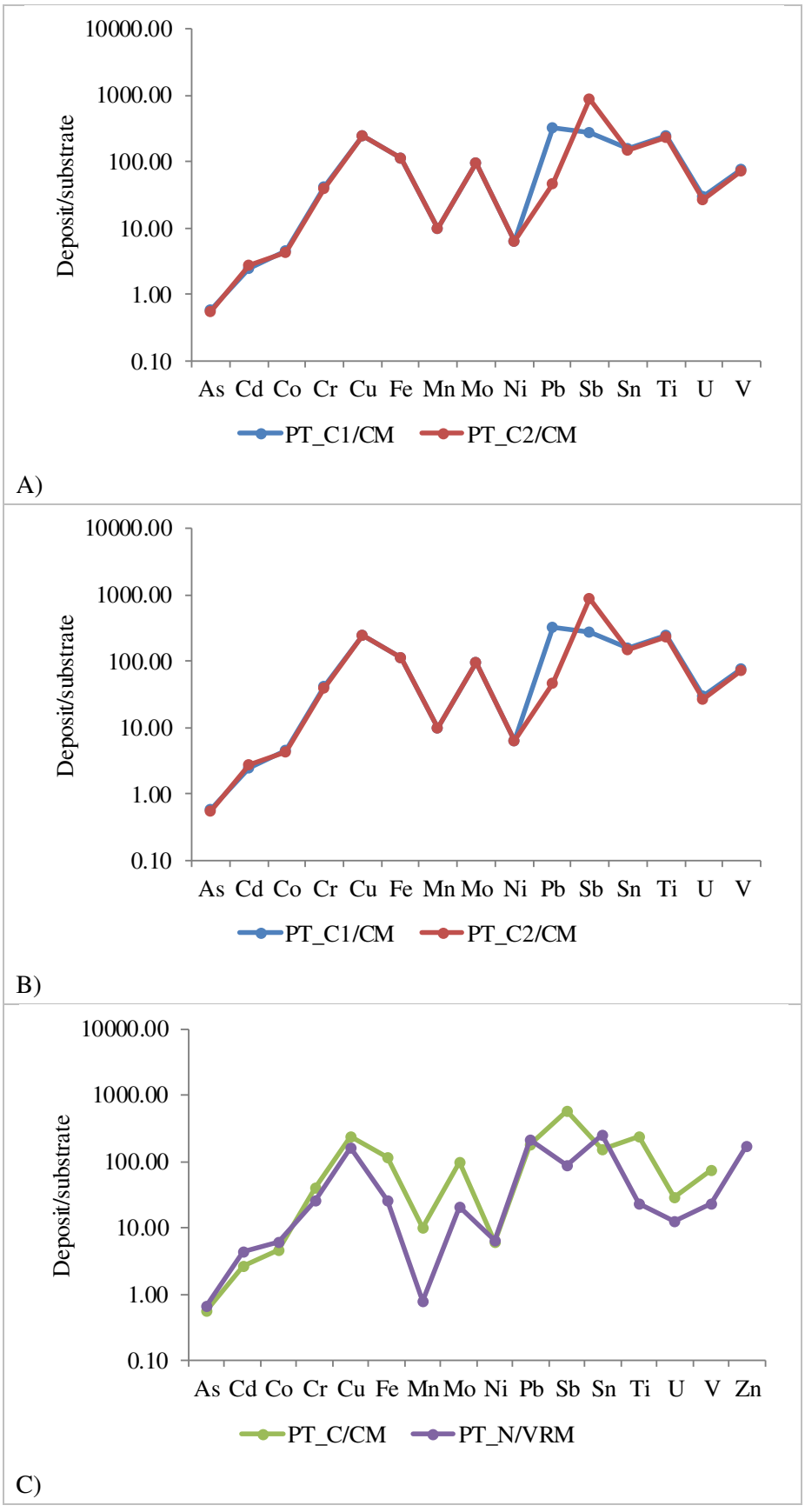

Figure 3.144 Ratio between heavy metals concentration measured in material deposited on samples exposed in Ferrara and in Carrara Marble substrate (A) and in Verona Red Marble substrate (B). C) Comparison of mean ratios between heavy metals concentrations measured on samples exposed in Ferrara and related substrates.

However, some differences can be detectable among heavy metals concentration in deposit collected in Ferrara if the two lithotypes are compared (Figure 3.144 C). Considering mean values of the ratio deposit/substrate, material accumulated on Carrara Marble samples were more enriched in Fe, Mo, Mn, Sb, Ti, U, V than those measured on material deposited on Verona Red Marble specimens. Therefore, it can be deduced that the deposition of heavy metals is influenced by the kind of stone substrate.

Samples exposed in Florence for 24 months were significantly enriched in Sn, reaching values 4556 and 3659 times higher than those measured in the marble substrate. In addition, Cu, Sn, Ti, Fe, Mo and V were assessed in the deposit with a concentration 1000-100 times higher than that measured in the substrate while lower amount of Cr, Mn and Pb were detected in the deposit (with values between 100 and 10 times higher than the substrate) (Figure 3.145). Deposit was characterised also by high concentration of Zn (419 and 641) as it was below limit of detection in marble substrate. The substantial enrichment in these elements suggests the vehicular traffic as the main source of heavy metals detected in the deposit, both from abrasion of tires and brakes (Sb, Sn, Cu, Zn) and from fuel combustion (Zn, V, Pb, Fe, Cr). Even if samples exposed in San Marco Museum are positioned in a controlled traffic zone, many buses, automobiles and mopeds drive along the opposite street (via G. La Pira) thus influencing the composition of particulate matter deposited on samples.

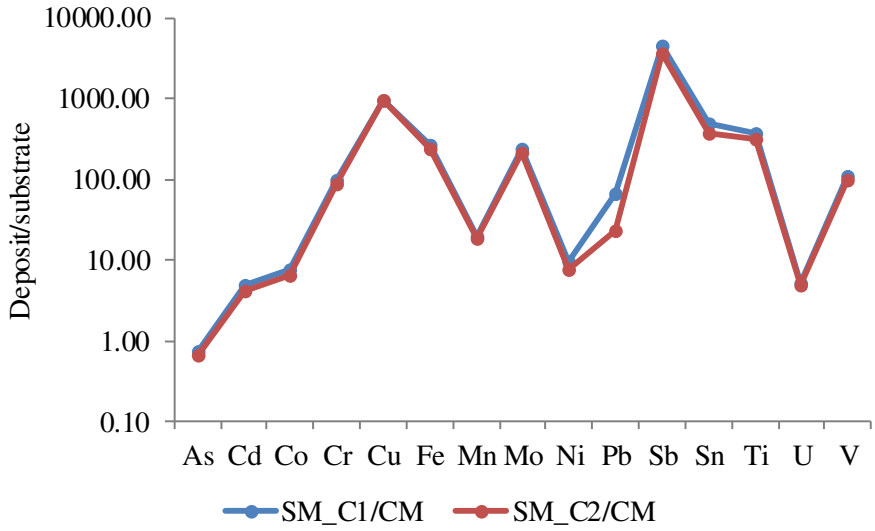

Figure 3.145 Ratio of heavy metals concentration measured in material deposited on samples exposed in Florence and in Carrara Marble substrate.

Finally, Figure 3.146 shows the mean enrichment of heavy metals observed in material deposited in samples exposed in Bologna, Ferrara and Florence for 24 months respect to Carrara Marble substrate. In general, samples exposed for 24 months in all sites underwent an enrichment mostly in Sb, Cu, Ti, Sn, Fe, Mo as well as in Zn totally derived from atmospheric deposition, confirming as traffic pollution source significantly influenced the composition of the deposited particulate matter. In particular, deposit/substrate ratio assessed for samples exposed in Florence resulted higher for all heavy metals, particularly for Sb and Cu and with exception of As, Pb and U, than those measured in Ferrara and Florence. This means higher emissions of heavy metals in Florence. Moreover, specimens exposed in Ferrara displayed the highest enrichment in Pb, usually associated to worn tires and lead gasoline while As is mainly related to the stone substrate in all sites. Besides heavy metals, samples exposed in all sites were affected by an enrichment in Ba, mostly in Ferrara and Florence (usually added with Ca to diesel in order to inhibit the formation of soot during the combustion

process or deriving from brake pad wear - Comite et al., 2017), Na (connected to sea-salt or de-icing salt) and Al (typical of soil dust) (Table 3.45).

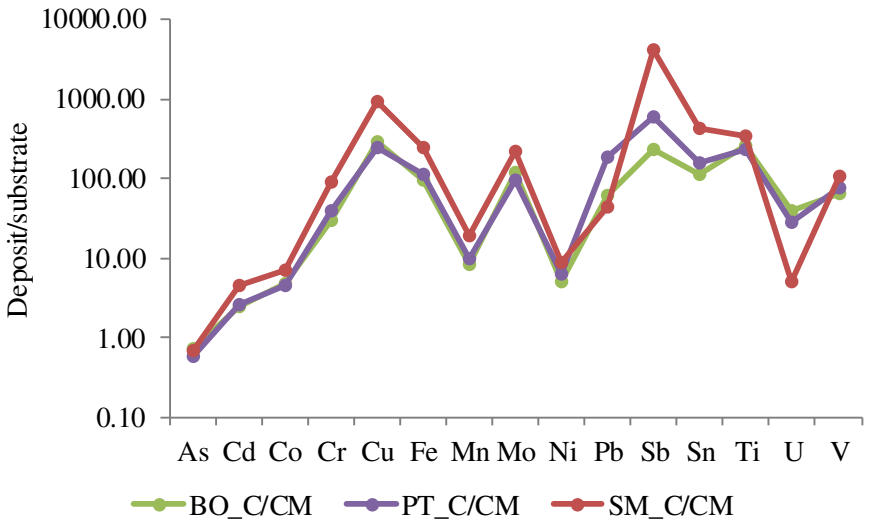

Figure 3.146 Comparison of mean ratios between heavy metals concentration measured on material deposited on samples exposed in Bologna (green), Ferrara (purple) and Florence (red) and on marble substrate.

Final remarks:

- Concentrating upon heavy metal content that are mainly related to anthropogenic emissions, the exposure outdoor of stone samples in all sites for 24 months led them to an enrichment mostly in Sb, Cu, Ti, Sn, Fe, Mo and Zn, highlighting as vehicular traffic influenced the composition of the deposited particulate matter. Indeed, emissions related to road traffic can derive from abrasion of tires and brakes (Sb, Sn, Cu, Zn) and fuel combustion (Zn, V, Pb, Fe, Cr) (Lucarelli et al., 2004; Thorpe and Harrison, 2008; Belfiore et al., 2013).
- Higher gain of heavy metals, with exception of As, Pb and U, was observed in samples exposed in Florence respected to those placed in Bologna and Ferrara.
- Comparing the composition of material accumulated on samples exposed in Ferrara, Carrara Marble samples were more enriched in Fe, Mo, Mn, Sb, Ti, U, V than those of Verona Red Marble, proving that the different kind of stone substrate can influence the deposition of heavy metals.
- Additionally, all samples underwent a significant enrichment in Ba, added to diesel to reduce soot or related to brake pad wear.

3.2. FIELD EXPOSURE TESTS OF PASSIVE FITERS

3.2.1. TOTAL DEPOSITED PARTICULATE (TDP)

The amount of particulate matter deposited per surface unit on passive quartz filters was calculated dividing the deposition mass of particulate matter (weighing quartz fibre filters before and after field exposure) by the real deposition area of the filters without gasket.

BOLOGNA

Table 3.46 displays the amount of PM deposited per surface unit (TDP) on quartz fibre filters exposed in Bologna after different exposure time. In general, it can be observed a slight gradual increase of TDP over time, passing from 2567.16 µg cm^{-2} calculated after the first 6 months of exposure to 3086.52 µg cm^{-2} after 24 months of exposure.

SAMPLE	EXPOSURE TIME (month)	TDP (µg cm^{-2})
PC84	6	2567.16
PC85	12	2916.81
PC86	18	2751.79
PC87	24	3086.52

Table 3.46 Total deposited particulate (TDP) accumulated on passive quartz fibre filters exposed in Bologna at different exposure time (6, 12, 18, 24 months).

FERRARA

Quantity of PM deposited per surface unit on quartz filters exposed in Ferrara gradually increased after 12 months of exposure changing from 1760.11 µg cm^{-2} after 6 months to 1930.46 µg cm^{-2} (Table 3.47). After 18 months of exposure, total deposited matter significantly increased (4690.57 µg cm^{-2}) while a removal of PM from quartz filters, probably due to wind or wind-driven rain, reduced TDP measured after 24 months of exposure to 1279.67 µg cm^{-2}.

SAMPLE	EXPOSURE TIME (month)	TDP (µg cm^{-2})
PTF1	6	1760.11
PTF2	12	1930.46
PTF3	18	4690.57
PTF5	24	1279.67

Table 3.47 Total deposited particulate (TDP) accumulated on passive quartz fibre filters exposed in Ferrara at different exposure time (6, 12, 18, 24 months).

FLORENCE

TDP on quartz filters exposed in Florence increased over time, reaching the highest value after 18 months of exposure (3755.97 µg cm^{-2}), while it underwent a slight decrease after 24 months of exposure (3468.03 µg cm^{-2}) (Table 3.48).

SAMPLE	EXPOSURE TIME (month)	TDP (µg cm^{-2})
SMF1	6	223.24
SMF2	12	996.32
PC94	18	3755.97
SMF4	24	3468.03

Table 3.48 Total deposited particulate (TDP) accumulated on passive quartz fibre filters exposed in Florence at different exposure time (6, 12, 18, 24 months).

COMPARISON

The comparison of total deposited particulate matter measured on passive quartz filters in all sites showed the highest value in Bologna, followed by Ferrara and Florence, after 6 and 12 months of exposure (Figure 3.147). In general, TDP detected in Bologna remained rather similar to the previous values also after 18 and 24 months of exposure (mean value equal to 2830.57 ± 222.51 µg cm^{-2}). On the contrary, TDP on passive quartz filters exposed in Ferrara and Florence increased after 18 months of exposure over the Bologna value, the first reaching the highest value ever (4690.57 µg cm^{-2}). After 24 months of exposure, passive quartz filter exposed in Florence underwent higher accumulation of PM per surface unit than Bologna and Ferrara.
Concluding, supply and removal of PM per surface unit remained rather constant over time in Bologna. In Ferrara there was a significant deposition of PM after 18 months followed by PM removal after 24 months while passive filters exposed in Florence underwent a gradual increasing deposition of PM per surface unit up to 3755.97 µg cm^{-2} after 18 months with a slight decrease after 24 months.

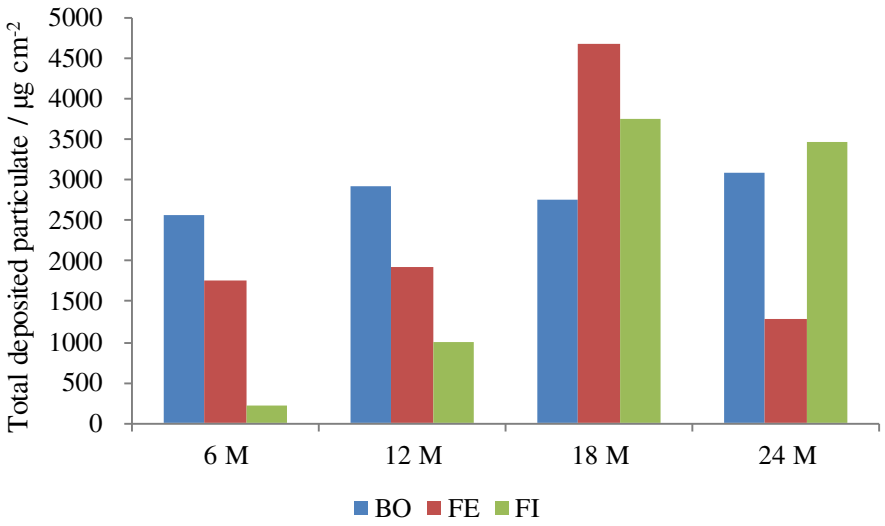

Figure 3.147 Comparison of the amount of particulate matter deposited per surface unit on passive quartz fibre filters exposed in Bologna (blue), Ferrara (red) and Florence (green) at different exposure time (6, 12, 18, 24 months).

Final remarks:

- In general, the amount of particulate matter deposited on passive filters exposed in Bologna remained rather constant over time (mean value equals to 2830.57 ± 222.51 µg cm^{-2}), being higher than TDP measured in Ferrara and Florence after 6 and 12 months of exposure.
- TDP identified in passive filter exposed in Ferrara after 18 months reached the highest value ever (4690.57 µg cm^{-2}) and of all sites while there was a higher accumulation of PM per surface unit in Florence than in the other sites after 24 months.

3.2.2. ION CHROMATOGRAPHY (IC)

BOLOGNA

Table 3.49 displays the detected amount of water soluble fractions (in ppm) in passive filters exposed in Bologna after 6, 12, 18 and 24 months while the corresponding ion concentration per surface unit (µg cm^{-2}) is reported in Table A5.1 (Annex 5).

SAMPLE	EXPOSURE TIME (month)	Cl^- (ppm)	NO_3^- (ppm)	SO_4^{2-} (ppm)	Na^+ (ppm)	NH_4^+ (ppm)	K^+ (ppm)	Mg^{2+} (ppm)	Ca^{2+} (ppm)
PC84	6	3.44	0.19	1.40	1.78	0.09	0.22	0.24	3.90
PC85	12	0.75	2.32	0.81	0.70	<LOD	0.54	0.14	6.53
PC86	18	6.44	3.21	0.42	0.27	0.04	0.16	<LOD	4.71
PC87	24	1.75	0.82	0.38	0.28	0.07	0.31	0.09	3.71

Table 3.49 Main soluble ions measured on passive filters exposed in Bologna for 6, 12, 18 and 24 months. <LOD means below limit of detection.

Cl^- was the anion detected with most significant concentration per surface unit over time (up to 64.40 µg cm^{-2} reached after 18 months of exposure), with exception after 12 months of exposure when NO_3^- prevailed (Figure 3.148). The amount of NO_3^- increased over time till 32.10 µg cm^{-2} after 18 months of exposure and decrease after 24 months while that of SO_4^{2-} showed a gradual decreasing trend from 14.03 µg cm^{-2} to 3.81 µg cm^{-2} (Figure 3.148). Moreover, the amount of Ca^{2+} measured per surface unit was always higher than the other cations showing a value up to 65.30 µg cm^{-2} after 12 months of exposure. Also Na^+ displayed rather high values mainly after 6 months of exposure (17.79 µg cm^{-2}). All the other cations never reached values higher than 5.50 µg cm^{-2}.

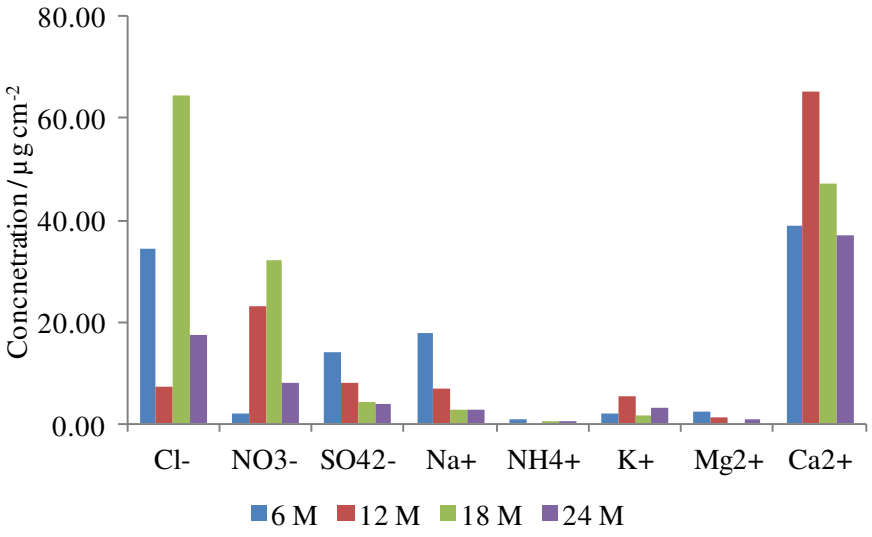

Figure 3.148 Concentration of soluble ions per surface unit measured in passive filters exposed in Bologna after 6 (blue), 12 (red), 18 (green) and 24 (purple) months.

FERRARA

Table 3.50 displays the detected amount of water soluble fractions (in ppm) in passive filters exposed in Ferrara after 6, 12, 18 and 24 months and the related calculated ion concentration per surface unit (µg cm^{-2}) is available in Table A5.2 (Annex 5).

SAMPLE	EXPOSURE TIME (month)	Cl^- (ppm)	NO_3^- (ppm)	SO_4^{2-} (ppm)	Na^+ (ppm)	NH_4^+ (ppm)	K^+ (ppm)	Mg^{2+} (ppm)	Ca^{2+} (ppm)
PTF1	6	0.31	0.05	0.48	5.38	0.18	1.04	1.01	8.25
PTF2	12	3.62	2.17	6.44	2.86	<LOD	0.74	0.16	6.87
PTF3	18	20.05	17.99	31.96	11.00	<LOD	3.44	1.45	24.50
PTF5	24	2.83	2.75	1.48	0.98	0.16	0.50	0.15	6.57

Table 3.50 Main soluble ions measured on passive filters exposed in Ferrara for 6, 12, 18 and 24 months. <LOD means below limit of detection.

Ion chromatography performed on passive filters exposed in Ferrara highlighted the most important increase of all ions after 18 months of exposure, with exception of NH_4^+ that remained below limit of detection. In particular, SO_4^{2-} (319.62 µg cm^{-2}) and Ca^{2+} (244.98 µg cm^{-2}) prevailed over the other ions (Figure 3.149). This was likely possible because of higher emissions of precursors of these species as well as environmental conditions proper for the deposition and accumulation of these soluble ions on filter surface.
After 6 months of exposure, all anions never reached a concentration per surface unit equals to 4.00 µg cm^{-2} while it was exceeded during all the other period. In this context, higher amount of SO_4^{2-} per surface unit was identified after 12 (42.95 µg cm^{-2}) and 18 (319.62 µg cm^{-2}) months than that of the other anions while it was almost half the concentration of Cl^- (28.34 µg cm^{-2}) and NO_3^- (27.53 µg cm^{-2}) after 24 months (Figure 3.149).
Concentrating upon cations, Ca^{2+} was detected always with the highest concentration per surface unit, followed by Na^+ that gradually decreased over time up to 9.75 after 24 months of exposure, with exception after 18 months (Figure 3.149).

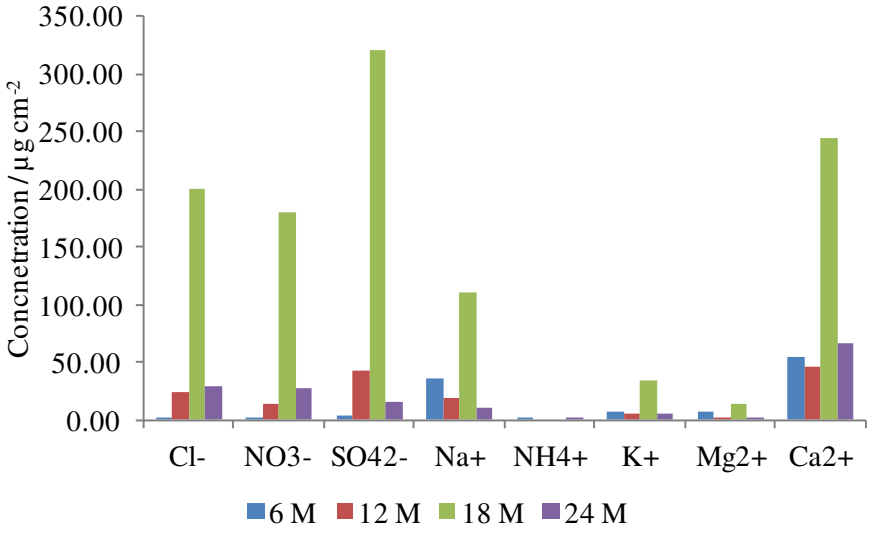

Figure 3.149 Concentration of soluble ions per surface unit measured in passive filters exposed in Ferrara after 6 (blue), 12 (red), 18 (green) and 24 (purple) months.

FLORENCE

Table 3.51 shows the detected amount of water soluble fractions (in ppm) measured in passive filters exposed in Florence after 6, 12, 18 and 24 months while the related ion concentration per surface unit (µg cm^{-2}) is presented in Table A5.3 (Annex 5).

SAMPLE	EXPOSURE TIME (month)	Cl^- (ppm)	NO_3^- (ppm)	SO_4^{2-} (ppm)	Na^+ (ppm)	NH_4^+ (ppm)	K^+ (ppm)	Mg^{2+} (ppm)	Ca^{2+} (ppm)
SMF1	6	2.56	0.15	1.26	1.20	0.06	0.22	0.19	3.79
SMF2	12	2.05	0.92	1.41	2.00	<LOD	0.87	0.27	11.76
PC94	18	5.78	2.32	2.59	3.64	<LOD	0.61	0.29	7.63
SMF4	24	6.05	2.62	3.82	3.77	<LOD	0.74	0.26	14.40

Table 3.51 Main soluble ions measured on passive filters exposed in Florence for 6, 12, 18 and 24 months. <LOD means below limit of detection.

Observing the concentration of anions detected per surface unit on passive filter (Figure 3.150), it gradually increased over time. In particular, Cl^- reached always the highest value (up to 60.55 µg cm^{-2}) followed by SO_4^{2-} and NO_3^-. Comparing each analysed period, Ca^{2+} displayed always the highest value, up to 144.03 µg cm^{-2} after 24 months of exposure (Figure 3.150). Among cations, also Na^+ was detected with significant amount per surface unit, with an increasing trend over time.

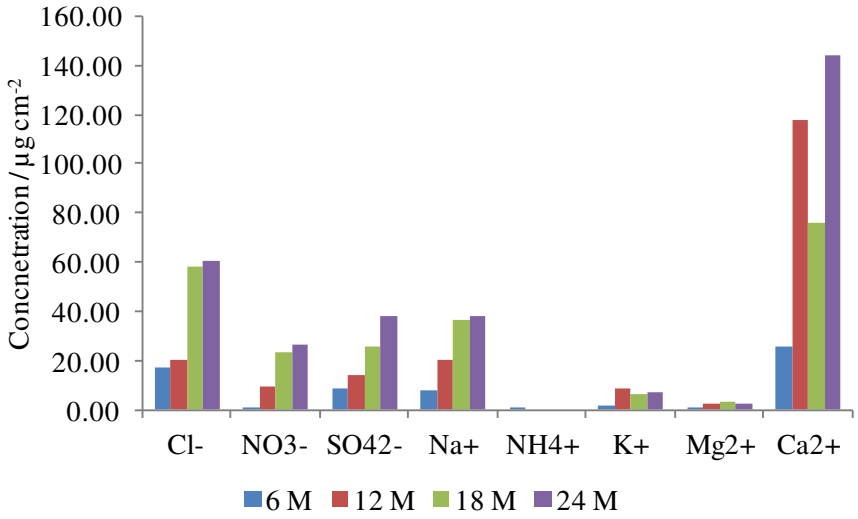

Figure 3.150 Concentration of soluble ions per surface unit measured in passive filters exposed in Florence after 6 (blue), 12 (red), 18 (green) and 24 (purple) months.

COMPARISON

Figure 3.151 shows the comparison of soluble ions concentration measured in passive filters exposed in Bologna, Ferrara and Florence for 6, 12, 18 and 24 months. During the first 6 months of exposure, Bologna reached the highest concentration of anions per surface unit respect to the other exposure sites, never exceeding 35.00 µg cm^{-2} (Figure 3.151 A). In general, the amount of Cl^- per surface unit was the highest,

followed by SO_4^{2-} and NO_3^-, in Bologna and Florence while quite similar values of Cl^- and SO_4^{2-} were observed in Ferrara. After 12 months, a general increase of all anions concentration per surface unit was detected in all sites, with exception of Bologna where NO_3^- significantly increased till to 23.17 µg cm^{-2} while Cl^- and SO_4^{2-} decreased below 9.00 µg cm^{-2}. In particular, SO_4^{2-} and Cl^- prevailed in Ferrara and Florence, respectively. A general increase of anions concentration was observed in all sites after 18 months of exposure, with exception of SO_4^{2-} in Bologna. Specifically, passive filter exposed in Ferrara reached the highest concentration of anions per surface unit ever, mostly for SO_4^{2-} (319.62 µg cm^{-2}). Moreover, anions concentration underwent a general reduction after 24 months of exposure in Bologna and Ferrara while it slightly increased in Florence never overcoming 61.00 µg cm^{-2} (Figure 3.151 A).

Considering cations (Figure3.151 B), Ca^{2+} was always detected with the highest concentration per surface unit in all sites, reaching the maximum value equals to 244.98 µg cm^{-2} in Ferrara after 18 months of exposure. Significant concentration of Na^+ was also measured during the whole considered period mainly in Florence and Ferrara, where it reached 110.00 µg cm^{-2} after 18 months of exposure. NH_4^+ never reached 2.00 µg cm^{-2} as well as K^+ and Mg^{2+} rarely exceeded 10.00 µg cm^{-2}.

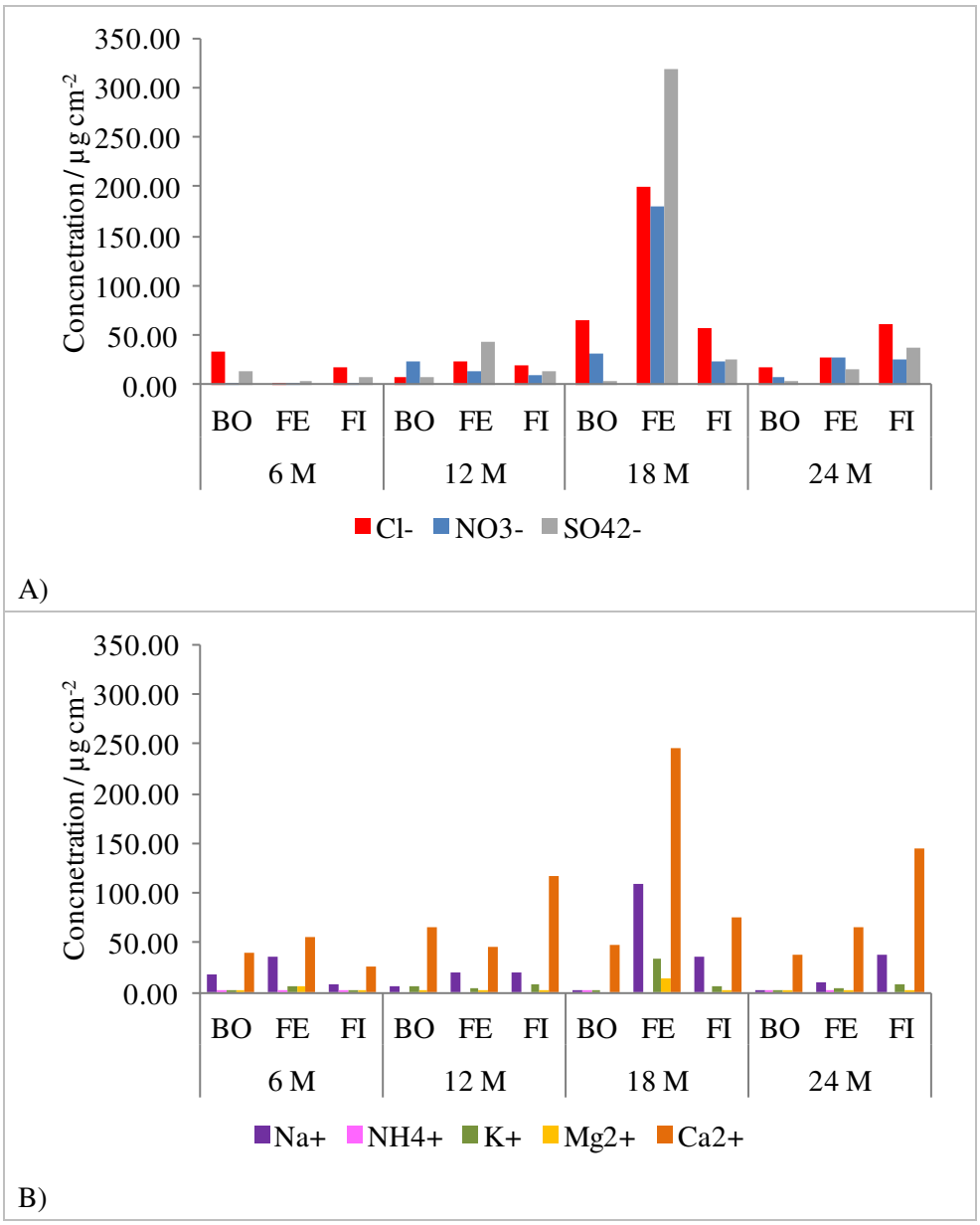

Figure 3.151 Concentration of anions (A) and cations (B) per surface unit measured in passive filters exposed in Bologna (BO), Ferrara (FE) and Florence (FI) for 6, 12, 18 and 24 months.

Final remarks:

- The highest concentration of all soluble ions per surface unit was measured in Ferrara after 18 months of exposure (till to 319.62 µg cm^{-2} for SO_4^{2-}).
- In general, ion chromatography showed that Cl^- and SO_4^{2-} prevailed among anions and Ca^{2+} and Na^+ among cations in all sites during the whole exposure period. These can be attributable both to natural (e.g. marine origin, resuspended dust) and anthropogenic (e.g. traffic and industry) emissions.
- The most abundant ions (Cl^-, SO_4^{2-}, Ca^{2+} and Na^+) identified in passive filters exposed in Florence underwent a general increase over time.

3.2.3. CARBON SPECIATION

BOLOGNA

Total carbon content (calculated as OC + EC) measured per surface unit in passive quartz filter exposed in Bologna remained between 70.35 µg cm^{-2} and 120.84 µg cm^{-2} measured after 6 and 12 months of exposure, respectively (Table 3.52). An increase in TC was observed after 12 and 24 months of exposure (120.84 µg cm^{-2} and 113.28 µg cm^{-2}, respectively) while filters exposed for 6 and 18 months displayed similar values (70.35 µg cm^{-2} and 78.71 µg cm^{-2}). Moreover, OC always prevailed over EC, reaching till to 120.82 µg cm^{-2} after 12 months of exposure while EC was always below limit of detection of the technique (equal to 0.15 µg cm^{-2}) (Table 3.52).

SAMPLE	EXPOSURE TIME (month)	OC (µg cm^{-2})	EC (µg cm^{-2})	TC (µg cm^{-2})
PC84	6	70.34	<LOD	70.35
PC85	12	120.82	<LOD	120.84
PC86	18	78.69	<LOD	78.71
PC87	24	113.26	<LOD	113.28

Table 3.52 Carbon fractions per surface unit measured on passive filters exposed in Bologna for 6, 12, 18 and 24 months. <LOD means below limit of detection.

FERRARA

Passive filters exposed in Ferrara underwent a significant accumulation of total carbon, increasing over time till after 18 months of exposure when the maximum value was reached (885.14 µg cm^{-2}) (Table 3.53). After 24 months the amount of TC per surface unit decreased to 194.96 µg cm^{-2}. Considering single carbon fractions, EC was always below limit of detection of the technique (0.15 µg cm^{-2}) while OC was between 194.93 µg cm^{-2} and 885.09 µg cm^{-2} measured after 24 months and 18 months, respectively. However, it should be highlighted that OC values detected in passive filters exposed for 12 and 18 moths are off-scale because filters were over-concentrated. Thus these values of OC and consequently of TC could not be considered reliable but it can be stated that a significant concentration of OC and TC per surface unit was detected after 12 and 18 months.

SAMPLE	EXPOSURE TIME (month)	OC (µg cm^{-2})	EC (µg cm^{-2})	TC (µg cm^{-2})
PTF1	6	260.83	<LOD	260.85
PTF2	12	436.19 *	<LOD	436.22 *
PTF3	18	885.09 *	<LOD	885.14 *
PTF5	24	194.93	<LOD	194.96

*Table 3.53 Carbon fractions per surface unit measured on passive filters exposed in Ferrara for 6, 12, 18 and 24 months. <LOD means below limit of detection. * value considered off-scale for the technique.*

FLORENCE

Table 3.54 displays the amount of TC, OC and EC measured per surface unit in passive filters exposed in Florence. Total carbon gradually increased over time passing from 76.35 µg cm^{-2} after 6 months of exposure to 372.30 µg cm^{-2} after 24 months. In particular, EC was always below limit of detection of the technique (0.15 µg cm^{-2}) while OC concentration per surface unit increased over time from 76.33 µg cm^{-2} to 372.25 µg cm^{-2} measured after 6 and 24 months of exposure, respectively. It should be note that the amount of OC (and thus of TC) measured after 24 months of exposure is off-scale because the filter was over-concentrated.

SAMPLE	EXPOSURE TIME (month)	OC (µg cm^{-2})	EC (µg cm^{-2})	TC (µg cm^{-2})
SMF1	6	76.33	<LOD	76.35
SMF2	12	154.43	<LOD	154.45
PC94	18	217.64	<LOD	217.66
SMF4	24	372.25 *	<LOD	372.30 *

*Table 3.54 Carbon fractions per surface unit measured on passive filters exposed in Florence for 6, 12, 18 and 24 months. <LOD means below limit of detection. * value considered off-scale for the technique.*

COMPARISON

OC and TC concentrations per surface area measured in passive filters in all sites at different exposure time are shown in Figure 3.152. EC values have not been reported as they were always below limit of detection of the technique in all sites. Therefore, TC values, resulting by the sum of OC plus EC, was always almost equal to those of OC. The amounts of OC measured per surface unit in passive filters exposed in Ferrara were always higher than those detected in Florence and Bologna after the same exposure period, with exception of OC measured after 24 months that reached the highest value in Florence. Concentration of carbon fractions measured in Bologna were always the lowest.

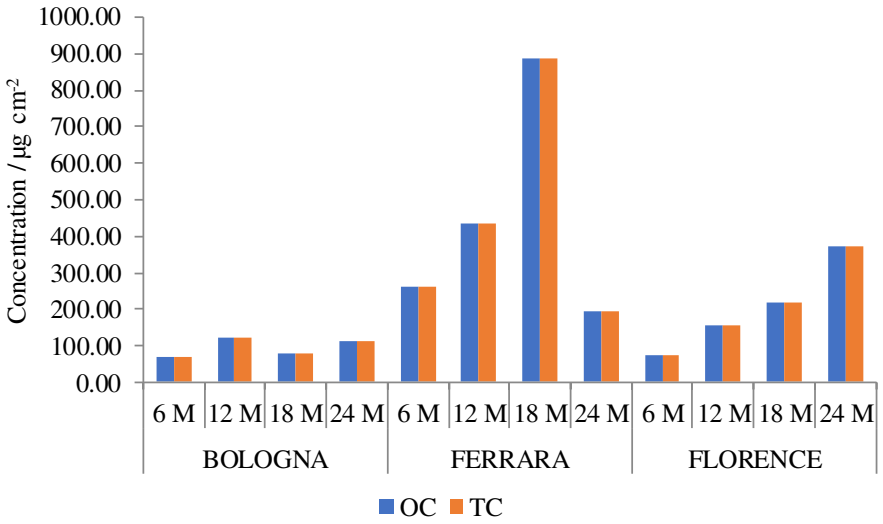

Figure 3.152 Concentration of OC (blue) and TC (orange) per surface unit measured in passive filters exposed in Bologna, Ferrara and Florence for 6, 12, 18 and 24 months.

However, particulate matter deposited on passive filters after 12 and 18 months of exposure in Ferrara and after 24 months in Florence was over-concentrated that OC and TC values cannot be considered reliable because they are off-scale. Anyway, it can be confirmed a significant concentration per surface unit of OC and TC in these filters. Indeed, also by visual assessment these filters (i.e. PTF2, PTF3 and SMF4) appeared really concentrated and characterised by a brownish/dark colour (Figure 3.153).

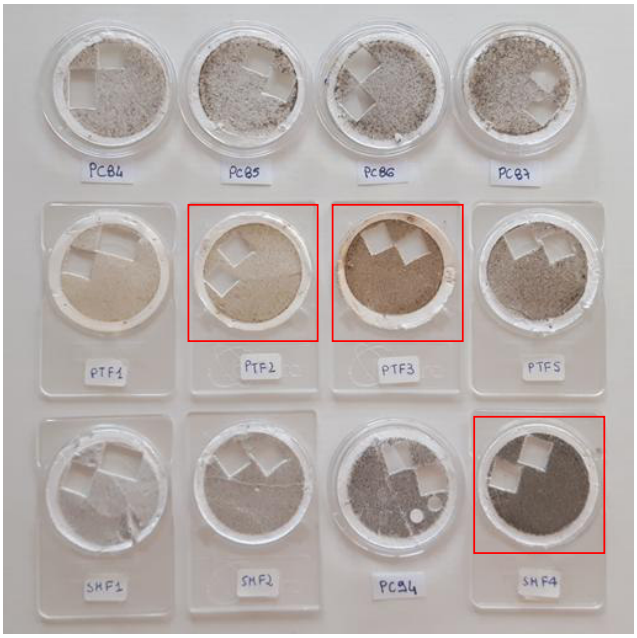

Figure 3.153 Picture of passive filters exposed in Bologna (PC84, PC85, PC86, PC87), Ferrara (PTF1, PTF2, PTF3, PTF5) and Florence (SMF1, SMF2, PC94, SMF4) for 6, 12, 18 and 24 months. Filters with off-scale OC and TC values are highlighted by red rectangles.

Final remarks:

- Considering each exposure period, passive filters exposed in Ferrara displayed the highest concentration of TC per surface unit, with exception of TC measured after 24 months that reached the most significant amount in Florence. The amount of TC per surface unit exposed in Florence gradually increased over time till to 372.30 µg cm^{-2} after 24 months while that of Bologna never exceeded 120.84 µg cm^{-2}.
- TC values, resulting by the sum of OC plus EC, was always almost equal to those of OC as EC was always below limit of detection of the technique in all sites.
- TC and OC deposited on passive filters after 12 and 18 months of exposure in Ferrara and after 24 months in Florence was so much concentrated that their concentration is considered off-scale.

3.3. PARTICULATE MATTER MONITORING CAMPAIGNS

3.3.1. CHARACTERISATION OF EXPOSURE SITES

BOLOGNA

Equipments for air pollution monitoring in the area of Bologna have been active from 1998 but data relative to air pollutants monitored by the Regional Environmental Protection Agency for Emilia-Romagna region (Agenzia Regionale per la Protezione Ambientale dell'Emilia-Romagna – ARPAE) are accessible from 2001 in its webpage (https://www.arpae.it/). For evaluating the background of aerosol condition relative to the exposure site in Bologna, I selected data of monitoring stations closer to the CNR (Figure 3.154). Their main characteristics are presented in Table 3.55. Nevertheless, some of them are no more active due to the adjustment of the Regional Monitoring Network to the EU directives designed to make comparable the environmental information of all member states.

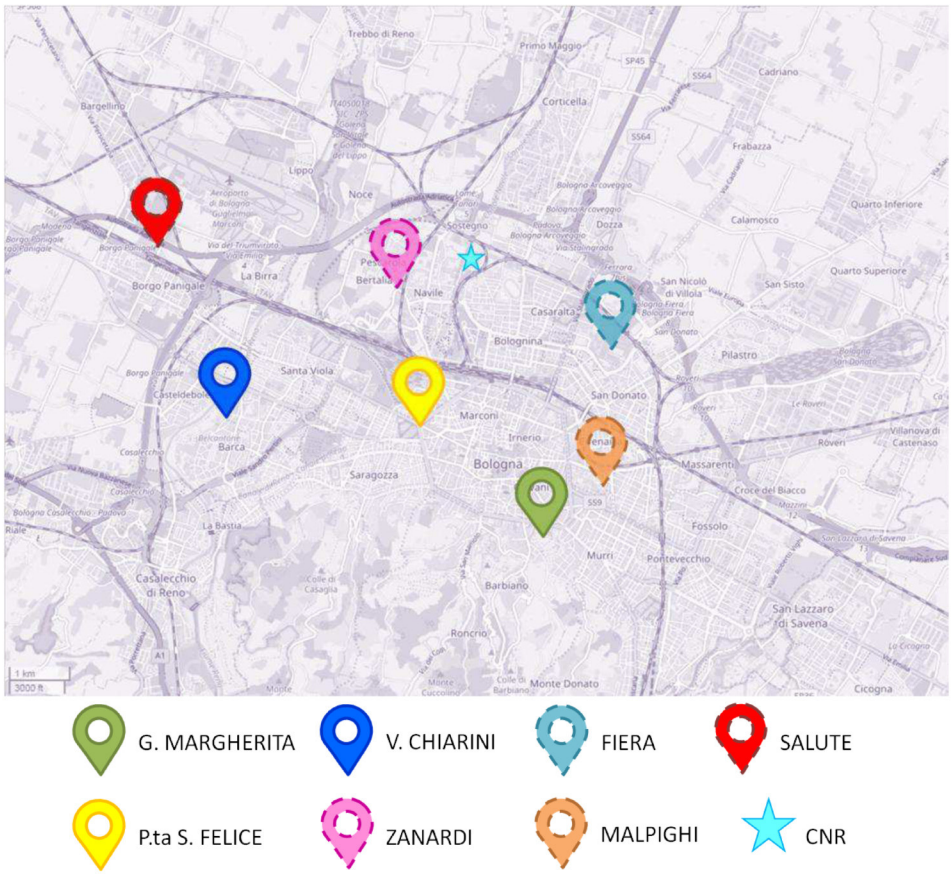

Figure 3.154 Location of monitoring stations of air quality in Bologna by ARPAE. Abandoned stations are indicated by dotted outline.

Among still active monitoring stations, Porta San Felice station is located at the intersection between the main street that circumscribes the city centre (characterised by two carriageway road with three lanes for each direction) and another road that join the urban centre with outskirts. The background station of Via Chiarini is placed in a residential area in the suburb of Bologna while the other operative background station (Giardini Margherita) is located in an urban park of a residential area of the city.

MONITORING STATION	FEATURES	AVAILABLE DATA	DISTANCE FROM THE PALACE (in straight line)	PM_{10}	$PM_{2.5}$	NO_2	CO	BENZENE
FIERA	urban traffic-oriented	2001-2006	around 2000 m	YES	-	YES	-	-
G.MARGHERITA	urban background	from 2001	4400 m	YES	YES	YES	YES	-
MALPIGHI	urban traffic-oriented	2001-2008	around 3800 m	-	-	YES	-	.-
P.ta s. FELICE	urban traffic-oriented	from 2001	2700 m	YES	YES	YES	YES	YES
SALUTE		2001-2004	around 5000 m	-	-	YES	-	-
Via CHIARINI	suburban background	from 2011	5000 m	YES		YES		
ZANARDI	urban background	2001-2008	1400 m	-	-	YES	-	YES

Table 3.55 The closest monitoring stations to CNR in Bologna and their measured pollutants.

The concentration of PM_{10} has generally decreased in all considered area of Bologna over the years, as shown in Figure 3.155. A part from the first years of sampling, P.ta S. Felice has maintained the highest concentration of particulate with a diameter lower than 10 µm but all the other stations has followed its trend. Considering the yearly limit value for human health protection fixed by Legislative Decree no. 250/2012 (40 µg m^{-3}) (see Table 3.56), no override was detected from 2008. Nevertheless, the guideline annual value for PM_{10} (20 µg m^{-3}) determined by the World Health Organisation (WHO) was sporadically respected only by G. Margherita.

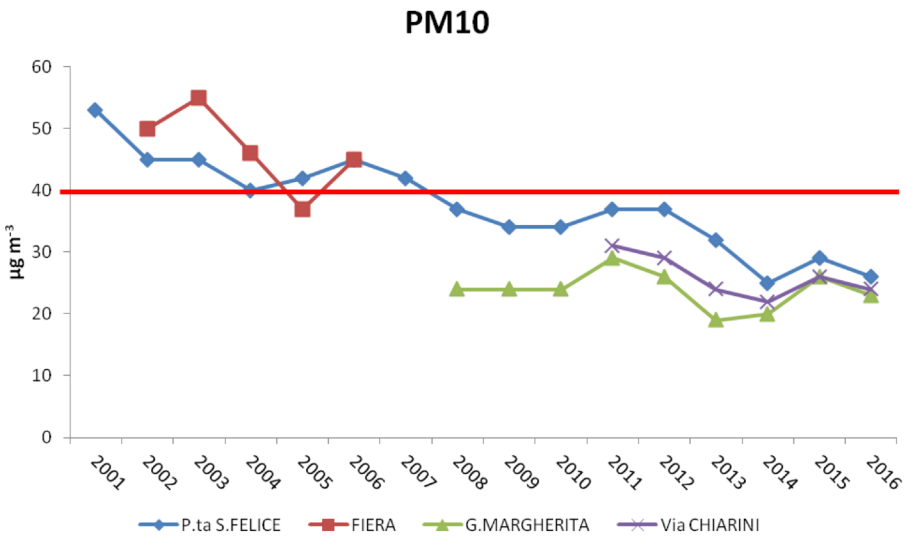

Figure 3.155 Mean annual concentration of PM_{10} measured by monitoring stations closest to CNR. Red line indicates the yearly limit value for human health protection fixed by Legislative Decree no. 250/2012.

POLLUTANT	AVAREGING PERIOD for human health protection	LIMIT VALUE	MAXIMUM NUMBER OF ALLOWED OCCURENCES
PM_{10}	24 hours	50 μg m^{-3}	35 per year
	year	40 μg m^{-3}	0
$PM_{2.5}$	year	25 μg m^{-3}	0
NO_2	24 hours	200 μg m^{-3}	18 per year
	year	40 μg m^{-3}	0
CO	maximum daily 8-hour mean	10 mg m^{-3}	0
SO_2	1 hour	350 μg m^{-3}	24 per year
	24 hour	125 μg m^{-3}	3 per year
O_3	maximum daily 8-hour mean	125 μg m^{-3}	25 per year
Benzene	year	5 μg m^{-3}	0
Benzo(a)pirene	year	1 ng m^{-3}	0
Arsenic	year	6.0 ng m^{-3}	0
Cadmium	year	5.0 ng m^{-3}	0
Nickel	year	20.0 ng m^{-3}	0
Lead	year	0.5 μg m^{-3}	0

Table 3.56 Summary of air-quality directive limit values and maximum number of allowed occurrences for the protection of human health fixed by the Italian legislative decree law 250/2012, which has transposed EU Directive no. 2008/50/EC on ambient air quality. For NO_x the Italian legislation limit the emission to 30 μg m^{-3} per year considering the vegetation protection.

Also the amount of $PM_{2.5}$ has diminished, displaying a trend very comparable to that of PM_{10} (Figure 3.156). This highlights the influent contribution of fine fraction particulate in PM_{10}. Moreover, taking into consideration the ratio $PM_{2.5}/PM_{10}$ of each year (https://www.arpae.it/), it shows minimum values during summer, when resuspension and long-distance transport of coarse fraction prevail, and maximum in wintertime, characterized by higher concentration of fine particles due to combustion processes and more air stagnation. Comparing the detected values with the yearly limit value for human health protection fixed by Legislative Decree no. 250/2012 (25 μg m^{-3}), no override was measured from 2008. However, no stations respected the guideline annual value of $PM_{2.5}$ (10 μg m^{-3}) fixed by WHO.

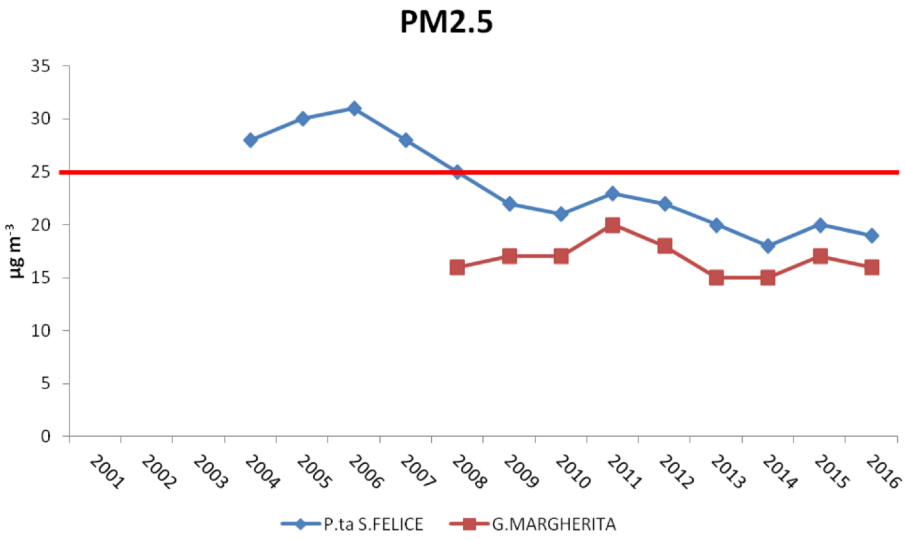

Figure 3.156 Mean annual concentration of $PM_{2.5}$ measured by monitoring stations closest to CNR. Red line indicates the yearly limit value for human health protection fixed by Legislative Decree no. 250/2012.

Further information about the particulate matter could be provided by Tositti et al. (2014) within the national project SITECOS (Integrated Study on national Territory for the characterisation and COntrol on atmospheric pollutantS), aimed at evaluating the different effects of climatic and emission features on pollutants dynamics of North, Centre, and South Italy. PM_{10} (on PTFE with support ring) and $PM_{2.5}$ (with quartz fibre filter) were sampled at Chemistry Department of the University of Bologna (located in the city centre, around 3 km far from the CNR) during different periods: fall (26 Sept-19 Oct) 2005, winter (23 Jan-05 Mar) and summer (20 Jun-20 Jul) 2006. Considering the amount of particulate matter monitored in each period, the minimum mean value was recorded during summer 2006 (35 µg m^{-3} for PM_{10} and 21 µg m^{-3} for $PM_{2.5}$) while winter 2006 displayed the highest average concentration (51 µg m^{-3} for PM_{10} and 41 µgm^{-3} for $PM_{2.5}$). Moreover, the $PM_{2.5}/PM_{10}$ ratio varied seasonally, showing values of 0.5-0.6 during summer and 0.8-0.9 during wintertime. This difference could be due to the increase in coarse fraction during warm season for higher resuspended dust and to different combustion sources in the two periods. In particular, chemical elements were analysed in PM_{10} filters by particle-induced X-ray emission (PIXE) while CHN elemental analysis and ion chromatography allowed to detect carbon speciation and soluble ions, respectively. The analyses revealed that OC account for about 60-70% of total carbon while EC only for 40-30% (cold versus warm values). Beyond carbonaceous fraction, the most abundant species in $PM_{2.5}$ in the considered periods were nitrate, sulphate and ammonium (Figure 3.157). It is noteworthy that NO_3^- contributed more than SO_4^{2-} to $PM_{2.5}$ during cold season. During summer, the photochemical oxidation of SO_2 causes a relative increase of the connected ionic species while the incomplete collection of NH_4NO_3 due to thermal instability is likely the responsible of lower contribution of nitrates into atmosphere. The assessment of the degree of neutralisation in the aerosol samples highlighted the acid feature of aerosol during the cold season. Furthermore, the analysis of the concentration of elements detected in PM_{10} showed this order: Ca>S>Si>Cl>Fe>K>Na>Al>Mg>Zn>Ti>Pb>P>Br>Mn>Cu>Cr>Ni>V.

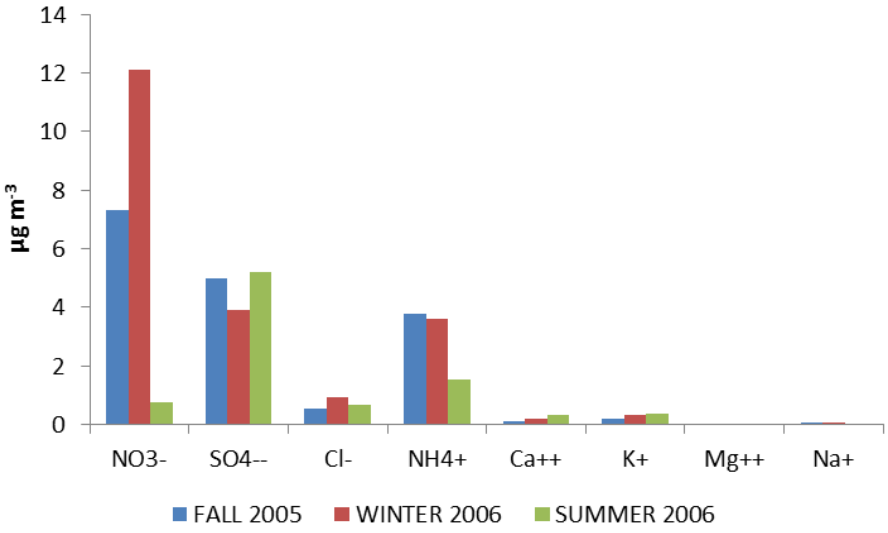

Figure 3.157 Mean ion concentration of $PM_{2.5}$ measured in Bologna (Tositti et al., 2014).

To better understand pollution condition and health effect, the Emilia-Romagna Region and its Agency for Prevention and Environment took part in the project Supersito (www.supersito-er.it). It aimed to study the chemical composition, source apportionment and toxicological properties of fine ($PM_{2.5}$ and PM_1) and ultrafine particulate ($<PM_{0.1}$). Samples were collected in different monitoring stations, including one located in the area of the CNR. It is considered an urban background site and it is important to maximize the representativeness of population exposure to particulate matter, avoiding sites characterised by strong local sources. Routine measurement started in November 2011 and finished in March 2015. Ricciardelli et al. (2017) reported average winter (December-February) and summer (June-august) values of daily monitoring of $PM_{2.5}$ at the station located at the CNR. Mean $PM_{2.5}$ winter concentration varied from 49 µg m^{-3} (in winter 2011-2012) and 30 µg m^{-3} (in winter 2013-2014), showing generally higher values than those measured in other European urban sites (Ricciardelli et al., 2017). As expected, during summer the concentration of $PM_{2.5}$ decreased, ranging from about 13 µg m^{-3} (in 2012) and 10 µg m^{-3} (in 2014). Analysing the composition, among detected species, winter $PM_{2.5}$ showed to be mainly composed of nitrate and OC and secondly of ammonium, sulphate, EC and the sum other ions while during summer sulphate and OC prevailed on the other species. Higher $PM_{2.5}$ amount in winter 2011-2012 seemed to be also influenced by particularly cold and snowy conditions that determined high ammonium nitrate concentration in the studied area. During winter, precursors of nitrate (NO_x) are indeed released by traffic, domestic heating and industries while the main source of atmospheric NH_3 is agriculture (90%), as evaluated by the regional emission inventory (Tugnoli et al., 2013). In addition, the ammonia-rich atmosphere that characterised the Po valley bypasses the favoured neutralisation of sulphuric acid as well as the low temperature and high humidity of Po plain promote the reaction between NH_3 and HNO_3 to form ammonium nitrate. Meteorological parameters influence the atmospheric composition also in warm season as the high temperature inhibits the formation of ammonium nitrate, as aforementioned by Tositti et al. (2014). Focusing on carbonaceous species, Ricciardelli et al. (2017) measured higher OC concentration in winter than in summer, likely due to the dispersion capacity of the atmosphere. Considering that OC emissions by traffic remain constant over the year, biogenic emissions and secondary aerosol formation contribute to summer OC concentration while during winter residential heating and biomass burning affect OC mass. In support of biomass burning correlation, a good correspondence between OC and K^+ was observed. EC, emitted by incomplete combustion of traffic and residential heating, revealed summer minimum and winter maximum, too.

In addition to this information, the Agency for Protection and Environment of Emilia-Romagna region provided further data about particulate matter monitored in the area of the National Research Council. PM_{10}

was monitored in different periods from 2011 to 2014 and its mean chemical composition is reported in Table 3.57. Unfortunately, PM_{10} mass concentration levels for the considered period were not supplied.

	Cl^-	NO_2^-	NO_3^-	SO_4^{2-}	Na^+	NH_4^+	K^+	Mg^{2+}	Ca^{2+}	WSOM (*1.8)	OC
FALL 2011	0.90	0.02	15.78	2.82	2.37	5.27	0.34	0.03	0.51	18.81	10.45
SUMMER 2012	0.23	0.03	2.03	2.61	0.49	0.99	0.05	0.08	0.54	3.74	2.08
WINTER 2013	0.76	0.02	11.54	2.21	0.23	3.98	0.21	0.03	0.52	9.11	5.06
SPRING 2013	0.11	0.04	1.47	0.61	0.20	0.49	0.02	0.03	0.19	1.93	1.07
FALL 2013	0.39	0.03	6.35	2.05	0.12	2.61	0.07	0.02	0.27	4.65	2.58
WINTER 2014	0.55	0.03	7.52	1.71	0.29	2.56	0.22	0.03	0.34	4.96	2.76
SPRING 2014	0.15	0.09	1.63	1.28	0.26	0.55	0.04	0.05	0.42	4.14	2.30

Table 3.57 Average concentration ($\mu g\ m^{-3}$) of the chemical composition of PM_{10} monitored at the CNR (data supplied by ARPAE).

As shown in Figure 3.158, measured PM_{10} was mainly composed by water soluble organic matter (WSOM), nitrate, sulphate and ammonium. In particular, NO_3^- confirmed higher values during cold seasons and lower level in warmer period while the concentration of sulphate remain almost constant independently from the season. Sulphate, in the form of ammonium sulphate and bisulphate, is indeed mainly produced in summer by photochemical processes while winter concentration could be attributed to episodic transport of polluted air masses from Balkan area (Perrino et al., 2014). Among cations NH_4^+ displayed the highest concentration, showing a reduction during warm periods. In the same periods, a slight decrease in organic component of PM is observable, too.

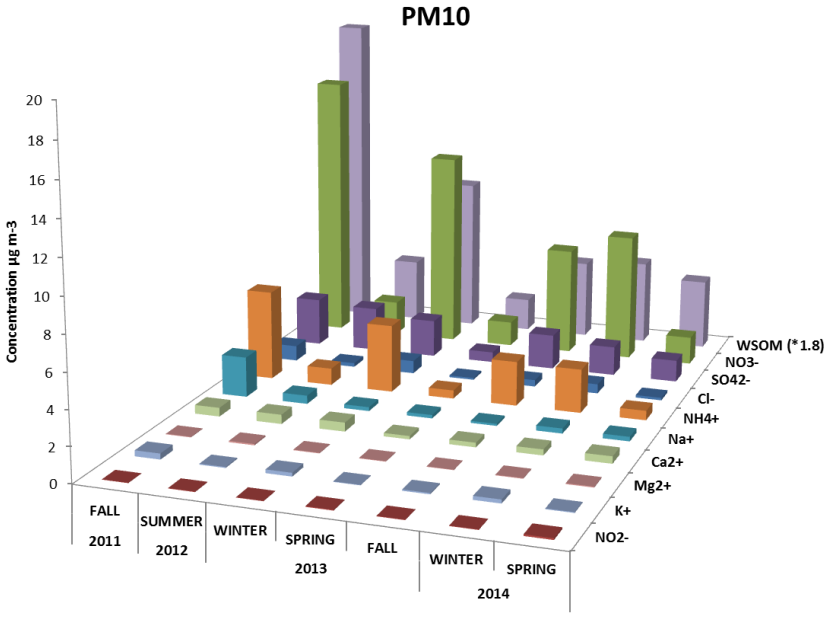

Figure 3.158 Average concentration of the chemical composition of PM10 monitored at the CNR (data supplied by ARPAE).

Moreover, $PM_{2.5}$ and PM_1 mass amount were measured at the CNR monitoring station by ARPAE from January 2013 till to March 2015, within the framework of Supersito Project. These fine fractions of

particulate matter displayed general higher amount during cold seasons and lower concentration in summer (Figure 3.159). During warm periods, PM_1 seemed to have a slightly higher influence on the total $PM_{2.5}$ mass.

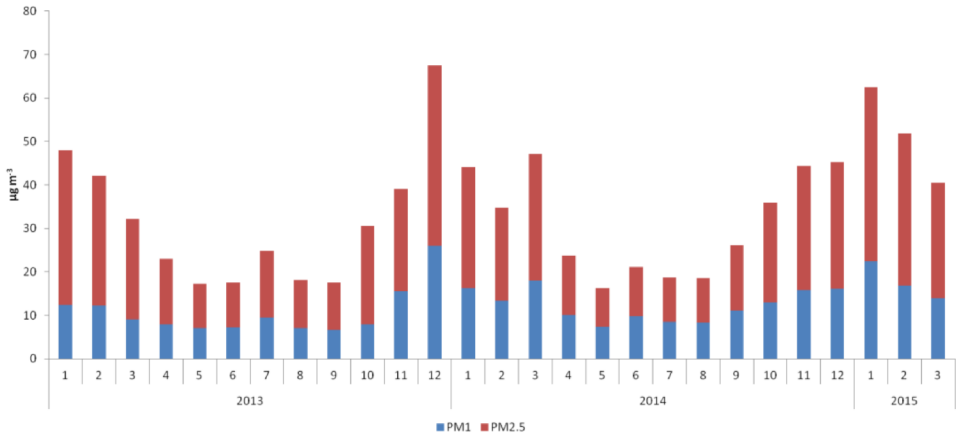

Figure 3.159 Monthly mean concentrations of $PM_{2.5}$ (red) and PM_1 (blue)(µg m^{-3}) monitored at CNR by ARPAE.

In addition, the comparison among $PM_{2.5}$ concentrations measured by the permanent monitoring stations of ARPAE and that located at CNR within the Supersito Project are reported in Figure 3.160. The monitoring station located at CNR displayed the highest values for both years among the considered monitoring centres and a similar trend to that located in Porta San Felice: a slight reduction in $PM_{2.5}$ concentration is appreciable in 2014.

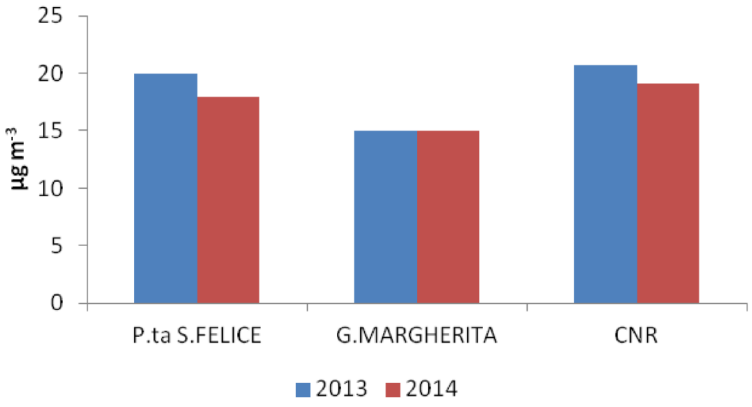

Figure 3.160 Comparison among the annual mean concentration of $PM_{2.5}$ measured at CNR and in the permanent monitoring station of ARPAE.

The main constituents of $PM_{2.5}$ monitored at the CNR are reported in Table 3.58, as monthly mean values. Analysing carbon speciation, OC always prevailed in all the considered months, showing generally higher concentration during cold months (Figure 3.161). EC displayed a very regular trend, with decreasing values during warmer period and increasing amount in winter.

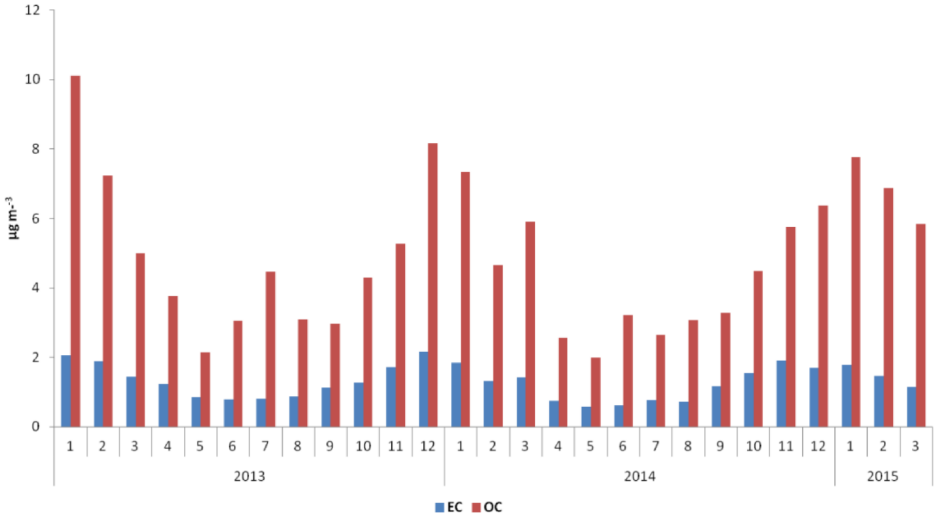

Figure 3.161 Monthly mean amount of OC (red) and EC (blue)measured (µg m^{-3}) in $PM_{2.5}$ at CNR.

YEAR	MONTH	EC	OC	TC	Na^+	$NH4^+$	K^+	Mg^{2+}	Ca^{2+}	Cl^-	Br^-	NO_3^-	SO_4^{2-}	PO_4^{3-}
2013	1	2.06	10.12	12.32	0.06	3.57	0.30	0.09	0.06	0.44	9.07	4.51	2.05	0.37
	2	1.88	7.23	9.27	0.15	3.16	0.17	<LOD	0.11	0.33	8.13	<LOD	2.26	0.36
	3	1.45	4.99	6.56	0.25	2.30	0.16	<LOD	0.21	0.50	5.36	<LOD	1.95	<LOD
	4	1.23	3.77	5.15	0.26	1.30	0.11	<LOD	0.25	<LOD	2.00	<LOD	2.14	<LOD
	5	0.85	2.15	2.99	0.25	0.84	0.09	<LOD	0.22	0.68	1.20	<LOD	1.73	<LOD
	6	0.79	3.04	3.84	0.24	0.94	0.07	<LOD	<LOD	<LOD	0.62	<LOD	2.01	<LOD
	7	0.81	4.47	5.29	0.09	1.54	0.05	<LOD	<LOD	<LOD	0.36	<LOD	3.41	<LOD
	8	0.87	3.10	3.97	<LOD	1.06	0.05	<LOD	<LOD	0.11	0.33	<LOD	2.11	<LOD
	9	1.13	2.97	4.12	0.13	0.97	0.04	0.03	<LOD	0.28	0.48	<LOD	1.90	<LOD
	10	1.28	4.29	6.86	0.10	2.48	0.06	0.02	<LOD	0.22	6.20	0.05	2.64	0.24
	11	1.72	5.26	8.06	0.10	2.12	0.16	0.02	<LOD	0.21	4.72	<LOD	1.54	0.40
	12	2.15	8.16	13.49	0.09	3.81	0.34	<LOD	<LOD	0.46	10.40	<LOD	1.80	0.72
2014	1	1.84	7.34	9.19	0.07	3.44	0.25	0.09	<LOD	0.26	8.49	<LOD	1.53	0.52
	2	1.31	4.65	5.97	0.14	2.73	0.13	0.04	0.09	0.27	6.41	<LOD	1.43	0.39
	3	1.42	5.91	7.47	0.14	3.33	0.15	0.02	0.14	0.25	8.13	<LOD	3.29	0.30
	4	0.75	2.56	3.31	0.11	1.42	0.07	0.03	0.17	0.10	1.59	<LOD	1.78	<LOD
	5	0.57	1.98	2.56	0.14	0.85	0.05	0.03	0.21	0.11	0.50	<LOD	1.30	<LOD
	6	0.61	3.23	3.83	<LOD	1.32	0.05	<LOD	0.11	<LOD	0.26	<LOD	2.58	<LOD
	7	0.76	2.65	3.41	0.16	0.99	0.05	0.04	0.13	0.08	0.28	<LOD	1.88	<LOD
	8	0.73	3.08	3.80	0.15	1.05	0.06	0.06	0.12	<LOD	0.22	<LOD	2.11	<LOD
	9	1.16	3.28	4.82	0.14	1.64	0.09	0.03	0.10	0.24	1.16	<LOD	2.79	0.20
	10	1.55	4.48	6.38	<LOD	2.95	0.10	<LOD	0.12	0.12	4.89	0.03	3.78	0.24
	11	1.90	5.75	7.65	0.13	3.00	0.21	0.02	0.13	0.21	6.63	<LOD	2.10	0.37
	12	1.70	6.37	8.05	0.13	2.83	0.27	<LOD	0.11	0.29	6.16	<LOD	1.75	0.35
2015	1	1.78	7.77	10.69	<LOD	3.92	0.42	0.04	0.16	0.38	9.98	<LOD	1.65	0.29
	2	1.47	6.87	8.34	0.18	3.66	0.25	<LOD	0.12	0.22	8.77	<LOD	2.28	<LOD
	3	1.15	5.84	6.99	0.19	2.85	0.16	<LOD	0.13	0.11	5.01	<LOD	2.85	<LOD

Table 3.58 Monthly mean concentration ($\mu g\ m^{-3}$) of the main components in $PM_{2.5}$ monitored at the CNR (data supplied by ARPAE). Continued

YEAR	MONTH	Al	As	Cr	Fe	Mn	Ni	V	Zn	Cd	Pb	Sn	Sb	Ba	Ca	K	Mg	La
2013	1	<LOD	0.00070	0.00132	0.09484	0.00341	0.00248	0.00072	0.02768	0.00021	0.00714	0.00183	0.00096	0.09346	<LOD	0.79667	<LOD	0.00008
	2	<LOD	0.00058	0.00140	0.09520	0.00324	0.00292	0.00048	0.02358	0.00020	0.00521	0.00141	0.00068	<LOD	<LOD	0.47000	<LOD	0.00005
	3	<LOD	0.00044	0.00115	0.08105	0.00426	0.00260	0.00081	0.01973	0.00016	0.00752	0.00109	0.00098	<LOD	<LOD	<LOD	<LOD	0.00008
	4	<LOD	0.00038	0.00122	0.08465	0.00227	0.00277	0.00191	0.01793	0.00013	0.00351	0.00087	0.00090	<LOD	<LOD	<LOD	<LOD	0.00005
	5	<LOD	0.00024	0.00090	0.07464	0.00201	0.00328	0.00138	0.01518	0.00015	0.00288	0.00077	0.00040	<LOD	<LOD	<LOD	<LOD	0.00008
	6	<LOD	0.00024	<LOD	0.06448	0.00161	0.00150	0.00095	0.01353	0.00008	0.00195	0.00078	0.00062	0.01943	<LOD	<LOD	<LOD	0.00007
	7	<LOD	0.00032	<LOD	0.05994	0.00187	0.00130	0.00105	0.01293	0.00011	0.00282	0.00082	0.00072	0.01235	<LOD	<LOD	<LOD	0.00010
	8	<LOD	0.00021	<LOD	0.06915	0.00142	0.00117	0.00071	0.01198	0.00005	0.00196	0.00077	0.00057	0.00740	<LOD	<LOD	<LOD	0.00006
	9	<LOD	0.00026	0.00115	0.08395	0.00248	0.00181	0.00122	0.01603	0.00007	0.00280	0.00113	0.00094	0.01982	<LOD	<LOD	<LOD	0.00006
	10	<LOD	0.00054	0.00112	0.09429	0.00290	0.00162	0.00103	0.02469	0.00030	0.00793	0.00168	0.00335	0.02591	<LOD	<LOD	<LOD	0.00007
	11	<LOD	0.00059	0.00134	0.10343	0.00357	0.00147	0.00053	0.03270	0.00037	0.00632	0.00188	0.00111	<LOD	<LOD	0.46000	<LOD	0.00004
	12	<LOD	0.00080	0.00170	0.15432	0.00460	0.00178	0.00077	0.03644	0.00038	0.01141	0.00257	0.00101	<LOD	<LOD	0.62500	<LOD	0.00008
2014	1	<LOD	0.00042	0.00170	0.08442	0.00274	0.00162	0.00041	0.02107	0.00017	0.00486	0.00156	0.00065	0.04909	<LOD	0.30320	0.33000	0.00009
	2	<LOD	0.00048	0.00139	0.07890	0.00291	0.00145	0.00045	0.02359	0.00016	0.00479	0.00125	0.00067	<LOD	<LOD	0.23727	<LOD	0.00003
	3	<LOD	0.00049	<LOD	0.11044	0.00533	0.00184	0.00106	<LOD	0.00023	0.00675	0.00104	0.00079	<LOD	<LOD	0.22000	<LOD	0.00006
	4	0.21289	0.00027	0.00124	0.08477	0.00241	0.00118	0.00133	0.01875	0.00008	0.00240	0.00073	0.00066	0.05417	<LOD	0.17364	<LOD	0.00006
	5	0.25465	0.00022	0.00127	0.06331	0.00158	0.00122	0.00089	0.01943	0.00005	0.00208	0.00055	0.00048	0.02786	<LOD	<LOD	<LOD	0.00009
	6	<LOD	0.00031	0.00165	0.05514	0.00151	0.00163	0.00102	0.02032	0.00009	0.00211	0.00062	0.00044	<LOD	<LOD	0.14500	<LOD	0.00003
	7	<LOD	0.00029	<LOD	0.07524	0.00198	0.00152	0.00080	0.02113	0.00008	0.00198	0.00079	0.00058	<LOD	<LOD	0.16000	<LOD	0.00006
	8	<LOD	0.00018	<LOD	0.06060	0.00118	0.00143	0.00130	0.02905	0.00006	0.00139	0.00076	0.00034	0.05258	<LOD	<LOD	<LOD	0.00007
	9	<LOD	0.00043	0.00138	0.10823	0.00258	0.00122	0.00090	0.02024	0.00013	0.00358	0.00116	0.00075	0.02489	<LOD	0.20889	0.35000	0.00004
	10	<LOD	0.00065	<LOD	0.11115	0.00300	0.00119	0.00110	0.02099	0.00017	0.00427	0.00151	0.00078	0.04908	<LOD	0.18824	<LOD	0.00004
	11	<LOD	0.00106	0.00205	0.10291	0.00395	0.00140	0.00048	0.03453	0.00024	0.00638	0.00195	0.00115	0.01608	<LOD	0.31474	<LOD	0.00004
	12	<LOD	0.00067	<LOD	0.10812	0.00323	0.00180	0.00047	0.02659	0.00026	0.00505	0.00192	0.00089	<LOD	<LOD	0.35286	<LOD	0.00009
2015	1	<LOD	0.00078	<LOD	0.17671	0.00549	0.00178	0.00068	0.03924	0.00027	0.00912	0.00347	0.00152	<LOD	<LOD	0.44000	<LOD	0.00009
	2	<LOD	0.00069	0.00176	0.13176	0.00384	0.00149	0.00066	0.02565	0.00019	0.00610	0.00179	0.00078	0.00484	<LOD	0.34533	<LOD	0.00006
	3	<LOD	0.00059	0.00189	0.10547	0.00337	0.00184	0.00091	0.02449	0.00017	0.00489	0.00119	0.00077	0.00913	<LOD	0.38000	<LOD	0.00005

Table 3.58 Mean concentration ($\mu g\ m^{-3}$) of the main components in $PM_{2.5}$ monitored at the CNR (data supplied by ARPAE).

Taking into consideration the old town centre where more historic buildings and monuments were constructed, ARPAE, on demand of Bologna Municipality, carried out winter campaigns in the corner between Via Rizzoli and Piazza del Nettuno, really close to San Petronio Cathedral (ARPAE, 2014). The one-month monitoring campaigns were executed between February and March in 2012, 2013 and 2014 by a mobile laboratory. For the features of its position, this monitoring station could be considered as an urban traffic-oriented one. The mean concentration of particulate matter ($PM_{2.5}$ and PM_{10}) sampled in 2014 confirmed the values of the previous year, albeit with a slight growth, characterised by a sharp decrease compared to 2012 levels (Figures 3.162, 3.163). In this context, the introduction of the so-called "T-days" in 2013, which have avoided the circulation of traffic (with exception of emergency vehicles) during Saturday and Sunday in the area of Via Rizzoli, Via Ugo Bassi and Via Indipendenza, seems to have favoured a reduction of air pollution in the selected area. However, its influence appears limited in comparison to that exerted by environmental conditions, in particular precipitation pattern.
Comparing PM_{10} concentration of the mobile station with that of the traffic-oriented station of Porta San Felice and of the background monitoring centre of Giardini Margherita, a continuous decrease from 2012 is observed in the two permanent stations (Figure 3.162). Furthermore, the area of Via Rizzoli appeared to be quite polluted as it documented the highest concentration of PM_{10} in 2012 and 2014, limited to the brief monitoring period.

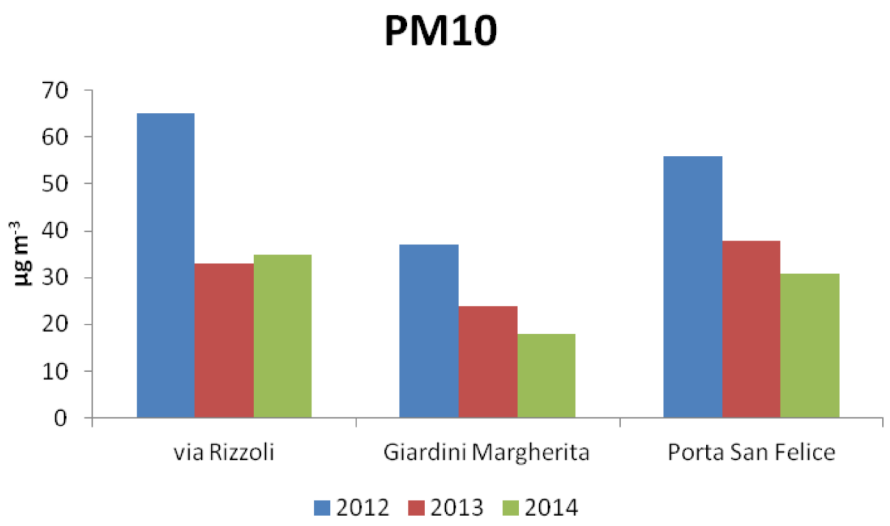

Figure 3.162 Comparison of the mean concentration of PM_{10} measured in Via Rizzoli, Giardini Margherita and Porta San Felice.

Considering $PM_{2.5}$ amount of the studied period, the trend of mean values is quite similar among the different stations: after a general decrease of the concentration from 2012 to 2013, the variation of mean $PM_{2.5}$ recorded in 2014 is similar or slightly higher (at max 2 µg m^{-3}) than that of the previous year (Figure 3.163). In addition, the comparison of $PM_{2.5}$ concentration analysed in Via Rizzoli, Porta San Felice, Giardini Margherita stations and at CNR during the same period in 2013 and 2014 highlighted the highest amount of the latter for both years, even if it is considered a urban background station (Figure 3.163). Even if this assessment is relative to one-month monitoring, it seems to corroborate the average annual higher amount of fine particulate matter at CNR in respect to the two stable monitoring centres described in Figure 3.160.

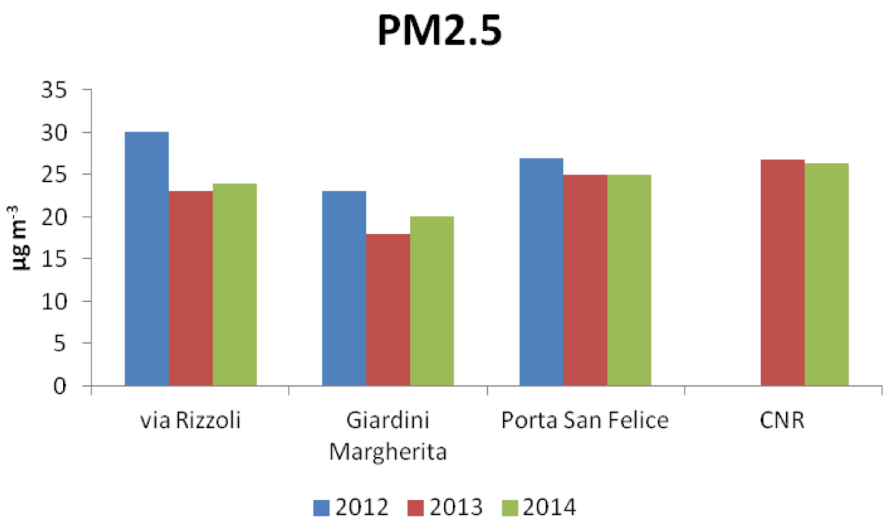

Figure 3.163 Comparison of the mean concentration of $PM_{2.5}$ measured in Via Rizzoli, Giardini Margherita, Porta San Felice and CNR.

Finally, EC concentration measured in $PM_{2.5}$ in Via Rizzoli in 2012 during the one-month period of study was slightly less than that measure at CNR (2.6 µg m^{-3} and 3.4 µg m^{-3}, respectively) while they were very similar in 2013 (1.8 µg m^{-3} and 1.7 µg m^{-3}, respectively) (ARPAE, 2012; ARPAE, 2013a). Moreover, for via Rizzoli measurement carried out in 2012, also the amount of OC (8.9 µg m^{-3}) is available, demonstrating as OC could represent about 75-80% of the total carbon analysed in $PM_{2.5}$ (ARPAE, 2012).

NO_2 is a pollutant that has been monitored by different stations during the last 15 years. Its concentration has not displayed the foreseen decrease as the only monitoring stations that recently recorded mean annual values below the yearly limit for human health protection fixed by Legislative Decree no. 250/2012 and WHO (40 µg m^{-3}) were G. Margherita and Via Chiarini (Figure 3.164). On the contrary, P.ta S. Felice continues to observe rather constant values over 50 µg m^{-3} also during last campaigns.

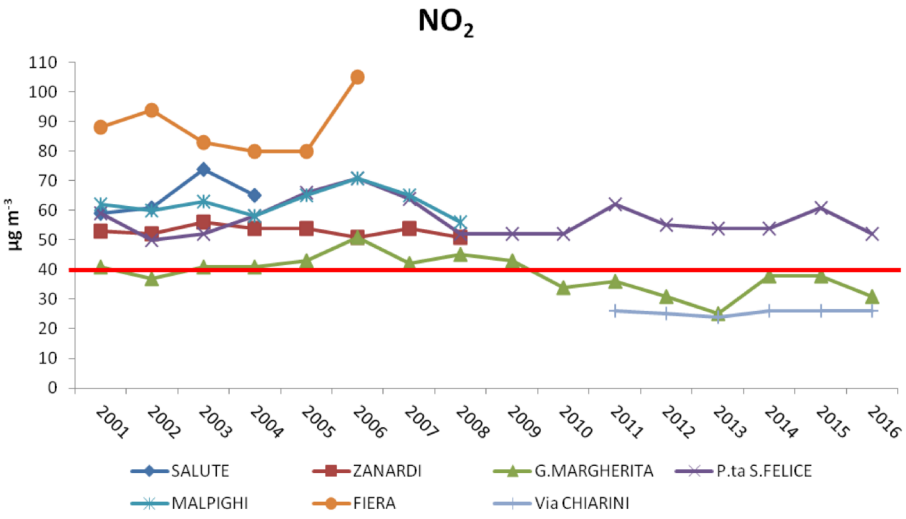

Figure 3.164 Mean annual concentration of NO_2 measured by monitoring stations closest to CNR. Red line indicates the yearly limit value for human health protection fixed by Legislative Decree no. 250/2012 and WHO.

From data available by ARPAE, NO_2 has proven to be more abundant during winter, when its formation reaches the maximum value due to heating systems, while in summer upward flows and favourable environmental conditions allow both its dispersion and transformation into nitric acid and nitrates. Observing the daily trend, a correlation is also appreciable with peak hours of traffic.

The amount of CO has been measured only in P.ta S. Felice station. Figure 3.165 shows a general decreasing trend over the years.

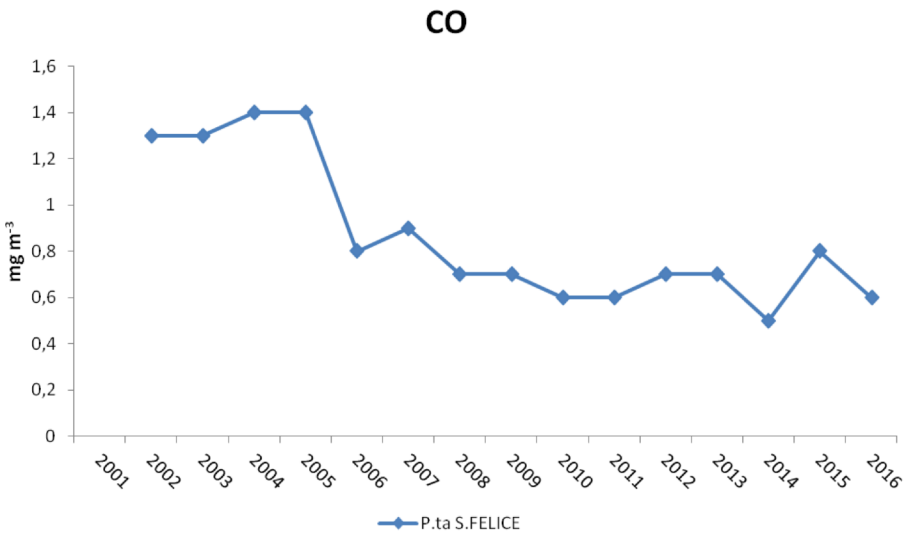

Figure 3.165 Mean annual concentration of CO measured by monitoring stations closest to CNR.

Benzene, added to gasoline as antiknock additive, is also used as a raw material for the production of secondary materials useful in the industry of plastic, cleansers, pesticides, varnishes, adhesives and inks. In Bologna it shows a diminishing trend and, in particular, it remained always below the yearly limit value fixed by the Legislative Decree no. 250/2012 (5 µg m^{-3}) in background stations and from 2004 also in the traffic-oriented station of P.ta S. Felice (Figure 3.166).

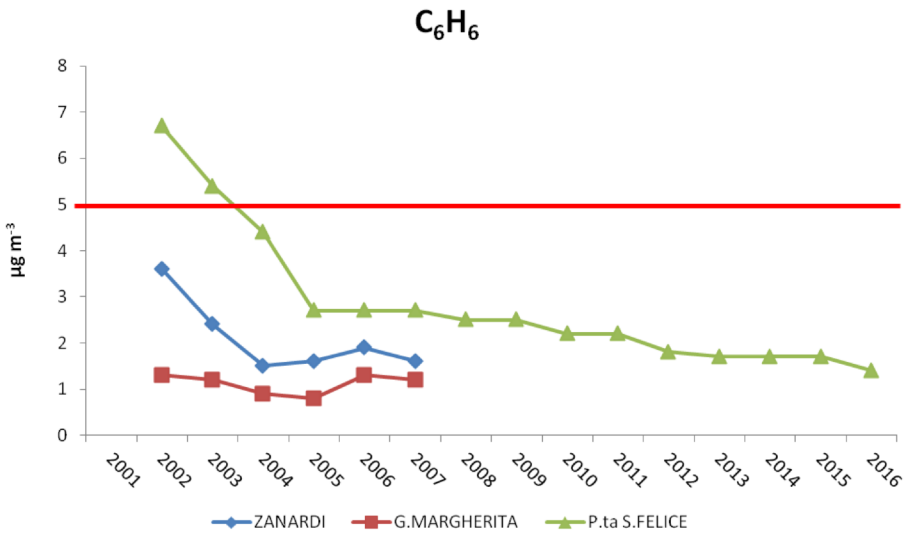

Figure 3.166 Mean annual concentration of C_6H_6 measured by monitoring stations closest to CNR. Red line indicates the yearly limit value for human health protection fixed by Legislative Decree no. 250/2012.

The study of the main pollutants origin is really important to better understand the emission dynamics of each contributing sector and to focus where changes should be apply in order to improve air quality. In this context, Tositti et al. (2014) evaluated the main sources contributing to PM_{10} by widely used receptor models on data achieved during the monitoring campaigns carried out at Chemistry Department of the University of Bologna in 2005 and 2006. In this study, the first cause of PM_{10} was attributable to *traffic* (35% of PM_{10}), detectable by emissions of NO_3^-, NH_4^+, Ni, Zn, K^+, Cr, Cu, OC and EC. Traffic exerted its influence mainly during cold season due to atmospheric stability. The second source was ascribable to *secondary aerosol* (26% of PM_{10}), linked to SO_4^{2-}, Mg^{2+}, NH_4^+ and K^+, while the third one to *mineral dust* (15%), linked to Al, Si, Ti, K, Ca, Fe and Mn. *Road dust* contributed to 11% of PM_{10} due to the abrasion of mechanical parts of vehicles and thus associated to Ca, Cu, Mn, Fe, Zn, Ni and Na while "*pseudo-marine*" (8% of PM_{10}), whose emissions of Na, Cl, Mg were attributed to the use of sea salt as de-icing agents on roads during wintertime. Finally, *biomass burning* (connected to OC, EC and K^+ and Mg^{2+}, in a lesser extent) was responsible of only 5% of PM_{10}. The high correlation observed in this case among K^+, SO_4^{2-}, Cl^- and to a less extent Zn measured in $PM_{2.5}$ suggested a likely influence of the municipal waste incinerator. Moreover, the mixed combustion source showed higher contribution during warm period, supporting its possible origin from waste incinerator and agricultural biomass burning at the end of the harvest rather than to domestic heating.
Emission inventory of Emilia-Romagna Region updated to 2010 (Tugnoli et al., 2013) divided the different sources in 11 parts, which in turn could be gathered in 4 macro branches:

1. Industry (combustion deriving from energy industry, transformation of sources of energy, production processes and industrial combustion systems);
2. Heating (non-industrial combustion systems);
3. Traffic (road transport and other movable sources);
4. Other (extraction and distribution of fossil fuels and geothermal energy, use of solvents, waste disposal plant, nature and farming).

Considering Bologna territory, traffic fallowed by industry seem to have released the highest concentration of pollutants into atmosphere (Table 3.59). In particular, traffic was the responsible of emission of CO, NO_x, CO_2 and PM10 while high production of SO_2 was ascribable to industry. Nevertheless, the report doesn't

account for the influence of non-industrial combustion systems even if its pressure on particulate matter emission is continuously increasing. In this regard, Ranzi and Lauriola (2015) declared that wood combustion in Emilia-Romagna region is responsible of 27% of total PM_{10} emissions.

	CO	SO_2	NMVOC	CH_4	NO_x	TSP	CO_2	N_2O	PM_{10}	NH_3	TOTAL
INDUSTRY	1363	1338	2622	1233	2751	327	2086600	84	217	277	2096810
TRAFFIC	15070	134	2851	244	14461	1427	2937000	117	1174	191	2972669
OTHER	72	2	11528	25995	293	0	-870000	749	15	4278	-827068

Table 3.59 Annual concentration of monitored pollutants (t y-1) emitted by different macro-sources in the territory of Bologna in 2010.

Moreover, the Municipality of Bologna and the Regional Agency for Prevention and Environment worked together for providing information about the main sources of emissions relative to 2012-2013 (ARPAE, 2013b). In this case, the presented data refers only to the municipality of Bologna and not more to its territory. Taking into consideration the four macro-branches of pollutants origin, *traffic* is responsible of 6668 t y^{-1}, followed by *heating* (3411 t y^{-1}), *other sources* (2184 t y^{-1}) and *industry* (1908 t y^{-1}). In particular, Figure 3.167 displays the amount of each pollutant released by each source. It should be highlighted that the emissions from *treatment and disposal of waste* was not considered (even if its impact should be reckoned with, as reported later) and that the negative value of *other natural sources and absorptions* referred to absorption of CO_2 by forests.

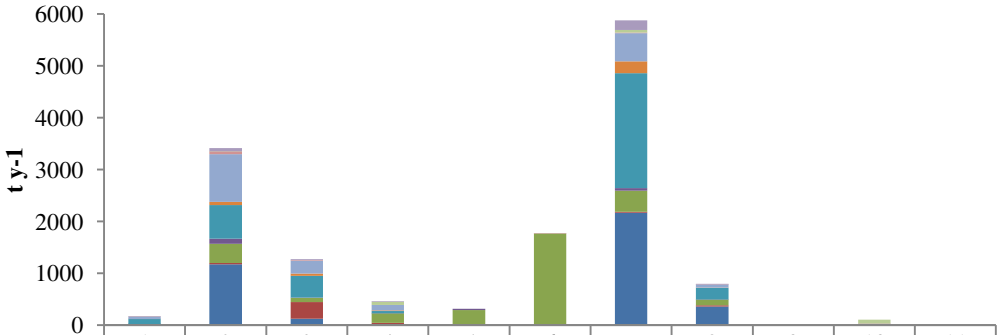

	1	2	3	4	5	6	7	8	9	10	11
PM10	0.2	58.8	18.4	10.3		0.1	183.7	7.1		0	
NH3		1.4	0.0	58.4			45.7	0		72.4	
N2O	0.1	54.6	15.2	0.0			15.8	0.9		12.3	
CO2	52.3	916.8	244.1	107.8			541.2	63.1			-10.2
TSP	0.2	61.3	45.5	13.9		0.2	230.6	7.3		0	
NOx	93.6	650.3	417.7	40.2			2213.6	219		3.4	
CH4	2.3	96.7	10.6	0.1	24.8		48	0.1		19.3	
VOCs	2.3	370.4	77.4	187.5	295.5	1765.7	409.7	113.7		0.0	
SO2	0.2	29.3	318.5	30.4			15.4	27.2			
CO	18.7	1171.7	128.5	13.9			2168.4	357.6			

Figure 3.167 Emission of pollutants (t y-1) in Bologna municipality distributed among different source branches. 1 refers to energy production and transformation of sources of energy, 2 to non-industrial combustion systems, 3 to industrial combustion systems and combustion deriving from energy industry, 4 to production processes, 5 to extraction, distribution of fossil fuels and geothermal energy, 6 to use of solvents, 7 to road transport, 8 to other movable sources, 9 to treatment and disposal of waste, 10 to farming and 11 to other natural sources and absorptions.

ARPAE (2013b) shows that non-industrial heating emitted mainly CO, CO_2, NO_x and VOCs, to less extent, while the whole industrial processes were responsible of NO_x, SO_2 and VOCs. Transport sector released high concentration of mainly CO and NO_x, farming of NH_3 and CH_4 and activities linked to extraction and distribution of fossil fuels or use of solvents released mostly VOCs. Finally, the analyses of PM_{10} emissions revealed the main responsibility of traffic (68%) and non-industrial heating (21%) sectors.

Additional information about emissions from civil heating highlighted its relevant importance in the total release of N_2O (55%), CO_2 (48%), CH_4 (48%), CO (30%), NO_x (18%) and VOCs (11%). Precisely the highest influence was ascribed to residential heating systems while institutional and commercial ones had less bearing. Moreover, considering the emissions by residential heating, systems powered by methane emitted 94% of NO_x and 97% of CO_2 while those powered by wood and by-products were identified as responsible of emissions of PM_{10} and TSP (93%), VOCs (78%) and CO (65%). In this regard, Tugnoli and Deserti (2011) identified fireplace as the most polluting wooden system (contributing till to 90% of emissions of this sector), whereas better performance were recognised in closed and more advanced systems.

The report (ARPAE 2013b) examined also the influence of different road vehicles, responsible mainly of CO, VOCs and CH_4 in urban roads and of other pollutants (such as SO_2, NO_x, CO_2, N_2O, NH_3 and PM_{10}) in trunk roads. On the contrary, lower impact in exhaust emissions was ascribable to motorway. Also the so-called "non-exhaust emissions" produced by the wear of tires, brakes and road surface are noteworthy as represented almost 50% of PM_{10} in the vehicular traffic sector. Further information about the influence of each kind of vehicle are described in the report. Taking into consideration the other movable sources, a international airport (*Guglielmo Marconi Airport*) is located close to Bologna, only around 3 km far from the CNR. Considering the Landing–Take Off (LTO) cycle, it results that airplanes emitted important concentrations of CO, SO_2, VOCs, NO_x and CO_2 in the non-vehicular traffic sector while they are responsible of the 63% of SO_2 amount released by the traffic macro-branch.

Finally, close to the city centre and the CNR (around 7 km far), there is a Municipal Waste to Energy Incinerator, located north of Bologna in the municipality of Granarolo dell'Emilia. It mainly burns solid urban, medical and sometimes also special nonhazardous wastes of Bologna and surroundings. ARPAE (2013b) showed that this incinerator was responsible of emission of atmospheric pollutants: 23.2 t y^{-1} of CO; 0.9 t y^{-1} of SO_2; 4.1 t y^{-1} of VOCs, 107.7 t y^{-1} of NO_x, 0.8 t y^{-1} of TSP, 23.8 t y^{-1} of CO_2, 20.6 t y^{-1} of N_2O; 3.9 t y^{-1} of NH_3 and 0.8 t y^{-1} of PM_{10}. Nevertheless, the report of ARPAE didn't account for the emissions from dumps, cremation, waste water treatment, composting and biogas production, which belong to *treatment and disposal of waste* sector. In this context, further studies on the possible effects observable in the neighbourhoods of this incinerator were carried out by Sarti et al. (2015, 2017) in order to quantify PM_1 and $PM_{2.5}$ and identify their composition in terms of metals, soluble ions, polycyclic aromatic hydrocarbons (PAHs), nitro-PAHs and n-alkanes. However, no clear evidences could be ascribable only to the incinerator.

FERRARA

As Bologna, Ferrara is situated in the Po Valley, densely populated and one of the most polluted areas of Italy. The main sources of pollution in the Ferrara municipality are attributable to industry, presents in many facilities, especially as chemical plants (Gerdol et al., 2014). Moreover, automotive, railway and flying transports have been recognised as important emission sources in the Po Valley as well as extensive agricultural activity and related food industry are widely developed in this area. In particular, Ferrara suffers also from pollutants released by point sources such as domestic heating plants, agricultural practices, vehicular traffic, car repair and paint shops. The poor air quality in this area is also influenced by its topography: Alps and Appenini mountain chains, indeed, behave as shield against atmospheric circulation, causing weak winds, low mixing heights and the development of temperature inversion during winter time. Consequently this condition of prolonged atmospheric stability is responsible of air mass stagnation and reduced pollutant dispersal both in warm seasons, with high level of photochemical smog, and in cold months, characterised by significant level of PM concentrations.

The Emilia-Romagna region started during the 1970s to monitor air quality through the constitution of a regional monitoring network (Coppi, 2007). Nevertheless, concentration of air pollutants measured in Ferrara area are available from the 1990s by the Regional Environmental Protection Agency for Emilia-Romagna region (Agenzia Regionale per la Protezione Ambientale dell' Emilia-Romagna – ARPAE) (https://www.arpae.it/). My research centres on data acquired by urban monitoring stations while neglects results from rural background stations (Gherardi, Cento and Ostellato), too far away from Palazzo Turchi di Bagno.
At the beginning, pollutants present in the city atmosphere were collected from monitoring stations located in Corso Isonzo, Via Bologna and Piazzale San Giovanni, all of them located within 2 km in straight line from Palazzo Turchi di Bagno (see Figure 3.168 and Table 3.60).

MONITORING STATION	FEATURES	PERIOD OF ACTIVITY	DISTANCE FROM THE PALACE (in straight line)	PM_{10}	$PM_{2.5}$	SO_2	NO_2	CO	BENZENE
BARCO	industrial	from 1994	2360 m	YES	YES	YES	YES	YES	YES
CASSANA	industrial	from 2011	4850 m	YES	YES	YES	YES	YES	-
C. ISONZO	urban traffic-oriented	from 1991	802 m	YES	YES	YES	YES	YES	YES
MIZZANA	industrial	1991-2011	3120 m	-	-	YES	YES	-	-
P.LE SAN GIOVANNI	urban traffic-oriented	1996-2007	1000 m	YES	-	-	YES	YES	YES
V. BOLOGNA	urban traffic-oriented	1996-2007	1940 m	-	-	-	YES	YES	-
VILLA FULVIA	urban background	from 2009	2930 m	YES	YES	-	YES	-	-

Table 3.60 The closest monitoring stations to Palazzo Turchi di Bagno in Ferrara and their measured pollutants.

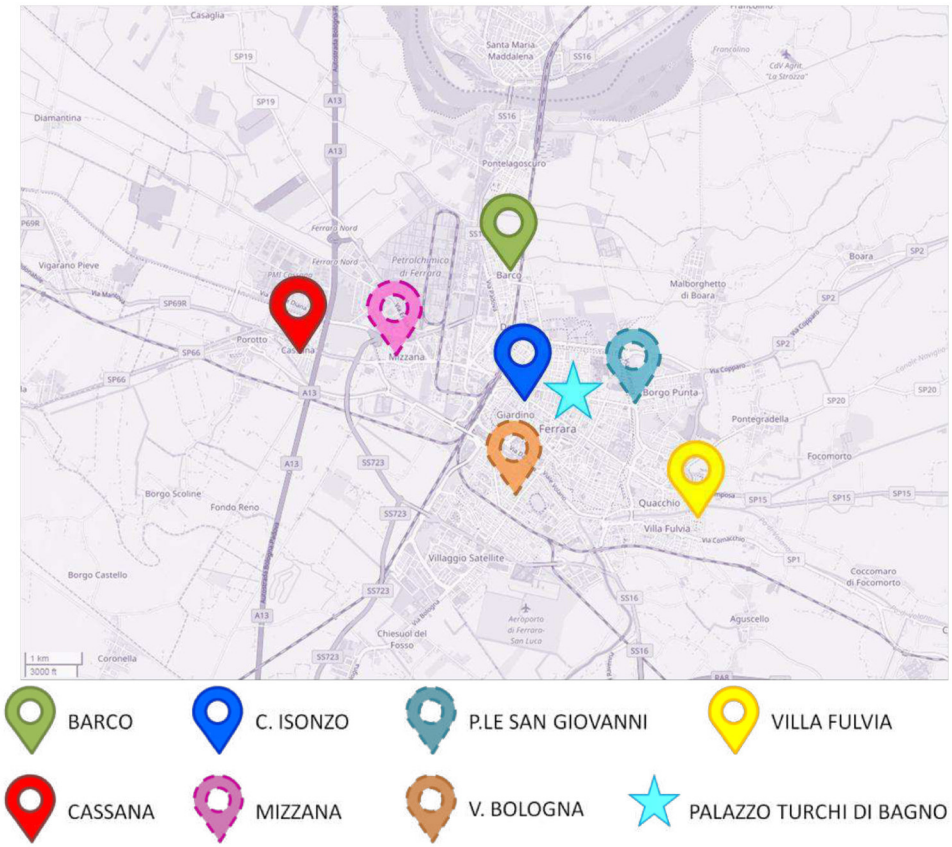

Figure 3.168 Location of monitoring stations of air quality by ARPAE. Abandoned stations are indicated by dotted outline.

However, the restoration of the monitoring network led to the closure of some stations, i.e. V. Bologna (in 2007) and P.le San Giovanni (in 2007), and the opening of Villa Fulvia station (from 2009). These years in brackets refer to period of data availability and not to the physical installation or cessation of the stations. Additionally, urban industrial monitoring stations (Barco and Mizzana, the latter moved to Cassana in 2011) are here considered because of the proximity of city centre to the important industrial area.

Isonzo urban traffic-oriented station is located in a residential area of Ferrara in the corner between Corso Isonzo and Viale Cavour. The latter is a busy two carriageway road with three lanes for each direction. Piazzale San Giovanni and Via Bologna are important node to connect the city centre with the east and south-west suburbs, respectively. Villa Fulvia station is located in a park of a residential area of Ferrara, close to Po di Volano river and is considered as urban background monitoring station. Industrial stations are those most close to the highway A13, power plant, urban waste incinerator, and many small and medium size enterprises.

Airborne particulate matter represents a complex mixture of organic and inorganic substances, covering a wide range of diameters. Some preliminary data monitored at Barco and Isonzo stations during the period 1991-1994 are shown in Figure 3.169 as total suspended particulate (TSP) (Magnavacca, 1996) . In this short interval there was a slight decrease in the amount of particulate present into atmosphere. Analysing the seasonal concentration of TSP for these years, no clear trend was appreciable.

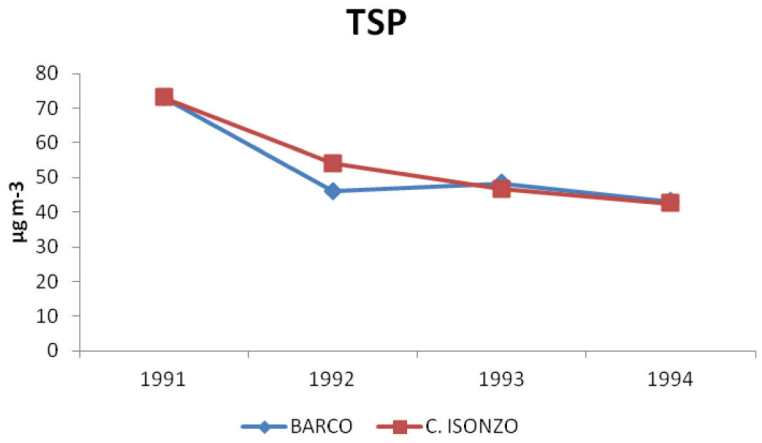

Figure 3.169 Mean annual concentration of TSP measured in Ferrara.

More detailed information about air particulate matter is obtained by ARPAE monitoring stations and provided as size-related subsets PM_{10} and $PM_{2.5}$.

As shown in Figure 3.170, a similar decreasing trend is observable for PM_{10} in all the monitoring stations, without any influence by their position of monitoring. Anyway, the decrease in the last decades results slight and not constant, with peaks of the mean annual concentration during 2011-2012 and 2015. These three years were characterised by a general environmental critical situation at a regional level induced by atmospheric stability and negative weathering conditions of the Po Valley (prolonged absence of rain and wind) as well as by anthropogenic pressure.

Considering the human health protection, the yearly limit value fixed by Legislative Decree no. 250/2012 (40 µg m^{-3}) was never exceeded from 2008. Nevertheless, the comparison with the more restrictive guideline value for PM_{10} set by the World Health Organisation (WHO, 20 µg m^{-3}) displays a clear overrun for all the monitored years, independently by the location of the stations.

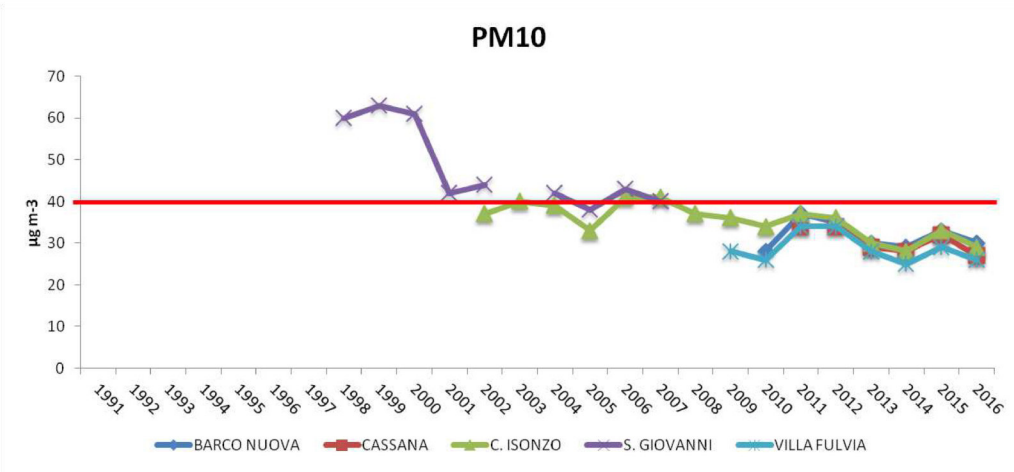

Figure 3.170 Mean annual concentration of PM_{10} measured in Ferrara. Red line indicates the yearly limit value for human health protection fixed by Legislative Decree no. 250/2012.

First data of $PM_{2.5}$ available from ARPAE dated back to 2005 and display a general diminishing tendency over the years (Figure 3.171). Always in wider terms, trend of $PM_{2.5}$ likely follows that of PM_{10}, confirming critical situations during the years 2011 and 2015 probably induce by environmental conditions. First results are available only for the urban traffic station of Corso Isonzo, substituted by Villa Fulvia station in 2009.

Whenever the comparison is possible, industrial monitoring stations of Cassana and Barco reveal slightly higher concentration of $PM_{2.5}$ in respect to Villa Fulvia.

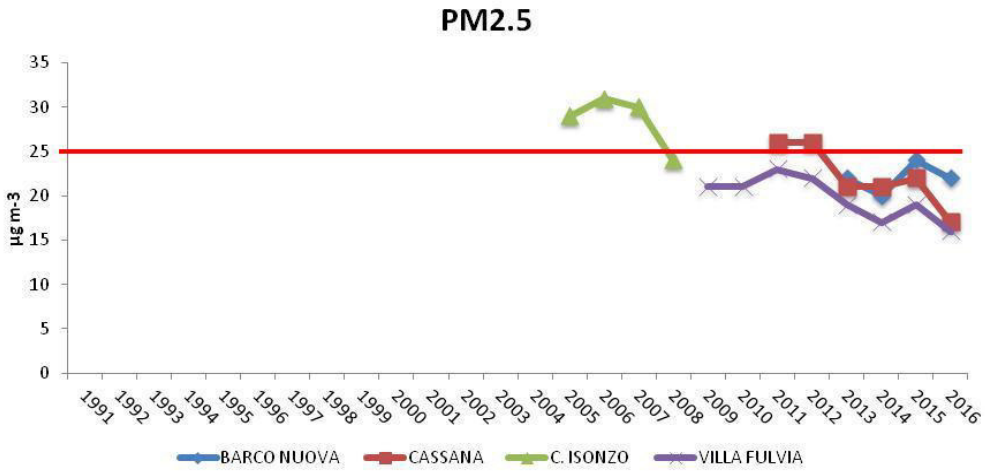

Figure 3.171 Mean annual concentration of $PM_{2.5}$ measured in Ferrara. Red line indicates the yearly limit value for human health protection fixed by Legislative Decree no. 250/2012.

Considering the human health protection, the yearly limit value fixed by Legislative Decree no. 250/2012 (25 µg m^{-3}) was never exceeded from 2013 while monitored data are always much higher the limit value of 10 µg m^{-3} determined by World Health Organisation (WHO) for all the monitoring stations.

Useful investigation of concentration and chemical composition of PM_{10} and $PM_{2.5}$ in Ferrara was carried out by Perrino et al. (2014) between October 2010 and September 2012 with four 1-month observations during summer and winter time. The studied area consisted of an industrial site (close to a power plant, a waste incinerator and companies), a rural site and a residential site located in Cassana. During the 2-year period of study, mean concentration of particulate matter was similar in the three sites and it increased during winter in respect to summertime: 48.5 µg m^{-3} and 29.0 µg m^{-3} for PM_{10} and 38.5 µg m^{-3} and 17.7 µg m^{-3} for $PM_{2.5}$, respectively. This trend confirms the high atmospheric stability as well as the increase in contribution of some seasonal PM sources. Evaluating the chemical composition of the sampled particulate matter (see Table 3.61), Al, Si, Mg and Ca (soil components) were find with higher concentration in the coarse PM fraction and mainly during summer while NH_4^+, EC and OC pertained mostly to $PM_{2.5}$ and their concentration increased during the winter. Potassium seems to have two sources: probably domestic heating due to its high amount in fine particles during winter and soil as it was considerably present in PM_{10} during summer. Moreover, NO_3^- is detectable both in $PM_{2.5}$ mainly in winter due to the secondary formation of ammonium nitrate and in coarse part over the year (natural sources). Considering the carbon fractions, organic portion was predominant than EC in all seasons, becoming almost double in wintertime (Table 3.61).

	WINTER_PM_{10}	WINTER_$PM_{2.5}$	SUMMER_PM_{10}	SUMMER_$PM_{2.5}$
Al	0.14	0.06	0.21	0.08
Si	0.54	0.15	0.92	0.27
Fe	0.25	0.06	0.20	0.02
Na	0.66	0.18	0.40	0.14
K	0.62	0.53	0.23	0.10
Mg	0.26	0.03	0.41	0.08
Ca	0.90	0.20	1.30	0.27
Cl^-	0.55	0.21	0.16	0.05
NO_3^-	9.30	6.60	2.00	0.53
SO_4^{2-}	3.50	2.80	3.10	2.80
Na^+	0.39	0.12	0.42	0.09
NH_4^+	3.80	2.90	1.00	0.86
K^+	0.49	0.42	0.14	0.11
Mg^{2+}	0.11	0.03	0.10	0.03
Ca^{2+}	0.55	0.14	0.90	0.22
OC	10.00	9.30	4.30	3.50
EC	1.20	1.00	0.61	0.52

Table 3.61 Average concentration ($\mu g\ m^{-3}$) of the main components in PM_{10} and $PM_{2.5}$ of the three sites (Perrino et al., 2014).

SO_2 was the first monitored pollutant in Ferrara area because of its riskiness for human health and cultural heritage. First data acquisitions were performed in 1979 by the industrial monitoring station of Barco. As explained by Magnavacca (1996), the concentration of SO_2 in the atmosphere over the decade 1984-1994 clearly decreased thanks to the substitution of fossil fuels with natural gas for domestic heating as well as the exploitation of geothermal energy (Figure 3.172). V. Giovecca and V. Cavour are consecutive, congested, central streets of Ferrara that divide into two parts the city while V. Canapa refers to a peripheral area close to a big urban park.

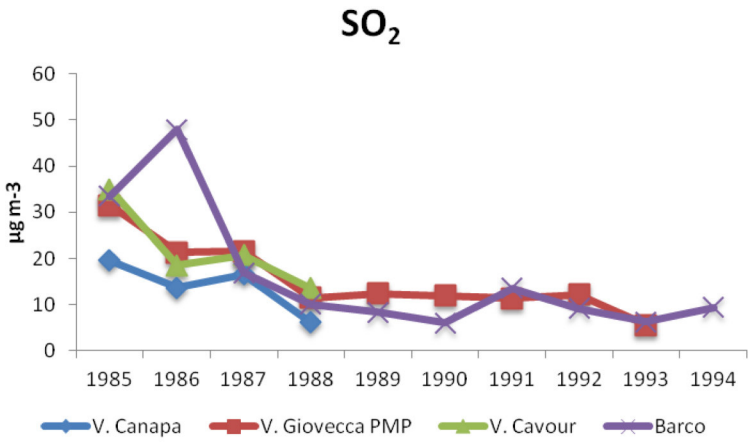

Figure 3.172 Mean annual concentration of SO_2 measured during the decade 1984-1994 in Ferrara.

Combining data released by Magnavacca (1996) with those supplied by ARPAE (see Figure 3.173), it is evident the change of monitoring stations over years, with Mizzana and Isonzo as the most long-lasting monitoring sites. In general, SO_2 atmospheric amount displays a decreasing trend, which has been stabilised around 7µg m^{-3} in the last years. Moreover, recently SO_2 seems to be a problem more related to industrial areas even if the measured values are small. In 2010, it was decided to interrupt its monitoring in the city centre as its concentration is lower than the instrumental limit of detection.

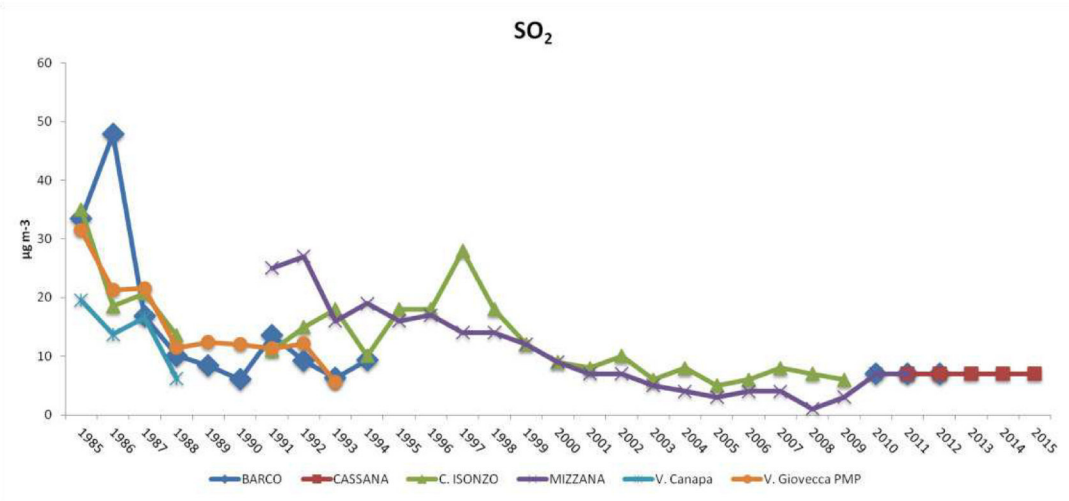

Figure 3.173 Mean annual concentration of SO2 measured in Ferrara.

NO_2 is the main source of nitrate aerosols, forming an important fraction of $PM_{2.5}$ and, in the presence of ultraviolet light, of ozone. Comparing the concentration of this pollutant from the 1990s till nowadays, it is observable a good representativeness of data and a decreasing trend (Figure 3.174). In particular, monitoring of NO_2 has been recorded in Corso Isonzo station from 1991 showing lately lower concentration that remains anyway over or equal to the yearly limit value fixed by the Legislative Decree no. 250/2012 and WHO for NO_2 (40 µg m^{-3}). No crossing of limit value was recorded in the industrial and urban background stations in the last 9 years.

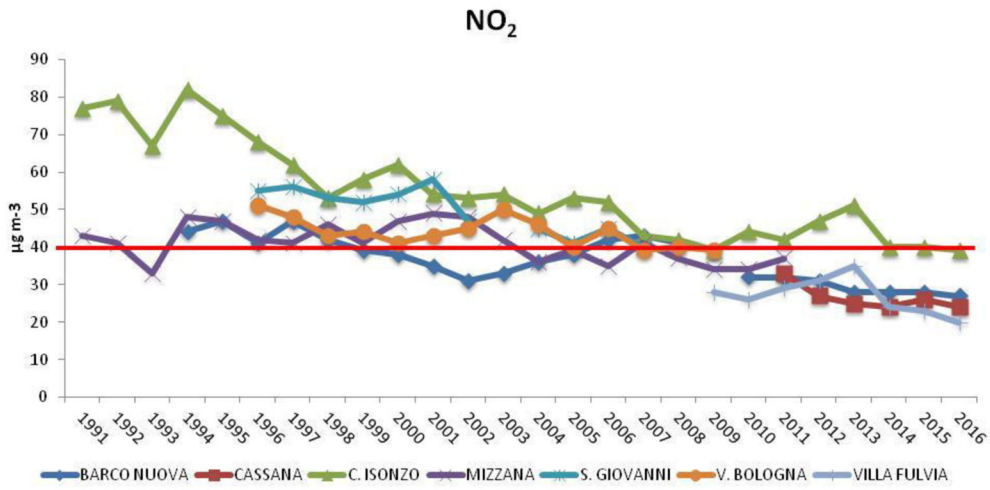

Figure 3.174 Mean annual concentration of NO_2 measured in Ferrara. Red line indicates the yearly limit value for human health protection fixed by Legislative Decree no. 250/2012 and WHO.

Even if carbon monoxide is no more considered a risky pollutant, it is continuously monitored. CO is mainly associated with vehicular traffic emissions as its highest daily concentration is recorded during the main congested hours (i.e. 8-10 a.m. and 18-20 p.m.) and during the wintertime. However, Figure 3.175 highlights the evident decrease of this pollutant over the years, reaching values lower the detection limit of the instrument (i.e. 0.6 mg m^{-3}).

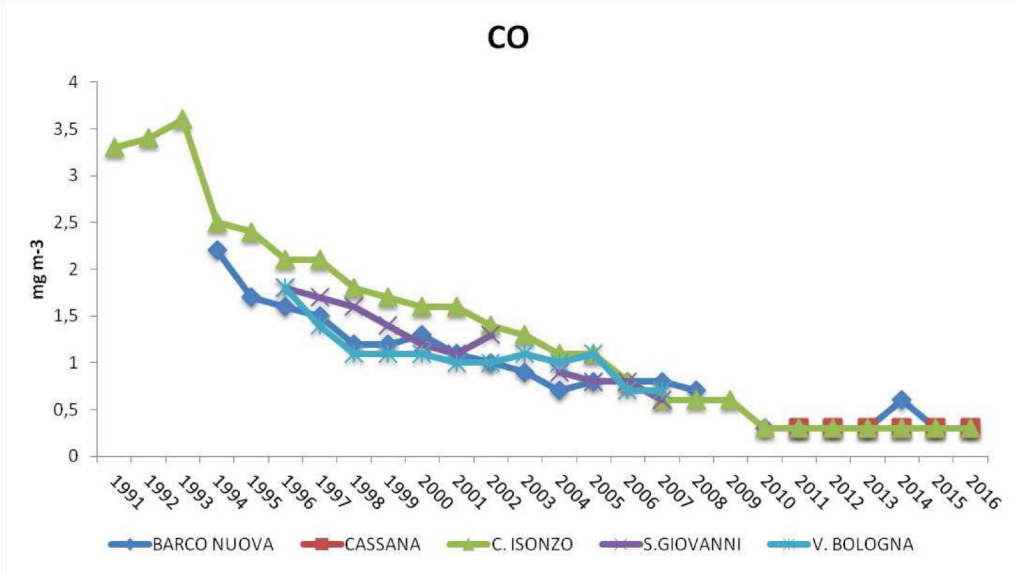

Figure 3.175 Mean annual concentration of CO measured in Ferrara.

Also benzene, emitted mainly by traffic, has decreased remaining below the yearly limit value fixed by the Legislative Decree no. 250/2012 (Figure 3.176).

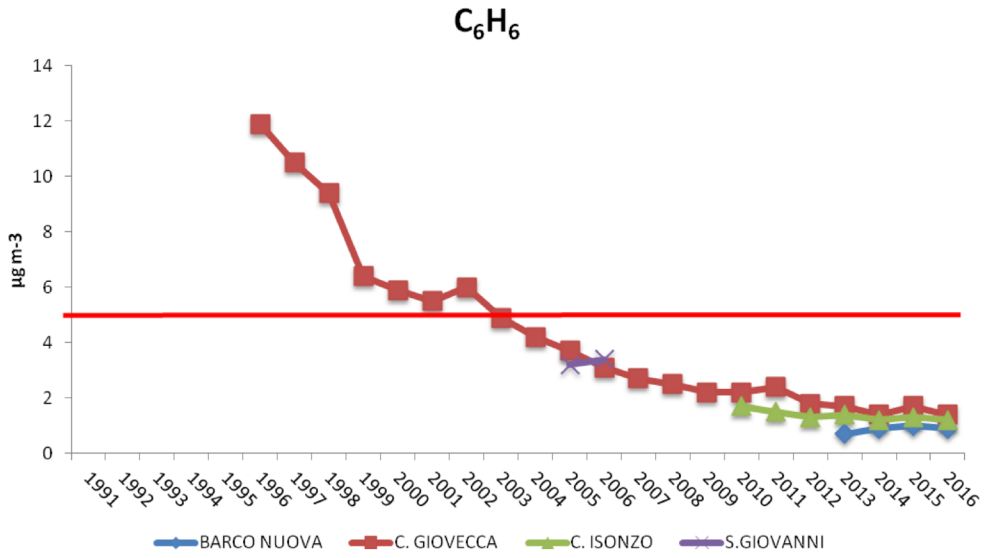

Figure 3.176 Mean annual concentration of C_6H_6 measured in Ferrara. Red line indicates the yearly limit value for human health protection fixed by Legislative Decree no. 250/2012.

Information relative to the presence of pollution induced by traffic was provided by the annual mean concentration of lead measured in the monitoring stations of Barco and Corso Isonzo for the period 1991-1994 (Magnavacca, 1996). Lead was indeed emitted in atmosphere by the combustion of antiknock additive in gasoline as well as by foundry and ceramics industry.

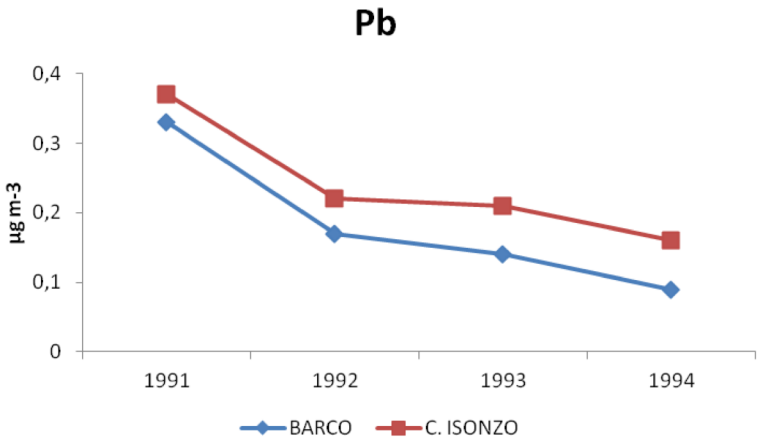

Figure 3.177 Mean annual concentration of Pb measured in Ferrara.

Both monitoring sites show a similar decreasing trend, with lower amount recorded in the industrial site (Figure 3.177). This higher concentration detected in Corso Isonzo was more probably ascribable to the heavy traffic, even if the use of unleaded gasoline was spreading out in those years.

A recent study by Canepari et al. (2014) assessed the results of 5-year (2008-2012) monitoring study carried out in the same area investigated by Perrino et al. (2013) concerning the concentration and solubility of micro- and trace-elements in atmospheric PM. Despite the presence of a high number of factories, industrial emissions, usually traced by these micro- and trace-pollutants, were not the main responsible for the high PM concentrations typically recorded in the studied site. Moreover, pollutants concentration measured at the three sites were similar, proving the considerable homogeneity of the air masses in the selected area and the

low contribution of local emissions. With the exception of S detected in the soluble fine fraction as product of secondary reactions, almost all the other considered elements were identified in PM_{10} and $PM_{2.5}$ both in soluble and residual fractions. Nevertheless, fine fraction, mainly associated to anthropogenic combustion processes, contains more soluble, and thus particularly accessible to environmental and biological systems, species than the coarse fraction, associated to abrasive and mechanical processes. Seasonal variability was mainly due to the poor atmospheric mixing occurring during the cold season even if some additional winter sources influenced the concentration of some elements (Pb, Sn, Li, Rb, and Ni). It is noteworthy the impact exercised by fog episodes, very frequent in the studied area, as it could occasionally decrease the concentration of most elements and significantly change their dimensional distribution, going beyond the cut-point of the sampling heads (i.e. 2.5 and 20 μm).

However, the environmental monitoring performed by ARPAE stations in Ferrara does not concern the old city centre where the main historic buildings are concentrated. The narrowness of medieval alleys does not allow the installation of the conventional equipment. To face this lack, researchers of the University of Ferrara designed new small detectors for gaseous pollutants exploiting the change in electrical conductivity induced by the interaction between sensor surface and the surrounding atmosphere (Carotta and Vaccaro, 2001). The modest dimension of these sensors permitted their position in two sites close to buildings of historic-artistic importance and characterised by different exposure to vehicular traffic: “Teatro Comunale” (Communal Theatre) , located in the corner of congested streets, and “Casa Romei”, affected by less traffic. The sensors monitored the concentration of atmospheric CO from March till October 2000. CO was indeed selected as marker of vehicular traffic since other pollutants such as ozone and nitrogen oxides are more subject to other pollution sources as well as weather conditions. Data processing from sensor located at the Theatre showed two maxima concentration of CO at around 9 a.m. and 8 p.m. and mean value (maximum mean value of ~2.7 mg m^{-3}) generally higher than that measured in the reference ARPAE station of Corso Isonzo (maximum mean value of ~1.7 mg m^{-3}). Moreover, the amount of CO remained high also during night proving the persistence of traffic also at night-time. Also monitoring campaign carried out at Casa Romei, considered as low traffic area, recorded values similar to those monitored in the other two congested areas. In this context, buildings height and street wideness have to be considered as they may contribute to less dispersion of pollutants (street canyon).
The same chemoresistive gas sensors were used to monitor the environmental condition of CO and NO_2 in Palazzo Turchi di Bagno, located in front of the famous Palazzo dei Diamanti (Ferrari, 2003). The sensors, placed on the ground and first floors (2 m and 8 m, respectively) of the building facing to Corso Porta Mare (a main road that crosses the city), monitored the environmental condition of limited periods in autumn 2002 and spring 2003, measuring values sometimes over those monitored in ARPAE urban station. This monitoring proves that pollutants concentration is influenced by road topography and amount of traffic (more heavy during working days than public holidays). Furthermore, also the height of monitoring is significant because ground floor is more affected by vehicular traffic than first floor as proved by higher monitored concentration of pollutants.

Another interesting monitoring approach of air pollution that has received increasing attention in recent years is the biomonitoring technique. With this method, living organisms are used to study pollutants both passively, based on their different sensitivity to air pollution (such as in the case of epiphytic lichens), or actively through their capacity to accumulate pollutants in the tissues (such as for mosses). Gerdol et al. (2014) took advantage of mosses (Tortula muralis Hedw. sp.) and lichens (Tilia spp. And Quercus spp.) for analysing respectively trace metals, total N and ^{15}N concentration and air quality through Lichen Diversity Value (LDV) in the area of Ferrara during a five-year interval (2006-2011). In general, metal concentration in moss tissues diminished in 2006 and 2011 in respect to 1999 in accordance with the decreasing trend observed in most European countries. However, some differences have been recorded from 2006 to 2011

reflecting affinity for different emission sources. From the first monitoring campaign till the second one, the amount of elements derived from vehicular traffic and incinerations increased (such as Cr, Ni, Sb from deterioration of tire, brake and engine and Cd, Cr, Ni and Zn from incinerators). Also the concentration of Li and Sr, linked to electronic waste, raised as well as As, emitted by waste incinerators, herbicides and insecticides. On the contrary particles related to industrial factories and coal-fired plants (i.e. Co, Se, Mo and Mn) showed a diminishing trend over the years, implying that the contribution of these pollution sources declined during this period. However, Mo and Co in the industrial area displayed a less strongly decreasing amounts as they derive from industrial plants.

The identification of emission sources represents an important part in a pollution assessment. The origin of emissions could be organised in four macro branches:

1. Industry (combustion deriving from energy industry, transformation of sources of energy, production processes and industrial combustion systems);
2. Heating (non-industrial combustion systems);
3. Traffic (road transport and other movable sources);
4. Other (extraction and distribution of fossil fuels and geothermal energy, use of solvents, waste disposal plant, nature and farming).

Report about emissions inventory of Emilia-Romagna Region in 2010 (Tugnoli et al., 2013) displays that industry and traffic were the main sources of pollutants. Considering each pollutant share emitted in atmosphere, it is possible to notice that industry was the major responsible of SO_2 and CO_2, traffic of NO_x and PM10 while heating systems realised high concentration of CO, non-methane volatile organic compound (NMVOC) and PM_{10} at regional level (Figure 3.178). Looking at the other pollutants, farming was in charge of relevant emissions of N_2O, NH_3 and CH_4 (the latter emitted also by distribution of energy and waste disposal plant) while use of solvents emanated rather high concentration of volatile organic compounds.

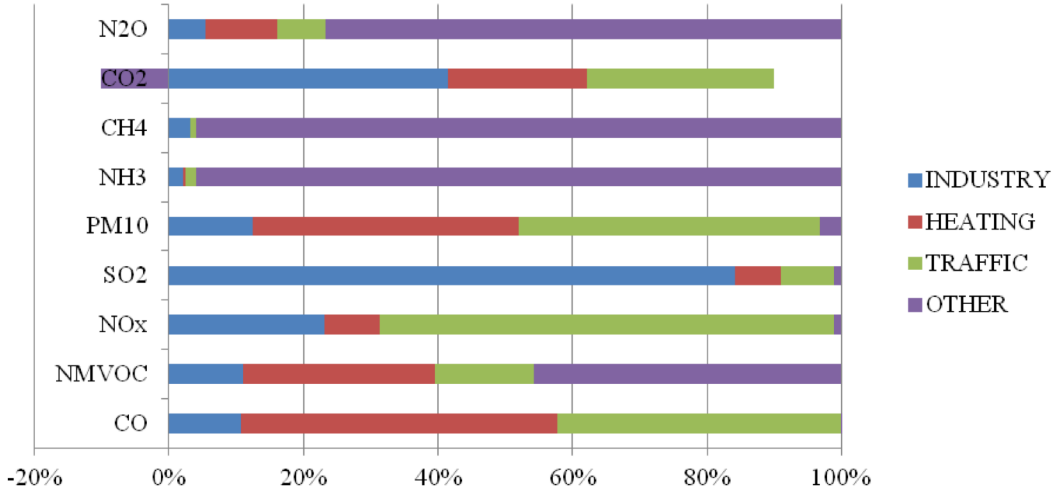

Figure 3.178 Percent distribution of emissions of main pollutants per macro-area in Emilia-Romagna region during 2010.

Focusing on Ferrara territory, industry and traffic proved to be the main sources of pollution released in 2010 (Table 3.62).

	CO	SO_2	NMVOC	CH_4	NO_x	TSP	CO_2	N_2O	PM_{10}	NH_3	TOTAL
INDUSTRY	4378	619	1587	2296	4869	224	3627300	33	137	421	3641864
TRAFFIC	6944	54	1387	104	6550	729	1185000	80	625	72	1201545
OTHER	28	0	2915	11071	190	0	63000	639	29	4601	82473

Table 3.62 Annual concentration of monitored pollutants (t y^{-1}) emitted by different macro-sources in the territory of Ferrara in 2010.

Table 3.62 misses data about pollutants emitted by non-industrial combustion systems but a previous document pertinent to 2004 (http://www.comune.fe.it/attach/superuser/docs/piano_aria_provincia_sintesi .pdf) reported the poor influence of heating in comparison to the other anthropogenic sources. However, a 2-years field study (2010-2012) in Ferrara highlighted an increase of mass concentration of particulate matter during wintertime, mainly due to the fine fraction: $PM_{2.5}$ (Perrino et al., 2014). In particular, the calculation of the contribution of residential wood burning disclosed that roughly half of the organic matter and a significant fraction of $PM_{2.5}$ (20%) during winter was attributable to this source, going beyond the emission from traffic in this part of year. This change of trend in respect to the previous research could be explained by a rapid diffusion of wood as primary source of heating also in plain and urban areas from 2010 because of the economic crisis (Zinoni, 2015). Even if biomass burning in Emilia-Romagna region covered energy requirements of only 8% in 2014, the relative estimation of non-industrial combustions displayed that 40% of PM_{10} in 2012 is ascribable to biomass domestic heating while only 34% to vehicular traffic (Deserti et al., 2015).

FLORENCE

Florentine environmental framework has became critical in the last 70 years because of the progressive population growth to the detriment of green spaces with the related problem of waste disposal, increased air pollution and overexploitation of groundwater. Paolini (2014) found the main driving force of the Florentine environmental deterioration in the great project of reconstruction after the II World War. In particular, three factors should fundamentally be worth considering: i) the frenetic and disorganised urban drift due to the migrant flow from the countryside and the southern part of Italy, ii) the rapid industrial development characterised by small/medium company as well as iii) the cultural behaviour aimed to a fast business expansion underestimating the risks for the environment (Paolini, 2014). The most important sectors involved in the industrialisation expansion of Florence were the textile, mechanical, clothing, footwear, petrochemical, wooden and leather ones. The booming economy of the 1950s led to the exploitation of the natural resource, with severe consequences for the water basin of Arno and the air but the local authorities became aware of the seriousness of the ecological problems only from the 1970s. In that period the main causes of detrimental pollutants were heating systems and vehicular traffic: bear in mind that motor vehicles increased from 26433 in 1951 to 593415 in 1980 only in the province of Florence. Furthermore monitoring campaigns realised between autumn 1972 and winter 1973 displayed relevant concentration of SO_2 (0.0035 kg m^{-3}), Pb (around 7 μm^{-3}) and PAH released from tailpipes while factories were the responsible of emissions of metals as Ca, Si, Mg, Mn, Fe, V, Cu, Zn, Ni (from the manufacturing of metals), S, phenols, fatty acids (from tannery and food industry), Cl, F, aldehydes (from chemical, plastic and rubber industries). In this context, the regional plan provided for the conversion to methane of the urban centre and the development of clean energy[1]. Nevertheless the adopted provisions resulted to be not sufficiently efficient to solve these problems.
It was only from the 1980s that first real interventions started to practically act to deal with environmental emergency. This antipollution process was time-consuming and its effects were real as highlighted also by the Florentine municipality that defined the environmental problems serious and obvious[2]. Considering the air quality, the main responsible of air pollution was the vehicular traffic that inlet into the atmosphere 15000 t of CO, 1500 t of unburned hydrocarbons and 3500 t of NO_x. Heating systems, mainly gas-driven, released 300 t of SO_2 while the industry were not such influential (Paolini, 2007). Also a national paper (La Repubblica, 24 February 1989) found one of the main cause of air pollution trouble in urban sites in the proliferation of vehicular traffic:

> *"**La guerra chimica dentro la citta'** - Dopo l' allarme dei milanesi oppressi dallo smog, miscela d'inquinamento in espansione continua e nebbia stagnante, l' informazione ha divulgato qualche notizia in più sullo stato delle città italiane. Risulta che i fattori d' inquinamento dell' aria, in larga misura, derivano dall' immane proliferazione dei veicoli a motore. Milano appare la città più inquinata solo perché là operano 49 stazioni di monitoraggio computerizzato, ma l' inquinamento non è minore a Torino, Genova, Bologna, Firenze, Roma, Napoli, Bari, Catania e Palermo. Tuttavia nessuno può, sa o vuole fare quel che dovrebbe, non i poteri pubblici, non quelli dell' industria e nemmeno gli ambientalisti.[...]"*

Those years were also characterised by the problem of acid rain (caused mostly by nitric, sulphuric and hydrochlor acids) with visible consequences on vegetation and stone monuments of the city centre.
To face this impending situation, the Regional Environmental Protection Agency (Agenzia Regionale per la Protezione Ambientale della Toscana – ARPAT) was found in 1995 in order to provide an adequate standard

[1] Contributo alla conoscenza della composizione chimica del pulviscolo atmosferico campionato nell'area urbana di Firenze, in "Inquinamento", luglio-agosto 1973.

[2] Comune di Firenze, *Firenzecologia*, Il Ventaglio, Roma, 1987, p. 85.

for air and water (http://www.arpat.toscana.it/). In addition to the monitoring and analysis of air quality, ARPAT enabled the introduction of some temporary actions, such as to limit traffic according to even and odd numbers of license plates on alternate days or to avoid the access to motor vehicles in the city centre during the so called “ecological Sunday”. These measures are useful to manage acute situation while there is still not a serious ecological policy probably due to the fear of impeding the economical growth (Paolini, 2007).

Monitoring campaigns performed by ARPAT over the years have supplied useful information to observe the trend of the concentration of some pollutants in the Florentine atmosphere. The monitoring network of the Florentine area consist of 7 permanent stations distributed in the city and its suburbs, as shown in Figure 3.179. They could be divided in urban and suburban stations, considering the kind of area, and in background or traffic-oriented ones, on the basis of the main pollutants. Nevertheless, it misses a monitoring station in the old town, which could provide fruitful data about the air condition surrounding historic buildings and thus plan a better management of them. Even if the city centre is a restricted traffic zone, there is a huge transit of motor vehicles, many of them are heavy duty diesel vehicle (such as buses of public urban/suburban transportation, tour buses and load/unload cargo lorry). Furthermore the configuration of the city itself, with quite high buildings and narrow streets typical of the medieval age, hinders pollution dispersion (Grechi, 2014).

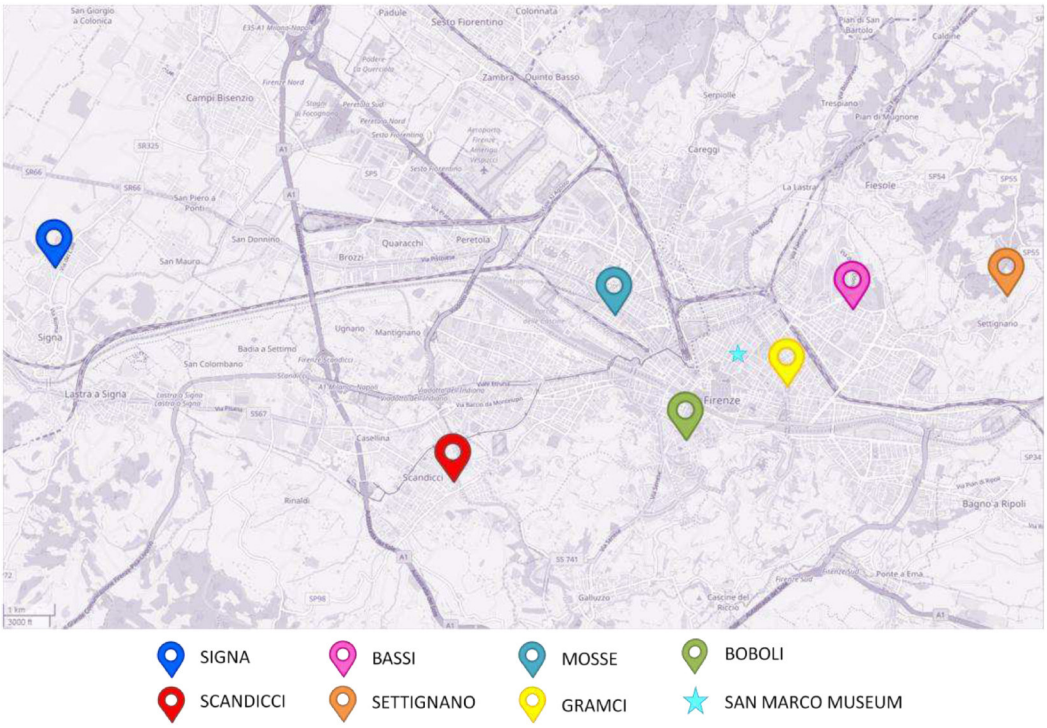

Figure 3.179 Location of monitoring stations of air quality by ARPAT.

Considering the position of San Marco Museum, I decided to consider the data measured from the closest monitoring stations, reported in the table below:

MONITORING STATION	FEATURES	DISTANCE FROM THE MUSEUM (in straight line)	PM_{10}	$PM_{2.5}$	SO_2	NO_2	CO	BENZENE
GRAMSCI	Urban, traffic-oriented	1200 m	YES	YES	-	YES	YES	YES
BOBOLI	Urban, background	1800 m	YES	-	-	-	-	-
BASSI	Urban, background	2300 m	YES	YES	YES	YES	-	YES
MOSSE	Urban, traffic-oriented	2400 m	YES	-	-	YES	-	-

Table 3.63 The closest monitoring stations to San Marco Museum in Florence and their measured pollutants.

The Gramsci urban traffic-oriented station is located beside the large open road of Viale Gramsci, which is a two carriageway road with three lanes for each direction, basically N–S oriented while the Boboli Station is an urban background station, located in Boboli Garden. The Bassi station is placed in Via Ugo Bassi, influenced by traffic (it is close to the Florence stadium) while the Mosse urban traffic-oriented station is located within the street canyon of Via Ponte alle Mosse. Via Ponte alle Mosse is a one-way, two-lane road with traffic priority over the crossing roads.

As observable in Figure 3.180, the analysis of the concentration of PM_{10} in the Florentine urban area displays a slight downward trend in respect to the measurements performed during the 1990s. The improvement is more evident in traffic-oriented areas even though the lowest concentration of PM_{10} was recorded in background sites during last years. Considering the yearly limit value for human health protection fixed by Legislative Decree no. 250/2012 (40 µg m^{-3}), no override was detected in the last three years. Nevertheless, the World Health Organisation (WHO) determined 20 µg m^{-3} as long-term (annual mean) guideline value for PM_{10} based on known health effects (WHO, 2006). Considering this value, all traffic-oriented stations recorded annual values over 20 µg m^{-3} while values slightly lower were measured during 2016 in background stations (18 µg m^{-3} in Boboli and 19 µg m^{-3} in Bassi stations).

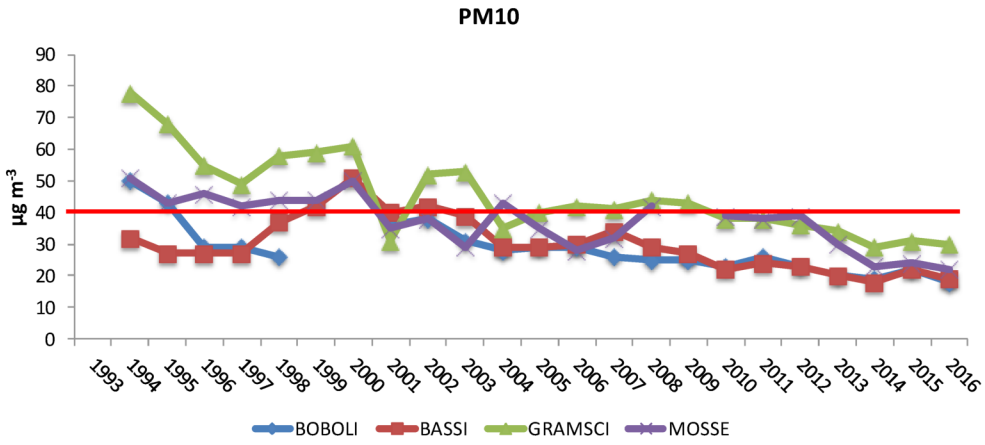

Figure 3.180 Mean annual concentration of PM_{10} measured by monitoring stations closest to San Marco Museum. Red line indicates the yearly limit value for human health protection fixed by Legislative Decree no. 250/2012.

Even if the measured values for $PM_{2.5}$ are less both from spatial and temporal point of view, Figure 3.181 shows a varying trend with a tendency quite similar to the one of PM_{10} at least for the last 6 years.

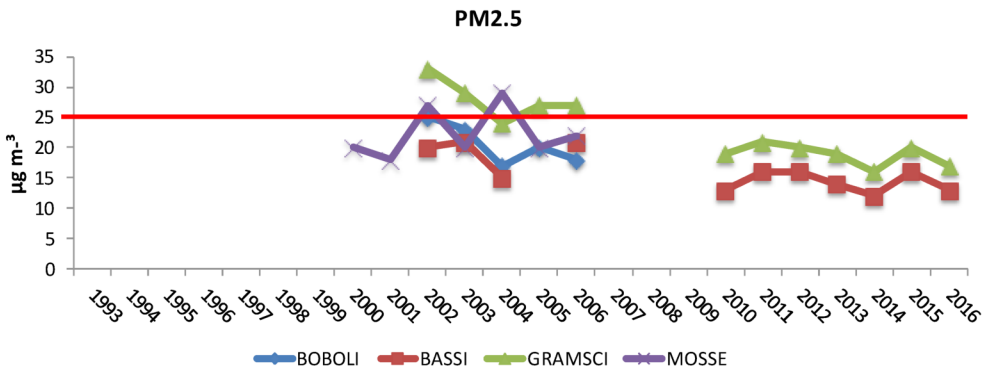

Figure 3.181 Mean annual concentration of $PM_{2.5}$ measured by monitoring stations closest to San Marco Museum. Red line indicates the yearly limit value for human health protection fixed by Legislative Decree no. 250/2012.

Even for $PM_{2.5}$ the World Health Organisation (WHO) determined a limit value of emission much lower (10 µg m^{-3}) that of the national law (25 µg m^{-3}). This discrepancy happens because WHO considers only healthcare perspectives: negative effects for human health start to arise over the defined values. On the contrary the European legislation considers both human health and environment. If we take into consideration the WHO limit value, none of registered data respected the threshold value.

The importance to consider also $PM_{2.5}$ concentration is driven by the fact that it is an atmospheric component very abundant in urban area since it is principally of anthropogenic origin: mainly from traffic (diesel exhaust emissions, brake and tyres exploitation and resuspension from road surface released as primary pollutants) or from the interaction with nitrogen and sulphur oxides present in the atmosphere. It has a long residence time in the atmosphere and has been recognised as an important fraction in the deposition mechanism occurring on vertical surfaces (Nazaroff and Cass, 1989). Moreover, carbon fractions (responsible for soiling and blackening of monuments) and soluble aerosols, such as sulphates, are generally abundant in fine particulate matter and thus $PM_{2.5}$ consists of a large fraction of PM_{10} in urban areas. In addition to consequences of $PM_{2.5}$ to cultural heritage, fine particles are noteworthy also for negative effects on human health because their small dimension allows them to deeply penetrate the respiratory system. In this context and for the necessity to make up for the lack of monitoring stations in controlled traffic zone, an initiative promoted and supported by some Florentine residents aims to locate a monitoring station for $PM_{2.5}$ in a private garden located in Via della Scala (in restricted traffic zone close to S. Maria Novella train station and at only 600 m far from San Marco Museum in straight line, see Figure 3.182).

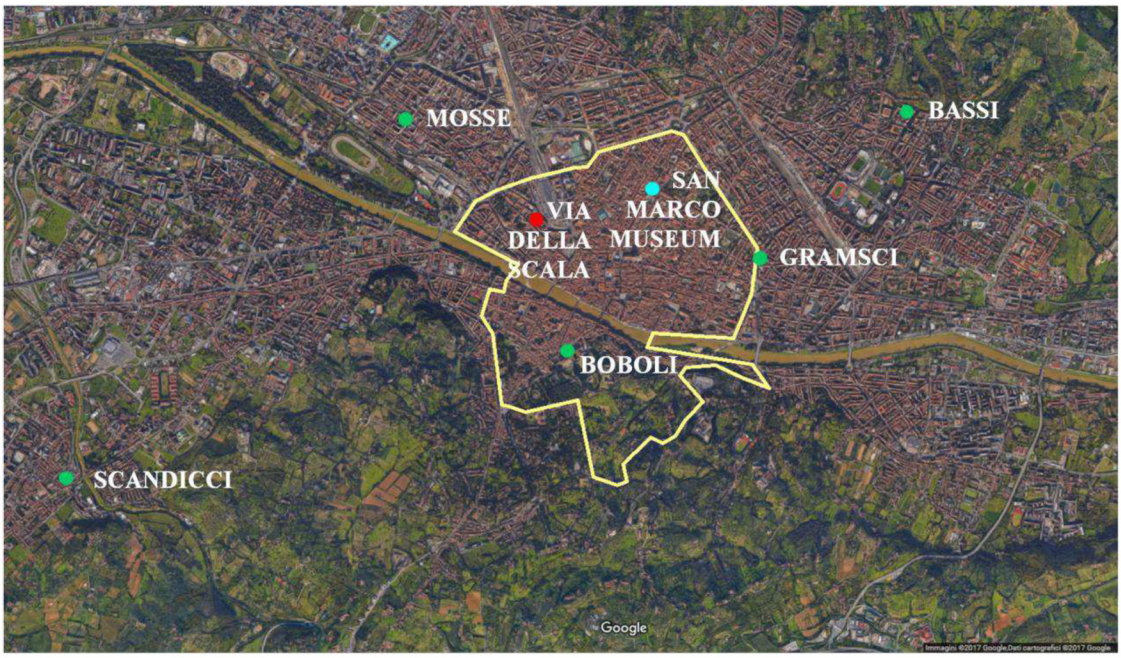

Figure 3.182 Map of Florence with the boundary of restricted traffic zone (in yellow), ARPAT monitoring stations (in green) and $PM_{2.5}$ monitoring station of Via della Scala (in red).

The station, classified as urban background station and based on light scattering technique, is operative from mid-December 2012 and all the data are available in real time at the website http://www.pm2.5firenze.it. Figure 3.183 reports the average monthly concentration of $PM_{2.5}$ measured from December 2012 till July 2017.

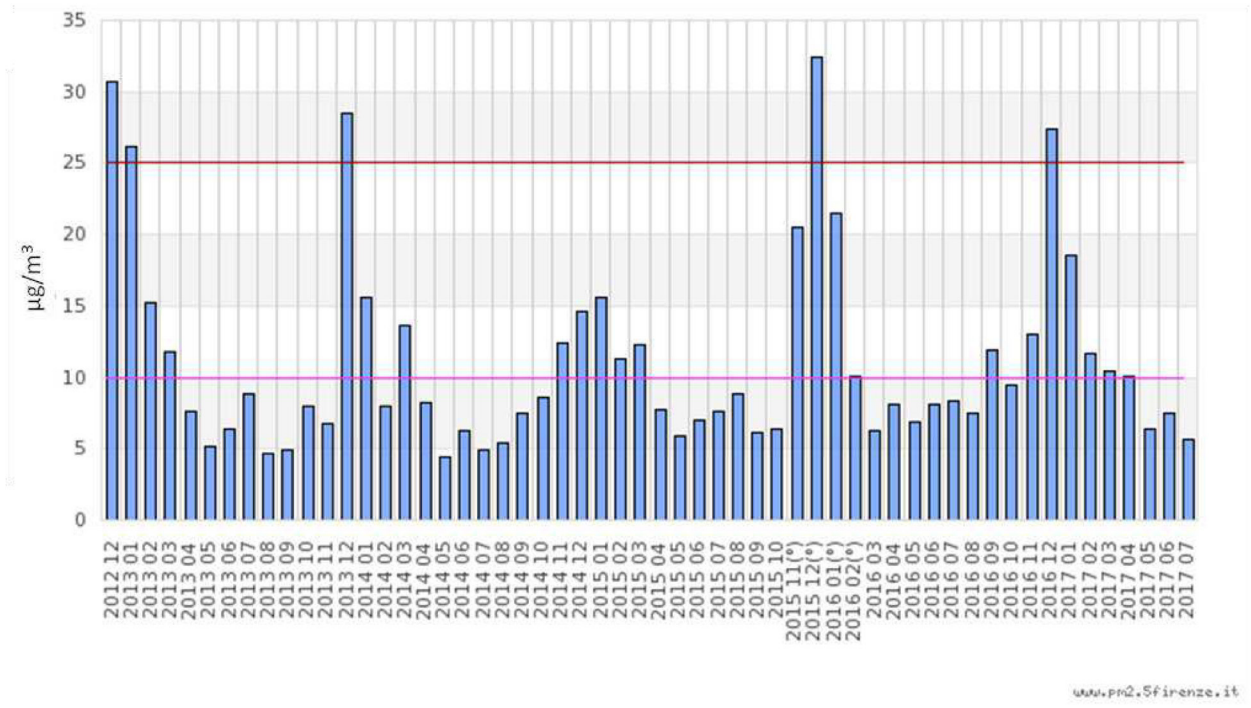

Figure 3.183 Mean monthly concentration of $PM_{2.5}$ recorded by the monitoring station of Via della Scala. Red line indicates the mean annual limit value fixed by Legislative Decree no. 250/2012 while in pink the limit value determined by WHO.

The measured data shows a trend suitable with measurements carried out with the monitoring stations of Via Bassi and Via Gramsci. As expected, the amount of $PM_{2.5}$ is lower during warmer months (approximately from April till October), remaining below the limit value established by WHO, while it increases in winter months exceeding also the national current regulation in December 2012, 2013, 2015 and 2016. This tendency is strictly influenced by the higher burning of biomass and other fuel for residential heating as well as the reduction of boundary layer height during winter.

The concentration of SO_2 has been decreasing from the 1993 with a similar tendency in all the stations, independently from the kind of monitoring stations (Figure 3.184). SO_2 values respected all the parameters fixed by the national and WHO legislations. SO_2 emissions, produced mainly by combustion of consumables and liquid fuels (e.g. charcoal, fuel oils), plastic production and waste burning, have been significantly decreased thanks to the improvement in fuel quality and the methanisation process of heating systems.

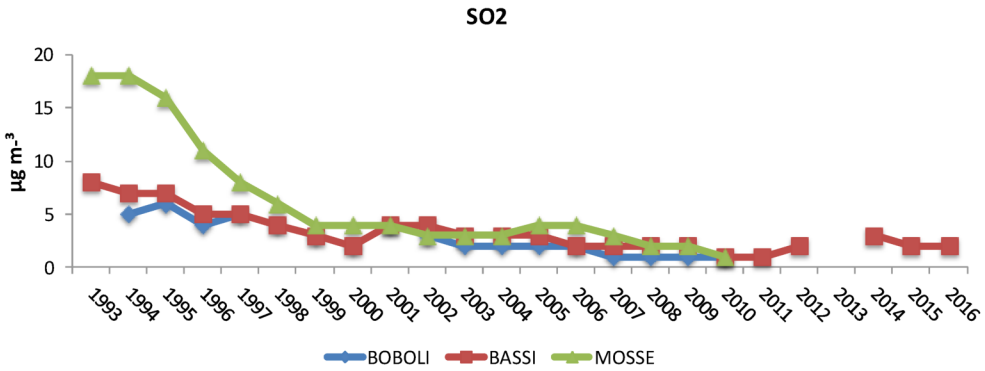

Figure 3.184 Mean annual concentration of SO_2 measured by monitoring stations closest to San Marco Museum.

Although in general the trend has decreased from the 1990s, NO_2 and NO_x concentration remains a problem to solve mainly for traffic-oriented stations. These last always exceeded the limit value fixed by the Legislative Decree no. 250/2012 for NO_2 (40 µg m^{-3}) from 1993 till 2016 while background stations never exceeded the limit value during the last 7 years. The general trend of NO_2 concentration is comparable in all sites with very similar values for the same kind of stations (traffic and background): an important reduction is observable in 2001, characterised by the absence of long period of atmospheric stability (ARPAT, 2002), followed by an amount of NO_2 almost constant with a temporary slight increase around 2010 (Figure 3.185).

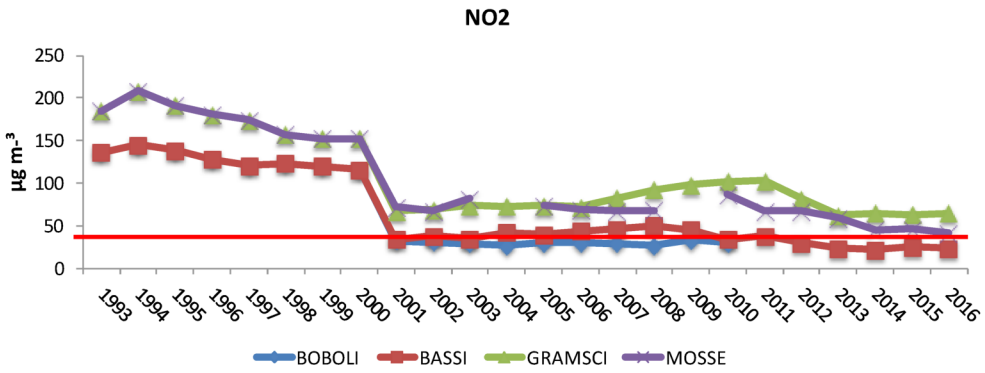

Figure 3.185 Mean annual concentration of NO_2 measured by monitoring stations closest to San Marco Museum. Red line indicates the yearly limit value for human health protection fixed by Legislative Decree no. 250/2012.

The available mean annual amounts of NO_x highlight a reduction in all the stations, with the exception of an increase between 2006-2007 (Figure 3.186). Nevertheless, all stations have surpassed the limit value established for the protection of vegetation.

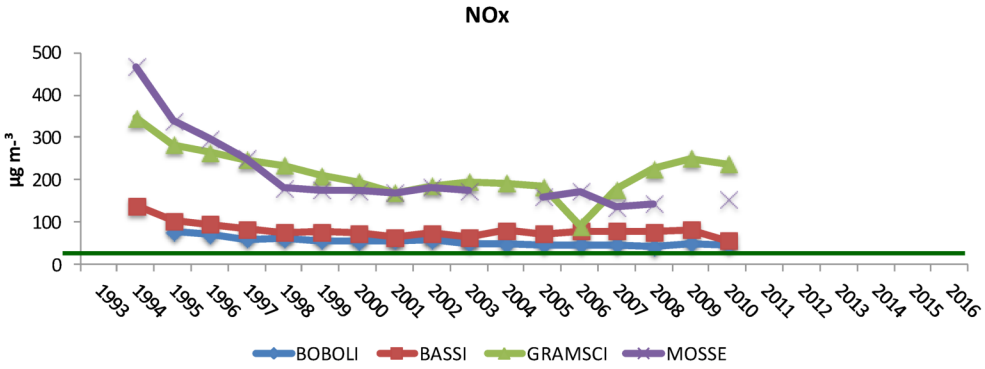

Figure 3.186 Mean annual concentration of NO_X measured by monitoring stations closest to San Marco Museum. Green line indicates the yearly limit value for vegetation protection fixed by Legislative Decree no. 250/2012.

Figure 3.187 shows the annual mean maximum concentration of carbon monoxide calculated on 8 hours. There is a general reduction in the amount of CO in Florence, even if a slight increase was recorded by Gramsci station in 2013. Considering the period 2004-2010 when four different monitoring stations measured the atmospheric CO concentration, it is possible to appreciate slightly higher values in traffic oriented stations (Gramsci and Mosse), confirming the close relationship of this pollutant with vehicular traffic.

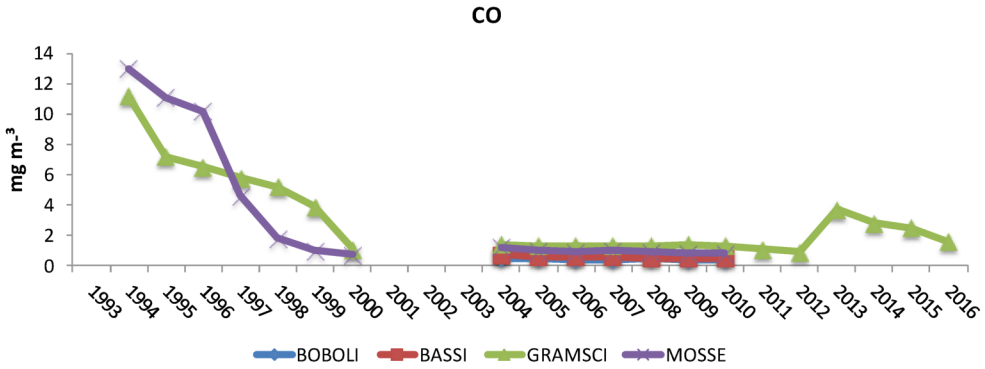

Figure 3.187 Mean annual maximum concentration of CO calculated on 8 hours measured by monitoring stations closest to San Marco Museum.

Mean annual concentration of benzene has generally decreased over the years, not exceeding the limit value fixed by the Legislative Decree no. 250/2012 also in the traffic oriented stations in recent times (Figure 3.188).

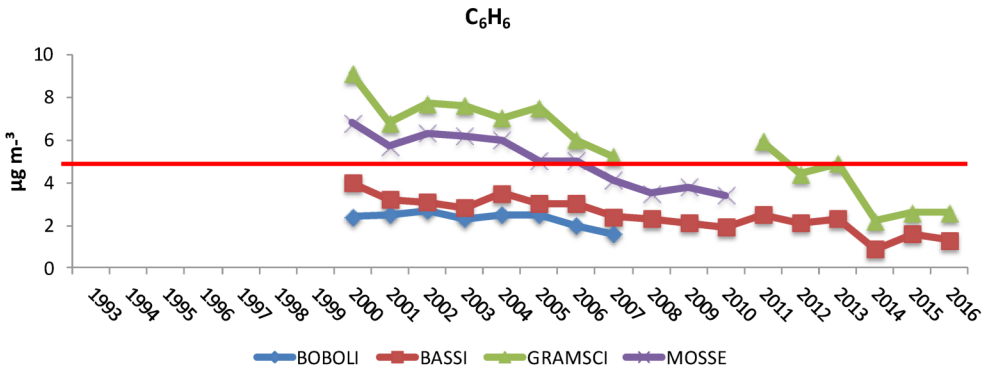

Figure 3.188 Mean annual concentration of C_6H_6 measured by monitoring stations closest to San Marco Museum. Red line indicates the yearly limit value for human health protection fixed by Legislative Decree no. 250/2012.

Besides the mean annual concentration of the main pollutants, it is important to assess the elemental concentrations to identify the different sources and estimate their impact on the ambient air quality. In 1997, an extensive investigation aiming at the characterisation of source appointment of PM_{10} aerosol in Florence urban area was started (Lucarelli et al., 2004). The urban areas involved in the research were briefly described in the table below.

SITE NAME	BRIEF DESCRIPTION	TIME OF SAMPLING
Site A	close to a heavy traffic road (Viale Gramsci)	February 1997 – January 1998
Site B	background site (close to Boboli Park)	January 1997 – January 1998
Site C	residential suburban area, closer to the industrial part of the district (Sesto Fiorentino)	December 1997 – May 1998

Table 3.64 Brief characterisation of sampling sites (Lucarelli et al., 2004).

The analysis of cellulose acetate filters by Particle-Induced X-Ray Emission (PIXE) and Particle-Induced γ-Ray Emission (PIGE) revealed traffic as the main aerosol contribution in sites A and B. Traffic is mostly characterized by high loadings of Pb and Br (tracer elements for leaded oil), Cu (emitted from diesel engines) and Zn (originated from the wearing down of vehicle tires). On the contrary, site C, closer to the industrial area, is mainly affected by the influence of oil source represented by high concentration of S, V and Ni (emitted by fossil-fuel combustion). However, airborne particulate levels of S, Br and Pb have decreased over a period of 10 years since 1988. Comparing these data with that of a previous study carried out in a traffic-oriented station (in Via Ponte alle Mosse) in September 1988 and January 1989 (Del Carmine et al., 1990), the concentrations of Pb and Br were 5 times lower than those found 10 years before, probably because of the increasing use of unleaded gasoline from the beginning of the 1990s. Also S amount strongly dropped in winter (6 times) and slightly in summer. The progressive substitution of oil combustion for domestic heating by methane fuel had certainly influenced S concentration.

The impact of traffic is highlighted also in a study executed by Tuscany Region (Forni, 2010) that recorded the amount of the main pollutants and heavy metals by direct measuring and estimate, considering different periods (1995, 2000, 2003, 2007, 2007, 2010) and sources. These last could be organised in four macro branches:

1. Industry (combustion deriving from energy industry, transformation of sources of energy, production processes and industrial combustion systems)
2. Heating (non-industrial combustion systems)
3. Traffic (road transport and other movable sources)
4. Other (extraction and distribution of fossil fuels and geothermal energy, use of solvents, waste disposal plant, nature and farming).

Figure 3.189 reports the annual relative emissions from different sources of the monitored pollutants: particulate matter (PM_{10}, $PM_{2.5}$), non-methane volatile organic compound (NMVOC), methane (CH_4), carbon oxides (CO, CO_2), hydrogen sulphide (H_2S), nitrogen oxides (NO_x), nitrous oxide (N_2O), ammonia (NH_3) and sulphur oxides (SO_X). It is possible to observe that traffic and heating macro-branches predominated in the emissions of pollutants in all the considered years. Moreover, pollutants released by traffic and industry show a fluctuating trend with a slight decrease in 2010 while heating system and other sources show a general diminishing concentrations.

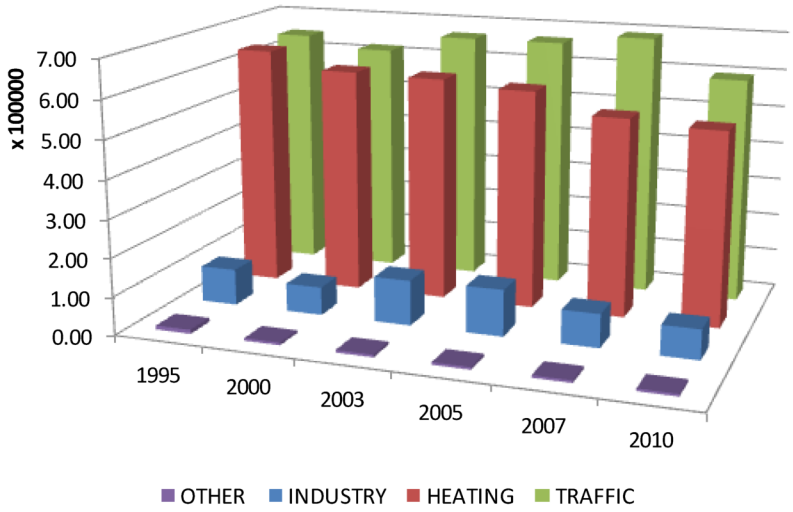

Figure 3.189 Relative load of total monitored pollutants (t) emitted by different sources.

Considering more in details each monitored pollutant (Figure 3.190), PM_{10} and $PM_{2.5}$ show a similar trend for all the emitting sources: high emissions of particulate matter released by traffic have decreased during last years while rather stable emissions pertained to heating system. Industry and other sources contributed less in the production of PM, displaying a decreasing or a very slight increasing trend, respectively. NMVOC underwent a substantial drop from 1995 to 2010, caused mainly by transport field, while methane emissions do not display a regular decreasing trend. CO emissions, whose main responsible is the traffic, decreased; a slight improvement is also appreciable for CO_2 in all emission sources. As expected, a clear drop in SO_X and H_2S is observed. Nevertheless, the control of sulphur oxides emission is important because they participate to the formation of secondary PM_{10} and $PM_{2.5}$. Despite the decrease during the period 1995-2010, traffic emissions of NO_x remains elevated and their concentration deviates from the amount released by all the other sources. Also N_2O and NH_3 are mainly emitted by traffic but recently emissions released by livestock and farming have been increasing.

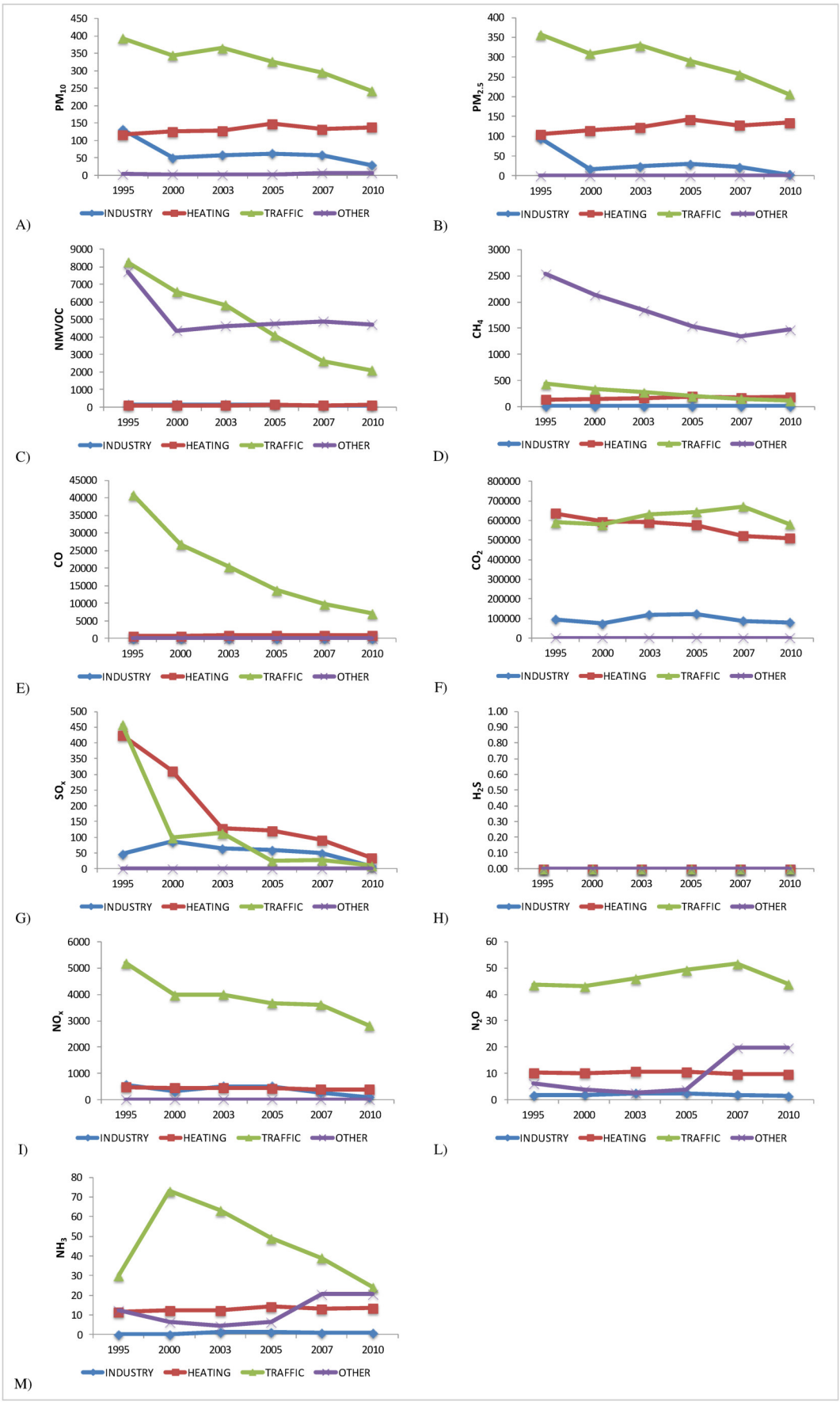

Figure 3.190 Mean annual concentration (t) of PM_{10} (A), $PM_{2.5}$ (B), NMVOC (C), CH_4 (D), CO (E), CO_2 (F), SO_X (G), H_2S (H), NO_x (I), N_2O (L), NH_3 (M) emitted by different sources.

Further information about the chemical characterisation and source apportionment of PM present in Florence are provided by EC AIRUSE LIFE+ project, aimed to characterise PM sources and contributions across the Southern Europe (AIRUSE summary report, 2016). In the urban background site of Florence monitored in 2013, annual mean level of PM_{10} and $PM_{2.5}$ were 19 µg m^{-3} and 13 µg m^{-3}, respectively. These data respected the limit values, but it should be considered that 2013 was particularly rainy, restraining the resuspension of particulate matter. The main aerosol sources in Florence were: sea salt, Saharan dust, secondary particles, particles released from road traffic, heavy oil combustion, biomass burning and local dust (Figure 3.191). In particular, *road traffic*, which comprises emissions from vehicle exhaust, vehicle non-exhaust and vehicle secondary nitrate, represented the major source of Florentine atmospheric pollution (31% of PM_{10} and $PM_{2.5}$). Its role was even more remarked during high pollution events (PM_{10} > 50 µg m^{-3} occurring in winter) being responsible for 43% of PM_{10} and 36% for $PM_{2.5}$. Another conspicuous contribution (27% of PM_{10} and 33% of $PM_{2.5}$) belonged to *non-traffic secondary particles* (sulphate, nitrate and organics) formed in the atmosphere from gaseous precursors (non-traffic NO_x, SO_2, VOCs, NH_3 and H_2S which is emitted by geothermal power plants located in Tuscany). In addition, *biomass burning* represented a relevant anthropogenic source (16% and 21% for PM_{10} and $PM_{2.5}$, respectively) that increased its influence during high pollution events (30% of PM_{10} and 33% of $PM_{2.5}$). Less weight came from other sources such as *local dust* (12% and 2% for PM_{10} and $PM_{2.5}$, respectively), *heavy oil combustion* (5% and 6%, mostly from activities that are located outside the city, like energy production, refinery, industrial plants and shipping) and *natural sources*, including sea salt and Saharan dust (8% of PM_{10} and 1.5% of $PM_{2.5}$).

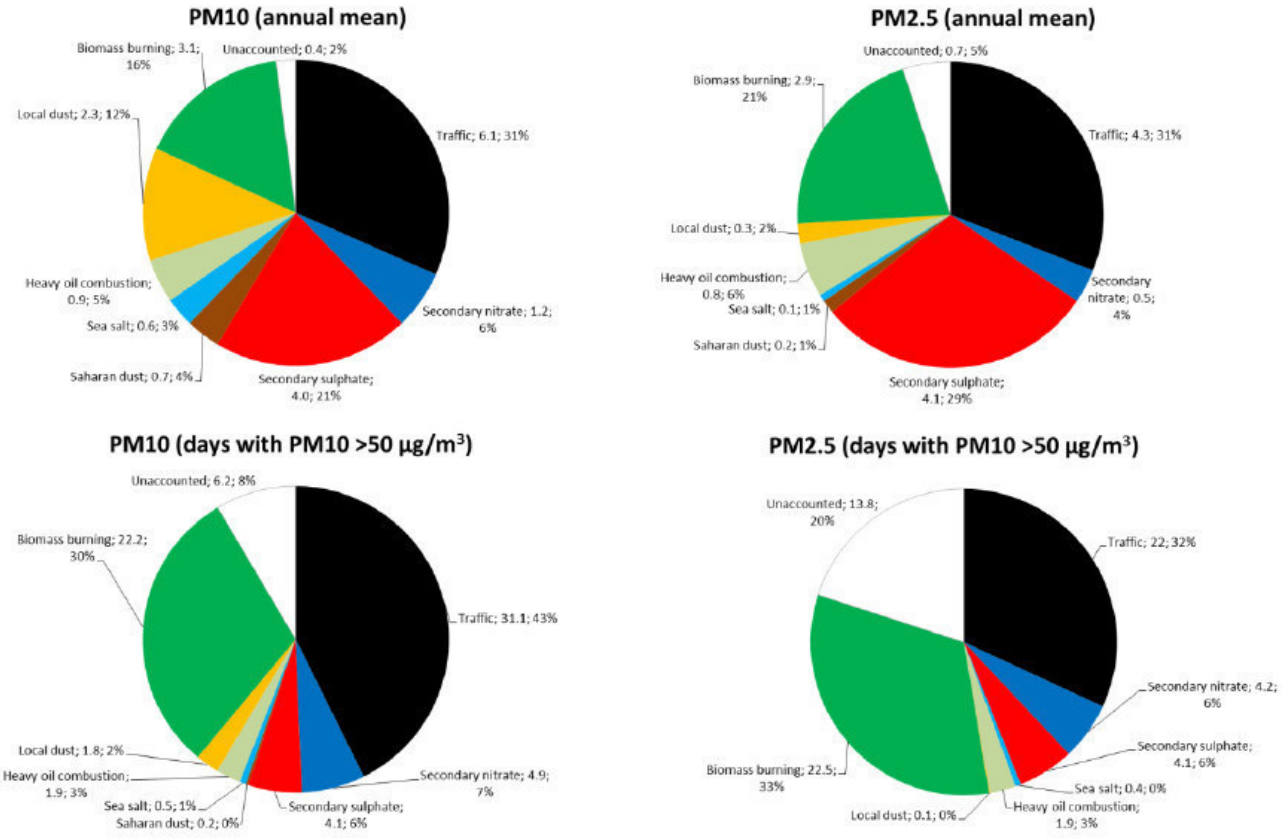

Figure 3.191 Source contributions in Florence in PM_{10} and $PM_{2.5}$. Values are expressed in µg m^{-3} and %. (AIRUSE summary report, 2016).

Most pollutant monitoring campaigns performed in urban areas aim to assess air quality for the protection of human health without considering the importance to evaluate the temporal variations of pollutants on immediate vicinity of an artistic monument. However, some examples are present in literature for the

Florentine case study and are mainly focused to characterise the atmospheric environment close to S. Maria del Fiore complex and Palazzo Vecchio (Cachier et al., 2004; Ozga et al., 2009; Nava et al., 2010; Ghedini et al., 2011).

Monitoring campaigns executed during 2003 at the Northern and Southern Door of S. Giovanni Baptistery, realized by Lorenzo Ghiberti and Andrea Pisano respectively, denoted a strong influence of sources nearby (such as traffic and tourist-related sources) as well as of very local meteorological conditions (i.e. enhancement of street-canyon effect) in the re-suspension of dust, dangerous for the conservation of artworks (Ghedini et al., 2011). This attitude is confirmed by the high level of total suspended particulate (TSP) detected during summer in contrast to its expected reduction due to the combination of increased thermal dispersion with a subsequent enhancement of the planetary boundary layer (PBL), on one hand, and a reduction of domestic heating sources, on the other. Comparing these data with TSP concentration of a city centre background situation (Cachier et al., 2004), the latter resulted to be lower than at the Baptistery, even more in summertime, i.e. tourist season. Therefore, tourists not only contributed to re-suspend deposited particles from the ground but proved to be themselves a major source of other diverse particles (such as fabric fibres, organic material, etc.), mainly when queuing for long time prior to entry (as in the case of the Northern Door of the Baptistery). Ozga et al. (2009) observed an appreciable decrease of sulphate anion at the Baptistery during 2003 and 2004 on the contrary of NO_3^- that was on the rise during the two years period. In general, these anions showed a rather similar trend with mean seasonal concentrations (winter, followed by summer, recorded the maximum concentration) higher at Northern Door, closer to vehicular traffic source, than at the Southern Door. These results confirm the gradual decrease of sulphur content in fuels but also their simultaneous enlarged consumption. Chloride is always present with higher concentrations in winter, spring and autumn at Northern Door while it prevailed at the Southern Door during summer. Prevailing winds flow mainly from marine west direction in summer/autumn and thus could had influenced the concentration of chloride. Acetates, formats and oxalates were also present without evidencing strong spatial differences. Considering cations, Ca^{2+} and Mg^{2+} were always present at the highest concentrations in the sampled aerosol while Na^+, K^+ and NH_4^+ were recorded in lower amount. Substantial concentrations of non-carbonate carbon (NNC) were analysed, higher at the Northern Door than the Southern one in all the seasons (Ozga et al., 2009). Comparing the seasonal mean values of NCC, the hot and droughty summer of 2003 might explain the highest values of NCC in summer in contrast to the wintry record values of 2004.

Besides evaluation of air quality conditions in Piazza della Signoria and Piazza del Duomo, Barbagallo (2014) characterised the atmospheric particulate matter in another area of the city centre, which hosts the exposure of stone samples and the aerosol monitoring campaigns described in this thesis: San Marco Museum close to the Accademia. Monitoring campaigns were carried out in summer (July) and winter (December) 2013 in order to evaluate the chemical composition of the aerosol. TSP measured during summer (mean: 45.39 ± 8.35 $\mu g\ m^{-3}$) is less than that collected during winter (mean: 53.72 ± 4.66 $\mu g\ m^{-3}$). These values are slightly decreased in respect to the results of analyses performed at S. Giovanni Baptistery in 2003 (74.3 $\mu g\ m^{-3}$ in summer and 61.2 $\mu g\ m^{-3}$) but however they proved to be higher than those measured in other European urban areas such as Milan (43 $\mu g\ m^{-3}$) and Paris (43 $\mu g\ m^{-3}$) (Gedini et al., 2011). The evaluation of ionic species show that there were some discrepancy between summer and winter amount of sulphate and nitrate (Table 3.65). The higher concentration of SO_4^{2-} during the warmer period could be explained by the increase in photochemical oxidation as sulphate is a typical secondary pollutant. On the contrary nitrate is more abundant in winter likely because of more intense traffic and use of domestic heating It should be considered also the possible evaporation during sampling of the semi-volatile ammonium nitrate (i.e. nitrate artifact) that occurs when temperature exceeds 25°C and in less extent between 20°C and 25°C (Schaap et al., 2004). The concentration of Ca^{2+} remained rather high during the year as an effect of dust re-suspension and the proximity to quarries.

	SITE	Na^+	NH_4^+	K^+	Mg^{2+}	Ca^{2+}	$C_2H_3O_2^-$	CHO_2^-	Cl^-	NO_3^-	SO_4^{2-}	$C_2O_4^{2-}$
Summer 2003	ND	0.86	0.11	0.21	0.22	5.10	0.13	0.03	0.81	4.13	5.10	0.04
	SD	0.72	0.12	0.14	0.15	4.03	0.22	0.02	1.79	1.56	5.00	0.20
Winter 2003	ND	0.34	0.38	0.13	0.08	2.11	0.13	0.04	0.27	5.20	6.33	0.22
	SD	0.29	0.37	0.15	0.09	2.48	0.09	0.04	0.21	5.90	6.20	0.34
Summer 2013	S. Marco Museum	0.53	0.95	0.72	0.06	2.48	0.03	0.50	0.19	0.77	2.84	0.21
Winter 2013	S. Marco Museum	0.15	1.21	0.44	0.04	2.56	0.04	0.05	0.31	5.50	0.81	0.21

Table 3.65 Mean air concentration (μg m^{-3}) of soluble ions measured during summer and winter campaigns at the North (ND) and South Door (SD) of the Baptistery in 2003 and at the San Marco Museum in 2013 (Barbagallo, 2014).

Comparing these data with ions concentration measured at the Baptistery in 2003, it is possible to observe a recent reduction of sulphate probably induced by the progressive substitution of heating systems with lower-sulphur fuels. Nevertheless, the concentration of nitrate did not undergo big changes implying a stable contribution of pollution from traffic (Barbagallo, 2014).

Focusing one's attention to the different components of carbon detected in aerosol, the EC CARAMEL Project (EVK4-CT2000-00029) analysed the carbon speciation of aerosol collected during one-year campaign (July 2002-July 2003) on the roof of the "Museo dell'Opera del Duomo" close to the Cathedral (Cachier et al., 2004). The results reveal the prevalence of OC (2.51 μg m^{-3}) in respect to EC (0.48 μg m^{-3}) in the mean mass concentration. In particular, both OC and EC were found predominantly in the fine fraction of aerosol (PM_2): 5.86 μg m^{-3} and 1.92 μg m^{-3}, respectively. The copious presence of scooters (2-stroke engines) in the Cathedral surroundings should explain the overproduction of fine OC particles. The daily pattern of EC displays the highest concentration during the morning and the late afternoon traffic peaks, highlighting the importance of regional traffic activity of workers beside the tourism activity.
In view of new restorations, air quality was measured in Michelozzo's Courtyard (in Palazzo Vecchio, headquarters of the communality) (Nava et al., 2010). It is a semi-confined environment, subjected to both urban pollution and heavy microclimatic conditions. During the monitoring campaigns (December 2003-January 2004 and June-July 2004), PM2.5 displayed the highest mass concentrations (up to 76 μg m^{-3}, mean value 32 μg m^{-3}) during stable meteorological conditions of wintertime while the lowest ones in summer (17 μg m^{-3}). Also in this case study, OC prevailed (13.6 μg m^{-3} in winter and 4.6 μg m^{-3} in summer) on EC concentration (1.8 μg m^{-3} in winter and 0.7 μg m^{-3} in summer). Comparing this data with the results obtained by Cachier et al. (2004) in the centre of Florence one year before, it is noteworthy a similar trend but with a general slight decrease in values. Nevertheless, this reduction cannot be firmly stated because of the difference in environment: partially sheltered in Michelozzo's Courtyard and exposed in the roof of Cathedral Museum. By contrast, data reported by Barbagallo (2014) referring to aerosol monitoring campaigns at the covered roof-terrace of San Marco Museum show a much higher amount of both EC and OC during 2013 sampling. EC values doubled throughout the year (from 1.8 μg m^{-3} to 4.81 μg m^{-3} in winter and from 0.7 μg m^{-3} to 1.68 μg m^{-3} in summer) as well as OC recorded higher values (in winter 13.6 μg m^{-3} and 19.14 μg m^{-3} and summer 4.6 μg m^{-3} and 7.52 μg m^{-3}, in 2003-04 and 2013 respectively). This could prove the increase of carbon emissions during the 10-year period.
A high correlation between OC and K amount was measured in $PM_{2.5}$ samples only during winter, suggesting a significant contribution from biomass burning (Nava et al., 2010). Sulphate concentrations were higher in summer (5.2 μg m^{-3}) than in winter (2.2 μg m^{-3}) because of a more efficient photochemical summer activity in the atmosphere that favours the oxidation of SO_2 into sulphate. On the contrary, nitrate amount decreased in summer likely because of its volatile nature and the lack of additional winter sources (i.e.

domestic heating). Therefore Nava et al. (2010) suggested a mainly local origin (i.e. combustion sources) for NO_3^- while a regional one for SO_4^{2-}, observing higher nitrate concentrations in reduced air circulation conditions and prevailing sulphate in uncovered situations.

3.3.2. TOTAL SUSPENDED PARTICULATE

Total suspended particulate (TSP) gives information about the total amount of atmospheric particles sampled in a specific volume, without any limitation of particles size. TSP value is calculated by the following equation:

$$TSP\ (\mu g\ m^{-3}) = W\ (\mu g) / V\ (m^{-3})$$

where W is the weight of total particulate measured by weight difference of filter after and before sampling while V is the monitored volume.

BOLOGNA

The amount of total suspended particulate measured during different monitoring campaigns in Bologna is reported in Table A6.1 (Annex 6).

Winter 2017 PM monitoring campaign

PM monitoring campaign was performed in the period 9-16 February 2017. TSP ranged between 24.76 µg m^{-3} and 57.53 µg m^{-3}, reaching the highest concentration during the weekend (Figure 3.192).

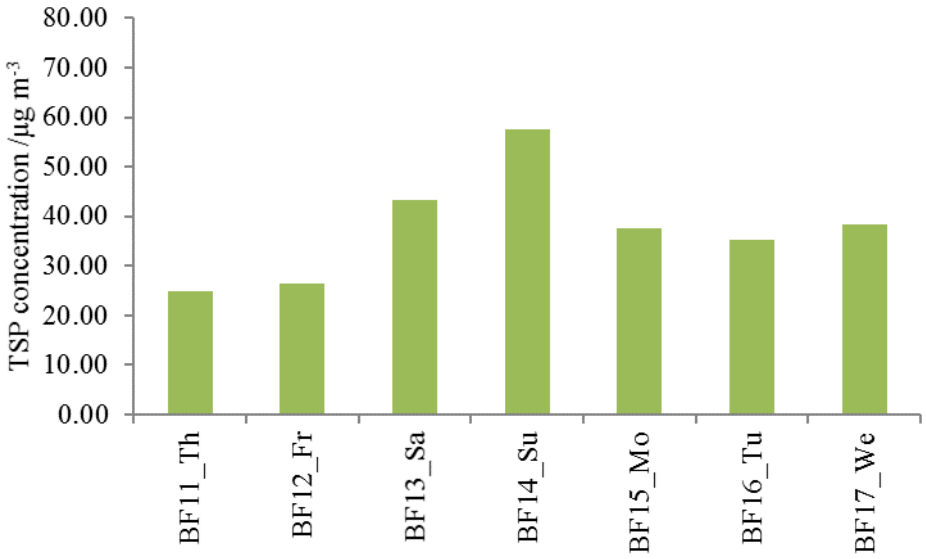

Figure 3.192 Daily atmospheric concentration of TSP measured in Bologna during winter 2017 campaign.

Summer 2017 PM monitoring campaign

Particulate matter was monitored in the period 13-19 June 2017. In general, TSP was quite constant throughout the analysed period showing a mean value of 17.60 µg m^{-3} (Figure 3.193).

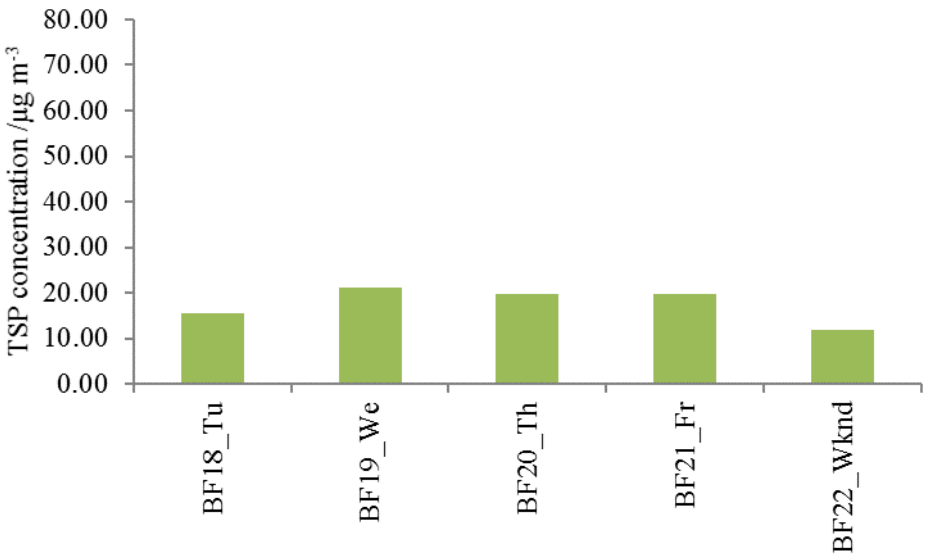

Figure 3.193 Daily atmospheric concentration of TSP measured in Bologna during summer 2017 campaign.

Winter 2018 PM monitoring campaign

PM monitoring campaign was carried out between 24 January and 1 February 2018. Figure 3.194 shows that the calculated TSP was between 16.72 µg m^{-3} and 74.45 µg m^{-3}, with higher values on Thursday and Friday.

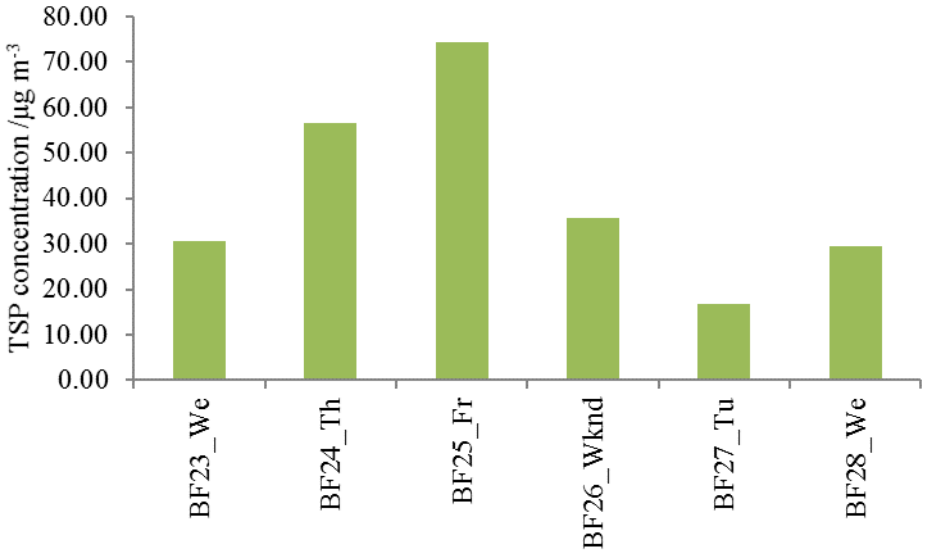

Figure 3.194 Daily atmospheric concentration of TSP measured in Bologna during winter 2018 campaign.

Summer 2018 PM monitoring campaign

Last monitoring campaign was performed in the period 7-14 June 2018. The detected particulate doesn't show particular differences among analysed days even if a slight increase till 23.18 µg m^{-3} happened during Monday (Figure 3.195). Unfortunately, no data about TSP of BF30 is available because of a mistake in measuring the weight of the filter before sampling.

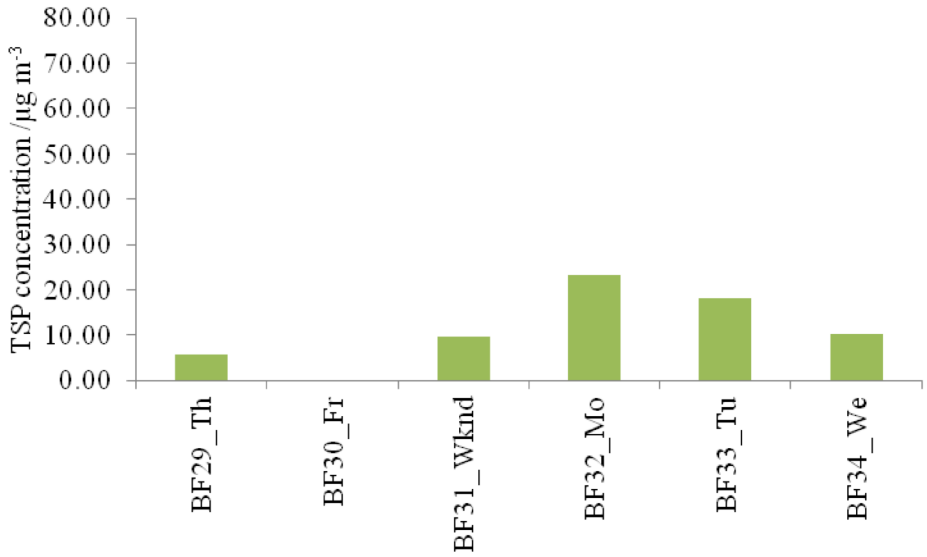

Figure 3.195 Daily atmospheric concentration of TSP measured in Bologna during summer 2018 campaign.

Comparison

The comparison of different PM monitoring campaigns performed in Bologna shows in general that TSP was higher and more variable during the monitoring campaigns carried out during cold season than data acquired during the summer ones (Figure 3.196). In particular, TSP mean value of winter campaigns is equal to 37.62 ± 10.99 µg m^{-3} in 2017 and 40.53 ± 21.06 µg m^{-3} in 2018 while lower values were detected during summer monitoring campaigns (17.60 ± 3.75 µg m^{-3} in 2017 and 13.38 ± 7.10 µg m^{-3} in 2018). Moreover, considering different day of week, no clear trend in the amount of TSP was detected over the analysed period.

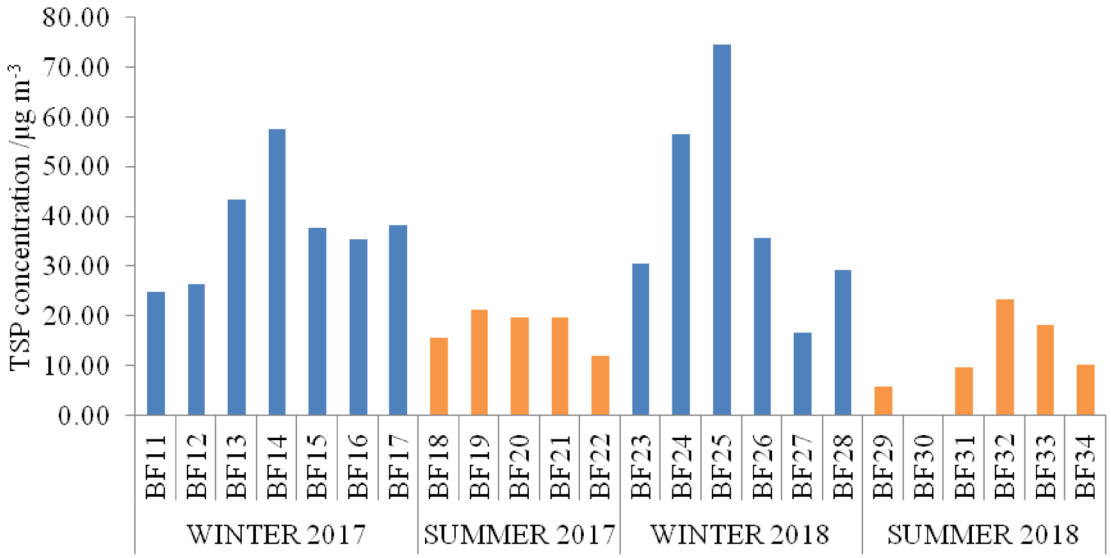

Figure 3.196 Daily concentration of total suspended particulate (TSP) acquired during PM monitoring campaigns performed in Bologna during winter (blue) and summer (orange) 2017 and 2018.

FERRARA

The concentration of total suspended particulate measured during different monitoring campaigns in Ferrara is reported in Table A6.2 (Annex 6).

Winter 2017 PM monitoring campaign

PM monitoring campaign affected the period between 22 February 2017 and 8 March 2017. In particular, the first part of the campaign (PTF11, PTF12, PTF13, PTF14, PTF15 and PTF17) was performed on the roof terrace of Palazzo Turchi di Bagno where stone samples are exposed while a change of position of the monitoring device to the ground floor in the Botanic Garden was necessary for other filters (PTF16, PTF18, PTF19 and PTF20) due to logistic problems.

TSP measured in the period remained between 5.20 µg m^{-3} and 29.04 µg m^{-3}, without displaying any clear trend related to different day of the week (Figure 3.197). Moreover, PM monitoring was carried out at both roof terrace and ground floor during the weekend 4-5 March 2017 in order to compare the acquired data. In this regard, the detected TSP was similar in both sites (Figure 3.197).

Figure 3.197 Daily atmospheric concentration of TSP measured in Ferrara during winter 2017 campaign.

Summer 2017 PM monitoring campaign

PM monitoring campaign was performed in the period 21-28 June 2017. The detected TSP ranged between 23.50 µg m^{-3} and 33.81 µg m^{-3}, with slightly higher amount on Thursday and Friday while characterised by constant and lower values during the other days (Figure 3.198).

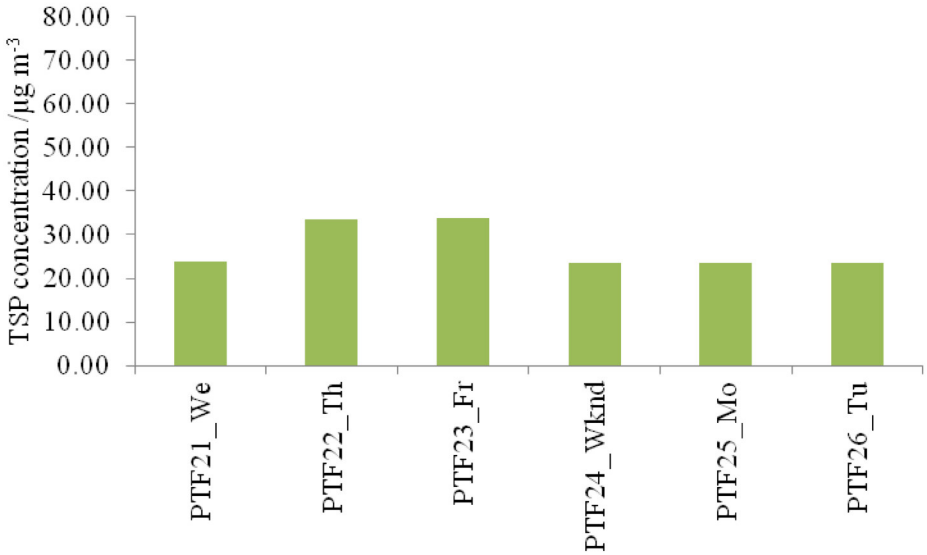

Figure 3.198 Daily atmospheric concentration of TSP measured in Ferrara during summer 2017 campaign.

Winter 2018 PM monitoring campaign

Aerosol monitoring affected the period 16-23 January 2018. TSP values were between 21.14 µg m^{-3} and 46.91 µg m^{-3}, with slightly lower value on Wednesday (Figure 3.199).

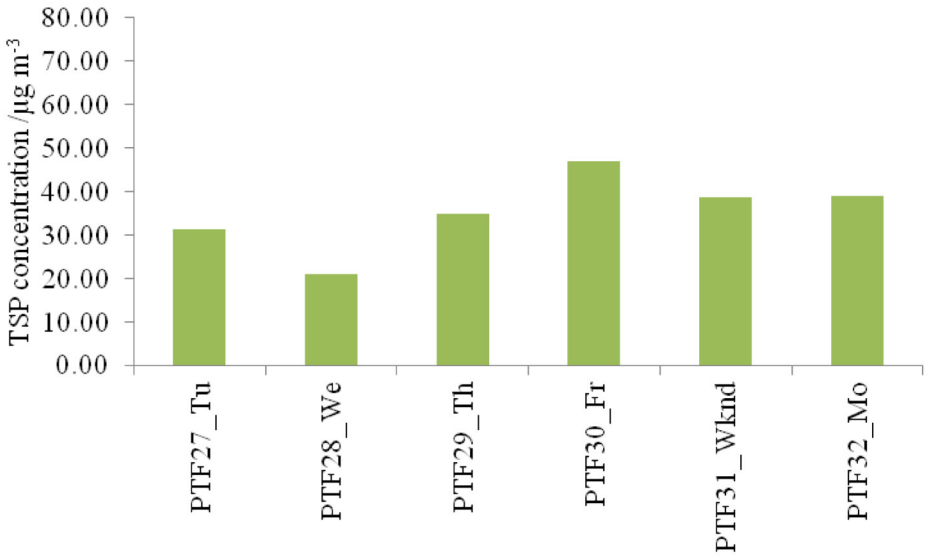

Figure 3.199 Daily atmospheric concentration of TSP measured in Ferrara during winter 2018 campaign.

Summer 2018 PM monitoring campaign

This monitoring campaign was carried out in the period 22-29 June 2018. TSP remained almost constant over the period with values always below 20.00 µg m^{-3} (Figure 3.200).

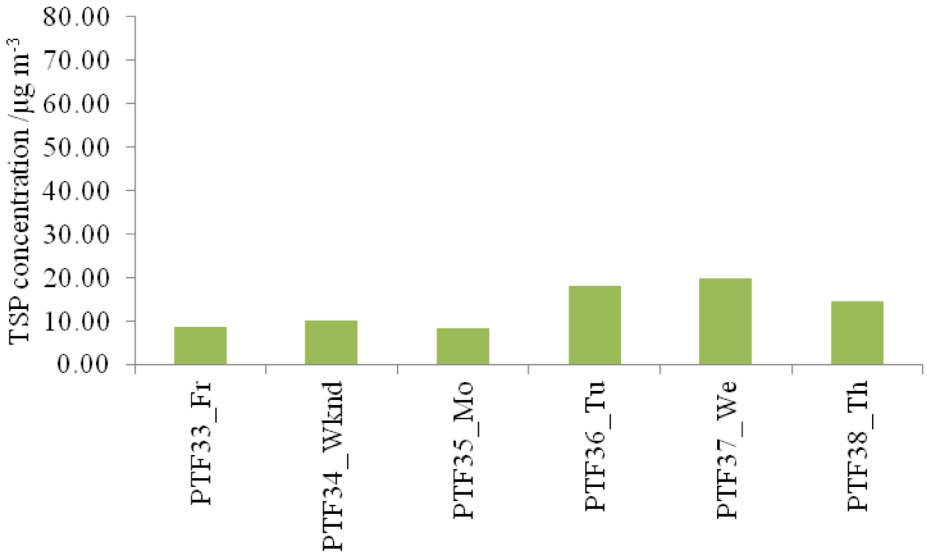

Figure 3.200 Daily atmospheric concentration of TSP measured in Ferrara during summer 2018 campaign.

Comparison

TSP acquired during the different PM monitoring campaigns in Ferrara shows higher amount during summer 2017 and winter 2018 periods (Figure 3.201). Specifically, mean value of TSP detected in winter 2018 recorded the highest amount (35.26 ± 8.67 µg m^{-3}), followed by that calculated from summer 2017 campaign data (26.98 ± 5.17 µg m^{-3}). TSP average values of winter 2017 and summer 2018 campaigns were lower (14.95 ± 8.03 µg m^{-3} and 13.24 ± 5.03 µg m^{-3}, respectively).

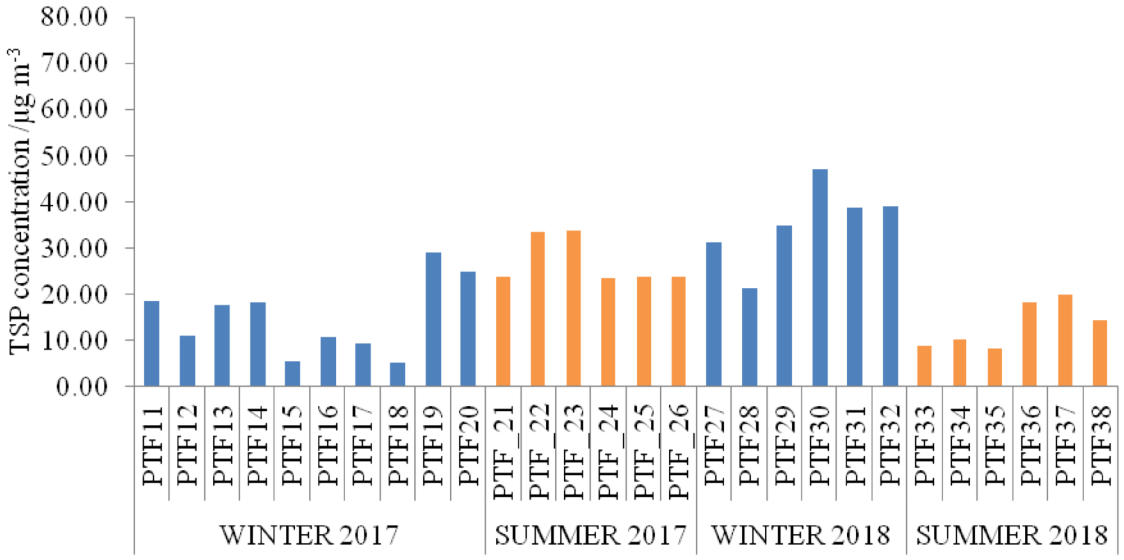

Figure 3.201 Daily concentration of total suspended particulate (TSP) acquired during PM monitoring campaigns performed in Ferrara during winter (blue) and summer (orange) 2017 and 2018.

FLORENCE

The amount of total suspended particulate measured during different monitoring campaigns in Florence is shown in Table A6.3 (Annex 6).

Winter 2017 PM monitoring campaign

Monitoring campaign of particulate matter started on 16 February and ended on 21 February 2017. Figure 3.202 displays the calculated total amount of PM. TSP remained between 14.75 µg m^{-3} and 31.66 µg m^{-3} without underwent to high changes over the period (Figure 3.202).

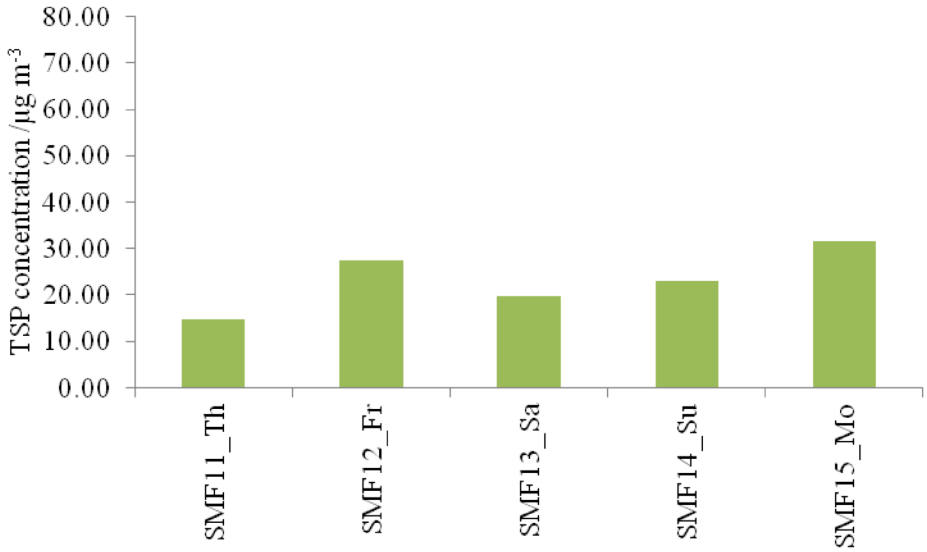

Figure 3.202 Daily atmospheric concentration of TSP measured in Florence during winter 2017 campaign.

Summer 2017 PM monitoring campaign

PM was collected during the period 6-12 June 2017. TSP was detected around 22.00 µg m^{-3} for almost all days with just a light lower amount on Thursday (13.03 µg m^{-3}) (Figure 3.203).

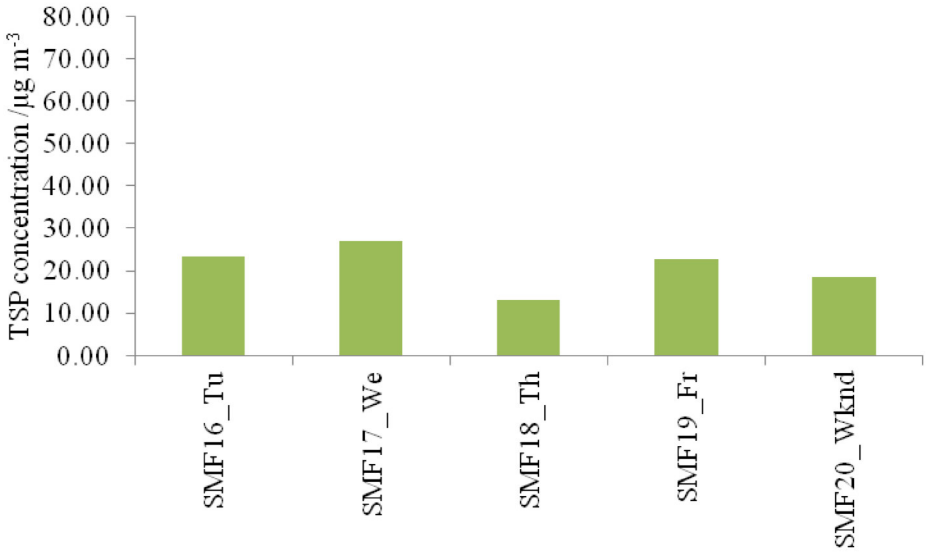

Figure 3.203 Daily atmospheric concentration of TSP measured in Florence during summer 2017 campaign.

Winter 2018 PM monitoring campaign

During winter PM monitoring campaign, performed between 2 and 8 February 2018, TSP ranged from 4.58 µg m^{-3} to 26.84 µg m^{-3}. Considering the different day of the week, weekend and Monday displayed higher TSP concentration (Figure 3.204).

Figure 3.204 Daily atmospheric concentration of TSP measured in Florence during winter 2018 campaign.

Summer 2018 PM monitoring campaign

PM was monitored between 15 and 21 June 2018. The analysed TSP resulted to be quite stable over the period with values between 16.19 µg m^{-3} and 24.75 µg m^{-3} (Figure 3.205).

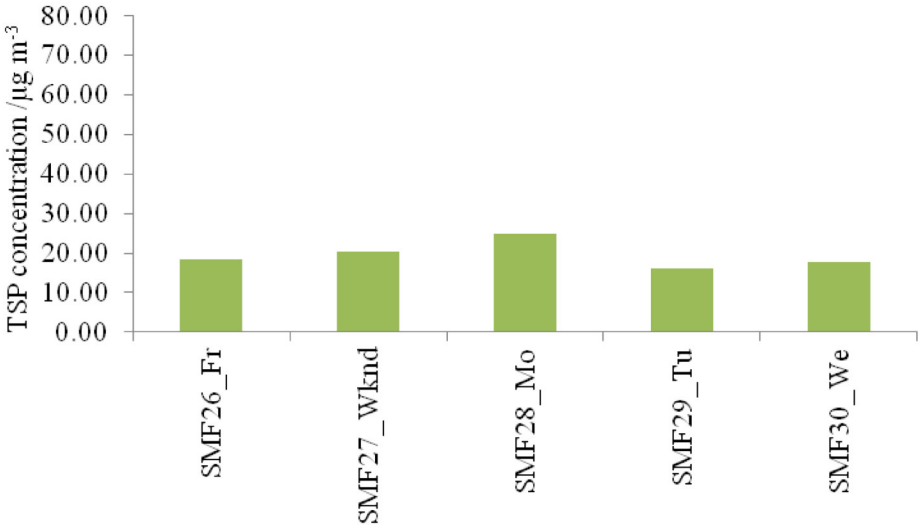

Figure 3.205 Daily atmospheric concentration of TSP measured in Florence during summer 2018 campaign.

Comparison

The comparison of the different monitoring campaigns of PM performed in Florence in 2017 and 2018 shows in general stable values of TSP around 20.00 µg m^{-3} all over the period (Figure 3.206). Some analysed filters differed from the mean TSP (for example SMF15 and SMF21) but they are sporadic.

Considering mean TSP values of each monitoring campaign (i.e. 23.30 ± 6.58 µg m^{-3} in winter 2017, 20.88 ± 5.34 µg m^{-3} in summer 2017, 18.27 ± 9.17 µg m^{-3} in winter 2018 and 19.48 ± 3.29 µg m^{-3} in summer 2018) no season differences was detected.

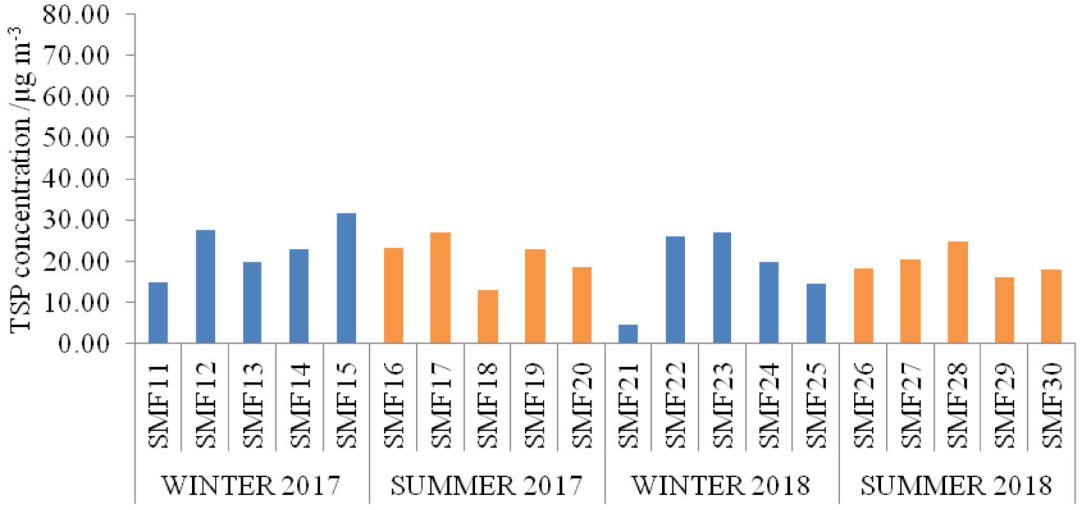

Figure 3.206 Daily concentration of total suspended particulate (TSP) acquired during PM monitoring campaigns performed in Florence during winter (blue) and summer (orange) 2017 and 2018.

GENERAL COMPARISON

The comparison of mean values of TSP detected during all monitoring campaigns for each site shows that Bologna was the site with the highest value (28.76 ± 17.04 µg m^{-3}) followed by Ferrara (21.51 ± 11.18 µg m^{-3}) and Florence (20.48 ± 6.23 µg m^{-3}). However, it is important to evaluate the season trend of each selected site because there could be some variations due to differences in emission sources and in the height of planetary boundary layer. In this regard, as indicated above, Bologna displays higher mean TSP values measured during both winter campaigns of 2017 and 2018 respect to the summer ones. On the contrary, mean TSP detected in Florence resulted rather stable all over the analysed period while in Ferrara higher average TSP was measured during summer 2017 and winter 2018.
In particular, considering the trend of mean TSP of each site during the winter campaigns in 2017, Bologna showed the highest TSP concentration (37.62 ± 10.99 µg m^{-3}) followed by Ferrara (14.95 ± 8.03 µg m^{-3}) and Florence (23.30 ± 6.58 µg m^{-3}) (Figure 3.207). During summer 2017 campaigns, mean TSP measured in Bologna (17.60 ± 3.75 µg m^{-3}) was lower respect to Ferrara (26.98 ± 5.17 µg m^{-3}) and Florence (20.88 ± 5.34 µg m^{-3}). Winter 2018 monitoring campaigns displayed the highest concentration of TSP in Bologna (40.53 ± 21.06 µg m^{-3}), as in the previous winter campaign, while the lowest TSP amount was detected in Florence (18.27 ± 9.17 µg m^{-3}). Finally, summer 2018 monitoring campaigns was characterised by similar values of TSP in Bologna (13.38 ± 7.10 µg m^{-3}) and Ferrara (13.24 ± 5.03 µg m^{-3}) while Florence reached higher mean value (19.48 ± 3.29 µg m^{-3}).

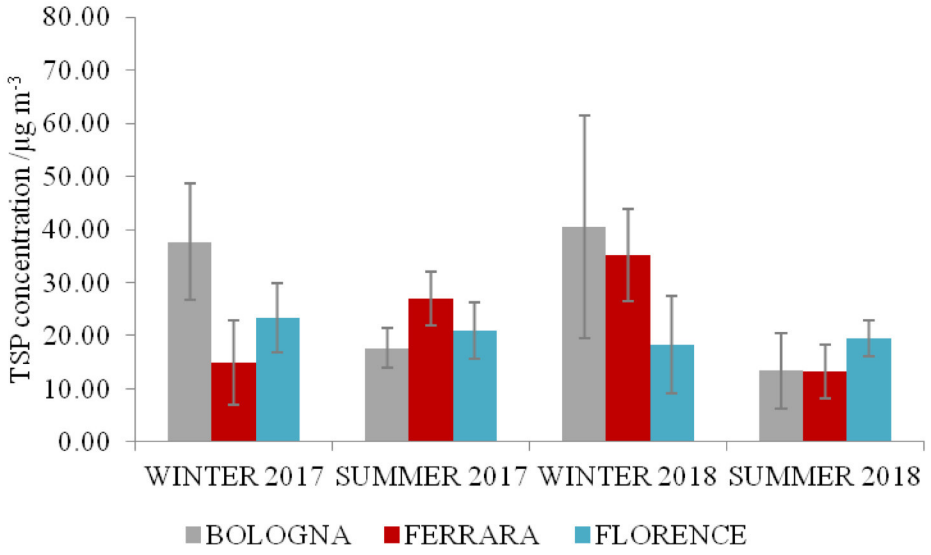

Figure 3.207 Mean TSP acquired during PM monitoring campaigns performed in Bologna (grey), Ferrara (red) and Florence (light blue) during winter and summer 2017 and 2018.

3.3.3. ION CHROMATOGRAPHY (IC)

BOLOGNA

Results of water-soluble ions detected in Bologna PM during different monitoring campaigns are displayed in Table A7.1 (Annex 7).

Winter 2017 PM monitoring campaign

The monitoring campaign was characterised by the prevalence of NO_3^- than the other ions all over the considered period, reaching higher values during the weekend (till 16.18 µg m^{-3}) (Figure 3.208). Among anions, also sulphate stood out for its concentration between 1.29 µg m^{-3} and 4.72 µg m^{-3}. NH_4^+ showed a concentration higher than the other cations, with values till to 4.98 µg m^{-3} reached during Sunday. Ca^{2+} concentration remained rather constant over the period (between 0.56 µg m^{-3} and 1.52 µg m^{-3}) while the amount of the other cations was negligible.

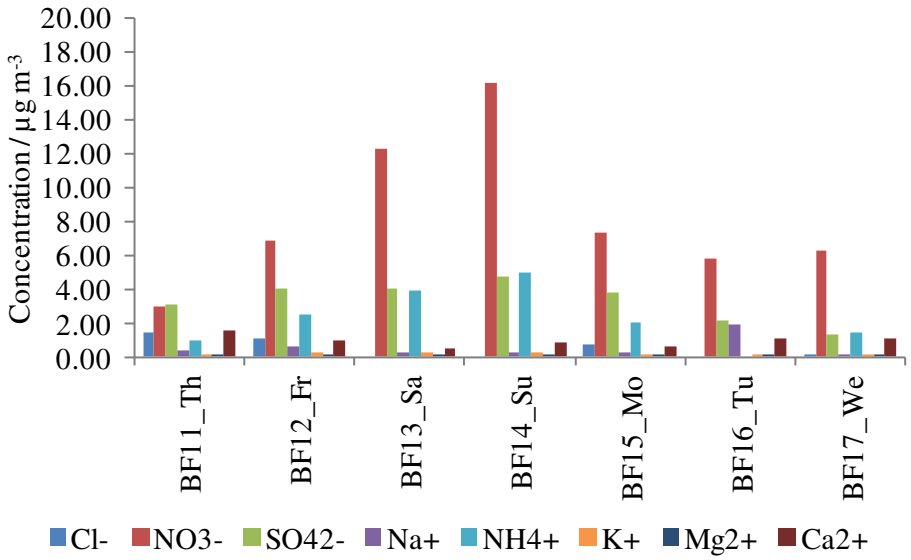

Figure 3.208 Daily atmospheric concentration of water-soluble ions measured in Bologna during winter 2017 campaign.

Summer 2017 PM monitoring campaign

The concentration of ions monitored during summer 2017 campaign never reached values higher than 2.14 µg m^{-3} (Figure 3.209). Within this range, SO_4^{2-}, NO_3^- and Ca^{2+} displayed slightly higher concentration then the other ions with maximum values of 2.14 µg m^{-3}, 2.13 µg m^{-3} and 1.38 µg m^{-3}, respectively.

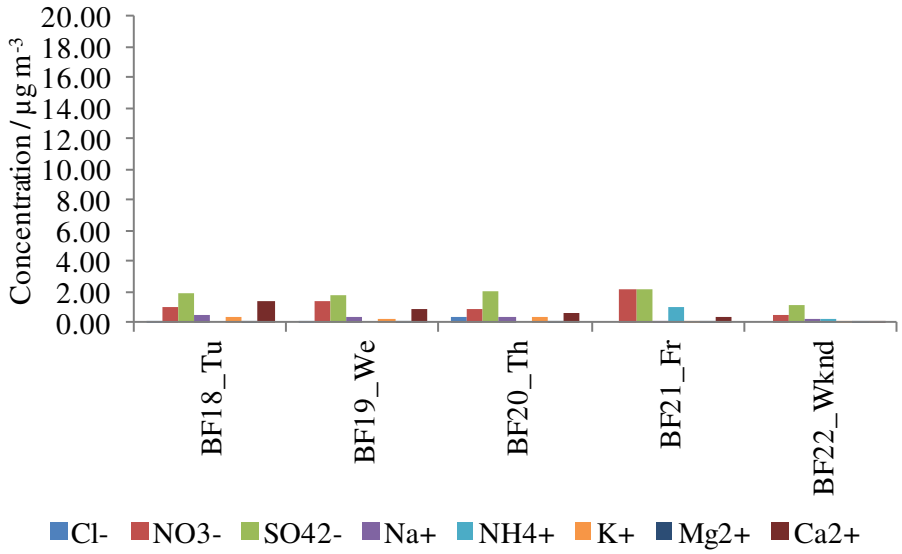

Figure 3.209 Daily atmospheric concentration of water-soluble ions measured in Bologna during summer 2017 campaign.

Winter 2018 PM monitoring campaign

NO_3^- reached higher concentration during every monitored day than the other ions, showing values between 4.88 µg m^{-3} and 18.91 µg m^{-3} (Figure 3.210). SO_4^{2-} was detected in concentration between 1.25 µg m^{-3} and 3.04 µg m^{-3} while the measured amount of chloride was much lower (below 1 µg m^{-3}).

Among cations, NH_4^+ prevailed over the others, showing a concentration between 1.50 µg m^{-3} and 5.02 µg m^{-3}.

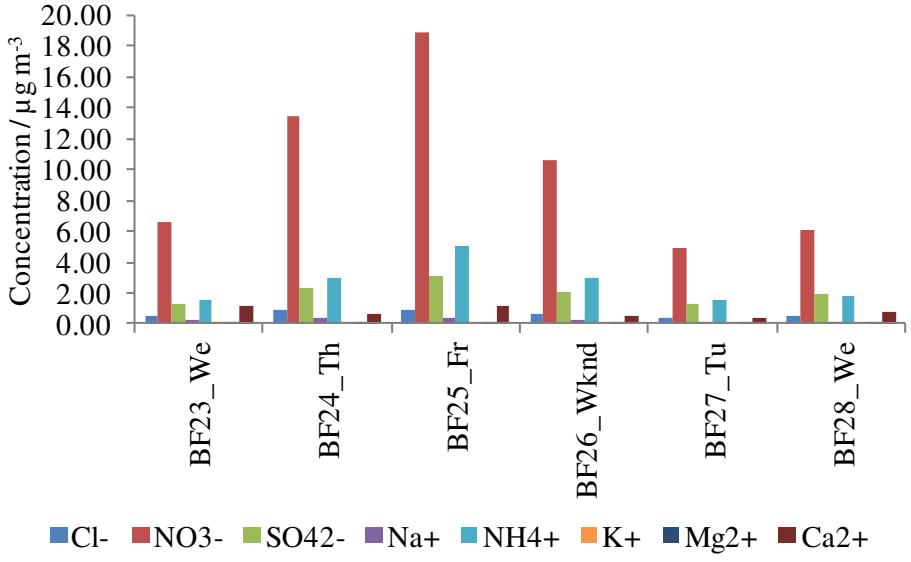

Figure 3.210 Daily atmospheric concentration of water-soluble ions measured in Bologna during winter 2018 campaign.

Summer 2018 PM monitoring campaign

The concentration of all ions detected during summer 2018 monitoring campaign remained always below 1.00 µg m^{-3} (Figure 3.211).

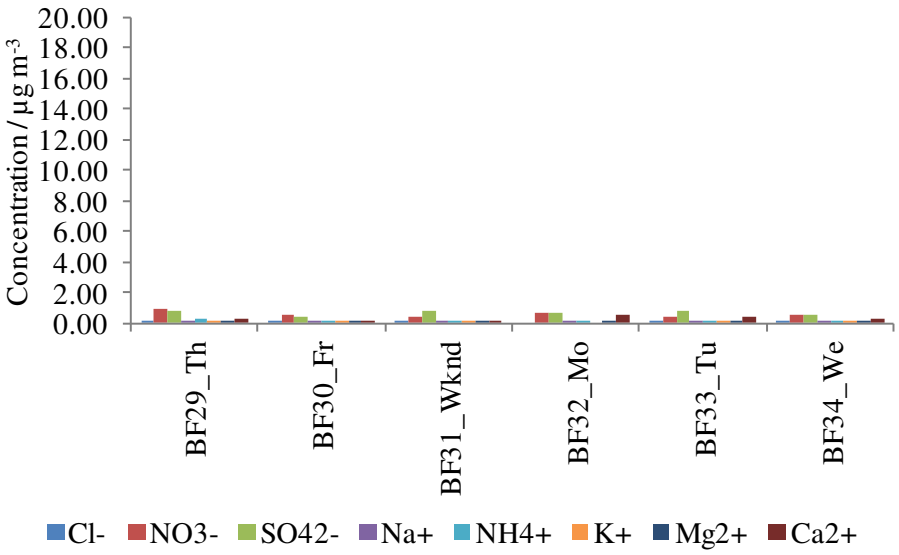

Figure 3.211 Daily atmospheric concentration of water-soluble ions measured in Bologna during summer 2018 campaign.

Comparison

The comparison of mean concentration of water-soluble ions detected during different monitoring campaigns performed in Bologna shows that NO_3^-, SO_4^{2-} and NH_4^+ were in general more abounding than the other ions, reaching higher values during winter campaigns (Figure 3.212). Specifically, mean NO_3^- amount was between 0.57 ± 0.19 µg m^{-3} (in summer 2018) and 10.08 ± 5.37 µg m^{-3} (in winter 2018), followed by SO_4^{2-} (from 0.67 ± 0.16 µg m^{-3} in summer 2018 and 3.30 ± 1.22 µg m^{-3} in winter 2017) and NH_4^+ (0.16 ± 0.05 µg m^{-3} in summer 2018 and 2.65 ± 1.52 µg m^{-3} in winter 2017).

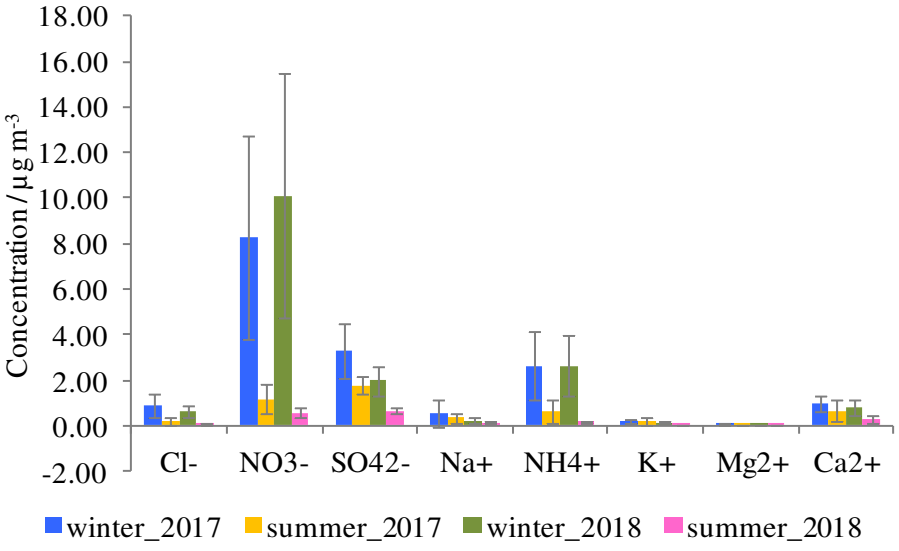

Figure 3.212 Mean atmospheric concentration of water-soluble ions measured in Bologna during different monitoring campaigns.

FERRARA

IC results measured in PM monitored in Ferrara during different monitoring campaigns are presented in Table A7.2 (Annex 7).

Winter 2017 PM monitoring campaign

Soluble ions measured in winter 2017 displayed the predominance of NO_3^- over the other ions, which reached 6.48 µg m^{-3} (Figure 3.213). Cl^- slightly exceeded the concentration of SO_4^{2-} for some filters (PTF16-20) but remaining always below 2.00 µg m^{-3}.

Among cations, concentrations of NH_4^+ and Ca^{2+} were slightly higher than the others although they rarely overcome 2.00 µg m^{-3}.

PM monitoring during the weekend performed both on the roof terrace of Palazzo Turchi di Bagno (PTF17) was slightly richer in soluble ions than those monitored at the ground floor in the Botanic Garden (PTF18), even if ion concentration was in general low.

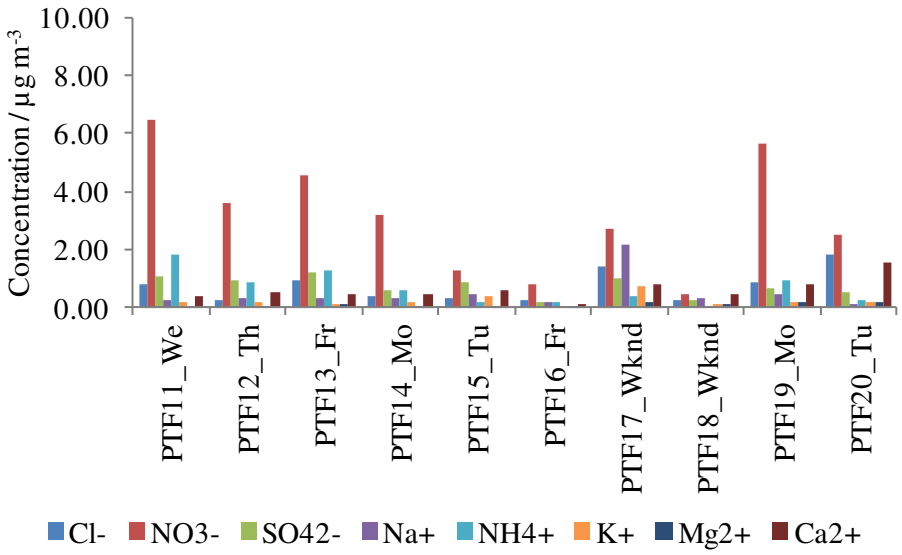

Figure 3.213 Daily atmospheric concentration of water-soluble ions measured in Ferrara during winter 2017 campaign.

Summer 2017 PM monitoring campaign

During summer 2017 monitoring campaign the concentration of ions remained below 3.05 µg m^{-3} (Figure 3.214). In particular, nitrate and sulphate prevailed among detected anions showing similar concentration (from 1.56 µg m^{-3} to 3.05 µg m^{-3} SO_4^{2-} and from 1.21 µg m^{-3} to 2.55 µg m^{-3} for NO_3^-). Moreover, Ca^{2+} was detected with a concentration around 1 µg m^{-3} and NH_4^+ remained between 0.41 µg m^{-3} and 0.92 µg m^{-3} while the concentration of other cations was negligible.

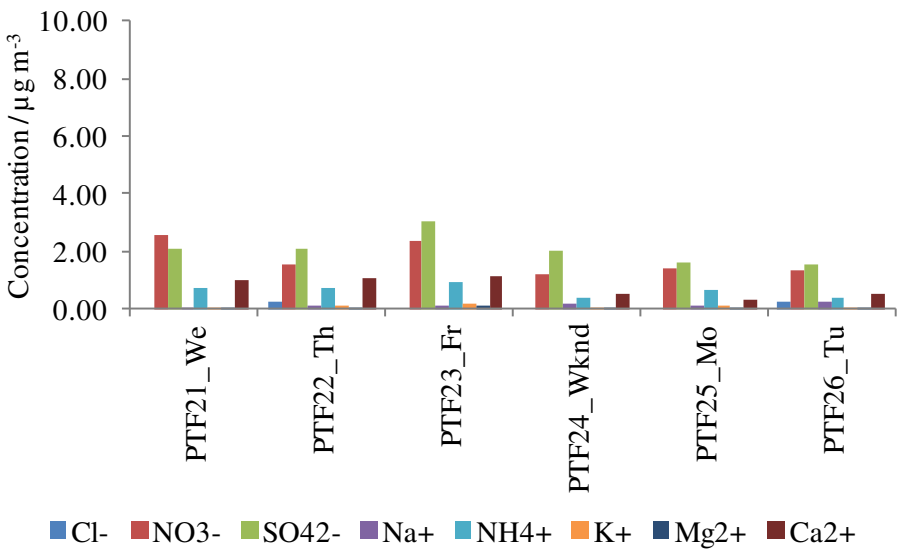

Figure 3.214 Daily atmospheric concentration of water-soluble ions measured in Ferrara during summer 2017 campaign.

Winter 2018 PM monitoring campaign

Ion concentration determined during winter 2018 campaign was below 7.00 µg m^{-3} (Figure 3.215). Specifically, NO_3^- dominated over all detected ions, displaying concentration from 2.52 µg m^{-3} and 6.70 µg m^{-3}. Considering the other anions, sulphate was measured between 0.58 µg m^{-3} and 2.66 µg m^{-3} and sometimes Cl^- concentration slightly overcame that of SO_4^{2-} (i.e. for PTF29, PTF30 and PTF32) reaching a maximum value equal to 1.15 µg m^{-3}.

Among cations, NH_4^+ and Ca^{2+} prevailed over the others with values below 2.00 µg m^{-3}. However, a slightly higher concentration of Na^+ was observed in those days characterised by higher amount of Cl^- (Thursday, Friday and Monday).

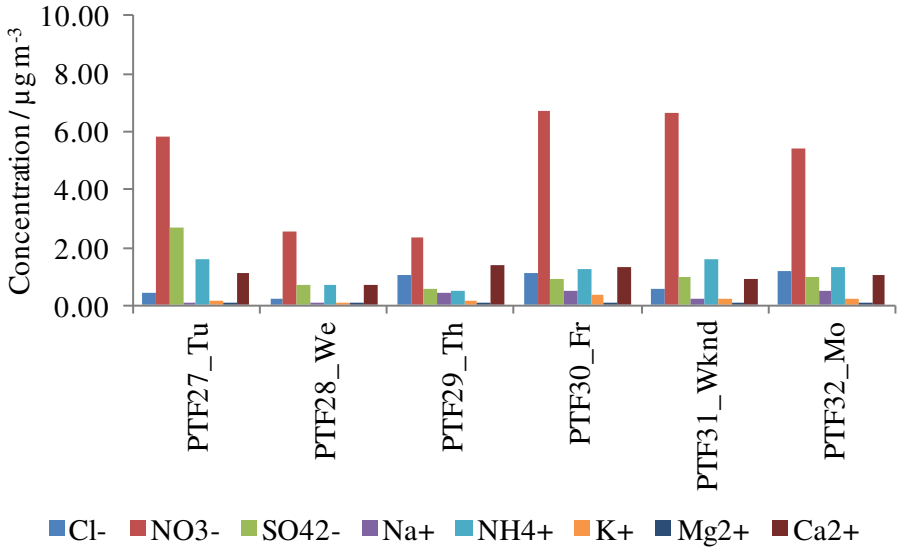

Figure 3.215 Daily atmospheric concentration of water-soluble ions measured in Ferrara during winter 2018 campaign.

Summer 2018 PM monitoring campaign

Concentration of all detected ions remained below 1 µg m^{-3} for all the duration of summer 2018 campaign (Figure 3.216). In general, NO_3^-, SO_4^{2-} and Ca^{2+} were identified in slightly higher amount reaching at most 0.90 µg m^{-3}, 0.58 µg m^{-3} and 0.37 µg m^{-3}, respectively.

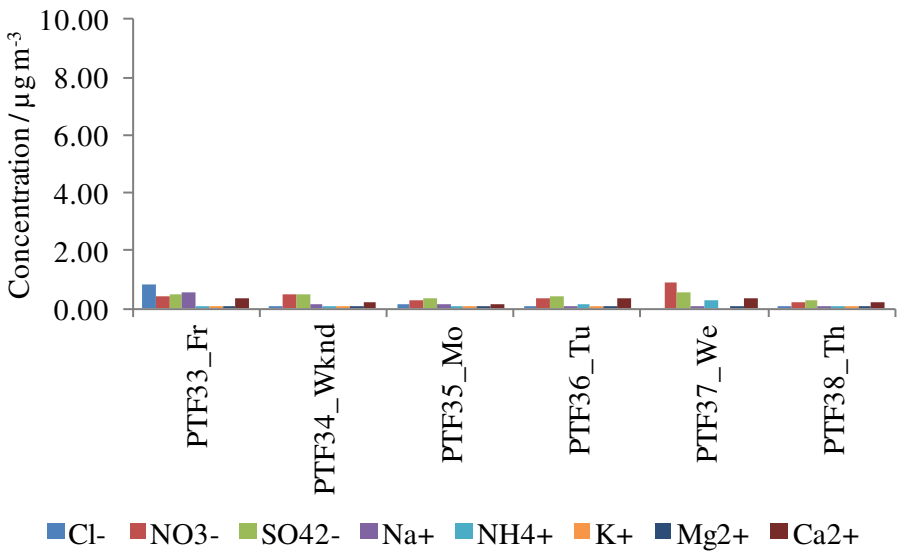

Figure 3.216 Daily atmospheric concentration of water-soluble ions measured in Ferrara during summer 2018 campaign.

Comparison

The comparison of soluble ions detected during different monitoring campaigns in Ferrara displays in general a prevalence of NO_3^- followed by SO_4^{2-} among anions and NH_4^+ and Ca^{2+} among cations (Figure 3.217). In particular, NO_3^- concentration was higher during both winter campaigns with mean values equal to 3.12 ± 2.01 µg m^{-3} in 2017 and 4.91 ± 1.99 µg m^{-3} in 2018. SO_4^{2-} was measured in higher amount during summer 2017 (2.06 ± 0.54 µg m^{-3}) and winter 2018 (1.14 ± 0.77 µg m^{-3}). Furthermore, both NH_4^+ and Ca^{2+} had a similar trend over the considered period with stable mean values in 2017 (around 0.65 ± 0.46 µg m^{-3} and 0.67 ± 0.36 µg m^{-3}, respectively), increased amount in winter 2018 (1.16 ± 0.45 µg m^{-3} and 1.08 ± 0.27 µg m^{-3}, respectively) and drop in summer 2018 (0.15 ± 0.08 µg m^{-3} and 0.28 ± 0.09 µg m^{-3}, respectively).

Finally, both Cl^- and Na^+ were identified with slightly higher concentration during winter campaigns but remaining always below 1.00 µg m^{-3}, suggesting a possible contribution of de-icing salt in winter that was added to sea spray effect.

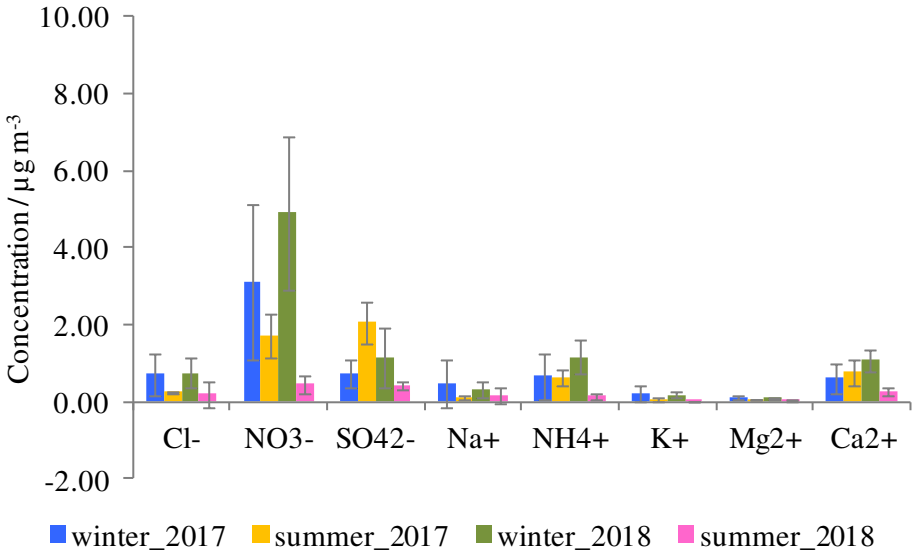

Figure 3.217 Mean atmospheric concentration of water-soluble ions measured in Ferrara during different monitoring campaigns.

FLORENCE

Soluble ions measured in PM monitored in Florence during different monitoring campaigns are displayed in Table A7.3 (Annex 7).

Winter 2017 PM monitoring campaign

Figure 3.218 shows that soluble ions measured in winter 2017 with higher concentration were NO_3^- (from 0.86 µg m^{-3} to 3.15 µg m^{-3}), SO_4^{2-} (from 0.53 µg m^{-3} to 2.21 µg m^{-3}) and Ca^{2+} (from 1.16 µg m^{-3} to 1.53 µg m^{-3}) while the amount of other ions remained below 1.00 µg m^{-3}.

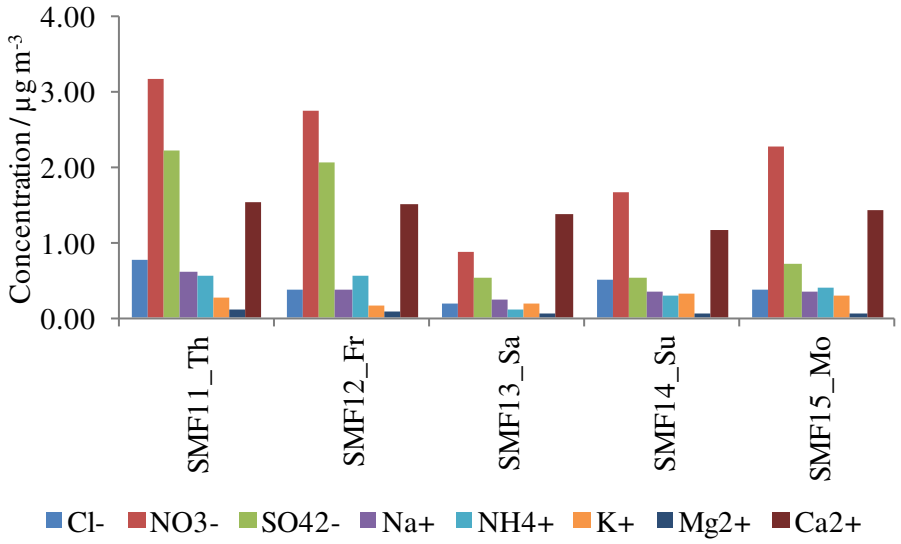

Figure 3.218 Daily atmospheric concentration of water-soluble ions measured in Florence during winter 2017 campaign.

Summer 2017 PM monitoring campaign

Summer 2017 monitoring campaign was characterised in general by the prevalence of SO_4^{2-} (from 0.91 µg m^{-3} to 1.17 µg m^{-3}) and Ca^{2+} (from 0.78 µg m^{-3} to 1.67 µg m^{-3}) over other ions (Figure 3.219). Also NO_3^- was identified but it remained almost always below 1.00 µg m^{-3}. Nevertheless, SMF6 and SMF7 revealed a peculiar ion concentration as rather high amount of Cl^- (1.05 µg m^{-3} and 2.57 µg m^{-3}, respectively) and Na^+ (1.23 µg m^{-3} and 2.30 µg m^{-3}, respectively) was measured. Considering that the prevailing wind direction during summertime in Florence is from south-west, it stands to reason that this higher concentration of Cl^- and Na^+ could originate from sea spray impact.

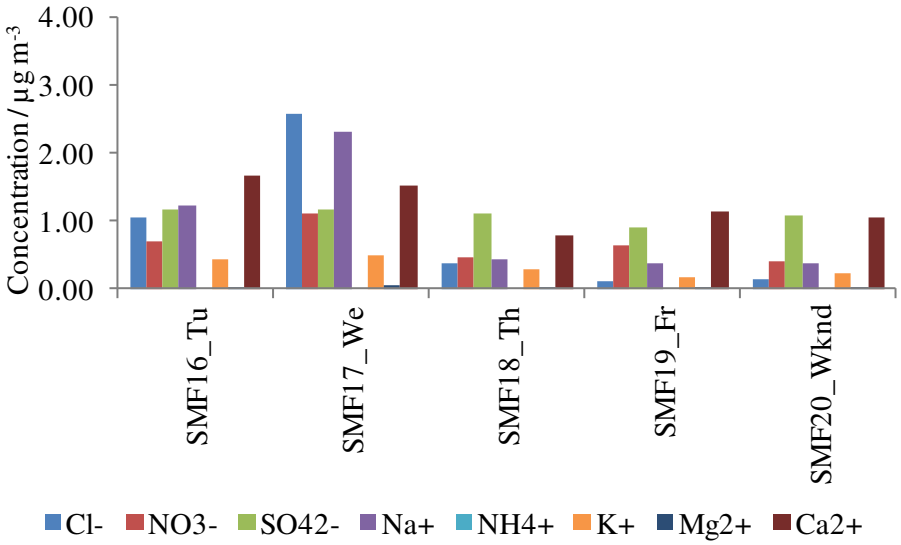

Figure 3.219 Daily atmospheric concentration of water-soluble ions measured in Florence during summer 2017 campaign.

Winter 2018 PM monitoring campaign

Figure 3.220 displays that the concentration of the monitored ions during winter 2018 campaign remained always below 2.00 µg m^{-3} and Ca^{2+} was the prevalent ion (from 0.14 µg m^{-3} to 1.91 µg m^{-3}).

Among anions, NO_3^- (from 0.16 µg m^{-3} to 1.37 µg m^{-3}) prevailed followed by SO_4^{2-} (from 0.06 µg m^{-3} to 0.38 µg m^{-3}) and Cl^- (from 0.05 µg m^{-3} to 0.63 µg m^{-3}).

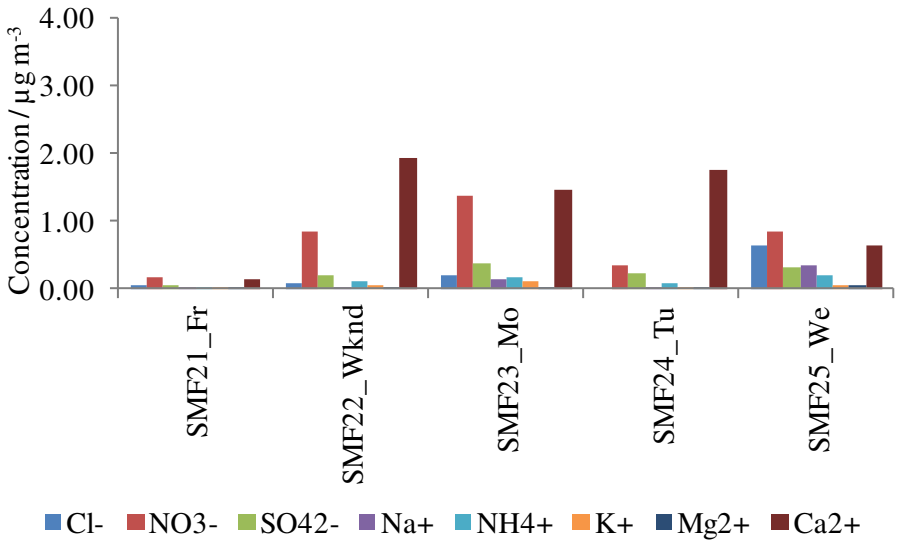

Figure 3.220 Daily atmospheric concentration of water-soluble ions measured in Florence during winter 2018 campaign.

Summer 2018 PM monitoring campaign

In general, ion concentration never exceeded 1.03 µg m^{-3}, reached by Ca^{2+} in SMF26 (Figure 3.221). Among anions, the concentration of SO_4^{2-} (from 0.59 µg m^{-3} to 0.99 µg m^{-3}) was generally double or at least three times (SMF28) higher than that of NO_3^- (from 0.25 µg m^{-3} to 0.33 µg m^{-3}) while Cl^- was negligible. Moreover, Ca^{2+} (from 0.54 µg m^{-3} to 1.03 µg m^{-3}) and NH_4^+ (from 0.17 µg m^{-3} to 0.26 µg m^{-3}), which prevailed among detected cations, remained almost stable during the monitored period.

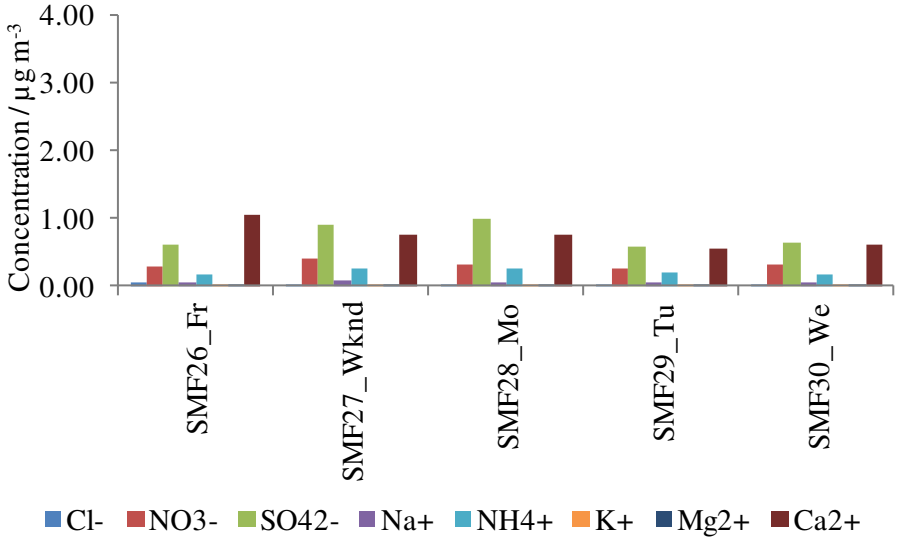

Figure 3.221 Daily atmospheric concentration of water-soluble ions measured in Florence during summer 2018 campaign.

Comparison

The comparison of mean anion concentration monitored during different campaigns in Florence highlights a general prevalence of NO_3^- during wintertime (2.14 ± 0.90 µg m^{-3} in 2017 and 0.71 ± 0.48 µg m^{-3} in 2018) and of SO_4^{2-} in summertime (1.08 ± 0.10 µg m^{-3} in 2017 and 0.74 ± 0.19 µg m^{-3} in 2018) (Figure 3.222). Among cations was detected in higher amount in all analysed period with a decreasing trend over time (from

0.74 ± 0.19 µg m^{-3} to 1.40 ± 0.15 µg m^{-3}). Furthermore, mean concentration of each ion resulted higher during winter 2017 campaign, with exception of Cl^-, Na^+ and K^+ that reached higher amount in summer 2017 (0.85 ± 1.04 µg m^{-3}, 0.94 ± 0.84 µg m^{-3} and 0.32 ± 0.14 µg m^{-3}, respectively) likely due to sea spray contribution. However, no ions exceeded the mean value of 2.14 µg m^{-3}, reached by NO_3^- in winter 2017.

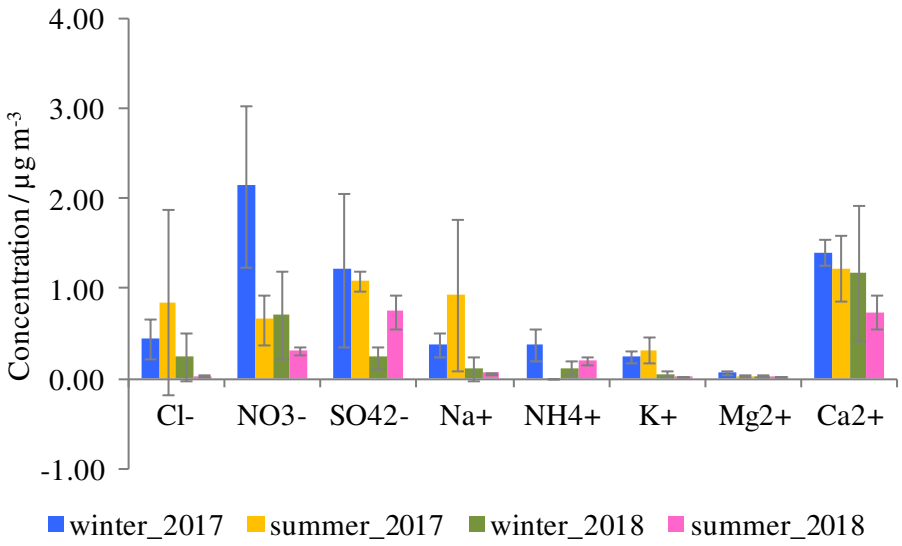

Figure 3.222 Mean atmospheric concentration of water-soluble ions measured in Ferrara during different monitoring campaigns.

GENERAL COMPARISON

The comparison of mean soluble ions detected in all sites during different monitoring campaigns highlights high concentration of NO_3^- during both winter campaigns mainly in Bologna and Ferrara while a notable decrease (till 18 times in Bologna in 2018) was measured during summer campaigns (Figure 3.223). Considering the other anions, SO_4^{2-} showed slight variations among sites during different monitoring campaigns, with a general lightly higher values during 2017 than 2018, and Cl^- remained generally constant (lower than 1 µg m^{-3}) during different periods in all sites.
Among cations, each site displayed a mean concentration of atmospheric Ca^{2+} rather stable during time, with higher values detected in Florence (Figure 3.223). NH_4^+ was rather abundant in Bologna and Ferrara during winter monitoring campaigns while it decreased during summer, showing a trend very similar to that of NO_3^-. Mean amount of Na^+ remained always below 1 µg m^{-3} and showed a trend similar to that of chloride in each site. Finally, constant values over time and in different sites were measured for K^+ and Mg^{2+}.

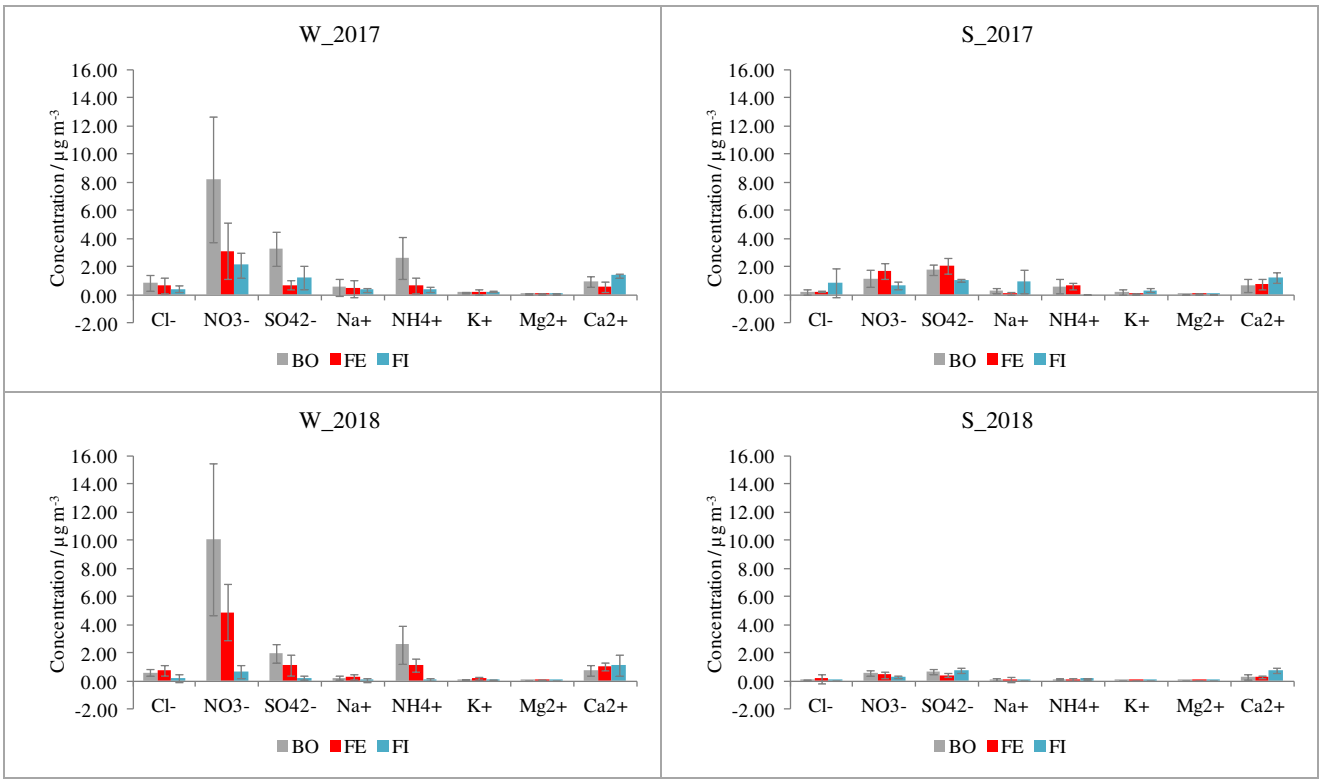

Figure 3.223 Mean atmospheric concentration of water-soluble ions measured in Bologna (grey), Ferrara (red) and Florence (light blue) during winter (W) and summer (S) 2017 and 2018 monitoring campaigns.

In this context, statistical elaboration by Pearson correlation of soluble ions detected in different sites during each monitoring campaign confirms a strong linear relationship among NO_3^-, SO_4^{2-} and NH_4^+ with exception of summer 2018 monitoring campaign (Table 3.66-3.69). Sulphate, nitrate and ammonium are indicative of traffic emissions and are generally present in atmosphere as ammonium sulphate or ammonium nitrate deriving from the neutralisation of sulphuric and nitric acids by ammonia. It is generally asserted that in warm period ammonia is almost exclusively dedicated to the production of ammonium sulphate as ammonium nitrate is inhibited by high temperature (Ricciardelli et al., 2017). Results show indeed a higher correlation coefficients between SO_4^{2-} and NH_4^+ during summer campaigns while between NO_3^- and NH_4^+ during cold periods. Moreover, a positive linear correlation was also evaluated between Cl^-, Na^+, Mg^{2+} and sometimes also K^+ as they can derive from sea spray.

W_2017	**Cl^-**	**NO_3^-**	**SO_4^{2-}**	**Na^+**	**NH_4^+**	**K^+**	**Mg^{2+}**	**Ca^{2+}**
Cl^-	**1.00**	0.25	0.35	0.38	0.23	0.28	**0.82**	0.32
NO_3^-		**1.00**	**0.79**	-0.05	**0.98**	-0.04	-0.03	-0.14
SO_4^{2-}			**1.00**	0.04	**0.84**	0.03	0.11	0.12
Na^+				**1.00**	-0.14	0.61	0.34	0.08
NH_4^+					**1.00**	-0.05	-0.07	-0.17
K^+						**1.00**	0.33	0.11
Mg^{2+}							**1.00**	0.37
Ca^{2+}								**1.00**

Table 3.66 Pearson correlation among values measured in all sites during winter 2017 campaign.

S_2017	Cl^-	NO_3^-	SO_4^{2-}	Na^+	NH_4^+	K^+	Mg^{2+}	Ca^{2+}
Cl^-	**1.00**	0.05	-0.30	**0.97**	-1.00	0.68	0.39	0.53
NO_3^-		**1.00**	**0.80**	-0.31	**0.86**	-0.37	0.47	-0.07
SO_4^{2-}			**1.00**	-0.42	**0.78**	-0.30	0.39	-0.11
Na^+				**1.00**	-0.83	**0.82**	-0.16	0.62
NH_4^+					**1.00**	**0.89**	-0.22	0.53
K^+						**1.00**	-0.53	**0.73**
Mg^{2+}							**1.00**	-0.18
Ca^{2+}								**1.00**

Table 3.67 Pearson correlation among values measured in all sites during summer 2017 campaign.

W_2018	Cl^-	NO_3^-	SO_4^{2-}	Na^+	NH_4^+	K^+	Mg^{2+}	Ca^{2+}
Cl^-	**1.00**	0.52	0.37	**0.95**	0.46	**0.71**	**0.79**	0.15
NO_3^-		**1.00**	**0.87**	0.48	**0.98**	0.51	0.38	-0.17
SO_4^{2-}			**1.00**	0.25	**0.90**	0.41	0.35	-0.20
Na^+				**1.00**	0.40	**0.72**	**0.77**	0.06
NH_4^+					**1.00**	0.44	0.32	-0.22
K^+						**1.00**	**0.84**	0.11
Mg^{2+}							**1.00**	0.29
Ca^{2+}								**1.00**

Table 3.68 Pearson correlation among values measured in all sites during winter 2018 campaign.

S_2018	Cl^-	NO_3^-	SO_4^{2-}	Na^+	NH_4^+	K^+	Mg^{2+}	Ca^{2+}
Cl^-	**1.00**	-0.06	-0.27	**0.95**	-0.50	-0.05	**0.92**	-0.21
NO_3^-		**1.00**	0.24	0.01	0.40	0.13	0.11	-0.22
SO_4^{2-}			**1.00**	-0.23	**0.72**	0.47	-0.09	0.52
Na^+				**1.00**	-0.56	0.05	**0.88**	-0.33
NH_4^+					**1.00**	0.34	-0.31	0.47
K^+						**1.00**	0.11	-0.06
Mg^{2+}							**1.00**	-0.16
Ca^{2+}								**1.00**

Table 3.69 Pearson correlation among values measured in all sites during summer 2018 campaign.

Final remarks:

- The concentration of water-soluble ions was in general higher during winter monitoring campaigns than that detected in summertime, never exceeding the mean value of 11.00 µg m^3.
- NO_3^-, SO_4^{2-} and NH_4^+, likely due to emission from traffic, prevailed in all sites.
- Noticeable seasonal variation of NO_3^-, more abundant in wintertime.
- Mean concentration of Ca^{2+} remained rather stable during time in all sites.
- The measured Cl^- and Na^+ suggest a possible contribution of de-icing salt in winter that is added to sea spray origin.
- Also the height of planetary boundary layer (PBL), lower during winter and higher in the warm season due to thermal expansion of atmospheric gases, as well as the meteorological conditions may have influenced the amount of detected ions.

3.3.4. CARBON SPECIATION

BOLOGNA

Winter 2017 PM monitoring campaign

Observing carbon fractions, OC was always more abundant than EC (Figure 3.224). In particular, OC was detected between 3.64 µg m^{-3} and 6.09 µg m^{-3}, with higher concentration during Saturday. On the contrary, the analysed amount of EC was lower and more constant over time (mean value around 0.57 µg m^{-3}). Therefore, OC/EC resulted lower for BF11 (equal to 5) while it reached the highest value during Saturday (equal to 13).

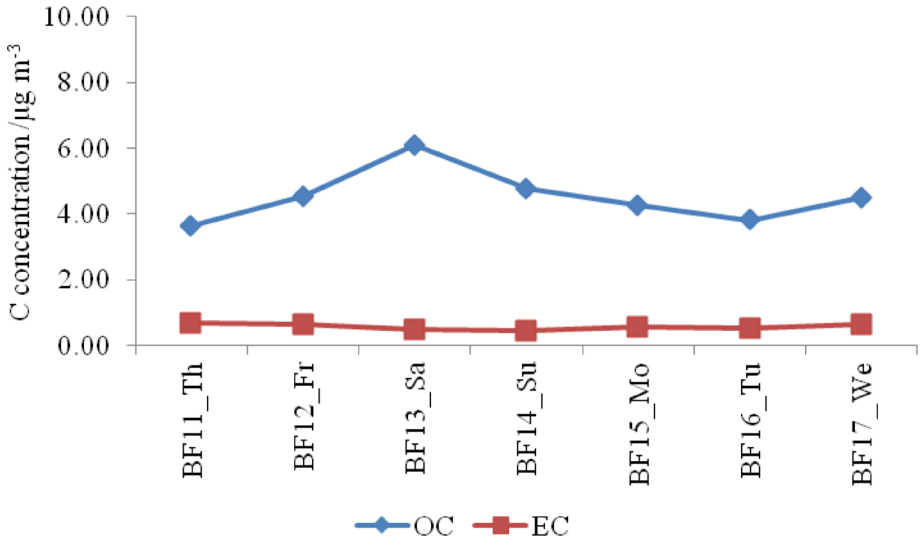

Figure 3.224 Daily atmospheric concentration of OC (blue rhombuses) and EC (red squares) measured in Bologna during winter 2017 campaign.

Summer 2017 PM monitoring campaign

Carbon fractions measured in summer 2017 campaign had a decreasing trend during the analysed period, more evident for OC (Figure 3.225). In particular, OC passed from 4.08 µg m^{-3} on Tuesday to 1.93 µg m^{-3} during the weekend while EC concentration was more stable over the period even if it underwent a slight reduction (from 0.31 µg m^{-3} at the beginning of the campaign till to 0.19 µg m^{-3} of the last day). OC/EC ratio remained always between 8 and 13.

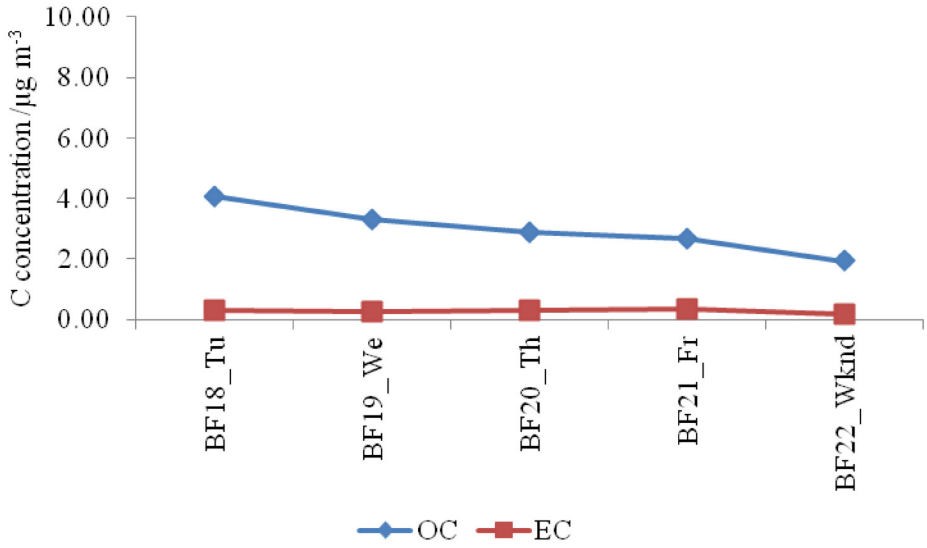

Figure 3.225 Daily atmospheric concentration of OC (blue rhombuses) and EC (red squares) measured in Bologna during summer 2017 campaign.

Winter 2018 PM monitoring campaign

PM monitoring highlighted the prevalence of OC over EC during the considered period. OC ranged from 3.77 µg m^{-3} and 8.14 µg m^{-3} while EC from 0.66 µg m^{-3} and 1.27 µg m^{-3} (Figure 3.226). The highest value of OC was measured on Friday while that of EC on Thursday while both displayed the lowest data on Tuesday. As a consequence, OC/EC ratio changed from 8 detected on Friday to 6 Tuesday.

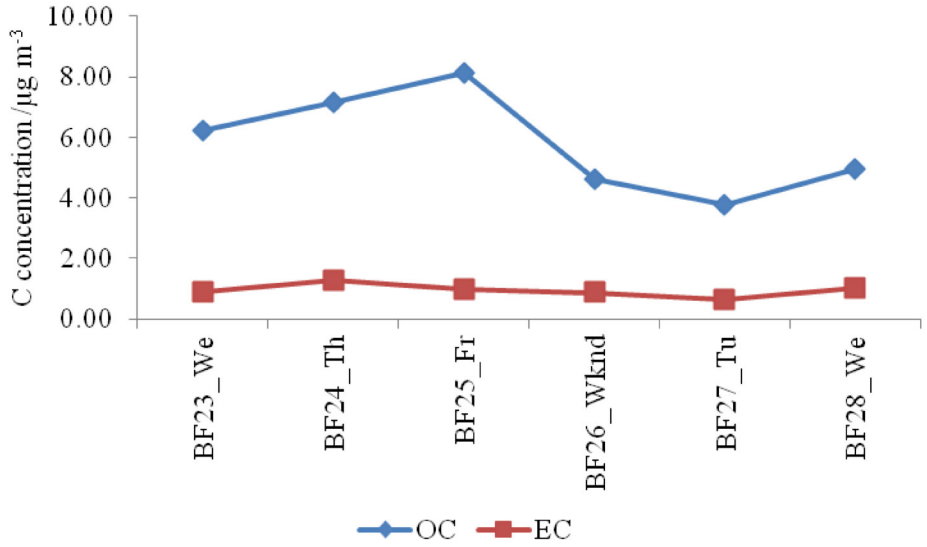

Figure 3.226 Daily atmospheric concentration of OC (blue rhombuses) and EC (red squares) measured in Bologna during winter 2018 campaign.

Summer 2018 PM monitoring campaign

OC amount monitored during this summer campaign was slightly higher that related to EC, with values between 1.46 µg m^{-3} and 3.66 µg m^{-3} for OC and between 0.17 µg m^{-3} and 0.63 µg m^{-3} for EC (Figure 3.227). Moreover, both carbon fractions showed a similar amount trend, more stable during the first 3 days and last 2 ones of monitoring but with an increase on Monday.

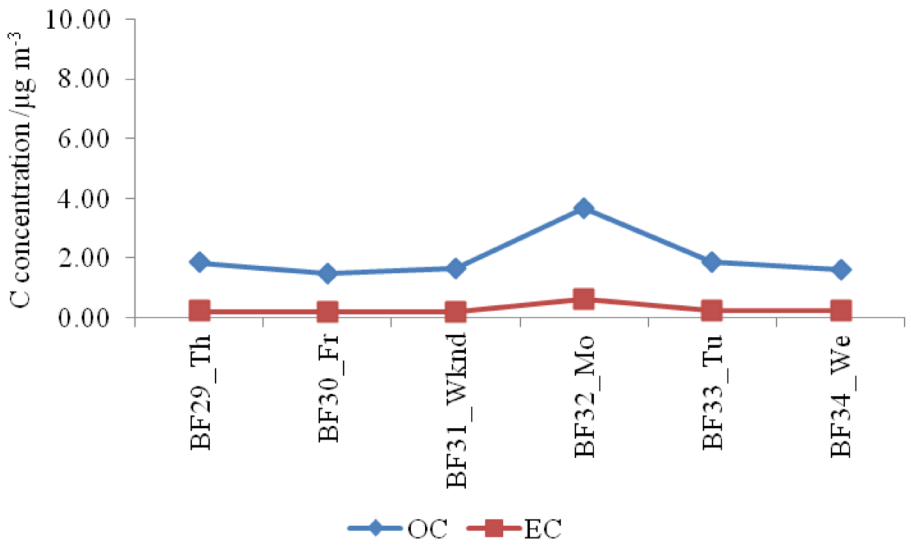

Figure 3.227 Daily atmospheric concentration of OC (blue rhombuses) and EC (red squares) measured in Bologna during summer 2018 campaign.

Comparison

The comparison of carbon fractions during all monitoring campaigns performed in Bologna during 2017 and 2018 shows that OC concentration always prevailed over EC amount (Figure 3.228). In particular, EC had a more constant trend in each monitored period, displaying slightly higher values during both winter monitoring campaigns. In general terms, a growth in concentration was reported also for OC during cold season in 2017 and 2018 but it underwent more variations during the same monitoring campaign. Furthermore, good affinity can be observed among carbon fractions and total suspended particulate (TSP), mainly for monitoring campaigns carried out in 2018 (Figure 3.228).

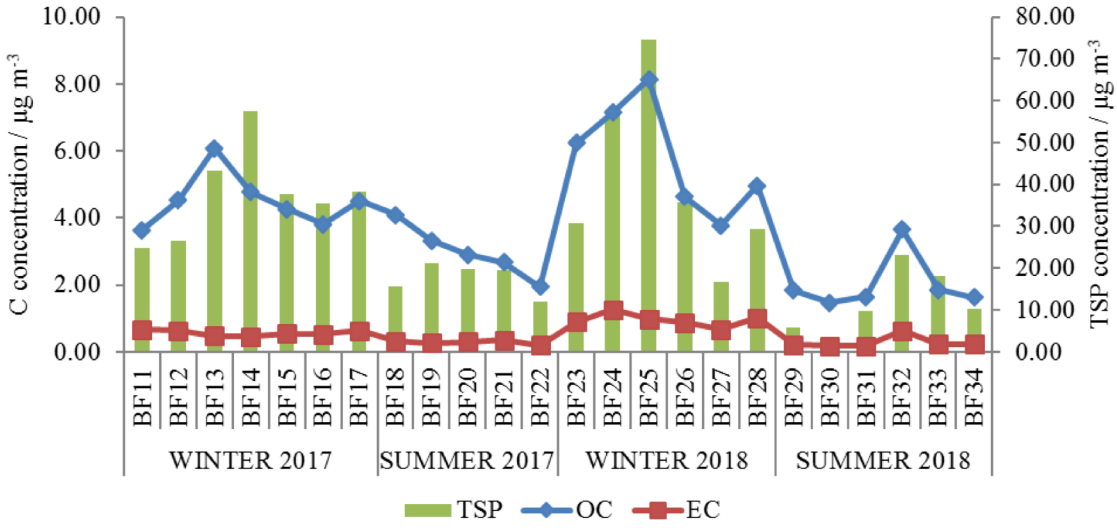

Figure 3.228 Daily atmospheric concentration of OC (blue rhombuses), EC (red squares) and TSP (green bars) measured in Bologna during PM monitoring campaigns in winter and summer 2017 and 2018.

FERRARA

Winter 2017 PM monitoring campaign

Carbon fractions measured in winter 2017 were generally low, with higher amount of OC (from 1.32 µg m^{-3} to 4.29 µg m^{-3}) respect to EC (more stable and ranging between 0.21 µg m^{-3} and 0.64 µg m^{-3}) (Figure 3.229). In particular, a slight increase of both carbon fractions was detected during the beginning of the week (see PTF14, PTF19 and PTF20) while lower values during the weekend (PTF17 and PTF18). In this regard, PM monitoring during the weekend, performed both on the roof terrace of Palazzo Turchi di Bagno (PTF17) and at the ground floor in the Botanic Garden (PTF18), showed similar values but with a slightly higher concentration of carbon fractions at the ground floor (i.e. 1.32 µg m^{-3} vs. 1.50 µg m^{-3} of OC and 0.21 µg m^{-3} vs. 0.28 µg m^{-3} of EC, respectively at the roof terrace and the ground floor). OC/EC ratio ranged between 4 of PTF13 and 12 of PTF20.

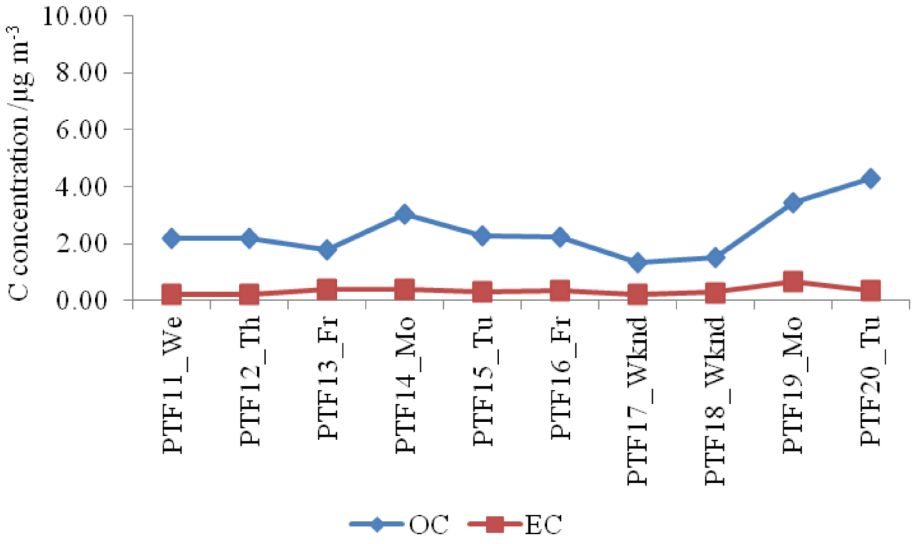

Figure 3.229 Daily atmospheric concentration of OC (blue rhombuses) and EC (red squares) measured in Ferrara during winter 2017 campaign. Filters PTF11, PTF12, PTF13, PTF14, PTF15 and PTF17 refer to PM monitoring at the roof terrace of Palazzo Turchi di Bagno while PTF16, PTF18, PTF19 and PTF20 to the ground floor in the Botanic Garden.

Summer 2017 PM monitoring campaign

Figure 3.230 displays in general a decreasing trend of OC amount over the analysed period, changing from 5.45 µg m^{-3} on Thursday to 2.42 µg m^{-3} of Tuesday. EC, always lesser than OC, had a concentration more constant over the analysed period with values between 0.80 µg m^{-3} on Friday and 0.41 µg m^{-3} on Monday and Tuesday. Moreover, OC/EC ratio ranged between 8 of PTF22 and 6 of PTF23, PTF24, PTF25, PTF26.

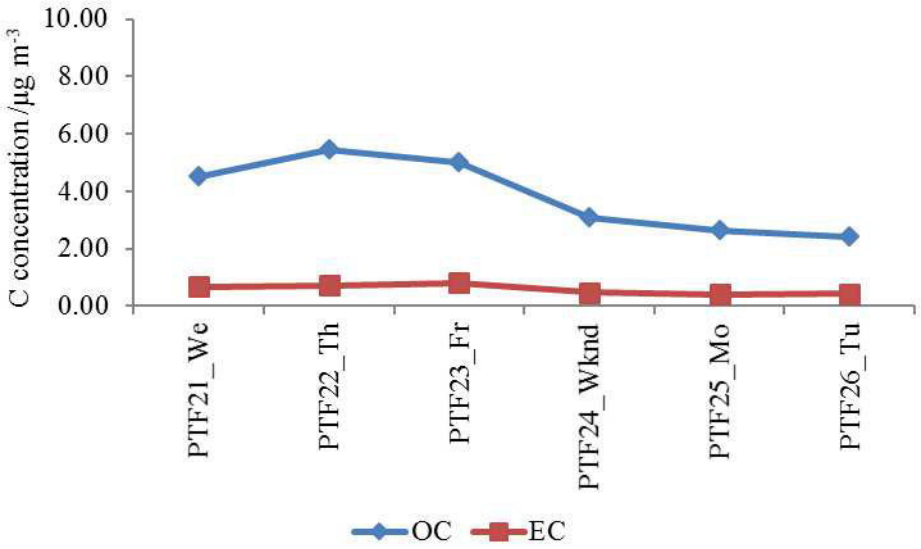

Figure 3.230 Daily atmospheric concentration of OC (blue rhombuses) and EC (red squares) measured in Ferrara during summer 2017 campaign.

Winter 2018 PM monitoring campaign

During winter 2018 campaign, OC prevailed over EC with a OC/EC ratio ranging from 4 on Thursday to 6 during Tuesday, Friday and weekend. In particular, OC concentration was higher during Friday (8.18 µg m^{-3}) and lower on Wednesday (3.17 µg m^{-3}) while EC underwent a general slight growth over the period, with values between 0.68 µg m^{-3} on Wednesday and 1.49 µg m^{-3} on Thursday (Figure 3.231).

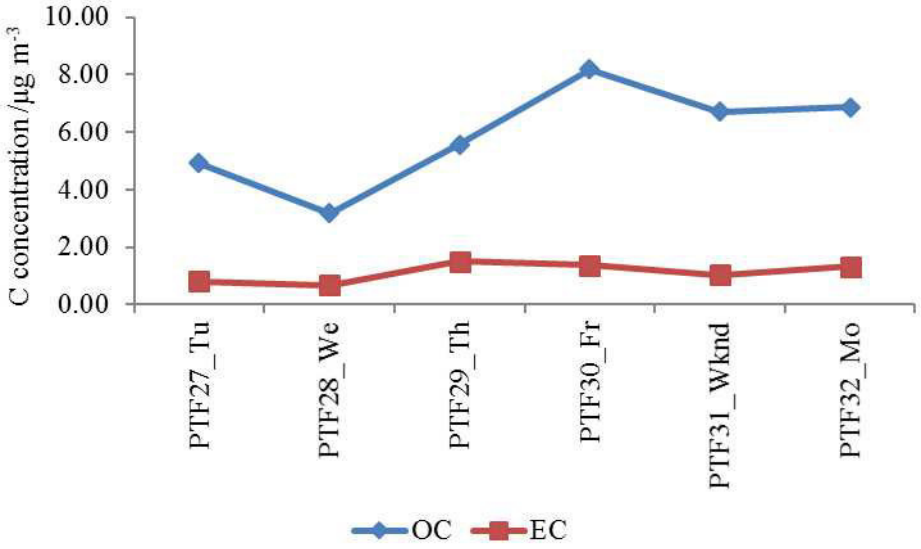

Figure 3.231 Daily atmospheric concentration of OC (blue rhombuses) and EC (red squares) measured in Ferrara during winter 2018 campaign.

Summer 2018 PM monitoring campaign

The amount of carbon fractions detected during this period is in general low. OC ranged indeed from 1.22 µg m^{-3} on Monday to 2.94 µg m^{-3} on Wednesday while EC was between 0.16 µg m^{-3} on Friday and 0.51 µg m^{-3} on Wednesday (Figure 3.232). Moreover, observing the trend of concentration, both fractions underwent an overall increase over time with exception of OC on Monday that experienced a slight decrease. OC/EC ratio was higher at the beginning of the monitoring (equal to 12) and decreased over time till to 5.

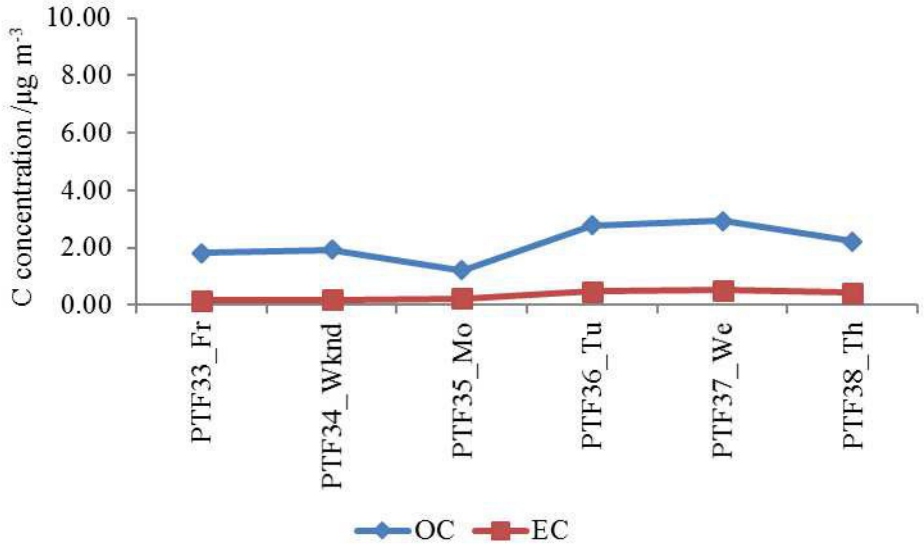

Figure 3.232 Daily atmospheric concentration of OC (blue rhombuses) and EC (red squares) measured in Ferrara during summer 2018 campaign.

Comparison

The comparison of the amount of carbon fractions acquired during the different monitoring campaigns highlights the prevalence of OC over EC throughout the considered period (Figure 3.233). In particular, carbon fractions were generally higher during summer 2017 and winter 2018 campaigns, when also total particulate matter was detected with higher concentration (Figure 3.233). Overall, OC ranged from 1.22 µg m^{-3} of PTF35 and 8.18 µg m^{-3} of PTF30 while EC from 0.16 µg m^{-3} of PTF33 and 1.49 µg m^{-3} of PTF29.

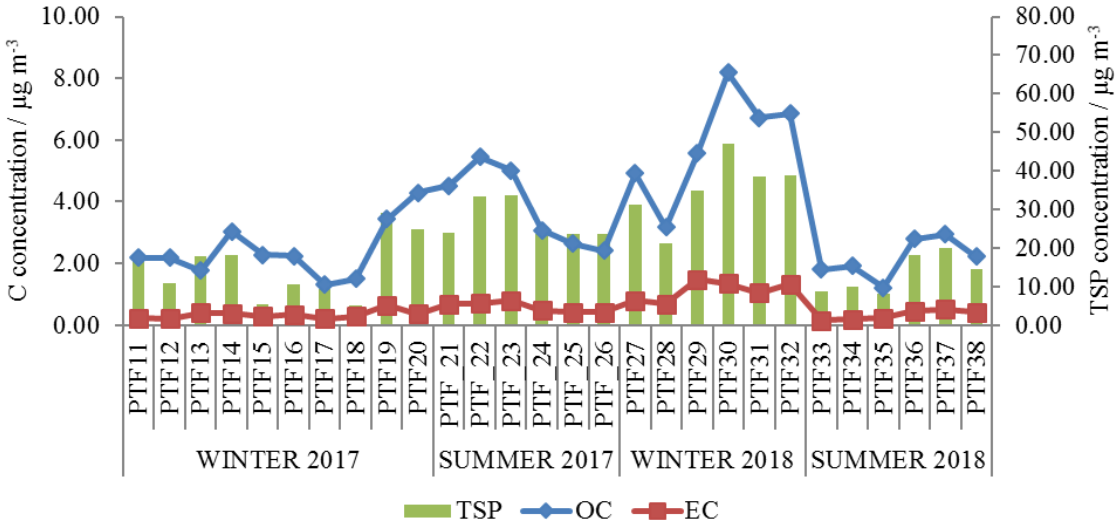

Figure 3.233 Daily atmospheric concentration of OC (blue rhombuses), EC (red squares) and TSP (green bars) measured in Ferrara during PM monitoring campaigns in winter and summer 2017 and 2018.

FLORENCE

Winter 2017 PM monitoring campaign

Figure 3.234 shows a predominance of OC over EC. In particular, OC ranged from 3.39 µg m^{-3} of SMF12 and 6.23 µg m^{-3} of SMF15 while EC was more constant (between 0.17 µg m^{-3} of SMF13 and 1.03 µg m^{-3} SMF11). OC/EC ratio was between 4 (SMF12) and 8 (SMF13).

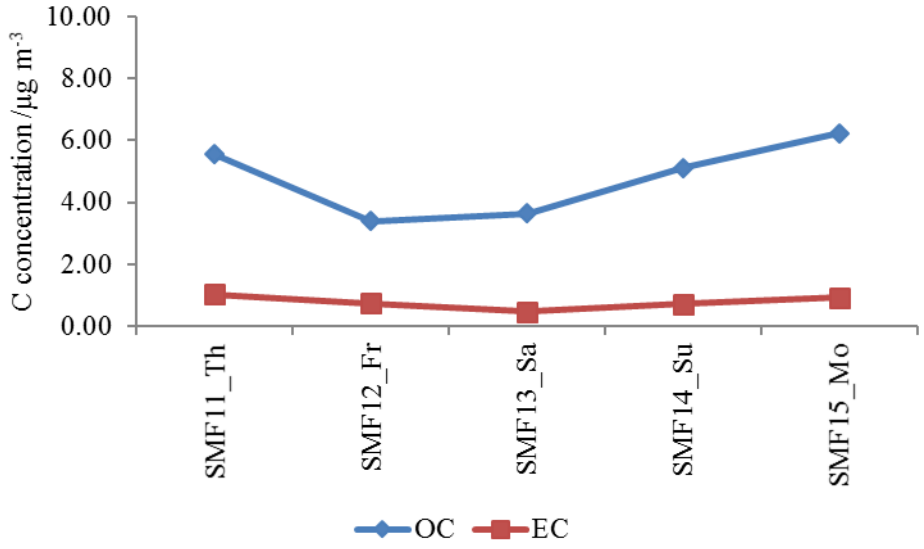

Figure 3.234 Daily atmospheric concentration of OC (blue rhombuses) and EC (red squares) measured in Florence during winter 2017 campaign.

Summer 2017 PM monitoring campaign

OC was always present with higher concentration than EC and each carbon fraction was rather constant throughout the analysed period (Figure 3.235). In particular, OC ranged from 2.76 µg m^{-3} of SMF18 to 3.77 µg m^{-3} of SMF19 while EC from 0.40 µg m^{-3} of SMF18 to 0.69 µg m^{-3} SMF19. Therefore, a slightly higher concentration of carbon fraction was detected on Friday. Finally, OC/EC ratio was between 4 (SMF17) and 7 (SMF20).

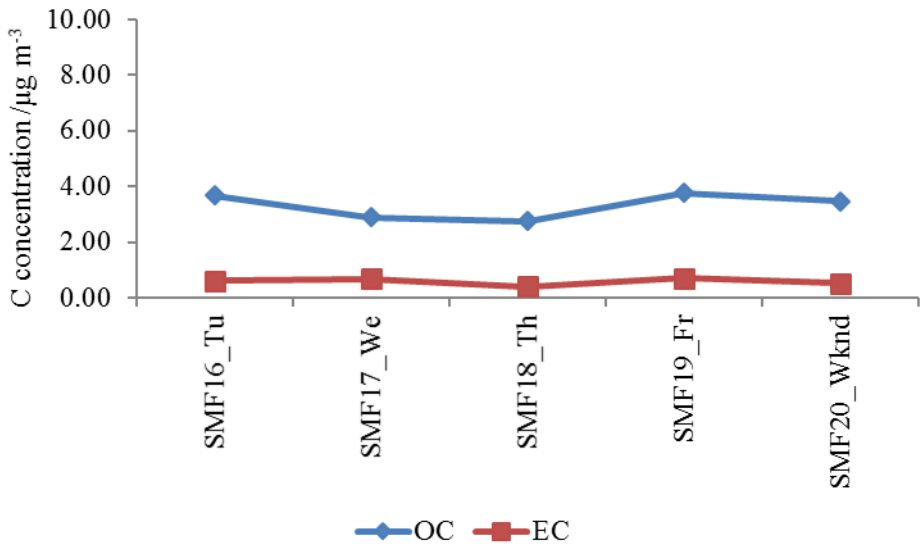

Figure 3.235 Daily atmospheric concentration of OC (blue rhombuses) and EC (red squares) measured in Florence during summer 2017 campaign.

Winter 2018 PM monitoring campaign

Figure 3.236 shows the prevalence of OC over EC during the considered period. In particular, OC, which ranged between 1.01 µg m^{-3} and 4.07 µg m^{-3}, was higher during the weekend and the beginning of the week (3.81 µg m^{-3} and 4.07 µg m^{-3}, respectively) while EC, in general between 0.26 µg m^{-3} and 0.88 µg m^{-3}, showed a slightly higher concentration on Wednesday. OC/EC ratio remained between 3 (SMF25) and 6 (SMF22).

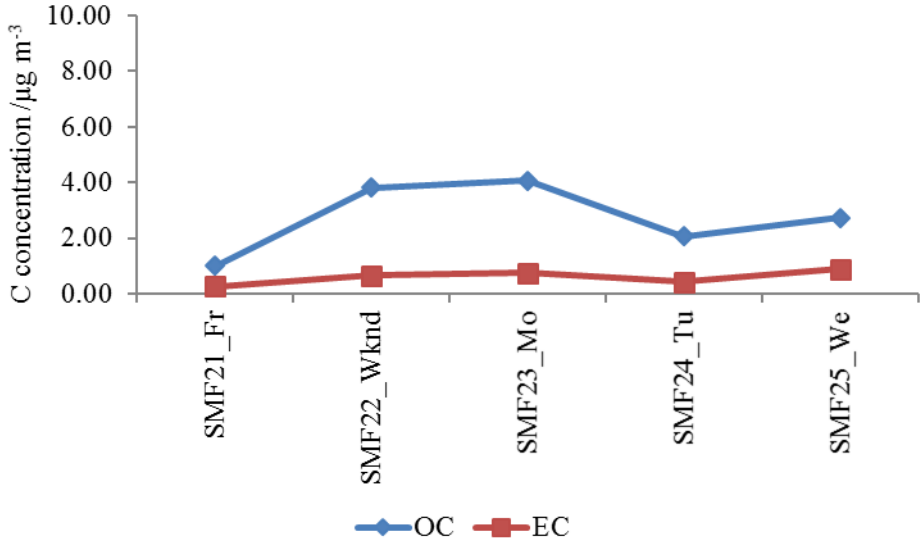

Figure 3.236 Daily atmospheric concentration of OC (blue rhombuses) and EC (red squares) measured in Florence during winter 2018 campaign.

Summer 2018 PM monitoring campaign

OC amount monitored during this campaign was higher that related to EC, with values between 2.87 µg m^{-3} (SMF30) and 4.15 µg m^{-3} (SMF28) for OC and between 0.59 µg m^{-3} (SMF27) and 0.95 µg m^{-3} (SMF28) for

EC (Figure 3.237). For both carbon fractions, the highest value was measured on Monday. Moreover, OC/EC ratio was between 4 of (SMF28 and SMF29) and 6 (SMF27).

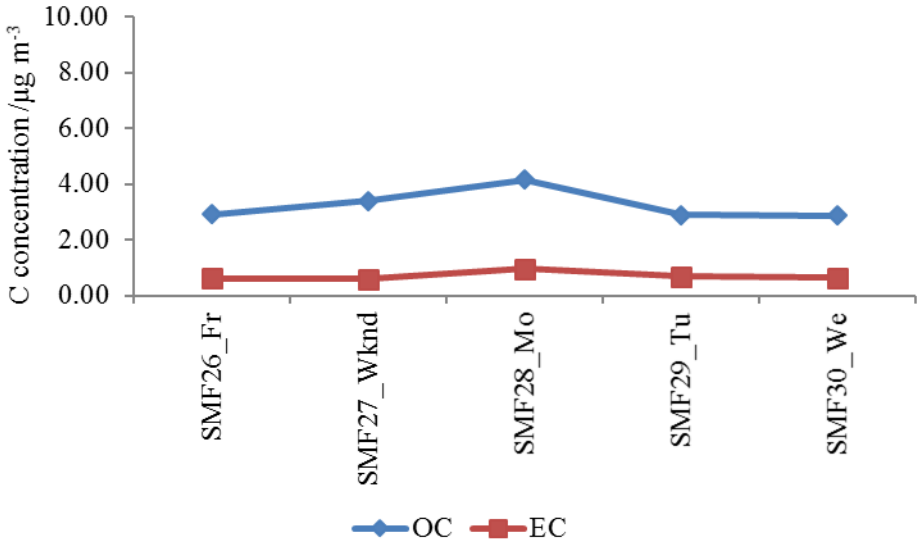

Figure 3.237 Daily atmospheric concentration of OC (blue rhombuses) and EC (red squares) measured in Florence during summer 2018 campaign.

Comparison

The comparison of carbon fractions measured during all monitoring campaigns in Florence displays a general higher amount of OC over EC (Figure 3.238). In particular, EC did not undergo considerable variations over time with an average value of 0.66 µg m^{-3} while OC ranged from 1.01 µg m^{-3} and 6.23 µg m^{-3}. Moreover, OC concentration underwent higher changes during the winter campaigns while it remained more stable during summer overall. Finally, good affinity can be detected among carbon fractions and total suspended particulate (TSP), mainly for OC fraction (Figure 3.238).

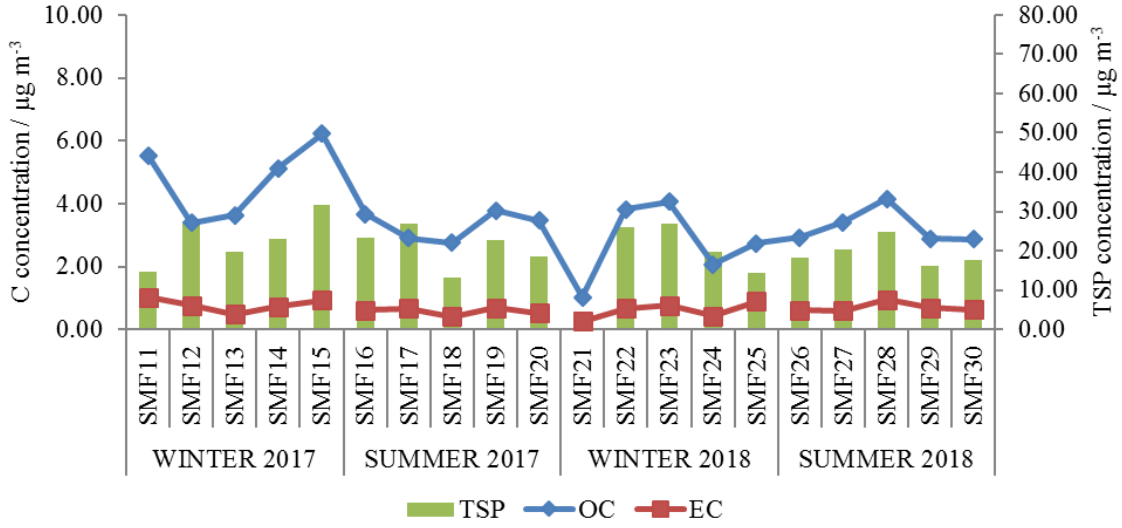

Figure 3.238 Daily atmospheric concentration of OC (blue rhombuses), EC (red squares) and TSP (green bars) measured in Florence during PM monitoring campaigns in winter and summer 2017 and 2018.

GENERAL COMPARISON

Comparing the mean values of carbon fractions amount measured in each site during different monitoring campaigns it is evident that the organic portion is always more abundant than the elemental one. This is clearly appreciable in Figure 3.239 that compare the average percentage values of each carbon fraction over TC (where TC represents the sum of OC and EC). In particular, the concentration of OC never decreased lower than 81 % while EC ranged always between 9 % and 19 %. In general, there were no big differences of OC/TC and EC/TC among the different monitoring campaigns. However, OC/TC resulted with higher value in Bologna followed by Ferrara and Florence during each period of campaign and thus Florence always experienced a higher concentration of EC/TC respect to the other investigated sites.

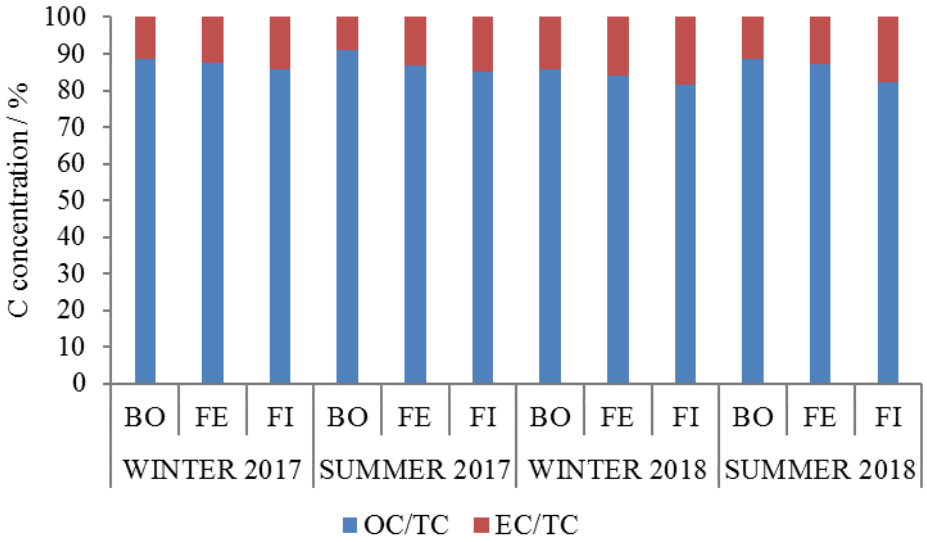

Figure 3.239 Mean values of OC/TC (blue) and EC/TC (red) calculated in each site during different monitoring campaigns. TC refers to the sum of OC and EC.

Nevertheless, the amount of each carbon fraction measured per volume of monitored air did not display a so clear and recurring trend. As shown in Figure 3.240, mean OC concentration of each site was higher during the winter campaigns but this is true in Bologna and Florence for 2017 and in Bologna and Ferrara for 2018. The monitored mean amount of OC in different sites ranged between 2.01 ± 0.82 µg m^{-3} measured in Bologna during summer 2018 and 5.90 ± 1.75 µg m^{-3} measured in Ferrara during winter 2018 while mean values of EC were between 0.28 ± 0.06 µg m^{-3} monitored in Bologna during summer 2017 and 1.12 ± 0.33 µg m^{-3} measured in Ferrara in winter 2018 (Figure 3.240).

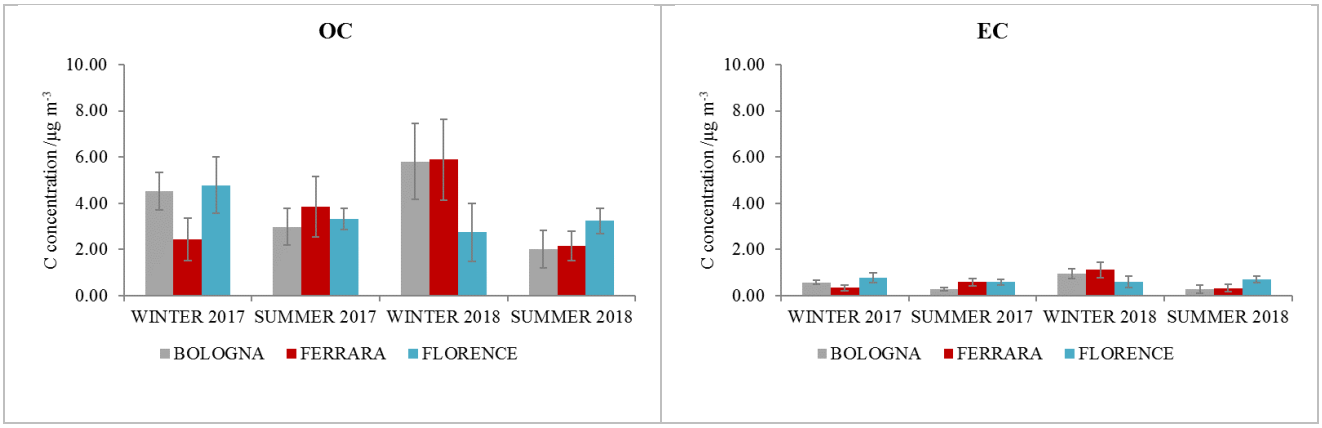

Figure 3.240 Mean concentrations of OC and EC measured in Bologna (grey), Ferrara (red) and Florence (light blue) during winter and summer 2017 and 2018.

Final remarks:

- OC was always more abundant than EC in all sites. In general, TC (equals to OC + EC) was constituted by more than 81% of OC and at most 19% of EC.
- Considering the ratio of each carbon fraction over TC, Florence always experienced the highest concentration of EC/TC while Bologna the highest amount of OC/TC, suggesting a higher contribution of fuel combustion and a combination of anthropogenic and biological emissions, respectively.

3.3.5. BIOAEROSOL

Atmospheric aerosol is a complex and dynamic mixture of solid and liquid particles that beside inorganic and organic components is made up also of biological component, called *bioaerosol*. This last consists of phatogenic or non-phatogenic, live or dead, entire or broken bacteria, fungi, algae, viruses, pollen, plant fibres, high molecular weight allergens, bacterial endotoxins, mycotoxins, peptidoglycans or glucans, etc., passively carried by air (thus insects are not included) (Douwes et al., 2003). Bioaerosol, also known as *primary biological aerosol particles* (PBAPs), has different size and morphology and could be appreciated with a magnifying glass or microscope. It can range from 0.05 µm till to 100 µm: for instance viruses (0.05-0.15 µm), bacteria (0.1-4 µm), fungal spores (0.5-15 µm), algae (<10 µm) and pollen (10-100 µm) (Bonazza et al., 2017). Often biological particles could be aggregated each other or incorporated in non-biological suspended solid particle or in liquids. This last case fosters atmospheric oxidation and gas-to-particle conversion of volatile organic compounds released from biological organisms, leading to the formation of the so-called *secondary biological aerosol particles* (SBAPs) (Després et al., 2012). A typical example of SBAPs happens when microorganisms are included into fog droplets and here could quickly grow. These particles make a substantial contribution mainly to sub-micron aerosol mass and thus it does not influence much PM_{10} amount (Fuzzi et al., 2015).

The concentration of bioaerosol changes with season and site. Dry periods determines a low hydration of the cells, making them lighter and promoting their dispersion, whereas dump conditions promote the fall of the spores and their accumulation on the ground (Caneva et al., 2003). The number density concentration of biogenic aerosol particles is close to 1% of the total aerosol in remote oceanic regions while it can contribute from around 2% to 25% in continental areas, reaching sometimes also 50% of total aerosol mass (Tomasi and Lupi, 2017). Bioaerosol represents a small portion of the whole aerosol particles from a numerical point of view while it is more similar to other kind of particles from the mass point of view. A variation is also appreciable between rural and urban area. De Nuntiis et al. (2003) reported that the mean mass concentration of biological particles in urban area during spring is around 20 µg m^{-3} out of a total of about 100 µg m^{-3}. In particular, urban areas show during spring an estimation of 10-10^3 bacteria m^{-3}, 10^3-10^4 fungal spores m^{-3} and 10-10^3 pollen grains m^{-3}.

Bioaerosol arises in areas characterised by biological activity exposed to air circulation and thus the major part of Earth's surface is a potential source of aerobiological matter. Moreover, anthropic sources, such as farming and agricultural activities, livestock, production and treatment of waste and some industrial activities, may contribute to the release of bioaerosol (Caneva et al., 2003). Natural airborne biological material could be produced by physiological processes by microorganisms themselves or physical mechanisms of disaggregation and fragmentation of organisms. Moreover, it could be released into atmosphere by typical processes of the living organism (such as the catapult expulsion mechanism of *Parietaria* pollen) or through winds and rain (De Nuntiis and Palla, 2017). Once in the atmosphere, bioaerosol could be transported and disperse by the kinetic energy exchanged when fast-moving air molecules impact bioaerosol particles (De Nuntiis and Palla, 2017). The global transport of desert dust has been identified as an important responsible for the transport of biological aerosol, too (Bonazza et al., 2017). Generically the smaller the particles, the more suspended in the air for a longer time; on the contrary, bigger particles tend to set down more quickly due to higher mass (with some exception such as Pinaceae pollen). In addition, the possible reachable distance can change due to the vicinity to particles sources and to resuspension of deposited particles. Nevertheless, the biogenic aerosol is generally widespread in the whole troposphere and could reach also different kilometres in height, such as some mould spores that can be detected also at 11 km altitude. Thus PBAPs could participate in the cloud and ice nucleation processes (Tomasi and Lupi, 2017). In general, the mean residence time of bioaerosol ranges from less than a day to few weeks, depending on their size and aerodynamic shape (De Nuntiis et al., 2003). Biological particles can be removed from air by sedimentation and collision to all surfaces or more efficiently by wash out of

precipitation. After deposition, biological particles can interact with aquatic or terrestrial ecosystems likely causing bioaerosol growth and reproduction.
The survival of microorganisms, or parts of it, is controlled by physical and chemical parameters, such as temperature, relative humidity, ultraviolet radiation and concentration of some gases (e.g. O_2, CO, NO_2). Favourable conditions for most organisms ranges between 20°C to 30°C and a relative humidity over 65% (MIBAC, 2001). Nevertheless, in atmosphere there are not only vegetative forms but also resistant ones, like fungal and bacterial spores, able to ensure the continuation of the species even in hostile environmental conditions. With improving environmental parameters, the dormant spore will reactivate itself to the vegetative state. In addition, there are also special environmental condition able to promote a rapid increase: for example, during radiation fog typical of the Po Valley, microorganism could be included in fog droplets and find suitable circumstances for its growth (De Nuntiis et al., 2003).

The study of bioaerosol in the field of cultural heritage has to be connected to the possible alteration processes induced by the growing and metabolic activities of microorganisms that can colonise both organic and inorganic materials. This damage could be induced by the penetration and thus formation of micro-cracks within the material (physical damage), by the chemical interaction of products of metabolic activity with the substrate (chemical damage) or by the releasing of pigmented substance (aesthetic damage). The danger of bioaerosol to artworks is regularly joined to other parameters, such as microclimatic conditions, chemical composition of the substrate and its conservation state. Biological degradation is usually caused not only by a single microorganism but by complex communities of microorganisms often organised as microbial biofilm that covers and penetrates the surface of the material (Bonazza et al., 2017). Biofilms often secrete extracellular polymeric substances (i.e. polysaccharides, proteins, lipids and humic substances), creating an extracellular matrix that provides structural and biochemical support to the surrounding cells.
Referring to stone materials, it is known that many factors influence the bio-colonisation of this kind of substrate. The mineral composition, texture and porosity of stone as well as environmental factors (T, RH and light) may influence the diffusion of these organisms on monuments (De Nuntiis and Palla, 2017). Under favourable conditions, the bioaerosol deposited on stone surface can grow and reproduce using the substratum as nutrient (heterotrophic organisms) or support (autotrophic organisms). However, as reported in Bonazza et al. (2017), the so-called biodeteriogens do not represent all the deposited bioaerosol harmful for cultural heritage. In effects, the former includes only viable organisms but in bioaerosol there are also resistant forms (i.e. biological spores), able to survive even in adverse conditions and to become active in proper environment. Since stone materials are inorganic, the most potentially detrimental biodeteriogens are the autotrophic ones, e.g. some bacteria of the sulphur and nitrogen cycles, *Cyanobacteria*, algae, lichens, mosses and higher plants. Heterotrophic organisms, such as fungi and *Actinomycetes*, may attack subsequently stone substrate, when organic substances of different origin and constitution have already been deposited (Caneva et al., 2003). The penetration in the stone substrate of biological structures (e.g. roots, rhizines and hyphae) may cause physical and mechanical stress with clear effects such as fragmentation, loss of cohesion of stone, delamination and shrinkage of surface. For example, lithophytic lichens can penetrate rock down to many millimetres. Moreover, many organisms secrete pigmented products, able to alter the colour of the substrate, such in the case of fungi that can develop visible films and spots. Besides pigments, also chemical substances may be produced by biological colonizers. In this circumstance, biodeteriogens exploit stone as nourishment by means of extracellular enzyme activity and ion exchange or secrete metabolic substances with an inhibitory or waste function. These excreted matters lead to the alteration, transformation and decomposition of the substrate and are much more common than in the past (Bonazza et al., 2017). Fungi showed to be among the most harmful biodeteriogens for stone. Among these, black meristematic fungi highly threaten stone materials and are so much common on rock that are also called *rock-inhabiting fungi* (RIF). As example, patinas of calcium oxalates (whewellite and weddelite) are commonly detect on carbonate stones. Among the possible causes (Bonazza et al., 2005), biological

organisms (mainly lichens and fungi) secrete oxalic acid not only as waste metabolite but also, for example, as metal detoxification and electron donor in wood degradation (Gadd et al., 2014). This acid could dissolve minerals and cause physical damage due to expansive formation of secondary oxalate products but it seems to behave also as protective for the underlying marble and limestone (Del Monte et al., 1987).

It is noteworthy that often biological organisms prefer to colonise surfaces that first underwent bioaccumulation (for example of metabolic products, droppings and dead microorganisms). This provides both a rough surface, more easy to occupy, and nutritive substances. Therefore, regular and adequate cleaning of surfaces and dusting should be included in maintenance protocols of cultural heritage.

It should bear in mind that atmospheric composition can affect the biocolonization of substrate of buildings and monuments. Thus particular attention should be paid to urban environment, generally more polluted than rural sites and where cultural heritage are more concentrated. For example, *Cyanobacteria* and lichens are considered as pioneer organisms of stone because they are nutritionally undemanding and can overcome water and thermal stresses. However, lichens are really susceptible to air pollutants, acting even as an indicator of air quality (Favali et al., 2003). The same authors referred the possibility that "...acid rain (generally referring to precipitation with pH less that 5) inhibits the growth of some microorganisms also on stone materials...". Therefore high concentration of CO_2, SO_2 and NO_x lowers the pH of rain, with visible consequences also on microorganisms. Nevertheless, it is wrong to state that a component or element inhibits growth in absolute terms but it should be rather considered the amount of pollutant and the kind of biological organisms. For examples, heavy metals are generally strong growth inhibitors but there are some bacteria able to convert lead carbonate into lead oxide (Appolonia et al., 2003). Overall, sulphur dioxide and chlorinated organic compounds show to be phytotoxic, thus organisms, especially lichens, grow more effectively on buildings in atmospheres with less sulphur. However, exceptions are often present, mainly for the domain of bacteria: for instance sulphobacteria are able to oxides SO_2.

Nowadays a lower concentration of SO_2 is measured in contemporary European atmosphere as well as a greater rate of delivery of nitrate and organic compounds to buildings surfaces (usually poor in this nutrients) behave as airborne fertiliser, increasing the amount of biological attack (Brimblecombe and Grossi, 2009).

Even if bioaerosol is ubiquitous, the Mediterranean climate and topography of south Europe foster the growth of numerous vegetal species whose flowering period is longer than in other bioclimatic area, implying the world's highest rate of bioaerosol (Tomasi and Lupi, 2017). However, it is rather difficult to estimate which are the mean bioaerosol components of each bioclimatic zone that may attack and deteriorate stone materials because the microclimate of building/monument is really influential. For examples, algae are present mainly close to wet environments, such as fountains and wells. However, some reference reviews of specific species detected in a certain area are provided by Després et al. (2012). More often pollen calendar are shared by aerobiology association (such as AIA, REA, IAA), as those relative to Po Valley and specifically to Bologna shown in Figure 3.241. The mean monthly pollen concentration measured in Po Valley and Bologna, site selected in this work for bioaerosol monitoring, highlights that pollen as a whole is present almost all year with higher concentration during spring and summer. Moreover, Figure 3.241b displays also mean concentration of fungi spore of *Alternaria* monitored in Bologna during the period 1999-2016, higher between June and October.

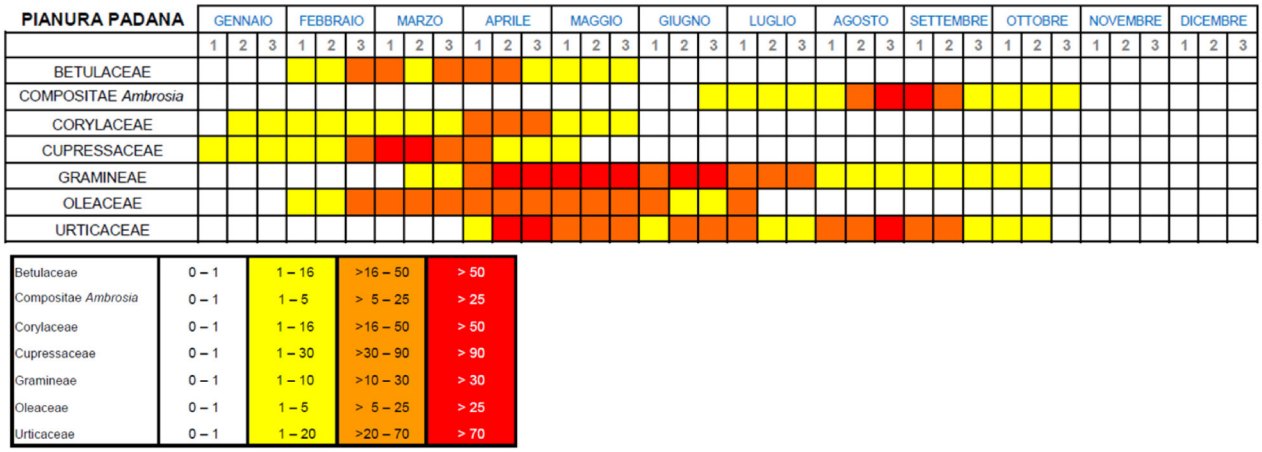

a)

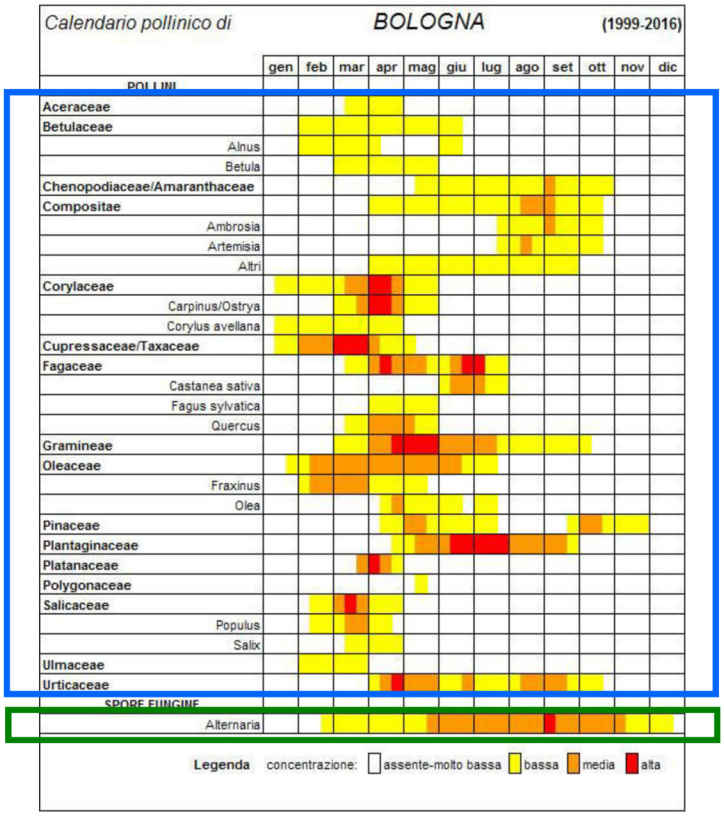

b)

Figure 3.241 a) calendar of mean pollen concentration per month of Po Valley (http://www.ilpolline.it/wp-content/uploads/2008/02/calendario-per-sito.pdf). b) calendar of mean concentration of pollen (framed in blue) and fungi spore (squared in green) per month measured in Bologna during the period 1999-2016. White boxes mean no or scarce concentration, yellow low, orange medium and red high (http://www.pollnet.it/Stations/cal_it_11.aspx).

In this research project, monitoring campaigns of bioaerosol were planned in Bologna in order to identify the potential biological risk factors for stone conservation. It is noteworthy that biodeterioration can be induced directly by the detected microorganisms or indirectly, as they could behave as biofilm suitable for the growth of other biological organisms more harmful for stone conservation.

Among the different sampling methods present in the market (see review in De Nuntiis and Palla, 2017 and INAIL 2010, 2011), the Surface Air System (SAS), in combination with laboratory culture methods, was selected to determine the atmospheric concentration of the potentially biodeteriogenic airborne viable components, thank to its high capture rate capability. In particular, the investigation focused on total

microbial load (bacteria and fungi). Further information about the chosen device and the adopted approach procedure are provided in subchapter 2.2.1. During the first year of field tests, two weekly monitoring campaigns were performed in the CNR area: one in winter and the other one in summer, sampling in double (two for fungi and two for bacteria) and repeating the measure in the morning and in the afternoon.
First campaign was carried out in the period 9-12 February 2017. Figure 3.242 represents the daily average of measured bacterial, fungal and total microbial load. Generally, fungal microbial load (FML) was more abundant than the bacterial one (BML), with exception of Thursday 9 February and Monday 13 February 2017. BML was detected in a concentration between 15 and 203 CFU m^{-3} while FML between 45 and 255 CFU m^{-3}. The mean Total Microbial Load (TML) remained always below 350 CFU m^{-3}, without showing a specific trend. Unfortunately, there are no regulation or limits relative to outdoor microbial load while some concentration ranges exist for indoor environment, as reported by CEC (1993) that however it is related to human health. The latter informs that indoor bacterial load below 100 CFU m^{-3} is considered a very low concentration and low below 500 CFU m^{-3} while for fungal load it is <50 CFU m^{-3} and <200 CFU m^{-3}, respectively. Therefore, just to get an idea of the detected biological microorganisms in comparison with indoor thresholds, bacterial and fungal microbial load measured outdoor in Bologna resulted quite low. Currently there are no threshold limits of total microbial load defined for the preservation of cultural heritage.

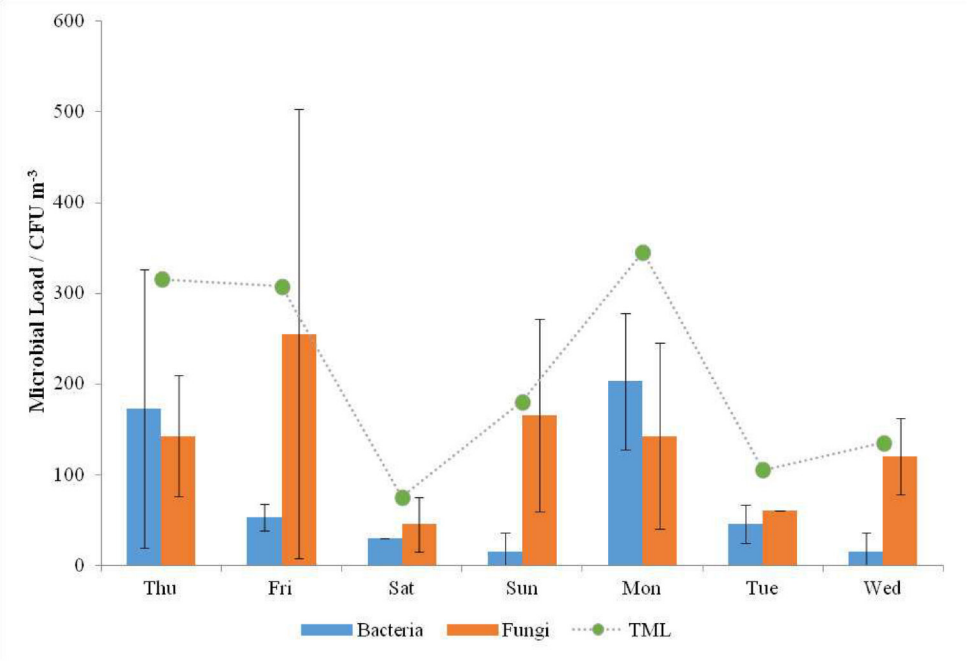

Figure 3.242 Mean daily bacterial (blue) and fungal (orange) microbial load measured during winter campaign 2017. Green dots represent mean daily total microbial load. Black bars indicate the relative standard deviation.

Summer bioaerosol monitoring campaign was carried out between 12 and 17 June 2017. Mean total microbial load ranged between 676 CFU m^{-3} of Tuesday and 2387 CFU m^{-3} of Friday. Fungal microbial load analysed in this period were substantial (between 571 and 2312 CFU m^{-3}) while the bacterial one remained more similar to that measured during the winter campaign (between 38 and 330 CFU m^{-3}). Thus the number of measured fungal colonies was much higher that of bacteria (Figure 3.243). Differences are appreciable also comparing the measured data with limits reported by CEC (1993) for indoor: fungal load ranged from low to high concentration while bacterial load remained within the threshold of low/very low concentration.

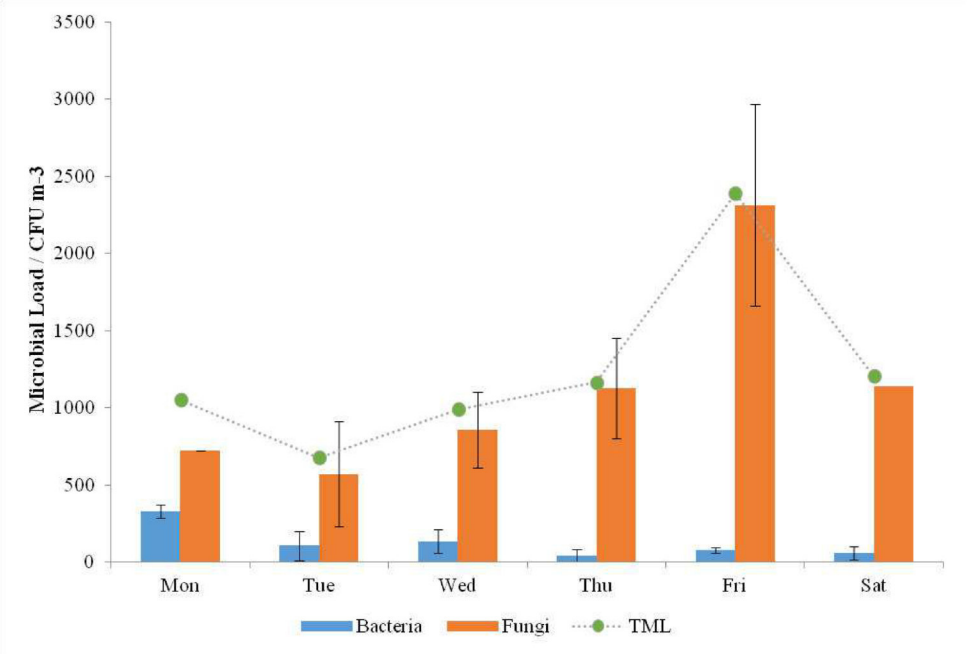

Figure 3.243 Mean daily bacterial (blue) and fungal (orange) microbial load measured during summer campaign 2017. Green dots represent mean daily total microbial load. Black bars indicate the relative standard deviation.

Comparing the two different monitoring campaigns (Figure 3.244), total microbial load measured in summer resulted much higher than that recorded during the cold period, as expected, reaching values till 13 times higher (i.e. on the 5th day). As previously shown, the increase of the total microbial load has to be attributed to the higher concentration of fungi during the warmer period.

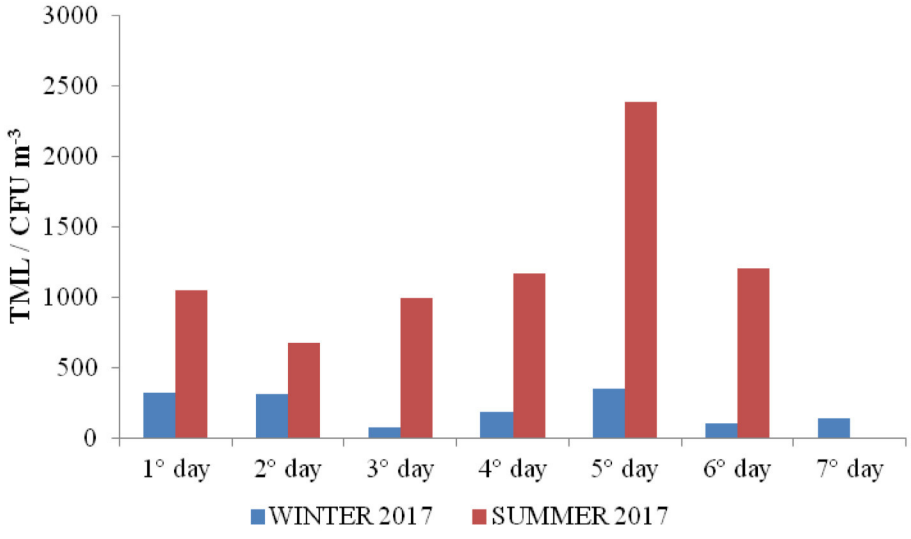

Figure 3.244 Mean daily Total Microbial Load (TML) measured during winter (blue) and summer (red) campaigns 2017.

As previously mentioned, environmental variables may affect the survival of biological microorganisms, whose favourable temperature for most organisms ranges between 20°C and 30°C and relative humidity over 65% (MIBAC, 2001). However, some microorganisms have special metabolic and adaptation capacities

useful for their survival also at temperature around 0°C (spychrophile organisms) or more than 60°C (thermophile organisms). In addition, fungal spores may resist also at RH < 60%, remaining inactive until environmental conditions allow their germination. Also wind has shown to influence the dispersal of bioaerosol, taking into consideration both speed and direction. In particular, the concentration of atmospheric bacteria seems to logarithmically decrease with increasing wind speed (except at the coastal site), probably due to atmospheric dilution, while wind represent an important parameter for the dispersal of other biological particles, like pollens. For these reasons, Table 3.70 reports the daily mean environmental parameters measured during the sampling campaigns.

WINTER CAMPAIGN 2017			
	T (C°)	RH (%)	W_S (m s^{-1})
Thu, 09/02/2017	4	78	1,5
Fri, 10/02/2017	5	76	1,1
Sat, 11/02/2017	6	79	1,3
Sun, 12/02/2017	8	78	1,0
Mon, 13/02/2017	8	81	1,4
Tue, 14/02/2017	8	71	1,5
Wed, 15/02/2017	9	64	2,6
MEAN	**7**	**75**	**1,5**

SUMMER CAMPAIGN 2017			
	T (C°)	RH (%)	W_S (m s^{-1})
Mon, 12/06/2017	26	42	2,4
Tue, 13/06/2017	28	41	2,9
Wed, 14/06/2017	27	53	3,1
Thu, 15/06/2017	25	73	1,7
Fri, 16/06/2017	28	56	2,0
Sat, 17/06/2017	26	59	2,8
MEAN	**27**	**54**	**2,5**

Table 3.70 Daily mean environmental conditions (temperature T, relative humidity RH and wind speed W_s) measured in Bologna during winter and summer bioaerosol monitoring campaigns 2017. In cream the corresponding mean values of the environmental parameters.

During the winter campaign, mean relative humidity was around 75% but temperature was too low for the growth of most microorganisms. In the summer campaign, the measured relative humidity decreased while temperature reached more suitable condition for the germination of biological particles. Therefore, these meteorological parameters may explain the higher concentration of colony forming units measured in summer. On the contrary, a minor influence over the development of biological microorganisms was exerted by wind speed as both campaigns were characterised by light air considering the Beaufort wind force scale, with summer wind speed increased of one unit in respect to that of the winter test.
Figure 3.245 shows the colonies grown on some cultured Petri dishes of the two bioaerosol campaigns after incubation time. In general, despite the presence in PCA Petri dishes of an antibiotic for preventing the growth of fungi, these latter are however present. The higher concentration of microbial colonies during the warmer period is already observable at first sight.

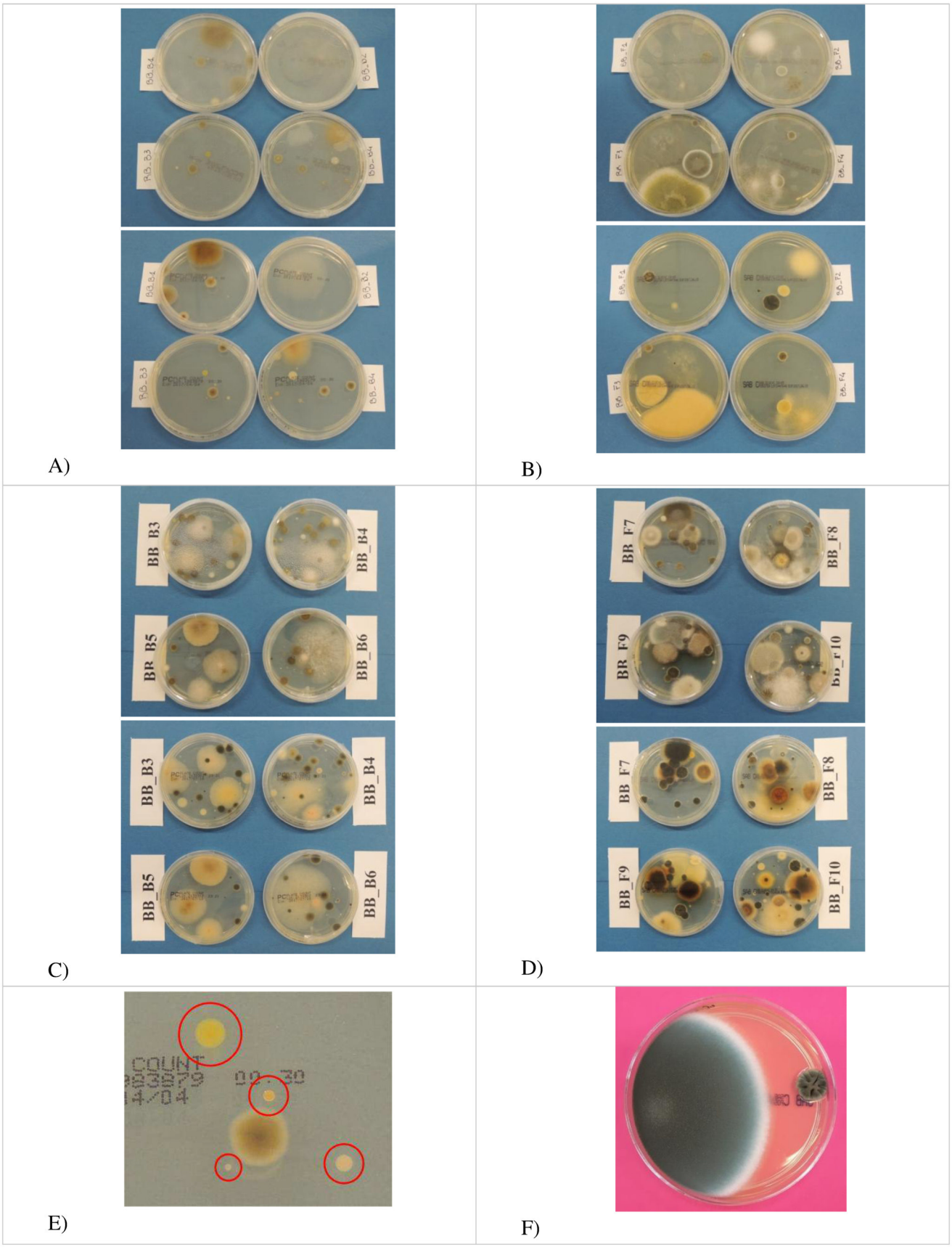

Figure 3.245 Colonies of bacteria (A,C,E - circled in red) and fungi (B, D, F) of winter (A, B) and summer (C, D) campaigns detectable after incubation time. The upper and the lower pictures in A, B, C, D represent respectively both sides of the Petri dishes.

Even if the aim of bioaerosol campaigns in this work was to evaluate the bacterial and fungi microbial load detectable in winter and summer condition in Bologna, optical microscopy was carried out on some colonies just to recognise the most abundant fungi that can grow and not to perform a specie-specific analysis. When morphological characteristic parameters (such as spores and sporangium) were detected, it was possible to identify the genus of fungi. The differences between cold and warm sampling periods seem to have affected only the number of colonies and not the genera. Fungi identified within this research belonged mainly to *Cladosporium* and *Aspergillus* genera. For example, Figure 3.246 A displays a wrinkled, grey fungi and the observation with optical microscope showed the presence of spherical to barrel-like spores, some of which are also septate (Figure 3.246 B, C). Therefore, it can be assumed that this fungi belongs to *Cladosporium* genus.

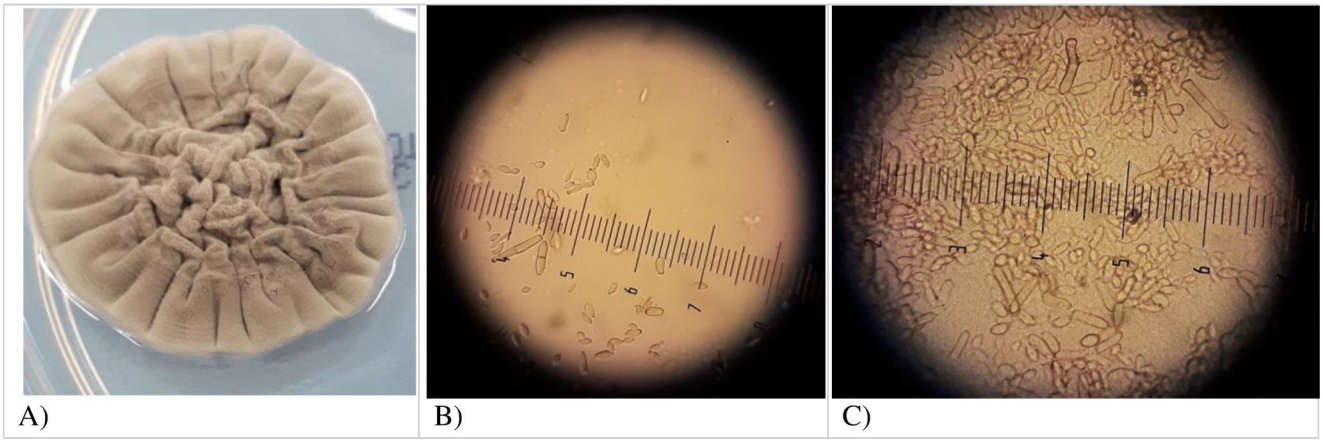

Figure 3.246 A) Visual observation of fungi detected on cultured Petri dish BB_F1. B and C) Optical microscope (40x) images of spores belonging to the same fungi.

Other fungi often grown on the Petri dishes had a cottony appearance, characterised by a grey-aquamarine colour in the centre and surrounded by a white ring (Figure 3.247). In this case, the fruiting body with the typical shape of aspergillum (like a holy water sprinkler), called conidiophores, was diagnostic of the *Aspergillus* genus (Figure 3.247 B, C). Small rounded spores, named conidia, surrounded the observed area.

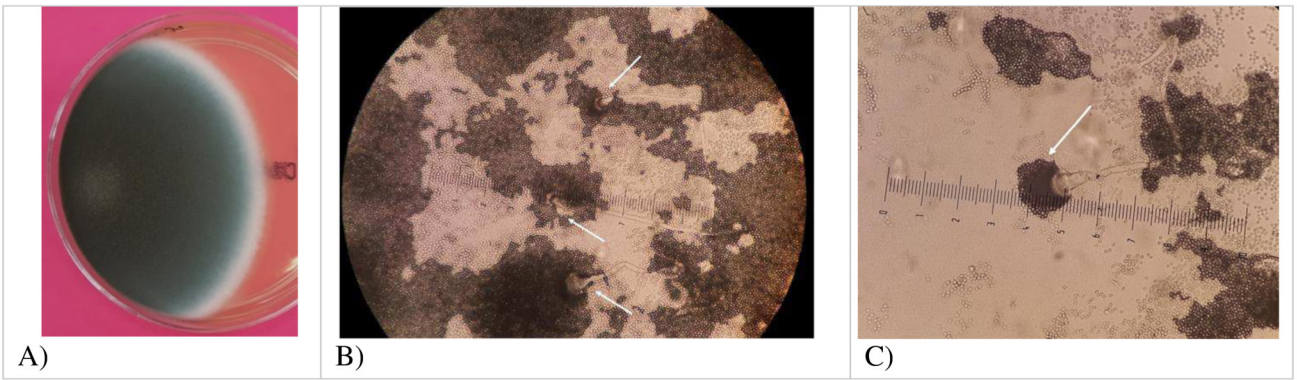

Figure 3.247 A) Visual observation of fungi detected on cultured Petri dish BB_F17. B and C) Optical microscope (40x) images of conidiophores (white arrows) and spores belonging to the same fungi.

Another kind of fungi observable during the monitoring campaigns, with a cottony look and green-yellow coloured, belongs to the same genus *Aspergillus* but probably to a different specie (Figure 3.248 A). The conidia are small, roudish, with a raised edge (see Figure 3.248 B, C).

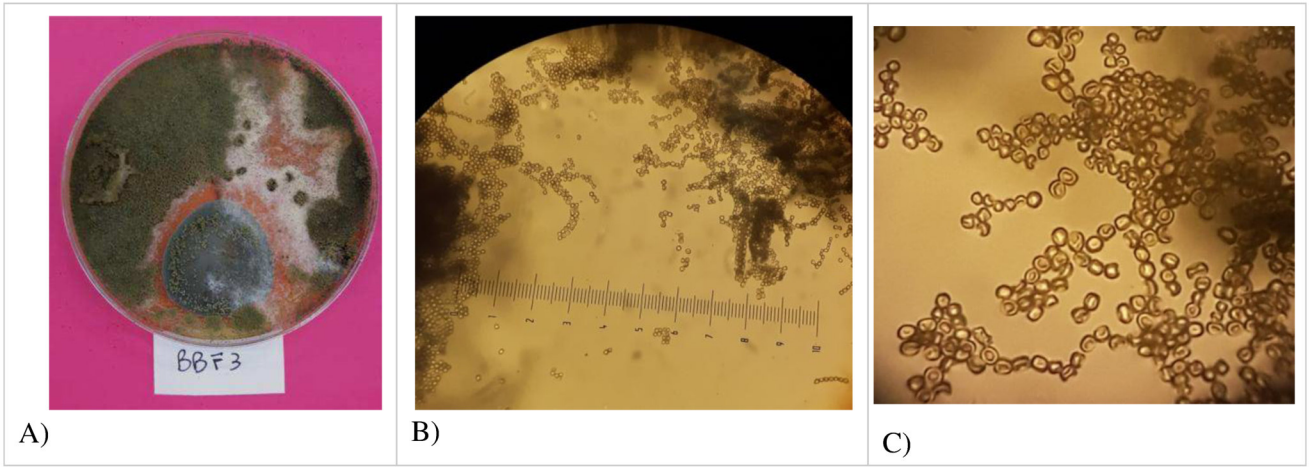

Figure 3.248 A) Visual observation of green fungi detected on cultured Petri dish BB_F3. B) Optical microscope (40x) image of spores belonging to the same fungi and corresponding enlargement (C).

Final remarks:

- Total microbial load measured in summer resulted much higher than that recorded during the cold period because of more suitable condition for the germination of biological particles. The increase of TML has to be attributed to the higher concentration of fungi during the warmer period.
- The differences between cold and warm sampling periods seem to have affected only the number of colonies and not the genera. Fungi identified within this research belonged mainly to *Cladosporium* and *Aspergillus* genera.

4. CHAPTER 4 - SIGNIFICANCE OF CHANGES OF EXPOSED MATERIALS

As field exposure tests were planned to simultaneously expose stone samples and passive quartz filters in a horizontal position, comparison of deposition rate, chemical composition and carbon fractions detected in different substrates is hereafter proposed.
Deposition rate (DR) provides information about the quantity of particulate matter deposited per surface area in a known period. The deposition rate of particulate matter accumulated on surface of passive quartz fibre filters and stone samples per month was calculated dividing the respective total deposited particulate per months of exposure (Ferrero et al., 2018) (Table 4.1).

	EXPOSURE TIME (month)	DEPOSITION RATE ($\mu g\ cm^{-2}\ month^{-1}$)		
		PF	CM	VRM
BOLOGNA	6	427.86	21.06	-
	12	243.07	18.63	-
	18	152.88	3.59	-
	24	128.60	7.09	-
FERRARA	6	293.35	35.53	23.26
	12	160.87	36.92	27.08
	18	260.59	46.60	28.43
	24	53.32	41.03	33.10
FLORENCE	6	37.21	43.29	-
	12	83.03	33.39	-
	18	208.67	41.13	-
	24	144.50	56.18	-

Table 4.1 Deposition rate of passive filters (PF), Carrara Marble (CM) and Verona Red Marble (VRM) samples calculated after different exposure time in Bologna, Ferrara and Florence.

Figure 4.1 shows the comparison of the deposition rate on different substrate horizontally exposed.

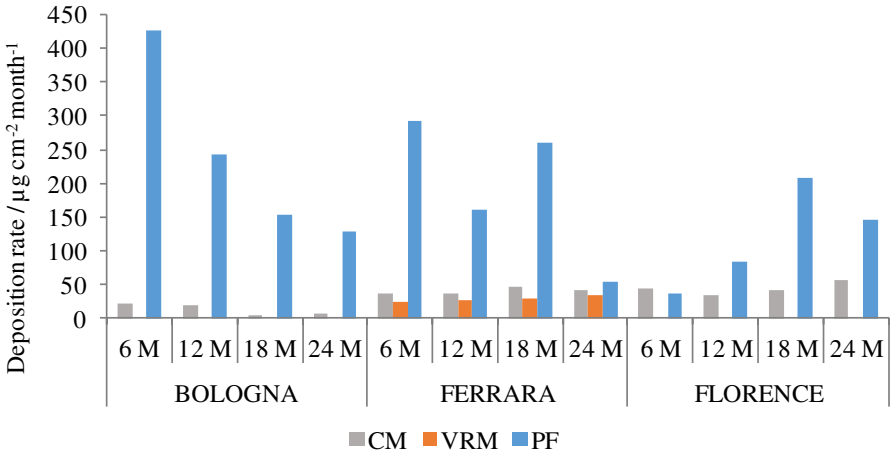

Figure 4.1 Deposition rate of particulate matter deposited on Carrara Marble (CM), Verona Red Marble (VRM) samples and passive filters (PF) in Bologna, Ferrara and Florence after 6, 12, 18 and 24 months of exposure.

In general, the deposition rate on passive filters in all sites (between 37.21 µg cm^{-2} $month^{-1}$ and 427.86 µg cm^{-2} $month^{-1}$) was always much higher than that on stone samples, with exception in Florence after 6 months of exposure when DR on Carrara Marble sample was slightly higher than that on passive filter (37.21 µg cm^{-2} $month^{-1}$ and 43.29 µg cm^{-2} $month^{-1}$, respectively). The higher deposition rate on quartz filters can be explained by the fibrous structure of quartz, characterised by a significant surface roughness, able to trap more particles than the polished stone sample surface (Casuccio et al., 2004). In particular, more difference among DR on different substrates was observed in Bologna where DR of passive filters was from 13 (after 12 months) to 43 (after 18 months) times higher that measured on marble specimens, even if both substrates underwent a general reduction of DR over time.
Concentrating upon Ferrara, DR on stone specimens and passive filters was characterised by a general decrease after 12 and 24 months of exposure. It should be noted that DR on Carrara Marble remained always slightly higher respected to that of Verona Red Marble probably because the slight higher open porosity detected in marble able to hold more particles (see subchapter 3.1.1.4).
In Florence, DR on stone samples was characterised by a continuous slight increase from 33.39 µg cm^{-2} $month^{-1}$ to 56.18 µg cm^{-2} $month^{-1}$ after 12 and 24 months of exposure, respectively, while DR on passive filters increased up to 208.67 µg cm^{-2} $month^{-1}$ after 18 months followed by a modest decrease (to 144.50 µg cm^{-2} $month^{-1}$).
Moreover, mean values of deposition rate on Carrara Marble identified in Ferrara (40.02 ± 4.97 µg cm^{-2} $month^{-1}$) and Florence (43.50 ± 9.46 µg cm^{-2} $month^{-1}$) are comparable to DR measured on Carrara Marble samples exposed in partially sheltered conditions in Milan in 2013-2014 (between 33± 10 µg cm^{-2} $month^{-1}$ and 69 ± 8 µg cm^{-2} $month^{-1}$) (Ferrero et al., 2018) and in German cities (i.e. Bamberg, Würzburg, Essen, Mainz and Munich) in 2013-2014 (Auras et al., 2018). On the contrary, mean DR marble value detected in Bologna (12.59 ± 8.56 µg cm^{-2} $month^{-1}$) was the lowest ever. However, average DR on passive quartz filters detected in Bologna (238.10 ± 135.75 µg cm^{-2} $month^{-1}$), Ferrara (192.03 ± 108.29 µg cm^{-2} $month^{-1}$) and Florence (118.35 ± 74.55 µg cm^{-2} $month^{-1}$) were much higher the DR values measured on quartz filters exposed in Milan (lower than 100 µg cm^{-2} $month^{-1}$) by Ferrerro et al. (2018) in 2013-2014 and Fermo et al. (2018) during the period 2014-2017.

The comparison of anions measured in particulate deposited on passive filters and stone samples highlights that chloride prevailed in Bologna in passive filters after 6, 18 and 24 months of exposure and in material deposited on stone surface after 6, 12 and 18 months (Figure 4.2 A). In general, also NO_3^- was identified in considerable concentration per surface unit in both substrates while SO_4^{2-} reached the highest amount only in deposit of stone specimens after 24 months of exposure (Figure 4.2 A).
In general terms, Cl^- was detected in significant concentration per surface unit in all the substrates exposed in Ferrara, too (Figure 4.2 B). However, SO_4^{2-} prevailed in passive filters in the first three periods of detection while it decreased after 24 months when, on the contrary, it slightly predominated in deposit on stone specimens over the other anions. This suggests that SO_4^{2-} identified on stones surface can be attributable not only to atmospheric deposition abut also to an ongoing sulphation process on marble and limestone.
Passive filters and marble samples exposed in Florence were characterised by higher deposition of Cl^- than the other anions during all periods, with exception of deposit on marble sample after 24 months of exposure (Figure 4.2 C). Furthermore, also SO_4^{2-} was measured in significant concentration per surface unit mainly in passive filters.
In general, it can be argued that Cl^- is the anionic specie detected with a significant concentration per surface unit in deposit of both passive filters and stone samples over time in different exposure sites. Passive filters generally underwent a higher accumulation of anions than that identified on stones surface, mainly after 18 months. Moreover, material deposited on stone samples after 24 months of exposure was characterised by higher concentration of SO_4^{2-} than the other anions in all sites even if Cl^- prevailed in the corresponding passive filters. This can indicate a possible ongoing sulphation process on the surface of stone specimens.

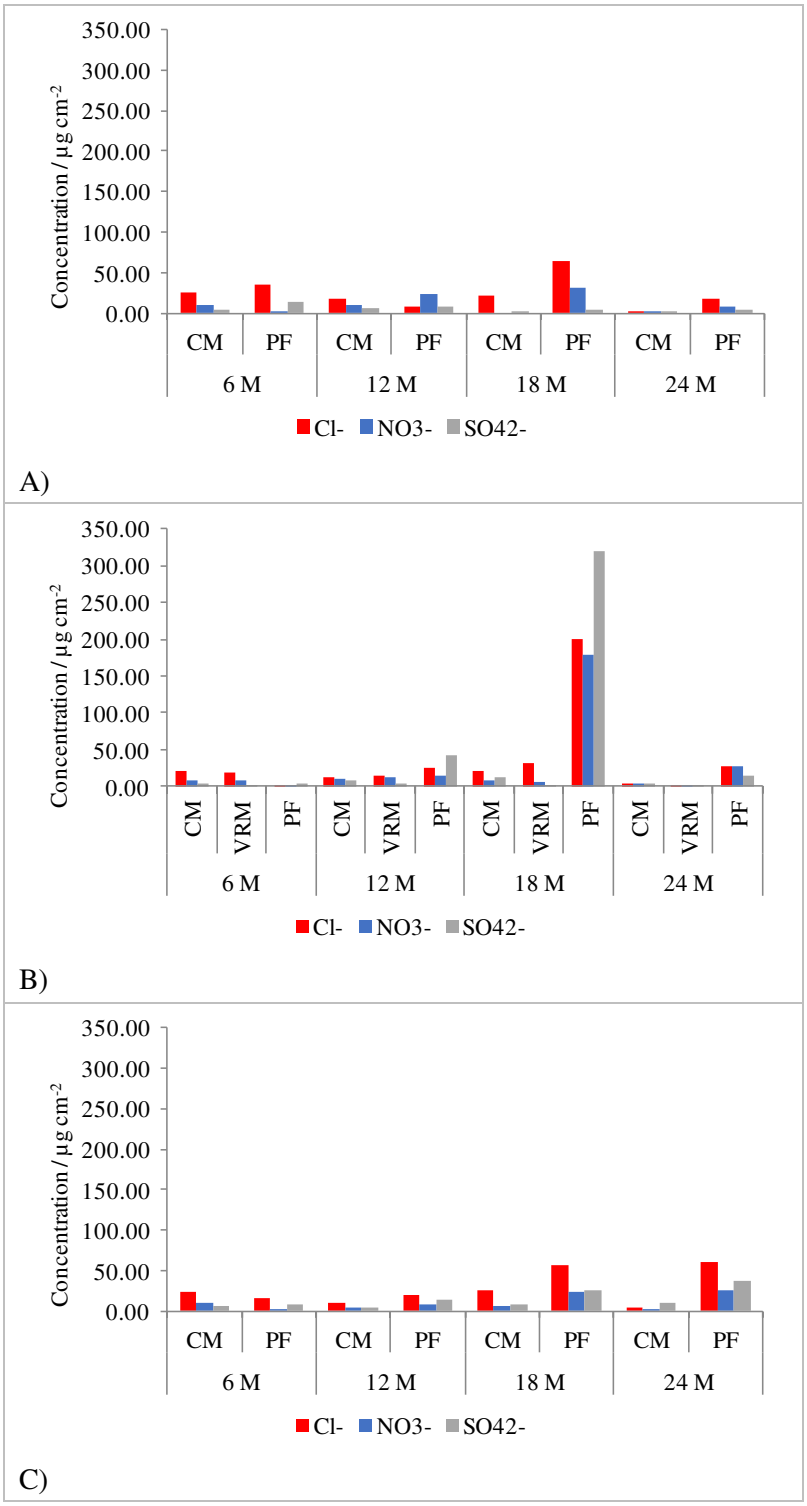

Figure 4.2 Concentration of anions per surface unit identified in particulate deposited on Carrara Marble (CM), Verona Red Marble (VRM) samples and passive filters (PF) in Bologna (A), Ferrara (B) and Florence (C) after 6, 12, 18 and 24 months of exposure.

The comparison of cations highlighted the prevalence of Na^+ and Ca^{2+} in all sites over time (Figure 4.3). In particular, deposit on stone samples underwent higher accumulation of Na^+ per surface unit till to 18 months

of exposure respect to the corresponding passive filter, which, on the contrary, was enriched mainly in Ca^{2+}. This suggests a higher interaction among stone substrate and Na^{+} and between quartz filters and Ca^{2+}.

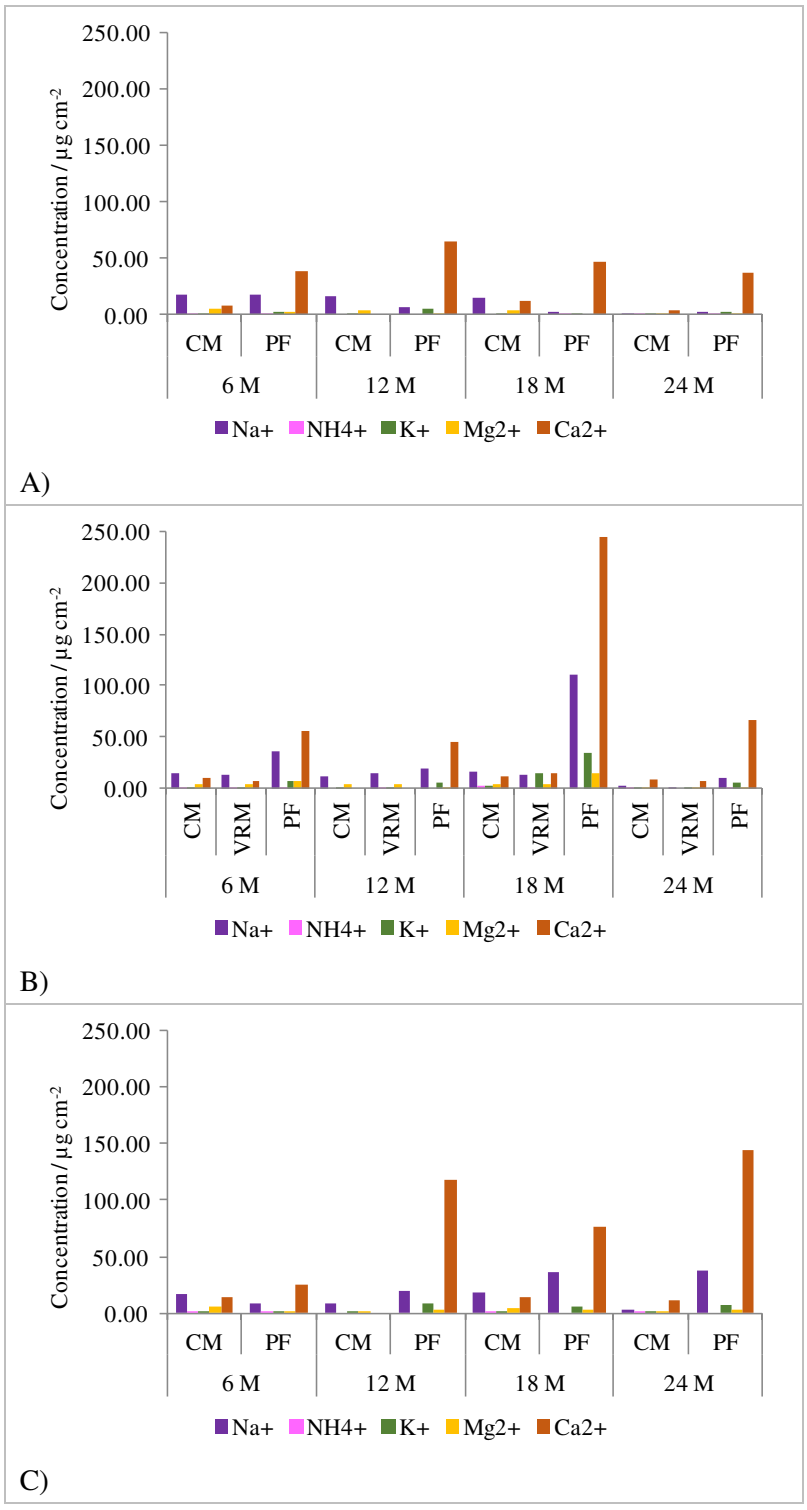

Figure 4.3 Concentration of cations per surface unit identified in particulate deposited on Carrara Marble (CM), Verona Red Marble (VRM) samples and passive filters (PF) in Bologna (A), Ferrara (B) and Florence (C) after 6, 12, 18 and 24 months of exposure.

However, cations concentration per surface unit decreased both in passive filters and deposit accumulated on stone specimens after 24 months of exposure, with exception of those exposed in Florence. Anyway, a slight predominance of Ca^{2+} per surface unit over other cations was detected in both substrates in all sites after 24 months of exposure.

It is possible to assume that the rather high concentration of Na^+ and Cl^- detected both on stone samples and in passive filters mainly within 18 months of exposure is related to a deposition of NaCl, a hygroscopic salt that can be easily solubilised when relative humidity reaches 75% at 20°C. In this context, Auras et al. (2018) found chloride in fresh road dust specimens while much lower amount of Cl^- was detected in older dust collected from road-near positions in Munich, suggesting the most likely wash-out with time of chlorides. Also Comite et al. (2017) identified significant concentration of Cl^- on Carrara plaques exposed in Catania mainly after the first year of exposure than the second one. They argue that chlorides could be penetrated below stone surface over time besides a lower deposition of Cl^- during the second year. However, it should be considered that the low porosity measured in Carrara Marble samples (see subchapter 3.3.4) reduces the decohesion linked to salt crystallisation. Moreover, it is noteworthy that the presence of NaCl allows to increase the solubility of some salts such as gypsum (Camuffo, 2014). When NaCl is present on a stone as crystal or solubilised in absorbed water vapour, the solubility of gypsum begins at 75 % of relative humidity and will increase up to RH = 90 %, likely causing a further damage to stone. Therefore, the detection of SO_4^{2-} and Ca^{2+} on stone deposit after 24 months suggests a possible ongoing sulphation process that could have been favoured also by the presence of NaCl.

In order to better understand the possible origin of soluble ions, ion chromatography data of passive filters and stones deposit are compared with the characteristic elemental ratio of marine origin: Cl^-/Na^+ (1.80), K^+/Na^+ (0.04), Mg^{2+}/Na^+ (0.12), Ca^{2+}/Na^+ (0.04) and SO_4^{2-}/Na^+ (0.25) (Karthikeyan and Balasubramanian, 2006; Fermo et al., 2018) (Table 4.2). In particular, Cl^-/Na^+ typical of marine source is equal to 1.80. Smaller ratio of Cl^-/Na^+ indicates the fractionation of sea-salt and modification by non-marine constituents found in re-suspended dust and de-icing salts. Karthikeyan and Balasubramanian (2006) suggested a possible loss of chloride by heterogeneous reaction of airborne sea-salt with acid atmospheric components (e.g. HNO_3 and H_2SO_4). On the contrary, significant concentration of Cl^- can lead to exceed the sea water ratio (as clearly observable in passive filters exposed in Bologna after 18 and 24 months of exposure) and can be related to industrial activities, including coal combustion and incineration, and also to biomass burning (Hossaini et al., 2016 and related references). Therefore, results highlight the prevalence of additional sources of Cl^- and Na^+ to the marine origin.

		CM				PF			
		6 M	12 M	18 M	24 M	6 M	12 M	18 M	24 M
BOLOGNA	Cl^-/Na^+	1.44	1.25	1.41	1.87	1.93	1.07	23.47	6.29
	K^+/Na^+	0.06	0.05	0.06	0.13	0.12	0.77	0.57	1.11
	Mg^{2+}/Na^+	0.31	0.04	0.25	0.12	0.13	0.20	n.d.	0.33
	Ca^{2+}/Na^+	0.82	n.d.	0.75	4.94	2.19	9.29	17.18	13.32
	SO_4^{2-}/Na^+	0.37	0.48	0.53	4.29	0.79	1.16	1.55	1.37
FERRARA	Cl^-/Na^+	1.47	1.05	1.33	1.87	0.06	1.27	1.82	2.91
	K^+/Na^+	0.07	0.12	0.16	0.56	0.19	0.26	0.31	0.51
	Mg^{2+}/Na^+	0.29	0.31	0.27	0.16	0.19	0.06	0.13	0.15
	Ca^{2+}/Na^+	0.76	n.d.	0.72	3.40	1.53	2.40	2.23	6.74
	SO_4^{2-}/Na^+	0.35	0.75	0.80	1.88	0.09	2.25	2.91	1.51
FLORENCE	Cl^-/Na^+	1.46	1.15	1.42	1.57	2.14	1.03	1.59	1.61
	K^+/Na^+	0.04	0.08	0.03	0.12	0.18	0.44	0.17	0.20
	Mg^{2+}/Na^+	0.28	0.22	0.27	0.29	0.15	0.14	0.08	0.07
	Ca^{2+}/Na^+	0.49	n.d.	0.84	9.54	3.17	5.88	2.10	3.82
	SO_4^{2-}/Na^+	0.24	0.35	0.20	4.36	1.05	0.71	0.71	1.01

Table 4.2 Elemental ratios useful to determine the possible marine source of inorganic ions detected for marble deposit and passive filters exposed in Bologna, Ferrara and Florence after 6, 12, 18 and 24 months of exposure. n.d. means not detected as the numerator was below limit of detection.

Moreover, sea-salt ($SS\_SO_4^{2-}$) and anthropogenic ($NSS\_SO_4^{2-}$) origin of sulphate has been calculated for stones deposit and passive filters according to the mass concentrations of the reference ionic species using the following formula:

$$[NSS\_SO_4^{2-}] = [SO_4^{2-}] - (0.14 \cdot [Cl^-])$$

where 0.14 is the weight ratio of SO_4^{2-}/Cl^- in sea water (Mayer and Krouse, 2004). The $SS\_SO_4^{2-}$ amount is then obtained by subtracting the amount of $NSS\_SO_4^{2-}$ from the total concentration of SO_4^{2-} (Comite et al., 2017; Fermo et al., 2018). Figure 4.4 shows that the contribution of sulphate of particulate deposited on marble samples and passive filters was mostly of anthropogenic origin, with exception of stone deposit detected in all sites after 6 months of exposure and that collected from stone sample and passive filter in Bologna after 18 months. In general, the concentration per surface unit of $NSS\_SO_4^{2-}$ measured in passive filters was always much higher than that identified in stone deposit, reaching the highest value in Ferrara after 18 months of exposure (i.e. 291.56 µg cm^{-2}) (Figure 4.4). Moreover, a general increase over time of anthropogenic source of sulphate was observed mostly in Florence, independently from the substrate. The anthropogenic source of sulphate is related to combustion of fuel oils and coal, confirming vehicular traffic as a significant emissions source beside industry.

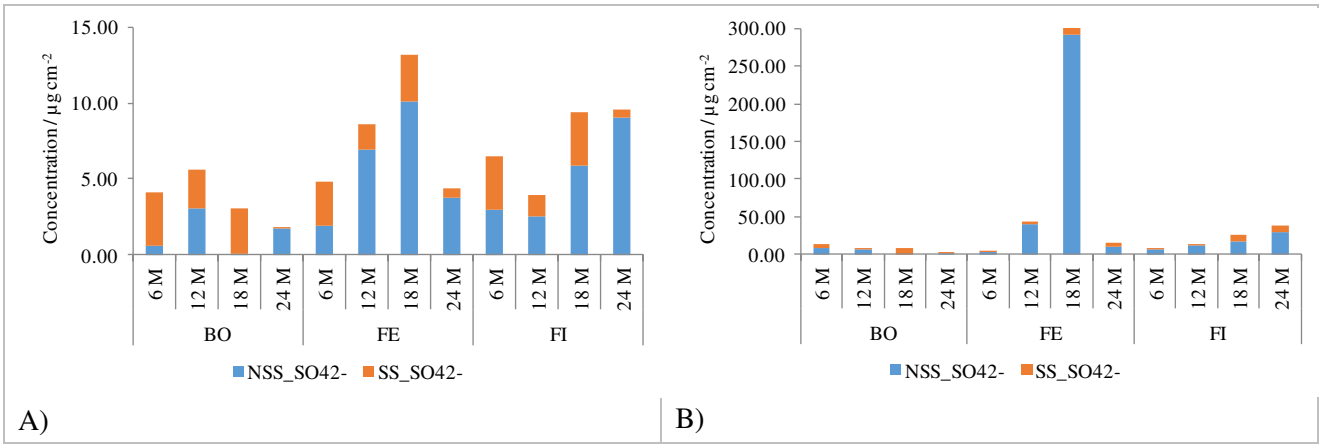

Figure 4.4 $NSS\_SO_4^{2-}$ (non-sea salt sulphate)and $NSS\_SO_4^{2-}$ (sea salt sulphate) contributions calculated for Carrara Marble samples (A) and passive filters (B) in Bologna, Ferrara and Florence after 6, 12, 18 and 24 months of exposure.

Concentrating upon carbon speciation, total carbon amount per surface unit measured in passive filters (from 70.35 µg cm^{-2} to 885.14 µg cm^{-2}) was always higher than that identified in the particulate deposited on stone samples surface (in a range of 9.46 – 152.75 µg cm^{-2} for Carrara Marble and 23.54 – 106.47 µg cm^{-2} in limestone specimens) in all sites (Figure 4.2 A). In general, stone samples and passive quartz filters exposed in Ferrara underwent a more significant accumulation of TC per surface unit respect to the corresponding ones exposed in Bologna and Florence, with exception of passive filter exposed for 24 months whose highest TC amount was in Florence. Moreover, it is appreciable a good relation between the trend of TC measured in passive filters over time and that identified in stone samples as an increase of TC in passive filters corresponded to a growth of TC measured in deposit accumulated on stone samples.

Considering carbon fractions (OC and EC as CC was not detected by Sunset Laboratory OC/EC analyser utilised for the analysis of filters), OC was always detected with the highest concentration per surface unit in all sites independently from the kind of substrate (Figure 4.2 B). OC measured in passive filters (between 70.34 and 885.09 µg cm^{-2}) was always higher that detected in particulate accumulated on marble (from 3.71 to 68.94 µg cm^{-2}) and limestone (from 30.10 µg cm^{-2} to 36.56 µg cm^{-2}) samples in all exposure sites. Also monitoring campaigns of atmospheric PM performed during winter and summer 2017 and 2018 displayed the prevalence of the organic component of carbon (see subchapter 3.3.4). This highlights as mostly vehicular traffic along with biological particles were the main sources of carbon emissions detected in Bologna, Ferrara and Florence.

Elemental carbon remained always below 70.00 µg cm^{-2} in powder deposit of stone samples and lower than limit of detection in passive filters (Figure 4.2 C).

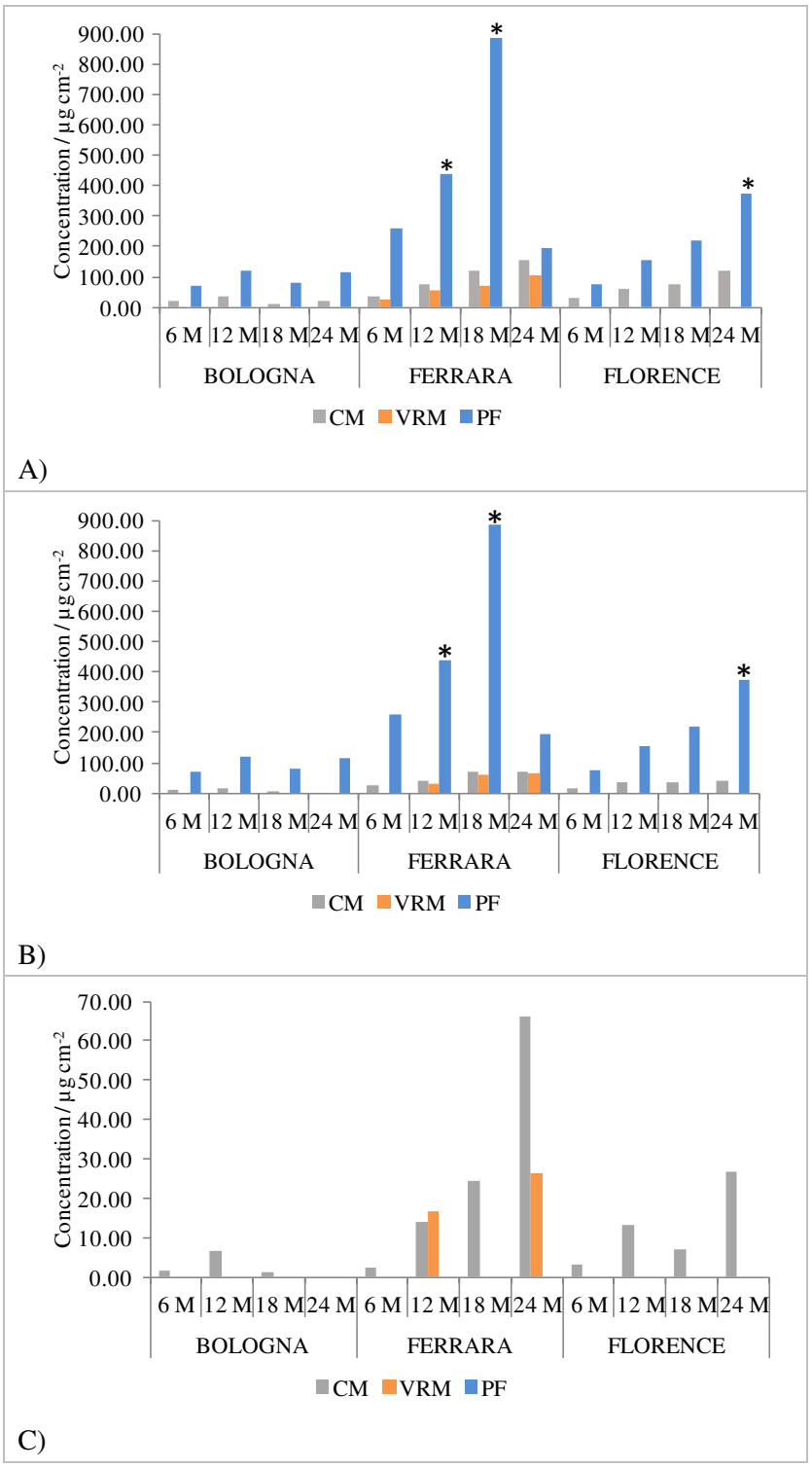

Figure 4.5 Concentration of TC (A), OC (B) and EC (C) per surface unit identified in particulate deposited on Carrara Marble (CM), Verona Red Marble (VRM) samples and passive filters (PF) in Bologna, Ferrara and Florence after 6, 12, 18 and 24 months of exposure. stands for off-scale values.*

It is widely recognised that the composition of deposit accumulated on stone samples can affect the aesthetic appearance of stone surface (Brimblecombe and Grossi, 2004; Bonazza et al., 2007; Brimblecombe and Grossi, 2009; Bonazza and Brimblecombe 2016; Grossi, 2016). In particular, blackening of stone surface is recognised to be mainly due to the accumulation of carbonaceous particles produced by incomplete

combustion of fossil fuels (i.e. EC) (Brimblecombe and Grossi, 2004). Figure 4.6 shows the relationship between the amount of EC per surface unit measured in deposit accumulated on horizontal and oblique marble samples surface at different exposure time and the related lightness value (L*). It was decided to make this comparison for Carrara Marble because of its higher initial lighter colour and aesthetic homogeneity than the Verona Red Marble. In general, it can be observed a reduction of lightness (i.e. darkening) in correspondence with higher concentration of EC in horizontal and oblique marble samples mainly exposed in Ferrara and Florence after different exposure time (Figure 4.6). In particular, the darkening effect with enhanced EC amount per surface unit appeared also to increase over time in samples exposed in Ferrara and in Florence (with exception of analysis after 18 months of exposure) (Figure 4.6 B, C) that experienced a general higher EC deposition respect to Bologna (Figure 4.5 C), confirming as an accumulation of carbonaceous particles over time led to higher darkening effect of stone surface.

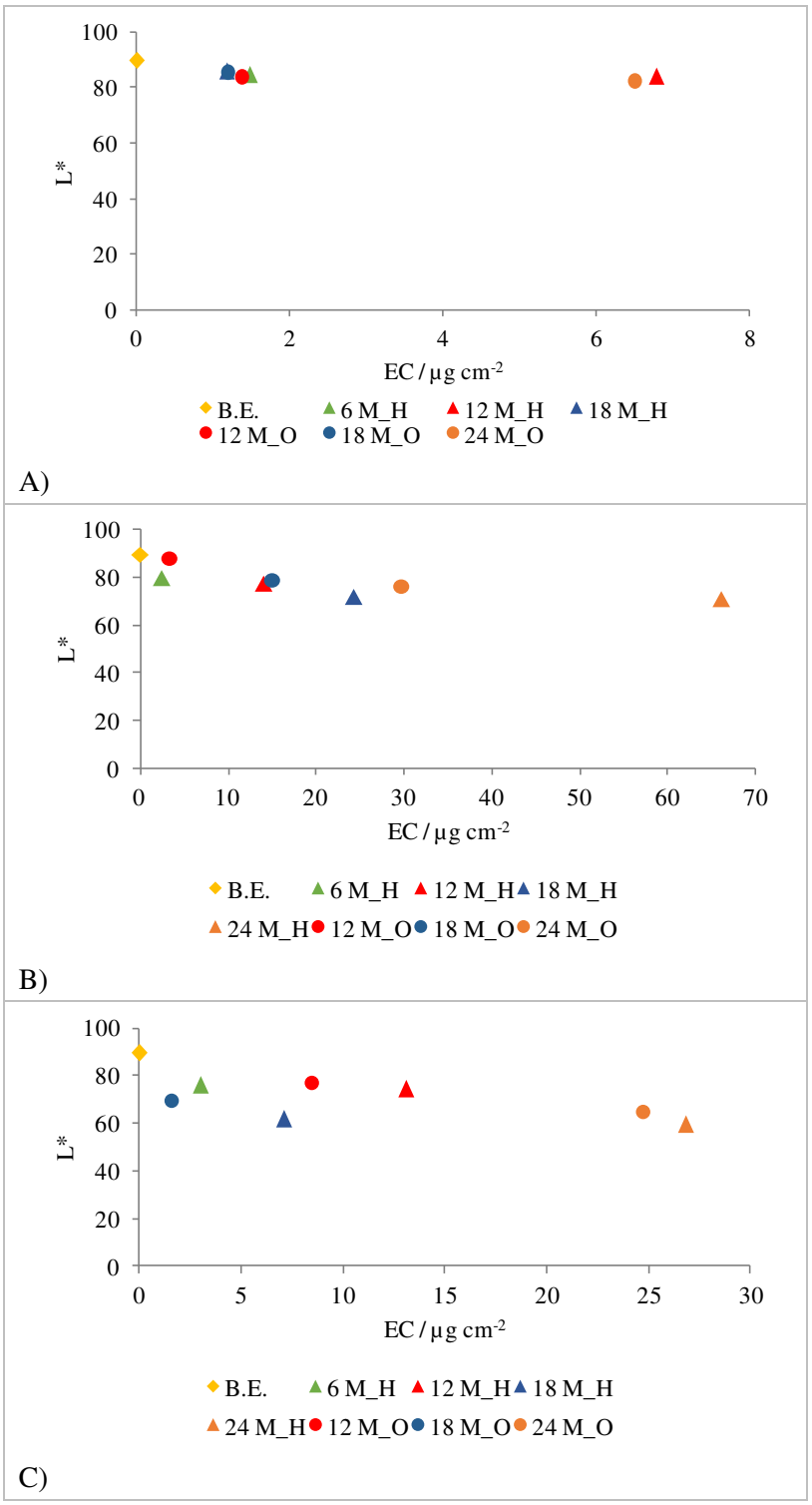

Figure 4.6 Lightness (L) versus amount of elemental carbon per surface unit (EC) measured in horizontal (H) and oblique (O) Carrara Marble samples exposed in Bologna (A), Ferrara (B) and Florence (C) before exposure (B.E.) and after 6, 12, 18 and 24 months of exposure. Consider that carbon fraction of samples exposed for 24 months were measured with the new methodological approach (OC determined at 400°C).*

Moreover, a shift of b* parameter toward more positive values was detected on marble samples in correspondence with higher concentration of OC per surface unit of stone deposit in all exposure sites (Figure 4.7).

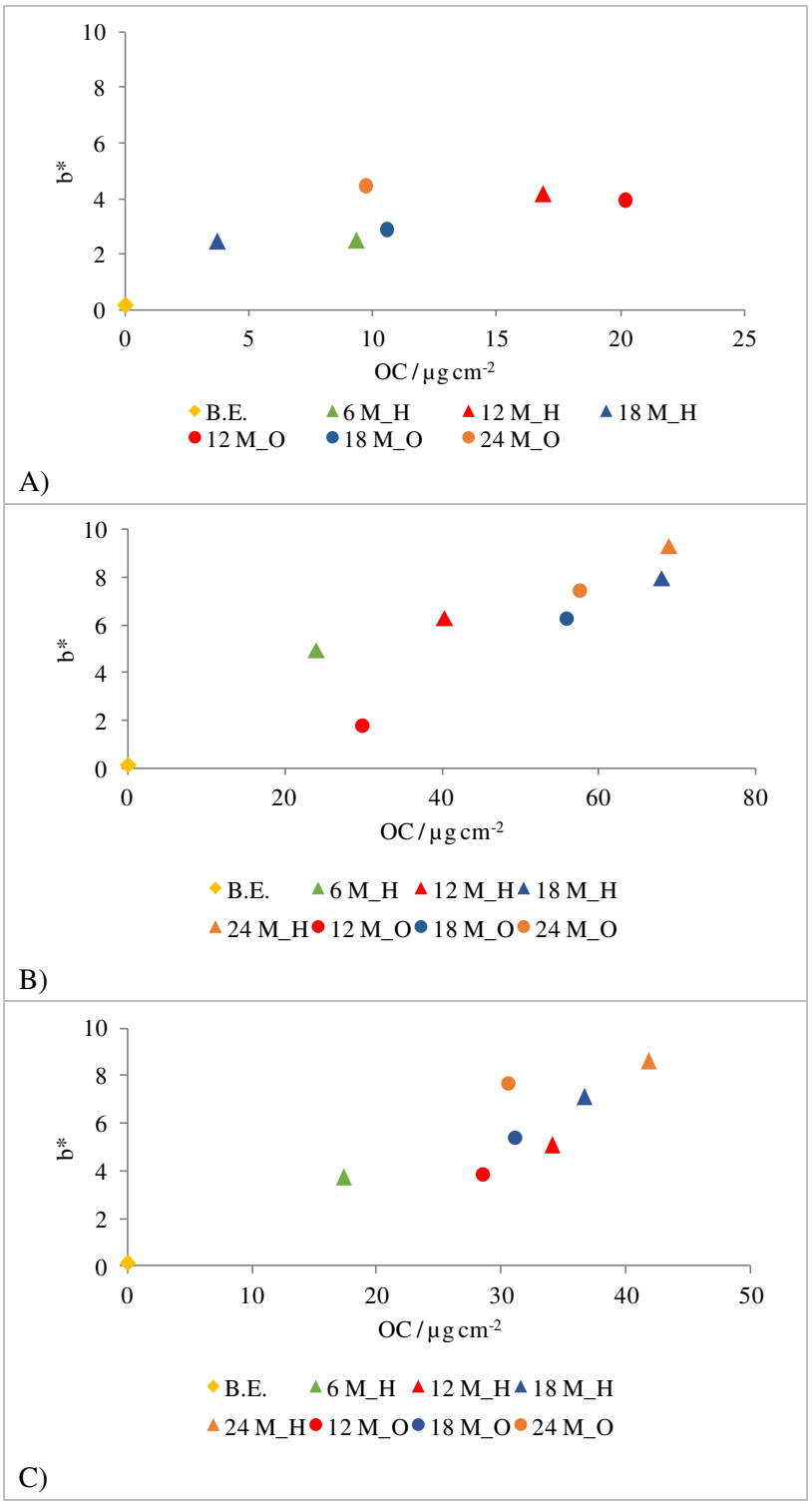

Figure 4.7 Blue-yellow component (b) versus amount of organic carbon per surface unit (OC) measured in horizontal (H) and oblique (O) Carrara Marble samples exposed in Bologna (A), Ferrara (B) and Florence (C) before exposure (B.E.) and after 6, 12, 18 and 24 months of exposure. Consider that carbon fraction of samples exposed for 24 months were measured with the new methodological approach (OC determined at 400°C).*

This is in accordance with studies on damage layers collected from monuments in European cities that revealed as recent damage layer have brownish tones and greater OC concentration than old black crusts (Bonazza et al., 2005). Grossi and Brimblecombe (2008) declared that a yellowing process of stone built

heritage may be of greater concern in the near future as urban atmospheric deposit is increasingly richer in oily organics relative to elemental carbon. In stone samples exposed in Ferrara and Florence, it is also possible to observe an increasing trend over time of the yellowing effect in relation to an enrichment of OC in the deposited material (Figure 4.7 B, C).

Finally, Grossi et al. (2007) identified that dry deposition of SO_2 (precursor for the formation of SO_4^{2-}) on carbonate stone in climate chamber resulted in an increase of b* parameter and consequently of the chroma on light limestone surfaces. In this context, the diagram that relates b* of stone surface with sulphate concentration per surface unit measured in deposited particulate matter highlights in general as a deposition of SO_4^{2-} led to a shift of b* parameter toward the yellow component, with some exceptions of Bologna where b* remained always below 5 even if SO_4^{2-} concentration reached up to 6 µg cm^{-2} (Figure 4.8).

As consequence, an accumulation on the surface of stone specimens of EC as well as of OC and SO_4^{2-} yielded, in most cases, a change of colorimetric appearance of stone toward a blackening effect and a shift of chroma to yellowing, respectively.

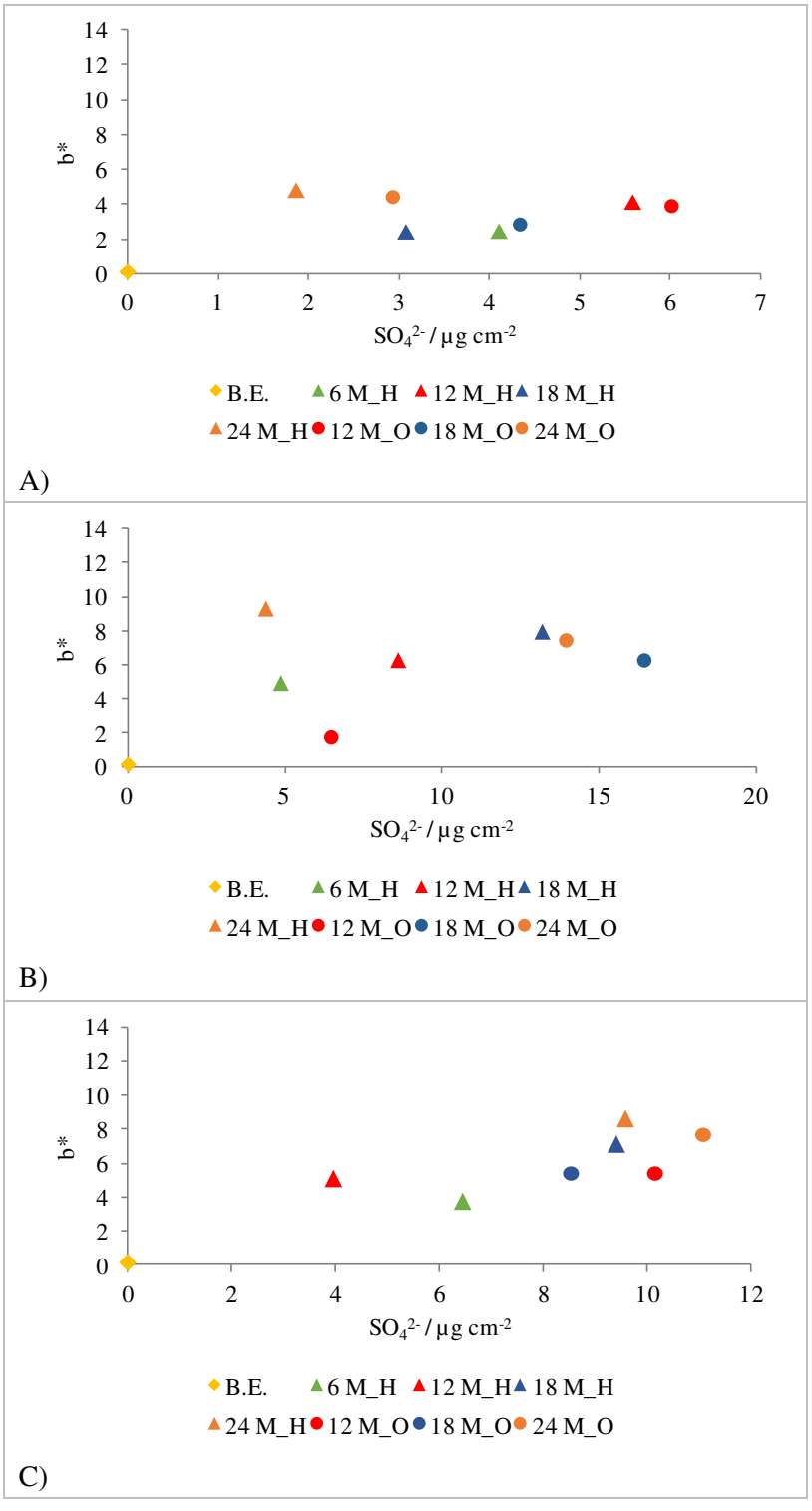

Figure 4.8 Blue-yellow component (b) versus amount of SO_4^{2-} measured in horizontal (H) and oblique (O) Carrara Marble samples exposed in Bologna (A), Ferrara (B) and Florence (C) before exposure (B.E.) and after 6, 12, 18 and 24 months of exposure.*

5. CHAPTER 5 - FINAL CONSIDERATIONS

5.1. CONCLUSIONS

Atmospheric particulate matter in urban sites represents a hazard for stone surfaces since it can deposit and interact with stone substrate leading to physic-chemical interactions and aesthetical variations. Field exposure tests in partially sheltered condition combined with atmospheric PM monitoring campaigns were selected as methodological approach for assessing the effect of atmospheric pollution on carbonate stone substrates in different environmental sites in Italy (Ferrara, Firenze and Bologna).

Concentrating upon atmospheric particulate matter, the analysed water-soluble portion of PM is mainly composed by NO_3^-, SO_4^{2-} and NH_4^+ in all sites, showing higher concentration in winter campaigns than in summer ones. These soluble fractions are typical of vehicular traffic emissions. Moreover, the carbon fraction of PM resulted to be mostly composed by OC respect to EC in all sites with a general higher concentration measured during winter campaigns, confirming a major contribution from mobile combustion sources. The prevalence of both soluble and carbon fractions in winter campaigns may be explained by the lower height of the planetary boundary layer and by further emissions sources, e.g. heating system.

Results obtained from stone samples highlighted a higher colour vulnerability of Carrara Marble than Verona Red Marble. In this regard, an increasing trend of soling over time was observed in all sites, higher on horizontal samples but detectable also on oblique specimens, often exceeding the acceptability limit of total colour change for human sight. The variation of total colour is more significant on samples exposed in Florence, followed by Ferrara and Bologna. This variation of ΔE^* is related mainly by a change of lightness (L^*) and secondly by a variation of the blue-yellow parameter (b^*) that lead to a blackening and a shift towards yellow component of the marble surface.

Ion chromatography on stone deposit allowed to quantify the amount of soluble ions per surface unit detected at different exposure periods. Mostly Cl^- and also NO_3^- prevailed in horizontal and oblique samples within 18 months of exposure while a general reduction of all soluble ions was measured on samples after 24 months of exposure. In particular, deposit accumulated on stone surface after 24 months was characterised by the prevalence of SO_4^{2-} over the other anions, suggesting an ongoing sulphation process. It is interesting to note that higher amount of SO_4^{2-} was detected on Carrara Marble than on limestone on equal exposure conditions in all analysed period, indicating a higher reactivity of the marble to sulphation process.

Results showed a non strict relation among these soluble ions and those detected in atmosphere. Further elaboration of data allowed to identify the possible sources of the detected anions: re-suspended dust and de-icing salts along with marine origin for Cl^- and the prevalence of anthropogenic origin for SO_4^{2-}.

Considering carbon fractions measured on material accumulated on stone samples, the concentration of TC per surface unit increased in general over time, mainly in Florence and Ferrara. In particular, OC prevailed over EC in all sites both in horizontal and oblique samples confirming the prevailing emissions from vehicular traffic. Emissions from fossil fuels combustion were also proved by the isotopic ratio of OC and EC over time. The choice to assess soluble and carbon fractions of the deposited powdered material from the whole exposed surface of a sample every 6 months, when possible, led to quantify the real deposition of atmospheric particulate per surface unit providing useful data for future elaboration of damage functions.

It was also observed that the accumulation of OC and SO_4^{2-} on marble surface led to a general shift of b^* parameter toward the yellow component while a decrease of lightness (blackening) was observed in correspondence with an accumulation of elemental carbon. Therefore, products of combustion of fossil fuels resulted to induce colorimetric changes of stone substrate.

ESEM-EDX allowed to detect the presence of mineral and soil dust particles along with fly-ash, carbonaceous and spherical dendritic Fe-rich particles related to anthropogenic processes (mostly combustion of fossil fuels) in the deposit collected after 24 months in all sites. Also high concentration of

heavy metals (specifically Sb, Cu, Ti, Sn, Fe, Mo and Zn) identified in deposit revealed as vehicular traffic influenced the composition of the accumulated particulate matter, mainly in Florence. It is worth noting that Carrara Marble samples were more enriched in Fe, Mo, Mn, Sb, Ti, U, V than those of Verona Red Marble, proving that the different kind of stone substrate can influence the deposition of heavy metals.

Even if both selected lithotypes have a carbonate composition (mostly calcite and dolomite), polished surfaces, low porosity (< 1.5 %) and were exposed to the same environmental conditions, Carrara Marble samples showed a slightly higher vulnerability to outdoor exposure respect to the limestone. This is likely due to stone texture as Carrara Marble has a granoblastic texture with average size crystals of 300 μm while Verona Red Marble, geologically classified as a limestone, has a micritic texture that causes greater compactness and resistance to degradation.

Passive filters always underwent higher deposition rate of particulate matter respect to stone samples probably because of the fibrous structure of quartz filters, able to trap more particles than the polished stone samples surface. Even if with higher amount per surface unit, passive filters confirmed the significant presence of Cl^-, SO_4^{2-}, Na^+ and Ca^{2+} among soluble ions detected in all sites as in stone deposit as well as the clear prevalence of OC over EC. This shows once again as vehicular traffic can directly (combustion of fossil fuels) or indirectly (re-suspended dust and de-icing salts) affected the composition of the deposited particulate matter.

5.2. FUTURE PERSPECTIVES

This study has provided an important contribution to create a database related to the real deposition of particulate matter (in terms of soluble and carbon fractions) on stone surface and to the consequent variation of the colorimetric parameters. Moreover, the monitoring of particulate matter carried out in the same location of stone exposure has supplied useful data to understand the relationship among carbon and soluble fractions of PM measured in atmosphere with those deposited on stone surface and that can interact with the substrate material. All these data will be prone to develop and/or improve existing damage functions suitable for planning the frequency of cleaning and maintenance interventions of stone material and identifying threshold level of air quality suitable for the conservation of cultural heritage.

The continuation of stone samples exposure can provide more data to identify a possible trend of colour change of substrate with respect to the concentration of soluble ions and carbon fractions of deposited particulate as well as the comparison of results obtained from this research with those of previous studies related to built heritage mainly of Bologna, Ferrara and Florence can allow to better understand any possible variation in composition from the past deposited particulate matter.

This research contributed also to an improvement of the methodology for carbon fractions discrimination and measurement in damage layers published by Ghedini et al in 2006 by application of the existing approaches for quantifying carbon fractions in soils purposely modified and implemented. The new developed method is based on a thermal process and permits the carbon fractions quantification by avoiding any chemical attack. In this context, the determination of isotopic ratio of each carbon fraction helped in validating the proper temperature of combustion and assess the possible emission sources. The additional ongoing adjustment of the methodology with a reduced temperature for organic carbon detection (400 °C rather than 430 °C) will be employed also to repeat the analysis on stone deposit before 24 months of exposure, whenever possible, in order to correct the available data.

ACKNOWLEDGMENTS

I would like to express my sincere gratitude to my supervisors, Alessandra Bonazza and Carmela Vaccaro, who assisted me during these three years with patience, motivation and encouragement in reaching the goals of my Ph.D study and related research.

My sincere thanks also goes to Institute of Atmospheric Science and Climate of the National Research Council of Italy that allowed me to deal with this research, in particular to Paola De Nuntiis, Chiara Ciantelli, Alessandro Sardella, Nadia Ghedini, Francesca Volpi, Francesco Manarini, Daniele Contini, Adelaide Dinoi.

I thank Claudio Natali, Massimo Coltorti, Salvatore Pepi, Annalisa Martucci, Renzo Tassinari, Renzo Tamoni and all my PhD colleagues of the University of Ferrara for helping me in performing analyses and processing data.

Moreover, I want to thank Paola Fermo and Valeria Comite of the Univeristy of Milan for part of IC and carbon speciation performed on quartz filters, Orlando Favoni of the Università Politecnica delle Marche for the support in MIP and to Franco Corticelli of IMM-CNR for the ESEM-EDX support.

I gratefully acknowledge Testi Group S.r.l. to supply stone samples, Simonetta Pancaldi and the Botanical Garden of Ferrara, Marilena Tamassia and all the staff of San Marco Museum, CNR of Bologna and ARPAE to allow me racks exposure and the performance of PM monitoring campaigns.

Last but not the least, I would like to really thank my family, in particular my parents and Federico, for their love and continuous support.

REFERENCES

CHAPTER 1

Amoroso G.G. (Ed.), 2002. Trattato di scienza della conservazione dei monumenti: etica della conservazione, degrado dei monumenti, interventi conservativi, consolidanti e protettivi. ALINEA Editrice, Florence, 416. ISBN 8881254107

Auras M., Bundschuh P., Eichhorn J., Kirchner D., Mach M., Seewald B., Scheuvens D. and Snethlage R., 2018. Salt deposition and soiling of stone facades by traffic-induced immissions. Environmental Earth Sciences 77: 323.

Ausset P., Crovisier J.L., Del Monte M., Furlan V., Girardet F., Hammecker C., Jeannette D. and Lefevre R.A., 1996. Experimental study of limestone and sandstone sulphation in polluted realistic conditions: The Lausanne Atmospheric Simulation Chamber (LASC). Atmospheric Environment 30 (18), 3197-3207.

Ausset P., Bannery F., Del Monte M., Lefevre R.A., 1998. Recording of preindustrial atmospheric-environment by ancient crusts on stone monuments. Atmospheric environment 32(16), 2859-2863.

Barca D., Belfiore C.M., Crisci G.M., La Russa M.F., Pezzino A. and Ruffolo S.A., 2010. Application of laser ablation ICP-MS and traditional techniques to the study of black crusts on building stones: a new methodological approach. Environmental Science and Pollution Research 17(8), 1433-1447.

Belfiore C.M., Barca D., Bonazza A., Comite V., La Russa M. F., Pezzino A., Ruffolo A. and Sabbioni C., 2013. Application of spectrometric analysis to the identification of pollution sources causing cultural heritage damage. Environmental Science and Pollution Research 20, 8848-8859.

Beloin N.J. and Haynie F.H., 1975. Soiling of Building Materials. Journal of the Air Pollution Control Association 25 (4), 399-403.

Bonazza A., Sabbioni C. and Ghedini N., 2005. Quantitative data on carbon fractions in interpretation of black crusts and soiling on European built heritage. Atmospheric Environment 39, 2607-2618.

Bonazza A., Sabbioni C., Ghedini N., Hermosin B., Jurado V., Gonzalez J.M. and Saiz-Jimenez C., 2007a. Did Smoke from the Kuwait Oil Well Fires Affect Iranian Archaeological Heritage? Environmental Science & Technology 41 (7), 2378-2386.

Bonazza A., Brimblecombe P., Grossi M.C. and Sabbioni C., 2007b. Carbon in Black Crusts from the Tower of London. Environmental Science & Technology 41 (12), 4199-4204.

Bonazza A., Messina P., Sabbioni C., Grossi C.M. and Brimblecombe P., 2009. Mapping the impact of climate change on surface recession of carbonate buildings in Europe. Science of The Total Environment 407 (6), 2039-2050.

Bonazza A., Natali I., Ozga I., Bartolozzi G., Cucci C., Marchiafava V., and Picollo M., 2013. Pollution effects on typical Florentine lithotypes: a multidisciplinary approach. In: Boriani M., Gabaglio R. and Gulotta D. (Eds.) online proceedings of Conference Built Heritage 2013 - Monitoring Conservation and Management, 18-20 November 2013, Milan, Italy, 1164-1169. ISBN 978-88-908961-0-1

Bonazza A. and Sabbioni C., 2016. Composition and Chemistry of Crusts on Stone, in Brimblecombe P. (Ed.), Urban Pollution and Changes to Materials and Building Surfaces, Imperial College Press, Singapore, 103-126.

Brimblecombe P., 2000. Air Pollution and Architecture: Past, Present and Future. Journal of Architectural Conservation 6 (2), 30-46.

Brimblecombe P. and Camuffo D., 2003. Long Term Damage to the Built Environment, in Brimblecombe P. (Ed.), The Effect of Air pollution on the Built Environment, Imperial College Press, Singapore, 1-30.

Brimblecombe P. and Grossi C.M., 2004. The rate of darkening of material surfaces, in Saiz-Jimenez C. (Ed.), Air Pollution and Cultural Heritage, Taylor & Francis Group, London, 193-198.

Brimblecombe P., Grossi C.M. and Harris I., 2006. The effect of long-term trends in dampness on historic buildings. Weather 61, 278-281.

Brimblecombe P. and Grossi C.M., 2007. Damage to Buildings from Future Climate and Pollution. APT Bulletin: Journal of Preservation Technology 38 (2-3), 13-18.

Brimblecombe P. and Grossi C.M., 2009. Millennium-long damage to building materials in London. Science of The Total Environment 407 (4), 1354-1361.

Butlin R.N., Yates T.J.S., Murray M. and Ashall G., 1995. THE UNITED KINGDOM NATIONAL MATERIALS EXPOSURE PROGRAMME. Water, Air and Soil Pollution 85, 2655-2660.

Camuffo D., Daffara C. and Sghedoni M., 2000. Archaeometry of Air Pollution: Urban Emission in Italy during the 17th Century. Journal of Archaeological Science 27, 685-690.

Camuffo D., Bertolin C., Schenal P., 2014. Climate change, sea level rise and impact on monuments in Venice. In: Rogerio-Candelera M.A. (Ed.), Science, Technology and Cultural Heritage, Proceedings of the 2nd International Congress on Science and Technology for the Conservation of Cultural Heritage, 24-27 June 2014, Sevilla, Spain, CRC Press/Balkema, Leiden, The Nederland, 1-17.

Chabas A., Fouqueau A., Attoui M., Alfaro S.C., Petitmangin A., Bouilloux A. et al., 2015. Characterisation of CIME, an experimental chamber for simulating interactions between materials of the cultural heritage and the environment. Environmental Science and Pollution Research 22 (23), 19170-19183.

Climate and Clean Air Coalition. http://www.ccacoalition.org/, last update: 23/08/2016.

Comite V., Álvarez de Buergo M., Barca D., Belfiore C.M., Bonazza A., La Russa M.F. et al., 2017. Damage monitoring on carbonate stones: Field exposure tests contributing to pollution impact evaluation in two Italian sites. Construction and Building Materials 152, 907-922.

Creighton P.J., Lioy P.J., Haynie F.H., Lemmons T.J., Miller J.L. and Gerhart J., 1990. Soiling by Atmospheric Aerosols in an Urban Industrial Area. Journal of the Air & Waste Management Association 40 (9), 1285-1289.

Doehne E. and Price C.A. (Eds.), 2010. Stone Conservation: An Overview of Current Research (2nd ed.). Getty Conservation Institute, Los Angeles, U.S.A.,158. ISBN 978-1-60606-046-9

EEA, 2016. Explaining road transport emissions - A non-technical guide. European Environment Agency ISBN: 978-92-9213-723-6

Elfving P., Panas I. and Lindqvist O., 1994. Model study of the first steps in the deterioration of calcareous stone II. Sulphate formation on calcite. Applied Surface Science 78 (1), 83-92.

Fermo P., Turrion R.G., Rosa M. and Omegna A., 2015. A new approach to assess the chemical composition of powder deposits damaging the stone surfaces of historical monuments. Environmental Science and Pollution Research 22 (8), 6262-6270. DOI: 10.1007/s11356-014-3855-y

Fermo P., Goidanich S., Comite V., Toniolo L. and Gulotta D., 2018. Study and Characterization of Environmental Deposition on Marble and Surrogate Substrates at a Monumental Heritage Site. Geosciences 8(9), 349.

Ferrero L., Casati M., Nobili L., D'Angelo L., Rovelli G., Sangiorgi G., et al., 2018. Chemically and size-resolved particulate matter dry deposition on stone and surrogate surfaces inside and outside the low emission zone of Milan: application of a newly developed "Deposition Box". Environmental Science and Pollution Research 25, 9402-9415.

Fronteau G., Schneider-Thomachot C., Chopin E., Barbin V., Mouze D. and Pascal A., 2010. Black-crust growth and interaction with underlying limestone microfacies, in Přikryl R. and Török Á. (Eds.), Natural Stone Resources for Historical Monuments, Geological Society, London, Special Publications 333, 25-34.

Gaddi R., Cusano M., Bonanni P., Cacace C., Giovagnoli A., Barbini F. et al., 2017. Inquinamento atmosferico e beni culturali: effetti sui materiali a Roma - Rapporti 270/2017. ISBN 978-88-448-0847-1

Ghedini N., Gobbi G., Sabbioni C., Zappia G., 2000. Determination of elemental and organic carbon on damaged stone monuments. Atmospheric Environment 34, 4383-4391.

Ghedini N., Sabbioni C., Pantani M., 2003. Thermal analysis in cultural heritage safeguard: an application. Thermochimica Acta 406, 105-113.

Ghedini N., Sabbioni C., Bonazza A., Gobbi G., 2006. Chemical-Thermal quantitative methodology for carbon speciation in damage layers on building surfaces. Environmental Science and Technology 40, 939-944.

Ghedini N., Ozga I., Bonazza A., Dilillo M., Cachier H., Sabbioni C., 2011. Atmospheric aerosol monitoring as a strategy for the preventive conservation of urban monumental heritage: The Florence Baptistery. Atmospheric Environment 45, 5979-5987.

Gieré R. and Querol X., 2010. Solid Particulate Matter in the Atmosphere. Elements 6, 215-222.

Gordon A., Tidblad J. and Lombardo T., 2012. Report No 71 The effect of black carbon on soiling of materials. Convention on long-range transboundary air pollution international co-operative programme on

effects on materials, including historic and cultural monuments. file:///C:/Users/Giorgia/Downloads/Report%2071%20Black%20carbon.pdf

Graber E.R. and Rudich Y., 2006. Atmospheric HULIS: How humic-like are they? A comprehensive and critical review. Atmospheric Chemistry and Physics 6, 729-753.

Graue B., Siegesmund S., Oyhantcabal P., Naumann R., Licha T. and Simon K., 2013. The effect of air pollution on stone decay: the decay of the Drachenfels trachyte in industrial, urban, and rural environments—a case study of the Cologne, Altenberg and Xanten cathedrals. Environmental Earth Sciences 69, 1095–1124.

Grossi C.M., Esbert R.M., Díaz-Pache F. and Alonso F.J., 2003. Soiling of building stones in urban environments. Building and Environment 38, 147-159.

Grossi C.M. and Brimblecombe P., 2004. Aesthetics of Simulated Soiling Patterns on Architecture. Environmental Science and Technology 38(14), 3971-3976.

Grossi C.M., Bonazza A., Brinblecombe P., Harris I., Sabbioni C., 2008. Predicting twenty-first century recession of architectural limestone in European cities. Environmental Geology 56, 455-461.

Grossi C.M., 2016. Soiling and Discolouration, in Brimblecombe P. (Ed.), Urban Pollution and Changes to Materials and Building Surfaces, Imperial College Press, Singapore, 127-142.

Haynie F.H. and Lemmons T.J., 1990. Particulate Matter Soiling of Exterior Paints at a Rural Site. Aerosol Science and Technology 13(3), 356-367.

Hamilton R.S. and Mansfield T.A., 1991. Airborne particulate elemental carbon: its sources, transport and contribution to dark smoke and soiling. Atmospheric Environment 25A (3/4), 715-723.
http://ep.yimg.com/ay/artsheaven/grand-canal-looking-south-west-from-the-palazzo-grimani-to-the-palazzo-foscari-9.jpg

http://iscs.icomos.org/glossary.html

http://www.corr-institute.se/

http://www.nettinc.com/information/emissions-faq/what-are-diesel-emissions

Kim S.T., Maeda Y., Tsujino Y., 2004. Assessment of the effect of air pollution on material damages in Northeast Asia. Atmospheric Environment 38 (1), 37–48.

Kramer R.P., Van Schijndel A.W.M., Schellen H.L., 2013. Inverse modeling to predict and characterize indoor climates. In: Mahdavi A., Martens B. (Eds.), proceedings of The 2nd Central European Symposium on Building Physics, 9-11 September 2013, Vienna, Austria, 101-108.

Kucera V., Tidblad J., Samie F., Schreiner M., Melcher M., Kreislov K., Lefevre R.A, Ionescu A., Snethlage R., Varotsos C., De Santis F., Mezinskis G., Sidraba I., Henriksen J., Kobus J., Ferm M., Faller M., Yates T., Watt J., Hamilton R., O'Hanlon S., 2005. Publishable final report of the EU 5FP RTD Project: Model for

multi-pollutant impact and assessment of threshold levels for cultural heritage, pp. 52. http://www.corr-institute.se/MULTI-ASSESS/

Lipfert F.W., 1989. Dry deposition velocity as an indicator for SO_2 damage to materials. Journal of Air Pollution Control Association 39, 446-452.

Mansfield T.A. and Hamilton R.S., 1989. The soiling of materials: models and measurement in a road tunnel in Man and his ecosystem. In: Brasser L.J. and Mulder W.C. (Eds.), proceedings of the 8th World Clean Air Congress, 11 - 15 September 1989, Hague, The Netherlands, Elsevier Science Publishers B.V., Amsterdam, The Netherlands, 353-357.

Massey S.W., 1999. The effects of ozone and NO_x on the deterioration of calcareous stone. Science of The Total Environment 227 (2-3), 109–121.

Nava S., Becherini F., Bernardi A., Bonazza A., Chiari M., García-Orellana I., Lucarelli F., Ludwig N., Migliori A., Sabbioni C., Udisti R., Valli G. and Vecchi R., 2010. An integrated approach to assess air pollution threats to cultural heritage in a semi-confined environment: The case study of Michelozzo's Courtyard in Florence (Italy). The Science of the Total Environment 408, 1403–1413.

Nicholson K.W., 1988. The dry deposition of small particles: A review of experimental measurements. Atmospheric Environment 22 (12), 2653-2666.

Ozga I., Bonazza A., Ait Lyazidi S., Haddad H., Ben-Ncer A., Ghedini N. and Sabbioni C., 2013. Pollution impact on the ancient ramparts of the Moroccan city Salé. Journal of Cultural Heritage, special issue 14S, S25–S33.

Pantani M., Sabbioni C., Bruzzi L. and Manco D., 1998. Air pollution deposition on stones of artistic Interest. Transactions on Ecology and the Environment 21, 675-684.

Pio C.A., Ramosa M.M., Duarte A.C., 1998. Atmospheric aerosol and soiling of external surfaces in an urban environment. Atmospheric Environment 32 (11), 1979-1989.

Přikryl R., Svobodová J., Žák K. and Hradil D., 2004. Anthropogenic origin of salt crusts on sandstone sculptures of Prague's Charles Bridge (Czech Republic): Evidence of mineralogy and stable isotope geochemistry. European journal of mineralogy 16 (4), 609-618.

Realini M., Negrotti R., Appollonia L. and Vaudan D., 1995. Deposition of particulate matter on stone surfaces: an experimental verification of its effects on Carrara marble. The Science of the Total Environment 167 (1-3), 67-72.

Sabbioni C. and Zappia G., 1992a. Decay of sandstone in urban areas correlated with atmospheric aerosol. Water, Air, and Soil Pollution 63 (3), 305-316.

Sabbioni C. and Zappia G., 1992b. Atmospheric-derived element tracers on damaged stone. The Science of the Total Environment 126, 35-48.

Sabbioni C., 1995. Contribution of atmospheric deposition to the formation of damage layers. The Science of the Total Environment 167, 49-55.

Sabbioni C., Zappia G. and Gobbi G., 1996. Carbonaceous particles and stone damage in a laboratory exposure system. Journal of Geophysical Research 101 (D14), 19621-19627.

Sabbioni C., 2000. Aerosol and Stone Monuments, in K.R. Spurny (Ed.), Aerosol Chemical Processes in the Environment, CRC Press LLC, Florida, pp. 327-345.

Sabbioni C., 2003. Mechanisms of air pollution damage to stone, in Brimblecombe P. (Ed.), The Effect of Air pollution on the Built Environment, Imperial College Press, Singapore, pp. 63-106.

Sabbioni C., Brimblecombe P., Bonazza A., Grossi C. M., Harris I., Messina P., 2007. Mapping climate change and cultural heritage. In: Drdacky M. (Ed.), proceedings of the 7th EC Prague Conference on Safeguarded Cultural Heritage - Understanding & Viabiliy for the Enlarged Europe, Prague, Czech Republic, 119-124.

Sabbioni C., Brimblecombe P., Cassar C. (Eds.), 2012. The Atlas of Climate Change Impact on European Cultural Heritage. Scientific Analysis and Management Strategies. Anthem Press, London, 160. ISBN 9780857282835

Schiavon N., 2007. Kaolinisation of granite in an urban environment. Environmental Geology 52 (2), 399-407.

Serra M. and Starace G., 1978. Study of the reactions between gaseous sulphur dioxide and calcium carbonate. In UNESCO/RILEM International Symposium on the Deterioration and Protection of Stone Monuments. UNESCO/RILEM, Paris, 3.7., 1-19.

Silva Hermo B., Prieto Lamas B., Rivas Brea T. and Pereira Pardo L., 2010. Gypsum-induced decay in granite monuments in Northwestern Spain. Materiales de Construcción 60 (297), 97-110.

Simão J., Ruiz-Agudo E., Rodriguez-Navarro C., 2006. Effects of particulate matter from gasoline and diesel vehicle exhaust emissions on silicate stones sulfation. Atmospheric Environment 40, 6905-6917.

Smith B.J., McCabe S., McAllister D., Adamson C., Viles H.A. and Curran J.M., 2011. A commentary on climate change, stone decay dynamics and the 'greening' of natural stone buildings: new perspectives on 'deep wetting'. Environmental Earth Sciences 63 (7), 1691-1700.

Tang W., Davidson C.I., Finger S. and Vance K., 2004. Erosion of limestone building surfaces caused by wind driven rain: 1. Field measurements. Atmospheric Environment 38, 5589-5599.

Tang W. and Davidson C.I., 2004. Erosion of limestone building surfaces caused by wind-driven rain: 2. Numerical modeling. Atmospheric Environment 38, 5601-5609.

Tidblad J., Kucera V., Ferm M., Kreislova K., Brüggerhoff S., Doytchinov S., et al., 2012. *Review Article* Effects of Air Pollution on Materials and Cultural Heritage: ICP Materials Celebrates 25 Years of Research. International Journal of Corrosion, vol. 2012, Article ID 496321, 16 pages. doi:10.1155/2012/496321

Tidblad J., Kreislova K., Faller M., De la Fuente D., Yates T. and Verney-Carron A., 2016. Convention On Long-Range Transboundary Air Pollution International Co-Operative Programme On Effects On Materials, Including Historic And Cultural Monuments, Report No 78 Results on corrosion and soiling from the 2011–2015 exposure programme for trend analysis. Swerea KIMAB AB, Stockholm, Sweden, 36.

Toniolo L., Zerbi C.M., Bugini R., 2009. Black layers on historical architecture. Environmental Science and Pollution Research 16 (2), 218-226.

Török Á., 2003. Surface strength and mineralogy of weathering crusts on limestone buildings in Budapest. Building and Environment 38, 1185-1192.

Török Á. and Rozgonyi N., 2004. Morphology and mineralogy of weathering crusts on highly porous oolitic limestones, a case study from Budapest. Environmental Geology 46, 333-349.

Török Á., 2008. Black crusts on travertine: factors controlling development and stability. Environmental Geology 56, 583-594.

Viles H.A., Taylor M.P., Yates T.J.S. and Massey S.W., 2002. Soiling and decay of N.M.E.P. limestone tablets. The Science of the Total Environment 292 (3), 215-229.

Urosevic M., Yebra-Rodríguez A., Sebastián-Pardo E. and Cardell C., 2012. Black soiling of an architectural limestone during two-year term exposure to urban air in the city of Granada (S Spain). Science of the Total Environment 414, pp. 564-575.

Viles H.A. and Gorbushina A.A., 2003. Soiling and microbial colonisation on urban roadside limestone: a three year study in Oxford (England), Building and Environment 38, 1217-1224.

Watt J. and Hamilton R., 2003. The Soiling of Buildings by Air Pollution. In: The Effects of Air Pollution on the Built Environment. Brimblecombe P. (Ed.), London, Imperial college press; 289-334. ISBN: 978-1-86094-291-4

Watt J., Jarrett D. and Hamilton R., 2008. Dose–response functions for the soiling of heritage materials due to air pollution exposure. Science of The Total Environment 400 (1–3), 415–424.

Watt J., Tidblad J., Kucera V., Hamilton R. (Eds.), 2009. The Effects of Air Pollution on Cultural Heritage. Springer, New York; 306. DOI 10.1007/978-0-387-84893-8

Weinbruch S., Worringen A., Ebert M., Scheuvens D., Kandler K., Pfeffer U. and Bruckmann P., 2014. A quantitative estimation of the exhaust, abrasion and resuspension components of particulate traffic emissions using electron microscopy. Atmospheric Environment 99, 175-182.

Wrigley E.A. (Ed.), 1990. Continuity, Chance and Change: The Character of the Industrial Revolution in England. Cambridge University Press, Cambridge, 156. ISBN 0-521-39657-3.

Yates T.J.S., Coote A.T. and Butlin R.N., 1988. The Effect of Acid Deposition on Buildings and Building Materials. Construction & Building Materials 2 (1), 20-26.

Zappia G., Sabbioni C., Riontino C., Gobbi G. and Favoni O., 1998. Exposure tests of building materials in urban atmosphere. The Science of the Total Environment 224 (1-3), 235-244.

CHAPTER 2

Birch M.E. and Cary R.A., 1996. Elemental carbon-based method for monitoring occupational exposures to particulate diesel exhaust. Aerosol Science and Technology 25 (3), 221–241.

Carbone C., Decesari S., Mircea M., Giulianelli L., Finessi E., Rinaldi M. et al., 2010. Size-resolved aerosol chemical composition over the Italian Peninsula during typical summer and winter conditions. Atmospheric Environment 44, 5269-5278.

Cardell C., Delalieux F., Roumpopoulos K., Moropoulou A., Auger F. and Van Grieken R., 2003. Salt-induced decay in calcareous stone monuments and buildings in a marine environment in SW France. Construction and Building Materials 17, 165-179.

Cesari D., Merico E., Dinoi A., Marinoni A., Bonasoni P. and Contini D., 2018. Seasonal variability of carbonaceous aerosols in an urban background area in Southern Italy. Atmospheric Research 200, 97-108.

Cuccia E., Piazzalunga A., Bernardoni V., Brambilla L., Fermo P., Massabò D., et al., 2011. Carbonate measurements in PM10 near the marble quarries of Carrara (Italy) by infrared spectroscopy (FT-IR) and source apportionment by positive matrix factorization (PMF). Atmospheric Environment 45 (35), 6481-6487.

Del Monte M., 2800. Materiale architettonico di spoglio: uso e reimpiego dell'antico a Bologna. il Geologo dell'Emilia-Romagna 30, 5-22.

De Nuntiis P. and Palla F., 2017. Bioaerosol. In: Palla F. and Barresi G. (eds.), Biotechnology and Conservation of Cultural Heritage, Springer International Publishing, Switzerland, 31-48. ISBN 978-3-319-46168-7

Fermo P., Gonzalez Turrion R., Rosa M. and Omegna A., 2015. A new approach to assess the chemical composition of powder deposits damaging the stone surfaces of historical monuments. Environmental Science and Pollution Research 22, 6262-6270.

Galloway G., Seminara G., Blöschl G., Garcia M., Montanari A. and Solari L. 2017. Saving a World Treasure: Protecting Florence from Flooding. Report of the international technical and scientific committee of Florence 2016 on the protection of Florence from flooding. Firenze University Press, Firenze , Italy, pp. 156. ISBN 978-88-6453-677-4

Ghedini N., Sabbioni C., Bonazza A. and Gobbi G., 2006. Chemical-Thermal Quantitative Methodology for Carbon Speciation in Damage Layers on Building Surfaces. Environmental Science and Technology 40, 939-944.

Grillini G.C., 2006. Due singolari pietre nelle architetture estensi e malatestiane: il calcare grigio di Noriglio e il marmo di Candoglia, in Zerbini M., Fabbri R., Bevilacqua F. (Eds.), Antichi mestieri della Tradizione Edilizia Ferrarese-Terrecotte e Dipinti Murali, SATE S.r.l., Ferrara, 87-93.

https://www.google.it/maps

http://whc.unesco.org/en/list/

https://www.worldweatheronline.com

http://www.meteoblue.com

https://www.openstreetmap.org

https://upload.wikimedia.org/wikipedia/commons/d/d2/Delta-P%C3%B4-1568.jpg

http://www.bonificaferrara.it

http://www.fe.camcom.it/cciaa/cenni-sull-economia-provinciale

http://statistica.fi.it/opencms/opencms/MenuPrincipale/Dati/Popolazione_ Firenze

http://www.climatemps.com/

http://www.eurometeo.com

https://www.wunderground.com/

https://www.tuttitalia.it

http://vincoliinretegeo.beniculturali.it

INAIL Il monitoraggio microbiologico negli ambienti di lavoro. Campionamento e analisi, (Edizioni INAIL, Milano, Italy, 2010) ISBN 978-88-7484-162-2.

INAIL La qualità del dato analitico nel monitoraggio ambientale del bioaerosol. L'esperienza INAIL di intercalibrazione dei conteggi microbici su piastra (Edizioni INAIL, Milano, Italy, 2011) ISBN 978-88-7484-214-8.

La Russa M.F., Fermo P., Comite V., Belfiore C.M., Barca D., Cerioni A., et al., 2017. The Oceanus statue of the Fontana di Trevi (Rome): The analysis of black crust as a tool to investigate the urban air pollution and its impact on the stone degradation. Science of the Total Environment 593-594, 297-309.

Natali C. and Bianchini G., 2015. Thermally based isotopic speciation of carbon in complex matrices: a tool for environmental investigation. Environmental Science and Pollution Research 22 (16), 12162-12173.

Natali C., Bianchini G. and Vittori Antisari L., 2018. Thermal separation coupled with elemental and isotopic analysis: A method for soil carbon characterisation. CATENA 164, 150-157.

Perrino C., Catrambone M., Dalla Torre S., Rantica E., Sargolini T. and Canepari S., 2014. Seasonal variations in the chemical composition of particulate matter: a case study in the Po Valley. Part I: macro-components and mass closure. Environmental Science and Pollution Research 21, 3999–4009.

Pio C.A., Cerqueira M., Harrison R.M., Nunes T., Mirante F., Alves C., et al., 2011. OC/EC ratio observations in Europe: Re-thinking the approach for apportionment between primary and secondary organic carbon. Atmospheric Environment 45, 6121-6132.

Ricciardelli I., Bacco D., Rinaldi M., Bonafè G., Scotto F., Trentini A. et al., 2017. A three-year investigation of daily PM2.5 main chemical components in four sites: the routine measurement program of the Supersito Project (Po Valley, Italy). Atmospheric Environment 152, 418-430.

Rubel F., Brugger K., Haslinger K., and Auer I., 2017. The climate of the European Alps: Shift of very high resolution Köppen-Geiger climate zones 1800-2100. Meteorologische Zeitschrift 26 (2): 115-125.

Sağlar Onay N. and Ricci M., 2013. Stone as a Determinant of Architectural Identity in the Florence of Renaissance, AZ ITU Journal of the Faculty of Architecture 9 (2), 121-134 ISSN: 1302-8324

Tositti L., Brattich E., Masiol M., Baldacci D., Ceccato D., Parmeggiani S. et al., 2014. Source apportionment of particulate matter in a large city of southeastern Po Valley (Bologna, Italy). Environmental Science and Pollution Research 21, 872-890.

UNI 15886:2010 Conservation of cultural property - Test methods - Colour measurement of surfaces

CHAPTER 3

Amoroso G.G. (Ed.), 2002. Diffusione e trasporto dei fluidi nei materiali porosi. In: Trattato di scienza della conservazione dei monumenti: etica della conservazione, degrado dei monumenti, interventi conservativi, consolidanti e protettivi. ALINEA Editrice, Florence, 131-165.

Appolonia L., Ranalli G., Sabbioni C. and Sorlini C., 2003. Chemical parameters and development of biodeteriogens. The Biological Aerosol as a Factor of Biodeterioration. In: Mandrioli P., Caneva G. and Sabbioni C. (Eds.), Cultural Heritage and Aerobiology Methods and Measurement Techniques for Biodeterioration Monitoring, Springer, Dordrecht, 81-103. ISBN: 1-4020-1622-0

Arnold A. and Zehnder K., 1991. Monitoring wall paintings affected by soluble salts. In: Cather S. (Ed.), The Conservation of Wall Paintings, proceedings of a symposium organized by the Courtauld Institute of Art and the Getty Conservation Institute, London, July 13-16 1987. Getty Conservation Institute, 103-135.

ARPAE, 2012. CAMPAGNA DI MONITORAGGIO DELLA QUALITA' DELL'ARIA EFFETTUATA NEL COMUNE DI BOLOGNA ANGOLO VIA F. RIZZOLI – PIAZZA DEL NETTUNO 21 Febbraio – 28 Marzo 2012.

ARPAE, 2013a. CAMPAGNA DI MONITORAGGIO DELLA QUALITA' DELL'ARIA EFFETTUATA NEL COMUNE DI BOLOGNA ANGOLO VIA F. RIZZOLI – PIAZZA DEL NETTUNO 14 Febbraio – 26 Marzo 2013.

ARPAE, 2013b. CONVENZIONE TRA COMUNE DI BOLOGNA E ARPA RELATIVA ALLE ATTIVITA' DI MONITORAGGIO INTEGRATIVO SULLA QUALITA' DELL'ARIA. Attività di monitoraggio e supporto tecnico per il periodo novembre 2012 – novembre 2013.

ARPAE, 2014. MONITORAGGIO DELLA QUALITÁ DELL'ARIA COMUNE DI BOLOGNA VIA F. RIZZOLI – PIAZZA DEL NETTUNO VIA IRNERIO – SFERISTERIO 20 FEBBRAIO – 19 MARZO 2014.

Ausset P., Bannery F., Del Monte M., Lefevre R.A., 1998. Recording of preindustrial atmospheric-environment by ancient crusts on stone monuments. Atmospheric environment 32(16), 2859-2863.

Barbagallo L. F., 2014. Monitoraggio di particolato atmosferico al fine della conservazione del patrimonio culturale urbano: il caso di Firenze. Thesis in Chemistry, University of Milan, A.Y. 2013-2014.

Belfiore C.M., Barca D., Bonazza A., Comite V., La Russa M. F., Pezzino A., Ruffolo A. and Sabbioni C., 2013. Application of spectrometric analysis to the identification of pollution sources causing cultural heritage damage. Environmental Science and Pollution Research 20, 8848-8859.

Bonazza A., Sabbioni C. and Ghedini N., 2005. Quantitative data on carbon fractions in interpretation of black crusts and soiling on European built heritage. Atmospheric Environment 39, 2607-2618.

Bonazza A. and Sabbioni C., 2016. Composition and Chemistry of Crusts on Stone, in Brimblecombe P. (Ed.), Urban Pollution and Changes to Materials and Building Surfaces, Imperial College Press, Singapore, 103-126.

Bonazza A., De Nuntiis P., Mandrioli P. and Sabbioni C., 2017. Aerosol Impact on Cultural Heritage: Deterioration Processes and Strategies for Preventive Conservation. In: Tomasi C., Fuzzi S. and Kokhanovsky A. (eds.), Atmospheric Aerosols: Life Cycles and Effects on Air Quality and Climate, Wiley-VCH Verlag GmbH & Co. KGaA, Weinheim, Germany, 645-670. ISBN: 978-3-527-33645-6

Bosellini A., Carraro F., Corsi M., De Vecchi G.P., Gatto G.O., Malaroda R., Sturani C., Ungaro S., Zanettin B., 1967. Note illustrative della Carta Geologica d'Italia alla scala 1.100.000, 49. Verona. Servizio Geologico d'Italia, pp. 61.

Brimblecombe P. And Grossi C.M., 2009. Deposition, Transformation, and Remobilization of Soot and Diesel Particulates on Building Surfaces. In: Moreira D. and Vilhena M. (Eds.), Air Pollution and Turbulence: Modeling and Applications, CRC Press Taylor & Francis Group, Boca Raton, Florida, 1-14. ISBN-13: 978-1-4398-4712-1

Cachier H., 1989. Isotopic characterization of carbonaceous aerosols. Aerosol Science Technology 10, 379-385.

Cachier H., Sarda-Estève R., Oikonomou K., Sciare J., Bonazza A., Sabbioni C., Greco M., Reyes J., Hermosin B. and Saiz-Jimenez C., 2004. Aerosol characterization and sources in different European urban

atmospheres: Paris, Seville, Florence and Milan. In: Saiz-Jimenez C. (Ed.), Air Pollution and Cultural Heritage, BALKEMA, Leiden, 3-14.

Cal-Prieto M. J., Carlosena A., Andrade J. M., Martínez M. L., Muniategui S., López-Mahía P. and Prada D., 2001. Antimony as a tracer of the anthropogenic influence on soils and estuarine sediments. Water, Air, and Soil Pollution 129, 333-348.

Camuffo D. (Ed.), 2014. Micropore condensation and stone weathering. In: Microclimate for Cultural Heritage, Conservation, Restoration, and Maintenance of Indoor and Outdoor Monuments (2nd Edition). Elsevier Science, 182-191.

Canepari S., Astolfi M. L., Farao C., Maretto M., Frasca D., Marcoccia M. and Perrino C., 2014. Seasonal variations in the chemical composition of particulate matter: a case study in the Po Valley. Part II: concentration and solubility of micro- and trace-elements. Environmental Science and Pollution Research 21 (6), 4010-4022.

Caneva G., Maggi O., Nugari M. P. , Pietrini A. M., Piervittori R., Ricci S., Roccardi A., 2003. The Biological Aerosol as a Factor of Biodeterioration. In: Mandrioli P., Caneva G. and Sabbioni C. (Eds.), Cultural Heritage and Aerobiology Methods and Measurement Techniques for Biodeterioration Monitoring, Springer, Dordrecht, 3-41. ISBN: 1-4020-1622-0.

Cardell C., Delalieux F., Roumpopoulos K., Moropoulou A., Auger F. and Van Grieken R., 2003. Salt-induced decay in calcareous stone monuments and buildings in a marine environment in SW France. Construction and Building Materials 17, 165-179.

Carotta M.C. and Vaccaro C., 2001. Monitoraggio degli inquinanti atmosferici e caratterizzazione dei prodotti di degrdo riscontrati negli elementi in cotto a Ferrara. In: Il progetto di conservazione: linee metodologiche per le analisi preliminari, l'intervento, il controllo di efficacia. Pesenti S. (Ed.), Firenze, Alinea Editrice; 276-283, ISBN 88-8125-537-5

CEC, 1993. Commission of the European Communities, Biological Particles in Indoor Environments, European Collaborative Action, Indoor Air Quality & Its Impact on Man, COST Project 613, Report No.12, EUR 14988 EN, Luxembourg.

Coppi S., 2007. Rapporto sulla Qualità dell'Aria della provincia di Ferrara anno 2006. pp. 133.

Chabas A. and Lefevre R.A., 2000. Chemistry and microscopy of atmospheric particulates at Delos (Cyclades-Greece). Atmospheric Environment 34 (2), 225-238.

Comite V., Álvarez de Buergo M., Barca D., Belfiore C.M., Bonazza A., La Russa M.F. et al., 2017. Damage monitoring on carbonate stones: Field exposure tests contributing to pollution impact evaluation in two Italian sites. Construction and Building Materials 152, 907-922.

Del Carmine P., Lucarelli F., Mandò P.A., Moscheni G. and Pecchioli A., 1990. PIXE measurements of air particulate elemental composition in the urban area of Florence, Italy. Nuclear Instruments and Methods in Physics Research Section B: Beam Interactions with Materials and Atoms 45 (1-4), 341-346.

Del Monte M., Sabbioni C. and Zappia G., 1987. The origin of calcium oxalates on historical buildings, monuments and natural outcrops. Science of The Total Environment 67 (1), 17-39.

De Nuntiis P., Maggi O., Mandrioli P., Ranalli G., Sorlini C., 2003. Monitoring the Biological Aerosol. In: Mandrioli P., Caneva G. and Sabbioni C. (Eds.), Cultural Heritage and Aerobiology Methods and Measurement Techniques for Biodeterioration Monitoring, Springer, Dordrecht, 107-144. ISBN: 1-4020-1622-0

De Nuntiis P. and Palla F., 2017. Bioaerosol. In: Palla F. and Barresi G. (eds.), Biotechnology and Conservation of Cultural Heritage, Springer International Publishing, Switzerland, 31-48. ISBN 978-3-319-46168-7

Deserti M., Maccaferri S., Stortini M., 2015. Politiche ambientali e uso di biomassa in Pianura padana (Environmental policies and use of biomass in the Po valley). Ecoscienza 1, 46-49.

Després V.R., Huffman J.A., Burrows S.M., Hoose C., Safatov A.S., Buryak G. et al., 2012. Primary biological aerosol particles in the atmosphere: a review. Tellus B: Chemical and Physical Meteorology 64 (1), 15598, 1-58.

Douwes J., Thorne P., Pearce N. and Heederik D., 2003. Bioaerosol health effects and exposure assessment: progress and prospects. The Annals of Occupational Hygiene 47 (3), 187–200.

Dunham R.J., 1962. Classification of carbonate rocks according to depositional texture. In: Ham W.E. (Ed.), Classification of Carbonate Rocks: A Symposium, American Association of Petroleum, Geologists Memoir 1, Tulsa, U.S.A., 108-121.

Ebert M., Müller-Ebert D., Benker N. and Weinbruch S., 2012. Source apportionment of aerosol particles near a steel plant by electron microscopy. Journal of Environmental Monitoring 14 (12), 3257-3266.

Esbert R.M., Dìaz-Pache F., Grossi C.M., Alonso F.J. and Ordaz J., 2001. Airborne particulate matter around the Cathedral of Burgos (Castilla y Leòn, Spain). Atmospheric Environment 35, 441-452.

Favali M. A., Gallo F., Maggi O., Mandrioli P., Pacini E., Pasquariello G., Piervittori R., Pietrini A.M., Ranalli G., Ricci S., Roccardi A. Sorlini C., 2003. Analysis of the Biological Aerosol. In: Mandrioli P., Caneva G. and Sabbioni C. (Eds.), Cultural Heritage and Aerobiology Methods and Measurement Techniques for Biodeterioration Monitoring, Springer, Dordrecht, 145-172. ISBN: 1-4020-1622-0

Ferrari E., 2003. Valutazione dell'impatto su superfici lapidee degli inquinanti atmosferici misurati in situ tramite sensori chemiresistivi. Thesis in Innovative Physical Technologies, Faculty of Mathematical, Physical and Natural Sciences, University of Ferrara, A.Y. 2002-2003.

Forni F., 2010. Inventario Regionale sulle Sorgenti di Emissione in aria ambiente IRSE - Rapporto aggiornamento anno 2010.

Fuzzi S., Baltensperger U., Carslaw K., Decesari S., Denier van der Gon H., Facchini M. C., et al., 2015. Particulate matter, air quality and climate: lessons learned and future needs. Atmospheric Chemistry and Physics 15, 8217-8299.

Gadd G.M., Bahri-Esfahani J., Li Q., Rhee Y.J., Wei Z., Fomina M. and Liang X, 2014. Oxalate production by fungi: significance in geomycology, biodeterioration and bioremediation. Fungal Biology Reviews 28, 36-55.

Gerdol R., Marchesini R., Iacumin P. and Brancaleoni L., 2014. Monitoring Temporal Trends of Air Pollution in an Urban Area Using Mosses and Lichens as Biomonitors. Chemosphere 108, 388-395.

Ghedini N., Ozga I., Bonazza A., Dilillo M., Cachier H. and Sabbioni C., 2011. Atmospheric aerosol monitoring as a strategy for the preventive conservation of urban monumental heritage: The Florence Baptistery. Atmospheric Environment 45 (33), 5979-5987.

Grechi D., 2014. EpiChange: Chi controlla la qualità dell'aria a Firenze? (Who is monitoring air pollution in Florence?). Epidemiologia e Prevenzione, 38 (3-4), 154-158.

https://www.arpae.it/

http://www.arpat.toscana.it/

http://www.bonificaferrara.it

http://www.comune.fe.it/attach/superuser/docs/piano_aria_provincia_sintesi.pdf

https://www.esrl.noaa.gov/

http://www.ilpolline.it/wp-content/uploads/2008/02/calendario-per-sito.pdf, accessed 08 Oct 2018

http://www.pollnet.it/Stations/cal_it_11.aspx, accessed 08 Oct 2018

INAIL Il monitoraggio microbiologico negli ambienti di lavoro. Campionamento e analisi, (Edizioni INAIL, Milano, Italy, 2010) ISBN 978-88-7484-162-2

INAIL La qualità del dato analitico nel monitoraggio ambientale del bioaerosol. L'esperienza INAIL di intercalibrazione dei conteggi microbici su piastra (Edizioni INAIL, Milano, Italy, 2011) ISBN 978-88-7484-214-8

Istat, Statistiche ambientali, Volume I, Roma 1984.

La Repubblica, 24 February 1989.

Lucarelli F., Mandò P.A., Nava S., Prati P. and Zucchiatti A., 2004. One-Year Study of the Elemental Composition and Source Apportionment of PM10 Aerosols in Florence, Italy. Journal of the Air and Waste Management Association 54 (11), 1372-1382.

Magnavacca M., 1996. Valutazione del degrado superficiale di edifici storici di Ferraraad opera di agenti inquinanti. Thesis in Geological Sciences, Faculty of Mathematical, Physical and Natural Sciences, University of Ferrara, A.Y. 1995-1996.

Martinsson J., Andersson A., Sporre M. K., Friberg J., Kristensson A., Swietlicki E., et al., 2017. Evaluation of $\delta^{13}C$ in Carbonaceous Aerosol Source Apportionment at a Rural Measurement Site. Aerosol and Air Quality Research 17, 2081-2094.

Mašalaitė A., Garbaras A. and Remeikis V., 2012. Stable isotopes in environmental investigations. Lithuanian Journal of Physics 52 (3), 261-268.

Mašalaitė A., Holzinger R., Remeikis V., Röckmann T., Dusek U., 2017. Characteristics, sources and evolution of fine aerosol (PM1) at urban, coastal and forest background sites in Lithuania. Atmospheric Environment 148, 62-76.

MIBAC (2001), Atto di Indirizzo sui criteri tecnico-scientifici e sugli standard di funzionamento e sviluppo dei musei, D. Lgs. 112/1998, art. 150, comma 6, G. U. n. 244.

Miliani C., Velo-Simpson M.L. and Scherer G.W., 2007. Particle-modified consolidants: a study on the effect of particles on sol-gel properties and consolidation effectiveness. Journal of Cultural Heritage 8 (1), 1-6. http://dx.doi.org/10.1016/j.culher.2006.10.002.

Nava S., Becherini F., Bernardi A., Bonazza A., Chiari M., García-Orellana I., Lucarelli F., Ludwig N., Migliori A., Sabbioni C., Udisti R., Valli G. and Vecchi R., 2010. An integrated approach to assess air pollution threats to cultural heritage in a semi-confined environment: The case study of Michelozzo's Courtyard in Florence (Italy). Science of the Total Environment 408 (6), 1403-1413.

Nazaroff W.W. and Cass G.R., 1989. Mass-transport aspects of pollutant removal at in door surfaces. Environment International 15, 567-84.

Ozga I. and Ghedini N., 2009. The importance of atmospheric particle monitoring in the protection of cultural heritage. Air Pollution XVII, 259-269.

Paolini F., 2007. I territori dello sviluppo. L'area fiorentino-pratese (1946-1995). In: Corona G. and Neri Serneri S., Storia e ambiente. Città, risorse e territori nell'Italia contemporanea, Roma, Carocci, pp. 179-194.

Paolini F., 2014. Firenze 1946-2005. Una storia urbana e ambientale: Una storia urbana e ambientale. Franco Angeli Edizioni (Ed.), Milan, 417.

Peré-Trepat E., Kim E., Paatero P., Hopke P.K., 2007. Source apportionment of time and size resolved ambient particulate matter measured with a rotating DRUM impactor. Atmospheric Environment 41, 5921-5933.

Perrino C., Catrambone M., Dalla Torre S., Rantica E., Sargolini T. and Canepari S., 2014. Seasonal variations in the chemical composition of particulate matter: a case study in the Po Valley. Part I: macro-components and mass closure. Environmental Science and Pollution Research 21, 3999–4009.

Primavori P., 2015. Carrara Marble: a nomination for "Global Heritage Stone Resource" from Italy. In: Pereira D., Marker B.R., Kramar S., Cooper B.J., Schouenborg B.E. (Eds.) Global Heritage Stone: Towards International Recognition of Building and Ornamental Stones, Geological Society of London, Bath, UK, 137-154.

Ranzi A. and Lauriola P., 2015. L'impatto sulla salute della combustione di legna. Ecoscienza 1, 60-61.

Ricciardelli I., Bacco D., Rinaldi M., Bonafé G., Scotto F., Trentini A., et al., 2017. A three-year investigation of daily PM2.5 main chemical components in four sites: the routine measurement program of the Supersito Project (Po Valley, Italy). Atmospheric Environment 152, 418-430.

Sabbioni C. (1995) Contribution of atmospheric deposition to the formation of damage layers. The Science of the Total Environment 167, 49-55.

Salminen P., 2014. Carbon isotope records of sedimentary carbonate rocks in the Pechenga belt, NW Russia: implications for the Precambrian carbon cycle. Unigrafia, Helsinki, pp. 39. ISBN 978-952-10-9462-0

Sarti E., Pasti L., Rossi M., Ascanelli M., Pagnoni A., Trombini M. and Remelli M., 2015. The composition of PM1 and PM2.5 samples, metals and their water soluble fractions in the Bologna area (Italy). Atmospheric Pollution Research 6, 708-718.

Sarti E., Pasti L., Scaroni I., Casali P., Cavazzini A. and Rossi M., 2017. Determination of n-alkanes, PAHs and nitro-PAHs in PM2.5 and PM1 sampled in the surroundings of a municipal waste incinerator. Atmospheric Environment 149, 12-23.

Schaap M., Spindler G., Schulz M., Acker K., Maenhaut W., Berner A., et al., 2004. Artefacts in the sampling of nitrate studied in the ''INTERCOMP'' campaigns of EUROTRAC-AEROSOL. Atmospheric Environment 38, 64876496.

Telloli C., 2014. Metal Concentrations in Snow Samples in an Urban Area in the Po Valley. International Journal of Geosciences 5, 1116-1136.
Thorpe A. and Harrison R.M., 2008. Sources and properties of non-exhaust particulate matter from road traffic: A review. Science of the Total Environment 400, 270-282.

Tomasi C. and Lupi A., 2017. Primary and Secondary Sources of Atmospheric Aerosol. In: Tomasi C., Fuzzi S. and Kokhanovsky A. (eds.), Atmospheric Aerosols: Life Cycles and Effects on Air Quality and Climate, Wiley-VCH Verlag GmbH & Co. KGaA, Weinheim, Germany, 1-86. ISBN: 978-3-527-33645-6

Tositti L., Brattich E., Masiol M., Baldacci D., Ceccato D., Parmeggiani S. et al., 2014. Source apportionment of particulate matter in a large city of southeastern Po Valley (Bologna, Italy). Environmental Science and Pollution Research 21, 872–890.

Tugnoli S. and Deserti M., 2011. Risultati dell'indagine sul consumo domestico di biomassa legnosa in Emilia-Romagna, ARPA Emilia-Romagna.

Tugnoli S., Rumberti V., Ansaloni F., Veronesi P., Stortini M and Maccaferri M, 2013. AGGIORNAMENTO INVENTARIO REGIONALE DELLE EMISSIONI IN ATMOSFERA ANNO 2010 (INEMAR-ER), https://www.arpae.it/cms3/documenti/_cerca_doc/aria/inventario_emissioni_2010.pdf

Urosevic M., Yebra-Rodríguez A., Sebastián-Pardo E. and Cardell C., 2012. Black soiling of an architectural limestone during two-year term exposure to urban air in the city of Granada (S Spain). Science of the Total Environment 414, pp. 564-575.

Weinbruch S., Worringen A., Ebert M., Scheuvens D., Kandler K., Pfeffer U. and Bruckmann P., 2014. A quantitative estimation of the exhaust, abrasion and resuspension components of particulate traffic emissions using electron microscopy. Atmospheric Environment 99, 175-182.

WHO-World Health Organisation, 2006. Air Quality Guidelines. Particulate matter, ozone, nitrogen dioxide and sulfur dioxide. Global Update 2005, Copenhagen, WHO Regional Office for Europe Regional Publications.

Widory D, 2006. Combustibles, fuels and their combustion products: A view through carbon isotopes, Combustion Theory and Modelling 10 (5), 831-841.

www.supersito-er.it

Zanoni F., 2015. Biomasse e riscaldamento, tra opportunità e rischio (Heating from biomass, opportunities and risks). Ecoscienza 1, 44-45.

CHAPTER 4

Auras M., Bundschuh P., Eichhorn J., Kirchner D., Mach M., Seewald B., Scheuvens D. and Snethlage R., 2018. Salt deposition and soiling of stone facades by traffic-induced immissions. Environmental Earth Sciences 77: 323.

Bonazza A., Sabbioni C. and Ghedini N., 2005. Quantitative data on carbon fractions in interpretation of black crusts and soiling on European built heritage. Atmospheric Environment 39, 2607-2618.

Bonazza A., Brimblecombe P., Grossi M.C. and Sabbioni C., 2007. Carbon in Black Crusts from the Tower of London. Environmental Science and Technology 41 (12), 4199-4204.

Bonazza A. and Brimblecombe P., 2016. Climate and the Changing Appearance of Buildings. In: Lefevre R., Sabbioni C. (Eds.), Cultural Heritage from Pollution to Climate Change, EDIPUGLIA, Italy, 17-24.

Brimblecombe P. and Grossi C.M., 2004. The rate of darkening of material surfaces, in Saiz-Jimenez C. (Ed.), Air Pollution and Cultural Heritage, Taylor & Francis Group, London, 193-198.

Brimblecombe P. and Grossi C.M., 2009. Millennium-long damage to building materials in London. Science of The Total Environment 407 (4), 1354-1361.

Camuffo D. (Ed.), 2014. Atmospheric Water and Stone Weathering. In: Microclimate for Cultural Heritage, Conservation, Restoration, and Maintenance of Indoor and Outdoor Monuments (2nd Edition). Elsevier Science, pp. 203-243.

Casuccio G.S., Schlaegle S.F., Lersch T.L., Huffman G.P., Chen Y., Shah N., 2004. Measurement of fine particulate matter using electron microscopy techniques. Fuel Processing Technology 85, 763-779.

Comite V., Álvarez de Buergo M., Barca D., Belfiore C.M. , Bonazza A., La Russa M.F. et al., 2017. Damage monitoring on carbonate stones: Field exposure tests contributing to pollution impact evaluation in two Italian sites. Construction and Building Materials 152, 907–922.

Fermo P., Goidanich S., Comite V., Toniolo L. and Gulotta D., 2018. Study and Characterization of Environmental Deposition on Marble and Surrogate Substrates at a Monumental Heritage Site. Geosciences 8(9), 349.

Ferrero L., Casati M., Nobili L., D'Angelo L., Rovelli G., Sangiorgi G., et al., 2018. Chemically and size-resolved particulate matter dry deposition on stone and surrogate surfaces inside and outside the low emission zone of Milan: application of a newly developed "Deposition Box". Environmental Science and Pollution Research 25, 9402-9415.

Grossi C.M., Brimblecombe P., Esbert R.M. and Alonso F.J., 2007. Color changes in architectural limestones from pollution and cleaning. Color research and application 32 (4), 320-331.

Grossi C.M. and Brimblecombe P., 2008. Past and future colouring patterns of historic stone buildings. Materiales de Construcción 58 (289-290), 143-160.

Grossi C.M., 2016. Soiling and Discolouration, in Brimblecombe P. (Ed.), Urban Pollution and Changes to Materials and Building Surfaces, Imperial College Press, Singapore, 127-142.

Hossaini R., Chipperfield M.P., SaizLopez A., Fernandez R., Monks S., Feng W., et al., 2016. A global model of tropospheric chlorine chemistry: Organic versus inorganic sources and impact on methane oxidation. Journal of Geophysical Research: Atmospheres 121, 14271-14297.

Karthikeyan S. and Balasubramanian R., 2006. Determination of water-soluble inorganic and organic species in atmospheric fine particulate matter. Microchemical Journal 82, 49-55.

Mayer B. and Krouse H.R., 2004. Procedures for sulfur isotope abundance studies. In: De Groot P.A. (Ed.), Handbook of stable isotope analytical techniques, vol.1, Elsevier, Amsterdam, The Nederland, 538-596.